Calpains in the Molecular Pathogenesis of Polyglutamine Disorders and their Potential as a Therapeutic Target

Dissertation

der Mathematisch-Naturwissenschaftlichen Fakultät

der Eberhard Karls Universität Tübingen

zur Erlangung des Grades eines

Doktors der Naturwissenschaften

(Dr. rer. nat.)

vorgelegt von

Jonasz Jeremiasz Weber

aus Gera

Tübingen

2017

Gedruckt mit Genehmigung der Mathematisch-Naturwissenschaftlichen Fakultät der Eberhard Karls Universität Tübingen.

Tag der mündlichen Qualifikation:	23.02.2018
Dekan:	Prof. Dr. Wolfgang Rosenstiel
1. Berichterstatter:	Prof. Dr. Olaf Rieß
2. Berichterstatter:	Prof. Dr. Ludger Schöls
3. Berichterstatter:	Prof. Dr. Susann Schweiger

Meiner Familie

"...to boldly go where no man has gone before."

James Tiberius Kirk

Table of contents

Abbreviations

aa	amino acid
Aβ	amyloid-β
AD	Alzheimer disease
ALS	amyotrophic lateral sclerosis
ALLN	N-acetyl-L-leucyl-L-leucyl-L-norleucinal
APP	amyloid precursor protein
BACE1	β-site APP cleaving enzyme 1
BACHD	bacterial artificial chromosome containing full-length huntingtin
bdp	breakdown product
Ca^{2+}	calcium (ions)
$CaCl_2$	calcium chloride
CAPN	calpain
CAPNS1	calpain small subunit 1
CAST	calpastatin
CI III	calpain inhibitor III
CMA	chaperone-mediated autophagy
CNS	central nervous system
DRPLA	dentatorubropallidoluysian atrophy
DUB	deubiquitinating enzyme
ER	endoplasmic reticulum
FTLD	frontotemporal lobar degeneration
HD	Huntington disease
Hdh	mouse huntingtin gene
HTT	human huntingtin gene
Htt	huntingtin protein
iCN	iPSC-derived differentiated cortical neuron
iHF	SV40-immortalised human fibroblast
IP_3R	1,4,5-trisphosphate receptor
iPSC	induced pluripotent stem cell
JD	Josephin domain
MAM	mitochondria-associated membrane
MJD1	human ataxin-3 gene
mPT	mitochondrial permeability transition
MSNs	medium-sized spiny neurons
NES	nuclear export signal
NLS	nuclear localisation signal
NMDA	N-methyl-D-aspartate
PC	protease core domain
PD	Parkinson disease
PEF	penta-EF-hand domain PD
polyQ	polyglutamine
ROS	reactive oxygen species
RyR	ryanodine receptor

Abbreviations

SBMA	spinal and bulbar muscular atrophy
SCA3	spinocerebellar ataxia type 3
SMA	spinal muscular atrophy
ST*Hdh*	SV40-immortalised striatal mouse precursor cells
SV40	*Simian virus* 40
TDP-43	TAR DNA-binding protein-43
TR-FRET	time-resolved Förster resonance energy transfer
TSPO	translocator protein/ tryptophan-rich sensory protein
UPS	ubiquitin-proteasome system
UTR	untranslated region
VDAC	voltage-dependent anion channel
YAC	yeast artificial chromosome

Summary

Summary (English)

Together with cancer and cardiovascular disorders, neurodegenerative diseases such as Alzheimer and Parkinson disease are an increasingly important medical issue for the aging society of the 21st century. Multiple factors such as environmental influences and individual living conditions act as important modulators of neuropathology. Despite various forms of neurodegenerative diseases, many similarities exist in the underlying molecular pathomechanisms. These are thus promising targets for medical interventions. Therefore, research on genetically determined forms featuring a singular trigger allows to understand these common processes and to transfer acquired knowledge to other neurological diseases.

In view of this fact, the current work investigates the validity of the *toxic fragment hypothesis* using the example of two polyglutamine diseases, Huntington disease and spinocerebellar ataxia type 3. This widely-described theory assumes that molecularly processed disease proteins in the form of toxic and aggregation-prone fragments enhance neurodegenerative effects. Amongst others, endogenous enzymes such as caspases and calcium-dependent calpains have been associated with the proteolytic cleavage of the disease-causing proteins, a source for toxic fragments. The present study focused on the analysis of the calpain-mediated fragmentation of the mutant proteins huntingtin and ataxin-3, as well as on the detection of the enzymatic overactivation of calpains in cell and animal models of Huntington disease and spinocerebellar ataxia type 3.

The investigations carried out here confirmed the influence of calpains on neurodegenerative processes in both polyglutamine diseases. Moreover, huntingtin and ataxin-3 were found to be cleaved at specific amino acid positions within the protein, and the resulting fragments exhibited both an increased toxicity and aggregation propensity. In addition, direct as well as indirect pharmacological inhibition of calpains and genetic modification of cleavage sites within the disease protein attenuated these processes, yielding positive effects on the respective molecular pathology. Future studies including the extension to other neurodegenerative diseases are necessary to further investigate the general validity of this pathomechanism. In this way, therapeutically applicable and effective strategies against neurodegeneration may be developed.

Zusammenfassung (Deutsch)

Zusammen mit Krebs und kardiovaskulären Erkrankungen, stellen neurodegenerative Krankheiten wie Alzheimer und Parkinson ein immer wichtiger werdendes medizinisches Problem der alternden Gesellschaft des 21. Jahrhunderts dar. Multiple Faktoren wie Umwelteinflüsse und individuelle Lebensbedingungen agieren hierbei als bedeutende Modulatoren der Neuropathologie. Trotz diverser Ausprägungen neurodegenerativer Erkrankungen, existieren viele Gemeinsamkeiten in den zugrundeliegenden molekularen Pathomechanismen. Diese stellen somit vielversprechende Angriffspunkte für medizinische Interventionen dar. Insbesondere die Forschung an genetisch bedingten Formen, die einen singulären Auslöser besitzen, ermöglicht es diese gemeinsamen Prozesse zu verstehen und erworbene Kenntnisse auf andere neurologische Krankheitsbilder zu übertragen.

In Anbetracht dessen ergründet diese Arbeit die Gültigkeit der *Hypothese der toxischen Fragmente* am Beispiel zweier Polyglutamin-Erkrankungen, der Chorea Huntington und der Spinozerebellären Ataxie Typ 3. Diese weithin beschriebene Theorie stützt sich auf die Annahme, dass Krankheitsproteine, bedingt durch molekulare Prozesse, als toxische und zur Aggregation neigende Fragmente neurodegenerative Effekte verstärken können. Unter anderem wurden endogene Enzyme wie Caspasen und Calcium-abhängige Calpaine mit der proteolytischen Spaltung krankheitsauslösender Proteine assoziiert, einer Quelle für toxische Fragmente. Der Fokus der vorliegenden Studie lag hierbei auf der Analyse der Calpain-vermittelten Fragmentierung der pathologisch-veränderten Proteine Huntingtin und Ataxin-3, wie auch auf dem Nachweis der enzymatischen Überaktivierung von Calpainen in Zell- und Tiermodellen des Morbus Huntington und der Spinozerebellären Ataxie Typ 3.

Die hier vorgenommenen Untersuchungen bestätigten zum einen den Einfluss von Calpainen auf die neurodegenerativen Prozesse beider Polyglutamin-Erkrankungen. Zum anderen wurde gezeigt, dass Huntingtin und Ataxin-3 an spezifischen Aminosäurepositionen im Protein geschnitten werden und daraus resultierende Fragmente sowohl eine erhöhte Toxizität als auch Aggregationsneigung besitzen. Darüber hinaus schwächten die direkte wie auch indirekte pharmakologische Inhibition von Calpainen und die genetische Modifikation von Schnittstellen im Erkrankungsprotein diese Prozesse ab, mit positiven Auswirkungen auf den jeweiligen molekularen Krankheitsverlauf. Zukünftige Untersuchungen wie auch die Ausweitung auf andere neurodegenerative Erkrankungen sind nötig, um die Allgemeingültigkeit dieses Pathomechanismus weiter zu erforschen. Auf diese Weise könnten therapeutisch anwendbare und wirksame Strategien gegen Neurodegeneration entwickeln werden.

List of publications

All publications are listed chronologically. The author position in the sequence of contributors is highlighted in bold. A co-first authorship is indicated by an asterisk (*) after respective names.

a. J. Hübener*, **J. J. Weber***, C. Richter, L. Honold, A. Weiss, F. Murad, P. Breuer, U. Wüllner, P. Bellstedt, F. Paquet-Durand, J. Takano, T. C. Saido, O. Riess, and H. P. Nguyen, “Calpain-mediated ataxin-3 cleavage in the molecular pathogenesis of spinocerebellar ataxia type 3 (SCA3),” *Hum. Mol. Genet.*, vol. 22, no. 3, pp. 508–18, Feb. 2013.

b. H. P. Nguyen, J. Hübener, **J. J. Weber**, S. Grueninger, O. Riess, and A. Weiss, “Cerebellar soluble mutant ataxin-3 level decreases during disease progression in spinocerebellar ataxia type 3 mice,” *PLoS One*, vol. 8, no. 4, p. e62043, Apr. 2013.

c. **J. J. Weber***, A. S. Sowa*, T. Binder*, and J. Hübener*, “From pathways to targets: Understanding the mechanisms behind polyglutamine disease,” *BioMed Research International*, vol. 2014. pp. 1–22, 2014.

d. L. E. Clemens*, **J. J. Weber***, T. T. Wlodkowski, L. Yu-Taeger, M. Michaud, C. Calaminus, S. H. Eckert, J. Gaca, A. Weiss, J. C. D. Magg, E. K. H. Jansson, G. P. Eckert, B. J. Pichler, T. Bordet, R. M. Pruss, O. Riess, and H. P. Nguyen, “Olesoxime suppresses calpain activation and mutant huntingtin fragmentation in the BACHD rat,” *Brain*, vol. 138, no. 12, pp. 3632–3653, Dec. 2015.

e. **J. J. Weber**, M. M. Ortiz Rios, O. Riess, L. E. Clemens, and H. P. Nguyen, “The calpain-suppressing effects of olesoxime in Huntington’s disease,” *Rare Dis.*, vol. 4, no. 1, p. e1153778, Jan. 2016.

f. J. Schmidt, T. Schmidt, M. Golla, L. Lehmann, **J. J. Weber**, J. Hübener-Schmid, and O. Riess, “*In vivo* assessment of riluzole as a potential therapeutic drug for spinocerebellar ataxia type 3,” *J. Neurochem.*, vol. 138, no. 1, pp. 150–162, Jul. 2016.

g. **J. J. Weber**, M. Golla, G. Guaitoli, P. Wanichawan, S. N. Hayer, S. Hauser, A.C. Krahl, M. Nagel, S. Samer, E. Aronica, C. R. Carlson, L. Schöls, O. Riess, C. J. Gloeckner, H. P. Nguyen, J. Hübener-Schmid. "A combinatorial approach to identify calpain cleavage sites in the Machado-Joseph disease protein ataxin-3," *Brain*, vol. 140, no. 5, pp. 1280-1299, May 2017.

Personal Contribution

The following section contains the statement of personal contribution to the above listed accepted papers.

a. Main investigator (together with J. Hübener). Performed cell culture experiments and established *in vitro* calpain cleavage assays. Conducted all western blot analyses. Involved in data analysis & interpretation, and in writing the manuscript.

b. Performed experiments. Involved in cell culture experiments, western blotting, TR-FRET analysis and quantification of calbindin staining.

c. Contributed equally to the preparation of the manuscript together with A. S. Sowa, T. Binder, and J. Hübener.

d. Main investigator (together with L. E. Clemens). Performed analysis of the calpain activation, calpain-dependent huntingtin cleavage, huntingtin aggregation, and expression of mitochondrial proteins. Conducted western blot analyses. Involved in data analysis & interpretation, and in writing the manuscript.

e. Main investigator. Analysis of the calpain activation, calpain-dependent huntingtin cleavage, and huntingtin aggregation. Conducted western blot analyses. Involved in data analysis & interpretation, and in writing the manuscript.

f. Performed experiments. Analysed ataxin-3 expression and fragmentation by western blotting.

g. Main investigator. Shared main role in study design. Performed *in silico* predictions, cell culture experiments, and protein biochemical analysis including western blotting, filter retardation assays and microscopy. Established DDAGE and cytoplasmic/nuclear fractionation assays. Interpreted the data and prepared the manuscript.

Introduction

Neurodegenerative diseases: the quest for new therapies

Preface

Enabled by a strong synergy of the scientific disciplines biology, chemistry and physics with applied medical research, our understanding of human physiology and pathology has been immensely widened in the last two centuries. One of the most important achievements in public healthcare constitutes the control of infectious diseases, which were the scourge of mankind over the last millennia and contributed to a high mortality and decreased lifespan. This development, which grounded on Louis Pasteur's (1822 – 1895) germ theory, was facilitated by the combination of sanitation (Edwin Chadwick, 1800 – 1890) and hygiene (Ignaz Semmelweis, 1818 – 1865), vaccination (Edward Jenner, 1749 – 1823) and discovery of antimicrobial medicines, with penicillin leading the way (Alexander Fleming, 1881 – 1955) (Chew and Sharrock, 2007). While human life expectancy gradually increases as a result of the advances in medicine and improvements in living conditions, the ageing mankind is now confronted with new health-threatening challenges: cancer, cardiovascular diseases, and neurodegenerative disorders (Harper, 2014). To provide adequate answers to these problems is one of the most important endeavours of medicine and medicine research in the 21st century.

Neurodegeneration and ageing

In the latest report on world population ageing, the United Nations projected that the percentage of people aged 60 or over will account for more than 20 per cent of the global population by the middle of the 21st century. In highly developed industrial nations, such as Japan or Germany, the proportion of people of this age has already reached one third of the total inhabitants in 2015 (United Nations, 2015). This demographic evolution is attributed to economic and social improvements, rising living standards, and medical advancements. In summary, the result is not only a prolonged but also healthier human life. However, ageing is also accompanied by the occurrence of age-related diseases, which, in particular, also include neurological manifestations. Unipolar depressive disorders, stroke, neuropathy, Parkinson disease (PD), Alzheimer disease (AD) and other dementias are among these highly disabling or life-threatening health conditions (Fratiglioni and Qiu, 2009; Hindle, 2010; United Nations, 2015).

AD, Lewy body dementia (LBD) and PD are the most common neurodegenerative disorders amongst the elderly (Bertram and Tanzi, 2005; de Lau and Breteler, 2006). In 2012, 5.4 million cases of AD were reported in the U.S. and AD prevalence is predicted to reach 13.8 million by 2050 (Alzheimer Association, 2016). Worldwide, 47 million people are suffering from dementia and this number will increase to over 100 million until the mid-21st century (Prince *et al.*, 2016). The prevalence estimates of PD in industrial nations range between 0.3% of the total population and approximately 1% in people aged 60 years and over and will double by 2030 (de Lau and Breteler, 2006; Dorsey *et al.*, 2007). All these figures presage the massive impact of neurodegenerative diseases not only on the individual but also social well-being and call for a clarification of the determinants underlying neurodegeneration.

Factors contributing to neuronal ageing and neurodegeneration

A variety of general environmental factors and individual living conditions are known to affect neuronal ageing and induce neurodegeneration throughout our lives. Equally, the efficiency of cellular rejuvenation and the maintenance of biological functions dwindle with advancing age rendering the organism more susceptible to external deleterious stressors. Based on aetiological considerations from the fields of AD, amyotrophic lateral sclerosis (ALS), dementia, depressive disorders, and PD (Fratiglioni *et al.*, 2004; Mattson and Magnus, 2006; Fratiglioni and Qiu, 2009), a set of hypotheses might explain the causes of age-dependent neurodegeneration (FIGURE 1).

Psychosocial stress

Human life is characterised and imprinted by the interactions with its social environment and influencing life events. Negative experiences, acute anxiety reactions, and persistent severe psychological stress were shown to trigger depression-like behaviours, neuronal aging and the onset of degenerative diseases (Tsolaki *et al.*, 2009; Alkadhi, 2011; Kubera *et al.*, 2011; Tran *et al.*, 2011; Miller and Sadeh, 2014; Austin *et al.*, 2016). These observations can be linked to the release of stress-related corticosteroids, which are known to increase the vulnerability and mediate neuronal damage of specific brain areas through various cellular pathways (Swaab *et al.*, 2005; Toda *et al.*, 2016; Vyas *et al.*, 2016). Correspondingly, antidepressant therapies, cognitive enrichments and socially integrated lifestyles can protect against these pathologies (Fratiglioni *et al.*, 2004; Alkadhi, 2011; Kubera *et al.*, 2011).

Obesity and diabetes

Rising living standards in the western world are accompanied by an increasing percentage of people with obesity, which is considered as the single most important predictor of type 2 diabetes (Chan *et al.*, 1994; Hu *et al.*, 2001; Hjerkind *et al.*, 2017). In the U.S., more than one third of adults aged 65 and over is obese and the prevalence of diabetes amongst people of the same age ranges from 22-33% (Fakhouri *et al.*, 2012; Kirkman *et al.*, 2012). Aside from the implications on health such as cardiovascular diseases, both obesity and diabetes have been associated with accelerated neuronal aging and an elevated risk of cognitive impairments, dementia, AD and PD (Whitmer *et al.*, 2005; Epel, 2009; Doherty, 2011; Strachan *et al.*, 2011; Awada *et al.*, 2013; Rajamani, 2014). In addition, obesity was shown to constitute a risk factor for chemically induced neurodegeneration (Sriram *et al.*, 2002). On the other hand, a healthier lifestyle as defined by caloric restriction and increased physical activity, or bariatric interventions can be protective against neurodegenerative diseases like AD or PD (Wu *et al.*, 2008; Contestabile, 2009; Ashrafian *et al.*, 2013; Gräff *et al.*, 2013).

Vascular risks

The maintenance of brain functions is dependent on its cerebral circulation, which provides oxygenated blood and glucose, and removes unwanted metabolites. Ageing contributes to an impairment of the vascular system, which can lead to a chronic hypoperfusion of neuronal tissues an eventually to a cognitive decline (Akinyemi *et al.*, 2013; Bangen *et al.*, 2014). Moreover, ischemic and hemorrhagic stroke can be the consequence of a poor blood flow and survivors of stroke are reportedly at a high long-term risk for dementia (Corraini *et al.*, 2016). As vascular dysfunctions represent a risk factor for neurodegeneration, there is, however, a gradual transition from post-stroke and vascular dementia to AD (Viswanathan *et al.*, 2009). Furthermore, elevated blood pressure and high serum cholesterol are known to increase the chance to develop AD (Skoog *et al.*, 1996; Kivipelto *et al.*, 2001). Improving cerebral blood supply or reducing additional risk factors for vascular deficits, such as diabetes or obesity, constitute a potential intervention to sustain cerebral function and counteract neurodegeneration (Forette *et al.*, 1998; Akinyemi *et al.*, 2013).

Environmental neurotoxins

Nutrition and the living environment entail the exposure to natural and synthetic toxins which, in turn, can compromise human health. The accumulation of certain neurotoxins was shown to induce neurodegeneration and thereby conditions reminiscent of specific disorders. A classic example is 1-methyl-4-phenyl-1,2,3,6-tetrahydropyridine (MPTP), a by-product of desmethylprodine synthesis, whose metabolite MPP+ selectively kills dopaminergic neurons and induces Parkinsonism (Langston *et al.*, 1983). Moreover, pesticides like paraquat or rotenone were shown to have comparable effects, and like MPP+ act via the impairment of mitochondrial function (Cicchetti *et al.*, 2009). The excitatory amino acids kainic acid and domoic acid, which act as glutamate receptor agonists, can damage hippocampal pyramidal neurons and cause AD-like symptoms (Perl *et al.*, 1990; Ben-Ari and Cossart, 2000). Likewise, N-methyl-D-aspartate (NMDA) injection into neuronal tissue leads to an NMDA receptor-mediated excitotoxicity and neuronal lesioning (Dong *et al.*, 2009; Rambousek *et al.*, 2016). 3-nitropropionic acid (3-NP) was shown to induce a striatal phenotype reminiscent of Huntington disease (HD) and the endogenous neurotoxin quinolinic acid (QA) has been linked to various neurological disorders including AD, ALS, HD, and PD (Ludolph *et al.*, 1991; Guillemin, 2012; Lugo-Huitrón *et al.*, 2013). Despite all the negative effects of neurotoxins on human health, the elucidation of the corresponding causalities provided new possibilities to explore – with certain limitations - principles of neurological diseases. To this day, toxin-induced cell and animal models are used to investigate pathological mechanisms of neurodegeneration and to develop therapeutic approaches (Bové *et al.*, 2005; Ramaswamy *et al.*, 2007; Toledano and Álvarez, 2011).

Neuroinflammation

A further contributing factor of neurodegeneration in the elderly is the age-dependent dysregulation of the immune system, which comprises chronic low-grade inflammation and dystrophic microglia in the central nervous system (CNS). The so called *inflammaging* and *immunosenescence* have been associated with clinical conditions like mild cognitive impairment, AD, ALS, PD, and MS (Franceschi *et al.*, 2007; von Bernhardi *et al.*, 2010; Deleidi *et al.*, 2015). On the other hand, an inflammatory response can be an effect of an emerging neurodegenerative disorder and has been described as a concomitant feature of neurodegeneration (Frank-Cannon *et al.*, 2009; Amor *et al.*, 2010; Glass *et al.*, 2010). Neuroinflammation can, moreover, impair regulatory pathways of metabolism and energy balance in the brain (Cai, 2013). The thereby induced obesity, diabetes, and vascular

dysfunction can conversely amplify neurodegeneration and neuroinflammation, thus forming a vicious circle. However, neuroinflammation itself can represent a therapeutic target to potentially reverse or slow down the process of neurodegeneration (Amor *et al.*, 2010; Glass *et al.*, 2010).

Genetics

The environmental effects and individual circumstances which are linked to neuronal ageing and degeneration show a large spectrum in their manifestation. Diseases like AD, ALS, HD or PD are different in their symptoms, age of onset or pathophysiology. These variations are also characterised by the selective neuronal vulnerability which is specific for every single disorder. An important player in this determination of neuronal ageing and degeneration is the individual genetic background. Several evolutionarily conserved genes are playing an important role in cellular aging processes. These genes are involved in pathways or represent regulatory elements such as DNA repair and modification, insulin/IGF1 signalling, lipid metabolism, mitochondrial function, mTOR signalling and sirtuins (Wolkow, 2002; Yehuda *et al.*, 2002; Mattson, 2003; Lu *et al.*, 2004; Bishop *et al.*, 2010; Alcedo *et al.*, 2013; Chow and Herrup, 2015). Furthermore, changes in the expression of these genes are reported to accompany neuronal ageing and emerge as an upregulation of inflammatory and stress response, or a downregulation of protein turnover and growth factors (Lee *et al.*, 2000). Several genes have been shown to increase the risk for developing a neurodegenerative disorder depending on the occurrence of certain polymorphisms. In sporadic late-onset AD, the ε4 allele of the apolipoprotein E gene (*APOE*) has been identified as significant risk factor (Bird, 2008; Liu *et al.*, 2013). Variants of genes like α-synuclein (*SNCA*), leucine-rich repeat kinase 2 (*LRRK2*) and β-glucocerebrosidase (*GBA*) are considered as risk factors of late-onset PD (Klein and Westenberger, 2012). Intermediate-length CAG repeat expansions in the *ATXN2* gene were associated with increased risk for ALS (Elden *et al.*, 2010). Around 25% of AD patients, 10% of PD patients and 10-15% of ALS patients have a positive family history, leaving the majority of sporadic cases genetically unsolved (Thomas and Beal, 2007; Bird, 2008; Byrne *et al.*, 2011). However, a set of genetic mutations have been linked with the recessive or dominant form of these diseases. Amongst them, mutations in the genes for amyloid precursor protein (*APP*), presenilin 1 (*PSEN1*) and presenilin 2 (*PSEN2*) are causative for autosomal dominant early-onset forms of familial AD (Blennow *et al.*, 2006). Mutations in the previously mentioned genes *SNCA* and *LRRK2* together with at least five other genes, e.g. encoding parkin (*PARK2*) and PTEN-induced

putative kinase 1 (*PINK1*), cause monogenic forms of PD (Trinh and Farrer, 2013). Familial forms of ALS include mutations in genes of superoxide dismutase 1 (*SOD1*), the TAR DNA-binding protein-43 (TDP-43; *TARBDP*), and the protein C9orf72 (*C9orf72*) (Renton *et al.*, 2013). In addition, multiple rare neurodegenerative diseases have a solely monogenic background, including the polyglutamine (polyQ) disorders HD, dentatorubropallidoluysian atrophy (DRPLA), spinal and bulbar muscular atrophy (SBMA), and six different forms of spinocerebellar ataxia (SCA) (Gusella and MacDonald, 2000). The identification of mutations underlying monogenic neurodegenerative diseases has enabled scientists to generate adequate model organisms which reproduce disease-related characteristics (Marsh *et al.*, 2009; Jucker, 2010). These disease models have, furthermore, paved the way for exploring common pathomechanisms and, thereby, for developing future treatment approaches including therapies, which directly target mutant genes or respective disease proteins (Ciechanover and Kwon, 2015; Heidenreich and Zhang, 2015; O'Connor and Boulis, 2015).

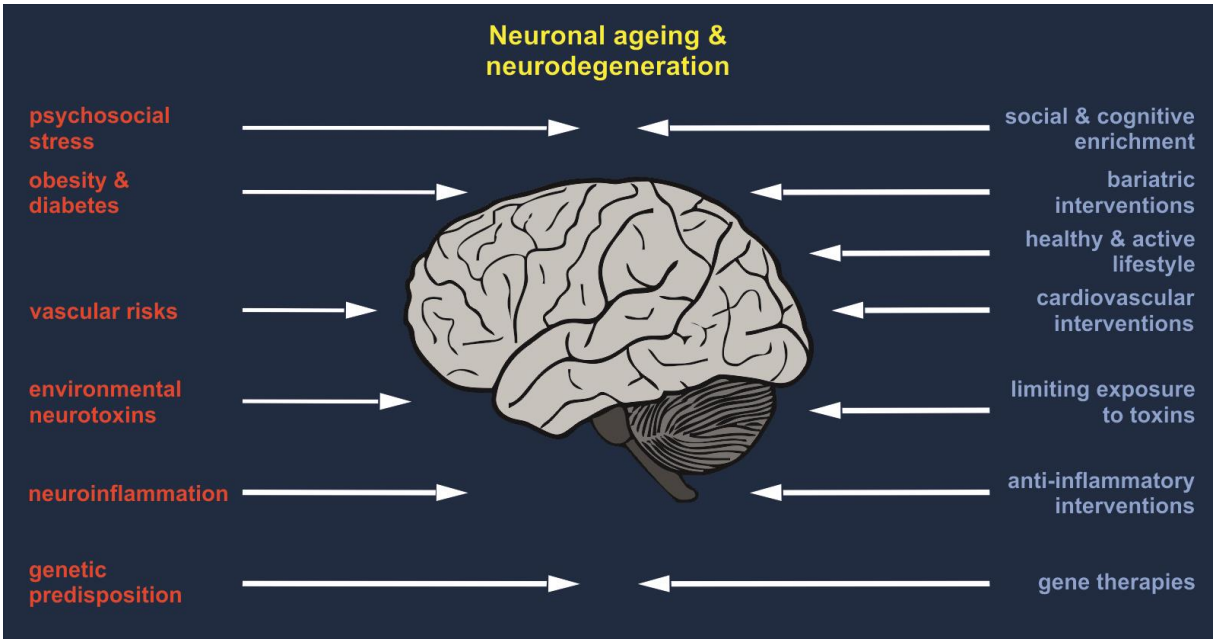

Figure 1. Overview of factors contributing to neuronal ageing and neurodegeneration. Environmental factors, living and health conditions and the individual genetic background (highlighted in red) form the basis of neuronal ageing and susceptibility to neurodegeneration. These factors can be countered by a healthier, enriched lifestyle and medical interventions (highlighted in blue).

Cellular and molecular changes during neuronal ageing and degeneration

External and internal effectors of neuronal ageing and neurodegeneration are triggering alterations on cellular and molecular level. These markers can be utilized to characterise the disease, to monitor disease progression and to delve into potential therapeutic points of action. Typical molecular alterations comprise disturbances of energy metabolism, mitochondrial function, elevation in levels of oxidatively modified molecules, Ca^{2+} dyshomeostasis and accumulation and aggregation of dysfunctional proteins (FIGURE 2) (Mattson and Magnus, 2006).

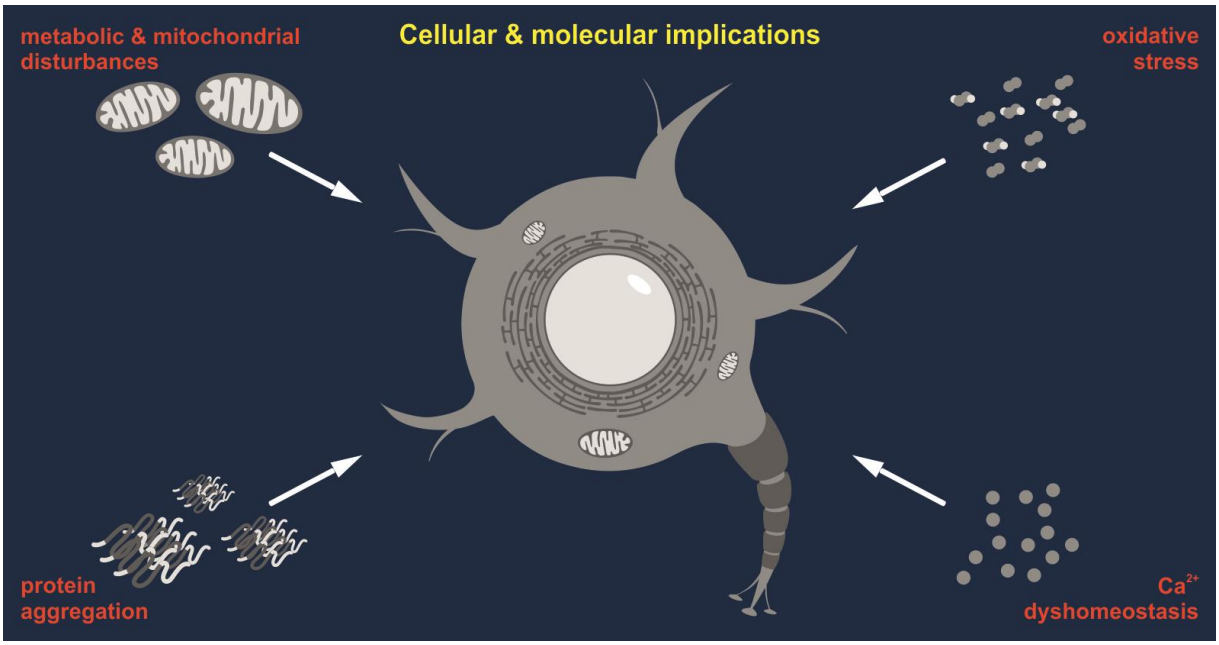

Figure 2. Cellular and molecular changes during neuronal ageing and degeneration. Ageing and degeneration is accompanied by molecular disturbances in affected neurons (highlighted in red), which represent mediators or consequences of detrimental processes.

Disturbances in energy metabolism and mitochondrial function

Brain function is highly dependent on the unconfined supply of neurons with energy. The main source for this energy is glucose which is provided by the glucose metabolism. Although the human brain accounts for only 2% of the total body weight, it consumes nearly 20% of the glucose-derived physiological energy (Raichle and Gusnard, 2002; Mergenthaler *et al.*, 2013). However, with ageing, glucose uptake and utilization decrease in many brain areas (Mosconi, 2013). In a more drastic form, these effects precede the clinical onset in

patients suffering from neurodegenerative diseases like AD, PD or HD (De Volder *et al.*, 1988; Feigin *et al.*, 2001; Patel and Brewer, 2003; Cunnane *et al.*, 2011; Borghammer, 2012; Niethammer *et al.*, 2012). In addition to these alterations, mitochondria, the main producers of the cellular energy currency adenosine triphosphate (ATP), and important regulators of energy metabolism, are compromised in their function. Especially, the activity of mitochondrial enzymes and enzymatic complexes, which are implemented in ATP production, have been shown to be negatively affected (Henchcliffe and Beal, 2008; Oliveira, 2010; Hroudová *et al.*, 2014). Moreover, many disease proteins like APP cleavage-derived amyloid-β (Aβ), α-synuclein or huntingtin have been directly linked with damaging mitochondria (Lin and Beal, 2006). PD-associated loss-of-function mutations in PINK1 and parkin were shown to impair mitophagy, a mitochondrial quality control mechanism (Youle and Narendra, 2011). As a consequence, energy-dependent cellular processes are impaired, neuronal structures like axons and synaptic termini degenerate and the functionality of neurons declines (Dutta *et al.*, 2006; Du *et al.*, 2010; Friese *et al.*, 2014). Finally, as mitochondria play a central role in regulation of apoptosis, their impaired viability leads to an activation of the cell death-linked caspase cascades, eventually leading to neuronal demise (Mattson, 2000).

Impact of oxidative stress

Metabolism of glucose and environmental toxins are the main source for reactive oxygen species (ROS), which – if not eliminated beforehand by antioxidative mechanisms – have the potential to harm the cell. A direct effect of ROS is the oxidative modification of different biomolecules like proteins and lipids, which can render them dysfunctional (Birben *et al.*, 2012). Furthermore, the accumulation oxidatively mutated DNA in neurons, which lack many DNA repair mechanisms due to their post-mitotic nature, can determine neuronal ageing and death (Chow and Herrup, 2015). The additional loss of mitochondrial integrity during ageing and in neurodegenerative disorders can lead to progressive amplification of ROS levels and their damaging effects, thereby feeding a detrimental loop (Lin and Beal, 2006). Interestingly, mutations of the ALS disease protein SOD1, a superoxide radical-removing enzyme, mainly induce a toxic gain-of-function, which leads to a mislocalisation of SOD1 to the mitochondrial intermembrane space and thereby to an increased production of hydrogen peroxide (Goldsteins *et al.*, 2008; Pickles *et al.*, 2013; Vehviläinen *et al.*, 2014). Ultimately, a permanent oxidative stress of mitochondria can trigger apoptosis by promoting excessive mitochondrial Ca^{2+} uptake and loss of membrane integrity (Mattson and Kroemer, 2003). On

the other hand, a downregulation of the mitochondrial activity by a dietary restriction-based reduction of glucose uptake has been shown to lower ROS levels and even exert anti-ageing effects (Walsh *et al.*, 2014; Ruetenik and Barrientos, 2015).

Calcium dyshomeostasis

Calcium ions (Ca^{2+}) represent one of the most important intracellular signals, regulating many essential physiological processes, which range from cell cycle regulation and gene transcription to ATP production and muscle contraction (Lu and Means, 1993; Dulhunty, 2006; Bading, 2013; Brini *et al.*, 2014). In neurons, Ca^{2+} is fundamentally involved in transmission of depolarization, neurotransmitter release, and synaptic plasticity (Zucker, 1999; Neher and Sakaba, 2008; Brini *et al.*, 2014). Cytosolic Ca^{2+} concentrations range from approximately 100 nM under resting conditions up to transient peaks of 1–10 µM upon membrane depolarization and opening of Ca^{2+} channels (Berridge *et al.*, 2000). Ca^{2+} levels are strongly regulated within all cells and dysfunctional Ca^{2+} homeostasis may fatally perturb cell function and viability leading to apoptosis (Orrenius *et al.*, 2003; Pinton *et al.*, 2008). Important regulatory elements of Ca^{2+} homeostasis comprise cell compartments like the endoplasmic reticulum (ER) and mitochondria, Ca^{2+}-binding proteins and a multitude of Ca^{2+} pumps and channels (Berridge *et al.*, 2000; Clapham *et al.*, 2007). In ageing neurons, Ca^{2+} homeostasis is known to be impaired, which is attributed to deregulated Ca^{2+} influx and extrusion through the plasma membrane, and disturbances of the internal Ca^{2+} buffering compartments ER and mitochondria (Murchison *et al.*, 2004; Toescu *et al.*, 2004; Nikoletopoulou and Tavernarakis, 2012). Levels of Ca^{2+}-binding proteins like calbindin and calretinin are known to decrease, additionally affecting neuronal Ca^{2+} buffering capacity (Iacopino and Christakos, 1990; Bu *et al.*, 2003). Knowing that excessive cytosolic levels of Ca^{2+} can ultimately trigger apoptosis, these processes may, altogether, contribute to aging-dependent neuronal dysfunction and degeneration, which has been earlier conceived in *The calcium hypothesis of brain ageing and Alzheimer's disease* (Khachaturian, 1994). Likewise, Ca^{2+} dyshomeostasis has been observed in neurodegenerative disorders and partly associated with the gain-of-function of specific disease proteins. In familial AD, mutant presenilins were shown to interfere with activities of the Ca^{2+} channels and pumps inositol-1,4,5-trisphosphate receptor (IP_3R), ryanodine receptor (RyR), and the sarco/endoplasmic reticulum Ca^{2+}-ATPase (SERCA) in the ER (Honarnejad and Herms, 2012). Monomers and oligomers of α-synuclein were shown to impair efflux and increase influx of Ca^{2+} by their interaction with membranes in PD (Angelova *et al.*, 2016). PolyQ-expanded proteins like

mutant huntingtin were shown to sensitize IP_3R1 to activation by its ligand IP_3 (Tang *et al.*, 2003; Bezprozvanny, 2011).

Detrimental accumulation and aggregation of proteins

One of the most prominent hallmarks of neuronal ageing and neuronal proteinopathies is the accumulation of damaged and misfolded proteins in histologically traceable intracellular and extracellular insoluble aggregates. A typical example is lipofuscin, an autofluorescent age pigment of post-mitotic cells. These conglomerates are composed of oxidatively damaged, cross-linked proteins and lipids and may compromise cellular function and viability (Szweda *et al.*, 2003; Gray, 2005; Jung *et al.*, 2007). The formation of lipofuscin or other protein aggregates is linked to an age-dependent impairment of cellular quality control mechanisms such as the proteasomal system, autophagy or other degradative enzymes (Cuervo, 2008; Vilchez *et al.*, 2014). Additionally, the amount of damaged and misfolded proteins increases with ageing due to elevated oxidative stress and a decline of molecular chaperone activity (Calderwood *et al.*, 2009; Kikis *et al.*, 2010; Wang and Michaelis, 2010). In many sporadic and inherited neurodegenerative disorders like AD, ALS, PD and HD, the same mechanisms were shown to be impaired and to mediate the detrimental effects on affected neurons (Son *et al.*, 2012; Ciechanover and Kwon, 2015). In particular, these disorders are characterised by the accumulation and aggregation of specific proteins: For instance, Aβ forms extracellular amyloid plaques in AD, and tau intracellular neurofibrillary tangles not only in AD but also many other neurodegenerative diseases termed tauopathies, including progressive supranuclear palsy (PSP) or autosomal dominant frontotemporal lobar degeneration (FTLD) (Lee and Leugers, 2012; Bloom, 2014; Rojas and Boxer, 2016). The α-synuclein protein aggregates as Lewy bodies in PD, dementia with Lewy bodies, and multiple system atrophy (MSA), which are thereby classified as α-synucleinopathies (Goedert and Spillantini, 1998; Lashuel *et al.*, 2012). Protein aggregates in ALS are composed of FUS, optineurin, SOD1, TDP -43, ubiquilin-2, and C9orf72 (Blokhuis *et al.*, 2013). And polyQ-expanded proteins such as huntingtin, ataxin-3, and atrophin-1 form intranuclear or cytoplasmic aggregates in HD, spinocerebellar ataxia type 3 (SCA3) and DRPLA, respectively (Gusella and MacDonald, 2000). Whether these protein aggregates have a detrimental or a rather protective function within neurons by sequestering toxic soluble species of the disease protein is, however, controversially discussed among scientists (Michalik and Van Broeckhoven, 2003). Besides initial mutations, many disease proteins are modified by further post-translational modifications, which can alter their aggregation propensity. For instance, zinc and copper ions were shown to modulate Aβ oligomerization into fibrils (Tanzi and Bertram, 2005).

Hyperphosphorylation of tau was shown to induce its accumulation into neurofibrillary tangles (Stoothoff and Johnson, 2005). Oxidation, nitration and metal ions like aluminium induce conformational changes of α-synuclein and modulate its fibrillation and toxicity (Breydo *et al.*, 2012; Chavarría and Souza, 2013). A widely occurring mechanism among neurodegenerative diseases is proteolytic cleavage, which releases toxic and aggregation-prone fragments. Since the first description of the *toxic fragment hypothesis*, many enzymes have been associated with the detrimental fragmentation of disease proteins (Wellington and Hayden, 1997). For example, the β-site APP cleaving enzyme (BACE1) cleaves APP and releases Aβ, whereas desintegrins and metalloproteinases ADAM9, ADAM10 and ADAM17 generate non-toxic forms of APP reducing the formation of Aβ (Zhang and Tanzi, 2012). The apoptosis-mediating protease family of caspases and Ca^{2+}-activated calpains were associated with fragmentation of α-synuclein, tau, TDP-43 and of polyQ proteins like huntingtin and ataxin-3 (Dufty *et al.*, 2007; Y.-J. Zhang *et al.*, 2009; Hanger and Wray, 2010; Ehrnhoefer *et al.*, 2011; Matos *et al.*, 2011; Yamashita *et al.*, 2012).

Polyglutamine diseases as a monogenic model for neurodegeneration

The group of polyglutamine diseases

Amongst the vast number of neurodegenerative disorders, which are mostly defined by unknown, complex or polygenic aetiologies, polyQ diseases constitute a genetically unambiguous class of medical conditions. Although multiple genes are causative for this class of disorders, they share many common molecular characteristics and pathomechanisms, rendering them an ideal scientific field to explore the bedrock of neurodegeneration.

PolyQ diseases belong to a bigger group of disorders, whose genetics are based upon the pathological expansion of trinucleotide repeats. These disorders include, for instance, expansions of CGG repeats in the 5' untranslated region (UTR) of the fragile X mental retardation 1 (*FMR1*) gene in fragile X syndrome, GAA repeats in the intron of the frataxin (*FXN*) gene in Friedreich's ataxia, or CTG repeats in the 3' UTR of the dystrophia myotonica protein kinase (*DMPK*) gene in myotonic dystrophy type 1 (Verkerk *et al.*, 1991; Mahadevan *et al.*, 1992; Campuzano *et al.*, 1996; Budworth and McMurray, 2013). The distinctive characteristic of polyQ diseases, however, is the exonic localisation of a CAG triplet repeat, which is translated into an elongated polyQ motif rendering the encoded protein dysfunctional and aggregation-prone (Gusella and MacDonald, 2000). The underlying molecular mechanism of trinucleotide repeat expansions remains elusive. Well accepted explanations are the occurrence of polymerase slippages and DNA loop formations due to trinucleotide-dependent misalignments and replication restarts during germ line DNA replication. Arising loops can then be integrated via DNA repair mechanisms, leading to an elongation of the trinucleotide tracts (Mirkin, 2007; McMurray, 2010). The thereby evoked generational repeat instability is furthermore linked to a phenomenon called *anticipation*, a hallmark of trinucleotide disorders: repeat expansions show a propensity to further increase over generations, which leads to an earlier onset and greater severity of the disease (McMurray, 2010; Budworth and McMurray, 2013).

The first disease which was identified as a polyQ disorder was the X-linked SBMA, also known as Kennedy disease featuring a CAG repeat expansion in the androgen receptor (AR) gene (La Spada *et al.*, 1991). To the present day, nine polyQ disorders have been described, comprising DRPLA, HD, SBMA, and the spinocerebellar ataxias type 1, 2, 3, 6, 7 and 17, which exhibit a neuromuscular or neurodegenerative manifestation (Gusella and MacDonald, 2000; Shao and Diamond, 2007). In contrast to trinucleotide expansions in UTRs or introns, which influence splicing, stability and expression of the affected mRNA, elongated glutamine-

coding CAG repeats have a direct impact on structure and function of the encoded protein. These changes on the protein level are believed to be the main trigger of pathogenic effects. Moreover, cytoplasmic and intranuclear aggregation of the polyQ-expanded proteins are a typical histological feature of affected neurons in polyQ diseases (Shao and Diamond, 2007). However, several studies suggested that CAG repeat-containing mRNAs themselves may exhibit certain toxicity and the intrinsic repeats can lead to a mistranslation into deleterious proteinaceous by-products via a mechanism called repeat-associated non-ATG (RAN) translation (Li *et al.*, 2008; Zu *et al.*, 2011; Nalavade *et al.*, 2013; Bañez-Coronel *et al.*, 2015; Strzyz, 2016).

Clinical features of Huntington disease and spinocerebellar ataxia type 3

Huntington disease

HD is a neurodegenerative disorder with a long history. Its principal symptom chorea, which is characterised by jerky, involuntary movements named after the ancient Greek circle dance *choreia* (χορεία), had been already described in the middle ages (Vale and Cardoso, 2015). In 1872, the first detailed clinical description on late-onset hereditary chorea was authored by George Huntington, who became the eponym for the disease (reprinted in: Huntington, 2003).

Although being firstly termed Huntington's chorea, the disease was renamed HD due to its symptomatic complexity, which cannot be only reduced to the presence of chorea but consists of a clinical triad of progressive motor, cognitive, and psychiatric impairments (Roos, 2010; Paulson and Albin, 2011). Aside from the characteristic chorea, which starts in early stages of HD, the motor disorder comprises dystonia, rigidity, dysphagia and dysarthria, gait impairments, and impaired eye movement. Cognitive dysfunctions are composed of slowed thinking, problems in information manipulation, dementia, deficient executive function and lowered skill and motor learning. Finally, psychiatric abnormalities range from irritability and aggression, over apathy, depression, mania, and psychosis, to sleep disturbances (Anderson and Marder, 2001; Roos, 2010). HD is a fatal disorder, and the majority of patients die from aspiration pneumonia as a consequence of dysphagia (Heemskerk and Roos, 2012). It is noteworthy, that people at risk or diagnosed with HD are suffering from suicidal ideation, and thus suicide represents the second most common death cause of this devastating disorder (Farrer *et al.*, 1986; Paulsen *et al.*, 2005; Roos, 2010).

The clinical triad of HD is strongly linked to the dysfunction and degeneration of parts of the CNS (FIGURE 3). Despite being primarily detectable as a neuronal decline of striatal structures, represented by an up to 95% loss of striatal gamma-aminobutyric acid (GABA)-ergic medium spiny neurons (MSNs), neurodegeneration can spread throughout the whole brain: cerebral cortex, subcortical white matter, thalamus, and hypothalamic nuclei can undergo atrophy with different degrees of severity (Halliday *et al.*, 1998; Vonsattel, 2008; Costanzo and Zurzolo, 2013; Bañez-Coronel *et al.*, 2015). Many of these features can be observed before clinical onset of HD and the variability of the degeneration accounts to a certain degree for the large spectrum of symptoms (Tabrizi *et al.*, 2009, 2011). With the steady progress in medical sciences, many other and more subtle characteristics of HD on behavioural, physiological and molecular level are now detectable as biomarkers, which allow for improved and earlier diagnosis (Weir *et al.*, 2011; Tabrizi *et al.*, 2013).

Classified as an autosomal-dominant inherited disorder, HD's genetic aetiology is the expansion of a polymorphic CAG triplet repeat in exon 1 of the *HTT* gene, which is also known as interesting transcript 15 (*IT15*) mapping to the short arm of chromosome 4 (4p16.3) (The Huntington's Disease Collaborative Research Group *et al.*, 1993). In unaffected humans, the CAG motif is ranging between 14 and 26 repeats. Exceeding the critical number of 40 repeats leads to a full penetrance, whereas 27-35 repeats constitute an intermediate, nonpathological range and 36-39 repeats are characterised by a reduced penetrance with a much later disease onset (Rubinsztein *et al.*, 1996; Potter *et al.*, 2004; Killoran *et al.*, 2013). The length of the CAG repeat inversely corresponds with the age of onset, which is 40 years on average (Duyao *et al.*, 1993; Myers, 2004). However, only around 60% of the variance in the age of onset can be attributed to the length of the repeat expansion, which is indicative for additional genetic and environment modifiers (Myers, 2004; Wexler *et al.*, 2004). Although a monoallelic CAG expansion is sufficient for causing HD, homozygous cases were reported, whose disease onset was in the range of heterozygous patients but clinical course of the disease was more severe (Squitieri *et al.*, 2003). The overall worldwide prevalence for HD is about 4 per 100.000, with its highest frequency in the Western world and the lowest in Asia amounting to 1-14 per 100.000 and <1 per 100.000, respectively (Pringsheim *et al.*, 2012; Baig *et al.*, 2016; Rawlins *et al.*, 2016).

Spinocerebellar ataxia type 3

In contrast to HD, the first descriptions of SCA3 were published one hundred years later in the 1970s. In the beginning, SCA3 was classified as three independent medical conditions named Machado disease, nigrospinodentatal degeneration, and autosomal dominant striatonigral degeneration, which reported in families of Azorean decent in the US (Nakano *et al.*, 1972; Woods and Schaumburg, 1972; Rosenberg *et al.*, 1976). After additional investigations of cases on the Azores, these diseases were unified and unlike other disorders, named Machado-Joseph disease (MJD, synonym for SCA3) as reference to two affected families: the Machado family from New England and the Californian Joseph family (Coutinho and Andrade, 1978; Lima and Coutinho, 1980).

The main clinical feature of SCA3 is ataxia, a deficit in voluntary coordination of muscle movements generally manifesting as gait abnormalities. However, the phenotype comprises many additional characteristics including ophthalmoplegia, diplopia, dystonia, faciolingual fasciculation, dysarthria and dysphagia (Riess *et al.*, 2008; Bettencourt and Lima, 2011). Cognitive dysfunction is rather mild and feature e.g. verbal and visual memory deficits or a visuospatial dysfunction (Bürk *et al.*, 2003; Kawai *et al.*, 2004). Due to its heterogeneity of symptoms, SCA3 was divided in four subtypes: type 1 (*type Joseph*) exhibits extrapyramidal and pyramidal signs with an early disease onset about 10-30 years; type 2 (*type Thomas*) features a true cerebellar deficit and other motor dysfunctions with an intermediate age of onset between 20 and 50 years; type 3 (*type Machado*) shows mainly cerebellar deficits and a peripheral neuropathy with a late disease onset of 40-75 years; the rare type 4 is characterised by a neuropathy and parkinsonism with a variable age of onset (Coutinho and Andrade, 1978; Suite *et al.*, 1986; Riess *et al.*, 2008; Bettencourt and Lima, 2011). Comparable to HD, early death from SCA3 is mainly caused by a dysphagia-dependent aspiration pneumonia (Rüb *et al.*, 2006).

Neuropathologically, SCA3 is characterised by an atrophy of different regions within the CNS, mainly restricted to the cerebellum, brainstem, and the spinal cord (FIGURE 3). However, further areas can be additionally impaired including the thalamus or the globus pallidus (Dürr *et al.*, 1996; Paulson, 2012; Rüb *et al.*, 2013). As for HD, search for accurate biomarkers as a tool for diagnosis and assessment of disease progression is ongoing, comprising studies, which focus on oculomotor deficits, functional magnetic resonance imaging (fMRI) or blood-based readouts (Raposo *et al.*, 2015; Duarte *et al.*, 2016; Wu *et al.*, 2017).

The polymorphic CAG trinucleotide repeat, which is expanded in SCA3, lies in exon 10 of the *MJD1* gene mapping to chromosome 14q32.1 (Takiyama *et al.*, 1993; Kawaguchi *et al.*, 1994; Schöls *et al.*, 1995). CAG motifs in unaffected individuals count 12-44 repeats, and 93.5% of those have fewer than 31 CAGs. In SCA3 patients the CAG number varies from 60-87 repeats. Accordingly, there is an intermediate range of 45-59 CAGs, which leads to a reduced penetrance (do Carmo Costa and Paulson, 2012). In contrast to HD, rare homozygous cases of SCA3 do not only exhibit an increased severity in disease phenotype but also an earlier age of onset, suggestive of a possibly dominant negative effect of the mutation in the *MJD1* gene (Takiyama *et al.*, 1995; Lerer *et al.*, 1996). As SCA3 is a very rare disorder, there is lack of precise and reliable data regarding its prevalence. However, with approximately 21% of all cases, SCA3 is considered as the most common form of autosomal dominant inherited cerebellar ataxias, with an estimated prevalence of 3 per 100.000 individuals worldwide (Schöls *et al.*, 2004). Strikingly, the number of SCA3 cases is the highest on the Azorean island Flores with a frequency of 1 per 239 in 2008 (Bettencourt *et al.*, 2008).

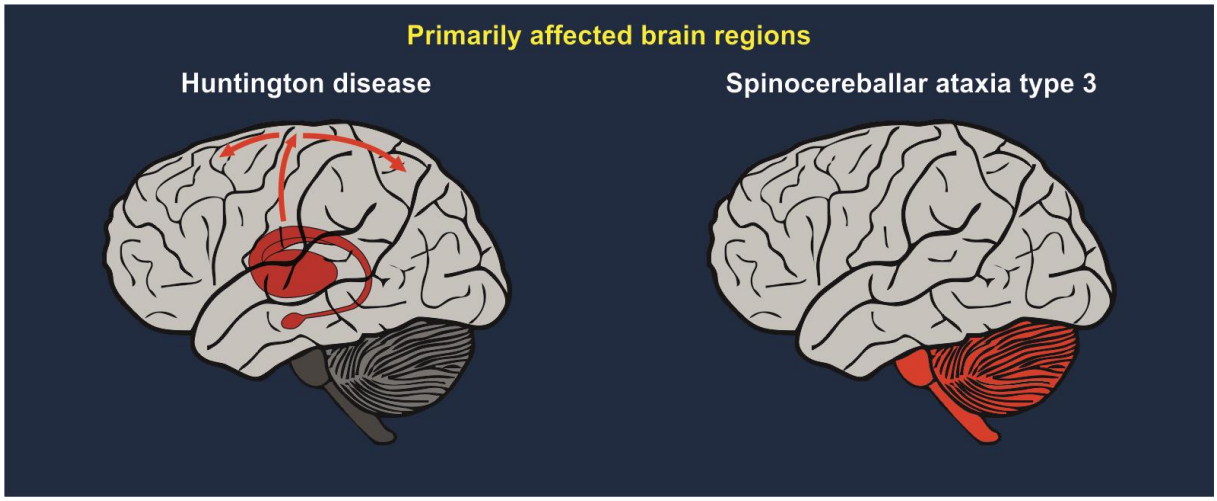

Figure 3. Brain regions primarily affected in Huntington disease and spinocerebellar ataxia type 3. The primary site of neurodegeneration in HD is the striatum (left side, red), however the degeneration can spread over the whole brain in late stages of the disease (indicated by red arrows). In SCA3-affected brain regions are mainly restricted to the cerebellum, brainstem and spinal cord (right side, red).

Molecular characteristics of Huntington disease and spinocerebellar ataxia type 3

The disease protein huntingtin

Characteristically for polyQ diseases in general, the CAG repeat in the *HTT* gene is translated into a polyQ tract, which is located at the N-terminus of huntingtin (UniProt identifier: P42858-1), a large soluble protein of more than 3100 amino acids. Huntingtin's exact size and molecular weight of roughly 350 kDa varies depending on the length of its polymorphic polyQ stretch.

HTT is an evolutionary old gene, which can be found in vertebrates, invertebrates but also some unicellular eukaryotes. Despite that, only in vertebrates, *HTT* is highly conserved sharing an 80% sequence homology (Baxendale *et al.*, 1995; Cattaneo *et al.*, 2005). In humans and rodents, huntingtin is expressed ubiquitously with high levels in brain neurons, but without enrichment in striatum, the site of greatest pathology in HD. On cellular level, huntingtin displays a mainly cytoplasmic distribution and was shown to be associated with membranes and the cytoskeleton. In neurons, the protein is found not only in the cell body, but also axons and dendrites, and is concentrated at nerve terminals (Sharp *et al.*, 1995; Trottier *et al.*, 1995). There, huntingtin was detected at microtubules and synaptic vesicles (DiFiglia *et al.*, 1995; Gutekunst *et al.*, 1995).

Aside from the N-terminal polyQ stretch, the structure of the protein contains a subsequent polyproline motif and 28-36 HEAT repeats (FIGURE 4) (Takano and Gusella, 2002; Ehrnhoefer *et al.*, 2011). These repeats are named after the first proteins in which these motifs were identified, namely huntingtin, elongation factor 3, protein phosphatase 2A and yeast target of rapamycin 1 (TOR1), and are organized in four main clusters (Andrade and Bork, 1995; Li *et al.*, 2006; Warby *et al.*, 2008). At its C-terminus, huntingtin features an active nuclear export signal (NES) (Xia *et al.*, 2003). Furthermore, the first 17 amino acids were shown to be important for subcellular localisation and represent a target for regulatory post-translational modifications (Cornett *et al.*, 2005; Arndt *et al.*, 2015). In general, huntingtin undergoes many different post-translational modifications, including acetylation, lipidation, phosphorylation, ubiquinitination, SUMOylation or proteolytic cleavage, which are known to modulate its localisation and interaction with other proteins (Ehrnhoefer *et al.*, 2011).

Due to its large size and characteristic occurrence of multiple HEAT repeats, huntingtin shows a big palette of interactions and functions within the cell, rendering it an important element of cellular function (Gusella and MacDonald, 1998; Goehler *et al.*, 2004). Well

investigated is the role of huntingtin as a scaffold protein in vesicle trafficking in endocytic and secretory pathways (Velier *et al.*, 1998). This function is mediated via the interaction with huntingtin-associated protein 1 (HAP1) and the dynein-dynactin complex (Li *et al.*, 1995; Caviston *et al.*, 2007, 2011; Zuccato and Cattaneo, 2009). In this regard, huntingtin was shown to facilitate vesicle transport from the ER to the Golgi apparatus, endosome motility, mitochondrial and in particular axonal transport (Gunawardena *et al.*, 2003; Pal *et al.*, 2006; Li *et al.*, 2010; Brandstaetter *et al.*, 2014; White *et al.*, 2015). Aside from this, the protein has been associated with many further functions. Huntingtin was shown to modulate transcription directly via binding to the genomic DNA or via interaction with transcription factors and regulators (Holbert *et al.*, 2001; S.-H. Li *et al.*, 2002; Zuccato *et al.*, 2003; Benn *et al.*, 2008). Furthermore, it is involved in mRNA biogenesis by binding spliceosome proteins, and in protein translation (Faber *et al.*, 1998; Passani *et al.*, 2000; Culver *et al.*, 2012). Huntingtin interacts in different ways with the cytoskeleton, and is involved in regulation of iron homeostasis, Ca^{2+} homeostasis, and energy metabolism (Bao *et al.*, 1996; Burke *et al.*, 1996; Kalchman *et al.*, 1997; Boutell *et al.*, 1998; Hilditch-Maguire *et al.*, 2000; Hoffner *et al.*, 2002; Tang *et al.*, 2003; Lumsden *et al.*, 2007; Rockabrand *et al.*, 2007). In addition, it regulates epidermal growth factor (EGF)- and mammalian TOR1 (mTOR1)-dependent signalling (Liu *et al.*, 1997; Pryor *et al.*, 2014). Recently, huntingtin has also been shown to act as a scaffold protein in autophagy (Ochaba *et al.*, 2014; Rui *et al.*, 2015).

Of particular interest are huntingtin's neuron-specific functions. In this regard, the protein was found to interact with protein kinase C and casein kinase substrate in neurons protein 1 (PACSIN1) or postsynaptic density 95 (PSD-95) and thereby regulate synaptic transmission (Sun *et al.*, 2001; Modregger *et al.*, 2002). Moreover, huntingtin was described as a neuroprotective protein. It amplifies the expression of brain-derived neurotrophic factor (BDNF), enhances the vesicular transport of BDNF and acts anti-apoptotic by inhibiting caspases-3 and -9 (Rigamonti *et al.*, 2000, 2001, Zuccato *et al.*, 2001, 2003; Gauthier *et al.*, 2004; Zhang *et al.*, 2006). Overexpression of normal huntingtin attenuates excitotoxic effects as mediated by NMDA or kainate receptors *in vitro* and *in vivo*, and protects against brain ischemia (Sun *et al.*, 2001; Zhang *et al.*, 2003; Leavitt *et al.*, 2006). Furthermore, wild type huntingtin was shown to reduce toxicity of its mutant counterpart in cell lines and *in vivo* (Ho *et al.*, 2001; Leavitt *et al.*, 2001).

The vital role of huntingtin was demonstrated in several studies which knocked out the protein or reduced its expression. The homozygous knockout of the *HTT* gene in mice led to embryonic death around day 8.5 of gestation (Duyao *et al.*, 1995; Nasir *et al.*, 1995; Zeitlin *et al.*, 1995). Heterozygous knockout animals, furthermore, exhibited cognitive deficits and

increased motor activity which was accompanied by a neuronal loss in the subthalamic nucleus (Nasir *et al.*, 1995). The conditional knockout of huntingtin in mouse forebrain and testes led to a progressive neuronal phenotype and sterility (Dragatsis *et al.*, 2000). A further indication for huntingtin's critical role in neurogenesis was shown in mice expressing huntingtin at a low level. These animals exhibited an aberrant brain development and perinatal lethality, whereas mice expressing polyQ-expanded huntingtin at normal levels did not feature these developmental impairments (White *et al.*, 1997). Further knockout studies discovered that, from the earliest stage of embryogenesis on, huntingtin is necessary for mitochondrial structure and function (Ismailoglu *et al.*, 2014). On the other hand, *HTT* knockout embryonic stem cells could be differentiated into functional post-mitotic neurons, demonstrating that huntingtin is not essential for neuronal differentiation *in vitro* (Metzler *et al.*, 1999). Latest *in vivo* studies based on conditional knockout of *HTT* have shown both vital and negligible roles of huntingtin in the adult mouse (G. Wang *et al.*, 2016; Dietrich *et al.*, 2017).

The disease protein ataxin-3

The CAG repeat in the *MJD1* gene encodes a polyQ stretch at the C-terminus of ataxin-3, a deubiquitinating enzyme (DUB). This cysteine protease consists of around 350 amino acids and is approximately 40 kDa in size, which not only depends on the length of the variable polyQ stretch but also on the respective isoform (Goto *et al.*, 1997).

The *ATXN3* gene is widely present amongst eukaryotic organisms, and many orthologues were identified in vertebrates and invertebrates, but also plants and unicellular eukaryotes (Albrecht *et al.*, 2002, 2004; do Carmo Costa *et al.*, 2004). The protein is not only expressed in neuronal tissues, like the SCA3-affected cerebellum or brainstem, but shows a ubiquitous tissue distribution which was found to be present at early stages of embryonic development (Paulson *et al.*, 1997a; do Carmo Costa *et al.*, 2004). On cellular level, ataxin-3 can be found in the cytoplasm, bound to mitochondria and inside of the nucleus. In neurons, ataxin-3 is localised mainly in the cell body, but also in processes like axons and dendrites (Tait *et al.*, 1998; Trottier *et al.*, 1998; Pozzi *et al.*, 2008).

The structure of ataxin-3 (FIGURE 4) is characterised by its N-terminal, 180 amino acid-long proteolytic Josephin domain (JD), which is the eponym for a whole group of enzymes sharing this domain, the Josephin family (Albrecht *et al.*, 2002). The JD exerts the deubiquinating activity based on cysteine residue at amino acid position 14 in the catalytic triad (Scheel *et*

al., 2003; Nicastro *et al.*, 2005). The interaction with ubiquitinated substrates is facilitated by ataxin-3's ubiquitin interacting motifs (UIMs) of which isoform 1 (UniProt identifier: P54252-1) carries two located between the JD and the polyQ stretch (UIM1 & UIM2), and isoform 2 (UniProt identifier: P54252-2) features a third one downstream of the glutamine repeat (UIM3) (Burnett *et al.*, 2003; Harris *et al.*, 2010). The JD and the UIMs allow ataxin-3 to bind and modify ubiquitin chains, which are linked via K48, K63 or mix-linked via K48 and K63 residues (Chai *et al.*, 2004; Winborn *et al.*, 2008). Furthermore, the ataxin-3 sequence was shown to contain two active NES within the JD, and a nuclear localisation signal (NLS) between UIM2 and the polyQ stretch (Tait *et al.*, 1998; Antony *et al.*, 2009; Macedo-Ribeiro *et al.*, 2009). Ataxin-3 is modified by various post-translational modifications, including phosphorylation, SUMOylation, neddylation, ubiquitination and proteolytic cleavage (Matos *et al.*, 2011). Phosphorylation by casein kinase-2 (CK2) and glycogen synthase kinase-3β (GSK 3β) were shown to modify its localisation and ubiquitination at lysine 117 regulates the DUB activity (Fei *et al.*, 2007; Mueller *et al.*, 2009; Todi *et al.*, 2009).

Ataxin-3 was found to interact with different proteins, which are also indicative for its cellular function. Important interactors are the human homologues of the yeast DNA repair protein RAD23 protein A and B (HHR23A & B), and valosin-containing protein (VCP/p97) (Wang *et al.*, 2000; Zhong and Pittman, 2006). These protein-protein interactions were shown to implicate ataxin-3 in the protein quality control mechanism by the ubiquitin-proteasome system (UPS), in particular the ER-associated protein degradation (ERAD) (Burnett *et al.*, 2003; Doss-Pepe *et al.*, 2003; Chai *et al.*, 2004).

As it is typical for DUBs, ataxin-3 is closely interacting with different E3 ubiquitin ligases, which allows to determine substrate specificities (Durcan and Fon, 2013). Amongst these E3 partners is C-terminus of Hsc70-interacting protein (CHIP), which is regulated by ataxin-3 in cooperation with the E2 ubiquitin conjugating enzyme Ube2w (Scaglione *et al.*, 2011). Moreover, ataxin-3 is an interactor of the autosomal recessive juvenile PD-associated E3 enzyme parkin, an important enzyme in the mitochondrial quality control mechanism of mitophagy. Ataxin-3 was shown to regulate parkin autoubiquitination and, through this, to play a role in regulating parkin's stability and turnover (Durcan *et al.*, 2011, 2012). However, a link between ataxin-3 and parkin-mediated mitophagy has not been investigated yet (Durcan and Fon, 2015; Nardin *et al.*, 2016). In addition, ataxin-3 plays a role in aggresome formation and exhibits a deneddylase activity by modifying the ubiquitin-like developmentally downregulated 8 protein (NEDD8) (Burnett and Pittman, 2005; Ferro *et al.*, 2007; H. Wang *et al.*, 2012). A further important function of the protein was found in transcriptional regulation, where ataxin-3 acts as a repressor of transcription by interacting with histones and recruiting

deacetylases (F. Li *et al.*, 2002; Evert *et al.*, 2006). Moreover, ataxin-3 is important in myogenic differentiation, participates in cell signalling and may represent a target in cancer (Rodrigues *et al.*, 2007; do Carmo Costa *et al.*, 2010; Kuhlbrodt *et al.*, 2011; Sacco *et al.*, 2013).

Due to its activity as a DUB in UPS, ataxin-3 was suggested to exert neuroprotective effects (Warrick *et al.*, 2005). In *Drosophila*, this neuroprotection was shown to depend on ubiquitination of ataxin-3 at amino acid position 117 and not on its E3 partner CHIP (Tsou *et al.*, 2013). In a HD model background, however, knockout of ataxin-3 did not elevate toxic effects of polyQ-expanded huntingtin *in vivo* (Zeng *et al.*, 2013). Likewise, overexpression of wild type ataxin-3 in SCA3 mice, could not mitigate the polyQ toxicity of the pathogenic variant (Hübener and Riess, 2010).

In contrast to various detrimental effects induced by a genetic ablation of huntingtin, the knockout of ataxin-3 has not been associated with an overt phenotype *in vivo*. Still, ataxin-3 knockout mice exhibited an increased anxiety and elevated levels of ubiquitinated proteins (Schmitt *et al.*, 2007; Switonski *et al.*, 2011). Furthermore, knockdown of ataxin-3 in murine and human cell lines led to defects in cytoskeletal organisation (Rodrigues *et al.*, 2010). Interestingly, *C. elegans* deficient for the orthologues of VCP/p97 and ataxin-3 showed extended lifespan due to an altered insulin-like growth factor 1 (IGF1) signalling pathway (Kuhlbrodt *et al.*, 2011).

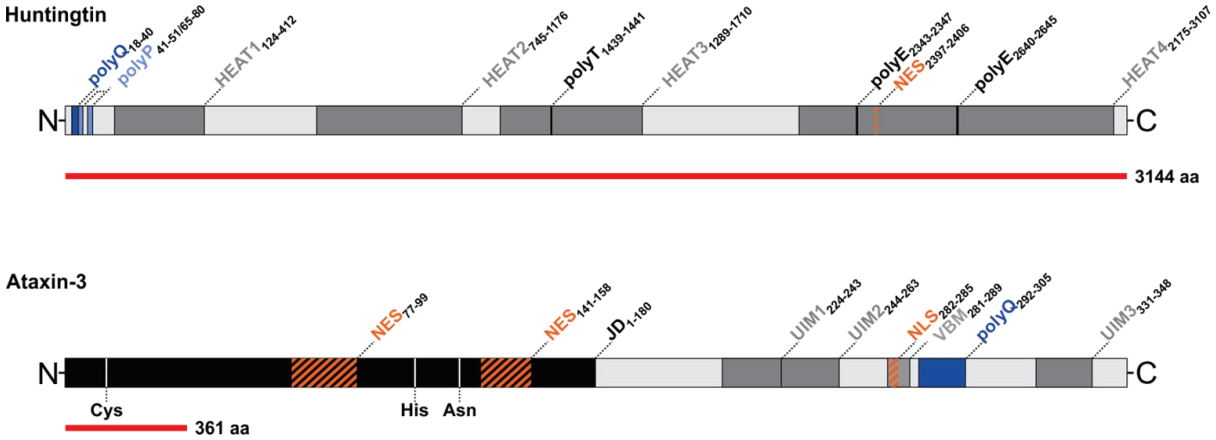

Figure 4. Comparison between the disease proteins huntingtin and ataxin-3. The huntingtin protein is characterised by its N-terminal polyQ domain, followed by a proline-rich region (polyP) and four clusters of HEAT repeats, which facilitate protein-protein interactions. A nuclear export signal (NES) is localised at the C-terminus. Further hallmarks are polythreonine (polyT) and polyglutamate (polyE) motifs. The deubiquitinase ataxin-3 is composed of its N-terminal proteolytic Josephin domain (JD) and up to three ubiquitin interacting motifs (UIMs) at the C-terminus of the enzyme. Two UIMs are located upstream and a third, isoform-specific UIM is located downstream of the polyQ repeat. The subcellular localisation of ataxin-3 is determined by two NES within the JD and one nuclear localisation signal (NLS) between UIM2 and the polyQ stretch. Amino acid positions of the catalytic triad of ataxin-3 are indicated by vertical white lines. A relative size comparison between huntingtin and ataxin-3 is indicated by the red lines below the structural illustrations.

Divergent and common molecular pathomechanisms

As described previously, huntingtin and ataxin-3 constitute two proteins, which significantly differ in their molecular weight, structure and function. On the other hand, both proteins cause neurodegeneration of the brain and share, as their main commonality, a polyQ stretch. The detrimental effects on neuronal health caused by the mutant protein can therefore be attributed to the specific negative impact of the polyQ expansion on their normal biological role. For both disease proteins a toxic gain or loss function have been hypothesised (Zuccato *et al.*, 2010; Li *et al.*, 2015). In the case of huntingtin, the protein's involvement in cellular trafficking was found to be disrupted due to the mutation of the polyQ stretch. This can have a negative impact on secretory pathways or mitochondrial transport (Gauthier *et al.*, 2004; Trushina *et al.*, 2004; Li *et al.*, 2010; Brandstaetter *et al.*, 2014). Furthermore, the recently discovered role of huntingtin as a scaffold protein in autophagy suggested a mutant huntingtin-driven impairment of the autophagic pathway (Martin *et al.*, 2015). In the same manner, specific functions of ataxin-3 may be compromised by the polyQ expansion. For instance, mutant ataxin-3 was shown to excessively bind its interaction partner VCP, thus pathologically deregulating its role in ERAD (Zhong and Pittman, 2006). Moreover, parkinsonian features of SCA3 are conceivably caused by an enhanced DUB activity of the polyQ-expanded protein, which increased deubiquitination and degradation of parkin (Durcan *et al.*, 2011).

Despite their functional disparities, the toxicity of mutant huntingtin and ataxin-3 are based on common molecular pathomechanisms. Hence, investigations on these pathways constitute an opportunity to unveil a general therapeutic approach not only for HD and SCA3, but also other polyQ or neurodegenerative disorders. Both mutant huntingtin and ataxin-3 were shown to accumulate in neuronal nuclei, which has been in particular associated with fragments of the disease proteins, and which is in contrast to the widely cytoplasmic distribution of the wild type full-length proteins (DiFiglia *et al.*, 1997; Hackam *et al.*, 1998; Schmidt *et al.*, 1998; Breuer *et al.*, 2010). A main common histological hallmark of the disease proteins is, however, the formation of intranuclear and cytoplasmic aggregates (DiFiglia *et al.*, 1997; Paulson *et al.*, 1997b; Gutekunst *et al.*, 1999; Seidel *et al.*, 2016). These aggregates were also shown to arise in axons and spatially block axonal transport, thereby contributing to neuronal dysfunction and degeneration (Gunawardena *et al.*, 2003; Chang *et al.*, 2006; Seidel *et al.*, 2010). Furthermore, intranuclear inclusions of ataxin-3 and huntingtin can sequester vital transcription factors and cause transcriptional deregulation (Kazantsev *et al.*, 1999; McCampbell *et al.*, 2000; Jiang *et al.*, 2003; Schaffar *et al.*, 2004). Likewise, this detrimental effect can be triggered by soluble forms of both polyQ proteins,

which were found to functionally interact with transcription factors (Zuccato *et al.*, 2001; F. Li *et al.*, 2002; S.-H. Li *et al.*, 2002). The proteotoxic stress, induced by the polyQ-dependent misfolding and aggregation of disease proteins, can additionally hamper protein quality control mechanisms. Chaperones, the UPS and autophagy were reportedly dysregulated and parts of the machinery depleted (Chai *et al.*, 1999; Hazeki *et al.*, 2000; Jana *et al.*, 2001; Sakahira *et al.*, 2002; Schmidt *et al.*, 2002; Koga *et al.*, 2011; Nascimento-Ferreira *et al.*, 2011; Park *et al.*, 2013; Martin *et al.*, 2015).

Interestingly, many common pathomechanisms are apparently consequences of soluble polyQ proteins rather than of aggregates. An initial point for neurodegeneration is mitochondrial dysfunction. Full-length forms and fragments of polyQ-expanded huntingtin and ataxin-3 were shown to directly interact with mitochondria and thereby negatively influence mitochondrial vitality, eventually leading to cell death (Chou *et al.*, 2006; Orr *et al.*, 2008; Yu *et al.*, 2009; Song *et al.*, 2011; Shirendeb *et al.*, 2012; Yano *et al.*, 2014). In addition, neuronal Ca^{2+} handling, which in a large part depends on mitochondrial function, was shown to be impaired in HD and SCA3. This dyshomeostasis of cellular Ca^{2+} levels can induce aberrant activation of Ca^{2+}-dependent enzymes and promote cell death (Tang *et al.*, 2003; Choo *et al.*, 2004; Rockabrand *et al.*, 2007; Chen *et al.*, 2008; Bezprozvanny, 2009, 2011; Czeredys *et al.*, 2013).

A further neurotoxicity-mediating feature of HD and SCA3 is the occurrence of huntingtin and ataxin-3 fragments. These by-products have been suggested to play a pivotal role in triggering many subsequent pathomolecular effects in HD and SCA3 (FIGURE 5) (Tarlac and Storey, 2003; Ehrnhoefer *et al.*, 2011; Matos *et al.*, 2011). The origin and the implications of these pernicious protein species are diverse and will be the subject of the following pages.

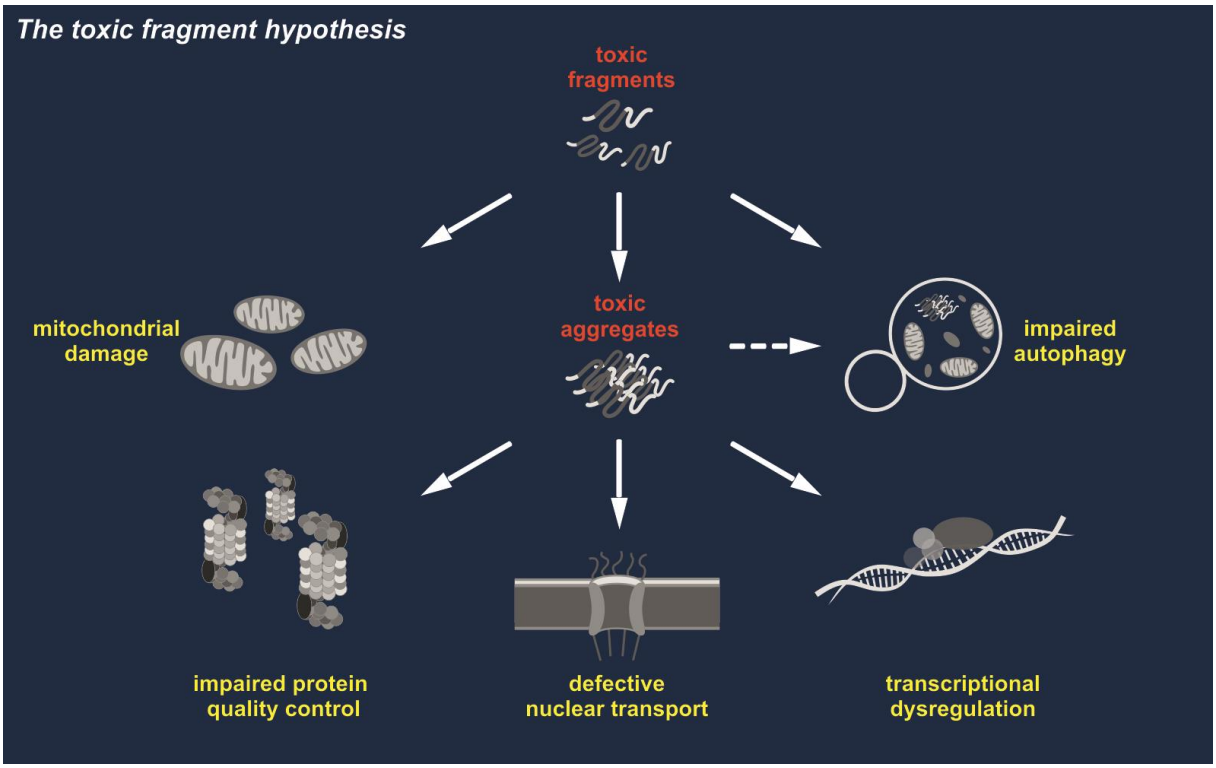

Figure 5. The toxic fragment hypothesis. Fragments of disease proteins like polyQ-expanded huntingtin or ataxin-3 may represent a starting point for molecular pathomechanisms. Due to their increased aggregation-propensity, fragments can increase the formation of aggregates, which consequently lead to impairments of cell function, such as defects in protein quality control mechanisms, nuclear-cytoplasmic transport and transcription. Furthermore, fragments by themselves can directly affect cellular vitality by, for instance, damaging mitochondria or impairing autophagy.

The role of proteolysis in neurodegenerative diseases

The toxic fragment hypothesis of neurodegeneration

Since the 1990s, our understanding of the molecular basis for neurodegeneration has been considerably widened. Notably, causative mutations for monogenic disorders like HD or SCA3 were unveiled due to technical achievements in molecular biology. However, the exact mechanism of neurodegeneration as mediated by polyQ-expanded proteins remains complex and elusive. The detailed analysis of patient tissue and disease models provided the indication that fragments of mutant proteins may be mediators of pathogenicity. These truncated species were shown to display an increased toxicity and aggregation propensity when compared to the respective full-length protein.

One of the first experimental proofs for the occurrence of toxic fragments was made in HD, when researchers performed immunohistochemical staining of huntingtin aggregates in post-mortem tissue. Neuronal deposits of the mutant protein were detected with antibodies binding the polyQ-containing N-terminus of huntingtin, but not with antibodies specific for the C-terminus, suggestive of a lack of the respective portion of the protein in aggregates (DiFiglia *et al.*, 1997). Together with the realization that the expression of an exon 1-based polyQ-expanded huntingtin fragment was sufficient to generate a severe progressive phenotype in mice, these findings led to formulation of the *toxic fragment hypothesis* (Mangiarini *et al.*, 1996; Davies *et al.*, 1997; Wellington and Hayden, 1997). The validity of this pathomolecular concept was corroborated by studies on additional neurodegenerative diseases. Early studies on SCA3 showed that the expression of polyQ-expanded truncated ataxin-3 in cell models and mice showed a markedly exacerbated phenotype compared to the expression of full-length ataxin-3 (Ikeda *et al.*, 1996). Analogously to findings in HD, ataxin-3 aggregates in SCA3 post-mortem tissue were clearly detectable with antibodies directed against the polyQ-containing C-terminus but not against the N-terminus of ataxin-3 (Schmidt *et al.*, 1998). Moreover, the presence and accumulation of soluble huntingtin or ataxin-3 fragments was demonstrated in brain tissue of animal models and patients, and even observed in lymphoblasts (Kim *et al.*, 2001; Toneff *et al.*, 2002; Goti *et al.*, 2004; Wang *et al.*, 2008). Further *in vitro* analyses confirmed the increased toxicity of polyQ-containing protein fragments in HD or SCA3 cell models, and showed that fragments and not the full-length protein formed intranuclear aggregates (Paulson *et al.*, 1997b; Hackam *et al.*, 1998; Martindale *et al.*, 1998; Haacke *et al.*, 2006). N-terminal fragments of huntingtin were found to accumulate at mitochondria and impair their function and trafficking (Orr *et al.*, 2008). Comparable findings regarding a potential pathogenic role of fragments were also described

for further polyQ disorders including DRPLA, SBMA, SCA7 and SCA17 (Butler *et al.*, 1998; Schilling, Wood, *et al.*, 1999; Yvert *et al.*, 2000; Garden *et al.*, 2002; Nucifora *et al.*, 2003; Friedman *et al.*, 2008; Young *et al.*, 2009). Interestingly, not all forms of polyQ-containing fragments show an increased toxicity. This has been reported for a transgenic mouse model of HD, where the expression of an N-terminal polyQ-expanded huntingtin fragment led to massive inclusions without evidence for neurodegeneration or behavioural abnormalities (Slow *et al.*, 2005). Ataxin-1 fragments, which observed in SCA1 transgenic mice, were excluded as component of the pathogenic process in this disease model (Klement *et al.*, 1998). Likewise contrary to the *toxic fragment hypothesis,* truncated mutant ataxin-2, which is present in post-mortem SCA2 brain tissue, exhibited reduced toxicity when compared to the full-length protein *in vitro* (Huynh *et al.*, 2000; Ng *et al.*, 2007). Moreover, the polyQ-dependency of fragment toxicity is not generally valid. A gene trap mouse model expressing the first 259 N-terminal amino acids fused to galactosidase and lacking the polyQ stretch developed cytoplasmic inclusion bodies and a neurological phenotype reminiscent of SCA3 (Hübener *et al.*, 2011). PolyQ-independent fragments of huntingtin were found to induce detrimental effects on autophagy and the ER, thus presumably contributing to neuronal cell death (Martin *et al.*, 2014; El-Daher *et al.*, 2015). Finally, in SCA6, it was hypothesized that the polyQ-expanded α1A Ca^{2+} channel is not toxic by itself, but renders arising toxic fragments resistant to further degradation by proteolysis (Kubodera *et al.*, 2003). Beyond polyQ diseases, pathogenic protein fragments are found in many different neurodegenerative disorders. The Aβ peptide, the breakdown product of APP, or toxic fragments of tau are involved in AD and tauopathies, respectively (Lee and Leugers, 2012; Zhang and Tanzi, 2012). Fragments of TDP-43 were present in post-mortem neuronal tissue of ALS and FTLD patients (Lee *et al.*, 2011). And the C-terminal truncation of α-synuclein was shown to occur *in vivo* and to promote α-synuclein aggregation in PD (Li *et al.*, 2005).

Two molecular mechanisms have been described as potential sources for disease protein fragments: Aberrant splicing and proteolytic cleavage (FIGURE 6). Alternative splicing is an important cellular tool for increasing the functional pallet of genes on protein level. This is achieved by exclusion or inclusion of exons during the processing of the final mRNA (Matlin *et al.*, 2005). Aberrant splicing, however, was described to produce truncated versions of proteins, which are toxic or tend to aggregate, as shown for huntingtin, TDP-43 or tau (Nishimoto *et al.*, 2010; Sathasivam *et al.*, 2013; Park *et al.*, 2016). The second, presumably more significant mechanism is the proteolytic fragmentation of disease proteins by endogenous enzymes, which will be discussed in detail in the following chapter.

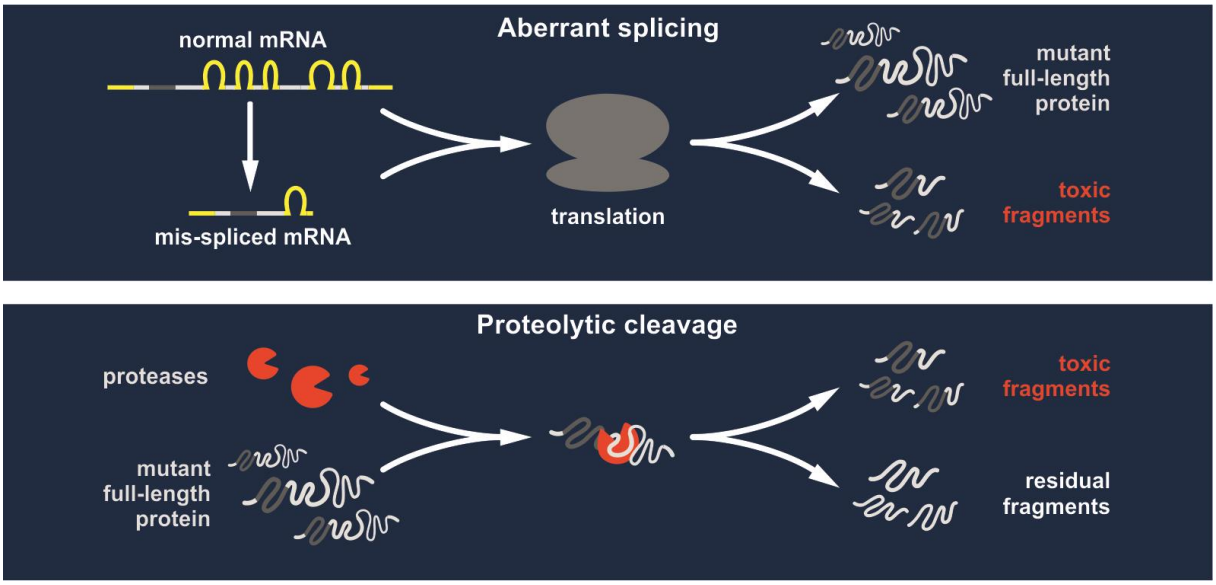

Figure 6. Sources for toxic protein fragments. Truncated forms of proteins can origin from aberrant splicing events omitting exons which normally ameliorate the toxicity or aggregation propensity. Alternatively, disease proteins can be fragmented by endogenous proteases, which separate toxic portions from the residual proteins.

Sources for toxic fragments

Proteolytic machineries of the cell

Protein homeostasis is an important key element of cellular integrity. Only the proper turnover of proteins, the interplay of degradation and synthesis, can guarantee removal and replacement of unnecessary or defective proteins. During a protein's life many different damages and unwanted modifications can occur, ranging from protein truncation, via deamination processes and carbonylation by oxidative stress, to aberrant disulphide crosslinking and protein aggregation (Toyama and Hetzer, 2012). Once detected by respective quality control mechanisms these impaired proteins are submitted to degradation by the two major catabolic mechanisms: the UPS and autophagy-lysosome system (FIGURE 7). In UPS, target proteins are tagged by ubiquitination and transported to the 26S proteasome, a proteolytic complex consisting of a barrel-shaped proteolytic 20S core particle and two 19S regulatory subunits. The 19S subunit recognizes ubiquitinated substrates, unfolds and deubiquitinates them, and mediates their translocation into the proteolytic 20S subunit, where the substrate is degraded to small peptides (Ciechanover, 2005). The second machinery, the autophagy-lysosome system, can be mainly divided into three sub-mechanisms: chaperone-mediated autophagy (CMA), microautophagy and macroautophagy.

The CMA is characterised by substrate recognition via Hsc70 and its co-chaperones based on the consensus sequence KFERQ in the target protein. The substrate-chaperone complex binds to the lysosome-associated membrane glycoprotein-2A (LAMP2A), a receptor on the lysosomal membrane. Finally, the substrate is unfolded, translocated into the lysosomal lumen and degraded down to amino acids by a battery of cathepsins (Kaushik *et al.*, 2011). Microautophagy is a mainly non-selective degradation process via the random engulfment of cytoplasmic cargo by membrane invagination at the lysosome (Li *et al.*, 2012). Macroautophagy, the most investigated form and major mode of autophagy, is based on a characteristic double-membrane vesicle, the autophagosome. The formation mechanism of this organelle is still a matter of debate and many origins have been discussed including the ER, the Golgi apparatus, mitochondria-associated membrane (MAM), or mitochondria themselves (Lamb *et al.*, 2013). Macroautophagy is regulated by two mechanisms, mTOR-ULK1 and the beclin-1 pathway, and its steps can be subdivided in vesicle nucleation and expansion, substrate recognition and autophagosome formation, docking and fusion with the lysosome, and, finally, vesicle and cargo breakdown and degradation (He and Klionsky, 2009; Lilienbaum, 2013). Once formed, autophagosomes can selectively engulf not only protein aggregates but also whole organelles like mitochondria, which are detected by p62 or neighbour of BRCA1 gene 1 (NBR1). These cargo receptors preferentially bind K63-polyubiquitin-tagged substrates and bring them in contact with the autophagosomes via a linker protein at the autophagosomal membrane, the phosphatidylethanolamine-amidated microtubule-associated protein 1A/1B light chain 3A (LC3-II), a marker for autophagosomes formation and autophagic flux (Kabeya *et al.*, 2000, 2004; Bjørkøy *et al.*, 2005; Mizushima and Yoshimori, 2007; Kirkin *et al.*, 2009).

All these processes are not only important for degrading dysfunctional elements of the cell but also to supply it with new nutrients by recycling expendable substrates. However, dysfunction of these degradative systems has been associated with neuronal ageing and degeneration, and is in the focus for therapeutic research (Ciechanover and Kwon, 2015). Regarding immediate production of toxic protein species of disease proteins, UPS and autophagy are rather playing a minor role as they ideally fully degrade substrate proteins without yielding certain deleterious breakdown products. Nevertheless, lysosomal cathepsins were associated with the fragmentation of mutant huntingtin in HD or APP in AD, and inhibition of these enzymes led to positive effects on the molecular disease phenotype (Ratovitski *et al.*, 2011; Kindy *et al.*, 2012).

The main source for toxic protein fragments is represented by non-UPS and non-lysosomal machineries, which comprise a large pallet of proteolytic enzymes. For instance, BACE1 or

the γ-secretase complex have been associated with APP truncation in AD, and matrix-metalloproteinases were shown to cleave huntingtin and α-synuclein in HD or PD, respectively (Miller *et al.*, 2010; Choi *et al.*, 2011; Zhang and Tanzi, 2012). However, the key players in this regard are two classes of cysteine proteases, caspases and calpains (FIGURE 7).

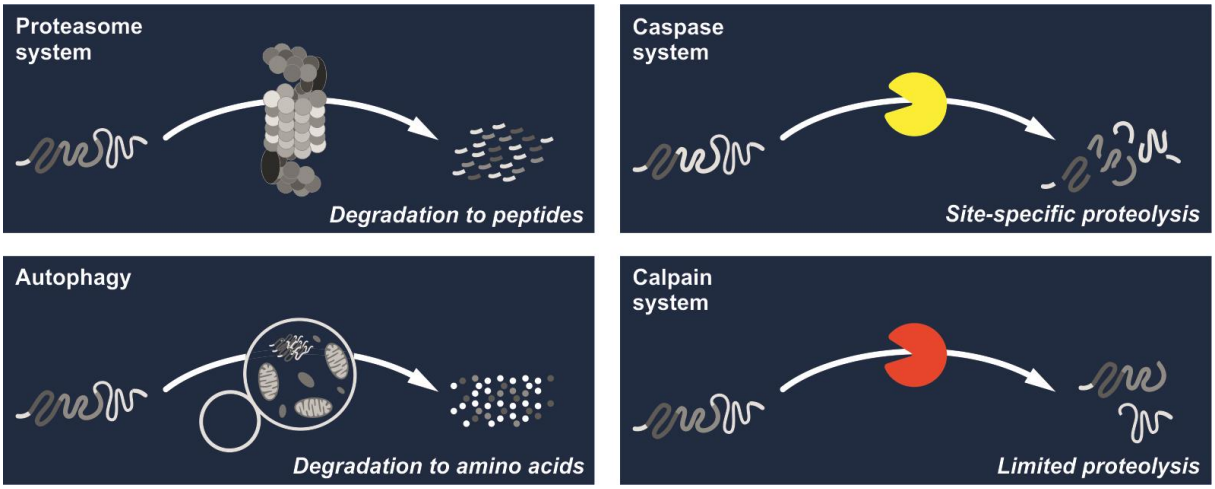

Figure 7. Proteolytic systems of the cell. Illustrative comparison between the degradative proteasome system and autophagy, which degrade substrate proteins to peptides and amino acids, with caspases and calpains, proteases which perform limited proteolysis and produce truncated forms of the target protein.

Caspases as mediators of apoptosis and disease protein cleavage

The name 'caspase' is an acronym for cysteine-dependent aspartate-specific protease. It summarized not only the occurrence of a cysteine residue in the enzyme's catalytic dyad but also the cleavage-specificity after an aspartate at the P_1 position, N-terminal of the scissile bond in the substrate protein (Pop and Salvesen, 2009). Caspases were firstly discovered as the mammalian interleukin-1β-processing enzyme (ICE), a pro-inflammatory cytokine processing protease (now caspase-1), and, at about the same time, the *C. elegans* cell death protein and ICE homologue cell death abnormality-3 (CED-3) (Cerretti *et al.*, 1992; Thornberry *et al.*, 1992; Yuan *et al.*, 1993).

As described for human and mice, there are 14 different caspases in mammals, of which caspase-11 is not present in humans and caspases-4, -5, and -10 lack in the mouse genome (Man and Kanneganti, 2015). The expression of caspases is relatively ubiquitous across all

tissues except for caspase-14 which is restricted to cornifying epithelia (Denecker *et al.*, 2008). Mammalian caspases can be divided in two groups based on the biological function: apoptotic and inflammatory caspases. The first group, which includes caspases-2, -3, and -6 to -10 can be further subdivided into initiator and executioner caspases, which cleave specific substrate proteins to cause cellular destruction. Caspases-2, -8, -9, and -10 are initiators, whereas caspases-3, -6, and -7 are executioners of apoptosis (Man and Kanneganti, 2015). The mechanism of programmed cell death can be enforced in an intrinsic or extrinsic manner. The intrinsic pathway is based on the release of cytochrome c from membrane-permeabilized mitochondria. Cytochrome c then interacts with apoptotic protease-activating factor 1 (Apaf-1) in the cytoplasm, which recruits initiator caspase-9, inducing the formation of the apoptosome and initiating the caspase cascade via executioner caspases-3 and -7 (Tait and Green, 2010). The extrinsic pathway, by contrast, is based on an external stimulus which is transmitted via death receptors like Fas receptor (FasR), tumour necrosis factor receptor 1 (TNFR1), or TNF-related apoptosis-inducing ligand (TRAIL) receptors. Binding of respective ligands leads to the recruitment, dimerization and activation of initiator caspase-8 and -10, which initiate the apoptotic cascade via activation of executioner caspase-3 (Guicciardi and Gores, 2009). Moreover, caspase-8 converts BH3 interacting-domain death agonist (BID) into tBID, which can in parallel activate the intrinsic apoptosis via mitochondria (Billen *et al.*, 2008). The second group consists of caspases-1, -4, -5, -11 and -12, and is associated with the inflammatory response via the inflammasome. This multi-protein complex activates caspase-1, which drives the conversion of cytokines such as pro-interleukin-1β and -18 to their active forms. Furthermore, inflammatory caspases are initiating pyroptosis, an inflammatory and lytic form of programmed cell death (Man and Kanneganti, 2015). Caspase-14 occupies a special position as it is neither involved in apoptotic nor inflammatory processes, but plays a role in terminal keratinocyte differentiation (Denecker *et al.*, 2008).

Structurally, initiator caspases consist of the C-terminal catalytic caspase domain and two different types of N-terminal, regulatory pro-domains, which are not present in executioner caspases-3, -6, -7, and -14 (FIGURE 8). Caspases-8 and -10 exhibit two death effector domains (DED) and the remainder feature a caspase activation and recruitment domain (CARD), which are crucial for caspase dimerization and activation. The catalytic caspase domain consists of a small (p10) and a large (p20) subunit connected by a linker region (Riedl and Shi, 2004). Upon dimerization initiator caspases undergo autoproteolysis, which removes the pro-domain and cleaves the linker. The separation of the small and large subunits leads to the rearrangement and formation of the active caspase heterotetramers.

Dimers of executioner caspases, however, require proteolysis by active initiator caspases for triggering subunit separation, rearrangement and activation (Yang *et al.*, 1998; Tait and Green, 2010). Several proteins were identified as direct or indirect inhibitors of caspases, which control their activation during cellular processes. The first potential inhibitor of caspases was the baculoviral p35 protein, which is known to potently inhibit most caspases and represents the prototype for the biggest group of endogenous mammalian inhibitors of apoptosis proteins (IAP) (Bump *et al.*, 1995; Xue and Robert Horvitz, 1995; Clem, 2001). They are characterised by their inhibitory baculoviral IAP repeat (BIR) domains. In addition, IAPs can feature a C-terminal really interesting new gene (RING) domain, which bears a E3 ubiquitin ligase function to tag themselves or targeted caspases for degradation via the UPS (Riedl and Shi, 2004; Vaux and Silke, 2005).

Besides their important role in regulating and executing apoptosis and inflammation, caspases are involved in many further biological processes including proliferation, differentiation, cell morphology and migration, and cell-autonomous immunity (Miura, 2012; Man and Kanneganti, 2015). In neurons, caspases control neuronal connectivity and signal transduction by mediating dendritic pruning, axon guidance, synaptogenesis and long-term depression (Hyman and Yuan, 2012).

Likewise, caspases are involved in various disease mechanisms. Interleukin-1 production by caspase-1 is implicated in inflammatory and autoinflammatory disorders including gout, arthritis or type 2 diabetes. Under certain pathological conditions caspases act as executioners of apoptosis in tissue degeneration. And mutations of caspases and overexpression of IAPs have been associated with cancer (Degterev *et al.*, 2003; McIlwain *et al.*, 2013). Furthermore, caspases are known to play a role in acute and chronic neurological diseases. For instance, they are involved in cell death and inflammatory response during cerebral ischemic injuries and inhibiting caspases pharmacologically was shown to reduce detrimental effects of ischemic and excitotoxic neuronal damage in animal models (Hara *et al.*, 1997; Fink *et al.*, 1998; Friedlander, 2003; García de la Cadena and Massieu, 2016). In many neurodegenerative disorders like AD, ALS, FTLD, HD, SCA3 and SCA7 caspases were found to mediate neuronal cell death and toxic fragmentation of disease proteins like tau, TDP-43, huntingtin, ataxin-3 or ataxin-7 (Goldberg *et al.*, 1996; Guégan *et al.*, 2001; Hartmann *et al.*, 2001; Berke *et al.*, 2004; Rissman *et al.*, 2004; Young *et al.*, 2007; Y.-J. Zhang *et al.*, 2009). Several cell and animal models treated with caspase inhibitors or expressing caspase-cleavage resistant variants of disease proteins furthermore showed improved molecular or behavioural phenotypes, underpinning the importance of caspases as

a potential therapeutic target in neurodegeneration (Graham *et al.*, 2006; Jung *et al.*, 2009; Leyva *et al.*, 2010; Rohn, 2010).

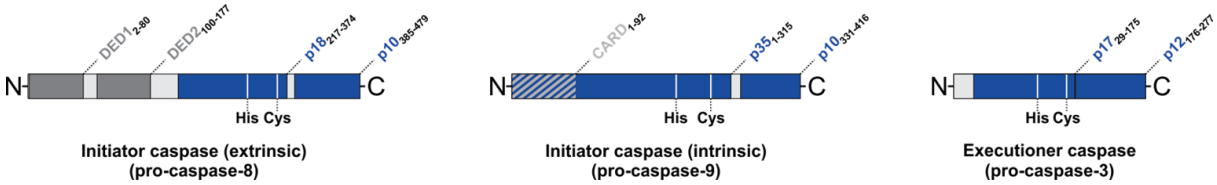

Figure 8. Domain composition of caspases. Caspases can be functionally subdivided in initiator and executioner caspases. Initiator caspases of the extrinsic apoptotic pathway like caspase-8, feature as a pro-enzyme two N-terminal death effector domains (DEDs), which are followed by a large and a small catalytic subunit, connected by a linker sequence. Upon interaction with an activator protein, the DEDs are cleaved off and the subunits are proteolytically separated. Initiator caspases triggering the intrinsic apoptosis, such as caspase-9, exhibit a caspase activation and recruitment domain (CARD) at their N-terminus. Comparably to the previous class, a linker sequence between the large and small subunit is cleaved, transforming the protease to its active state. Executioner caspases like caspase-3 do not feature pro-domains and are likewise activated by the proteolytic separation of their subunits. Amino acid positions of the catalytic dyad of caspases are indicated by vertical white lines. Illustrations of caspases are based on data retrieved from the UniProt database.

Calpains and their involvement in health and disease

The group of calpains was discovered and firstly described as a Ca^{2+}-activated, neutral proteinase (CANP) by Gordon Guroff more than half a century ago (Guroff, 1964). The established name ‘calpain’ was proposed later and is a portmanteau consisting of the elements ‘cal’ as a reference to Ca^{2+} and Ca^{2+}-binding proteins, and ‘pain’, which corresponds to structurally-related cysteine proteases from plants, papain or bromelain (Murachi *et al.*, 1980).

Calpains are characterised by their well conserved proteolytic domain (CysPc), which consist of two protease core domains (PC1 and PC2) (FIGURE 9). In a modular principle with more than 40 different other domains or motifs, the CysPc domain forms multiple variants of calpains, which are found in many species, from some bacteria via unicellular and multicellular eukaryotes through to vertebrates (Sorimachi *et al.*, 2011). In humans, 15 different calpains are described, which can be divided in conventional classical (calpain-1 and -2), unconventional classical (calpains-3, -8, -9, -11 to -14) and unconventional non-classical calpains (calpains-5, -6, -7, -10, -15, and -16). The main differences between these

groups are as follows: Conventional classical calpains are characterised by a C-terminal Ca^{2+}-binding penta-EF-hand (PEF) domain and their vital interaction with the regulatory calpain small subunit 1 (CAPNS1, formerly known as calpain-4). Unconventional non-classical calpains share the same structure as classical calpains including the PEF domain but without interacting with CAPNS1. Lastly, unconventional non-classical calpains lack both PEF domains and the regulatory subunit (Dayton *et al.*, 1976; Sorimachi *et al.*, 2011; Ono *et al.*, 2016). Together with calpastatin (CAST), the only known endogenously expressed and highly specific, proteinaceous calpain inhibitor, they form the intracellular calpain system (FIGURE 9) (Nishiura *et al.*, 1978; Wendt *et al.*, 2004). The expression of calpains depends on the respective isoform. For instance, calpain-1, -2, or -10 are expressed ubiquitously or at least in most cells, whereas calpain-3 is solely expressed in skeletal muscle, calpain-11 and -13 can be found in testes, and expression of calpain-12 is restricted to the skin (Ono *et al.*, 2016).

How calpains are activated was controversially discussed and different explanatory scenarios were suggested, including autoproteolysis, protease dimerization, or dissociation from the regulatory subunit (Campbell and Davies, 2012). However, X-ray crystallography of Ca^{2+}-bound calpain-2 together with CAPNS1 and CAST gave information about the precise mechanism: In a fully active state, calpain binds ten Ca^{2+} ions of which eight bind to the two PEF domains, and one Ca^{2+} binds each PC domain. This triggers structural rearrangements which then lead to the connection of the two protease core domains PC1 and PC2 to a closed active state (Moldoveanu *et al.*, 2002, 2008; Hanna *et al.*, 2008). *In vitro* studies normally utilize micro to millimolar Ca^{2+} concentrations to activate calpains, which are rather divergent from the nanomolar levels in cells under normal physiological conditions. However, this apparent contradiction is resolved, as sufficient Ca^{2+} concentration may be reached in the cellular microenvironment (Campbell and Davies, 2012).

Calpains perform many regulatory functions in cells by executing limited proteolysis, a specific recognition motif-dependent cleavage of substrate proteins (Tompa *et al.*, 2004; DuVerle *et al.*, 2011). This allows them to modulate the activity of enzymes or structural proteins. Calpains are known to play a role in remodelling cytoskeletal elements, modulation of cell motility, cell cycle control and proliferation, regulation of gene expression, inflammation, autophagy, apoptosis, signal transduction, and synaptic plasticity in neurons (Goll *et al.*, 2003; Ravikumar *et al.*, 2010; Baudry and Bi, 2016; Ji *et al.*, 2016).

The important role of calpains in healthy biological system becomes clear, when considering the wide-ranging implication of their malfunction in human diseases. In cardiovascular

disorders, myopathies, ophthalmic diseases or cancer, calpains were found to be deregulated or to mediate certain molecular pathomechanisms. A whole group of medical conditions based on dysfunctions of calpains was termed *calpainopathies* comprising many different pathological manifestations (Ono *et al.*, 2016). The first calpainopathy was limb-girdle muscular dystrophy 2A, which is caused by mutations in the gene of muscular calpain-3 (*CAPN3*) (Richard *et al.*, 1995). Missense mutations in the calpain-5 gene (*CAPN5*) were associated with a form of autosomal-dominant neovascular inflammatory vitreoretinopathy (Mahajan *et al.*, 2012). And an intriguing association of calpains was made with diabetes, when calpain 10 was identified as a susceptibility gene for type 2 diabetes (Horikawa *et al.*, 2000). Finally, calpains are also involved in neuronal injury, neurodegenerative disorders and neuronal ageing processes (Nixon, 2003; Mattson and Magnus, 2006). For instance, these proteases execute Wallerian degeneration, mediate degenerative effects in traumatic brain injury, and show detrimental overactivation or perform disease protein cleavage in neurodegenerative disorders like AD, ALS, or PD (Samantaray *et al.*, 2008; Saatman *et al.*, 2010; Ferreira and Adriana, 2012; J.T. Wang *et al.*, 2012; Ma *et al.*, 2013; Wright and Vissel, 2016). A neuronal calpainopathy caused by *CAPN1*-null mutations is characterised by cerebellar ataxia and limb spasticity (Y. Wang *et al.*, 2016). In addition to it, calpains play a significant role in polyQ diseases, which will be discussed in detail for HD and SCA3 in the subsequent chapter.

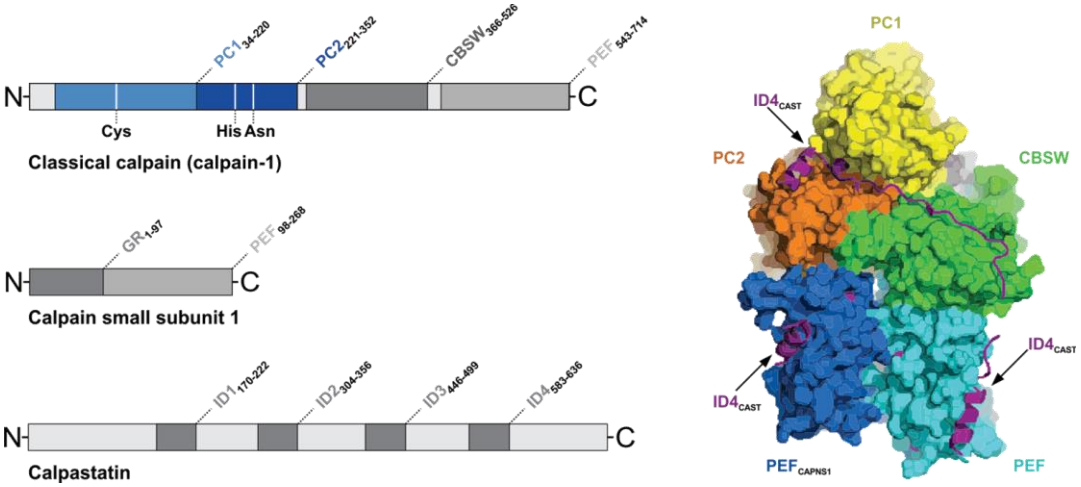

Figure 9. Domain composition and structure of calpains and calpastatin. Conventional classical calpains are present as a large protease unit, such as calpain-1, and the calpain small subunit 1 (CAPNS1). Both share a C-terminal Ca^{2+}-binding penta-EF-hand (PEF) domain. Calpain-1 further contains an N-terminal proteolytic CysPc domain, consisting of core domains PC1 and PC2, which also bind Ca^{2+} ions. Amino acid positions of the catalytic triad of calpains are indicated by vertical white lines. In addition, a calpain-like β-sandwich domain (CBSW) is located between the CysPc and the PEF domain. CAPNS1 features, moreover, an N-terminal glycine rich (GR) hydrophobic domain. Unconventional calpains lack the interaction with a small subunit and non-classical calpains do not have a PEF domain, but other characteristic structural elements. The endogenous inhibitor calpastatin contains four structurally flexible inhibitory domains (ID1-4) of which each can inhibit one calpain molecule. Illustrations of calpain-1, CAPNS1 and calpastatin are based on data retrieved from the UniProt database. The binding of calpastatin's ID4 (purple ribbon schematic) to a calpain-CAPNS1 heterodimer is illustrated as a space-filling crystal structure on the right side (adapted from Campbell and Davies, 2012).

Calpains and their role in Huntington disease and spinocerebellar ataxia type 3

Calpains and Huntington disease

Evidence for proteolytic fragmentation of huntingtin and ataxin-3 has been provided about 20 years ago, when caspases were shown to cleave both polyQ proteins and thereby contribute to the formation of toxic and aggregation-prone fragments (Goldberg *et al.*, 1996; Wellington *et al.*, 1998). The association of calpains with huntingtin was revealed shortly after, when a further processing of caspase-3 cleavage-derived fragments by calpains was detected in human HD brain, suggestive of a sequential huntingtin proteolysis by both classes of enzymes (Kim *et al.*, 2001). Additionally, further studies in different cell and animal models of HD demonstrated that wild type and mutant huntingtin are substrates of calpains (Gafni and Ellerby, 2002; Goffredo *et al.*, 2002; Gafni *et al.*, 2004; Landles *et al.*, 2010). This has been also shown for wild type huntingtin in rat cortex and striatum after transient ischemic injury and 55 kDa large fragments were observed to translocate from injured neurons to astrocytes (Kim *et al.*, 2003, 2011). In contrast to caspase-dependent fragmentation, the polyQ tract was shown to modulate the calpain cleavage propensity of huntingtin, rendering the polyQ-expanded protein more sensitive to fragmentation by calpains *in vitro* (Wellington *et al.*, 1998; Gafni and Ellerby, 2002). Moreover, arising N-terminal calpain cleavage-derived fragments accumulate in the nucleus of HD cell models, which has been correlated with increased cytotoxicity (Hackam *et al.*, 1998; Martindale *et al.*, 1998; Gafni *et al.*, 2004). On the other hand, researchers proposed a protective role of a calpain-dependent huntingtin degradation, which removes toxic N-terminal fragments arising from cleavage by enzymes such as bleomycin hydrolase or cathepsin Z (Ratovitski *et al.*, 2007, 2011; Southwell *et al.*, 2011). Only few investigations were done on the determination of cleavage sites within the huntingtin protein. Two main sites were identified at amino acids 469 and 536, and the existence of further site between amino acids 510 and 654 was presumed (Gafni *et al.*, 2004; Landles *et al.*, 2010). Furthermore, calpain cleavage at amino acids 8 and 15 was linked to the degradation of N-terminal huntingtin constructs (Southwell *et al.*, 2011). Aside from discovery of huntingtin as a calpain substrate, calpain activation has been shown to be a characteristic of the molecular pathogenesis of HD. Despite lacking a direct colocalisation of active calpain-2 with aggregates of mutant huntingtin in post-mortem tissue (Adamec *et al.*, 2002), calpain overactivation has been identified in human HD tissue and in cell and animal models of HD. This comprises increased expression levels of calpain-1, -5. -7, and -10 and an elevated enzyme activity as detected by increased breakdown of the calpain substrates α-spectrin and huntingtin (Gafni and Ellerby, 2002; Gafni *et al.*, 2004; Majumder *et al.*, 2007).

Furthermore, the endogenous proteinaceous inhibitor CAST was shown to be decreased in cells expressing mutant huntingtin (Reijonen *et al.*, 2010; Hyrskyluoto *et al.*, 2013). As calpains play a role upon neuronal lesioning, these enzymes have been described as major effectors of striatal cell death in 3-NP models of HD (Bizat *et al.*, 2003). The increased activation of calpains was shown to contribute to a loss of surface NMDA receptors and cleavage of striatal-enriched protein tyrosine phosphatase 61 in the YAC128 model of HD (Cowan *et al.*, 2008; Gladding *et al.*, 2012, 2014). Moreover, NMDA-induced calpain activation correlated with enhanced cell death in cultured MSNs (Cowan *et al.*, 2008). Interestingly, the detected calpain overactivation in the striatum of YAC128 was shown to undergo an age-dependent attenuation, pointing to alterations in Ca^{2+} signalling mechanism with disease progression (Dau *et al.*, 2014).

Calpains and spinocerebellar ataxia type 3

Analogous to the research history of huntingtin cleavage, ataxin-3 was firstly described as a substrate of caspases (Wellington *et al.*, 1998; Berke *et al.*, 2005). Although initial studies could not verify a role of calpains in the molecular pathogenesis of SCA3, subsequent investigations unequivocally demonstrated the occurrence of calpain-dependent ataxin-3 cleavage in established cell models, SCA3 mice and patient-derived neurons (Berke *et al.*, 2004; Haacke *et al.*, 2007; Koch *et al.*, 2011; Simões *et al.*, 2012). However, a direct proof for calpain-dependent ataxin-3 fragmentation in human MJD brain failed to materialize. First attempts to identify calpain cleavage sites within the ataxin-3 protein, narrowed the sites down to amino acid positions 60, 154, 190, 200, 220 and 260, without proving the exact localisation by site-specific mutagenesis (Colomer Gould *et al.*, 2007; Haacke *et al.*, 2007; Simões *et al.*, 2012). Interestingly, most of the proposed cleavage sites are located between two N-terminal NES and the C-terminal NLS, and the separation of these signals by proteolytic events was suggested to trigger the mislocalisation of polyQ-containing fragments into the nucleus as a prerequisite of an enhanced intranuclear aggregation of mutant ataxin-3 (Haacke *et al.*, 2006; Antony *et al.*, 2009). A clear general overactivation of the calpain system as a hallmark of the molecular pathogenesis of SCA3 has not been directly described yet as it was done for HD. However, levels of the CAST were shown to be lowered in SCA3 mice and human SCA3 brain, indicative of an increased calpain activity (Simões *et al.*, 2012). Furthermore, NMDA or glutamate treatment of neurons, derived from SCA3 patient-specific induced pluripotent stem cells (iPSCs), led to an excitotoxic activation of calpains, thus resulting in a fragmentation and aggregation of mutant ataxin-3 (Koch *et al.*, 2011).

Taken together, a multitude of studies revealed the important contribution of the calpain system and calpain-dependent proteolysis to the molecular pathogenesis of HD and SCA3. The thereby generated quantity of information on this specific disease mechanism points out new possibilities for a therapeutic approach for both polyQ disorders by modulating calpain activity and cleavage of the disease proteins huntingtin and ataxin-3.

How to target the calpain proteolytic pathway as a therapeutic approach

Direct and indirect modulation of calpain activity

The scientific evidence on contribution of the calpain system in polyQ disorders was consequently accompanied by developing and testing various strategies to suppress detrimental effects of calpain activation.

A direct approach is the pharmacological inhibition of calpain activity using selective compounds. These molecules target the enzyme's active site by mimicking a substrate or lower its activation allosterically by binding e.g. the PEF domain or protease core (Ono *et al.*, 2016). This strategy has been tested in several HD and SCA3 cell lines or animal models in order to decrease cleavage of the mutant protein or to counteract the negative effects of calpain overactivation. In HD cell lines, which exhibited an elevated calpain activation due to the expression of a polyQ-expanded huntingtin fragment, treatment with calpain inhibitors N-acetyl-L-leucyl-L-leucyl-L-norleucinal (ALLN) and Z-L-Abu-CONH$(CH_2)_3$-morpholine restored NF-κB-p65 levels and improved cell viability (Reijonen *et al.*, 2010). Intracerebroventricular infusion of ALLN in 3-NP-treated rats reduced huntingtin cleavage, rescued full-length huntingtin levels, and alleviated the 3-NP-induced striatal loss (Bizat *et al.*, 2003). Moreover, ALLN-treated primary cultures of MSNs derived from HD mice showed a normalized surface NMDA receptor expression and reduced NMDA-induced apoptosis to wild type levels (Cowan *et al.*, 2008). Calpain inhibitors such as ALLN and calpeptin attenuated calpain-dependent fragmentation of ataxin-3 in Ca^{2+}-treated cell lysates or in cells incubated with the Ca^{2+}-ionophore ionomycin (Haacke *et al.*, 2007). In neurons derived from SCA3 patient-specific iPSCs, incubation with calpain inhibitors abolished mutant ataxin-3 cleavage and aggregation upon excitotoxic stress by NMDA or glutamate treatment (Koch *et al.*, 2011). The oral administration of the calpain inhibitor BDA-410 to a lentiviral mouse model of SCA3 led to a diminished ataxin-3 cleavage, lower full-length levels and reduced aggregation of mutant ataxin-3. This was accompanied by an amelioration of striatal cells loss, rescue of cerebellar morphology, and improvement of motor behaviour deficits (Simões *et al.*, 2014).

However, the therapeutic use of pharmacologic calpain inhibitors is strongly limited to their lack of isoform selectivity and side-effects like binding to other cysteine proteases (Donkor, 2011). Peptides based on the only known selective calpain inhibitor, the endogenous CAST, might represent a promising alternative to other compounds (Gil-Parrado *et al.*, 2003; Wu *et al.*, 2003; Fiorino *et al.*, 2007). Further investigations and the development of a new generation of calpain inhibitors is demanded and ongoing, but can only be achieved by intensifying the research on calpain function and biology (Ono *et al.*, 2016).

Alternatively, activation of calpains can be attenuated by targeting pathways, which are known to be deregulated and thereby induce calpain activity. An example is the administration of memantine, an antagonist to NMDA receptors and therapeutic targeting glutamate excitotoxicity in AD. This compound has been previously shown to reduce calpain activation in different models of AD (Nimmrich *et al.*, 2008; Goñi-Oliver *et al.*, 2009). Respectively, in a 3-NP rat model of HD, memantine was found to be neuroprotective and to act extenuatingly on the calpain system (Lee *et al.*, 2006). On the other hand, treating the YAC128 mouse model of HD with memantine, attenuated, indeed, synaptic dysfunction and pro-death signalling, but without affecting the calpain system (Dau *et al.*, 2014). A further indirect target is the Ca^{2+}-sensitive sigma-1 receptor, which is known to be a regulator of Ca^{2+} homeostasis via interactions with binding immunoglobulin protein (BiP) and IP_3Rs. Overexpressing sigma-1 receptor or administration of its agonist PRE084 was shown to upregulate CAST and reduce calpain-dependent cleavage of α-spectrin in mutant huntingtin-expressing PC6.3 cells (Hyrskyluoto *et al.*, 2013).

Aside from these pharmacologic strategies, genetic approaches can be undertaken to target calpains like knocking-out specific calpain isoforms or overexpressing the endogenous inhibitor CAST. In PC6.3 cells, which express a polyQ-expanded fragment of huntingtin, co-transfection with CAST reduced calpain overactivation and normalized aberrant NF-κB-p65 signalling (Reijonen *et al.*, 2010). The involvement of calpains in the regulation of autophagy was targeted in HD fly and mouse models, where the knockdown of a calpain homologue in *Drosophila* and the overexpression of CAST in a fragment mouse model of HD were protective against aggregation and herewith linked toxicity. Concurrently, it was found, that the knockdown of calpain exerted protective effects in a *Drosophila* model expressing the AD-associated protein tau. This observation further underlined the general validity of this approach for neurodegenerative diseases. Most importantly, the same study demonstrated that a constant overexpression of CAST did not lead to any overt deleterious phenotype in mice (Menzies *et al.*, 2014). In SCA3, transfection with CAST abrogated fragmentation and aggregation of mutant ataxin-3 in cell culture (Haacke *et al.*, 2007). Moreover, the adeno-

associated virus (AAV)-based overexpression of CAST in a lentiviral mouse model of SCA3 resulted in lower ataxin-3 proteolysis, decreased size and amount of intranuclear ataxin-3 inclusions, and neuroprotection via calpain inhibition (Simões *et al.*, 2012).

All these positive results on pharmacological or genetic calpain inhibition in HD and SCA3 are particularly promising and they emphasize that following this strategy might lead to the development of a therapeutic treatment not only of polyQ disorders, but also further neurodegenerative diseases. Nevertheless, attention should be paid to potential adverse effects of calpain inhibition as well: Calpains were shown to contribute to the degradation of mutant huntingtin by removing the very N-terminus of exon 1 constructs, which is known to play a substantial role in modulating protein function, localisation and toxicity (Southwell *et al.*, 2011; Arndt *et al.*, 2015). Furthermore, decreasing the enzymatic activity of calpains induced the accumulation of N-terminal huntingtin species and thereby increased aggregation of the disease protein (Ratovitski *et al.*, 2007). Finally and most strikingly, as calpain-1 knockout animals were found to develop ataxia-like symptoms and calpain-2 mice exhibit embryonic lethality, special caution is demanded, when genetically targeting the calpain system as a therapeutic approach (Takano *et al.*, 2011; Lopez *et al.*, 2015).

Rendering disease proteins resistant to proteolysis by calpains

Following the *toxic fragment hypothesis*, proteolytic fragmentation of disease proteins like polyQ-expanded huntingtin or ataxin-3 generates breakdown products, which are more toxic and more aggregation-prone than the full-length protein. Thus, preventing the cleavage of disease proteins may ameliorate the molecular, physiological and behavioural disease phenotype. The inhibition of proteases responsible for the fragmentation represents a potential approach, especially, when these enzymes are known to be additionally upregulated in the disease context. However, the global downregulation of protease activity can interfere with their physiological function and lead to unwanted side effects (Howley and Fearnhead, 2008; Ono *et al.*, 2016). Therefore, targeting the disease protein itself to decrease its cleavage propensity can constitute are more specific strategy, which circumvents influencing the complex cellular machineries.

Proteases like caspases and calpains are known to cleave substrates at characteristic sites, which are defined by their amino acid sequence or three-dimensional appearance. A directed mutation or a targeted post-translational modification of these sites can render them unrecognizable for the respective proteases and block or, at least, diminish cleavage.

Caspase cleavage sites are highly conserved due to an aspartate residue at the P_1 position in a core tetrapeptide motif (P_4-P_3-P_2-P_1), which is N-terminal of the scissile bond. An additional amino acid preferences at the P_4 site was used for a cleavage site-based subclassification of caspases into three groups (Talanian *et al.*, 1997; Nicholson, 1999). Mutating the aspartate residue at the P_1 site to alanine or asparagine is sufficient to reduce caspase substrate recognition and thus cleavage, and was shown to reduce fragmentation, toxicity and aggregation of mutant huntingtin or ataxin-3 *in vitro* and *in vivo* (Wellington *et al.*, 2000; Berke *et al.*, 2004; Graham *et al.*, 2006; Jung *et al.*, 2009).

For calpains, the situation looks slightly different. Calpain substrate recognition was primarily reduced to a 'P_2-P_1 rule', with mainly arginine or tyrosine at the P_1 and leucine or valine at the P_2 position (Hirao and Takahashi, 1984; Sasaki *et al.*, 1984). Studies in which a single amino acid mutation in the consensus motif was sufficient to abolish proteolysis of calpain substrates like α-spectrin or short transient receptor potential channel 5 (TRPC5) firstly validated the 'P_2-P_1 rule'. However, other researchers could not confirm these observations on further calpain substrates such as histones, myelin basic protein, or tau (Sakai *et al.*, 1987; Banik *et al.*, 1994; Garg *et al.*, 2011). Reviewing these inconsistencies led to the conclusion that a combination of many features of the substrate protein, like primary and secondary protein structures, or the presence of sequences containing proline, glutamic acid, serine, and threonine (so called PEST regions), are determining the recognition by calpains (Tompa *et al.*, 2004; DuVerle *et al.*, 2011; Z. Liu *et al.*, 2011).

Due to the complexity of these motifs, many approaches to abolish calpain cleavage were based on polyalanine substitutions or cleavage site deletions, which can affect up to 10 amino acids surrounding the cleavage site (Gafni *et al.*, 2004; Wanichawan *et al.*, 2014). In this context, the deletion of two identified cleavage sites at amino acid position 469 and 536 in the polyQ-expanded human huntingtin resulted in a lowered calpain-dependent fragmentation, reduced aggregation and an attenuated toxicity (Gafni *et al.*, 2004). As post-translational modifications can also influence the steric nature of an adjacent calpain recognition motif, modulating these changes in a desirable direction can constitute an alternative option. For instance, the serine residue at the calpain cleavage site 536 in human huntingtin was shown to be phosphorylated, and substituting serine by aspartate to mimic phosphorylation inhibited cleavage and reduced toxicity of mutant huntingtin in cell culture (Schilling *et al.*, 2006). However, translation of these results into *in vivo* models still lacks proof-of-concept, although beneficial effects were demonstrated in the caspase cleavage context (Graham *et al.*, 2006; Jung *et al.*, 2009).

Another interesting strategy in preventing disease protein cleavage is based on exon skipping, which omits the translation of protein regions containing cleavage sites. Via administration of specific antisense oligonucleotides, the skipping of exon 12 or both exons 8 and 9 in huntingtin or ataxin-3, respectively, was prompted, which led to the expression of proteins lacking the known caspase or calpain recognition motifs (Evers *et al.*, 2014; Toonen *et al.*, 2016). Moreover, first *in vivo* trials for huntingtin exon 12 skipping in the YAC128 mouse model of HD yielded promising results (Casaca-Carreira *et al.*, 2016). Underlining the technical feasibility of this approach in patients, a therapeutic intervention for Duchenne muscular dystrophy using a morpholino antisense oligomer-mediated exon skipping has been recently approved by the FDA (Cirak *et al.*, 2011; Young and Pyle, 2016).

Objectives of the study

The well documented and frequently reported involvement of calpains in the molecular pathogenesis of many neurodegenerative disorders renders this group of Ca^{2+}-dependent proteases a promising therapeutic target. However, our relatively shallow knowledge regarding calpain function and missing comparative approaches demand further investigations. Therefore, the current study focussed on three main aspects to elucidate the role of calpains in the pathomechanisms of two polyQ diseases, HD and SCA3:

Aim 1: To investigate the calpain system activation in polyQ disease models

For validating the impact of calpains under pathophysiological conditions, several cell and animal models of HD or SCA3 were analysed regarding the expression and activation of proteinaceous elements of the calpain system. Additionally, activation of calpains was genetically amplified *in vivo* by knocking out the endogenous inhibitor CAST in HD and SCA3 mice to test its repercussion on the respective pathology.

Aim 2: To assess the potential benefit of targeting calpains as a therapeutic approach

Genetic and pharmacological strategies were pursued to attenuate the disease-relevant activation of calpains and calpain-mediated fragmentation of disease proteins *in cellulo* and *in vivo*. Calpain inhibitors were administered to HD and SCA3 cell lines to evaluate their protective effects. Two HD animal models were treated with the experimental compound olesoxime, which targets the mitochondrial Ca^{2+} channel VDAC1. Moreover, calpain-1 was knocked out in SCA3 mice to assess its impact on ataxin-3 fragmentation and aggregation *in vivo*.

Aim 3: To characterise the calpain-mediated fragmentation of polyQ disease proteins

Calpain cleavage sites within the disease proteins huntingtin and ataxin-3 were identified using a combinatorial approach. Strategies to reduce calpain-mediated polyQ protein breakdown based on modifications of cleavage sites were tested. Furthermore, the molecular impact of resulting fragments was analysed in cell-based assays for assessing their contribution to the molecular pathogenesis.

Results and discussion

Investigating calpain activation in cell and animal models of polyQ diseases

Preliminary considerations

The disease-associated overactivation of the calpain system has been described as an important feature in neurodegeneration and might mediate the pathology on the molecular level. In HD and SCA3, an increased activity of calpains and dysregulation of elements of the calpain system have been unequivocally described. Therefore, the reproducibility of this pathological hallmark by cell and animal models may not only validate calpains as a mediator of neurodegeneration in general but also represent a relevant evaluation or selection criterion for appropriate disease models.

To reliably ascertain calpain activity in cell lines and tissues, various molecular indicators can be utilized. An indirect approach is measuring the turnover of artificial fluorescent calpain substrates, which alter their emission properties upon cleavage (Rosser *et al.*, 1993; Tompa *et al.*, 2004). This method allows for tracking calpain activity even in living cells, but is currently limited to *in cellulo* experiments (Rosser and Gores, 2000; Niapour and Berger, 2007; Farr and Berger, 2010). Second, as calpains feature many cellular substrates, an increased or reduced activity will lead to changes in the breakdown of these proteins. These substrates and their proteolytic fragments can be assessed by immunodetection-based methods like western blotting or immunohistochemistry. A well described and characterised calpain substrate is α-spectrin, a cytoskeletal protein in eukaryotes, which lines the intracellular side of the plasma membrane. Calpain cleavage results in the formation of a 145 kDa and a 150 kDa fragment and neo-epitope antibodies directed against the cleavage site can specifically detect the occurring fragments. Interestingly, α-spectrin is also a substrate for caspases. However, proteolysis by the latter enzymes produces fragments of 120 kDa and 150 kDa. Thus, comparison of the fragmentation pattern can help to differentiate between calpain and caspase activation (Wang *et al.*, 1998; Warren *et al.*, 2005; Z. Zhang *et al.*, 2009). A substantial neuronal target of calpain cleavage is the cyclin-dependent kinase 5 (CDK5) activator 1, also known as p35. Calpains mediate the conversion of p35 to p25, which is not only an indicator of calpain activation but can also lead to a pathological deregulation of CDK5 activity, a characteristic in AD (M. S. Lee *et al.*, 2000; Taniguchi *et al.*, 2001). Finally, a third strategy is the direct immunodetection of calpains and their endogenous inhibitor CAST. Changes in CAST levels can give evidence about the inhibitory state of the calpain system. Decreased amounts of CAST can be due to lower

expression or increased turnover as CAST acts as a suicidal substrate and is also cleaved by caspases (Wang *et al.*, 1998; Kim *et al.*, 2007; Rao *et al.*, 2008). Likewise, expression levels of calpains can be analysed, but changes may not directly correlate with activity of the calpain system. Calpain-1 and calpain-2 were shown to undergo autoproteolysis, which can be detected by western blotting. For calpain-1, cleavage events at the protein's N-terminus lead to a transition from an 80 kDa full-length enzyme, via a 78 kDa intermediate, to a 75 kDa species (Michetti *et al.*, 1996). Despite previous assumptions and unlike the proteolytic activatory processing of caspases, autoproteolysis of calpains was shown to be irrelevant for enzyme activation (Li *et al.*, 2004; Campbell and Davies, 2012). However, as this process is a concomitant of protease activity, it is frequently used to evaluate calpain activation (Gafni and Ellerby, 2002; Yamashita *et al.*, 2012; Diepenbroek *et al.*, 2014).

Based on these preliminary considerations, this work utilized western blotting and immunohistochemistry to analyse the activation and the cellular distribution of members of the calpain system, respectively. As primary markers, calpain-1 processing, CAST protein levels, and α-spectrin cleavage were detected. For neuronal tissues, cleavage of p35 was additionally investigated. Only a comparative analysis of all aforementioned proteins assures a robust judgement on calpain activation in cell and animal models of HD and SCA3.

Calpain activation in cell models of HD and SCA3

(Covered in Unpublished project manuscript A; Weber *et al.*, 2017)

Cell lines and primary cells constitute a versatile, reproducible and relatively easy-to-use tool to investigate biological processes outside of the complexity of a multicellular tissue or organism. Therefore, first analyses on the calpain system were pursued in cell models of HD and SCA3. Protein lysates were assayed to detect expression and activation of representative calpain isoforms, levels of the endogenous inhibitor CAST and cleavage of the calpain substrate α-spectrin.

For HD, immortalised striatal precursor cell lines (ST*Hdh*) and murine embryonic fibroblasts (MEF*Hdh*) were utilised, which are both derived from *Hdh*^{Q111} knock-in (HDKI) mice and respective wild type littermates (Wheeler *et al.*, 1999; Trettel *et al.*, 2000; Walter *et al.*, 2016). The mutant ST*Hdh*^{Q111} cell line exhibited increased expression of full-length calpain-1 but reduced levels of full-length calpain-2 and -10 compared to wild type ST*Hdh*^{Q7} cells. Total amounts of CAST appeared unchanged. However, a putative breakdown product was increased in ST*Hdh*^{Q111} cells. Likewise, calpain cleavage-derived fragments of α-spectrin showed higher levels in the mutant cell line. Also of note is an elevation in α-spectrin full-length levels. A qualitatively increased calpain-mediated fragmentation of α-spectrin has been described before (Paoletti *et al.*, 2008). However, previous studies did not comment on alterations in full-length levels of α-spectrin (Trettel *et al.*, 2000; Paoletti *et al.*, 2008; Xifró *et al.*, 2008).

Comparative analyses were subsequently performed for MEF*Hdh*. Analogous to the situation in ST*Hdh*, MEF*Hdh*^{Q111} exhibited an overall activation of the calpain system featuring elevated levels of autoprocessed calpain-1, full-length calpain-2 and the calpain-dependent α-spectrin breakdown product. However, the observed effects did not reach statistical significance. This might be explained by the origin of embryonic fibroblasts, which usually represent a non-neuronal and heterogeneous population of mesenchymal cells (Singhal *et al.*, 2016). Nevertheless, further affirmative investigations on this fibroblast cell lines regarding calpain activation should be undertaken, in particular, as MEFs are commonly used as a reliable primary cell model in HD research.

In addition, both ST*Hdh* cells and MEF*Hdh* were immunocytochemically stained for calpain-1. Qualitative microscopy analysis confirmed the stronger expression of calpain-1 in ST*Hdh*^{Q111} cells as observed before by western blotting. Interestingly, calpain-1 signals showed a distinct subcellular distribution. Double labelling together with mitochondrial

translocase of outer membrane 20 (TOM20) revealed an entire colocalisation of calpain-1 with mitochondrial structures, which complies with previous findings on a mitochondrial targeting signal at the enzyme's N-terminus (Badugu *et al.*, 2008).

Finally, calpain activation was explored in an immortalised human fibroblast (iHF) cell line of SCA3. These fibroblasts are derived from skin biopsies of an SCA3 patient and a healthy control, which were transduced using the *Simian virus* 40 (SV40) (Pipas, 2009). The calpain system of iHFs was investigated in relationship with calpain-mediated cleavage of ataxin-3. Although the administration of the calpain-specific inhibitor III reduced overall calpain activation and ataxin-3 cleavage, there was no difference between SCA3 patient and control cell lines in baseline calpain-1 autoprocessing, CAST levels or α-spectrin cleavage. In contrast to this observation, rat cerebellar granule neurons overexpressing polyQ-expanded ataxin-3 were reported to exhibit a slightly increased calpain-mediated α-spectrin cleavage compared to cells expressing the wild type protein (Simões *et al.*, 2014). The lack of calpain overactivation in iHFs may be attributed to the strong molecular perturbations caused by their neoplastic character (Geraghty *et al.*, 2014). Therefore, further specific and conclusive research on calpain activation, especially in SCA3 patient-derived cell lines, is necessary, as current studies on calpain-dependent ataxin-3 cleavage in fibroblasts or iPSCs have omitted this pathomolecular aspect (Koch *et al.*, 2011; Hansen *et al.*, 2016).

The expression of mutant huntingtin in two investigated cell lines apparently caused elevated calpain activation, emphasizing the disease-related perturbation of this proteolytic system. Similar corroborative observations have been already described by other researchers, who analysed *in vitro* models of HD based on Neuro2a and PC6.3 cell lines, ST*Hdh* cells or cultured MSNs. On the other hand, no alterations in calpain activity were observed in immortalised SCA3 fibroblasts. Nevertheless, additional investigations on further SCA3 cell lines are demanded. The correct assessment of calpains in cell models of polyQ diseases can be conducive to reproduce and investigate the molecular aspects of these disorders. Furthermore, only selection of appropriate cell lines provides the basis for successfully testing calpain-targeting strategies as a therapeutic approach *in vitro*.

Calpain activation in animal models of HD

(Covered in Unpublished project manuscript B; Clemens *et al.*, 2015; Weber *et al.*, 2016)

In vivo models of human diseases do not only help to recapitulate pathological conditions for analysing their aetiology, they also serve as a means for screening and testing therapeutically promising interventions, which - not only from an ethical aspect - cannot be primarily tested in humans. Several, mainly rodent models have been developed and characterized for HD and SCA3, which, with certain limitations and variations, reproduce the known behavioural and molecular aspects of both diseases (Matos *et al.*, 2011; Pouladi *et al.*, 2013). To determine the role of calpain activation in disease-relevant tissues, three animal models of HD were analysed in this study: HDKI mice, YAC128 mice and BACHD rats (Wheeler *et al.*, 1999; Slow *et al.*, 2003; Yu-Taeger *et al.*, 2012).

HDKI mice represent a knock-in model carrying a chimeric murine huntingtin gene (*Hdh*), whose first exon was replaced by the human *HTT* exon 1 with 109 CAGs. The physiological expression of mutant huntingtin on an endogenous level resembles more the genetic condition in HD patients, and leads to a slow progressive phenotype with late gait abnormalities and mainly striatal nuclear huntingtin aggregation, which starts between 4 and 6 months of age (Wheeler *et al.*, 1999; Menalled, 2005). Therefore, the investigations on the calpain system were performed in striatal and cortical tissues of mice at 6 months of age using western blotting. Examination of calpain-1 autoprocessing and α-spectrin cleavage revealed an overactivation of the calpain system, which was interestingly restricted to HDKI striatum. By contrast, calpain activity and α-spectrin cleavage in cortex showed a trend towards reduction. It cannot be ruled out that with disease progression and spreading damage of adjacent neuronal tissues, increased calpain activation might be detected also in additional brain regions. However, respective analyses in HDKI mice at later time points are pending. Corresponding to this work, a previous study on HDKI mice featuring 150 CAGs and an aggravated phenotype showed an elevated, mutant huntingtin dose-dependent calpain activation, which was not only present in striatum but also cortex (Gafni *et al.*, 2004).

A second analysis was pursued in YAC128 mice, a yeast artificial chromosome (YAC)-based transgenic mouse model which carries the entire human *HTT* gene with 128 CAGs. This animal model features a motor phenotype beginning at 6 months, striatal neuronal loss by 9 months and nuclear aggregation detectable by 12 months (Slow *et al.*, 2003; Pouladi *et al.*, 2012). Investigations were performed on striatal and cortical lysates at presymptomatic stages (6 weeks) and on lysates and histological sections at symptomatic stages with 12 months of age. Despite covering two brain areas, two distinct time points and a palette of

different calpains and calpain substrates, YAC128 mice did not show any strong alterations of the calpain system as detected by western blotting. A clear calpain overactivation was neither present at 6 weeks of age nor at 12 months, which was demonstrated by unchanged levels of calpain-1, -2, -5, and -10. At 6 weeks of age, CAST levels, calpain-dependent cleavage of α-spectrin and p35-to-p25 conversion were comparable between wild type and transgenic animals. However, at 12 months of age, expression of CAST was significantly increased in YAC128 striatum. This was accompanied by a trend towards reduced calpain levels and substrate cleavage, pointing to a general attenuation of the calpain system. Qualitative immunofluorescence microscopy of brain sections at 12 months confirmed findings obtained by western blotting. These observations stand in contrast with previous reports on YAC128 animals, which demonstrated an increased calpain activation by elevated cleavage of α-spectrin, NMDA receptors or striatal-enriched protein tyrosine phosphatase 61 in presymptomatic 1- to 2-month-old transgenic mice (Cowan *et al.*, 2008; Gladding *et al.*, 2012, 2014). An age-dependent attenuation of calpain activation has been reported for YAC128 mice at 4 and 12 months of age, which does not explain the herein described findings in 6-week-old animals (Dau *et al.*, 2014; Gladding *et al.*, 2014).

Lastly, the in-house BACHD rat model was included in the analyses of the calpain system. This rodent model features a bacterial artificial chromosome (BAC)-based transgene, which encompasses the entire human *HTT* gene with 97 CAG/CAA repeats, but with shorter adjoining up- and downstream sequences than the YAC-based *HTT* construct. BACHD rats show a motor phenotype after 1 month, reduced brain volume by 12 month, and neuropil aggregates with a mainly cortical localisation by 3 months (Yu-Taeger *et al.*, 2012). The calpain system of BACHD rats was investigated by western blotting of cortical and striatal lysates obtained at 13 months of age. In opposition to observations in HDKI mice, striatum of BACHD rats did not feature any elevation in calpain activation compared to wild type animals. However, a clear overactivation of calpains was present in BACHD cortex, as detected by increased autoprocessing of calpain-1, decreased CAST levels and raised α-spectrin cleavage. It is noteworthy that the examination of heavy membrane fractions, isolated from cerebral hemispheres and enriched for mitochondrial and ER proteins, revealed the occurrence of calpain-1, CAST and α-spectrin, but without presenting differences in calpain activation. This finding suggests that the manifestation of calpain activation is rather limited to the cytosol or nucleus, excluding mitochondria and the ER. The specificity of calpain activation in cortex but not striatum correlates with the rather cortical accumulation of huntingtin aggregates despite equal expression of the mutant protein in both tissues (Yu-Taeger *et al.*, 2012). This might represent a characteristic of the BACHD rat model. In this

context, further analyses at earlier and later time points might help to identify time-dependent differences in the tissue specificity of calpain activation. In addition, a comparative exploration of the calpain system in the BACHD mouse model of HD, which is grounded on the identical transgene construct as the BACHD rat, can be useful to evaluate the transgene- and animal model-dependent variations in calpain overactivation (Gray *et al.*, 2008).

In total, two of three analysed HD animal models were showing a clear calpain overactivation in disease-affected brain tissues. HDKI mice exhibited a rather striatal and BACHD rats a cortical activation of calpains. However, further analysis of additional tissues at further time points might contribute to the discrimination of the overall activation pattern in these animal models. The general overactivation of the calpain system is in line with previous studies in knock-in and YAC128 mice (Gafni *et al.*, 2004; Cowan *et al.*, 2008; Dau *et al.*, 2014). The reinvestigation of YAC128 in this study did, surprisingly, not recapitulate the previous reports. This might be attributed to different factors such as artefacts of strain backgrounds and inbreeding, which are known to modulate the manifestation of disease phenotypes, and demands further investigations (Lloret *et al.*, 2006; Yoshiki and Moriwaki, 2006; Ehrnhoefer *et al.*, 2009). The principally well-documented participation of calpains in the molecular pathogenesis of HD points to a putatively altered activation of these proteases in the context of SCA3. However, the precise assessment of calpain activation is outstanding except for reports on decreased CAST levels in SCA3 mice and post-mortem patient tissue (Simões *et al.*, 2012). Future work on SCA3 models based on the methodology applied in HD research will complete our understanding of calpain activation and therapeutic targetability in polyQ diseases.

Amplifying calpain activity by genetically depleting calpastatin

(Covered in Unpublished project manuscript C; Hübener *et al.*, 2013)

Several studies including the current work demonstrated an involvement of calpains in the molecular pathogenesis of HD and SCA3. Calpains were shown to proteolytically cleave the disease proteins huntingtin and ataxin-3 and to be upregulated in the disease context (Gafni and Ellerby, 2002; Gafni *et al.*, 2004; Haacke *et al.*, 2007; Cowan *et al.*, 2008; Koch *et al.*, 2011; Simões *et al.*, 2012). A sophisticated way to further dissect the underlying pathway and to evaluate the contribution of these enzymes to the respective aetiology is the manipulation of the calpain system by molecular biological strategies. A commonly used target in this connection is CAST, the only known endogenous inhibitor of calpains. Modulation of CAST expression can alter calpain activity and thereby its impact on the molecular pathogenesis. Several studies have shown that overexpression of CAST leads to a reduction of disease protein fragmentation, aggregation and toxicity in cell and animal models of HD and SCA3 (Haacke *et al.*, 2007; Reijonen *et al.*, 2010; Simões *et al.*, 2012; Menzies *et al.*, 2014). To investigate the impact of CAST ablation and the herewith provoked amplification of calpain activity on polyQ diseases, two animal models were generated which, besides expression of the mutant polyQ protein, feature a genetic knockout of CAST.

For modelling this genetic situation in HD, HDKI animals were crossbred with a *Cast*$^{-/-}$ knockout mouse model (Takano *et al.*, 2005). To assess firstly the molecular outcome of the knockout, wild type and *Cast*$^{-/-}$ mice were sacrificed at 10 months of age and whole brain lysates were investigated regarding the activation of the calpain system by western blotting. As expected, *Cast*$^{-/-}$ showed generally elevated calpain system activation, which was represented by an increase of autoprocessed calpain-1 and an elevated cleavage of α-spectrin and p35. To evaluate the consequences of amplified calpain activation on mutant huntingtin, double mutant animals and their respective controls were sacrificed at 13 months of age. Whole brain lysates and homogenates were subjected to biochemical analysis for detection of calpain activation, huntingtin fragmentation and the aggregate load. Consistent with findings in mice at 10 months, 13-month-old *Cast*$^{-/-}$ and HDKI/*Cast*$^{-/-}$ mice exhibited an increased calpain activation when compared to wild type or HDKI controls. This overactivation led to a stronger fragmentation of wild type and polyQ-expanded huntingtin and to a higher amount of huntingtin aggregates. As fragments of huntingtin were shown to be more aggregation-prone, these findings are self-consistent (Hackam *et al.*, 1998; Martindale *et al.*, 1998; Gafni *et al.*, 2004). However, calpains are known to negatively regulate autophagy, and the enhanced calpain activation might lead to reduced autophagic

flux and impaired aggregate removal (Yousefi *et al.*, 2006; Williams *et al.*, 2008; Russo *et al.*, 2011). This could increase the occurrence of huntingtin deposits in a fragmentation-independent manner. In this context, an opposite effect of increased autophagy by CAST overexpression was described in a fragment model of HD, which resulted in reduced aggregation and polyQ toxicity (Menzies *et al.*, 2014). To assess the impact of the genetic CAST depletion on autophagy, levels of the marker proteins LC3-II and p62 were detected. Interestingly, levels of LC3-II showed rather an increase and levels of p62 a decrease in *Cast*$^{-/-}$ and HDKI/*Cast*$^{-/-}$ mice, which actually point to an increased autophagic flux or at least hint at perturbations of autophagy in these animals (Mizushima and Yoshimori, 2007). To analyse effects on the dysfunction of dopaminergic neurons in HDKI/*Cast*$^{-/-}$ mice, expression of dopamine- and cAMP-regulated neuronal phosphoprotein-32 (DARPP-32), a marker for dopaminergic neurons such as the HD-affected MSNs, was investigated by western blotting. Full-length levels of DARPP-32 dropped not only as expected in HDKI but also in *Cast*$^{-/-}$ mice. However, this effect was not further enhanced in HDKI/*Cast*$^{-/-}$ animals. Although the loss of DARPP-32 can be indicative of a demise of respective neurons, calpains were shown to cleave this protein and hereby additionally contribute to reduced DARPP-32 full-length levels (van Dellen *et al.*, 2000; Jiang *et al.*, 2012; Cho *et al.*, 2015).

For SCA3, *Cast*$^{-/-}$ animals were crossbred with mice overexpressing the cDNA of ataxin-3 isoform 2 (UniProt identifier: P54252-2) with 148 CAGs under the murine prion protein promoter. The SCA3 mouse model is characterised by early neurological symptoms starting at 2 months, a decreased life span and widespread intranuclear inclusions in all brain regions (Bichelmeier *et al.*, 2007). In contrast to analyses pursued in HDKI/*Cast*$^{-/-}$ animals, investigations on SCA3/*Cast*$^{-/-}$ mice mainly focused on the behavioural and neuropathological phenotype, two aspects which are still pending for modelling CAST depletion in the HD background. SCA3/*Cast*$^{-/-}$ animals showed an exacerbated phenotype regarding their motor performance as assessed by rotarod test and a trend towards decreased life span when compared to SCA3 mice. Furthermore, neuropathological analysis using toluidine blue staining of cerebellar sections revealed an increased number of atrophic and degenerated neurons in SCA3/*Cast*$^{-/-}$ mice. *Cast*$^{-/-}$ and wild type mice, on the other hand, did not show any neuronal degeneration. Also, the aggregate load was strongly enhanced in double mutant animals, correspondent with findings in HDKI/*Cast*$^{-/-}$ mice. Interestingly, *ex vivo* calpain activation assays demonstrated that the lack of CAST in lysates of SCA3/*Cast*$^{-/-}$ led to an intensified cleavage of ataxin-3, which might be considered as an indicator of the ongoing physiological processes *in vivo*.

The comparable observation of aggravated molecular, histological or behavioural phenotypes in HD and SCA3 caused by the genetic depletion of CAST is an important evidence for calpains as mediators of polyQ-dependent toxicity and neurodegeneration. It should be kept in mind that the knockout of CAST itself might cause a detrimental phenotype aside from the polyQ disease context. However, except for a decreased locomotor activity in stressful environments and impaired auditory startle response, *Cast*$^{-/-}$ mice did not exhibit negative effects regarding development, fertility or life span when compared to wild type animals. Interestingly, *Cast*$^{-/-}$ mice were shown to be more susceptible to kainate-induced excitotoxicity and thus suggesting CAST as a negative regulator of calpains under pathological conditions (Takano *et al.*, 2005; Nakajima *et al.*, 2008). Further behavioural analyses in HDKI/*Cast*$^{-/-}$ animals and molecular analyses in their SCA3 counterpart can help to complete the picture of the calpain-mediated pathogenesis and to draw conclusions about the molecular situation in other polyQ diseases.

Summary and outlook

The activation of the calpain system has been investigated thoroughly in cell and rodent models of HD and SCA3 (TABLE 1). In addition to baseline measurements, further *in vivo* analyses were performed in disease models which exhibited a genetic knockout of the endogenous calpain inhibitor CAST. Despite inconclusive results in YAC128 mice and SCA3 iHF cell lines, the general outcome of these investigations emphasises the important contribution of calpains to the molecular pathogenesis of both polyQ disorders and is consistent with previous findings. The herein undertaken research was, however, not exhaustive and is leaving further aspects unanswered, which can be employed as starting points for subsequent studies. The most interesting and important remaining questions are first, the further elucidation of a baseline calpain overactivation in cell and animal models of SCA3, and second, a more precise dissection of calpains' general role in autophagy regulation. Especially the latter subject can be useful for understanding the autophagy dysregulation in neurodegenerative disorders and thereby for developing additional treatment strategies.

Table 1. The calpain system in cell and rodent models of HD and SCA3. Summary of findings on the calpain system in polyQ disease models obtained in this study. ms = mouse; rt = rat; huc = human cell line; msc = mouse cell line, light blue = HD; dark blue = SCA3; ↑ = upregulation; ↓ = downregulation; ↕ = unchanged; () = tendency; ^{ctx} = only in cortex; ^{str} = only in striatum; * = global; $^{\#}$ = knockout effects relative to baseline; n/a = not available.

Disease model	*Calpain activation*	*CAST levels*	*Substrate cleavage*	*Disease protein cleavage*	*Remarks and conclusion*	*References*
ST*Hdh* msc	CAPN1 ↑ CAPN2 ↓ CAPN10 ↓	CAST ↕ (cleavage ↑)	Spectrin ↑	n/a	Increased overall calpain activation	Unpublished manuscript A
MEF*Hdh* msc	CAPN1 (↑) CAPN2 (↑)	n/a	Spectrin (↑)	n/a	Trend towards increased calpain system activation	Unpublished manuscript A
HDKI ms 6 months	CAPN1 ↑^{str}	n/a	Spectrin ↑^{str}	n/a	Elevated calpain activation in striatum but not cortex	Weber *et al.*, 2016
YAC128 ms 12 months	CAPN1 (↓) CAPN2 (↓) CAPN10 (↓)	CAST ↑	Spectrin (↓) NR2B (↓)	Huntingtin ↕ (at 6 weeks)	Attenuation of calpain activity especially in striatum	Unpublished manuscript B
BACHD rt 13 months	CAPN1 ↑^{ctx}	CAST (↓)^{ctx}	Spectrin ↑^{ctx}	Huntingtin ↑^{ctx}	Elevated calpain activation in cortex but not striatum	Clemens *et al.*, 2015
HDKI/*Cast*$^{-/-}$ ms,$^{\#}$ 13 months	CAPN1 ↑*	knockout	Spectrin ↑* p35 ↑*	Huntingtin ↑*	Increased huntingtin fragmentation and aggregation by CAST depletion	Unpublished manuscript C
iHFs huc	CAPN1 ↕	CAST ↕	Spectrin ↕	Ataxin-3 ↕	No differences in calpain activation in immortalised fibroblasts	Weber *et al.*, 2017
SCA3/*Cast*$^{-/-}$ ms,$^{\#}$ 12 months	n/a	knockout	n/a	Ataxin-3 ↑ (*ex vivo*)	Increased ataxin-3 aggregation and neurodegeneration by CAST depletion	Hübener *et al.*, 2013

Modulation of calpain activity as a therapeutic approach

Preliminary considerations

Since overactivation of calpains as well as calpain-mediated fragmentation of disease proteins evidentially contribute to the molecular pathogenesis of neurodegenerative disorders, specific inhibition of these enzymes might represent a promising therapeutic target. As discussed earlier, several approaches are conceivable to reduce calpain activity, which include the application of specific inhibitors, the administration of compounds which influence activating pathways, and genetic approaches which eliminate calpain isoforms or overexpress calpain inhibitor CAST (Ono *et al.*, 2016).

Although these options can be easily tested in the field of biomolecular research, translation into clinics is strongly limited to factors such as safety, efficacy and costs. In particular, highly promising gene therapies for neurodegenerative disorders of the CNS are still in early stages of development, despite a great technological progress and successful proofs of concept in the last twenty years (Simonato *et al.*, 2013; O'Connor and Boulis, 2015). For this reason, efforts must be intensified to allow this therapeutic strategy to be applied in the next decades. To bridge the gap between the current state of research and the future, it is important to make use of available pharmacological possibilities for treating neurodegenerative diseases. Although many calpain-targeting drugs are under preclinical or early clinical research, none of those has yet reached clinical applicability which might be also due to general limitations in translational research or obstacles in drug delivery (Jucker, 2010; Lang, 2010; Upadhyay, 2014; Ono *et al.*, 2016).

To evaluate calpain inhibition as a treatment strategy in this study, conventional inhibitors and olesoxime, a potential mitochondria-specific modulator of calpain-activating pathways, were tested in cell and animal models of HD and SCA3. Molecular effects of these compounds were monitored by measuring calpain activation as well as disease protein cleavage and aggregation. *In vivo* trials additionally comprised an assessment of the pharmacological impact on the behavioural phenotype. Aside from drug-based studies, a genetical approach targeting calpain-1 was investigated in an SCA3 mouse model.

Inhibition of calpains in cell models of HD and SCA3

(Covered in Unpublished project manuscript A and E; Weber *et al.* 2017)

The most direct way to reduce calpain activation is the treatment with specific inhibitors. In the current work, three inhibitors were tested in cell-free and cell-based models of HD and SCA3, namely ALLN (N-acetyl-L-leucyl-L-leucyl-L-norleucinal), calpain inhibitor III (CI III) and PD150606. ALLN, also known as calpain inhibitor I, is a cell-permeable peptide aldehyde inhibitor of calpains with a certain affinity to cathepsins (Saito *et al.*, 1987; Hiwasa *et al.*, 1990). CI III, also known as MBL-28170, is a synthetic, cell-penetrating inhibitor of calpains, but like ALLN also of cathepsins (Mehdi *et al.*, 1988; Mehdi, 1991). On the contrary, the alpha-mercaptoacrylic acid derivative PD150606 constitutes an non-active site-binding allosteric calpain inhibitor (Wang *et al.*, 1996).

In the HD context, calpain inhibitors ALLN and CI III were shown to reduce calpain-mediated cleavage of wild type and mutant huntingtin. The parallel incubation with these inhibitors abolished the formation of huntingtin fragments upon administration of exogenous calpains or when activating endogenous calpains by $CaCl_2$ addition to lysates. In cell-based experiments, preincubation of HEK 293T cells with CI III counteracted the Ca^{2+}-ionophore ionomycin-facilitated calpain activation and fragmentation of substrates α-spectrin and huntingtin. To investigate the protective effects of calpain inhibition in HD cell lines, viability of ST*Hdh*^{Q111} cells treated with ALLN or PD150606 was measured using a resazurin-based approach. Both inhibitors significantly improved cell viability of the mutant cell line, which was previously found to exhibit a calpain overactivation when compared to wild type ST*Hdh*^{Q7} cells. On the other hand, treating the ST*Hdh*^{Q7} line with the same inhibitors led to a reduction of their vitality, pointing to detrimental effects of reducing a non-pathological calpain activity. These observations regarding beneficial effects of calpain inhibition by ALLN accord to previous findings in other HD studies, which employed PC6.3 cells or cultured MSNs (Cowan *et al.*, 2008; Reijonen *et al.*, 2010). However, calpain inhibition in a PC12 cell line of HD was also shown to provoke negative effects as this might compromise a calpain-mediated clearance of mutant huntingtin (Ratovitski *et al.*, 2007).

Comparable to the afore-described effects of calpain inhibition in HD cell lines, administration of ALLN or CI III exerted beneficial effects on calpain-mediated ataxin-3 cleavage in SCA3 cell lysates. Likewise, CI III blocked wild type and polyQ-expanded ataxin-3 fragmentation in HEK 293T and iHF cell lines treated with ionomycin and showed that the detected predominant ataxin-3 fragments are all calpain cleavage-derived. Despite lacking a baseline overactivation between patient- and healthy control-derived cell lines, CI III-treated iHF cells

showed in addition to reduced ataxin-3 cleavage an attenuated fragmentation of α-spectrin and elevated levels of CAST. Especially the latter marker is reportedly reduced in SCA3 mouse brains and post-mortem patient brain tissue, suggestive of a calpain overactivation-dependent depletion of CAST in SCA3 pathogenesis (Simões *et al.*, 2012). Consistent with the results covered above, ALLN has been previously shown to prevent calpain-dependent cleavage of ataxin-3 in cell-free assays. Inhibitors like calpeptin and BDA-410 reduced calpain activation as well as mutant ataxin-3 fragmentation and aggregation in N2a cell lines or cultured rat cerebellar granule cells (Haacke *et al.*, 2007; Simões *et al.*, 2014).

Considering that analysis on further disease hallmarks like polyQ protein aggregation are still due, targeting calpains with inhibitors resulted in promising effects, i.e. lower calpain activation, disease protein cleavage and viability in cell models of two polyQ diseases. These observations accord with findings from studies utilising cell culture or *ex vivo* models not only of HD and SCA3 but also of other neurodegenerative disorders such as AD, ALS or PD (Samantaray *et al.*, 2006; Haacke *et al.*, 2007; Cowan *et al.*, 2008; Nimmrich *et al.*, 2010; Gladding *et al.*, 2012; Yamashita *et al.*, 2012; Gold *et al.*, 2015). Most importantly, further investigations have already applied specific calpain inhibitors *in vivo* with a largely positive outcome for prevention of neurodegeneration in multiple animal models (Trinchese *et al.*, 2008; Saatman *et al.*, 2010; Simões *et al.*, 2014; Samantaray *et al.*, 2015). However, chronic calpain inhibition has been also associated with diverse detrimental repercussions which might be due to impairments of the healthy physiological function or to side-effects, attributed to the lack of a specificity (Ono *et al.*, 2016). Therefore, continuing research on calpains and respective drug development is necessary. Novel molecules, like the α-ketoamide-based inhibitor A-705253 or its derivative ABT-957 as well as epoxide-based inhibitors such as NYC438 or NYC488, which have been already tested in AD research, might represent a subsequent step in the clinical applicability of pharmacological calpain inhibition (Lubisch *et al.*, 2003; Trumbeckaite *et al.*, 2003; Nikkel *et al.*, 2012; Fà *et al.*, 2015). On the other hand, focusing on calpain activating pathways might constitute an alternative approach, which circumvents the pitfalls of directly acting on calpains.

Calpain suppression by the VDAC1-targeting compound olesoxime in vivo

(Covered in Clemens *et al.* 2015; Weber *et al.* 2016)

Calpain overactivation in neurodegeneration might be a consequence of a pathological Ca^{2+} dyshomeostasis. In HD and SCA3, this cellular condition has been attributed to three different derangements: 1. PolyQ-expanded huntingtin or ataxin-3 have been shown to directly bind to the ER-located Ca^{2+} channel IP_3R1, which causes its sensitization to activation by IP_3 and the release of Ca^{2+} to the cytosol (Tang *et al.*, 2003; Chen *et al.*, 2008; Bezprozvanny, 2011). 2. Mutant huntingtin has been also reported to facilitate Ca^{2+} influx by enhancing NMDA receptor activity and thereby sensitise neurons to NMDA receptor-mediated excitotoxicity (Zeron *et al.*, 2002; Tang *et al.*, 2005; Shehadeh *et al.*, 2006). 3. Finally, mitochondria, which represent an important Ca^{2+} buffering compartment, are impaired in HD and SCA3 and their dysfunction may contribute to pathologically elevated cytosolic Ca^{2+} levels (Milakovic *et al.*, 2006; Oliveira *et al.*, 2006; Yu *et al.*, 2009; Laço *et al.*, 2012). Therefore, targeting one of these dysfunctional elements might consequently attenuate the excessive activation of calpains.

The HD-related mitochondrial impairment, its repercussion on the neuronal health and consequences on the behavioural phenotype were in the focus of a longitudinal therapeutic study, which applied the experimental, neuroprotective drug olesoxime. This cholesterol-derivative, also known as TRO19622, has been identified in a cell-based drug screen for compounds counteracting ALS-associated motor neuron death. Olesoxime localises at the outer mitochondrial membrane, where it binds two components of the mitochondrial permeability transition (mPT) pore, the voltage-dependent anion channel (VDAC) and the translocator protein (TSPO) (Bordet *et al.*, 2007). The compound has demonstrated therapeutic efficacy in cell and animal models of ALS, peripheral neuropathy, spinal muscular atrophy (SMA), and α-synucleinopathies (Bordet *et al.*, 2007, 2008, 2010, Xiao *et al.*, 2009, 2012; Sunyach *et al.*, 2012; Richter *et al.*, 2014; Gouarné *et al.*, 2015). Olesoxime's neuroprotective function has been shown to be exerted via inhibition of mPT-mediated apoptosis and by promoting remyelination of neurons (Martin *et al.*, 2011; Magalon *et al.*, 2012). Furthermore, in ST*Hdh*^{Q111} cells, isolated mitochondrial membranes of HDKI mice, and BACHD rats, olesoxime was shown to restore the pathologically increased mitochondrial membrane fluidity (Eckmann *et al.*, 2014).

To further assess olesoxime's therapeutic value in an HD animal model, the drug was administered to BACHD rats via the food from 5 weeks to 13 months of age. Subsequent analyses comprised behavioural tests as well as metabolic and neuropathological

measurements. Moreover, primary molecular investigations included expression profiling of mitochondrial proteins and the assessment of huntingtin protein and aggregation levels. Analysis of the BACHD rat motor phenotype confirmed previously reported impairments as shown by hind limb clasping and rotarod performance, but without detecting any improvements upon olesoxime administration (Yu-Taeger *et al.*, 2012). On the other hand, simple swim test and elevated plus maze demonstrated an amelioration of HD-reminiscent cognitive and psychiatric abnormalities by the treatment. Moreover, MRI scans of olesoxime-treated rats detected reduced cortical thinning but without reducing overall cerebral or striatal atrophy when compared to the placebo group.

Immunohistochemical analysis showed reduced amounts of mutant huntingtin aggregation and nuclear accumulation in cortex, hypothalamus, thalamus and amygdala of olesoxime-treated rats. Detergent-insoluble species of the disease protein were reduced in both cortex and striatum as shown by filter retardation assays. Interestingly, protein quantification via time-resolved Förster resonance energy transfer (TR-FRET), a method based on the energy transfer between fluorophores coupled to two target-specific antibodies, found that soluble levels of mutant huntingtin appeared to be elevated upon treatment. This was also confirmed by increased levels of full-length huntingtin via western blotting. Remarkably, this effect was accompanied by a strongly reduced mutant huntingtin fragmentation in cortex and striatum of treated BACHD rats. As caspases and calpains are known to cleave mutant huntingtin, both proteolytic systems were examined for their activation. Although caspases 3 and 6 showed no changes in expression or activity, the calpain system activation was significantly elevated in cortex of BACHD rats compared to wild type animals. This overactivation was significantly alleviated upon administration of olesoxime as detected by reduced calpain-1 autoprocessing, lower α-spectrin cleavage and increased levels of CAST.

Interestingly, olesoxime also reduced the activity of calpains in cerebral heavy membrane fractions enriched for mitochondrial and ER proteins, despite lacking a genotype-specific difference at baseline. Further investigations on mitochondria of olesoxime-treated rats, showed a reduced HD-related mitochondrial respiration deficit, increased levels of mitochondrial fusion proteins such as mitofusin-1 and -2 and elevated levels of TOM20. As olesoxime is known to bind VDAC and this protein is involved in ER-mitochondrial Ca^{2+} shuttling via an mortalin/grp75-bridged interaction with IP_3R, respective protein levels of both Ca^{2+} channels were investigated (Szabadkai *et al.*, 2006). The expression of VDAC1 and VDAC2 was markedly increased in olesoxime-treated wild type and BACHD cortex and in BACHD striatum. Baseline levels of IP_3R1 were elevated in cortex of BACHD rats, and reduced to wild type levels upon treatment. Overall, these findings suggest an olesoxime-

mediated improvement of mitochondrial function and neuronal Ca^{2+} handling, which attenuates the Ca^{2+}-dependent calpain overactivation. The lower activity of calpains resulted in a mitigated formation of toxic and aggregation-prone huntingtin fragments and thereby in reduced huntingtin aggregation. The rather cortex-restricted beneficial impact of olesoxime, which did not only occur on molecular but also behavioural level, might be explained by the compound enrichment in the prefrontal and frontal cortex as detected by high-performance liquid chromatography.

To verify the observed effects of olesoxime in a further animal model, the trials were repeated in HDKI mice. To achieve the earliest possible start of the treatment, olesoxime was already administered to parental animals during breeding. The offspring was further treated until 3 months of age. Subsequent analysis focused solely on the reinvestigation of molecular markers, which were found to be altered in treated BACHD rats. Western blot analysis of half brain lysates of untreated HDKI mice showed reduced levels of mutant huntingtin, accompanied by elevated huntingtin fragmentation. Similar to findings in BACHD rats at baseline, the activation of the calpain system was increased, which was substantiated by elevated α-spectrin cleavage and reduced CAST levels. Administration of olesoxime resulted in an attenuation of calpain overactivation and thus mutant huntingtin cleavage. Comparable, although not significant effects of the treatment were observed for IP_3R1 and VDAC1 levels. Surprisingly, detergent-insoluble huntingtin species were already detectable in half brain homogenates of HDKI mice at 3 months of age. However, olesoxime did only by tendency reduce their amount. Following these observations, olesoxime exerted similar beneficial effects in HDKI mice and BACHD rats on the molecular level. Nevertheless, molecular but also behavioural investigations at later time points with a clear manifestation of HD phenotype are necessary to fully evaluate the therapeutic efficacy of olesoxime in the HDKI mouse model.

The amelioration of the molecular and behavioural phenotype in two HD animal models by olesoxime revealed its potential as a therapeutic compound in the treatment of HD. This is encouraged by findings in phase I clinical studies, which showed that this experimental drug is well tolerated by human subjects (Martin, 2010). Furthermore, olesoxime is orally active and sufficiently crosses the blood brain barrier (Bordet *et al.*, 2010). In end stage ALS patients, a combinatorial treatment of olesoxime with riluzole in a phase II-III clinical trial did not show a significant beneficial effect, despite being well tolerated (Lenglet *et al.*, 2014). On the other hand, treatment of SMA patients at an early stage strikingly prevented loss of motor function for 2 years in a phase II clinical study (Dessaud *et al.*, 2014; Bertini *et al.*, 2017). Therefore, olesoxime might only reach efficacy at early disease stages, emphasising its

function as a disease-modifying compound. This idea is further supported by the herein described findings in BACHD rats whose treatment commenced at 5 weeks of age and thus after onset of the earliest symptoms.

Aside from the apparent effects on mitochondrial function, levels of VDACs and IP_3R1, and their consequences for the HD phenotype, olesoxime's precise molecular mode of action remains elusive. Nevertheless, the direct modulation of VDAC activity and mitochondrial Ca^{2+} is highly conceivable. First investigations on the Ca^{2+} retention capacity of isolated mitochondria found no alterations by olesoxime administration (Bordet *et al.*, 2010). However, this observation might be due to the experimental setup lacking the cellular and inter-organelle context of mitochondrial function. A neurodegenerative disease-modulating potential of VDAC has been shown earlier in an AD mouse model, where the heterozygous knockout of VDAC1 rescued mitochondrial function and synaptic deficiencies (Manczak *et al.*, 2013). Generally, the VDAC1-mortalin/grp75-IP_3R Ca^{2+} bridges between mitochondria and the ER are suggested to play a crucial role in neurodegeneration and represent a potential therapeutic target (Calì *et al.*, 2012; Krols *et al.*, 2016; Paillusson *et al.*, 2016). Correspondingly, modulation of proteins like sigma-1 receptor or RyR which both additionally mediate the ER-mitochondrial Ca^{2+} flux were shown to ameliorate disease-linked perturbations in cell or animal models of HD and SCA3. (Hayashi and Su, 2007; Chen *et al.*, 2008, 2011; Hyrskyluoto *et al.*, 2013; Del Prete *et al.*, 2014). An additional, herein not further investigated contribution of the second identified target of olesoxime TSPO is also very likely, as it bears a VDAC activating function (Veenman *et al.*, 2008; Gatliff and Campanella, 2012). Future research should therefore utilise pharmacological and genetical strategies to modulate both VDAC1 and TSPO. Comparison with olesoxime's effects and the assessment of the Ca^{2+} buffering capacities of treated cells might give a deeper insight in the underlying molecular pathways. Finally and most importantly, due to its highly probable impact on Ca^{2+} homeostasis, olesoxime should be tested in cell and animal models of further neurodegenerative disorders, as it might represent a widely useful candidate for therapeutic interventions.

Reduction of ataxin-3 fragmentation by genetic ablation of calpain-1 in vivo

(Covered in Unpublished project manuscript D)

Aside from pharmacological interventions, genetic approaches can be applied for modulating calpain activity. Corresponding to the administration of compounds, which inhibit calpains, the overexpression of the endogenous inhibitor CAST was shown to reduce calpain overactivation and linked detrimental effects in cell and animal models of neurodegenerative disorders including ALS, HD, PD, SCA3, and tauopathies (Rao *et al.*, 2008, 2014, 2016; Tradewell and Durham, 2010; Simões *et al.*, 2012; Diepenbroek *et al.*, 2014; Menzies *et al.*, 2014). Concurrently, this work showed that knockout of CAST exacerbates the molecular and behavioural phenotype in HD and SCA3 mice (Unpublished project manuscript C; Hübener *et al.*, 2013). Based on the findings from the CAST knockout study in a SCA3 mouse model, which additionally showed that calpain-1 is efficiently cleaving mutant ataxin-3 and might thereby contribute to the formation of toxic and aggregation-prone fragments, the genetic ablation of calpain-1 emerged as a promising target for ameliorating the disease phenotype.

To test this hypothesis, a transgenic SCA3 mouse model was crossbred with homozygous calpain-1 knockout mice. The employed SCA3 mice hemizygously carry a YAC-based construct encompassing the *MJD1* locus with 84 CAGs. This model features gait disturbances by 4 weeks, distinct neuronal loss by 12 months and nuclear ataxin-3 accumulation detectable by 8 weeks (Cemal *et al.*, 2002; do Carmo Costa *et al.*, 2013). Previous characterizations of calpain-1 knockout mice have shown an unaffected viability and fertility, except for certain disturbances in platelet function (Azam *et al.*, 2001). For confirmation of the knockout and its consequences on the calpain system, brain and skeletal muscle lysates of 3-month-old wild type, calpain-1 knockout, SCA3 and double mutant animals were investigated using western blotting. The analysis showed a successful depletion of the calpain-1 protein which was accompanied by a reduced cleavage of α-spectrin in both examined tissues. CAST levels were markedly elevated in knockout and double mutant animals, with the strongest increase detectable in skeletal muscle. Moreover, the conversion of neuronal p35 to p25 was significantly reduced due to the absence of calpain-1. Despite an at least conceivable compensation of the calpain system, solely the knockout of calpain-1 clearly reduced the overall activity, as demonstrated by the effects on substrate proteins. As expected, subsequent assessment of ataxin-3 cleavage in brain tissue revealed a reduced formation of endogenous and transgenic, polyQ-expanded ataxin-3 fragments. Interestingly, levels of a larger fragment increased upon calpain-1 knockout

pointing to a sequential cleavage of ataxin-3 by this protease. The cleavage pattern of ataxin-3 in skeletal muscle, on the other hand, differed from the pattern observed in brain, which might be due to a divergent involvement of muscle-specific proteases. Furthermore, the knockout of calpain-1 did not distinctly change fragmentation of ataxin-3 in muscle tissue but showed a trend comparable to the effects in brain of calpain-1 knockout and double mutant mice. TR-FRET analysis of brain homogenates found that depletion of calpain-1 resulted in elevated levels of total ataxin-3. This observation might be in line with the previously described age- and presumably calpain-dependent decrease of ataxin-3 levels in a second SCA3 mouse model (Hübener et al., 2013; Nguyen *et al.*, 2013). It was also demonstrated, that a decrease in soluble ataxin-3 levels correlates with elevated amounts of mutant ataxin-3 aggregates in SCA3 mouse brain (Nguyen *et al.*, 2013). Considering a reduced cleavage and increased soluble levels of ataxin-3, the impact of calpain-1 knockout on aggregate formation was investigated in a following step. Surprisingly, ataxin-3 aggregation at 3 months of age appeared unchanged as detected using filter retardation assays, when comparing double mutant animals with SCA3 mice. In respect to these findings, additional investigations at a later time point are necessary to fully assess the impact of an calpain-1 knockout on fragmentation and aggregation of ataxin-3.

Contrary to expectations for the here investigated genetic approach, recent research on calpain-1 null and missense mutations in humans and dogs as well as on the knockout in mice revealed that the absence of the protease causes an ataxic phenotype. This is accompanied by limp spasticity, abnormal cerebellar development, and impairments in metabotropic glutamate receptor-dependent long-term depression as well as fear memory extinction (Forman *et al.*, 2013; Y. Wang *et al.*, 2016; Zhu *et al.*, 2017). The negative impact of a loss of calpain-1 is corroborated by behavioural data in double mutant animals, which show a worsening of the motor phenotype.

Taken together, genetically targeting calpain-1 appears to be an inapplicable strategy for SCA3. An alternative could be focussing on calpain-2, whose homozygous knockout in the maternal placenta, on the other hand, was shown to cause embryonic lethality in mice (Takano *et al.*, 2011). Even the widely investigated overexpression of CAST has been recently linked to perturbations in scar healing during myocardial infarction, which can provoke an increased mortality, and to a higher susceptibility to lethal spleen tumours in mice (Wan *et al.*, 2015; Hanouna *et al.*, 2017). On this account, the genetic modification of the calpain system as a therapeutic approach in neurodegenerative disorders should be only followed with special caution.

Summary and outlook

Targeting calpains constitutes an auspicious therapeutic strategy for neurodegenerative diseases. This work has tested three different approaches for decreasing calpain activity in models of HD and SCA3 (TABLE 2): First, direct lowering of calpain activity by specific pharmacologic inhibitors in cell culture resulted in reduced calpain overactivation, disease protein fragmentation and improved cell viability in mutant cell lines. Second, indirect reduction of calpain activation by improving mitochondrial function and Ca^{2+} handling by the experimental drug olesoxime improved the molecular and behavioural phenotype in two animal models of HD. Last, the genetic ablation of calpain-1 attenuated the fragmentation of mutant ataxin-3 in an SCA3 mouse model. Although all three molecular concepts successfully achieved the primary objectives of attenuating global calpain activity and disease protein fragmentation, several issues need to be taken into consideration. Especially, application of calpain inhibitors is limited to their imperfect specificity, and knockout of calpain isoforms can lead to disturbances due to the loss of their vital physiological implications. Olesoxime emerged as a promising drug candidate, which is reemphasized by its simple applicability, pharmacologic tolerance and neuroprotective properties. However, further investigations are demanded to fully understand its molecular mode of action and to improve its efficacy.

Table 2. Targeting calpains in cell and rodent models of HD and SCA3. Comparison of pursued pharmacologic and genetic strategies. ms = mouse; rt = rat; huc = human cell line; msc = mouse cell line, light blue = HD; dark blue = SCA3; ↑ = upregulation; ↓ = downregulation; ↕ = unchanged; (p) = pharmacological approach; (g) = gene knockout; n/a = not available.

Study	*Disease model*	*Target*	*Molecular effects*	*Effects on phenotype*	*References*
Calpain inhibitor trials *in vitro* & *in cellulo*	**ST*Hdh*** msc **HEK 293T** huc	Calpains (p)	Reduced calpain system activation. Counteracting ionomycin-mediated calpain activation. Decreased huntingtin cleavage.	Increased viability of the mutant cell line	Unpublished manuscript A and E
Olesoxime treatment study I	**BACHD** rt 13 months	VDAC1 (p)	Increased VDAC1 and reduced IP_3R levels. Reduced calpain system activation. Decreased huntingtin cleavage and aggregation.	Alleviated cortical thinning. Improved cognitive and psychiatric phenotype.	Clemens *et al.*, 2015
Olesoxime treatment study II	**HDKI** ms 3 months	VDAC1 (p)	Reduced calpain system activation. Decreased huntingtin cleavage.	n/a	Weber *et al.*, 2016
Calpain inhibitor trials *in vitro* & *in cellulo*	**iHFs** huc **HEK 293T** huc	Calpains (p)	Reduced calpain system activation. Counteracting ionomycin-mediated calpain activation. Decreased ataxin-3 cleavage.	n/a	Weber *et al.*, 2017
Calpain-1 knockout	**YAC84/*Capn1*$^{-/-}$** ms 3 months	*Capn1* (g)	Reduced calpain system activation. Decreased ataxin-3 cleavage. No effects on aggregation.	Increased behavioural deficits in comparison to wild type and YAC84 mice.	Unpublished manuscript D

Characterisation of polyglutamine disease protein fragmentation by calpains

Preliminary considerations

The localisation of cleavage sites within a substrate protein can help to understand the physiological function of a protein and evaluate the repercussion of proteolytic events. In the special case of disease proteins like mutant huntingtin or ataxin-3, knowledge on the exact scissile bond allows not only for characterising the toxicity of emerging breakdown products but also for developing molecular strategies to therapeutically modulate proteolysis.

A set of different technical approaches can be utilised to first narrow down and then precisely determine the amino acid position of the specific cleavage site. An initial step is the confirmation of substrate recognition and proteolysis by the respective enzyme. This can be done in pure *in vitro* approaches by incubating recombinant substrate proteins with enzymes, but also in a more physiological context by inducing protease activity in cell-based or *ex vivo* experiments. Hereafter, samples can be analysed by western blotting ideally applying a set of antibodies specific for different portions of the substrate protein. The comparison of cleavage patterns, regarding the presence of certain antibody epitopes in detected protein fragments, represents a reference point for cleavage site localisation. In combination with *in silico* prediction tools like the ExPASy PeptideCutter, observed cleavage events can be spatially limited to a selection of computed sites (Gasteiger *et al.*, 2005). However, only methodologies based on Edman N-terminal sequencing or mass spectrometry of breakdown products are sufficient to determine the sequence and position of a cleavage site (Edman, 1950; Doucet and Overall, 2011; Van den Berg and Tholey, 2012). An indirect way for identifying recognition motifs is based on peptide libraries. Here, libraries of substrate peptides are used to reconstruct cleavage motifs and their sequences are then aligned with protein databases (Birkett *et al.*, 1991; Turk *et al.*, 2001; Schilling and Overall, 2008). To ultimately corroborate cleavage sites, site-directed mutagenesis or post-translational modifications are applied to block fragmentation of the substrate protein.

Based on these principles, many studies have devoted themselves to the characterisation of calpain cleavage in disease proteins such as α-synuclein, TDP-43 or tau (Dufty *et al.*, 2007; M. C. Liu *et al.*, 2011; Yamashita *et al.*, 2012). In this study, a combinatorial strategy consisting of several biochemical and cell biological methods has been deployed to further and robustly analyse calpain-dependent cleavage events in huntingtin and ataxin-3.

Identification of calpain cleavage sites in huntingtin

(Covered in Unpublished project manuscript E; Clemens *et al.*, 2015)

Since the first reports on calpain-mediated proteolysis of huntingtin as a player in the molecular pathogenesis of HD, a couple of cleavage sites at the N-terminus of the disease protein has been identified (Gafni *et al.*, 2004; Southwell *et al.*, 2011). To reinvestigate huntingtin fragmentation, this study focused on the confirmation of calpain-dependent cleavage in additional cell models and *ex vivo*, together with the analysis of the fragmentation pattern and localisation of yet unknown cleavage sites.

In a first experiment, proteolytic cleavage of wild type and mutant huntingtin was induced in lysates of respective ST*Hdh* cell lines by a time-dependent addition of exogenous recombinant calpain-1 or -2. Western blot analysis showed that both recombinant calpains could readily cleave murine huntingtin and generate comparable fragmentation patterns. This observation was confirmed in lysates of HEK 293T cells overexpressing human HA-tagged huntingtin with 15 and 128 glutamines and *ex vivo* in cortex samples of wild type and BACHD rats. Differences between the fragmentation of wild type and mutant huntingtin, on the other hand, could be explained by polyQ-dependent size shifts of certain cleavage bands. Thus, calpain-1 and -2 seem to generally target the same recognition motifs within the huntingtin protein.

To reproduce calpain cleavage of huntingtin in a cellular context, further experiments were performed in HA-tagged huntingtin 15Q and 128Q overexpressing HEK 293T cells, which were treated with the Ca^{2+}-ionophore ionomycin. This compound facilitates the increase of cytosolic Ca^{2+} levels and, hereby, calpain overactivation. The increased calpain activity led to a time-dependent accumulation of polyQ and non-polyQ fragments which were abolished by administration of the calpain inhibitor CI III. Interestingly, this cell-based approach and the *in vitro* cleavage assays revealed the formation of two large C-terminal huntingtin breakdown products lacking the polyQ stretch. Size estimations and detectability by different antibodies pointed to yet unknown calpain-mediated cleavage event downstream of amino acid position 1000 as the source for these fragments.

For identification of the cleavage site underlying the formation of the large C-terminal fragments, mass spectrometry analysis of calpain-cleaved human huntingtin was performed. Lysates of HEK 293T cells, which expressed HA-tagged huntingtin 15Q and 128Q, were incubated with $CaCl_2$ for activating calpains. Proteins were then separated by polyacrylamide gel electrophoresis and respective bands of interests excised for mass spectrometry.

Comparison of peptides resulting from tryptic and non-tryptic digest uncovered a novel cleavage site at amino acid T1175 of human huntingtin (UniProt identifier: P42858-1 with 23 glutamines), which was further corroborated by *in silico* predictions. Interestingly, this site colocalises with the C-terminal end of the HEAT cluster 2 (FIGURE 10). This corresponds to previous conjectures that caspase and calpain cleavage sites preferentially fall into the PEST motif-rich intervening sequences between huntingtin's HEAT domains (Warby *et al.*, 2008). However, further investigations are necessary to confirm calpain cleavage at this position and to evaluate the impact of the resulting fragments on the molecular pathogenesis of HD.

The here described results are in line with previous reports on calpain-mediated fragmentation of huntingtin. Earlier studies have identified cleavage sites at amino acids 8 and 15 and 469 and 536, respectively. Deletion mutagenesis of the latter sites did not only prevent cleavage of huntingtin but also reduced huntingtin aggregation and toxicity (Gafni *et al.*, 2004). On the other hand, antibody-based blocking of the very N-terminal cleavage sites abrogated a calpain-dependent degradation of a mutant huntingtin exon 1 construct (Southwell *et al.*, 2011). This rather protective effect of calpains has been also suggested by experiments, which pharmacologically inhibited these proteases (Ratovitski *et al.*, 2007). Moreover, it was demonstrated, that huntingtin fragments are not by itself pathogenic but their specific amino acid range and cleavage site-defined margin determine their toxicity (Slow *et al.*, 2005; Graham *et al.*, 2006). Together with findings, that C-terminal and non-polyQ-containing fragments of huntingtin can impair autophagy, ER function and endocytosis, the current work underlines the relevance of further research on calpain cleavage sites in huntingtin and fragment characterisation for understanding HD pathology (Martin *et al.*, 2014; Ochaba *et al.*, 2014; El-Daher *et al.*, 2015).

Identification of calpain cleavage sites in ataxin-3

(Covered in Hübener *et al.*, 2013; Nguyen *et al.*, 2013; Weber *et al.*, 2017)

Similar to developments in the field of HD research, scientists have investigated ataxin-3 cleavage by calpains more closely. The position of calpain recognition motifs, however, remained mainly unsolved. The first analyses applied Edman N-terminal sequencing of *in vitro* calpain-2-digested ataxin-3 and localised cleavage sites around amino acids 60, 200, and 260, but without further confirmation (Haacke *et al.*, 2007). Based on rough estimations or *in silico* prediction, several subsequent studies narrowed down additional sites around positions 154, 190, and 220 (Colomer Gould *et al.*, 2007; Simões *et al.*, 2012). Due to this insufficient evidence, this work aimed at precisely localising calpain recognition motifs in ataxin-3 and thereby reviewing the pathological relevance of calpain cleavage for SCA3.

In the first *in vitro* and *ex vivo* experiments, it was tested whether both calpain-1 and calpain-2 can cleave ataxin-3 and whether there are differences between the resulting fragmentation patterns. For this purpose, lysates of HEK 293T cells overexpressing ataxin-3 (UniProt identifier: P54252-2) with 15, 77 or 148 glutamines and of wild type and SCA3 mouse brains were incubated with each of the recombinant proteases. Western blotting showed that both calpain-1 and calpain-2 cleave ataxin-3 in a time-dependent manner. Interestingly, calpain-2 showed a more efficient proteolysis in contrast to calpain-1, which occurred even more rapidly for polyQ-expanded ataxin-3. The general cleavage pattern generated by both enzymes, however, did not apparently diverge. However, further *in vitro* cleavage assays employing purified ataxin-3 did not reproduce these findings but showed a rather equipollent, polyQ-independent fragmentation.

To proof that calpain cleavage of wild type and mutant ataxin-3 is a physiological and disease relevant process, patient-derived cells and SCA3 post-mortem brain tissue were investigated. Western blot analysis of fibroblasts, iHF cell lines, iPSCs and iPSC-derived differentiated cortical neurons (iCNs), all obtained from SCA3 patients and healthy controls, demonstrated the occurrence of calpain-cleaved ataxin-3 fragments at baseline. The observed fragmentation could be further amplified by addition of $CaCl_2$ to iHF lysates or by ionomycin administration to cultured iHFs, iPSCs and iCNs. Correspondingly, treating iHFs with the calpain inhibitor CI III reduced the formation of ataxin-3 fragments. Most remarkably, the presence of calpain-cleaved ataxin-3 was revealed in post-mortem brain tissue of SCA3 patients but also of healthy controls, confirming that this proteolytic process takes place under normal physiological conditions.

The calpain-mediated fragmentation of ataxin-3 was further tracked using a TR-FRET-based approach. This assay used two fluorophore-labelled antibodies, one binding to amino acids 214-233 of ataxin-3 and the second recognizing the expanded polyQ tract localized after amino acid 292. Incubation of SCA3 mouse brain homogenates with $CaCl_2$ for calpain activation led to a reduced FRET signal. This observation suggested a calpain-mediated separation of the bound antibodies and indicated the presence of a recognition motif between respective epitopes, consistent with reports on putative cleavage sites around positions 220 and 260 (Haacke *et al.*, 2007; Simões *et al.*, 2012).

To dissect the ataxin-3 fragmentation pattern, arising cleavage products were mapped using a panel of antibodies, which bind along the entire ataxin-3 protein. By this means, the occurrence of five major N-terminal fragments was revealed. Comparison with ataxin-3 deletion constructs, which lack C-terminal portions of the protein, narrowed down four recognition motifs to regions between amino acids 321–366, 244–259, 198–243, and just before position 198. To precisely map cleavage sites, quantitative mass spectrometry of heavy and light isotope-labelled ataxin-3 after calpain digest was performed. This analysis identified amino acids H187, D208, S256 and G259 as the P_1 sites of four calpain recognition motifs.

Validation of mapped cleavage sites was achieved by site-directed mutagenesis of amino acids within the recognition motif. For this purpose, two strategies were applied based on the substitution of five amino acids by alanine or three amino acids by tryptophan. The first approach has been commonly used (Wanichawan *et al.*, 2014), whereas tryptophan substitutions were conceived by computing effects of randomly replacing amino acids on the site-specific calpain cleavage likelihood. Both strategies were firstly tested via calpain overlay assays of 20-mer ataxin-3 peptides which comprise respective calpain recognition motifs with or without respective substitutions. Overlay assays confirmed binding of calpain-1 and calpain-2 to peptides containing the cleavage sites H187, D208 and S256, plus the additionally predicted position T277. Notably and according to *in silico* projections, triple tryptophan exchanges showed a more efficient reduction of calpain binding than quintuple alanine substitutions. In a next step, these mutations were introduced into ataxin-3 constructs and the overexpressed proteins were subjected to *in vitro* and cell-based calpain activation assays. In line with the overlay assays, modified ataxin-3 carrying triple tryptophan mutations at sites D208, S256 or both showed significantly reduced formation of respective fragments when compared to the non-mutated protein.

To evaluate the pathomolecular consequences of calpain-mediated ataxin-3 breakdown, a set of truncated ataxin-3 constructs was generated, which represents fragmentation at amino acid positions D208 and S256. HEK 293T cells transfected with these fragment constructs were examined using aggregation assays and FACS-based viability analysis. Overexpression of C-terminal polyQ-expanded constructs resulted in a massive formation of ubiquitinated aggregates and an increased cytotoxicity when compared to the full-length protein. Both effects were even enhanced for the shorter C-terminal construct, which corresponds to cleavage at the S256 site. On the other hand, N-terminal ataxin-3 fragment constructs, which lack the polyQ stretch, did not form insoluble protein species or microscopically traceable aggregates. This observation stands in contrast with a previous report on a transgenic mouse model expressing a fusion protein of the first 259 amino acids of ataxin-3 and β-galactosidase but accord to earlier cell-based investigations (Perez *et al.*, 1998; Hübener *et al.*, 2011). Furthermore, both N-terminal and C-terminal fragment constructs exhibited a mainly cytoplasmic or diffuse localisation as shown by subcellular fractionation assays and confocal microscopy. Other studies, however, demonstrated the nuclear occurrence of C-terminal ataxin-3 fragments or suggested their nuclear shift attributed to the absence of the N-terminally located NESs (Goti *et al.*, 2004; Antony *et al.*, 2009). On a final note, the here identified calpain cleavage site at amino acid D208 is adjacent to phospho-site T207, and S256 itself has been shown to be phosphorylated (Schmidt *et al.*, 1998; Trottier *et al.*, 1998; Mueller *et al.*, 2009). Two protein kinases, CK2 and GSK 3β, respectively, have been predicted or proven to mediate these phosphorylations, most likely having consequences for the cleavage likelihood. Corresponding implications have already been demonstrated for calpain or caspase cleavage of huntingtin (Luo *et al.*, 2005; Schilling *et al.*, 2006). Thus, modulating these specific post-translation modifications might represent a promising target to alter calpain-driven fragmentation of ataxin-3 as a potential treatment approach in SCA3.

Taken together, the here presented investigations showed for the first time that calpain-mediated fragmentation of ataxin-3 is present in patient-derived cells and SCA3 post-mortem brain tissue at baseline. Moreover, four cleavage sites were precisely localized. Mutating amino acids at two main recognition motifs to tryptophan nearly abrogated the formation of two predominant C-terminal fragments and their N-terminal counterparts. Further characterisation of these C-terminal breakdown products demonstrated an increased aggregation propensity and cytotoxicity compared to the polyQ-expanded full-length protein. The findings are in line with previous studies on the role of ataxin-3 fragmentation by calpains in the molecular pathogenesis of SCA3 (Haacke *et al.*, 2007; Koch *et al.*, 2011;

Simões *et al.*, 2012). However, additional *in vivo* validation of these results, particularly regarding herein generated calpain cleavage-resistant forms of polyQ-expanded ataxin-3, is still pending. These future investigations might reveal whether targeting ataxin-3 cleavage constitutes a valuable therapeutic strategy in treating SCA3.

Summary and outlook

Calpain-mediated fragmentation of disease proteins is a widely-described element of the molecular pathomechanism of neurodegenerative disorders. The current work on huntingtin and ataxin-3 cleavage emphasizes its general validity by proving its physiological occurrence, successfully localising novel cleavage sites and characterising emerging fragments. However, and despite ongoing efforts to identify further cleavage sites within these polyQ proteins, further steps need to be taken to enhance our understanding of consequent implications. *In silico* predictions yield 189 highly probable calpain cleavage sites for huntingtin and 36 sites for ataxin-3, which is in contrast with a relatively low number of yet confirmed sites (FIGURE 10). This complexity of proteolytic modifications is further enhanced by the circumstance that cleavage at distinct positions can result in various consequences for disease protein function, integrity and toxicity. Nonetheless, the herein before described results on calpain-resistant ataxin-3, together with therapeutically promising findings in other studies, remain encouraging for future investigations. Those efforts could also include the analysis of non-synonymous polymorphisms in the mutant *HTT* and *MJD1* genes, which lead to amino acid changes at calpain cleavage sites and thereby alterations in cleavage likelihood. A correlation of the polymorphisms with the patient's disease onset and progression might further unveil the clinical relevance of calpain-dependent disease protein fragmentation.

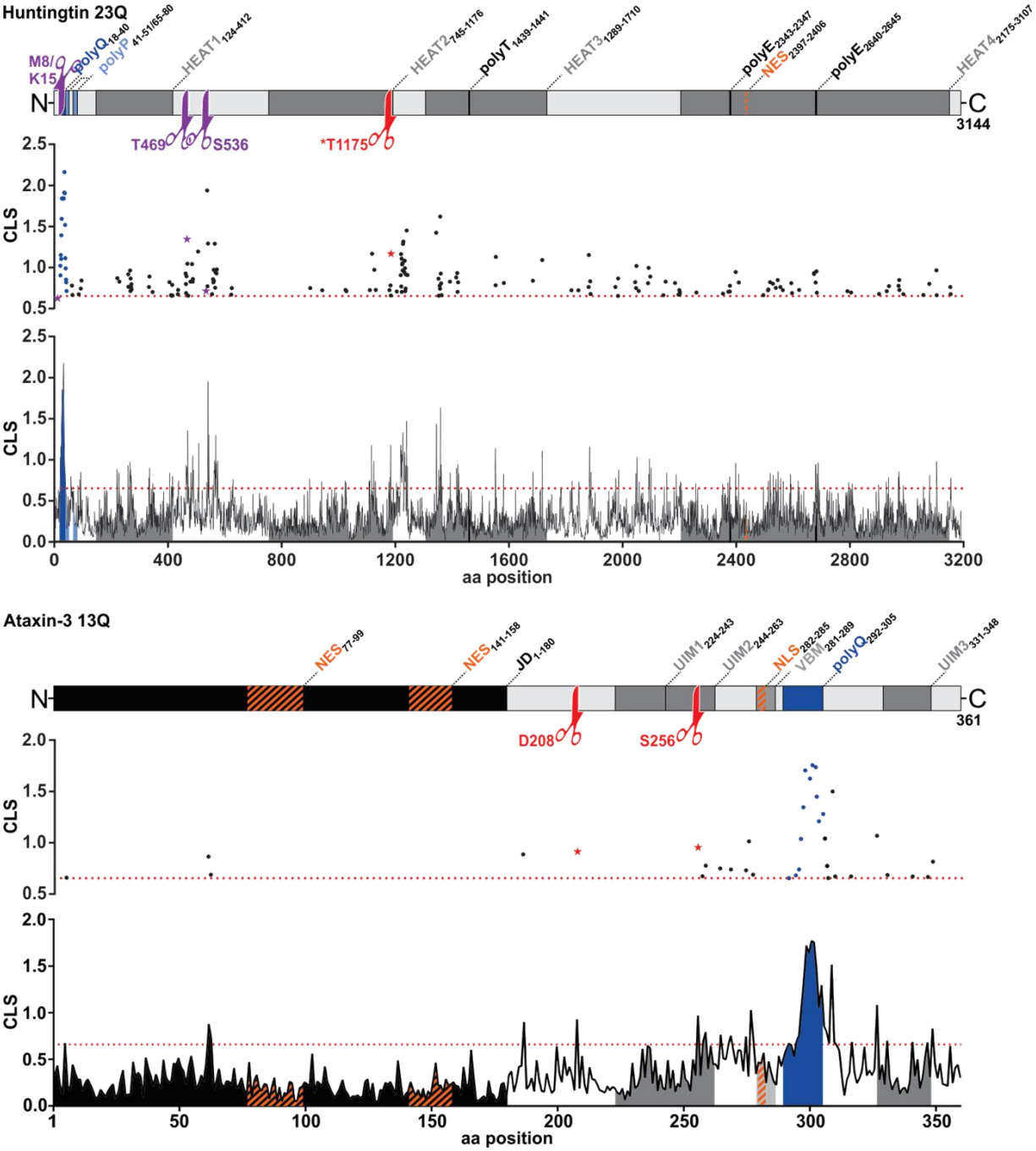

Figure 10. Overview of already known and newly identified calpain cleavage sites within huntingtin and ataxin-3. *In silico* prediction of calpain cleavage sites in huntingtin (UniProt identifier: P42858-1, 23Q) and ataxin-3 (UniProt identifier: P54252-2, 13Q) using the GPS-CCD tool. Cleavage likelihood scores (CLS) are plotted relative to their amino acid position. For comparison, respective protein structures are illustrated above. The red dotted line indicates maximum default cut-off value of 0.654. Scatter plots show amino acid positions with a CLS above the cut-off value. Cleavage sites identified in this work are highlighted with red scissors and stars, previously known sites are represented by purple scissors and stars. Asterisk (*) = lacks confirmation by site-directed mutagenesis. For a detailed description of the indicated protein domains see FIGURE 4.

Conclusion

The overall goal of this work was to shed new light on calpains as important players and therapeutic targets in neurodegeneration. Exemplified by investigations on the polyQ diseases HD and SCA3, three main aspects were scientifically covered, namely the pathologic overactivation of calpains, strategies to attenuate this activation, and characterisation of calpain-mediated disease protein cleavage.

Biochemical analysis revealed a general disease-related increase of the calpain system activity in different cell and animal models. Triggering further overactivation amplified the HD and SCA3 pathology in two mouse models, whereas genetic or pharmacological inhibition of calpains or their activating pathways effectuated an amelioration of pathological hallmarks *in vitro* and *in vivo*. Unveiling the therapeutic efficacy of the experimental drug olesoxime, moreover, constitutes a major and perhaps trailblazing finding in treatment of polyQ disorders. Despite all these important insights, this work is just another puzzle piece in the breakdown of disease mechanisms and related interventions in neurodegeneration.

The next decades will hopefully produce gene therapies capable of curing diseases with a clear monogenic aetiology such as HD and SCA3. On the other hand, genetic disorders represent only a fraction of neurodegenerative diseases and most of these medical conditions are still determined by environmental factors and the individual lifestyle. On these grounds, further efforts must be undertaken to explore common molecular pathomechanisms including calpains as mediators of neuronal demise.

Future studies on calpains need to broaden the comparative spectrum of molecular analyses and treatment strategies between diseases, thus enabling the development of generally applicable therapies for neurodegeneration.

Funding

The project on calpain cleavage of ataxin-3 was supported by the German Research Foundation DFG, research grant number HU1770/3-1). The olesoxime treatment study was funded by the European Union 7th Framework Program for RTD, Project MitoTarget (research grant number HEALTH F2-2008-223388). Analysis of calpain activation in YAC128 animals was funded by the Baden-Wuerttemberg Foundation (research grant number P-BWS-SPII/3-08).

Acknowledgements

The long journey of my doctoral thesis has finally come to an end, and this work would have never been accomplished without all the different forms of help and support, which I have gratefully received from so many, many people.

First and foremost, I would like to express my gratitude and appreciation to my supervisors Jeannette Hübener-Schmid, Hoa Nguyen and Olaf Rieß, who did not only convince me of doing my PhD in our institute and gave me all their trust and support, but have also opened my view on the exciting field of calpains in neurodegeneration and beyond, which I truly became a fan of. I strongly wish that my expertise, which I have developed under your guidance, will somehow and someday add to the understanding of those devastating diseases and contribute to the quest for new therapies.

Many thanks to all the collaborators and co-authors, especially Pimthanya Wanichawan and Cathrine Carlson from the Oslo University Hospital, Giambattista Guaitoli and Christian Johannes Glöckner as well as Stefanie Hayer, Stefan Hauser and Ludger Schöls from the DZNE in Tübingen, and Dagmar Ehrnhoefer and Michael Hayden from the CMMT in Vancouver, who prove once again that scientific research can only prosper, when many individuals jointly engage in a common endeavour.

I want to further thank all my students, Fabronia Murad, Lukas Klumpp, Midea Ortiz-Rios, Maike Nagel, Vivien Weber, Stefanie Anger and Simon Kloock, for their big contribution to this work, and for the great and fun times we spent together inside and outside the lab. Many advances in the projects would not have been possible without their special commitment to our research.

Many thanks to all the current and the former members of the HD and SCA3 working groups, and all the other people from the Institute of Medical Genetics and Applied Genomics for our (scientific) time together, particularly Mahkameh Abeditashi, Meike Diepenbroek, Ben Fabry, Matthias Golla, Eva Haas, Alex Kelp, Arianna Novati, Esteban Portal, Jana & Thorsten Schmidt, Ilnaz Sepahi, Lissy Singer, Janice Stricker-Shaver, Anna Sowa, Zijian Wang, and Libo Yu-Täger.

One of the great points about our institute, aside from representing the professional centre of your daily life, is that it became the home base of many wonderful friendships. Thus I would like to say a huge thank you for everything to all the guys from this “inner circle”: Nicolas Casadei (Thank you so much for all the inspiring time we spent discussing and sharing our scientific point of views, for all the lab stuff you taught me, for the common - nearly

professional, but always cheerful - interest in music, and for the great memorable moments we had outside the institute.), The Clemenssons (One of the prototypes of a happy and cool scientist couple/family who one loves to spend time with. Laura, endless thanks for allowing me to be part of your research life and for teaching me how important it is to scrutinize every experiment you do. And thank you, Erik, that you've never stopped trying to give me an understanding of all facets of animal behaviour analysis.), Tina & Florian Harmuth (Thank you, Tina, for always worrying and caring of my private and professional life. And thank you, Flo, my oldest university companion, for convincing me to choose human genetics as the main subject of my studies.), Janine Magg (Many thanks to you for steadily emphasizing how important it is that a scientist in our field never forgets about the consequences of his work for the patients.), Priscila Sena (Thank you, Pri, for bringing in all the joyous Brazilian vibes to us, which undeniably affected both my scientific and personal life in the most positive ways.), Zeina Wassouf (Thanks for our debates on principles in science and re-infecting me with your enthusiasm and energy for research, and also for being this cool girl.), and Daniel Weishäupl (Thank you for standing and answering my scientific and non-scientific questions as my desk neighbour, exchanging our knowledge on Corel, statistics and astronomy, and for still trying to do this one GST-pulldown.).

And what is a human being without a family? That is why my infinite thanks and love go to my German grandparents, Irma and Rudolf Weber, who sadly did not live to see the completion of my PhD (Wo auch immer Ihr jetzt seid, ich bin mir sicher, Ihr seid stolz auf mich.), to my Polish grandparents Zenobia and Leszek Florek (Dzięnkuję za wszystko, Babciu I Dziadku! Kocham Was!) and to my beloved parents Urszula and Roland Weber (Ohne Euch, Mama und Paps, wäre ich niemals dort, wo ich jetzt bin. Danke für wirklich alles! Ich liebe Euch!).

Finally, I would like to say thank you to Anne Krahl, who – not only as my girlfriend and best friend, but also colleague, collaboration partner and proofreader – unremittingly supported and encouraged me during the happy and hard times of my thesis. You are really the perfect partner for a frenetic biologist like me. I love you!

References

Adamec E, Mohan P, Vonsattel JP, Nixon R a. Calpain activation in neurodegenerative diseases: confocal immunofluorescence study with antibodies specifically recognizing the active form of calpain 2. Acta Neuropathol. 2002; 104: 92–104.

Akinyemi RO, Mukaetova-Ladinska EB, Attems J, Ihara M, Kalaria RN. Vascular risk factors and neurodegeneration in ageing related dementias: Alzheimer's disease and vascular dementia. Curr. Alzheimer Res. 2013; 10: 642–53.

Albrecht M, Golatta M, Wüllner U, Lengauer T. Structural and functional analysis of ataxin-2 and ataxin-3. Eur. J. Biochem. 2004; 271: 3155–3170.

Albrecht M, Hoffmann D, Evert BO, Schmitt I, Wüllner U, Lengauer T. Structural modeling of ataxin-3 reveals distant homology to adaptins. Proteins Struct. Funct. Bioinforma. 2002; 50: 355–370.

Alcedo J, Flatt T, Pasyukova EG. Neuronal Inputs and Outputs of Aging and Longevity. Front. Genet. 2013; 4: 71.

Alkadhi KA. Chronic stress and Alzheimer's disease-like pathogenesis in a rat model: prevention by nicotine. Curr. Neuropharmacol. 2011; 9: 587–97.

Alzheimer Association. 2016 Alzheimer's Disease Facts and Figures. Alzheimer's Dement. 2016 2016; 12: 1–80.

Amor S, Puentes F, Baker D, van der Valk P. Inflammation in neurodegenerative diseases. Immunology 2010; 129: 154–69.

Anderson KE, Marder KS. An overview of psychiatric symptoms in Huntington's disease. Curr. Psychiatry Rep. 2001; 3: 379–88.

Andrade MA, Bork P. HEAT repeats in the Huntington's disease protein. Nat. Genet. 1995; 11: 115–116.

Angelova PR, Ludtmann MHR, Horrocks MH, Negoda A, Cremades N, Klenerman D, et al. Calcium is a key factor in α-synuclein induced neurotoxicity. J. Cell Sci. 2016

Antony PMA, Mäntele S, Mollenkopf P, Boy J, Kehlenbach RH, Riess O, et al. Identification and functional dissection of localization signals within ataxin-3. Neurobiol. Dis. 2009; 36: 280–292.

Arndt JR, Chaibva M, Legleiter J. The emerging role of the first 17 amino acids of huntingtin in Huntington's disease. Biomol. Concepts 2015; 6: 33–46.

Ashrafian H, Harling L, Darzi A, Athanasiou T. Neurodegenerative disease and obesity: what is the role of weight loss and bariatric interventions? Metab. Brain Dis. 2013; 28: 341–353.

Austin KW, Ameringer SW, Cloud LJ. An Integrated Review of Psychological Stress in Parkinson's Disease: Biological Mechanisms and Symptom and Health Outcomes. Parkinsons. Dis. 2016; 2016: 1–15.

Awada R, Parimisetty A, Lefebvre d'Hellencourt C. Influence of Obesity on Neurodegenerative Diseases. In: Neurodegenerative Diseases. InTech; 2013.

Azam M, Andrabi SS, Sahr KE, Kamath L, Kuliopulos A, Chishti AH. Disruption of the mouse mu-calpain gene reveals an essential role in platelet function. Mol. Cell. Biol. 2001; 21: 2213–20.

Bading H. Nuclear calcium signalling in the regulation of brain function. Nat. Rev. Neurosci. 2013; 14: 593–608.

References

Badugu R, Garcia M, Bondada V, Joshi A, Geddes JW. N terminus of calpain 1 is a mitochondrial targeting sequence. J. Biol. Chem. 2008; 283: 3409–3417.

Baig SS, Strong M, Quarrell OW. The global prevalence of Huntington's disease: a systematic review and discussion. Neurodegener. Dis. Manag. 2016; 6: 331–343.

Bañez-Coronel M, Ayhan F, Tarabochia AD, Zu T, Perez BA, Tusi SK, et al. RAN Translation in Huntington Disease. Neuron 2015; 88: 667–677.

Bangen KJ, Nation DA, Clark LR, Harmell AL, Wierenga CE, Dev SI, et al. Interactive effects of vascular risk burden and advanced age on cerebral blood flow. Front. Aging Neurosci. 2014; 6: 159.

Banik NL, Chou CH, Deibler GE, Krutzch HC, Hogan EL. Peptide bond specificity of calpain: proteolysis of human myelin basic protein. J. Neurosci. Res. 1994; 37: 489–96.

Bao J, Sharp AH, Wagster M V, Becher M, Schilling G, Ross CA, et al. Expansion of polyglutamine repeat in huntingtin leads to abnormal protein interactions involving calmodulin. Proc. Natl. Acad. Sci. U. S. A. 1996; 93: 5037–42.

Baudry M, Bi X. Calpain-1 and Calpain-2: The Yin and Yang of Synaptic Plasticity and Neurodegeneration. Trends Neurosci. 2016; 39: 235–245.

Baxendale S, Abdulla S, Elgar G, Buck D, Berks M, Micklem G, et al. Comparative sequence analysis of the human and pufferfish Huntington's disease genes. Nat. Genet. 1995; 10: 67–76.

Beal MF, Kowall NW, Ellison DW, Mazurek MF, Swartz KJ, Martin JB. Replication of the neurochemical characteristics of Huntington's disease by quinolinic acid. Nature 1986; 321: 168–171.

Ben-Ari Y, Cossart R. Kainate, a double agent that generates seizures: two decades of progress. Trends Neurosci. 2000; 23: 580–7.

Benn CL, Sun T, Sadri-Vakili G, McFarland KN, DiRocco DP, Yohrling GJ, et al. Huntingtin modulates transcription, occupies gene promoters in vivo, and binds directly to DNA in a polyglutamine-dependent manner. J. Neurosci. 2008; 28: 10720–33.

Van den Berg BHJ, Tholey A. Mass spectrometry-based proteomics strategies for protease cleavage site identification. Proteomics 2012; 12: 516–529.

Berke SJS, Chai Y, Marrs GL, Wen H, Paulson HL. Defining the role of ubiquitin-interacting motifs in the polyglutamine disease protein, ataxin-3. J. Biol. Chem. 2005; 280: 32026–34.

Berke SJS, Schmied F a F, Brunt ER, Ellerby LM, Paulson HL. Caspase-mediated proteolysis of the polyglutamine disease protein ataxin-3. J. Neurochem. 2004; 89: 908–18.

von Bernhardi R, Tichauer JE, Eugenín J. Aging-dependent changes of microglial cells and their relevance for neurodegenerative disorders. J. Neurochem. 2010; 112: 1099–1114.

Berridge MJ, Lipp P, Bootman MD. The versatility and universality of calcium signalling. Nat. Rev. Mol. Cell Biol. 2000; 1: 11–21.

Bertini E, Dessaud E, Mercuri E, Muntoni F, Kirschner J, Reid C, et al. Safety and efficacy of olesoxime in patients with type 2 or non-ambulatory type 3 spinal muscular atrophy: a randomised, double-blind, placebo-controlled phase 2 trial. Lancet Neurol. 2017; 16: 513–522.

Bertram L, Tanzi RE. The genetic epidemiology of neurodegenerative disease. J. Clin. Invest. 2005; 115

Bettencourt C, Lima M. Machado-Joseph disease: From first descriptions to new perspectives. Orphanet J. Rare Dis. 2011; 6: 1–12.

Bettencourt C, Santos C, Kay T, Vasconcelos J, Lima M. Analysis of segregation patterns in Machado–Joseph disease pedigrees. J. Hum. Genet. 2008; 53: 920–923.

Bezprozvanny I. Calcium signaling and neurodegenerative diseases. Trends Mol. Med. 2009; 15: 89–100.

Bezprozvanny I. Role of inositol 1,4,5-trisphosphate receptors in pathogenesis of Huntington's disease and spinocerebellar ataxias. Neurochem. Res. 2011; 36: 1186–97.

Bichelmeier U, Schmidt T, Hübener J, Boy J, Rüttiger L, Häbig K, et al. Nuclear localization of ataxin-3 is required for the manifestation of symptoms in SCA3: in vivo evidence. J. Neurosci. 2007; 27: 7418–7428.

Billen LP, Shamas-Din A, Andrews DW. Bid: a Bax-like BH3 protein. Oncogene 2008; 27: S93–S104.

Birben E, Sahiner UM, Sackesen C, Erzurum S, Kalayci O. Oxidative stress and antioxidant defense. World Allergy Organ. J. 2012; 5: 9–19.

Bird TD. Genetic aspects of Alzheimer disease. Genet. Med. 2008; 10: 231–239.

Birkett AJ, Soler DF, Wolz RL, Bond JS, Wiseman J, Berman J, et al. Determination of enzyme specificity in a complex mixture of peptide substrates by N-terminal sequence analysis. Anal. Biochem. 1991; 196: 137–143.

Bishop NA, Lu T, Yankner BA. Neural mechanisms of ageing and cognitive decline. Nature 2010; 464: 529–35.

Bizat N, Hermel J-M, Boyer F, Jacquard C, Créminon C, Ouary S, et al. Calpain is a major cell death effector in selective striatal degeneration induced in vivo by 3-nitropropionate: implications for Huntington's disease. J. Neurosci. 2003; 23: 5020–30.

Bjørkøy G, Lamark T, Brech A, Outzen H, Perander M, Overvatn A, et al. p62/SQSTM1 forms protein aggregates degraded by autophagy and has a protective effect on huntingtin-induced cell death. J. Cell Biol. 2005; 171: 603–14.

Blennow K, de Leon MJ, Zetterberg H. Alzheimer's disease. Lancet 2006; 368: 387–403.

Blokhuis AM, Groen EJN, Koppers M, van den Berg LH, Pasterkamp RJ. Protein aggregation in amyotrophic lateral sclerosis. Acta Neuropathol. 2013; 125: 777–794.

Bloom GS. Amyloid-β and Tau. JAMA Neurol. 2014; 71: 505.

Bordet T, Berna P, Abitbol JL, Pruss RM. Olesoxime (TRO19622): A novel mitochondrial-targeted neuroprotective compound. Pharmaceuticals 2010; 3: 345–368.

Bordet T, Buisson B, Michaud M, Abitbol J-L, Marchand F, Grist J, et al. Specific antinociceptive activity of cholest-4-en-3-one, oxime (TRO19622) in experimental models of painful diabetic and chemotherapy-induced neuropathy. J. Pharmacol. Exp. Ther. 2008; 326: 623–32.

Bordet T, Buisson B, Michaud M, Drouot C, Galéa P, Delaage P, et al. Identification and characterization of cholest-4-en-3-one, oxime (TRO19622), a novel drug candidate for amyotrophic lateral sclerosis. J. Pharmacol. Exp. Ther. 2007; 322: 709–20.

Borghammer P. Perfusion and metabolism imaging studies in Parkinson's disease. Dan. Med. J. 2012; 59:

B4466.

Boutell JM, Wood JD, Harper PS, Jones AL. Huntingtin interacts with cystathionine beta-synthase. Hum. Mol. Genet. 1998; 7: 371–8.

Bové J, Prou D, Perier C, Przedborski S. Toxin-induced models of Parkinson's disease. NeuroRx 2005; 2: 484–94.

Brandstaetter H, Kruppa AJ, Buss F. Huntingtin is required for ER-to-Golgi transport and for secretory vesicle fusion at the plasma membrane. Dis. Model. Mech. 2014; 7: 1335–40.

Breuer P, Haacke A, Evert BO, Wüllner U. Nuclear aggregation of polyglutamine-expanded ataxin-3: fragments escape the cytoplasmic quality control. J. Biol. Chem. 2010; 285: 6532–7.

Breydo L, Wu JW, Uversky VN. α-Synuclein misfolding and Parkinson's disease. Biochim. Biophys. Acta - Mol. Basis Dis. 2012; 1822: 261–285.

Brini M, Calì T, Ottolini D, Carafoli E. Neuronal calcium signaling: function and dysfunction. Cell. Mol. Life Sci. 2014; 71: 2787–2814.

Bu J, Sathyendra V, Nagykery N, Geula C. Age-related changes in calbindin-D28k, calretinin, and parvalbumin-immunoreactive neurons in the human cerebral cortex. Exp. Neurol. 2003; 182: 220–31.

Budworth H, McMurray CT. A brief history of triplet repeat diseases. Methods Mol. Biol. 2013; 1010: 3–17.

Bump NJ, Hackett M, Hugunin M, Seshagiri S, Brady K, Chen P, et al. Inhibition of ICE family proteases by baculovirus antiapoptotic protein p35. Science 1995; 269: 1885–8.

Bürk K, Globas C, Bösch S, Klockgether T, Zühlke C, Daum I, et al. Cognitive deficits in spinocerebellar ataxia type 1, 2, and 3. J. Neurol. 2003; 250: 207–211.

Burke JR, Enghild JJ, Martin ME, Jou Y-S, Myers RM, Roses AD, et al. Huntingtin and DRPLA proteins selectively interact with the enzyme GAPDH. Nat. Med. 1996; 2: 347–350.

Burnett B, Li F, Pittman RN. The polyglutamine neurodegenerative protein ataxin-3 binds polyubiquitylated proteins and has ubiquitin protease activity. Hum. Mol. Genet. 2003; 12: 3195–3205.

Burnett BG, Pittman RN. The polyglutamine neurodegenerative protein ataxin 3 regulates aggresome formation. Proc. Natl. Acad. Sci. U. S. A. 2005; 102: 4330–4335.

Butler R, Leigh PN, McPhaul MJ, Gallo JM. Truncated forms of the androgen receptor are associated with polyglutamine expansion in X-linked spinal and bulbar muscular atrophy. Hum. Mol. Genet. 1998; 7: 121–7.

Byrne S, Bede P, Elamin M, Kenna K, Lynch C, McLaughlin R, et al. Proposed criteria for familial amyotrophic lateral sclerosis. Amyotroph. Lateral Scler. 2011; 12: 157–159.

Cai D. Neuroinflammation and neurodegeneration in overnutrition-induced diseases. Trends Endocrinol. Metab. 2013; 24: 40–47.

Calderwood SK, Murshid A, Prince T. The shock of aging: molecular chaperones and the heat shock response in longevity and aging--a mini-review. Gerontology 2009; 55: 550–8.

Calì T, Ottolini D, Brini M. Mitochondrial Ca(2+) and neurodegeneration. Cell Calcium 2012; 52: 73–85.

Campbell RL, Davies PL. Structure–function relationships in calpains. Biochem. J. 2012; 447: 335–351.

Campuzano V, Montermini L, Moltò MD, Pianese L, Cossée M, Cavalcanti F, et al. Friedreich's ataxia: autosomal recessive disease caused by an intronic GAA triplet repeat expansion. Science 1996; 271: 1423–7.

do Carmo Costa M, Bajanca F, Rodrigues A-J, Tomé RJ, Corthals G, Macedo-Ribeiro S, et al. Ataxin-3 Plays a Role in Mouse Myogenic Differentiation through Regulation of Integrin Subunit Levels. PLoS One 2010; 5: e11728.

do Carmo Costa M, Gomes-Da-Silva J, Miranda CJ, Sequeiros J, Santos MM, Maciel P. Genomic structure, promoter activity, and developmental expression of the mouse homologue of the Machado-Joseph disease (MJD) gene. Genomics 2004; 84: 361–373.

do Carmo Costa M, Luna-Cancalon K, Fischer S, Ashraf NS, Ouyang M, Dharia RM, et al. Toward RNAi Therapy for the Polyglutamine Disease Machado–Joseph Disease. Mol. Ther. 2013; 21: 1898–1908.

do Carmo Costa M, Paulson HL. Toward understanding Machado-Joseph disease. Prog. Neurobiol. 2012; 97: 239–257.

Casaca-Carreira J, Toonen LJA, Evers MM, Jahanshahi A, van-Roon-Mom WMC, Temel Y. In vivo proof-of-concept of removal of the huntingtin caspase cleavage motif-encoding exon 12 approach in the YAC128 mouse model of Huntington's disease. Biomed. Pharmacother. 2016; 84: 93–96.

Casadei N, Pöhler A-M, Tomás-Zapico C, Torres-Peraza J, Schwedhelm I, Witz A, et al. Overexpression of synphilin-1 promotes clearance of soluble and misfolded alpha-synuclein without restoring the motor phenotype in aged A30P transgenic mice. Hum. Mol. Genet. 2014; 23: 767–81.

Cattaneo E, Zuccato C, Tartari M. Normal huntingtin function: an alternative approach to Huntington's disease. Nat. Rev. Neurosci. 2005; 6: 919–930.

Caviston JP, Ross JL, Antony SM, Tokito M, Holzbaur ELF. Huntingtin facilitates dynein/dynactin-mediated vesicle transport. Proc. Natl. Acad. Sci. U. S. A. 2007; 104: 10045–10050.

Caviston JP, Zajac AL, Tokito M, Holzbaur ELF. Huntingtin coordinates the dynein-mediated dynamic positioning of endosomes and lysosomes. Mol. Biol. Cell 2011; 22: 478–492.

Cemal CK, Carroll CJ, Lawrence L, Lowrie MB, Ruddle P, Al-Mahdawi S, et al. YAC transgenic mice carrying pathological alleles of the MJD1 locus exhibit a mild and slowly progressive cerebellar deficit. Hum. Mol. Genet. 2002; 11: 1075–94.

Cerretti DP, Kozlosky CJ, Mosley B, Nelson N, Van Ness K, Greenstreet TA, et al. Molecular cloning of the interleukin-1 beta converting enzyme. Science 1992; 256: 97–100.

Chai Y, Berke SS, Cohen RE, Paulson HL. Poly-ubiquitin Binding by the Polyglutamine Disease Protein Ataxin-3 Links Its Normal Function to Protein Surveillance Pathways. J. Biol. Chem. 2004; 279: 3605–3611.

Chai Y, Koppenhafer SL, Shoesmith SJ, Perez MK, Paulson HL. Evidence for proteasome involvement in polyglutamine disease: localization to nuclear inclusions in SCA3/MJD and suppression of polyglutamine aggregation in vitro. Hum. Mol. Genet. 1999; 8: 673–82.

Chan JM, Rimm EB, Colditz GA, Stampfer MJ, Willett WC. Obesity, Fat Distribution, and Weight Gain as Risk Factors for Clinical Diabetes in Men. Diabetes Care 1994; 17

Chang DTW, Rintoul GL, Pandipati S, Reynolds IJ. Mutant huntingtin aggregates impair mitochondrial movement

and trafficking in cortical neurons. Neurobiol. Dis. 2006; 22: 388–400.

Chavarría C, Souza JM. Oxidation and nitration of α-synuclein and their implications in neurodegenerative diseases. Arch. Biochem. Biophys. 2013; 533: 25–32.

Chen X, Tang TS, Tu H, Nelson O, Pook M, Hammer R, et al. Deranged calcium signaling and neurodegeneration in spinocerebellar ataxia type 3. J Neurosci 2008; 28: 12713–12724.

Chen X, Wu J, Lvovskaya S, Herndon E, Supnet C, Bezprozvanny I. Dantrolene is neuroprotective in Huntington's disease transgenic mouse model. Mol. Neurodegener. 2011; 6: 81.

Chew M, Sharrock K. Medical Milestones: Celebrating Key Advances Since 1840. BMJ Publ. Group; 2007.

Cho K, Cho MH, Seo JH, Peak J, Kong KH, Yoon SY, et al. Calpain-mediated cleavage of DARPP-32 in Alzheimer's disease. Aging Cell 2015; 14: 878–886.

Choi DH, Kim YJ, Kim YG, Joh TH, Beal MF, Kim YS. Role of matrix metalloproteinase 3-mediated α-synuclein cleavage in dopaminergic cell death. J. Biol. Chem. 2011; 286: 14168–14177.

Choo YS, Johnson GVW, MacDonald M, Detloff PJ, Lesort M. Mutant huntingtin directly increases susceptibility of mitochondria to the calcium-induced permeability transition and cytochrome c release. Hum. Mol. Genet. 2004; 13: 1407–1420.

Chou AH, Yeh TH, Kuo YL, Kao YC, Jou MJ, Hsu CY, et al. Polyglutamine-expanded ataxin-3 activates mitochondrial apoptotic pathway by upregulating Bax and downregulating Bcl-xL. Neurobiol. Dis. 2006; 21: 333–345.

Chow H, Herrup K. Genomic integrity and the ageing brain. Nat. Rev. Neurosci. 2015; 16: 672–684.

Cicchetti F, Drouin-Ouellet J, Gross RE. Environmental toxins and Parkinson's disease: what have we learned from pesticide-induced animal models? Trends Pharmacol. Sci. 2009; 30: 475–483.

Ciechanover A. Intracellular protein degradation: from a vague idea thru the lysosome and the ubiquitin–proteasome system and onto human diseases and drug targeting*. Cell Death Differ. 2005; 12: 1178–1190.

Ciechanover A, Kwon YT. Degradation of misfolded proteins in neurodegenerative diseases: therapeutic targets and strategies. Exp. Mol. Med. 2015; 47: e147.

Cirak S, Arechavala-Gomeza V, Guglieri M, Feng L, Torelli S, Anthony K, et al. Exon skipping and dystrophin restoration in patients with Duchenne muscular dystrophy after systemic phosphorodiamidate morpholino oligomer treatment: an open-label, phase 2, dose-escalation study. Lancet (London, England) 2011; 378: 595–605.

Clapham DE, Abzhanov A, Kuo WP, Hartmann C, Grant BR, Grant PR, et al. Calcium signaling. Cell 2007; 131: 1047–58.

Clem RJ. Baculoviruses and apoptosis: the good, the bad, and the ugly. Cell Death Differ 2001; 8: 137–143.

Colomer Gould VF, Goti D, Pearce D, Gonzalez GA, Gao H, Bermudez de Leon M, et al. A mutant ataxin-3 fragment results from processing at a site N-terminal to amino acid 190 in brain of Machado-Joseph disease-like transgenic mice. Neurobiol. Dis. 2007; 27: 362–9.

Contestabile A. Benefits of caloric restriction on brain aging and related pathological States: understanding mechanisms to devise novel therapies. Curr. Med. Chem. 2009; 16: 350–61.

Cooper JK, Schilling G, Peters MF, Herring WJ, Sharp AH, Kaminsky Z, et al. Truncated N-terminal fragments of huntingtin with expanded glutamine repeats form nuclear and cytoplasmic aggregates in cell culture. Hum. Mol. Genet. 1998; 7: 783–790.

Cornett J, Cao F, Wang C-E, Ross CA, Bates GP, Li S-H, et al. Polyglutamine expansion of huntingtin impairs its nuclear export. Nat. Genet. Publ. online 16 January 2005; | doi10.1038/ng1503 2005; 37: 198.

Corraini P, Henderson VW, Ording AG, Pedersen L, Horváth-Puhó E, Sørensen HT. Long-Term Risk of Dementia Among Survivors of Ischemic or Hemorrhagic Stroke. Stroke 2016

Costanzo M, Zurzolo C. The cell biology of prion-like spread of protein aggregates: mechanisms and implication in neurodegeneration. Biochem. J. 2013; 452: 1–17.

Coutinho P, Andrade C. Autosomal dominant system degeneration in Portuguese families of the Azores Islands. A new genetic disorder involving cerebellar, pyramidal, extrapyramidal and spinal cord motor functions. Neurology 1978; 28: 703–9.

Cowan CM, Fan MMY, Fan J, Shehadeh J, Zhang LYJ, Graham RK, et al. Polyglutamine-Modulated Striatal Calpain Activity in YAC Transgenic Huntington Disease Mouse Model: Impact on NMDA Receptor Function and Toxicity. J. Neurosci. 2008; 28: 12725–12735.

Cuervo AM. Autophagy and aging: keeping that old broom working. Trends Genet. 2008; 24: 604–12.

Culver BP, Savas JN, Park SK, Choi JH, Zheng S, Zeitlin SO, et al. Proteomic analysis of wild-type and mutant huntingtin-associated proteins in mouse brains identifies unique interactions and involvement in protein synthesis. J. Biol. Chem. 2012; 287: 21599–614.

Cunnane S, Nugent S, Roy M, Courchesne-Loyer A, Croteau E, Tremblay S, et al. Brain fuel metabolism, aging, and Alzheimer's disease. Nutrition 2011; 27: 3–20.

Czeredys M, Gruszczynska-Biegala J, Schacht T, Methner A, Kuznicki J. Expression of genes encoding the calcium signalosome in cellular and transgenic models of Huntington's disease. Front. Mol. Neurosci. 2013; 6: 42.

Dau A, Gladding CM, Sepers MD, Raymond L a. Chronic blockade of extrasynaptic NMDA receptors ameliorates synaptic dysfunction and pro-death signaling in Huntington disease transgenic mice. Neurobiol. Dis. 2014; 62: 533–42.

Davies SW, Turmaine M, Cozens B a, DiFiglia M, Sharp a H, Ross C a, et al. Formation of neuronal intranuclear inclusions underlies the neurological dysfunction in mice transgenic for the HD mutation. Cell 1997; 90: 537–48.

Dayton WR, Goll DE, Zeece MG, Robson RM, Reville WJ. A Ca2+-activated protease possibly involved in myofibrillar protein turnover. Purification from porcine muscle. Biochemistry 1976; 15: 2150–8.

Degterev A, Boyce M, Yuan J. A decade of caspases. Oncogene 2003; 22: 8543–8567.

Deleidi M, Jäggle M, Rubino G. Immune aging, dysmetabolism, and inflammation in neurological diseases. Front. Neurosci. 2015; 9: 172.

van Dellen A, Welch J, Dixon RM, Cordery P, York D, Styles P, et al. N-Acetylaspartate and DARPP-32 levels decrease in the corpus striatum of Huntington's disease mice. Neuroreport 2000; 11: 3751–7.

Denecker G, Ovaere P, Vandenabeele P, Declercq W. Caspase-14 reveals its secrets. J. Cell Biol. 2008; 180: 451–8.

Dessaud E, André C, Scherrer B, Berna P, Pruss R, Cuvier V, et al. A Phase II study to assess safety and efficacy of olesoxime (TRO19622) in 3-25 year-old Spinal Muscular Atrophy (SMA) patients. Neuromuscul. Disord. 2014; 24: 920–921.

Diepenbroek M, Casadei N, Esmer H, Saido TC, Takano J, Kahle PJ, et al. Over expression of the calpain-specific inhibitor calpastatin reduces human alpha-Synuclein processing, aggregation and synaptic impairment in [A30P]αSyn transgenic mice. Hum. Mol. Genet. 2014; 23: 3975–3989.

Dietrich P, Johnson IM, Alli S, Dragatsis I. Elimination of huntingtin in the adult mouse leads to progressive behavioral deficits, bilateral thalamic calcification, and altered brain iron homeostasis. PLOS Genet. 2017; 13: e1006846.

DiFiglia M, Sapp E, Chase K, Schwarz C, Meloni A, Young C, et al. Huntingtin is a cytoplasmic protein associated with vesicles in human and rat brain neurons. Neuron 1995; 14: 1075–81.

DiFiglia M, Sapp E, Chase KO, Davies SW, Bates GP, Vonsattel JP, et al. Aggregation of huntingtin in neuronal intranuclear inclusions and dystrophic neurites in brain. Science 1997; 277: 1990–3.

Doherty GH. Obesity and the Ageing Brain: Could Leptin Play a Role in Neurodegeneration? Curr. Gerontol. Geriatr. Res. 2011; 2011: 1–8.

Dong X, Wang Y, Qin Z. Molecular mechanisms of excitotoxicity and their relevance to pathogenesis of neurodegenerative diseases. Acta Pharmacol. Sin. 2009; 30: 379–387.

Donkor IO. Calpain inhibitors: a survey of compounds reported in the patent and scientific literature. Expert Opin. Ther. Pat. 2011; 21: 601–636.

Dorsey ER, Constantinescu R, Thompson JP, Biglan KM, Holloway RG, Kieburtz K, et al. Projected number of people with Parkinson disease in the most populous nations, 2005 through 2030. Neurology 2007; 68: 384–386.

Doss-Pepe EW, Stenroos ES, Johnson WG, Madura K. Ataxin-3 Interactions with Rad23 and Valosin-Containing Protein and Its Associations with Ubiquitin Chains and the Proteasome Are Consistent with a Role in Ubiquitin-Mediated Proteolysis. Mol. Cell. Biol. 2003; 23: 6469–6483.

Doucet A, Overall CM. Broad coverage identification of multiple proteolytic cleavage site sequences in complex high molecular weight proteins using quantitative proteomics as a complement to edman sequencing. Mol. Cell. Proteomics 2011; 10: M110.003533.

Dragatsis I, Levine MS, Zeitlin S. Inactivation of Hdh in the brain and testis results in progressive neurodegeneration and sterility in mice. Nat. Genet. 2000; 26: 300–306.

Du H, Guo L, Yan S, Sosunov AA, McKhann GM, Yan SS. Early deficits in synaptic mitochondria in an Alzheimer's disease mouse model. Proc. Natl. Acad. Sci. U. S. A. 2010; 107: 18670–5.

Duarte JV, Faustino R, Lobo M, Cunha G, Nunes C, Ferreira C, et al. Parametric fMRI of paced motor responses uncovers novel whole-brain imaging biomarkers in spinocerebellar ataxia type 3. Hum. Brain Mapp. 2016; 37: 3656–3668.

Dufty BM, Warner LR, Hou ST, Jiang SX, Gomez-Isla T, Leenhouts KM, et al. Calpain-cleavage of alpha-synuclein: connecting proteolytic processing to disease-linked aggregation. Am. J. Pathol. 2007; 170: 1725–1738.

Dulhunty AF. Excitation-contraction coupling from the 1950s into the new millennium. Clin. Exp. Pharmacol.

Physiol. 2006; 33: 763–772.

Durcan TM, Fon EA. Ataxin-3 and its E3 partners: Implications for Machado-Joseph disease. Front. Neurol. 2013; 4 MAY: 46.

Durcan TM, Fon EA. The three 'P's of mitophagy: PARKIN, PINK1, and post-translational modifications. Genes Dev. 2015; 29: 989–999.

Durcan TM, Kontogiannea M, Bedard N, Wing SS, Fon E a. Ataxin-3 deubiquitination is coupled to parkin ubiquitination via E2 ubiquitin-conjugating enzyme. J. Biol. Chem. 2012; 287: 531–541.

Durcan TM, Kontogiannea M, Thorarinsdottir T, Fallon L, Williams AJ, Djarmati A, et al. The machado-joseph disease-associated mutant form of ataxin-3 regulates parkin ubiquitination and stability. Hum. Mol. Genet. 2011; 20: 141–154.

Dürr A, Stevanin G, Cancel G, Duyckaerts C, Abbas N, Didierjean O, et al. Spinocerebellar ataxia 3 and Machado-Joseph disease: Clinical, molecular, and neuropathological features. Ann. Neurol. 1996; 39: 490–499.

Dutta R, McDonough J, Yin X, Peterson J, Chang A, Torres T, et al. Mitochondrial dysfunction as a cause of axonal degeneration in multiple sclerosis patients. Ann. Neurol. 2006; 59: 478–489.

DuVerle DA, Ono Y, Sorimachi H, Mamitsuka H. Calpain cleavage prediction using multiple kernel learning. PLoS One 2011; 6: e19035.

Duyao M, Ambrose C, Myers R, Novelletto A, Persichetti F, Frontali M, et al. Trinucleotide repeat length instability and age of onset in Huntington's disease. Nat. Genet. 1993; 4: 387–392.

Duyao MP, Auerbach AB, Ryan A, Persichetti F, Barnes GT, McNeil SM, et al. Inactivation of the mouse Huntington's disease gene homolog Hdh. Science 1995; 269: 407–10.

Eckmann J, Clemens LE, Eckert SH, Hagl S, Yu-Taeger L, Bordet T, et al. Mitochondrial Membrane Fluidity is Consistently Increased in Different Models of Huntington Disease: Restorative Effects of Olesoxime. Mol. Neurobiol. 2014

Edman P. Method for determination of the amino acid sequence in peptides. Acta Chem. Scand. 1950; 4: 283–293.

Ehrnhoefer DE, Butland SL, Pouladi MA, Hayden MR. Mouse models of Huntington disease: variations on a theme. Dis. Model. Mech. 2009; 2: 123–9.

Ehrnhoefer DE, Sutton L, Hayden MR. Small changes, big impact: posttranslational modifications and function of huntingtin in Huntington disease. Neuroscientist 2011; 17: 475–92.

El-Daher M-T, Hangen E, Bruyère J, Poizat G, Al-Ramahi I, Pardo R, et al. Huntingtin proteolysis releases non-polyQ fragments that cause toxicity through dynamin 1 dysregulation. EMBO J. 2015; 34: 2255–71.

Elden AC, Kim H-J, Hart MP, Chen-Plotkin AS, Johnson BS, Fang X, et al. Ataxin-2 intermediate-length polyglutamine expansions are associated with increased risk for ALS. Nature 2010; 466: 1069–1075.

Epel ES. Psychological and metabolic stress: A recipe for accelerated cellular aging? Hormones 2009; 8: 7–22.

Evers MM, Tran H-D, Zalachoras I, Meijer OC, den Dunnen JT, van Ommen G-JB, et al. Preventing formation of toxic N-terminal huntingtin fragments through antisense oligonucleotide-mediated protein modification. Nucleic Acid Ther. 2014; 24: 4–12.

References

Evert BO, Araujo J, Vieira-Saecker AM, de Vos RAI, Harendza S, Klockgether T, et al. Ataxin-3 Represses Transcription via Chromatin Binding, Interaction with Histone Deacetylase 3, and Histone Deacetylation. J. Neurosci. 2006; 26: 11474–11486.

Fà M, Zhang H, Staniszewski A, Saeed F, Shen LW, Schiefer IT, et al. Novel Selective Calpain 1 Inhibitors as Potential Therapeutics in Alzheimer's Disease. J. Alzheimers. Dis. 2015; Preprint: 1–15.

Faber PW, Barnes GT, Srinidhi J, Chen J, Gusella JF, MacDonald ME. Huntingtin interacts with a family of WW domain proteins. Hum. Mol. Genet. 1998; 7: 1463–1474.

Fakhouri THI, Ogden CL, Carroll MD, Kit BK, Flegal KM. Prevalence of obesity among older adults in the United States, 2007-2010. NCHS Data Brief 2012: 1–8.

Farr C, Berger S. Measuring calpain activity in fixed and living cells by flow cytometry. J. Vis. Exp. 2010: 2–5.

Farrer LA, Opitz JM, Reynolds JF. Suicide and attempted suicide in Huntington disease: Implications for preclinical testing of persons at risk. Am. J. Med. Genet. 1986; 24: 305–311.

Fei E, Jia N, Zhang T, Ma X, Wang H, Liu C, et al. Phosphorylation of ataxin-3 by glycogen synthase kinase 3β at serine 256 regulates the aggregation of ataxin-3. Biochem. Biophys. Res. Commun. 2007; 357: 487–492.

Feigin A, Leenders KL, Moeller JR, Missimer J, Kuenig G, Spetsieris P, et al. Metabolic network abnormalities in early Huntington's disease: an [(18)F]FDG PET study. J. Nucl. Med. 2001; 42: 1591–5.

Ferreira A, Adriana. Calpain Dysregulation in Alzheimer's Disease. ISRN Biochem. 2012; 2012: 1–12.

Ferro A, Carvalho AL, Teixeira-Castro A, Almeida C, Tomé RJ, Cortes L, et al. NEDD8: A new ataxin-3 interactor. Biochim. Biophys. Acta - Mol. Cell Res. 2007; 1773: 1619–1627.

Fink K, Zhu J, Namura S, Shimizu-Sasamata M, Endres M, &NA; J, et al. Prolonged Therapeutic Window for Ischemic Brain Damage Caused by Delayed Caspase Activation. J. Cereb. Blood Flow Metab. 1998; 18: 1071–1076.

Fiorino F, Gil-Parrado S, Assfalg-Machleidt I, Machleidt W, Moroder L. A new cell-permeable calpain inhibitor. J. Pept. Sci. 2007; 13: 70–73.

Forette F, Seux ML, Staessen JA, Thijs L, Birkenhäger WH, Babarskiene MR, et al. Prevention of dementia in randomised double-blind placebo-controlled Systolic Hypertension in Europe (Syst-Eur) trial. Lancet (London, England) 1998; 352: 1347–51.

Forman OP, De Risio L, Mellersh CS, Guttman M, Lander E. Missense Mutation in CAPN1 Is Associated with Spinocerebellar Ataxia in the Parson Russell Terrier Dog Breed. PLoS One 2013; 8: e64627.

Franceschi C, Capri M, Monti D, Giunta S, Olivieri F, Sevini F, et al. Inflammaging and anti-inflammaging: A systemic perspective on aging and longevity emerged from studies in humans. Mech. Ageing Dev. 2007; 128: 92–105.

Frank-Cannon TC, Alto LT, McAlpine FE, Tansey MG, Rivest S, Crutcher K, et al. Does neuroinflammation fan the flame in neurodegenerative diseases? Mol. Neurodegener. 2009; 4: 47.

Fratiglioni L, Paillard-Borg S, Winblad B. An active and socially integrated lifestyle in late life might protect against dementia. Lancet Neurol. 2004; 3: 343–353.

Fratiglioni L, Qiu C. Prevention of common neurodegenerative disorders in the elderly. Exp. Gerontol. 2009; 44:

46–50.

Friedlander RM. Apoptosis and Caspases in Neurodegenerative Diseases. N. Engl. J. Med. 2003; 348: 1365–1375.

Friedman MJ, Wang C-EE, Li X-JJ, Li S. Polyglutamine expansion reduces the association of TATA-binding protein with DNA and induces DNA binding-independent neurotoxicity. J. Biol. Chem. 2008; 283: 8283–90.

Friese MA, Schattling B, Fugger L. Mechanisms of neurodegeneration and axonal dysfunction in multiple sclerosis. Nat. Rev. Neurol. 2014; 10: 225.

Gafni J, Ellerby LM. Calpain activation in Huntington's disease. J. Neurosci. 2002; 22: 4842–9.

Gafni J, Hermel E, Young JE, Wellington CL, Hayden MR, Ellerby LM. Inhibition of calpain cleavage of Huntingtin reduces toxicity: Accumulation of calpain/caspase fragments in the nucleus. J. Biol. Chem. 2004; 279: 20211–20220.

García de la Cadena S, Massieu L. Caspases and their role in inflammation and ischemic neuronal death. Focus on caspase-12. Apoptosis 2016; 21: 763–777.

Garden GA, Libby RT, Fu Y-H, Kinoshita Y, Huang J, Possin DE, et al. Polyglutamine-expanded ataxin-7 promotes non-cell-autonomous purkinje cell degeneration and displays proteolytic cleavage in ataxic transgenic mice. J. Neurosci. 2002; 22: 4897–905.

Garg S, Timm T, Mandelkow EM, Mandelkow E, Wang Y. Cleavage of Tau by calpain in Alzheimer's disease: The quest for the toxic 17 kD fragment. Neurobiol. Aging 2011; 32: 1–14.

Gasteiger E, Hoogland C, Gattiker A, Duvaud S, Wilkins M, Appel R, et al. Protein Identification and Analysis Tools on the ExPASy Server. Proteomics Protoc. Handb. 2005: 571–607.

Gatliff J, Campanella M. The 18 kDa translocator protein (TSPO): a new perspective in mitochondrial biology. Curr. Mol. Med. 2012; 12: 356–68.

Gauthier LR, Charrin BC, Borrell-Pagès M, Dompierre JP, Rangone H, Cordelières FP, et al. Huntingtin controls neurotrophic support and survival of neurons by enhancing BDNF vesicular transport along microtubules. Cell 2004; 118: 127–138.

Geraghty RJ, Capes-Davis A, Davis JM, Downward J, Freshney RI, Knezevic I, et al. Guidelines for the use of cell lines in biomedical research. Br. J. Cancer 2014; 111: 1021–46.

Gil-Parrado S, Assfalg-Machleidt I, Fiorino F, Deluca D, Pfeiler D, Schaschke N, et al. Calpastatin Exon 1B-Derived Peptide, a Selective Inhibitor of Calpain: Enhancing Cell Permeability by Conjugation with Penetratin. Biol. Chem. 2003; 384: 395–402.

Gladding CM, Fan J, Zhang LYJ, Wang L, Xu J, Li EHY, et al. Alterations in STriatal-Enriched protein tyrosine Phosphatase expression, activation, and downstream signaling in early and late stages of the YAC128 Huntington's disease mouse model. J. Neurochem. 2014; 130: 1–15.

Gladding CM, Sepers MD, Xu J, Zhang LYJ, Milnerwood AJ, Lombroso PJ, et al. Calpain and STriatal-Enriched protein tyrosine phosphatase (STEP) activation contribute to extrasynaptic NMDA receptor localization in a Huntington's disease mouse model. Hum. Mol. Genet. 2012; 21: 3739–52.

Glass CK, Saijo K, Winner B, Marchetto MC, Gage FH. Mechanisms underlying inflammation in

neurodegeneration. Cell 2010; 140: 918–34.

Goedert M, Spillantini MG. Lewy body diseases and multiple system atrophy as alpha-synucleinopathies. Mol. Psychiatry 1998; 3: 462–5.

Goehler H, Lalowski M, Stelzl U, Waelter S, Stroedicke M, Worm U, et al. A Protein Interaction Network Links GIT1, an Enhancer of Huntingtin Aggregation, to Huntington's Disease. Mol. Cell 2004; 15: 853–865.

Goffredo D, Rigamonti D, Tartari M, De Micheli A, Verderio C, Matteoli M, et al. Calcium-dependent cleavage of endogenous wild-type huntingtin in primary cortical neurons. J. Biol. Chem. 2002; 277: 39594–8.

Gold M, Koczulla AR, Mengel D, Koepke J, Dodel R, Dontcheva G, et al. Reduction of glutamate-induced excitotoxicity in murine primary neurons involving calpain inhibition. J. Neurol. Sci. 2015; 359: 356–362.

Goldberg YP, Nicholson DW, Rasper DM, Kalchman MA, Koide HB, Graham RK, et al. Cleavage of huntingtin by apopain, a proapoptotic cysteine protease, is modulated by the polyglutamine tract. Nat. Genet. 1996; 13: 442–9.

Goldsteins G, Keksa-Goldsteine V, Ahtoniemi T, Jaronen M, Arens E, Akerman K, et al. Deleterious Role of Superoxide Dismutase in the Mitochondrial Intermembrane Space. J. Biol. Chem. 2008; 283: 8446–8452.

Goll DE, Thompson VF, Li H, Wei W, Cong J. The calpain system. Physiol. Rev. 2003; 83: 731–801.

Goñi-Oliver P, Avila J, Hernández F. Memantine inhibits calpain-mediated truncation of GSK-3 induced by NMDA: implications in Alzheimer's disease. J. Alzheimers. Dis. 2009; 18: 843–8.

Goti D, Katzen SM, Mez J, Kurtis N, Kiluk J, Ben-Haïem L, et al. A Mutant Ataxin-3 Putative-Cleavage Fragment in Brains of Machado-Joseph Disease Patients and Transgenic Mice Is Cytotoxic above a Critical Concentration. J. Neurosci. 2004; 24: 10266–10279.

Goto J, Watanabe M, Ichikawa Y, Yee SB, Ihara N, Endo K, et al. Machado-Joseph disease gene products carrying different carboxyl termini. Neurosci. Res. 1997; 28: 373–7.

Gouarné C, Tracz J, Paoli MG, Deluca V, Seimandi M, Tardif G, et al. Protective role of olesoxime against wild-type α-synuclein-induced toxicity in human neuronally differentiated SHSY-5Y cells. Br. J. Pharmacol. 2015; 172: 235–245.

Gräff J, Kahn M, Samiei A, Gao J, Ota KT, Rei D, et al. A dietary regimen of caloric restriction or pharmacological activation of SIRT1 to delay the onset of neurodegeneration. J. Neurosci. 2013; 33: 8951–60.

Graham RK, Deng Y, Carroll J, Vaid K, Cowan C, Pouladi MA, et al. Cleavage at the 586 amino acid caspase-6 site in mutant huntingtin influences caspase-6 activation in vivo. J. Neurosci. 2010; 30: 15019–29.

Graham RK, Deng Y, Slow EJ, Haigh B, Bissada N, Lu G, et al. Cleavage at the caspase-6 site is required for neuronal dysfunction and degeneration due to mutant huntingtin. Cell 2006; 125: 1179–91.

Graham RK, Pouladi MA, Joshi P, Lu G, Deng Y, Wu N-P, et al. Differential Susceptibility to Excitotoxic Stress in YAC128 Mouse Models of Huntington Disease between Initiation and Progression of Disease. J. Neurosci. 2009; 29: 2193–2204.

Gray DA. Lipofuscin and Aging: A Matter of Toxic Waste. Sci. Aging Knowl. Environ. 2005; 2005: re1-re1.

Gray M, Shirasaki DI, Cepeda C, André VM, Wilburn B, Lu X-H, et al. Full-length human mutant huntingtin with a stable polyglutamine repeat can elicit progressive and selective neuropathogenesis in BACHD mice. J. Neurosci. 2008; 28: 6182–95.

Guégan C, Vila M, Rosoklija G, Hays a P, Przedborski S. Recruitment of the mitochondrial-dependent apoptotic pathway in amyotrophic lateral sclerosis. J. Neurosci. 2001; 21: 6569–6576.

Guicciardi ME, Gores GJ. Life and death by death receptors. FASEB J. 2009; 23: 1625–37.

Guillemin GJ. Quinolinic acid, the inescapable neurotoxin. FEBS J. 2012; 279: 1356–1365.

Gunawardena S, Her L-S, Brusch RG, Laymon RA, Niesman IR, Gordesky-Gold B, et al. Disruption of axonal transport by loss of huntingtin or expression of pathogenic polyQ proteins in Drosophila. Neuron 2003; 40: 25–40.

Guroff G. A Neutral, Calcium-activated Proteinase from the Soluble Fraction of Rat Brain. J. Biol. Chem. 1964; 239: 149–55.

Gusella JF, MacDonald ME. Huntingtin: a single bait hooks many species. Curr. Opin. Neurobiol. 1998; 8: 425–30.

Gusella JF, MacDonald ME. Molecular genetics: unmasking polyglutamine triggers in neurodegenerative disease. Nat. Rev. Neurosci. 2000; 1: 109–115.

Gutekunst CA, Levey AI, Heilman CJ, Whaley WL, Yi H, Nash NR, et al. Identification and localization of huntingtin in brain and human lymphoblastoid cell lines with anti-fusion protein antibodies. Proc. Natl. Acad. Sci. U. S. A. 1995; 92: 8710–4.

Gutekunst CA, Li SH, Yi H, Mulroy JS, Kuemmerle S, Jones R, et al. Nuclear and neuropil aggregates in Huntington's disease: relationship to neuropathology. J. Neurosci. 1999; 19: 2522–34.

Haacke A, Broadley S a., Boteva R, Tzvetkov N, Hartl FU, Breuer P. Proteolytic cleavage of polyglutamine-expanded ataxin-3 is critical for aggregation and sequestration of non-expanded ataxin-3. Hum. Mol. Genet. 2006; 15: 555–68.

Haacke A, Hartl FU, Breuer P. Calpain inhibition is sufficient to suppress aggregation of polyglutamine-expanded ataxin-3. J. Biol. Chem. 2007; 282: 18851–6.

Hackam AS, Hodgson JG, Singaraja R, Zhang T, Gan L, Gutekunst C, et al. Evidence for both the nucleus and cytoplasm as subcellular sites of pathogenesis in Huntington â€^{TM} s disease in cell culture and in transgenic mice expressing mutant huntingtin. Mol. Med. 1999; 8: 1047–1056.

Hackam AS, Singaraja R, Wellington CL, Metzler M, McCutcheon K, Zhang T, et al. The influence of huntingtin protein size on nuclear localization and cellular toxicity. J. Cell Biol. 1998; 141: 1097–1105.

Halliday GM, McRitchie DA, Macdonald V, Double KL, Trent RJ, McCusker E. Regional Specificity of Brain Atrophy in Huntington's Disease. Exp. Neurol. 1998; 154: 663–672.

Hanger DP, Wray S. Tau cleavage and tau aggregation in neurodegenerative disease. Biochem. Soc. Trans. 2010; 38

Hanna RA, Campbell RL, Davies PL. Calcium-bound structure of calpain and its mechanism of inhibition by calpastatin. Nature 2008; 456: 409–412.

Hanouna G, Mesnard L, Vandermeersch S, Perez J, Placier S, Haymann J-P, et al. Specific calpain inhibition protects kidney against inflammaging. Sci. Rep. 2017; 7: 8016.

Hansen SK, Stummann TC, Borland H, Hasholt LF, Tümer Z, Nielsen JE, et al. Induced pluripotent stem cell - derived neurons for the study of spinocerebellar ataxia type 3. Stem Cell Res. 2016; 17: 306–317.

Hara H, Friedlander RM, Gagliardini V, Ayata C, Fink K, Huang Z, et al. Inhibition of interleukin 1beta converting enzyme family proteases reduces ischemic and excitotoxic neuronal damage. Proc. Natl. Acad. Sci. U. S. A. 1997; 94: 2007–12.

Harper S. Economic and social implications of aging societies. Science (80-.). 2014; 346: 587–591.

Harris GM, Dodelzon K, Gong L, Gonzalez-Alegre P, Paulson HL. Splice Isoforms of the Polyglutamine Disease Protein Ataxin-3 Exhibit Similar Enzymatic yet Different Aggregation Properties. PLoS One 2010; 5: e13695.

Hartmann A, Troadec JD, Hunot S, Kikly K, Faucheux BA, Mouatt-Prigent A, et al. Caspase-8 is an effector in apoptotic death of dopaminergic neurons in Parkinson's disease, but pathway inhibition results in neuronal necrosis. J. Neurosci. 2001; 21: 2247–55.

Hayashi T, Su TP. Sigma-1 Receptor Chaperones at the ER- Mitochondrion Interface Regulate Ca2+ Signaling and Cell Survival. Cell 2007; 131: 596–610.

Hazeki N, Tukamoto T, Goto J, Kanazawa I. Formic acid dissolves aggregates of an N-terminal huntingtin fragment containing an expanded polyglutamine tract: applying to quantification of protein components of the aggregates. Biochem. Biophys. Res. Commun. 2000; 277: 386–393.

He C, Klionsky DJ. Regulation mechanisms and signaling pathways of autophagy. Annu. Rev. Genet. 2009; 43: 67–93.

Heemskerk AW, Roos RAC. Aspiration pneumonia and death in Huntington's disease. PLoS Curr. 2012; 4: RRN1293.

Heidenreich M, Zhang F. Applications of CRISPR–Cas systems in neuroscience. Nat. Rev. Neurosci. 2015; 17: 36–44.

Henchcliffe C, Beal MF. Mitochondrial biology and oxidative stress in Parkinson disease pathogenesis. Nat. Clin. Pract. Neurol. 2008; 4: 600–609.

Hilditch-Maguire P, Trettel F, Passani LA, Auerbach A, Persichetti F, MacDonald ME. Huntingtin: an iron-regulated protein essential for normal nuclear and perinuclear organelles. Hum. Mol. Genet. 2000; 9: 2789–97.

Hindle J V. Ageing, neurodegeneration and Parkinson's disease. Age Ageing 2010; 39: 156–161.

Hirao T, Takahashi K. Purification and characterization of a calcium-activated neutral protease from monkey brain and its action on neuropeptides. J. Biochem. 1984; 96: 775–84.

Hiwasa T, Sawada T, Sakiyama S. Cysteine proteinase inhibitors and ras gene products share the same biological activities including tranforming activity toward NIH3T3 mouse fibroblasts and the differentiation-inclucing activity toward PC12 rat pheochromocytoma cells. Carcinogenesis 1990; 11: 75–80.

Hjerkind KV, Stenehjem JS, Nilsen TIL. Adiposity, physical activity and risk of diabetes mellitus: prospective data from the population-based HUNT study, Norway. BMJ Open 2017; 7: e013142.

Ho LW, Brown R, Maxwell M, Wyttenbach A, Rubinsztein DC. Wild type Huntingtin reduces the cellular toxicity of mutant Huntingtin in mammalian cell models of Huntington's disease. J. Med. Genet. 2001; 38: 450–2.

Hoffner G, Kahlem P, Djian P. Perinuclear localization of huntingtin as a consequence of its binding to microtubules through an interaction with beta-tubulin: relevance to Huntington's disease. J. Cell Sci. 2002; 115: 941–948.

Holbert S, Denghien I, Kiechle T, Rosenblatt A, Wellington C, Hayden MR, et al. The Gln-Ala repeat transcriptional activator CA150 interacts with huntingtin: Neuropathologic and genetic evidence for a role in Huntington's disease pathogenesis. Proc. Natl. Acad. Sci. 2001; 98: 1811–1816.

Honarnejad K, Herms J. Presenilins: Role in calcium homeostasis. Int. J. Biochem. Cell Biol. 2012; 44: 1983–1986.

Horikawa Y, Oda N, Cox NJ, Li X, Orho-Melander M, Hara M, et al. Genetic variation in the gene encoding calpain-10 is associated with type 2 diabetes mellitus. Nat. Genet. 2000; 26: 163–175.

Howley B, Fearnhead HO. Caspases as therapeutic targets. J. Cell. Mol. Med. 2008; 12: 1502–1516.

Hroudová J, Singh N, Fišar Z. Mitochondrial dysfunctions in neurodegenerative diseases: relevance to Alzheimer's disease. Biomed Res. Int. 2014; 2014: 175062.

Hu FB, Manson JE, Stampfer MJ, Colditz G, Liu S, Solomon CG, et al. Diet, Lifestyle, and the Risk of Type 2 Diabetes Mellitus in Women. N. Engl. J. Med. 2001; 345: 790–797.

Hübener J, Riess O. Polyglutamine-induced neurodegeneration in SCA3 is not mitigated by non-expanded ataxin-3: Conclusions from double-transgenic mouse models. Neurobiol. Dis. 2010; 38: 116–124.

Hübener J, Vauti F, Funke C, Wolburg H, Ye Y, Schmidt T, et al. N-terminal ataxin-3 causes neurological symptoms with inclusions, endoplasmic reticulum stress and ribosomal dislocation. Brain 2011; 134: 1925–42.

Huntington G. On chorea. George Huntington, M.D. J. Neuropsychiatry Clin. Neurosci. 2003; 15: 109–12.

Huynh DP, Figueroa K, Hoang N, Pulst SM. Nuclear localization or inclusion body formation of ataxin-2 are not necessary for SCA2 pathogenesis in mouse or human. Nat. Genet. 2000; 26: 44–50.

Hyman BT, Yuan J. Apoptotic and non-apoptotic roles of caspases in neuronal physiology and pathophysiology. Nat. Rev. Neurosci. 2012; 13: 395–406.

Hyrskyluoto A, Pulli I, Törnqvist K, Huu Ho T, Korhonen L, Lindholm D. Sigma-1 receptor agonist PRE084 is protective against mutant huntingtin-induced cell degeneration: involvement of calpastatin and the NF-κB pathway. Cell Death Dis. 2013; 4: e646.

Iacopino AM, Christakos S. Specific reduction of calcium-binding protein (28-kilodalton calbindin-D) gene expression in aging and neurodegenerative diseases. Proc. Natl. Acad. Sci. U. S. A. 1990; 87: 4078–82.

Igarashi S, Morita H, Bennett KM, Tanaka Y, Engelender S, Peters MF, et al. Inducible PC12 cell model of Huntington's disease shows toxicity and decreased histone acetylation. Neuroreport 2003; 14: 565–8.

Ikeda H, Yamaguchi M, Sugai S, Aze Y, Narumiya S, Kakizuka A. Expanded polyglutamine in the Machado-Joseph disease protein induces cell death in vitro and in vivo. Nat. Genet. 1996; 13: 196–202.

Ismailoglu I, Chen Q, Popowski M, Yang L, Gross SS, Brivanlou AH. Huntingtin protein is essential for mitochondrial metabolism, bioenergetics and structure in murine embryonic stem cells. Dev. Biol. 2014; 391: 230–240.

Jana NR, Zemskov E a, Wang Gh, Nukina N. Altered proteasomal function due to the expression of polyglutamine-expanded truncated N-terminal huntingtin induces apoptosis by caspase activation through mitochondrial cytochrome c release. Hum. Mol. Genet. 2001; 10: 1049–59.

Ji J, Su L, Liu Z. Critical role of calpain in inflammation. Biomed. reports 2016; 5: 647–652.

Jiang H, Nucifora FC, Ross CA, DeFranco DB. Cell death triggered by polyglutamine-expanded huntingtin in a neuronal cell line is associated with degradation of CREB-binding protein. Hum. Mol. Genet. 2003; 12: 1–12.

Jiang M, Wang J, Fu J, Du L, Jeong H, West T, et al. Neuroprotective role of Sirt1 in mammalian models of Huntington's disease through activation of multiple Sirt1 targets. Nat. Med. 2012; 18: 153–158.

Jucker M. The benefits and limitations of animal models for translational research in neurodegenerative diseases. Nat. Med. 2010; 16: 1210–1214.

Jung J, Xu K, Lessing D, Bonini NM. Preventing Ataxin-3 protein cleavage mitigates degeneration in a Drosophila model of SCA3. Hum. Mol. Genet. 2009; 18: 4843–52.

Jung T, Bader N, Grune T. Lipofuscin: Formation, distribution, and metabolic consequences. In: Annals of the New York Academy of Sciences. 2007. p. 97–111.

Kabeya Y, Mizushima N, Ueno T, Yamamoto A, Kirisako T, Noda T, et al. LC3, a mammalian homologue of yeast Apg8p, is localized in autophagosome membranes after processing. EMBO J. 2000; 19: 5720–5728.

Kabeya Y, Mizushima N, Yamamoto A, Oshitani-Okamoto S, Ohsumi Y, Yoshimori T. LC3, GABARAP and GATE16 localize to autophagosomal membrane depending on form-II formation. J. Cell Sci. 2004; 117: 2805–2812.

Kalchman MA, Koide HB, McCutcheon K, Graham RK, Nichol K, Nishiyama K, et al. HIP1, a human homologue of S. cerevisiae Sla2p, interacts with membrane-associated huntingtin in the brain. Nat. Genet. 1997; 16: 44–53.

Kaushik S, Bandyopadhyay U, Sridhar S, Kiffin R, Martinez-Vicente M, Kon M, et al. Chaperone-mediated autophagy at a glance. J. Cell Sci. 2011; 124: 495–499.

Kawaguchi Y, Okamoto T, Taniwaki M, Aizawa M, Inoue M, Katayama S, et al. CAG expansions in a novel gene for Machado-Joseph disease at chromosome 14q32.1. Nat. Genet. 1994; 8: 221–228.

Kawai Y, Takeda A, Abe Y, Washimi Y, Tanaka F, Sobue G. Cognitive impairments in Machado-Joseph disease. Arch. Neurol. 2004; 61: 1757–60.

Kazantsev A, Preisinger E, Dranovsky A, Goldgaber D, Housman D. Insoluble detergent-resistant aggregates form between pathological and nonpathological lengths of polyglutamine in mammalian cells. Proc. Natl. Acad. Sci. U. S. A. 1999; 96: 11404–9.

Khachaturian ZS. Calcium hypothesis of Alzheimer's disease and brain aging. Ann. N. Y. Acad. Sci. 1994; 747: 1–11.

Kikis EA, Gidalevitz T, Morimoto RI. Protein homeostasis in models of aging and age-related conformational disease. Adv. Exp. Med. Biol. 2010; 694: 138–59.

Killoran A, Biglan KM, Jankovic J, Eberly S, Kayson E, Oakes D, et al. Characterization of the Huntington intermediate CAG repeat expansion phenotype in PHAROS. Neurology 2013; 80: 2022–2027.

Kim KA, Lee YA, Shin MH. Calpain-dependent calpastatin cleavage regulates caspase-3 activation during apoptosis of Jurkat T cells induced by Entamoeba histolytica. Int. J. Parasitol. 2007; 37: 1209–1219.

Kim M, Roh J-K, Yoon BW, Kang L, Kim YJ, Aronin N, et al. Huntingtin is degraded to small fragments by calpain after ischemic injury. Exp. Neurol. 2003; 183: 109–15.

Kim SC, Chung JY, Im W, Kim M, Kim M. Calpain cleaved-55kDa N-terminal huntingtin delocalizes from neurons

to astrocytes after ischemic injury. Cell. Mol. Biol. (Noisy-le-grand). 2011; 57 Suppl: OL1534-42.

Kim YJ, Yi Y, Sapp E, Wang Y, Cuiffo B, Kegel KB, et al. Caspase 3-cleaved N-terminal fragments of wild-type and mutant huntingtin are present in normal and Huntington's disease brains, associate with membranes, and undergo calpain-dependent proteolysis. Proc. Natl. Acad. Sci. U. S. A. 2001; 98: 12784–9.

Kindy MS, Yu J, Zhu H, El-Amouri SS, Hook V, Hook GR. Deletion of the cathepsin B gene improves memory deficits in a transgenic ALZHeimer's disease mouse model expressing AβPP containing the wild-type β-secretase site sequence. J. Alzheimers. Dis. 2012; 29: 827–40.

Kirkin V, Lamark T, Sou Y-S, Bjørkøy G, Nunn JL, Bruun J-A, et al. A Role for NBR1 in Autophagosomal Degradation of Ubiquitinated Substrates. Mol. Cell 2009; 33: 505–516.

Kirkman MS, Briscoe VJ, Clark N, Florez H, Haas LB, Halter JB, et al. Diabetes in older adults: a consensus report. J. Am. Geriatr. Soc. 2012; 60: 2342–56.

Kivipelto M, Helkala EL, Laakso MP, Hänninen T, Hallikainen M, Alhainen K, et al. Midlife vascular risk factors and Alzheimer's disease in later life: longitudinal, population based study. BMJ 2001; 322: 1447–51.

Klein C, Westenberger A. Genetics of Parkinson's disease. Cold Spring Harb. Perspect. Med. 2012; 2: a008888.

Klement IA, Skinner PJ, Kaytor MD, Yi H, Hersch SM, Clark HB, et al. Ataxin-1 nuclear localization and aggregation: role in polyglutamine-induced disease in SCA1 transgenic mice. Cell 1998; 95: 41–53.

Koch P, Breuer P, Peitz M, Jungverdorben J, Kesavan J, Poppe D, et al. Excitation-induced ataxin-3 aggregation in neurons from patients with Machado–Joseph disease. Nature 2011; 480: 543–6.

Koga H, Martinez-Vicente M, Arias E, Kaushik S, Sulzer D, Cuervo a. M. Constitutive Upregulation of Chaperone-Mediated Autophagy in Huntington's Disease. J. Neurosci. 2011; 31: 18492–18505.

Krols M, van Isterdael G, Asselbergh B, Kremer A, Lippens S, Timmerman V, et al. Mitochondria-associated membranes as hubs for neurodegeneration. Acta Neuropathol. 2016; 131: 505–523.

Kubera M, Obuchowicz E, Goehler L, Brzeszcz J. In animal models, psychosocial stress-induced (neuro)inflammation, apoptosis and reduced neurogenesis are associated to the onset of depression. Prog. Neuro-Psychopharmacology Biol. Psychiatry 2011; 35: 744–759.

Kubodera T, Yokota T, Ohwada K, Ishikawa K, Miura H, Matsuoka T, et al. Proteolytic cleavage and cellular toxicity of the human alpha1A calcium channel in spinocerebellar ataxia type 6. Neurosci. Lett. 2003; 341: 74–8.

Kuhlbrodt K, Janiesch PC, Kevei É, Segref A, Barikbin R, Hoppe T. The Machado-Joseph disease deubiquitylase ATX-3 couples longevity and proteostasis. Nat. Cell Biol. 2011; 13: 273–281.

Laço MN, Oliveira CR, Paulson HL, Rego AC. Compromised mitochondrial complex II in models of Machado–Joseph disease. Biochim. Biophys. Acta - Mol. Basis Dis. 2012; 1822: 139–149.

Lamb CA, Yoshimori T, Tooze SA. The autophagosome: origins unknown, biogenesis complex. Nat. Rev. Mol. Cell Biol. 2013; 14: 759–774.

Landles C, Sathasivam K, Weiss A, Woodman B, Moffitt H, Finkbeiner S, et al. Proteolysis of mutant huntingtin produces an exon 1 fragment that accumulates as an aggregated protein in neuronal nuclei in Huntington disease. J. Biol. Chem. 2010; 285: 8808–23.

Lang AE. Clinical trials of disease-modifying therapies for neurodegenerative diseases: the challenges and the

future. Nat. Med. 2010; 16: 1223–1226.

Langston JW, Ballard P, Tetrud JW, Irwin I. Chronic Parkinsonism in humans due to a product of meperidine-analog synthesis. Science 1983; 219: 979–80.

Lashuel HA, Overk CR, Oueslati A, Masliah E. The many faces of α-synuclein: from structure and toxicity to therapeutic target. Nat. Rev. Neurosci. 2012; 14: 38–48.

de Lau LM, Breteler MM. Epidemiology of Parkinson's disease. Lancet Neurol. 2006; 5: 525–535.

Leavitt BR, Guttman JA, Hodgson JG, Kimel GH, Singaraja R, Vogl AW, et al. Wild-Type Huntingtin Reduces the Cellular Toxicity of Mutant Huntingtin In Vivo. Am. J. Hum. Genet. 2001; 68: 313–324.

Leavitt BR, Raamsdonk JM, Shehadeh J, Fernandes H, Murphy Z, Graham RK, et al. Wild-type huntingtin protects neurons from excitotoxicity. J. Neurochem. 2006; 96: 1121–1129.

Lee CK, Weindruch R, Prolla T a. Gene-expression profile of the ageing brain in mice. Nat. Genet. 2000; 25: 294–297.

Lee E, Lee VM-Y, Trojanowski JQ. Gains or losses: molecular mechanisms of TDP43-mediated neurodegeneration. Nat. Rev. Neurosci. 2011; 13: 38–50.

Lee G, Leugers CJ. Tau and Tauopathies. In: Progress in Molecular Biology and Translational Science. NIH Public Access; 2012. p. 263–293.

Lee MS, Kwon YT, Li M, Peng J, Friedlander RM, Tsai LH. Neurotoxicity induces cleavage of p35 to p25 by calpain. Nature 2000; 405: 360–4.

Lee S-T, Chu K, Park J-E, Kang L, Ko S-Y, Jung K-H, et al. Memantine reduces striatal cell death with decreasing calpain level in 3-nitropropionic model of Huntington's disease. Brain Res. 2006; 1118: 199–207.

Lenglet T, Lacomblez L, Abitbol JL, Ludolph a., Mora JS, Robberecht W, et al. A phase II-III trial of olesoxime in subjects with amyotrophic lateral sclerosis. Eur. J. Neurol. 2014; 21: 529–536.

Lerer I, Merims D, Abeliovich D, Zlotogora J, Gadoth N. Machado-Joseph disease: correlation between the clinical features, the CAG repeat length and homozygosity for the mutation. Eur. J. Hum. Genet. 1996; 4: 3–7.

Leyva MJ, Degiacomo F, Kaltenbach LS, Holcomb J, Zhang N, Gafni J, et al. Identification and evaluation of small molecule pan-caspase inhibitors in Huntington's disease models. Chem. Biol. 2010; 17: 1189–200.

Li F, Macfarlan T, Pittman RN, Chakravarti D. Ataxin-3 is a histone-binding protein with two independent transcriptional corepressor activities. J. Biol. Chem. 2002; 277: 45004–45012.

Li H, Thompson VF, Goll DE. Effects of autolysis on properties of μ- and m-calpain. Biochim. Biophys. Acta - Mol. Cell Res. 2004; 1691: 91–103.

Li L-B, Yu Z, Teng X, Bonini NM. RNA toxicity is a component of ataxin-3 degeneration in Drosophila. Nature 2008; 453: 1107–1111.

Li S-H, Cheng AL, Zhou H, Lam S, Rao M, Li H, et al. Interaction of Huntington disease protein with transcriptional activator Sp1. Mol. Cell. Biol. 2002; 22: 1277–87.

Li S-H, Li XJ. Aggregation of N-terminal huntingtin is dependent on the length of its glutamine repeats. Hum. Mol. Genet. 1998; 7: 777–782.

Li W, Li J, Bao J. Microautophagy: lesser-known self-eating. Cell. Mol. Life Sci. 2012; 69: 1125–1136.

Li W, Serpell LC, Carter WJ, Rubinsztein DC, Huntington JA. Expression and characterization of full-length human huntingtin, an elongated HEAT repeat protein. J. Biol. Chem. 2006; 281: 15916–22.

Li W, West N, Colla E, Pletnikova O, Troncoso JC, Marsh L, et al. Aggregation promoting C-terminal truncation of alpha-synuclein is a normal cellular process and is enhanced by the familial Parkinson's disease-linked mutations. Proc. Natl. Acad. Sci. U. S. A. 2005; 102: 2162–7.

Li X-J, Li SH, Sharp AH, Nucifora FC, Schilling G, Lanahan A, et al. A huntingtin-associated protein enriched in brain with implications for pathology. Nature 1995; 378: 398–402.

Li X-J, Orr AL, Li S. Impaired mitochondrial trafficking in Huntington's disease. Biochim. Biophys. Acta - Mol. Basis Dis. 2010; 1802: 62–65.

Li X, Liu H, Fischhaber PL, Tang T-S. Toward therapeutic targets for SCA3: Insight into the role of Machado-Joseph disease protein ataxin-3 in misfolded proteins clearance. Prog. Neurobiol. 2015; 132: 34–58.

Lilienbaum A. Relationship between the proteasomal system and autophagy. Int. J. Biochem. Mol. Biol. 2013; 4: 1–26.

Lima L, Coutinho P. Clinical criteria for diagnosis of Machado-Joseph disease: report of a non-Azorena Portuguese family. Neurology 1980; 30: 319–22.

Lin MT, Beal MF. Mitochondrial dysfunction and oxidative stress in neurodegenerative diseases. Nature 2006; 443: 787–795.

Liu C-C, Liu C-C, Kanekiyo T, Xu H, Bu G. Apolipoprotein E and Alzheimer disease: risk, mechanisms and therapy. Nat. Rev. Neurol. 2013; 9: 106–18.

Liu MC, Kobeissy F, Zheng W, Zhang Z, Hayes RL, Wang KK. Dual vulnerability of tau to calpains and caspase-3 proteolysis under neurotoxic and neurodegenerative conditions. ASN Neuro 2011; 3: e00051.

Liu Y, Sun J, Wang Y, Lopez D, Tran J, Bi X, et al. Deleting both PHLPP1 and CANP1 rescues impairments in long-term potentiation and learning in both single knockout mice. Learn. Mem. 2016; 23: 399–404.

Liu YF, Deth RC, Devys D. SH3 Domain-dependent Association of Huntingtin with Epidermal Growth Factor Receptor Signaling Complexes. J. Biol. Chem. 1997; 272: 8121–8124.

Liu Z, Cao J, Gao X, Ma Q, Ren J, Xue Y. GPS-CCD: a novel computational program for the prediction of calpain cleavage sites. PLoS One 2011; 6: e19001.

Lloret A, Dragileva E, Teed A, Espinola J, Fossale E, Gillis T, et al. Genetic background modifies nuclear mutant huntingtin accumulation and HD CAG repeat instability in Huntington's disease knock-in mice. Hum. Mol. Genet. 2006; 15: 2015–2024.

Lopez D, Pinto V, Wang Y, Liu Y, Seinfeld J, Bi X, et al. Calpain-1 Knockout in Mice Causes Degeneration of Cerebellar Granule Cells and Ataxia [Internet]. FASEB J. vol. 29 no. 1 Suppl. 727.8 2015Available from: http://www.fasebj.org/content/29/1_Supplement/727.8

Lu KP, Means AR. Regulation of the cell cycle by calcium and calmodulin. Endocr. Rev. 1993; 14: 40–58.

Lu T, Pan Y, Kao S-Y, Li C, Kohane I, Chan J, et al. Gene regulation and DNA damage in the ageing human brain. Nature 2004; 429: 883–891.

Lubisch W, Beckenbach E, Bopp S, Hofmann H-P, Kartal A, Kästel C, et al. Benzoylalanine-Derived Ketoamides Carrying Vinylbenzyl Amino Residues: Discovery of Potent Water-Soluble Calpain Inhibitors with Oral Bioavailability. J. Med. Chem. 2003; 46: 2404–2412.

Ludolph AC, He F, Spencer PS, Hammerstad J, Sabri M. 3-Nitropropionic acid-exogenous animal neurotoxin and possible human striatal toxin. Can. J. Neurol. Sci. 1991; 18: 492–8.

Lugo-Huitrón R, Ugalde Muñiz P, Pineda B, Pedraza-Chaverrí J, Ríos C, Pérez-de la Cruz V. Quinolinic acid: an endogenous neurotoxin with multiple targets. Oxid. Med. Cell. Longev. 2013; 2013: 104024.

Lumsden AL, Henshall TL, Dayan S, Lardelli MT, Richards RI. Huntingtin-deficient zebrafish exhibit defects in iron utilization and development. Hum. Mol. Genet. 2007; 16: 1905–1920.

Luo S, Vacher C, Davies JE, Rubinsztein DC. Cdk5 phosphorylation of huntingtin reduces its cleavage by caspases: implications for mutant huntingtin toxicity. J. Cell Biol. 2005; 169: 647–56.

Ma M, Ferguson TA, Schoch KM, Li J, Qian Y, Shofer FS, et al. Calpains mediate axonal cytoskeleton disintegration during Wallerian degeneration. Neurobiol. Dis. 2013; 56: 34–46.

Macedo-Ribeiro S, Cortes L, Maciel P, Carvalho AL. Nucleocytoplasmic shuttling activity of ataxin-3. PLoS One 2009; 4: e5834.

Magalon K, Zimmer C, Cayre M, Khaldi J, Bourbon C, Robles I, et al. Olesoxime accelerates myelination and promotes repair in models of demyelination. Ann. Neurol. 2012; 71: 213–226.

Mahadevan M, Tsilfidis C, Sabourin L, Shutler G, Amemiya C, Jansen G, et al. Myotonic dystrophy mutation: an unstable CTG repeat in the 3' untranslated region of the gene. Science 1992; 255: 1253–5.

Mahajan VB, Skeie JM, Bassuk AG, Fingert JH, Braun TA, Daggett HT, et al. Calpain-5 Mutations Cause Autoimmune Uveitis, Retinal Neovascularization, and Photoreceptor Degeneration. PLoS Genet. 2012; 8: e1003001.

Majumder P, Raychaudhuri S, Chattopadhyay B, Bhattacharyya NP. Increased caspase-2, calpain activations and decreased mitochondrial complex II activity in cells expressing exogenous huntingtin exon 1 containing CAG repeat in the pathogenic range. In: Cellular and Molecular Neurobiology. 2007. p. 1127–1145.

Man SM, Kanneganti T-D. Converging roles of caspases in inflammasome activation, cell death and innate immunity. Nat. Rev. Immunol. 2015; 16: 7–21.

Manczak M, Sheiko T, Craigen WJ, Reddy PH. Reduced VDAC1 protects against alzheimer's disease, mitochondria, and synaptic deficiencies. J. Alzheimer's Dis. 2013; 37: 679–690.

Mangiarini L, Sathasivam K, Seller M, Cozens B, Harper A, Hetherington C, et al. Exon 1 of the HD gene with an expanded CAG repeat is sufficient to cause a progressive neurological phenotype in transgenic mice. Cell 1996; 87: 493–506.

Marsh JL, Lukacsovich T, Thompson LM. Animal Models of Polyglutamine Diseases and Therapeutic Approaches. J. Biol. Chem. 2009; 284: 7431–7435.

Martin DDO, Heit RJ, Yap MC, Davidson MW, Hayden MR, Berthiaume LG. Identification of a post-translationally myristoylated autophagy-inducing domain released by caspase cleavage of Huntingtin. Hum. Mol. Genet. 2014; 23: 1–14.

Martin DDO, Ladha S, Ehrnhoefer DE, Hayden MR. Autophagy in Huntington disease and huntingtin in autophagy. Trends Neurosci. 2015; 38: 26–35.

Martin LJ. Olesoxime, a cholesterol-like neuroprotectant for the potential treatment of amyotrophic lateral sclerosis. IDrugs 2010; 13: 568–580.

Martin LJ, Adams NA, Pan Y, Price A, Wong M. The Mitochondrial Permeability Transition Pore Regulates Nitric Oxide-Mediated Apoptosis of Neurons Induced by Target Deprivation. J. Neurosci. 2011; 31: 359–370.

Martindale D, Hackam A, Wieczorek A, Ellerby L, Wellington C, McCutcheon K, et al. Length of huntingtin and its polyglutamine tract influences localization and frequency of intracellular aggregates. Nat. Genet. 1998; 18: 150–4.

Martinez-Vicente M, Talloczy Z, Wong E, Tang G, Koga H, Kaushik S, et al. Cargo recognition failure is responsible for inefficient autophagy in Huntington's disease. Nat. Neurosci. 2010; 13: 567–576.

Matlin AJ, Clark F, Smith CWJ. Understanding alternative splicing: towards a cellular code. Nat. Rev. Mol. Cell Biol. 2005; 6: 386–398.

Matos CA., de Macedo-Ribeiro S, Carvalho AL. Polyglutamine diseases: the special case of ataxin-3 and Machado-Joseph disease. Prog. Neurobiol. 2011; 95: 26–48.

Mattson MP. Apoptosis in neurodegenerative disorders. Nat. Rev. Mol. Cell Biol. 2000; 1: 120–130.

Mattson MP. Methylation and acetylation in nervous system development and neurodegenerative disorders. Ageing Res. Rev. 2003; 2: 329–42.

Mattson MP, Kroemer G. Mitochondria in cell death: novel targets for neuroprotection and cardioprotection. Trends Mol. Med. 2003; 9: 196–205.

Mattson MP, Magnus T. Ageing and neuronal vulnerability. Nat. Rev. Neurosci. 2006; 7: 278–94.

McCampbell A, Taylor JP, Taye AA, Robitschek J, Li M, Walcott J, et al. CREB-binding protein sequestration by expanded polyglutamine. Hum. Mol. Genet. 2000; 9: 2197–2202.

McIlwain DR, Berger T, Mak TW. Caspase functions in cell death and disease. Cold Spring Harb. Perspect. Biol. 2013; 5: a008656.

McMurray CT. Mechanisms of trinucleotide repeat instability during human development. Nat. Rev. Genet. 2010; 11: 786–799.

Mehdi S. Cell-penetrating inhibitors of calpain. Trends Biochem. Sci. 1991; 16: 150–153.

Mehdi S, Angelastro MR, Wiseman JS, Bey P. Inhibition of the proteolysis of rat erythrocyte membrane proteins by a synthetic inhibitor of calpain. Biochem. Biophys. Res. Commun. 1988; 157: 1117–1123.

Menalled LB. Knock-in mouse models of Huntington's disease. NeuroRx 2005; 2: 465–470.

Mende-Mueller LM, Toneff T, Hwang SR, Chesselet MF, Hook VY. Tissue-specific proteolysis of Huntingtin (htt) in human brain: evidence of enhanced levels of N- and C-terminal htt fragments in Huntington's disease striatum. J. Neurosci. 2001; 21: 1830–7.

Menzies FM, Garcia-Arencibia M, Imarisio S, O'Sullivan NC, Ricketts T, Kent B a, et al. Calpain inhibition mediates autophagy-dependent protection against polyglutamine toxicity. Cell Death Differ. 2014; 22: 433–444.

Mergenthaler P, Lindauer U, Dienel GA, Meisel A. Sugar for the brain: the role of glucose in physiological and

pathological brain function. Trends Neurosci. 2013; 36: 587–97.

Metzler M, Chen N, Helgason CD, Graham RK, Nichol K, McCutcheon K, et al. Life without huntingtin: normal differentiation into functional neurons. J. Neurochem. 1999; 72: 1009–18.

Michalik A, Van Broeckhoven C. Pathogenesis of polyglutamine disorders: aggregation revisited. Hum. Mol. Genet. 2003; 12: R173–R186.

Michetti M, Salamino F, Tedesco I, Averna M, Minafra R, Melloni E, et al. Autolysis of human erythrocyte calpain produces two active enzyme forms with different cell localization. FEBS Lett. 1996; 392: 11–15.

Milakovic T, Quintanilla R a, Johnson GVW. Mutant huntingtin expression induces mitochondrial calcium handling defects in clonal striatal cells: functional consequences. J. Biol. Chem. 2006; 281: 34785–34795.

Miller JP, Holcomb J, Al-Ramahi I, de Haro M, Gafni J, Zhang N, et al. Matrix metalloproteinases are modifiers of huntingtin proteolysis and toxicity in Huntington's disease. Neuron 2010; 67: 199–212.

Miller MW, Sadeh N. Traumatic stress, oxidative stress and post-traumatic stress disorder: neurodegeneration and the accelerated-aging hypothesis. Mol. Psychiatry 2014; 19: 1156–62.

Mirkin SM. Expandable DNA repeats and human disease. Nature 2007; 447: 932–940.

Miura M. Apoptotic and nonapoptotic caspase functions in animal development. Cold Spring Harb. Perspect. Biol. 2012; 4: a008664.

Mizushima N, Yoshimori T. How to Interpret LC3 Immunoblotting. Autophagy 2007; 3: 542–5.

Modregger J, DiProspero NA, Charles V, Tagle DA, Plomann M. PACSIN 1 interacts with huntingtin and is absent from synaptic varicosities in presymptomatic Huntington's disease brains. Hum. Mol. Genet. 2002; 11: 2547–58.

Moldoveanu T, Gehring K, Green DR. Concerted multi-pronged attack by calpastatin to occlude the catalytic cleft of heterodimeric calpains. Nature 2008; 456: 404–408.

Moldoveanu T, Hosfield CM, Lim D, Elce JS, Jia Z, Davies PL. A Ca2+ switch aligns the active site of calpain. Cell 2002; 108: 649–660.

Mosconi L. Glucose metabolism in normal aging and Alzheimer's disease: Methodological and physiological considerations for PET studies. Clin. Transl. Imaging 2013; 1: 217–233.

Mueller T, Breuer P, Schmitt I, Walter J, Evert BO, Wüllner U. CK2-dependent phosphorylation determines cellular localization and stability of ataxin-3. Hum. Mol. Genet. 2009; 18: 3334–3343.

Murachi T, Tanaka K, Hatanaka M, Murakami T. Intracellular Ca2+-dependent protease (calpain) and its high-molecular-weight endogenous inhibitor (calpastatin). Adv. Enzyme Regul. 1980; 19: 407–24.

Murchison D, Zawieja DC, Griffith WH. Reduced mitochondrial buffering of voltage-gated calcium influx in aged rat basal forebrain neurons. Cell Calcium 2004; 36: 61–75.

Myers RH. Huntington's disease genetics. NeuroRx 2004; 1: 255–62.

Nakajima R, Takao K, Huang S-M, Takano J, Iwata N, Miyakawa T, et al. Comprehensive behavioral phenotyping of calpastatin-knockout mice. Mol. Brain 2008; 1: 7.

Nakano KK, Dawson DM, Spence a. Machado disease. A hereditary ataxia in Portuguese emigrants to Massachusetts. Neurology 1972; 22: 49–55.

Nalavade R, Griesche N, Ryan DP, Hildebrand S, Krau S. Mechanisms of RNA-induced toxicity in CAG repeat disorders. Cell Death Dis. 2013; 4: e752.

Nardin A, Schrepfer E, Ziviani E. Counteracting PINK/Parkin Deficiency in the Activation of Mitophagy: A Potential Therapeutic Intervention for Parkinson's Disease. Curr. Neuropharmacol. 2016; 14: 250–9.

Nascimento-Ferreira I, Santos-Ferreira T, Sousa-Ferreira L, Auregan G, Onofre I, Alves S, et al. Overexpression of the autophagic beclin-1 protein clears mutant ataxin-3 and alleviates Machado-Joseph disease. Brain 2011; 134: 1400–1415.

Nasir J, Floresco SB, O'Kusky JR, Diewert VM, Richman JM, Zeisler J, et al. Targeted disruption of the Huntington's disease gene results in embryonic lethality and behavioral and morphological changes in heterozygotes. Cell 1995; 81: 811–23.

Neher E, Sakaba T. Multiple Roles of Calcium Ions in the Regulation of Neurotransmitter Release. Neuron 2008; 59: 861–872.

Ng H, Pulst S-M, Huynh DP. Ataxin-2 mediated cell death is dependent on domains downstream of the polyQ repeat. Exp. Neurol. 2007; 208: 207–15.

Niapour M, Berger S. Flow cytometric measurement of calpain activity in living cells. Cytom. Part A 2007; 71A: 475–485.

Nicastro G, Menon RP, Masino L, Knowles PP, McDonald NQ, Pastore A. The solution structure of the Josephin domain of ataxin-3: structural determinants for molecular recognition. Proc. Natl. Acad. Sci. U. S. A. 2005; 102: 10493–10498.

Nicholson DW. Caspase structure, proteolytic substrates, and function during apoptotic cell death. Cell Death Differ. 1999; 6: 1028–1042.

Niethammer M, Feigin A, Eidelberg D. Functional neuroimaging in Parkinson's disease. Cold Spring Harb. Perspect. Med. 2012; 2: a009274.

Nikkel AL, Martino B, Markosyan S, Brederson J-D, Medeiros R, Moeller A, et al. The novel calpain inhibitor A-705253 prevents stress-induced tau hyperphosphorylation in vitro and in vivo. Neuropharmacology 2012; 63: 606–612.

Nikoletopoulou V, Tavernarakis N. Calcium homeostasis in aging neurons. Front. Genet. 2012; 3: 200.

Nimmrich V, Reymann K, Strassburger M, Schöder U, Gross G, Hahn A, et al. Inhibition of calpain prevents NMDA-induced cell death and β-amyloid-induced synaptic dysfunction in hippocampal slice cultures. Br. J. Pharmacol. 2010; 159: 1523–1531.

Nimmrich V, Szabo R, Nyakas C, Granic I, Reymann KG, Schröder UH, et al. Inhibition of Calpain Prevents N-Methyl-D-aspartate-Induced Degeneration of the Nucleus Basalis and Associated Behavioral Dysfunction. J. Pharmacol. Exp. Ther. 2008; 327: 343–52.

Nishimoto Y, Ito D, Yagi T, Nihei Y, Tsunoda Y, Suzuki N. Characterization of Alternative Isoforms and Inclusion Body of the TAR DNA-binding Protein-43. J. Biol. Chem. 2010; 285: 608–619.

Nishiura I, Tanaka K, Yamato S, Murachi T. The occurrence of an inhibitor of Ca2+-dependent neutral protease in rat liver. J. Biochem. 1978; 84: 1657–9.

Nixon RA. The calpains in aging and aging-related diseases. Ageing Res. Rev. 2003; 2: 407–418.

Nucifora FC, Ellerby LM, Wellington CL, Wood JD, Herring WJ, Sawa A, et al. Nuclear Localization of a Non-caspase Truncation Product of Atrophin-1, with an Expanded Polyglutamine Repeat, Increases Cellular Toxicity. J. Biol. Chem. 2003; 278: 13047–13055.

O'Connor DM, Boulis NM. Gene therapy for neurodegenerative diseases. Trends Mol. Med. 2015; 21: 504–512.

Ochaba J, Lukacsovich T, Csikos G, Zheng S, Margulis J, Salazar L, et al. Potential function for the Huntingtin protein as a scaffold for selective autophagy. Proc. Natl. Acad. Sci. U. S. A. 2014; 111: 16889–94.

Oliveira JMA. Nature and cause of mitochondrial dysfunction in Huntington's disease: Focusing on huntingtin and the striatum. J. Neurochem. 2010; 114: 1–12.

Oliveira JMA, Chen S, Almeida S, Riley R, Goncalves J, Oliveira CR, et al. Mitochondrial-Dependent Ca2+ Handling in Huntington's Disease Striatal Cells: Effect of Histone Deacetylase Inhibitors. J. Neurosci. 2006; 26: 11174–11186.

Ono Y, Saido TC, Sorimachi H. Calpain research for drug discovery: challenges and potential. Nat. Rev. Drug Discov. 2016; 15: 854–876.

Orr AL, Li S, Wang C-E, Li H, Wang J, Rong J, et al. N-terminal mutant huntingtin associates with mitochondria and impairs mitochondrial trafficking. J. Neurosci. 2008; 28: 2783–92.

Orrenius S, Zhivotovsky B, Nicotera P. Calcium: Regulation of cell death: the calcium–apoptosis link. Nat. Rev. Mol. Cell Biol. 2003; 4: 552–565.

Paillusson S, Stoica R, Gomez-Suaga P, Lau DHW, Mueller S, Miller T, et al. There's Something Wrong with my MAM; the ER-Mitochondria Axis and Neurodegenerative Diseases. Trends Neurosci. 2016; 39: 146–157.

Pal A, Severin F, Lommer B, Shevchenko A, Zerial M. Huntingtin–HAP40 complex is a novel Rab5 effector that regulates early endosome motility and is up-regulated in Huntington's disease. J. Cell Biol. 2006; 172: 605–618.

Paoletti P, Vila I, Rife M, Lizcano JM, Alberch J, Gines S. Dopaminergic and Glutamatergic Signaling Crosstalk in Huntington's Disease Neurodegeneration: The Role of p25/Cyclin-Dependent Kinase 5. J. Neurosci. 2008; 28: 10090–10101.

Park SA, Ahn S Il, Gallo J-M. Tau mis-splicing in the pathogenesis of neurodegenerative disorders. BMB Rep. 2016; 49: 405–13.

Park SH, Kukushkin Y, Gupta R, Chen T, Konagai A, Hipp MS, et al. PolyQ proteins interfere with nuclear degradation of cytosolic proteins by sequestering the Sis1p chaperone. Cell 2013; 154: 134–145.

Passani LA, Bedford MT, Faber PW, McGinnis KM, Sharp AH, Gusella JF, et al. Huntingtin's WW domain partners in Huntington's disease post-mortem brain fulfill genetic criteria for direct involvement in Huntington's disease pathogenesis. Hum Mol Genet 2000; 9: 2175–2182.

Patel JR, Brewer GJ. Age-related changes in neuronal glucose uptake in response to glutamate and beta-amyloid. J. Neurosci. Res. 2003; 72: 527–36.

Paulsen JS, Hoth KF, Nehl C, Stierman L. Critical Periods of Suicide Risk in Huntington's Disease. Am. J. Psychiatry 2005; 162: 725–731.

Paulson HL. Machado–Joseph disease/spinocerebellar ataxia type 3. In: Handbook of Clinical Neurology. 2012.

p. 437–449.

Paulson HL, Albin RL. Huntington's Disease: Clinical Features and Routes to Therapy. CRC Press/Taylor & Francis; 2011.

Paulson HL, Das SS, Crino PB, Perez MK, Patel SC, Gotsdiner D, et al. Machado-Joseph disease gene product is a cytoplasmic protein widely expressed in brain. Ann. Neurol. 1997; 41: 453–462.

Paulson HL, Perez MK, Trottier Y, Trojanowski JQ, Subramony SH, Das SS, et al. Intranuclear inclusions of expanded polyglutamine protein in spinocerebellar ataxia type 3. Neuron 1997; 19: 333–344.

Perez MK, Paulson HL, Pendse SJ, Saionz SJ, Bonini NM, Pittman RN. Recruitment and the role of nuclear localization in polyglutamine-mediated aggregation. J. Cell Biol. 1998; 143: 1457–70.

Perl TM, Bédard L, Kosatsky T, Hockin JC, Todd ECD, Remis RS. An Outbreak of Toxic Encephalopathy Caused by Eating Mussels Contaminated with Domoic Acid. N. Engl. J. Med. 1990; 322: 1775–1780.

Pickles S, Destroismaisons L, Peyrard SL, Cadot S, Rouleau GA, Brown RH, et al. Mitochondrial damage revealed by immunoselection for ALS-linked misfolded SOD1. Hum. Mol. Genet. 2013; 22: 3947–3959.

Pinton P, Giorgi C, Siviero R, Zecchini E, Rizzuto R. Calcium and apoptosis: ER-mitochondria Ca2+ transfer in the control of apoptosis. Oncogene 2008; 27: 6407–6418.

Pipas JM. SV40: Cell transformation and tumorigenesis. Virology 2009; 384: 294–303.

Pop C, Salvesen GS. Human Caspases: Activation, Specificity, and Regulation. J. Biol. Chem. 2009; 284: 21777–21781.

Potter NT, Spector EB, Prior TW. Technical standards and guidelines for Huntington disease testing. Genet. Med. 2004; 6: 61–5.

Pouladi MA, Morton AJ, Hayden MR. Choosing an animal model for the study of Huntington's disease. Nat. Rev. Neurosci. 2013; 14: 708–721.

Pouladi MA, Stanek LM, Xie Y, Franciosi S, Southwell AL, Deng Y, et al. Marked differences in neurochemistry and aggregates despite similar behavioural and neuropathological features of Huntington disease in the full-length BACHD and YAC128 mice. Hum. Mol. Genet. 2012; 21: 2219–2232.

Pozzi C, Valtorta M, Tedeschi G, Galbusera E, Pastori V, Bigi A, et al. Study of subcellular localization and proteolysis of ataxin-3. Neurobiol. Dis. 2008; 30: 190–200.

Del Prete D, Checler F, Chami M, Kriegstein A, Nicoll R, Takao K, et al. Ryanodine receptors: physiological function and deregulation in Alzheimer disease. Mol. Neurodegener. 2014; 9: 21.

Prince M, Comas-Herrera A, Knapp M, Guerchet M, Karagiannidou M. World Alzheimer Report 2016 Improving healthcare for people living with dementia. Coverage, Quality and costs now and in the future. Alzheimer's Dis. Int. 2016: 1–140.

Pringsheim T, Wiltshire K, Day L, Dykeman J, Steeves T, Jette N. The incidence and prevalence of Huntington's disease: A systematic review and meta-analysis. Mov. Disord. 2012; 27: 1083–1091.

Pryor WM, Biagioli M, Shahani N, Swarnkar S, Huang W-C, Page DT, et al. Huntingtin promotes mTORC1 signaling in the pathogenesis of Huntington's disease. Sci. Signal. 2014; 7: ra103-ra103.

Raichle ME, Gusnard DA. Appraising the brain's energy budget. Proc. Natl. Acad. Sci. U. S. A. 2002; 99: 10237–9.

Rajamani U. Causes of Neurodegeneration in Diabetes: Possible Culprits and Therapeutic Targets. Brain Disord. Ther. 2014; 3

Ramaswamy S, McBride JL, Kordower JH. Animal models of Huntington's disease. Ilar J 2007; 48: 356–373.

Rambousek L, Kleteckova L, Kubesova A, Jirak D, Vales K, Fritschy J-M. Rat intra-hippocampal NMDA infusion induces cell-specific damage and changes in expression of NMDA and GABAA receptor subunits. Neuropharmacology 2016; 105: 594–606.

Rao MV., Mohan PS, Peterhoff CM, Yang D-S, Schmidt SD, Stavrides PH, et al. Marked Calpastatin (CAST) Depletion in Alzheimer's Disease Accelerates Cytoskeleton Disruption and Neurodegeneration: Neuroprotection by CAST Overexpression. J. Neurosci. 2008; 28: 12241–12254.

Rao MV, Campbell J, Palaniappan A, Kumar A, Nixon RA. Calpastatin inhibits motor neuron death and increases survival of hSOD1 G93A mice. J. Neurochem. 2016; 137: 253–265.

Rao MV, McBrayer MK, Campbell J, Kumar A, Hashim A, Sershen H, et al. Specific Calpain Inhibition by Calpastatin Prevents Tauopathy and Neurodegeneration and Restores Normal Lifespan in Tau P301L Mice. J. Neurosci. 2014; 34: 9222–9234.

Raposo M, Bettencourt C, Maciel P, Gao F, Ramos A, Kazachkova N, et al. Novel candidate blood-based transcriptional biomarkers of machado-joseph disease. Mov. Disord. 2015; 30: 968–975.

Ratovitski T, Chighladze E, Waldron E, Hirschhorn RR, Ross C a. Cysteine proteases bleomycin hydrolase and cathepsin Z mediate N-terminal proteolysis and toxicity of mutant huntingtin. J. Biol. Chem. 2011; 286: 12578–89.

Ratovitski T, Nakamura M, D'Ambola J, Chighladze E, Liang Y, Wang W, et al. N-terminal proteolysis of full-length mutant huntingtin in an inducible PC12 cell model of Huntington's disease. Cell Cycle 2007; 6: 2970–81.

Ravikumar B, Sarkar S, Davies JE, Futter M, Garcia-Arencibia M, Green-Thompson ZW, et al. Regulation of mammalian autophagy in physiology and pathophysiology. Physiol. Rev. 2010; 90: 1383–435.

Rawlins MD, Wexler NS, Wexler AR, Tabrizi SJ, Douglas I, Evans SJW, et al. The Prevalence of Huntington's Disease. Neuroepidemiology 2016; 46: 144–153.

Reijonen S, Kukkonen JP, Hyrskyluoto A, Kivinen J, Kairisalo M, Takei N, et al. Downregulation of NF-kappaB signaling by mutant huntingtin proteins induces oxidative stress and cell death. Cell. Mol. Life Sci. 2010; 67: 1929–41.

Renton AE, Chiò A, Traynor BJ. State of play in amyotrophic lateral sclerosis genetics. Nat. Neurosci. 2013; 17: 17–23.

Richard I, Broux O, Allamand V, Fougerousse F, Chiannilkulchai N, Bourg N, et al. Mutations in the proteolytic enzyme calpain 3 cause limb-girdle muscular dystrophy type 2A. Cell 1995; 81: 27–40.

Richter F, Gao F, Medvedeva V, Lee P, Bove N, Fleming SM, et al. Chronic administration of cholesterol oximes in mice increases transcription of cytoprotective genes and improves transcriptome alterations induced by alpha-synuclein overexpression in nigrostriatal dopaminergic neurons. Neurobiol. Dis. 2014; 69: 263–75.

Riedl SJ, Shi Y. Molecular mechanisms of caspase regulation during apoptosis. Nat. Rev. Mol. Cell Biol. 2004; 5:

897–907.

Riess O, Rüb U, Pastore A, Bauer P, Schöls L. SCA3: neurological features, pathogenesis and animal models. Cerebellum 2008; 7: 125–37.

Rigamonti D, Bauer JH, De-Fraja C, Conti L, Sipione S, Sciorati C, et al. Wild-type huntingtin protects from apoptosis upstream of caspase-3. J. Neurosci. 2000; 20: 3705–13.

Rigamonti D, Sipione S, Goffredo D, Zuccato C, Fossale E, Cattaneo E. Huntingtin's neuroprotective activity occurs via inhibition of procaspase-9 processing. J. Biol. Chem. 2001; 276: 14545–8.

Rissman RA, Poon WW, Blurton-Jones M, Oddo S, Torp R, Vitek MP, et al. Caspase-cleavage of tau is an early event in Alzheimer disease tangle pathology. J. Clin. Invest. 2004; 114: 121–30.

Rockabrand E, Slepko N, Pantalone A, Nukala VN, Kazantsev A, Marsh JL, et al. The first 17 amino acids of Huntingtin modulate its sub-cellular localization, aggregation and effects on calcium homeostasis. Hum. Mol. Genet. 2007; 16: 61–77.

Rodrigues A-J, do Carmo Costa M, Silva T-L, Ferreira D, Bajanca F, Logarinho E, et al. Absence of ataxin-3 leads to cytoskeletal disorganization and increased cell death. Biochim. Biophys. Acta - Mol. Cell Res. 2010; 1803: 1154–1163.

Rodrigues A-J, Coppola G, Santos C, Costa M d. C, Ailion M, Sequeiros J, et al. Functional genomics and biochemical characterization of the C. elegans orthologue of the Machado-Joseph disease protein ataxin-3. FASEB J. 2007; 21: 1126–1136.

Rohn TT. The role of caspases in Alzheimer's disease; potential novel therapeutic opportunities. Apoptosis 2010; 15: 1403–1409.

Rojas JC, Boxer AL. Neurodegenerative disease in 2015: Targeting tauopathies for therapeutic translation. Nat. Rev. Neurol. 2016; 12: 74–76.

Roos RAC. Huntington's disease: a clinical review. Orphanet J. Rare Dis. 2010; 5: 40.

Rosenberg RN, Nyhan WL, Bay C, Shore P. Autosomal dominant striatonigral degeneration. A clinical, pathologic, and biochemical study of a new genetic disorder. Neurology 1976; 26: 703–14.

Rosser BG, Gores GJ. Cellular in vivo assay of calpain activity using a fluorescent substrate. Application to study of anoxic liver injury. Methods Mol. Biol. 2000; 144: 245–59.

Rosser BG, Powers SP, Gores GJ. Calpain activity increases in hepatocytes following addition of ATP. Demonstration by a novel fluorescent approach. J. Biol. Chem. 1993; 268: 23593–23600.

Rüb U, Brunt ER, Petrasch-Parwez E, Schöls L, Theegarten D, Auburger G, et al. Degeneration of ingestion-related brainstem nuclei in spinocerebellar ataxia type 2, 3, 6 and 7. Neuropathol. Appl. Neurobiol. 2006; 32: 635–649.

Rüb U, Schöls L, Paulson H, Auburger G, Kermer P, Jen JC, et al. Clinical features, neurogenetics and neuropathology of the polyglutamine spinocerebellar ataxias type 1, 2, 3, 6 and 7. Prog. Neurobiol. 2013; 104: 38–66.

Rubinsztein DC, Leggo J, Coles R, Almqvist E, Biancalana V, Cassiman JJ, et al. Phenotypic characterization of individuals with 30-40 CAG repeats in the Huntington disease (HD) gene reveals HD cases with 36 repeats and

apparently normal elderly individuals with 36-39 repeats. Am. J. Hum. Genet. 1996; 59: 16–22.

Ruetenik A, Barrientos A. Dietary restriction, mitochondrial function and aging: from yeast to humans. Biochim. Biophys. Acta - Bioenerg. 2015; 1847: 1434–1447.

Rui Y-N, Xu Z, Patel B, Chen Z, Chen D, Tito A, et al. Huntingtin functions as a scaffold for selective macroautophagy. Nat. Cell Biol. 2015; 17: 262–275.

Russo R, Berliocchi L, Adornetto a, Varano GP, Cavaliere F, Nucci C, et al. Calpain-mediated cleavage of Beclin-1 and autophagy deregulation following retinal ischemic injury in vivo. Cell Death Dis. 2011; 2: e144.

Saatman KE, Creed J, Raghupathi R. Calpain as a therapeutic target in traumatic brain injury. Neurotherapeutics 2010; 7: 31–42.

Saatman KE, Creed J, Raghupathi R, Saatman, Kathryn E; Creed, Jennifer; Raghupathi R, Saatman KE, Creed J, et al. Calpain as a Therapeutic Target in Traumatic Brain Injury. Society 2010; 7: 31–42.

Sacco JJ, Yau TY, Darling S, Patel V, Liu H, Urbé S, et al. The deubiquitylase Ataxin-3 restricts PTEN transcription in lung cancer cells. Oncogene 2013: 1–8.

Saito M, Kawaguchi N, Hashimoto M, Kodama T, Higuchi N, Tanaka T, et al. Purification and structure of novel cysteine proteinase inhibitors, staccopins P1 and P2, from Staphylococcus tanabeensis. Agric. Biol. Chem. 1987; 51: 861–868.

Sakahira H, Breuer P, Hayer-Hartl MK, Hartl FU. Molecular chaperones as modulators of polyglutamine protein aggregation and toxicity. Proc. Natl. Acad. Sci. 2002; 99: 16412–16418.

Sakai K, Akanuma H, Imahori K, Kawashima S. A unique specificity of a calcium activated neutral protease indicated in histone hydrolysis. J. Biochem. 1987; 101: 911–8.

Samantaray S, Knaryan VH, Shields DC, Cox AA, Haque A, Banik NL. Inhibition of Calpain Activation Protects MPTP-Induced Nigral and Spinal Cord Neurodegeneration, Reduces Inflammation, and Improves Gait Dynamics in Mice. Mol. Neurobiol. 2015; 52: 1054–1066.

Samantaray S, Ray SK, Ali SF, Banik NL. Calpain activation in apoptosis of motoneurons in cell culture models of experimental Parkinsonism. In: Annals of the New York Academy of Sciences. 2006. p. 349–356.

Samantaray S, Ray SK, Banik NL. Calpain as a potential therapeutic target in Parkinson's disease. CNS Neurol. Disord. Drug Targets 2008; 7: 305–12.

Sarkar S, Ravikumar B, Floto R a, Rubinsztein DC. Rapamycin and mTOR-independent autophagy inducers ameliorate toxicity of polyglutamine-expanded huntingtin and related proteinopathies. Cell Death Differ. 2009; 16: 46–56.

Sasaki T, Kikuchi T, Yumoto N, Yoshimura N, Murachi T. Comparative specificity and kinetic studies on porcine calpain I and calpain II with naturally occurring peptides and synthetic fluorogenic substrates. J. Biol. Chem. 1984; 259: 12489–12494.

Sathasivam K, Neueder A, Gipson TA, Landles C, Benjamin AC, Bondulich MK, et al. Aberrant splicing of HTT generates the pathogenic exon 1 protein in Huntington disease. Proc. Natl. Acad. Sci. U. S. A. 2013; 110: 2366–70.

Scaglione KM, Zavodszky E, Todi S V., Patury S, Xu P, Rodríguez-Lebrón E, et al. Ube2w and Ataxin-3

Coordinately Regulate the Ubiquitin Ligase CHIP. Mol. Cell 2011; 43: 599–612.

Schaffar G, Breuer P, Boteva R, Behrends C, Tzvetkov N, Strippel N, et al. Cellular toxicity of polyglutamine expansion proteins: mechanism of transcription factor deactivation. Mol. Cell 2004; 15: 95–105.

Scheel H, Tomiuk S, Hofmann K. Elucidation of ataxin-3 and ataxin-7 function by integrative bioinformatics. Hum. Mol. Genet. 2003; 12: 2845–52.

Schilling B, Gafni J, Torcassi C, Cong X, Row RH, LaFevre-Bernt M a., et al. Huntingtin phosphorylation sites mapped by mass spectrometry. Modulation of cleavage and toxicity. J. Biol. Chem. 2006; 281: 23686–97.

Schilling G, Becher MW, Sharp a H, Jinnah H a, Duan K, Kotzuk J a, et al. Intranuclear inclusions and neuritic aggregates in transgenic mice expressing a mutant N-terminal fragment of huntingtin. Hum. Mol. Genet. 1999; 8: 397–407.

Schilling G, Wood JD, Duan K, Slunt HH, Gonzales V, Yamada M, et al. Nuclear accumulation of truncated atrophin-1 fragments in a transgenic mouse model of DRPLA. Neuron 1999; 24: 275–86.

Schilling O, Overall CM. Proteome-derived, database-searchable peptide libraries for identifying protease cleavage sites. Nat. Biotechnol. 2008; 26: 685–694.

Schmidt T, Landwehrmeyer GB, Schmitt I, Trottier Y, Auburger G, Laccone F, et al. An isoform of ataxin-3 accumulates in the nucleus of neuronal cells in affected brain regions of SCA3 patients. Brain Pathol. 1998; 8: 669–79.

Schmidt T, Lindenberg KS, Krebs A, Scho L, Laccone F, Herms J, et al. Protein Surveillance Machinery in Brains with Spinocerebellar Ataxia Type 3 : Redistribution and Differential Recruitment of 26S Proteasome Subunits and Chaperones to Neuronal Intranuclear Inclusions. Ann. Neurol. 2002: 302–310.

Schmitt I, Linden M, Khazneh H, Evert BO, Breuer P, Klockgether T, et al. Inactivation of the mouse Atxn3 (ataxin-3) gene increases protein ubiquitination. Biochem. Biophys. Res. Commun. 2007; 362: 734–739.

Schöls L, Bauer P, Schmidt T, Schulte T, Riess O. Autosomal dominant cerebellar ataxias: clinical features, genetics, and pathogenesis. Lancet Neurol. 2004; 3: 291–304.

Schöls L, Vieira-Saecker a M, Schöls S, Przuntek H, Epplen JT, Riess O. Trinucleotide expansion within the MJD1 gene presents clinically as spinocerebellar ataxia and occurs most frequently in German SCA patients. Hum. Mol. Genet. 1995; 4: 1001–5.

Seidel K, den Dunnen WFA, Schultz C, Paulson H, Frank S, de Vos RA, et al. Axonal inclusions in spinocerebellar ataxia type 3. Acta Neuropathol. 2010; 120: 449–60.

Seidel K, Siswanto S, Fredrich M, Bouzrou M, den Dunnen WFAA, ??zerden I, et al. On the Distribution of Intranuclear and Cytoplasmic Aggregates in the Brainstem of Patients with Spinocerebellar Ataxia Type 2 and 3. Brain Pathol. 2016

Shao J, Diamond MI. Polyglutamine diseases: emerging concepts in pathogenesis and therapy. Hum. Mol. Genet. 2007; 16 Spec No: R115-23.

Sharp AH, Loev SJ, Schilling G, Li SH, Li XJ, Bao J, et al. Widespread expression of Huntington's disease gene (IT15) protein product. Neuron 1995; 14: 1065–1074.

Shehadeh J, Fernandes HB, Zeron Mullins MM, Graham RK, Leavitt BR, Hayden MR, et al. Striatal neuronal

apoptosis is preferentially enhanced by NMDA receptor activation in YAC transgenic mouse model of Huntington disease. Neurobiol. Dis. 2006; 21: 392–403.

Shirendeb UP, Calkins MJ, Manczak M, Anekonda V, Dufour B, McBride JL, et al. Mutant huntingtin's interaction with mitochondrial protein Drp1 impairs mitochondrial biogenesis and causes defective axonal transport and synaptic degeneration in Huntington's disease. Hum. Mol. Genet. 2012; 21: 406–20.

Simões AT, Goncalves N, Koeppen A, Deglon N, Kugler S, Duarte CB, et al. Calpastatin-mediated inhibition of calpains in the mouse brain prevents mutant ataxin 3 proteolysis, nuclear localization and aggregation, relieving Machado-Joseph disease. Brain 2012; 135: 2428–2439.

Simões AT, Gonçalves N, Nobre RJ, Duarte CB, Pereira de Almeida L. Calpain inhibition reduces ataxin-3 cleavage alleviating neuropathology and motor impairments in mouse models of Machado-Joseph disease. Hum. Mol. Genet. 2014; 23: 4932–44.

Simonato M, Bennett J, Boulis NM, Castro MG, Fink DJ, Goins WF, et al. Progress in gene therapy for neurological disorders. Nat. Rev. Neurol. 2013; 9: 277–91.

Singhal PK, Sassi S, Lan L, Au P, Halvorsen SC, Fukumura D, et al. Mouse embryonic fibroblasts exhibit extensive developmental and phenotypic diversity. Proc. Natl. Acad. Sci. U. S. A. 2016; 113: 122–7.

Skoog I, Lernfelt B, Landahl S, Palmertz B, Andreasson LA, Nilsson L, et al. 15-year longitudinal study of blood pressure and dementia. Lancet (London, England) 1996; 347: 1141–5.

Slow EJ, Graham RK, Osmand AP, Devon RS, Lu G, Deng Y, et al. Absence of behavioral abnormalities and neurodegeneration in vivo despite widespread neuronal huntingtin inclusions. Proc. Natl. Acad. Sci. U. S. A. 2005; 102: 11402–7.

Slow EJ, van Raamsdonk J, Rogers D, Coleman SH, Graham RK, Deng Y, et al. Selective striatal neuronal loss in a YAC128 mouse model of Huntington disease. Hum. Mol. Genet. 2003; 12: 1555–1567.

Smith MA, Schnellmann RG. Calpains, mitochondria, and apoptosis. Cardiovasc. Res. 2012; 96: 32–37.

Son JH, Shim JH, Kim K-H, Ha J-Y, Han JY. Neuronal autophagy and neurodegenerative diseases. Exp. Mol. Med. 2012; 44: 89.

Song W, Chen J, Petrilli A, Liot G, Klinglmayr E, Zhou Y, et al. Mutant huntingtin binds the mitochondrial fission GTPase dynamin-related protein-1 and increases its enzymatic activity. Nat. Med. 2011; 17: 377–382.

Sorimachi H, Hata S, Ono Y. Calpain chronicle--an enzyme family under multidisciplinary characterization. Proc. Jpn. Acad. Ser. B. Phys. Biol. Sci. 2011; 87: 287–327.

Southwell AL, Bugg CW, Kaltenbach LS, Dunn D, Butland S, Weiss A, et al. Perturbation with intrabodies reveals that calpain cleavage is required for degradation of huntingtin exon 1. PLoS One 2011; 6: e16676.

La Spada AR, Wilson EM, Lubahn DB, Harding AE, Fischbeck KH. Androgen receptor gene mutations in X-linked spinal and bulbar muscular atrophy. Nature 1991; 352: 77–79.

Squitieri F, Gellera C, Cannella M, Mariotti C, Cislaghi G, Rubinsztein DC, et al. Homozygosity for CAG mutation in Huntington disease is associated with a more severe clinical course. Brain 2003; 126: 946–55.

Sriram K, Benkovic SA, Miller DB, O'Callaghan JP. Obesity exacerbates chemically induced neurodegeneration. Neuroscience 2002; 115: 1335–46.

Stoothoff WH, Johnson GVW. Tau phosphorylation: physiological and pathological consequences. Biochim. Biophys. Acta - Mol. Basis Dis. 2005; 1739: 280–297.

Strachan MWJ, Reynolds RM, Marioni RE, Price JF. Cognitive function, dementia and type 2 diabetes mellitus in the elderly. Nat. Rev. Endocrinol. 2011; 7: 108–114.

Strzyz P. Translation: The features of pathologic RAN translation. Nat. Rev. Mol. Cell Biol. 2016; 17: 264–264.

Suite ND, Sequeiros J, McKhann GM. Machado-Joseph disease in a Sicilian-American family. J. Neurogenet. 1986; 3: 177–82.

Sun Y, Savanenin A, Reddy PH, Liu YF. Polyglutamine-expanded Huntingtin Promotes Sensitization of N-Methyl-D-aspartate Receptors via Post-synaptic Density 95. J. Biol. Chem. 2001; 276: 24713–24718.

Sunyach C, Michaud M, Arnoux T, Bernard-Marissal N, Aebischer J, Latyszenok V, et al. Olesoxime delays muscle denervation, astrogliosis, microglial activation and motoneuron death in an ALS mouse model. Neuropharmacology 2012; 62: 2346–52.

Swaab DF, Bao A-M, Lucassen PJ. The stress system in the human brain in depression and neurodegeneration. Ageing Res. Rev. 2005; 4: 141–194.

Switonski PM, Fiszer A, Kazmierska K, Kurpisz M, Krzyzosiak WJ, Figiel M. Mouse Ataxin-3 Functional Knock-Out Model. NeuroMolecular Med. 2011; 13: 54–65.

Szabadkai G, Bianchi K, Várnai P, De Stefani D, Wieckowski MR, Cavagna D, et al. Chaperone-mediated coupling of endoplasmic reticulum and mitochondrial Ca2+ channels. J. Cell Biol. 2006; 175: 901–911.

Szweda PA, Camouse M, Lundberg KC, Oberley TD, Szweda LI. Aging, lipofuscin formation, and free radical-mediated inhibition of cellular proteolytic systems. Ageing Res. Rev. 2003; 2: 383–405.

Tabrizi SJ, Langbehn DR, Leavitt BR, Roos RA, Durr A, Craufurd D, et al. Biological and clinical manifestations of Huntington's disease in the longitudinal TRACK-HD study: cross-sectional analysis of baseline data. Lancet. Neurol. 2009; 8: 791–801.

Tabrizi SJ, Scahill RI, Durr A, Roos RA, Leavitt BR, Jones R, et al. Biological and clinical changes in premanifest and early stage Huntington's disease in the TRACK-HD study: the 12-month longitudinal analysis. Lancet Neurol. 2011; 10: 31–42.

Tabrizi SJ, Scahill RI, Owen G, Durr A, Leavitt BR, Roos RA, et al. Predictors of phenotypic progression and disease onset in premanifest and early-stage Huntington's disease in the TRACK-HD study: analysis of 36-month observational data. Lancet Neurol. 2013; 12: 637–649.

Tait D, Riccio M, Sittler A, Scherzinger E, Santi S, Ognibene A, et al. Ataxin-3 is transported into the nucleus and associates with the nuclear matrix. Hum. Mol. Genet. 1998; 7: 991–7.

Tait SWG, Green DR. Mitochondria and cell death: outer membrane permeabilization and beyond. Nat. Rev. Mol. Cell Biol. 2010; 11: 621–632.

Takano H, Gusella JF. The predominantly HEAT-like motif structure of huntingtin and its association and coincident nuclear entry with dorsal, an NF-kB/Rel/dorsal family transcription factor. BMC Neurosci. 2002; 3: 15.

Takano J, Mihira N, Fujioka R, Hosoki E, Chishti AH, Saido TC. Vital role of the calpain-calpastatin system for placental-integrity-dependent embryonic survival. Mol. Cell. Biol. 2011; 31: 4097–4106.

Takano J, Tomioka M, Tsubuki S, Higuchi M, Iwata N, Itohara S, et al. Calpain mediates excitotoxic DNA fragmentation via mitochondrial pathways in adult brains: Evidence from calpastatin mutant mice. J. Biol. Chem. 2005; 280: 16175–16184.

Takiyama Y, Igarashi S, Rogaeva E a, Endo K, Rogaev EI, Tanaka H, et al. Evidence for inter-generational instability in the CAG repeat in the MJD1 gene and for conserved haplotypes at flanking markers amongst Japanese and Caucasian subjects with Machado-Joseph disease. Hum. Mol. Genet. 1995; 4: 1137–46.

Takiyama Y, Nishizawa M, Tanaka H, Kawashima S, Sakamoto H, Karube Y, et al. The gene for Machado-Joseph disease maps to human chromosome 14q. Nat. Genet. 1993; 4: 300–304.

Talanian R V, Quinlan C, Trautz S, Hackett MC, Mankovich JA, Banach D, et al. Substrate specificities of caspase family proteases. J. Biol. Chem. 1997; 272: 9677–82.

Tang T-S, Slow E, Lupu V, Stavrovskaya IG, Sugimori M, Llinás R, et al. Disturbed Ca2+ signaling and apoptosis of medium spiny neurons in Huntington's disease. Proc. Natl. Acad. Sci. U. S. A. 2005; 102: 2602–7.

Tang T-S, Tu H, Chan EYW, Maximov A, Wang Z, Wellington CL, et al. Huntingtin and huntingtin-associated protein 1 influence neuronal calcium signaling mediated by inositol-(1,4,5) triphosphate receptor type 1. Neuron 2003; 39: 227–239.

Taniguchi S, Fujita Y, Hayashi S, Kakita A, Takahashi H, Murayama S, et al. Calpain-mediated degradation of p35 to p25 in postmortem human and rat brains. FEBS Lett. 2001; 489: 46–50.

Tanzi RE, Bertram L. Twenty Years of the Alzheimer's Disease Amyloid Hypothesis: A Genetic Perspective. Cell 2005; 120: 545–555.

Tarlac V, Storey E. Role of proteolysis in polyglutamine disorders. J. Neurosci. Res. 2003; 74: 406–16.

The Huntington's Disease Collaborative Research Group, HD collaborative, research group. A novel gene containing a trinucleotide repeat that is expanded and unstable on Huntington's disease chromosomes. The Huntington's Disease Collaborative Research Group. Cell 1993; 72: 971–83.

Thomas B, Beal MF. Parkinson's disease. Hum. Mol. Genet. 2007; 16: R183–R194.

Thornberry NA, Bull HG, Calaycay JR, Chapman KT, Howard AD, Kostura MJ, et al. A novel heterodimeric cysteine protease is required for interleukin-1βprocessing in monocytes. Nature 1992; 356: 768–774.

Toda S, Iguchi Y, Lin Z, Nishikawa H, Nagasawa T, Watanabe H, et al. Reconsidering Animal Models of Major Depressive Disorder in the Elderly. Front. Aging Neurosci. 2016; 8: 188.

Todi SV, Winborn BJ, Scaglione KM, Blount JR, Travis SM, Paulson HL. Ubiquitination directly enhances activity of the deubiquitinating enzyme ataxin-3. EMBO J. 2009; 28: 372–82.

Toescu EC, Verkhratsky A, Landfield PW. Ca2+ regulation and gene expression in normal brain aging. Trends Neurosci. 2004; 27: 614–620.

Toledano A, Álvarez MI. Lesion-Induced Vertebrate Models of Alzheimer Dementia. 2011. p. 295–345.

Tompa P, Buzder-Lantos P, Tantos A, Farkas A, Szilágyi A, Bánóczi Z, et al. On the sequential determinants of calpain cleavage. J. Biol. Chem. 2004; 279: 20775–20785.

Toneff T, Mende-Mueller L, Wu Y, Hwang S-R, Bundey R, Thompson LM, et al. Comparison of huntingtin proteolytic fragments in human lymphoblast cell lines and human brain. J. Neurochem. 2002; 82: 84–92.

Toonen LJA, Schmidt I, Luijsterburg MS, van Attikum H, van Roon-Mom WMC. Antisense oligonucleotide-mediated exon skipping as a strategy to reduce proteolytic cleavage of ataxin-3. Sci. Rep. 2016; 6: 35200.

Toyama BH, Hetzer MW. Protein homeostasis: live long, won't prosper. Nat. Rev. Mol. Cell Biol. 2012; 14: 55–61.

Tradewell ML, Durham HD. Calpastatin reduces toxicity of SOD1G93A in a culture model of amyotrophic lateral sclerosis. Neuroreport 2010; 21: 1.

Tran TT, Srivareerat M, Alhaider IA, Alkadhi KA. Chronic psychosocial stress enhances long-term depression in a subthreshold amyloid-beta rat model of Alzheimer's disease. J. Neurochem. 2011; 119: 408–416.

Trettel F, Rigamonti D, Hilditch-Maguire P, Wheeler VC, Sharp a H, Persichetti F, et al. Dominant phenotypes produced by the HD mutation in STHdh(Q111) striatal cells. Hum. Mol. Genet. 2000; 9: 2799–2809.

Trinchese F, Liu S, Zhang H. Inhibition of calpains improves memory and synaptic transmission in a mouse model of Alzheimer disease. J. Clin. Invest. 2008; 118: 2796–2807.

Trinh J, Farrer M. Advances in the genetics of Parkinson disease. Nat. Rev. Neurol. 2013; 9: 445–454.

Trottier Y, Cancel G, An-Gourfinkel I, Lutz Y, Weber C, Brice a, et al. Heterogeneous intracellular localization and expression of ataxin-3. Neurobiol. Dis. 1998; 5: 335–347.

Trottier Y, Devys D, Imbert G, Saudou F, An I, Lutz Y, et al. Cellular localization of the Huntington's disease protein and discrimination of the normal and mutated form. Nat. Genet. 1995; 10: 104–110.

Trumbeckaite S, Neuhof C, Zierz S, Gellerich FN. Calpain inhibitor (BSF 409425) diminishes ischemia/reperfusion-induced damage of rabbit heart mitochondria. Biochem. Pharmacol. 2003; 65: 911–6.

Trushina E, Dyer RB, Badger JD, Ure D, Eide L, Tran DD, et al. Mutant Huntingtin Impairs Axonal Trafficking in Mammalian Neurons In Vivo and In Vitro. Mol. Cell. Biol. 2004; 24: 8195–8209.

Tsolaki M, Kounti F, Karamavrou S. Severe Psychological Stress in Elderly Individuals: A Proposed Model of Neurodegeneration and Its Implications. Am. J. Alzheimers. Dis. Other Demen. 2009; 24: 85–94.

Tsou WL, Burr A a., Ouyang M, Blount JR, Scaglione KM, Todi S V. Ubiquitination regulates the neuroprotective function of the deubiquitinase ataxin-3 in vivo. J. Biol. Chem. 2013; 288: 34460–34469.

Turk BE, Huang LL, Piro ET, Cantley LC. Determination of protease cleavage site motifs using mixture-based oriented peptide libraries. Nat. Biotechnol. 2001; 19: 661–667.

United Nations - Department of Economic and Social Affairs - Population Division. World Population Ageing 2015. 2015.

Upadhyay RK. Drug delivery systems, CNS protection, and the blood brain barrier. Biomed Res. Int. 2014; 2014: 869269.

Vale TC, Cardoso F. Chorea: A Journey through History. Tremor Other Hyperkinet. Mov. (N. Y). 2015; 5: 1–6.

Vaux DL, Silke J. IAPs, RINGs and ubiquitylation. Nat. Rev. Mol. Cell Biol. 2005; 6: 287–297.

Veenman L, Shandalov Y, Gavish M. VDAC activation by the 18 kDa translocator protein (TSPO), implications for apoptosis. J. Bioenerg. Biomembr. 2008; 40: 199–205.

Vehviläinen P, Koistinaho J, Gundars G. Mechanisms of mutant SOD1 induced mitochondrial toxicity in amyotrophic lateral sclerosis. Front. Cell. Neurosci. 2014; 8: 126.

Velier J, Kim M, Schwarz C, Kim TW, Sapp E, Chase K, et al. Wild-type and mutant huntingtins function in vesicle trafficking in the secretory and endocytic pathways. Exp. Neurol. 1998; 152: 34–40.

Verkerk AJ, Pieretti M, Sutcliffe JS, Fu YH, Kuhl DP, Pizzuti A, et al. Identification of a gene (FMR-1) containing a CGG repeat coincident with a breakpoint cluster region exhibiting length variation in fragile X syndrome. Cell 1991; 65: 905–14.

Vilchez D, Saez I, Dillin A. The role of protein clearance mechanisms in organismal ageing and age-related diseases. Nat. Commun. 2014; 5: 5659.

Viswanathan A, Rocca WA, Tzourio C. Vascular risk factors and dementia: how to move forward? Neurology 2009; 72: 368–74.

De Volder A, Bol A, Michel C, Cogneau M, Evrard P, Lyon G, et al. Brain glucose utilization in childhood Huntington's disease studied with positron emission tomography (PET). Brain Dev. 1988; 10: 47–50.

Vonsattel JPG. Huntington disease models and human neuropathology: similarities and differences. Acta Neuropathol. 2008; 115: 55–69.

Vyas S, Rodrigues AJ, Silva JM, Tronche F, Almeida OFX, Sousa N, et al. Chronic Stress and Glucocorticoids: From Neuronal Plasticity to Neurodegeneration. Neural Plast. 2016; 2016: 1–15.

Walsh ME, Shi Y, Van Remmen H. The effects of dietary restriction on oxidative stress in rodents. Free Radic. Biol. Med. 2014; 66: 88–99.

Walter C, Clemens LE, Müller AJ, Fallier-Becker P, Proikas-Cezanne T, Riess O, et al. Activation of AMPK-induced autophagy ameliorates Huntington disease pathology in vitro. Neuropharmacology 2016; 108: 24–38.

Wan F, Letavernier E, Le Saux CJ, Houssaini A, Abid S, Czibik G, et al. Calpastatin overexpression impairs postinfarct scar healing in mice by compromising reparative immune cell recruitment and activation. Am. J. Physiol. Heart Circ. Physiol. 2015; 309: H1883-93.

Wang CE, Tydlacka S, Orr AL, Yang SH, Graham RK, Hayden MR, et al. Accumulation of N-terminal mutant huntingtin in mouse and monkey models implicated as a pathogenic mechanism in Huntington's disease. Hum. Mol. Genet. 2008; 17: 2738–2751.

Wang G, Liu X, Gaertig MA, Li S, Li X-J. Ablation of huntingtin in adult neurons is nondeleterious but its depletion in young mice causes acute pancreatitis. Proc. Natl. Acad. Sci. 2016; 113: 3359–3364.

Wang G, Sawai N, Kotliarova S, Kanazawa I, Nukina N. Ataxin-3, the MJD1 gene product, interacts with the two human homologs of yeast DNA repair protein RAD23, HHR23A and HHR23B. Hum. Mol. Genet. 2000; 9: 1795–803.

Wang H, Ying Z, Wang G. Ataxin-3 regulates aggresome formation of copper-zinc superoxide dismutase (SOD1) by editing K63-linked polyubiquitin chains. J. Biol. Chem. 2012; 287: 28576–28585.

Wang JT, Medress ZA, Barres BA. Axon degeneration: Molecular mechanisms of a self-destruction pathway. J. Cell Biol. 2012; 196: 7–18.

Wang KKW, Nath R, Posner A, Raser KJ, Buroker-Kilgore M, Hajimohammadreza I, et al. An alpha-mercaptoacrylic acid derivative is a selective nonpeptide cell-permeable calpain inhibitor and is neuroprotective. Proc. Natl. Acad. Sci. U. S. A. 1996; 93: 6687–92.

Wang KKW, Posmantur R, Nadimpalli R, Nath R, Mohan P, Nixon R a, et al. Caspase-mediated fragmentation of calpain inhibitor protein calpastatin during apoptosis. Arch. Biochem. Biophys. 1998; 356: 187–196.

Wang KKW, Posmantur R, Nath R, McGinnist K, Whitton M, Talanian R V., et al. Simultaneous degradation of αII- and βII-spectrin by caspase 3 (CPP32) in apoptotic cells. J. Biol. Chem. 1998; 273: 22490–22497.

Wang X, Michaelis EK. Selective neuronal vulnerability to oxidative stress in the brain. Front. Aging Neurosci. 2010; 2: 12.

Wang Y, Hersheson J, Lopez D, Hammer M, Liu Y, Lee K-H, et al. Defects in the CAPN1 Gene Result in Alterations in Cerebellar Development and Cerebellar Ataxia in Mice and Humans. Cell Rep. 2016; 16: 79–91.

Wanichawan P, Hafver TL, Hodne K, Aronsen JM, Lunde IG, Dalhus B, et al. Molecular Basis of Calpain Cleavage and Inactivation of the Sodium-Calcium Exchanger 1 in Heart Failure. J. Biol. Chem. 2014; 289: 33984–33998.

Warby SC, Doty CN, Graham RK, Carroll JB, Yang Y-ZZ, Singaraja RR, et al. Activated caspase-6 and caspase-6-cleaved fragments of huntingtin specifically colocalize in the nucleus. Hum. Mol. Genet. 2008; 17: 2390–404.

Warren MW, Kobeissy FH, Liu MC, Hayes RL, Gold MS, Wang KKW. Concurrent calpain and caspase-3 mediated proteolysis of alpha II-spectrin and tau in rat brain after methamphetamine exposure: a similar profile to traumatic brain injury. Life Sci. 2005; 78: 301–9.

Warrick JM, Morabito LM, Bilen J, Gordesky-Gold B, Faust LZ, Paulson HL, et al. Ataxin-3 Suppresses Polyglutamine Neurodegeneration in Drosophila by a Ubiquitin-Associated Mechanism. Mol. Cell 2005; 18: 37–48.

Weir DW, Sturrock A, Leavitt BR. Development of biomarkers for Huntington's disease. Lancet Neurol. 2011; 10: 573–590.

Wellington CL, Ellerby LM, Hackam a S, Margolis RL, Trifiro M a, Singaraja R, et al. Caspase cleavage of gene products associated with triplet expansion disorders generates truncated fragments containing the polyglutamine tract. J. Biol. Chem. 1998; 273: 9158–67.

Wellington CL, Hayden MR. Of molecular interactions, mice and mechanisms: new insights into Huntington's disease. Curr. Opin. Neurol. 1997; 10: 291–8.

Wellington CL, Singaraja R, Ellerby L, Savill J, Roy S, Leavitt B, et al. Inhibiting caspase cleavage of huntingtin reduces toxicity and aggregate formation in neuronal and nonneuronal cells. J. Biol. Chem. 2000; 275: 19831–8.

Wendt A, Thompson VF, Goll DE. Interaction of calpastatin with calpain: A review. Biol. Chem. 2004; 385: 465–472.

Wexler NS, Lorimer J, Porter J, Gomez F, Moskowitz C, Shackell E, et al. Venezuelan kindreds reveal that genetic and environmental factors modulate Huntington's disease age of onset. Proc. Natl. Acad. Sci. U. S. A. 2004; 101: 3498–503.

Wheeler VC, Auerbach W, White JK, Srinidhi J, Auerbach A, Ryan A, et al. Length-dependent gametic CAG repeat instability in the Huntington's disease knock-in mouse. Hum. Mol. Genet. 1999; 8: 115–122.

White JA, Anderson E, Zimmerman K, Zheng KH, Rouhani R, Gunawardena S. Huntingtin differentially regulates the axonal transport of a sub-set of Rab-containing vesicles in vivo. Hum. Mol. Genet. 2015; 24: 7182–7195.

White JK, Auerbach W, Duyao MP, Vonsattel J-PP, Gusella JF, Joyner AL, et al. Huntingtin is required for neurogenesis and is not impaired by the Huntington's disease CAG expansion. Nat. Genet. 1997; 17: 404–410.

Whitmer R, Gunderson E, Barrett-Connor E, Quesenberry C, Yaffe K. Obesity in middle age and future risk of dementia: A 27 year longitudinal population based study. BMJ 2005; 330: 1360.

Williams A, Sarkar S, Cuddon P, Ttofi EK, Saiki S, Siddiqi FH, et al. Novel targets for Huntington's disease in an mTOR-independent autophagy pathway. Nat. Chem. Biol. 2008; 4: 295–305.

Winborn BJ, Travis SM, Todi S V., Scaglione KM, Xu P, Williams AJ, et al. The Deubiquitinating Enzyme Ataxin-3, a Polyglutamine Disease Protein, Edits Lys63 Linkages in Mixed Linkage Ubiquitin Chains. J. Biol. Chem. 2008; 283: 26436–26443.

Wolkow CA. Life span: getting the signal from the nervous system. Trends Neurosci. 2002; 25: 212–6.

Woods BT, Schaumburg HH. Nigro-spino-dentatal degeneration with nuclear ophthalmoplegia. A unique and partially treatable clinico-pathological entity. J. Neurol. Sci. 1972; 17: 149–66.

Wright AL, Vissel B. CAST your vote: is calpain inhibition the answer to ALS? J. Neurochem. 2016; 137: 140–141.

Wu C, Chen D-B, Feng L, Zhou X-X, Zhang J-W, You H-J, et al. Oculomotor deficits in spinocerebellar ataxia type 3: Potential biomarkers of preclinical detection and disease progression. CNS Neurosci. Ther. 2017

Wu H-Y, Lynch DR. Calpain and Synaptic Function. Mol. Neurobiol. 2006; 33: 215–236.

Wu H-Y, Tomizawa K, Matsushita M, Lu Y-F, Li S-T, Matsui H. Poly-arginine-fused calpastatin peptide, a living cell membrane-permeable and specific inhibitor for calpain. Neurosci. Res. 2003; 47: 131–5.

Wu P, Shen Q, Dong S, Xu Z, Tsien JZ, Hu Y, et al. Calorie restriction ameliorates neurodegenerative phenotypes in forebrain-specific presenilin-1 and presenilin-2 double knockout mice. Neurobiol. Aging 2008; 29: 1502–11.

Xia J, Lee DH, Taylor J, Vandelft M, Truant R. Huntingtin contains a highly conserved nuclear export signal. Hum. Mol. Genet. 2003; 12: 1393–1403.

Xiao WH, Zheng FY, Bennett GJ, Bordet T, Pruss RM. Olesoxime (cholest-4-en-3-one, oxime): analgesic and neuroprotective effects in a rat model of painful peripheral neuropathy produced by the chemotherapeutic agent, paclitaxel. Pain 2009; 147: 202–9.

Xiao WH, Zheng H, Bennett GJ. Characterization of oxaliplatin-induced chronic painful peripheral neuropathy in the rat and comparison with the neuropathy induced by paclitaxel. Neuroscience 2012; 203: 194–206.

Xifró X, García-Martínez JM, Del Toro D, Alberch J, Pérez-Navarro E. Calcineurin is involved in the early activation of NMDA-mediated cell death in mutant huntingtin knock-in striatal cells. J. Neurochem. 2008; 105: 1596–1612.

Xue D, Robert Horvitz H. Inhibition of the Caenorhabditis elegans cell-death protease CED-3 by a CED-3 cleavage site in baculovirus p35 protein. Nature 1995; 377: 248–251.

Yamashita T, Hideyama T, Hachiga K, Teramoto S, Takano J, Iwata N, et al. A role for calpain-dependent cleavage of TDP-43 in amyotrophic lateral sclerosis pathology. Nat. Commun. 2012; 3: 1307.

Yang X, Chang HY, Baltimore D. Autoproteolytic activation of pro-caspases by oligomerization. Mol. Cell 1998; 1: 319–25.

Yano H, Baranov S V, Baranova O V, Kim J, Pan Y, Yablonska S, et al. Inhibition of mitochondrial protein import by mutant huntingtin. Nat. Neurosci. 2014; 17: 822–831.

Yehuda S, Rabinovitz S, Carasso RL, Mostofsky DI. The role of polyunsaturated fatty acids in restoring the aging neuronal membrane. Neurobiol. Aging 2002; 23: 843–853.

Yoshiki A, Moriwaki K. Mouse phenome research: implications of genetic background. ILAR J. 2006; 47: 94–102.

Youle RJ, Narendra DP. Mechanisms of mitophagy. Nat. Rev. Mol. Cell Biol. 2011; 12: 9–14.

Young CS, Pyle AD. Exon Skipping Therapy. Cell 2016; 167: 1144.

Young JE, Garden GA, Martinez RA, Tanaka F, Sandoval CM, Smith AC, et al. Polyglutamine-expanded androgen receptor truncation fragments activate a Bax-dependent apoptotic cascade mediated by DP5/Hrk. J. Neurosci. 2009; 29: 1987–97.

Young JE, Gouw L, Propp S, Sopher BL, Taylor J, Lin A, et al. Proteolytic cleavage of ataxin-7 by caspase-7 modulates cellular toxicity and transcriptional dysregulation. J. Biol. Chem. 2007; 282: 30150–60.

Yousefi S, Perozzo R, Schmid I, Ziemiecki A, Schaffner T, Scapozza L, et al. Calpain-mediated cleavage of Atg5 switches autophagy to apoptosis. Nat. Cell Biol. 2006; 8: 1124–1132.

Yu-Taeger L, Petrasch-Parwez E, Osmand AP, Redensek A, Metzger S, Clemens LE, et al. A novel BACHD transgenic rat exhibits characteristic neuropathological features of Huntington disease. J. Neurosci. 2012; 32: 15426–38.

Yu Y-C, Kuo C-L, Cheng W-L, Liu C-S, Hsieh M. Decreased antioxidant enzyme activity and increased mitochondrial DNA damage in cellular models of Machado-Joseph disease. J. Neurosci. Res. 2009; 87: 1884–91.

Yuan J, Shaham S, Ledoux S, Ellis HM, Horvitz HR. The C. elegans cell death gene ced-3 encodes a protein similar to mammalian interleukin-1 beta-converting enzyme. Cell 1993; 75: 641–52.

Yvert G, Lindenberg KS, Picaud S, Landwehrmeyer GB, Sahel J a, Mandel JL. Expanded polyglutamines induce neurodegeneration and trans-neuronal alterations in cerebellum and retina of SCA7 transgenic mice. Hum. Mol. Genet. 2000; 9: 2491–506.

Zeitlin S, Liu J-P, Chapman DL, Papaioannou VE, Efstratiadis A. Increased apoptosis and early embryonic lethality in mice nullizygous for the Huntington's disease gene homologue. Nat. Genet. 1995; 11: 155–163.

Zeng L, Tallaksen-Greene SJ, Wang B, Albin RL, Paulson HL. The De-Ubiquitinating Enzyme Ataxin-3 does not Modulate Disease Progression in a Knock-in Mouse Model of Huntington Disease. J. Huntingtons. Dis. 2013; 2: 201–215.

Zeron MM, Hansson O, Chen N, Wellington CL, Leavitt BR, Brundin P, et al. Increased sensitivity to N-methyl-D-aspartate receptor-mediated excitotoxicity in a mouse model of Huntington's disease. Neuron 2002; 33: 849–60.

Zhang C, Tanzi RE. Natural Modulators of Amyloid-Beta Precursor Protein Processing. Curr. Alzheimer Res. 2012; 276: 391–402.

Zhang Y-J, Xu Y-F, Cook C, Gendron TF, Roettges P, Link CD, et al. Aberrant cleavage of TDP-43 enhances aggregation and cellular toxicity. Proc. Natl. Acad. Sci. U. S. A. 2009; 106: 7607–12.

Zhang Y, Leavitt BR, van Raamsdonk JM, Dragatsis I, Goldowitz D, MacDonald ME, et al. Huntingtin inhibits caspase-3 activation. EMBO J. 2006; 25: 5896–906.

Zhang Y, Li M, Drozda M, Chen M, Ren S, Mejia Sanchez RO, et al. Depletion of wild-type huntingtin in mouse models of neurologic diseases. J. Neurochem. 2003; 87: 101–6.

Zhang Z, Larner SF, Liu MC, Zheng W, Hayes RL, Wang KKW. Multiple alphaII-spectrin breakdown products distinguish calpain and caspase dominated necrotic and apoptotic cell death pathways. Apoptosis 2009; 14: 1289–1298.

Zhong X, Pittman RN. Ataxin-3 binds VCP/p97 and regulates retrotranslocation of ERAD substrates. Hum. Mol. Genet. 2006; 15: 2409–2420.

Zhu G, Briz V, Seinfeld J, Liu Y, Bi X, Baudry M. Calpain-1 deletion impairs mGluR-dependent LTD and fear memory extinction. Sci. Rep. 2017; 7: 42788.

Zu T, Gibbens B, Doty NS, Gomes-Pereira M, Huguet A, Stone MD, et al. Non-ATG-initiated translation directed by microsatellite expansions. Proc. Natl. Acad. Sci. U. S. A. 2011; 108: 260–5.

Zuccato C, Cattaneo E. Brain-derived neurotrophic factor in neurodegenerative diseases. Nat. Rev. Neurol. 2009; 5: 311–322.

Zuccato C, Ciammola A, Rigamonti D, Leavitt BR, Goffredo D, Conti L, et al. Loss of Huntingtin-Mediated BDNF Gene Transcription in Huntington's Disease. Science (80-.). 2001; 293: 493–498.

Zuccato C, Tartari M, Crotti A, Goffredo D, Valenza M, Conti L, et al. Huntingtin interacts with REST/NRSF to modulate the transcription of NRSE-controlled neuronal genes. Nat. Genet. 2003; 35: 76–83.

Zuccato C, Valenza M, Cattaneo E. Molecular Mechanisms and Potential Therapeutical Targets in Huntington ' s Disease. Physiol Rev 2010; 90: 905–981.

Zucker RS. Calcium- and activity-dependent synaptic plasticity. Curr. Opin. Neurobiol. 1999; 9: 305–13.

Appendix I: Unpublished project manuscripts

The following pages are dedicated to unpublished project manuscripts. The work described in these manuscripts is composed of additional or preliminary experiments, which were conducted as individual projects or as a part of the major published studies.

Every single project is divided into a brief introduction, a result part and a discussion. Material and methods are only included if not already described in the published manuscripts in Appendix II. However, references to the respective publications are enclosed. An author contribution statement is given at the end of each section.

The unpublished project manuscripts comprise:

A. The calpain system in cell models of HD

B. Calpain activation in the YAC128 mouse model of HD

C. Calpastatin ablation in the HDKI mouse model of HD

D. Calpain-1 ablation in the YAC84 mouse model of SCA3

E. Calpain-dependent cleavage of huntingtin

A. The calpain system in cell models of HD

Jonasz J. Weber[1,2], Lukas Klumpp[1,2], Laura E. Clemensson[1,2], Huu P. Nguyen[1,2]

[1] Institute of Medical Genetics and Applied Genomics, University of Tuebingen, Tuebingen, Germany
[2] Centre for Rare Diseases, University of Tuebingen, Tuebingen, Germany

Introduction

Proteolytic fragmentation of disease proteins has been discussed as an important step in the molecular pathogenesis not only of Huntington disease (HD) but also further neurodegenerative disorders (*Accepted paper c*). The so called *toxic fragment hypothesis* states that this post-translational modification represents an important source for breakdown products of disease proteins which, in comparison to the full-length protein, exhibit an increased toxicity and aggregation propensity (Wellington and Hayden, 1997). In HD, several groups of enzymes have been associated with the cleavage of mutant huntingtin such as caspases and calpains (Ehrnhoefer *et al.*, 2011). Calpains, a class of Ca^{2+}-dependent cysteine proteases, do not only cleave the disease protein, but also exhibit an overactivation in the molecular context of HD (Kim *et al.*, 2001; Gafni and Ellerby, 2002; Gafni *et al.*, 2004; Cowan *et al.*, 2008; Dau *et al.*, 2014; *Accepted paper d & e*). Furthermore, this overactivation seems be connected with synaptic dysfunctions via calpain-dependent loss of surface NMDARs (Cowan *et al.*, 2008; Gladding *et al.*, 2012; Dau *et al.*, 2014). These observations emphasize that calpains represent an important player in the molecular pathogenesis of HD and targeting these enzymes might constitute a promising therapeutic strategy to treat this dreadful disease.

To further assess the role of calpains, we analysed calpain activation in cell models of HD. By western blotting, we assessed expression levels of calpains and fragmentation of their substrates in ST*Hdh*^{Q7} and ST*Hdh*^{Q111} cells. These immortalized striatal precursor cells with a potential for an induced neuronal differentiation were generated from wild type mice and the homozygous *Hdh*^{Q111} knock-in (HDKI) mouse model of HD (Trettel *et al.*, 2000). To validate our results, we utilized primary murine embryonic fibroblasts, MEF*Hdh*^{Q7} and MEF*Hdh*^{Q111}, which were retrieved from the same animal model as ST*Hdh* cells. Furthermore, we tested the effect of a calpain activity reduction by measuring viability of ST*Hdh* cells treated with specific pharmacologic inhibitors.

Materials and Methods

Cell culture

Generation of MEF*Hdh*^{Q7} and MEF*Hdh*^{Q111} has been described elsewhere (Walter *et al.*, 2016). Cells were maintained in Dulbecco's Modified Eagle Medium (DMEM) supplemented with 10% fetal calf serum and 1% penicillin/streptomycin (all Thermo Fisher Scientific) at 37°C and 5% CO_2. Fibroblasts in passages 4–12 were used for the experiments. For pharmacologic calpain inhibition, undifferentiated ST*Hdh* cells were treated with 5 µM N-acetyl-L-leucyl-L-leucyl-L-norleucinal (ALLN) or 25 µM PD150606 (both Sigma-Aldrich) for 24 h. DMSO was used as a vehicle control. For measuring viability, ST*Hdh* were assayed using the resazurin-based PrestoBlue® Cell Viability Reagent (Thermo Fisher Scientific) and an Envision Multilabel Plate Reader (Perkin Elmer) according to the manufacturer's protocol.

Immunofluorescence staining of tissue culture cells

Undifferentiated ST*Hdh* cells or MEF*Hdh* were cultured on coverslips and pre-fixed in 0.4% paraformaldehyde in DMEM for 15 min at 37°C. Afterwards, cells were fixed in 4% paraformaldehyde in Dulbecco's phosphate buffered saline (DPBS) for 10 min and washed three times with DPBS. Blocking solution (DPBS supplemented with 1% normal donkey serum and 0.1% Triton X-100) was added for 1 h at room temperature. After blocking, cells were incubated with rabbit anti-calpain-1 (1:100; ab39170, Abcam) and mouse anti-TOMM20 (1:100; ab56783, Abcam) antibodies in blocking solution overnight. Subsequently, cells were washed three times with DPBS and incubated with the respective secondary antibodies goat anti-rabbit Alexa Fluor® 488 (1:1000; ab150077, Abcam) and goat anti-mouse Cy3 (1:1000; 115-165-146, Dianova) diluted in blocking solution for 1 h at room temperature. Afterwards, cells were washed again three times with DPBS and nuclear counterstaining was performed using Hoechst 33342. Cells were embedded in a solution of Mowiol containing 2.5% 1,4-diazobicyclo-[2.2.2]-octane (DABCO) (Sigma-Aldrich) and mounted on microscope slides. Images were taken with an Axioplan 2 microscope and imaging software AxioVision 4.7 (both Zeiss).

Antibodies for western blotting

The following list contains information on additional antibodies used for western blot analysis in this study, which were not mentioned elsewhere: rabbit anti-calpain-2 (1:500; ab39168, Abcam); rabbit anti-calpain-10 (1:500; ab28220, Abcam).

Further materials and methods

Information on cell lysis and western blot analysis can be found under *Accepted papers e* and *g.*

Results

Calpain-1 is overexpressed in STHdh^{Q111} cells

For a better insight into activation patterns of the calpain system in cell models of HD, we performed western blotting of undifferentiated ST*Hdh*^{Q7} and ST*Hdh*^{Q111} lysates (Fig. 1). Immunodetection showed a significant increase in total calpain-1 levels in ST*Hdh*^{Q111} compared to the wild type cell line. The calpain substrate α-spectrin showed an increased formation of cleavage fragment (Fig. 1a, upper black arrowhead). Interestingly, full-length levels of α-spectrin were also elevated in ST*Hdh*^{Q111}. On the contrary, calpain-2 and calpain-10 (bands a and b) showed a decrease in their full-length levels. The endogenous calpain inhibitor calpastatin (CAST) exhibited no differences in total levels (band a). However, levels of a probable fragment band of CAST (Fig. 1a, arrowhead b) appeared to be significantly increased. Taken together, ST*Hdh*^{Q111} cells exhibited elevated disturbances in the expression of members of the calpain system and an over-all increase in calpain activation.

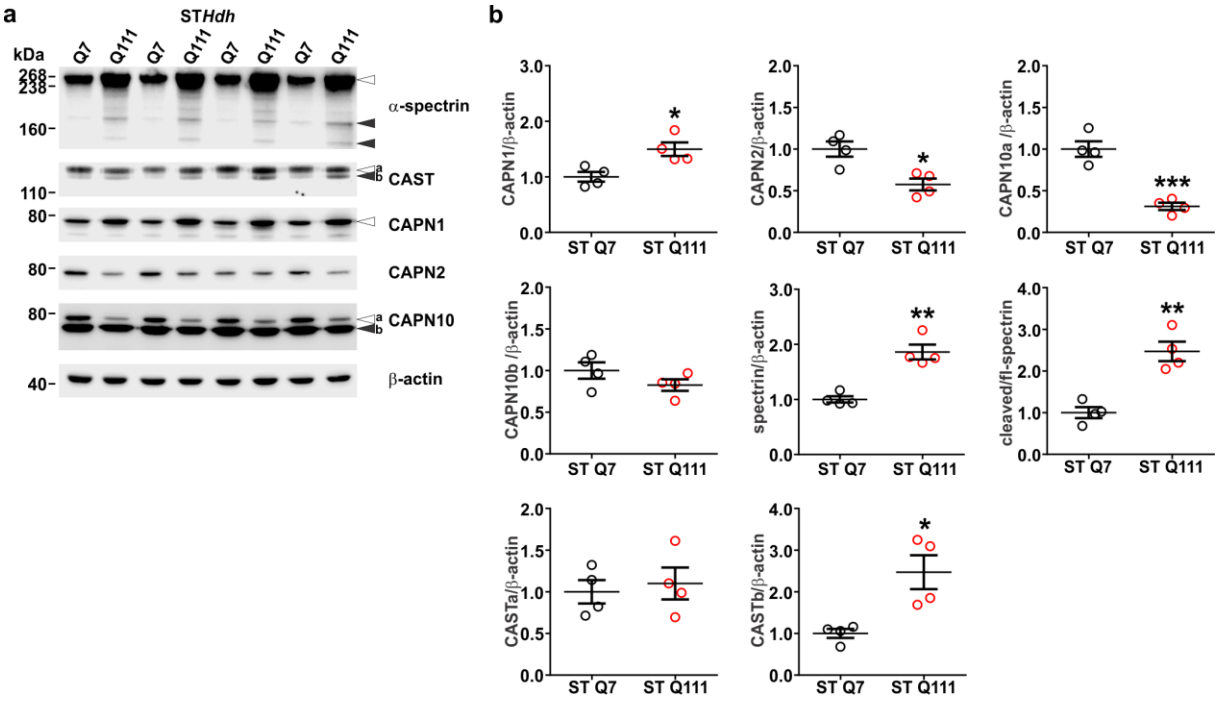

Figure 1. Western blot analysis shows an increased activation of the calpain system in undifferentiated ST*Hdh*^{Q111} cells. (**a**) Lysates of undifferentiated ST*Hdh* cells expressing huntingtin with 7 or 111 glutamines were analysed by western blotting. Blots were stained with calpain-1, calpain-2, calpain-10, and CAST antibodies. For evaluating the effects on calpain substrates, fragmentation of α-spectrin was investigated. Actin served as a loading control. White arrowheads indicate full-length proteins, black arrowheads highlight proteolytically processed proteins. (**b**) Protein levels were quantified using the NIH software ImageJ. The calpain cleavage-dependent α-spectrin fragment band (upper black arrowhead) was quantified relative to full-length levels of α-spectrin. Horizontal lines represent the means ± s.e.m. of four independent experiments. Statistical significance was assessed by Student's *t*-test, *: $P < 0.1$; **: $P < 0.01$.

Trend towards a calpain system overactivation in MEFHdh^{Q111}

To compare results of the calpain system activation as observed in ST*Hdh* cells, we analysed MEFs expressing wild type huntingtin (Q7) or mutant huntingtin (Q111) using western blotting. Immunodetection and quantification of calpain-1, calpain-2 and α-spectrin recapitulated by tendency the increased activation of the calpain system without reaching statistical significance (Fig. 2).

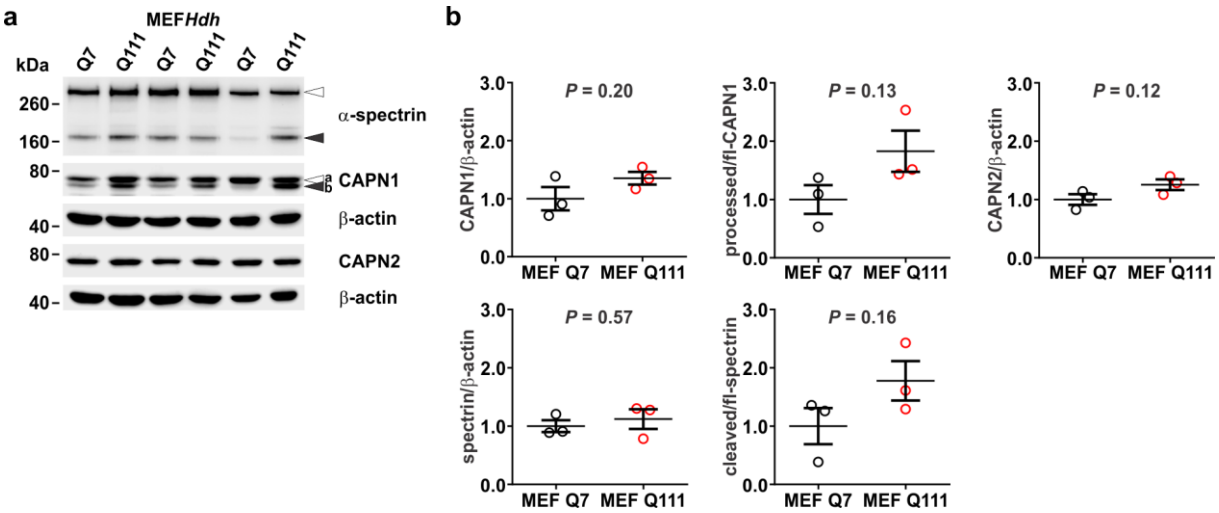

Figure 2. Western blot analysis shows a trend towards increased calpain activation in MEF*Hdh*^{Q111}. (**a**) MEFs expressing huntingtin with 7 or 111 glutamines were lysed using RIPA-buffer and analysed by western blotting to detect levels of calpain-1, calpain-2 and the calpain substrate α-spectrin. Actin served as a loading control. White arrowheads indicate full-length proteins, black arrowheads highlight proteolytically processed proteins. (**b**) Protein levels were quantified using the NIH software ImageJ. The calpain cleavage-dependent α-spectrin fragment band was quantified relative to full-length levels of α-spectrin. Calpain-1 activation was quantified by calculating the ratio of proteolytically cleaved (active) form to the inactive form of calpain-1. Horizontal lines represent the means ± s.e.m. of three independent experiments.

Calpain-1 colocalizes with mitochondria in STHdh cells and MEFHdhs

As we observed increased levels of calpain-1 in ST*Hdh*^{Q111} cells by western blotting, we aimed for validating these alterations by microscopy. To investigate the cellular levels and the distribution of calpain-1, we performed immunofluorescence analysis of ST*Hdh* cells and MEF*Hdh*s using an antibody specific to calpain-1. Fluorescence microscopy revealed, most strikingly, a distinct and organized distribution of calpain-1 reminiscent of mitochondrial structures in ST*Hdh* cells and MEF*Hdh*s (Fig. 3). Double staining of calpain-1 together with the mitochondrial outer membrane protein TOMM20 confirmed the colocalization with mitochondrial structures in MEF*Hdh*s (Fig. 3b). Furthermore, the intensity of calpain-1 staining in ST*Hdh*^{Q111} cells appeared to be increased compared to ST*Hdh*^{Q7} cells, endorsing the previous observations by western blot analysis of ST*Hdh* cells.

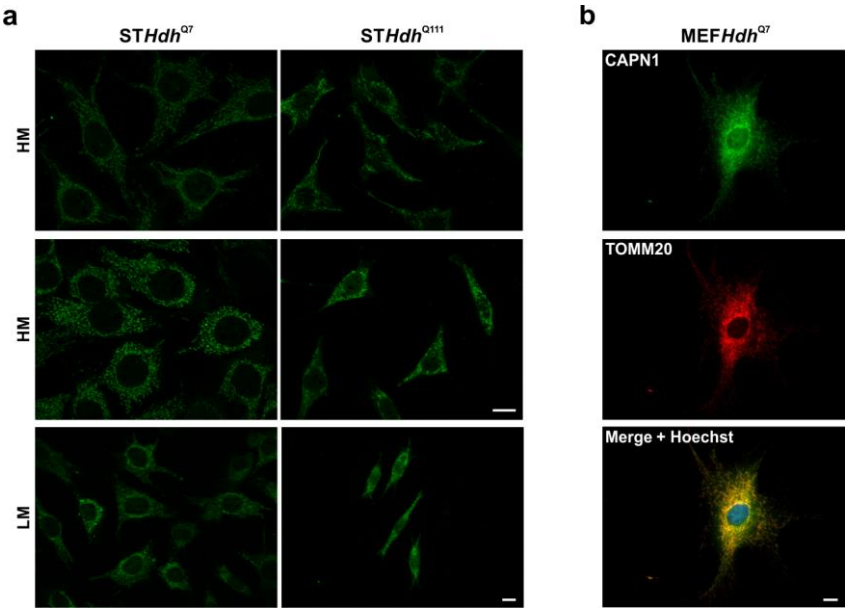

Figure 3. Immunofluorescence microscopy of ST*Hdh* cells and MEF*Hdh*s reveals a mitochondrial association of calpain-1. (**a**) ST*Hdh* cells expressing huntingtin with 7 or 111 glutamines were stained with an antibody specific for calpain-1 (green). (**b**) MEFs expressing huntingtin with 7 glutamines were double stained with antibodies specific to calpain-1 (green) and to the mitochondrial outer membrane protein TOMM20 (red). Both signals show a strong structural resemblance and colocalization (yellow). Nuclei were counterstained with Hoechst 33342 (blue). LM = low magnification; HM = high magnification. Scale bar = 20 µm.

Viability of HD cells increases upon calpain inhibition

As proteolytic cleavage of huntingtin is reported to produce toxic fragments, we sought to investigate whether pharmacologic inhibition of calpains in ST*Hdh*^{Q111} would lead to increased cell viability due to a reduced calpain-dependent huntingtin cleavage. For this, we incubated ST*Hdh*^{Q7} and ST*Hdh*^{Q111} cells with calpain inhibitors ALLN or PD150606 for 24 h and measured viability using a resazurin-based fluorescent assay (Fig. 4). As hypothesized, ST*Hdh*^{Q111} cells showed a significantly increased viability when incubated with one or the other calpain inhibitor when compared to DMSO treated controls. Interestingly, the viability of ST*Hdh*^{Q7} cells was significantly reduced.

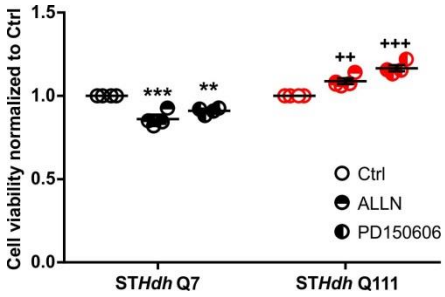

Figure 4. Calpain inhibition leads to an increased viability of ST*Hdh*^{Q111} cells, but reduces viability of ST*Hdh*^{Q7} cells. ST*Hdh* cells were grown in a 96 well plate and incubated with 5 µM ALLN or 25 µM PD150606 for 24 h. Afterwards, cell viability was measured fluorometrically using the resazurin-based PrestoBlue® assay. Horizontal lines represent the means ± s.e.m. of four independent experiments. Statistical significance was assessed using one-way-ANOVA with Tukey post-test. Q7 Ctrl vs. treated: *; Q111 Ctrl vs. treated +; **/++: $P < 0.01$; ***/+++: $P < 0.001$.

Discussion

Several studies have shown that calpain activity is upregulated in HD animal models and *post mortem* HD brain tissue (Gafni and Ellerby, 2002; Gafni *et al.*, 2004; *Accepted paper d & e*). In order to further investigate this condition and to identify cell-based models recapitulating calpain overactivation, we analysed two cell models of HD derived from HD knock-in animals, the HDKI mice (Wheeler *et al.*, 1999).

By performing western blot analysis of ST*Hdh*^{Q111} cells and their respective control line ST*Hdh*^{Q7}, we were able to reproduce the known dysregulation and increased activation of the calpain system. This observation is consistent with results retrieved from previous *in vivo* studies by other researchers and our lab, which investigated calpains in the HDKI animals, the source of ST*Hdh* cells, and in further mouse and rat models of HD (Gafni *et al.*, 2004; Cowan *et al.*, 2008; Dau *et al.*, 2014; *Accepted paper d & e*). Furthermore, a study on HD-associated dopamine and glutamate neurotoxicity qualitatively showed an increased calpain-dependent fragmentation of α-spectrin in ST*Hdh*^{Q111} cells at baseline (Paoletti *et al.*, 2008). When analysing fibroblasts generated from HDKI mice and wild type controls, MEF*Hdh*^{Q111} and MEF*Hdh*^{Q7}, we found a comparable trend towards an overactivation of calpains, but without reaching significance as for ST*Hdh*^{Q111} cells. The lacking reproducibility of the effects in MEF*Hdh* might be due to multiple factors like the differing tissue origin of MEFs and ST*Hdh* cells. While ST*Hdh* cells are of striatal origin, MEF cultures are primarily considered as mesenchymal cells composed of highly heterogeneous populations (Singhal *et al.*, 2016).

In addition, we performed immunofluorescence analysis of ST*Hdh* cells and MEF*Hdh*s to reassess the alterations of calpain-1 levels as seen in western blotting by microscopy. Most interestingly, we detected a specific spatial distribution of calpain-1 within the cell, which could be identified as a colocalization with mitochondria. Although it is known that calpains exhibit both a cytosolic and a mitochondrial distribution, and that calpain-1 is exhibiting a mitochondrial targeting sequence at its N-terminus, it was still surprising that the localization of calpain-1 appeared to be mainly mitochondrial (Badugu *et al.*, 2008; Smith and Schnellmann, 2012). This observation could highlight a subcellular link between calpain-1 activation and the effects of the compound olesoxime, which binds to the outer mitochondrial membrane protein VDAC1 and was shown to lead to an amelioration of calpain overactivation in animal models of HD in two of our studies (Bordet *et al.*, 2010; *Accepted paper d & e*).

As calpains are reported to be involved in the formation of toxic fragments of mutant huntingtin and, when overactivated, to trigger synaptic dysfunctions, we tested the effect of a

pharmacologic inhibition of calpains in ST*Hdh*^{Q7} and ST*Hdh*^{Q111} cell lines (Gafni *et al.*, 2004; Cowan *et al.*, 2008). Treatment with calpain inhibitors ALLN and PD150606 led to an increased viability of the mutant ST*Hdh*^{Q111} cells, whereas the wild type counterpart showed an impaired viability. These contrary effects could be due to a negative impact of inhibiting a non-pathologic calpain system in wild type cells, whereas the calpain overactivation in ST*Hdh*^{Q111} cells could be favourably decreased upon inhibitor addition. In this context, it is worth mentioning, that activation of the calpain system might not only trigger pathological conditions but may also mediate neuroprotective functions (Wu and Lynch, 2006; Baudry and Bi, 2016).

In summary, ST*Hdh* cells and, to a limited extent, MEF*Hdh*s constitute appropriate cellular models for investigating the HD-related calpain overactivation and for screening pharmacologic interventions, which target this condition as a therapeutic approach.

Author contribution statements

Experimental design: JJW, HPN

Conduction of experiments: JJW, LK, LEC

Data analysis: JJW, LEC

Acknowledgements

We want to thank our colleague Carolin Walter for establishing the MEF*Hdh* lines used in this study.

B. Calpain activation in the YAC128 mouse model of HD

Jonasz J. Weber[1,2], Dagmar E. Ehrnhoefer[3], Michael R. Hayden[3], Olaf Riess[1,2], Huu P. Nguyen[1,2]

[1] Institute of Medical Genetics and Applied Genomics, University of Tuebingen, Tuebingen, Germany

[2] Centre for Rare Diseases, University of Tuebingen, Tuebingen, Germany

[3] Department of Medical Genetics, University of British Columbia, Vancouver, Canada

Introduction

The identification and choice of an appropriate disease model is an important prerequisite for investigating molecular pathomechanisms and experimental treatment approaches not only in Huntington disease (HD) but medical life science in general. A long list of animal models has been generated for HD, which recapitulate to a greater or lesser extent the phenotypic and molecular hallmarks of this neurodegenerative disorder (Pouladi *et al.*, 2013). Calpain overactivation, which has been described for patient post-mortem tissue, has also been identified in a variety of cell and animal models of HD (Gafni and Ellerby, 2002; Cowan *et al.*, 2008; *Accepted paper d & e*; *Unpublished project manuscript A*). A widely used and well characterized HD rodent model is the YAC128 mouse (Slow *et al.*, 2003). Although calpain activation has previously been reported for these mice, we sought to investigate the calpain system more in detail (Cowan *et al.*, 2008). For this, we focussed on the analysis of activation and expression patterns of different calpains and calpain substrates in striatum and cortex of YAC128 mice at different ages.

Materials and Methods

Animals

All animal experiments were conducted in accordance with protocols approved by the University of British Columbia Committee on Animal Care and the Canadian Council on Animal Care. Wild type and YAC128 mice bred on a FVB/N background were genotyped and housed as previously described (Slow *et al.*, 2003). Animals were sacrificed at 6 weeks (presymptomatic) or 12 months (symptomatic) of age. Mouse brains were dissected for further western blot or histological analyses.

Immunofluorescence staining of brain sections

Dissected brains of YAC128 mice at 12 months of age were processed for fluorescence microscopy as described before (Casadei *et al.*, 2014). 7-µm-sagittal sections were stained with primary antibodies rabbit anti-calpain-1 (1:200; ab39170, Abcam), rabbit anti-calpain-2 (1:200; ab39168, Abcam), and rabbit anti-CAST (1:200; #4146, Cell Signaling) and the secondary antibody goat anti-rabbit Alexa Fluor® 488 (1:500; ab150077, Abcam). Nuclei were counterstained using 4′,6-diamidino-2-phenylindole (DAPI).

Antibodies for western blotting

The following list contains information on additional antibodies used for western blot analysis in this study, which were not mentioned elsewhere: rabbit anti-calpain-2 (1:500; ab39165, Abcam); rabbit anti-calpain-5 (1:500; ab38943, Abcam); rabbit anti-calpain-10 (1:500; ab28220, Abcam); mouse anti-NR2B (1:500; clone13/NMDAR2B, 610416, BD Biosciences); rabbit anti-p35 (1:500; clone C64B10, #2680, Cell Signaling).

Further materials and methods

Information on tissue preparation and lysis, western blot analysis, and antibodies can be found under *Accepted papers d, e*, and *g.*

Results

Analysis of calpain activation in the YAC128 mouse model of HD at 12 months of age

To assess calpain activity in cortex and striatum of YAC128 mice, we analysed the expression levels and activation state of members of the calpain system by western blotting. Furthermore, we detected fragmentation of the known calpain substrates α-spectrin and N-methyl D-aspartate receptor subtype 2B (NR2B) (Cowan *et al.*, 2008). As we expected an aggravation of calpain overactivation with aging as concluded from the previously analysed BACHD rats and HDKI mice, we first focused on investigating samples of 12-month-old animals (*Accepted paper d & e*). However, immunodetections did not show differences in the expression levels of calpains or in the fragmentation of their substrates in cortex (Fig. 1a). Interestingly, we observed a trend towards a reduced expression of calpains and a lowered formation of calpain cleavage-derived α-spectrin and NR2B fragments in striatum (Fig. 1b). Concordantly, CAST levels were significantly increased in striatum of 12-month-old YAC128 mice, suggesting an inhibiting effect on calpain activation in these animals compared to wild type.

To analyse calpain expression alterations in YAC128 mice at histological level, we performed immunofluorescence staining of paraffin-embedded brain sections of 12-month-old wild type and YAC128 mice. Using fluorescence microscopy, we evaluated signal distribution and intensity of calpain-1, calpain-2, and CAST (Fig. 2). Comparison of cortex, striatum and cerebellum showed no striking differences in signal intensities between genotypes. This observation accords to our results in western blotting, where calpain levels were unchanged or exhibited only tendencies in variation. Notably, the mainly cytoplasmic expression of all three immunodetected members of the calpain system appeared to be lower in striatum than in cortex and cerebellum.

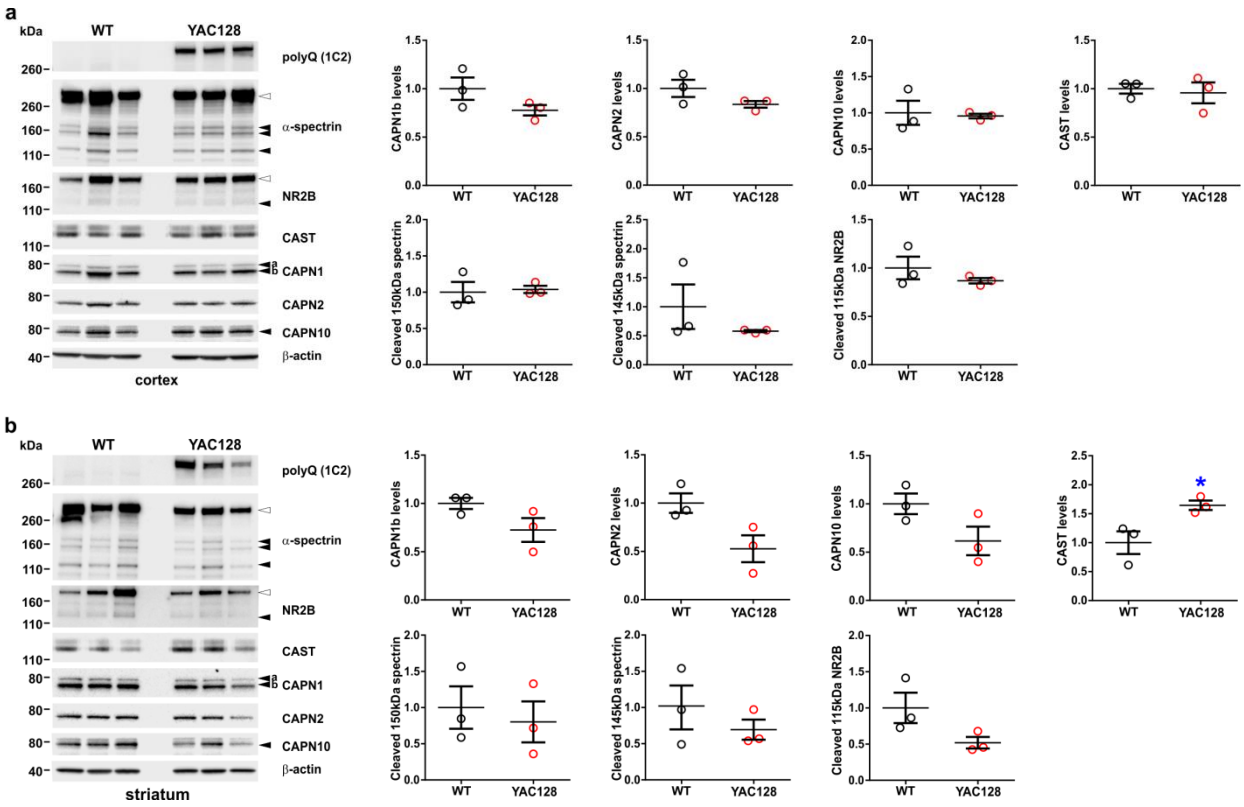

Figure 1. Western blot analysis shows a trend towards decreased calpain activation in striatum of 12-month-old YAC128 mice. Cortical (**a**) and striatal (**b**) lysates of 12-month-old wild type (WT) and YAC128 mice were analysed using western blotting and immunostaining with antibodies against calpain-1, calpain-2, calpain-10, α-spectrin, NR2B, and CAST. Genotyping was confirmed using the polyglutamine (polyQ)-specific antibody 1C2. Actin served as a loading control. Protein levels were quantified using the NIH software ImageJ. Horizontal lines represent the means ± s.e.m. of three animals per genotype. Statistical significance was assessed by Student's *t*-test, *: $P < 0.05$.

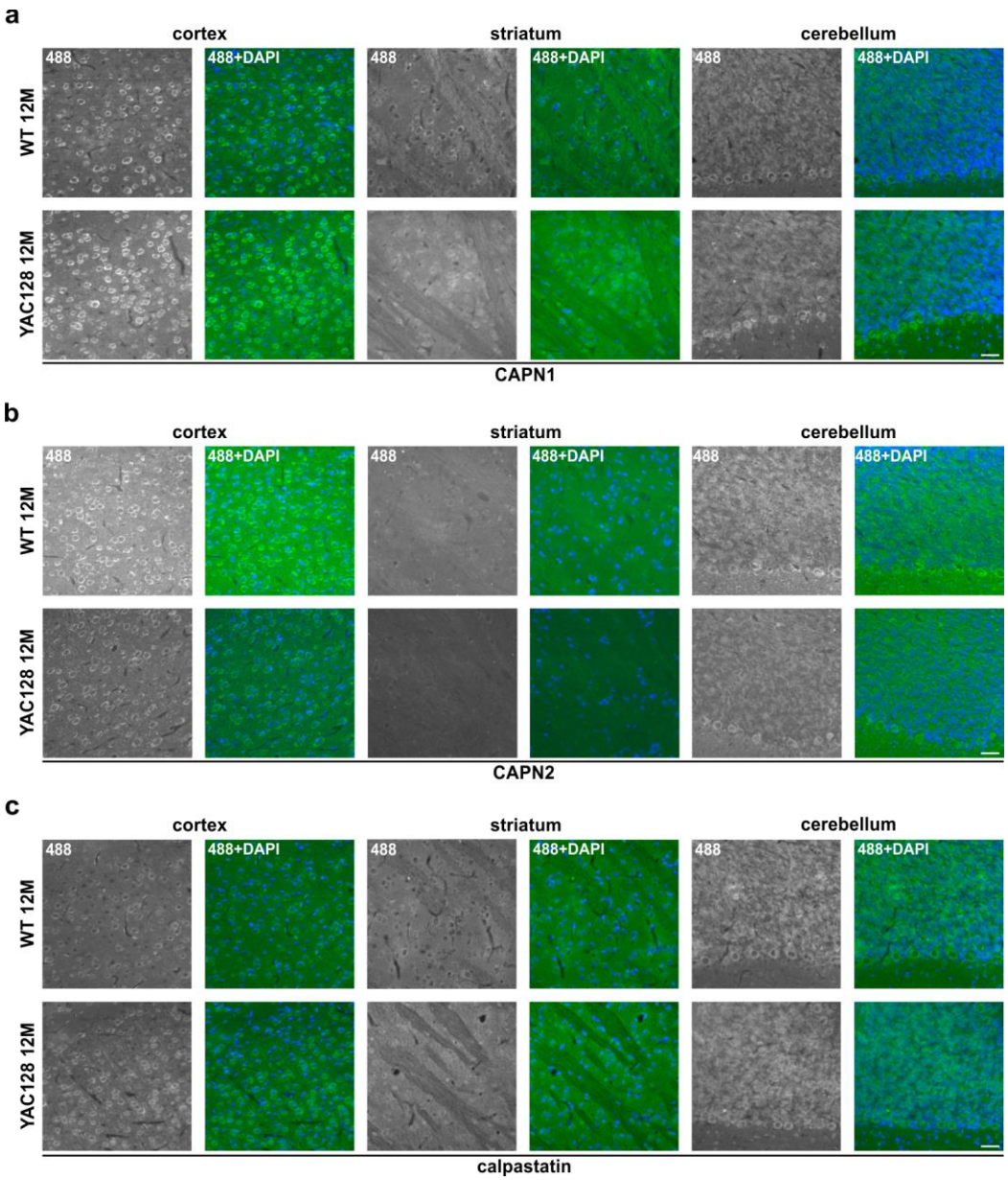

Figure 2. Immunofluorescence analysis of 12-month-old mouse brain sections show region-specific differences in calpain expression. Sagittal brain sections of 12-month-old wild type (WT) and YAC128 mice were immunostained using calpain-1 (**a**), calpain-2 (**b**) and CAST (**c**)-specific antibodies in combination with an Alexa® 488-coupled secondary antibody (greyscale and green). Nuclei were counterstained using DAPI (blue). All three markers of the calpain system show no strong differences when comparing genotypes. Focussing on differences between brain regions, calpain-1, calpain-2 and to a lesser extent CAST exhibit a weaker staining of cell bodies in striatum than in cortex or cerebellum. Scale bar = 50 µm.

Analysis of calpain activation in the YAC128 mouse model of HD at 6 weeks of age

In retrospect to absent calpain overactivation in 12-month-old YAC128 mice, we focused on analysing younger animals to examine possible age-dependent attenuation effects on calpain activity. For this purpose, we analysed cortical and striatal lysates of 6-week-old wild type and YAC128 mice by western blotting. Immunodetection of calpain-1, calpain-2, calpain-5 and calpain-10 did not show alterations in expression levels or activation in cortex (Fig. 3a) or striatum (Fig. 3b). The endogenous inhibitor CAST showed no changes in expression levels despite observing an increase in striatum of 12-month-old YAC128 animals. Likewise, neither calpain substrates α-spectrin and p35 nor huntingtin exhibited differences in fragmentation. Interestingly, expression levels of full-length α-spectrin were significantly increased in YAC128 cortex. Comparably, striatal α-spectrin levels showed a trend towards an elevation in YAC128 mice compared to wild type animals.

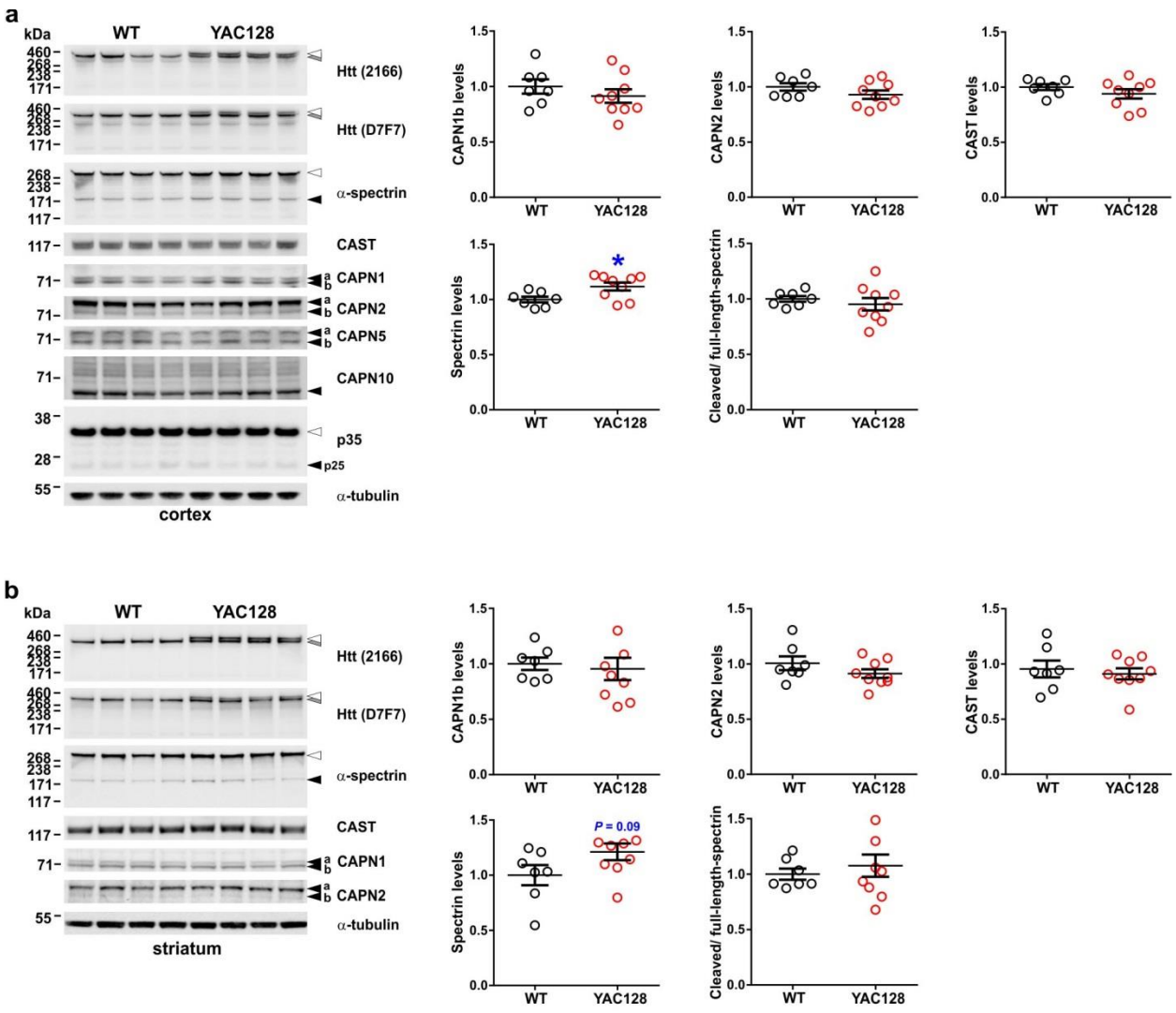

Figure 3. Western blot analysis of cortex and striatum of 6-week-old animals shows no differences in calpain activation between wild type and YAC128 mice. Cortical (**a**) and striatal (**b**) lysates of 6-week-old wild type (WT) and YAC128 mice were analysed using western blotting and immunostaining with antibodies against calpain-1, calpain-2, calpain-5, calpain-10, p35, α-spectrin, and CAST. Mouse genotypes were confirmed and huntingtin fragmentation was investigated using the huntingtin-specific antibodies 2166 and D7F7. Tubulin served as a loading control. Protein levels were quantified using the NIH software ImageJ. Horizontal lines represent the means ± s.e.m of 7 wild type and 9 YAC128 animals. Statistical significance was assessed by Student's *t*-test, *: $P < 0.05$.

Discussion

As previous studies demonstrated that calpains are overactivated in brain of two HD animal models, the BACHD rat and the *Hdh*^{Q111} knock-in (HDKI) mouse, we analysed the calpain activation in an additional, well characterized animal model, the YAC128 mouse (Slow *et al.*, 2003; *Accepted paper d & e*).

We performed our first analyses in YAC128 animals at an age of 12 months since we expected a stronger activation of the calpain system with disease progression. Surprisingly, we did not detect elevated levels of calpains, increased calpain activation or a higher fragmentation of typical calpain substrates like α-spectrin. Investigations of cortex samples by western blotting did not show any alterations. However, striatal samples exhibited a trend towards a reduced calpain activation accompanied by significantly increased levels of the endogenous calpain inhibitor CAST. The decreased activation of the calpain system in YAC128 striatum at 12 months of age is consistent with recent findings (Dau *et al.*, 2014), which showed elevated calpain activity in YAC128 mice at 6 weeks but not at 4 months of age. These observations suggest a possible attenuation of the calpain activity with aging in YAC128 mice. Therefore, we repeated our analyses using cortical and striatal samples of 6-week-old wild type and YAC128 mice. However, we neither detected an increase in calpain activity nor an elevation in CAST levels, as observed in striatum of 12-month-old YAC128 mice.

Taken together, our results are in contrast to the previously described overactivation of calpains in the YAC128 model and demand further validations (Cowan *et al.*, 2008; Gladding *et al.*, 2012; Dau *et al.*, 2014). A possible control experiment in this regard could be performed by altering the genetic background of YAC128 mice. It is known, that maintaining inbred mouse strains over many generations can lead to an accumulation of mutations, which can eventually alter the manifestation of a disease phenotype (Yoshiki and Moriwaki, 2006). For HD mouse models it has been reported that breeding onto C57BL/6 or FVB/N background strains can modify the severity of a HD phenotype (Lloret *et al.*, 2006; Ehrnhoefer *et al.*, 2009). Although earlier investigations on calpains were performed using YAC128 mice on the FVB/N background, changing to the C57BL/6 strain could be a promising strategy as HDKI mice, which feature calpain overactivation, were bred on the latter background.

Alternatively, an excitotoxic insult could be induced pharmacologically in YAC128 mice to trigger differences in the calpain activation. This can be performed by administering NMDA or

quinolinic acid, which both have been described as potent compounds for modelling HD or as an additional stressor in YAC128 animals (Beal *et al.*, 1986; Graham *et al.*, 2009).

In summary, a clear activation of the calpain system in YAC128 mice, as described in several previous studies, could not be reproduced in our investigations. This circumstance questions, at least to some extent, whether overactivation of the calpain system plays a major role during the entire lifespan of the YAC128 mouse model.

Author contribution statements

Experimental design: DEE, MRH; HPN, OR

Conduction of experiments: JJW

Data analysis: JJW

C. Calpastatin ablation in the HDKI mouse model of HD

Jonasz J. Weber[1,2], Maike Nagel[1,2], Julian Hofman[1,2], Huu P. Nguyen[1,2]

[1] Institute of Medical Genetics and Applied Genomics, University of Tuebingen, Tuebingen, Germany
[2] Centre for Rare Diseases, University of Tuebingen, Tuebingen, Germany

Introduction

One of the most investigated regulatory mechanisms for calpain activity is the inhibitory function of the endogenous proteinaceous calpain inhibitor calpastatin (CAST) (Wendt *et al.*, 2004; Hanna *et al.*, 2008). Two *in vivo* studies conducted in our institute investigated the effect of a genetic CAST depletion on the pathogenesis of mutant synuclein-linked Parkinson disease (PD) and Spinocerebellar ataxia type 3 (SCA3) (Diepenbroek *et al.*, 2014; *Accepted paper a*). Both studies showed that a CAST knockout led to an increase in calpain activation, an aggravation of disease-associated molecular hallmarks and a worsening of the disease phenotype. As calpains play an important role in Huntington disease (HD), we aimed for analysing the effect of a CAST ablation in a mouse model of HD. For this purpose, we crossbred *Hdh*^{Q111} knock-in (HDKI) with *Cast*$^{-/-}$ mice and analysed HD-related molecular characteristics including calpain activation, and both fragmentation and aggregation of mutant huntingtin.

Materials and Methods

Animals

All mouse experiments were conducted after approval by the local ethics committee at the Regierungspraesidium Tuebingen in accordance with the German Animal Welfare Act and the guidelines of the Federation of European Laboratory Animal Science Associations, based on European Union legislation (Directive 2010/63/EU). Homozygous calpastatin knockout (*Cast*$^{-/-}$) and heterozygous *Hdh*^{Q111} (HDKI) mice bred on a C57BL/6 background were maintained and genotyped as previously described (Wheeler *et al.*, 1999; Takano *et al.*, 2005). Both models were crossbred to obtain following groups of animals: wild type (WT), *Cast*$^{-/-}$, HDKI, and HDKI/*Cast*$^{-/-}$. Animals were sacrificed by CO_2 inhalation. Whole brains were immediately dissected on ice, snap-frozen in liquid nitrogen and stored at –80°C for further analysis.

Antibodies for western blotting

The following list contains information on additional antibodies used for western blot analysis in this study, which were not mentioned elsewhere: rabbit anti-DARPP-32 (1:10.000; clone EP720Y, 1710-1, Epitomics), mouse anti-LC3 (1:200, clone 5F10, NanoTools), and rabbit anti-p62 (1:500; #5114, Cell Signaling).

Further materials and methods

Information on tissue preparation and lysis, western blot analysis, filter retardation assays and antibodies can be found under *Accepted paper e.*

Results

Calpain activation is increased in brain of calpastatin knockout animals

To assess the baseline activation of the calpain system in *Cast*$^{-/-}$ mice, whole brain lysates of 10-month-old wild type and *Cast*$^{-/-}$ mice were analysed using western blotting (Fig. 1a). CAST knockout was confirmed by immunodetection. Calpain-1 autoprocessing and cleavage of calpain substrate α-spectrin were significantly elevated in *Cast*$^{-/-}$ animals compared to wild type controls. Correspondingly, the fragmentation of a second substrate protein p35 was increased as demonstrated by a higher p35-to-p25 conversion (Fig. 1b). These observations point towards a globally elevated calpain system activation upon genetic CAST depletion.

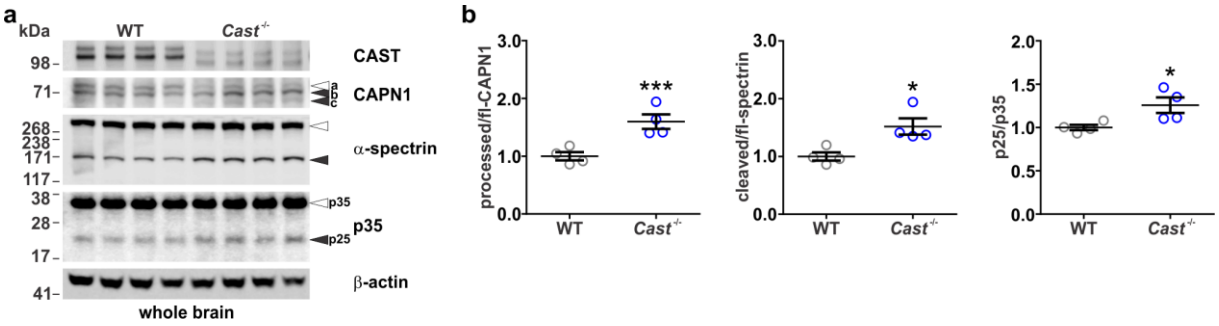

Figure 1. Western blot analysis of brain tissue of 10-month-old animals shows increased calpain activation in CAST knockout brains. (**a**) Whole brain lysates of wild type (WT) and *Cast*$^{-/-}$ mice at 10 months of age were analysed by western blotting and immunostaining with antibodies against calpain-1, α-spectrin and p35. Mouse genotypes were confirmed by detection of CAST. Actin served as a loading control. (**b**) Protein levels were quantified using the LI-COR Image Studio Software. Horizontal lines represent the means ± s.e.m. of 4 animals per genotype. Statistical significance was assessed by Student's *t*-test. *: $P < 0.05$, ***: $P < 0.001$.

Calpastatin ablation amplifies calpain activation in the HDKI brain

After corroborating the increased calpain activation in brains of *Cast*$^{-/-}$ mice at 10 months of age, we analysed the effect of a CAST knockout in HDKI animals. We first confirmed the successful knockout of CAST in single mutant (*Cast*$^{-/-}$) and double mutant (HDKI/*Cast*$^{-/-}$) animals and investigated its implication on the calpain system. For this purpose, we performed western blotting of whole brain lysates of animals at 13 months of age using antibodies directed against CAST, calpain-1, α-spectrin and p35 (Fig. 2a). Detection of CAST showed the complete ablation of the protein in *Cast*$^{-/-}$ and HDKI/*Cast*$^{-/-}$ mice compared to wild type and HDKI mice. Furthermore, CAST knockout led to a significantly increased activation of calpain-1, to elevated levels of the calpain cleavage-derived α-spectrin fragment and to higher proteolytic conversion of the calpain substrate p35 (Fig. 2b). The increased calpain activation at baseline, which has been already observed in HDKI striatum at 6 months (*Accepted paper e*), was, by tendency, reproduced in whole brain at 13 months but without reaching significance.

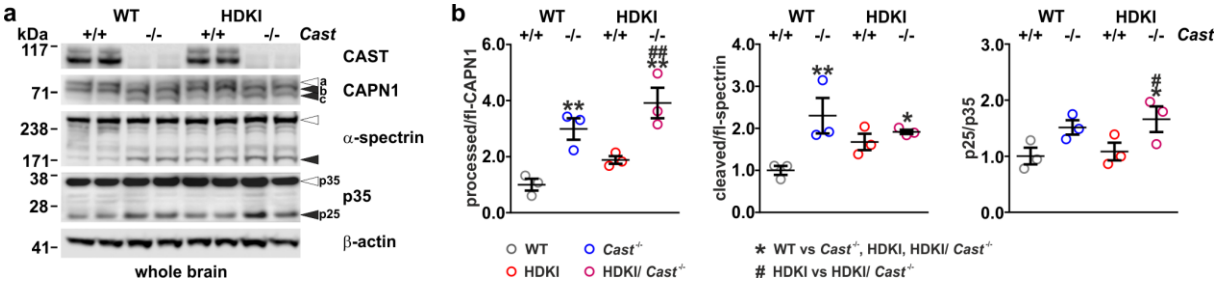

Figure 2. Western blot analysis of brain tissue of 13-month-old animals shows increased calpain activation upon CAST ablation. (**a**) Whole brain lysates of 13-month-old mice were analysed using western blotting and immunostaining with antibodies against calpain-1, CAST, α-spectrin and p35. Actin served as a loading control. (**b**) Protein levels were quantified using the NIH software ImageJ. Horizontal lines represent the means ± s.e.m. of three animals per genotype. Statistical significance was assessed by one-way ANOVA with Fisher's LSD post-hoc analysis, */#: $P < 0.05$ and **/##: $P < 0.01$.

Calpastatin knockout elevates the cleavage of wild type and mutant huntingtin in vivo

As CAST knockout led to an increased activation of the calpain system, we next analysed its impact on the fragmentation of wild type and mutant huntingtin *in vivo*. Western blotting and immunostaining for huntingtin using the antibodies 2166 (epitope between amino acids 443-457) and D7F7 (epitope surrounding amino acid 1220) revealed an increased formation of N-terminal, polyQ-dependent and C-terminal, polyQ-independent huntingtin fragments (Fig. 3; red and black arrowheads, respectively) in both *Cast*$^{-/-}$ and HDKI/*Cast*$^{-/-}$ animals. Interestingly, the majority of detected fragments appeared to originate from calpain-dependent cleavage and only a small portion of breakdown products remained unchanged due to CAST knockout.

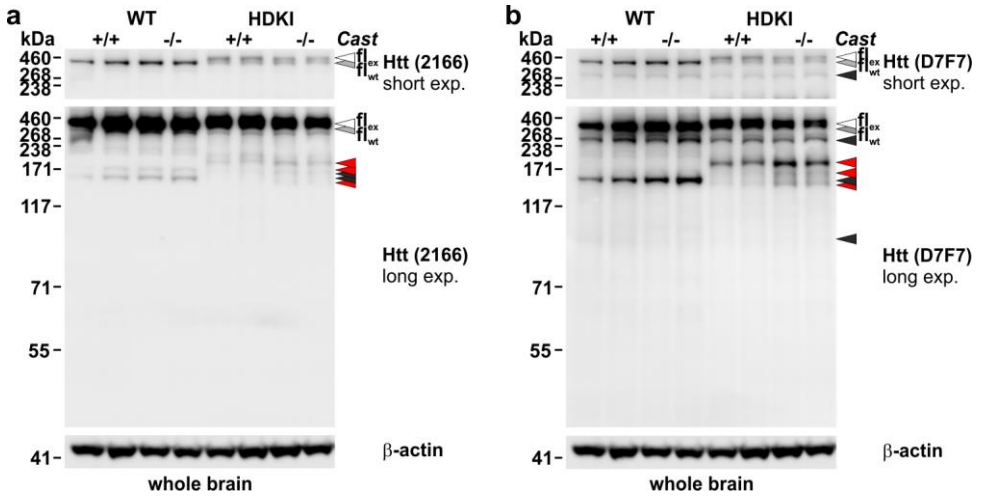

Figure 3. CAST ablation results in an increased fragmentation of wild type and polyQ-expanded huntingtin. Whole brain lysates of 13-month-old mice were analysed using western blotting and immunostaining with the huntingtin-specific antibodies 2166 (**a**) and D7F7 (**b**). Red arrowheads indicate N-terminal, polyQ-dependent fragments and black arrowheads C-terminal fragments, which do not contain the polyQ stretch. Actin served as a loading control. exp. = exposure; fl_{wt} = full-length wild type huntingtin; fl_{ex} = full-length expanded huntingtin.

Calpastatin knockout enhances aggregation of mutant huntingtin

N-terminal fragments of polyQ-expanded huntingtin have been shown to be more aggregation-prone than the full-length protein (Cooper *et al.*, 1998; Li and Li, 1998). Since genetic CAST ablation led to an increased formation of these fragments, we sought to study the aggregation of huntingtin in the brain of HDKI/*Cast*$^{-/-}$ mice in comparison to HDKI animals. For this, we performed filter retardation assays of whole brain homogenates and immunostaining with the 2166 antibody (Fig. 4a). While wild type and *Cast*$^{-/-}$ mice did not exhibit SDS-insoluble species of huntingtin, both HDKI and HDKI/*Cast*$^{-/-}$ mice featured an accumulation of huntingtin aggregates. As expected, CAST knockout led to elevated huntingtin aggregation, with levels 20% higher than in HDKI animals.

To investigate whether CAST knockout further promoted striatal dopaminergic dysfunction in HDKI animals, we detected levels of DARPP-32, a marker for dopaminergic neurons, in whole brain lysates by western blotting (van Dellen *et al.*, 2000; Slow *et al.*, 2003; Jiang *et al.*, 2012). Animals expressing polyQ-expanded huntingtin showed strongly reduced levels of DARPP-32 when compared to wild type animals (Fig. 4b). Interestingly, knockout of CAST alone led to lower amounts of DARPP-32 in *Cast*$^{-/-}$ mice, while an additional effect on HDKI/*Cast*$^{-/-}$ was unobvious. The decrease in DARPP-32 levels in *Cast*$^{-/-}$ mice was accompanied by a significant increase in fragments, suggestive of a calpain-mediated cleavage of the protein.

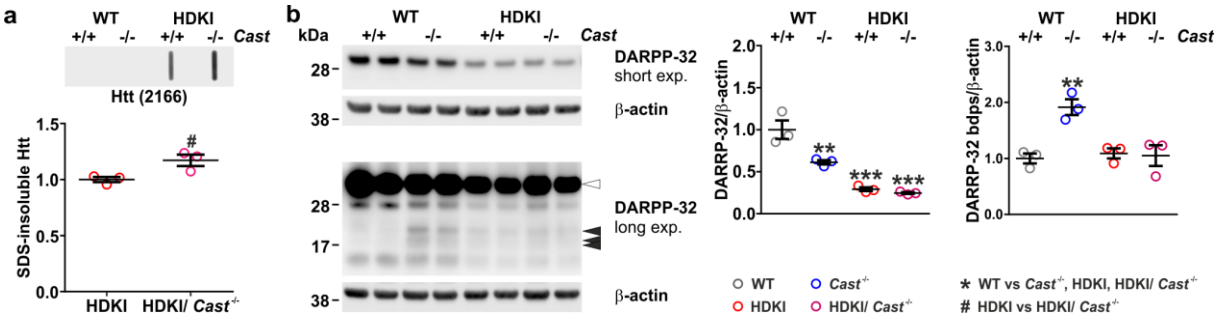

Figure 4. CAST ablation in HDKI animals leads to an increased formation of huntingtin aggregates. (**a**) The huntingtin aggregate load within whole brain homogenates of 13-month-old mice was analysed by filter retardation assay. Retained aggregates were stained using the 2166 antibody. Statistical significance was assessed by Student's *t*-test. #: $P < 0.05$. (**b**) Striatal dopaminergic dysfunction was assessed by western blot analysis of DARPP-32, a phosphoprotein enriched in different types of striatal neurons in the basal ganglia. Black arrowheads indicate DARPP-32 breakdown products (bdps), whereas the white arrow head points to the full-length protein. Actin served as a loading control. Aggregate and protein signals were quantified using the NIH software ImageJ. Horizontal lines represent the means ± s.e.m. of three animals per group. Statistical significance was assessed by one-way ANOVA with Fisher's LSD post-hoc analysis. **: $P < 0.01$; ***: $P < 0.001$.

Calpastatin knockout perturbs the autophagy system

A recent study reported on the degradation of mutant huntingtin aggregates via a calpain-dependent regulation of the autophagy system. Overexpression of CAST led to a lowered calpain activity, which in turn increased autophagosome levels and reduced the aggregate load in *Drosophila* and HD mice (Menzies *et al.*, 2014). Furthermore, calpains were shown to inhibit autophagy by inactivating key proteins of the autophagy pathway (Yousefi *et al.*, 2006; Russo *et al.*, 2011). Therefore, we investigated whether the observed increase of huntingtin aggregates in double mutant mice resulted not only from an elevated cleavage of polyQ-expanded huntingtin but, in addition, from a calpain-dependent impairment of the autophagy system. To assess the state of autophagy in our mice, we detected by western blotting levels of LC3-II, a modified variant of LC3 and marker for the amount of autophagosomes, and p62, an autophagy adaptor protein which is degraded during the process of autophagy (Fig. 5). Surprisingly, levels of LC3-II were raised in *Cast*$^{-/-}$, HDKI and double mutant animals, and p62 showed a significant decrease indicative of an upregulated autophagy system.

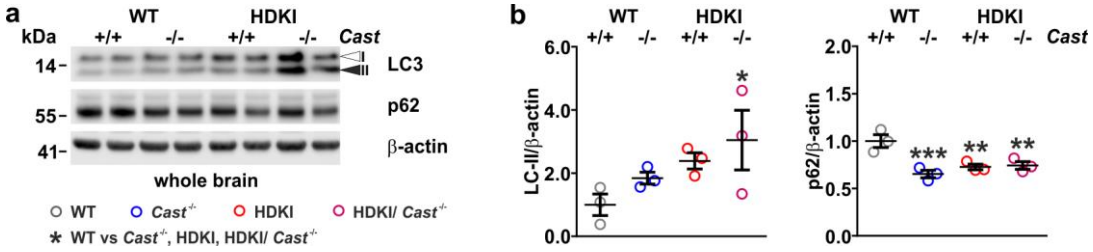

Figure 5. Western blot analysis of brain tissue of 13-month-old animals reveals increased levels of autophagy marker LC3-II despite calpain system overactivation. (**a**) Whole brain lysates of 13-month-old mice were analysed using western blotting and immunostaining with antibodies against p62 and LC3. Actin served as a loading control. (**b**) Protein levels were quantified using the NIH software ImageJ. Horizontal lines represent the means ± s.e.m. of three animals per group. Statistical significance was assessed by one-way ANOVA with Fisher's LSD post-hoc analysis, *: $P < 0.05$; **: $P < 0.01$; ***: $P < 0.001$.

Discussion

An increased activation of the calpain system is an important hallmark in the molecular pathogenesis of HD and might represent a key mediator of mutant huntingtin toxicity (Gafni and Ellerby, 2002; Gafni *et al.*, 2004). In addition, we have demonstrated increased calpain activation in BACHD rats and HDKI mice (*Accepted paper d & e*). A genetic countermeasure is the overexpression of the endogenous calpain inhibitor CAST, which has been shown to ameliorate disease phenotype not only in an animal model of HD, but also of other neurodegenerative diseases (Simões *et al.*, 2012; Diepenbroek *et al.*, 2014; Menzies *et al.*, 2014; Rao *et al.*, 2016). To further investigate the contribution of calpains in neurodegenerative processes in HD, we sought to increase calpain activity by knocking out CAST *in vivo*.

After confirming that calpain activity is elevated in CAST knock-out mice at baseline, we crossbred them with HDKI animals. The lack of the endogenous calpain inhibitor in HDKI animals led expectedly to a further activation of calpains *in vivo*, which eventually resulted in elevated huntingtin fragmentation and aggregate formation. These observations are in line with findings in other mouse models of neurodegenerative diseases, which showed enhanced disease protein cleavage and aggregation accompanied by an increased neuronal loss (Diepenbroek *et al.*, 2014; *Accepted paper a*). Regarding the latter, we investigated dysfunction of dopaminergic neurons by analysing levels of the specific marker DARPP-32. Interestingly, despite not observing an increased loss of DARPP-32 in HDKI/*Cast*$^{-/-}$ mice, we detected a reduction of the protein in *Cast*$^{-/-}$ mice, which was accompanied by an increased formation of presumably calpain-dependent fragments. Corresponding to our findings, DARPP-32 has been previously identified as a substrate protein of calpains in the context of Alzheimer disease (Cho *et al.*, 2015).

Active calpains have been shown to reduce autophagy and thereby contribute to the dysfunctional degradation of toxic protein species like mutant huntingtin aggregates (Yousefi *et al.*, 2006; Sarkar *et al.*, 2009; Russo *et al.*, 2011). To investigate these circumstances as an additional factor in our HDKI/*Cast*$^{-/-}$ mice, we analysed levels of the autophagy proteins LC3-II and p62. Our results for both markers suggest rather an increase than a decrease in autophagy levels, which cannot account for the increased huntingtin aggregate load. However, an increased autophagy might be a compensatory effect bracing against the elevated huntingtin aggregation in HDKI/*Cast*$^{-/-}$ mice. Nevertheless, it is of note that huntingtin itself was shown to act as a scaffold in macroautophagy (Ochaba *et al.*, 2014; Rui *et al.*, 2015). Furthermore, animal models and human HD cells displayed an impairment of

autophagy which was characterized by an impaired cargo recognition (Martinez-Vicente *et al.*, 2010). All these findings must be considered to correctly evaluate autophagy in a disease model like the HDKI/*Cast*$^{-/-}$ mouse.

Although we investigated many molecular characteristics in HDKI/*Cast*$^{-/-}$ mice, which point to the strong involvement of the calpain system in HD, further investigations on the behavioural phenotype are still remaining. These assessments are necessary to entirely judge the impact of a genetic CAST depletion in our HD animals as previously done in a comparable mouse model of SCA3 (*Accepted paper a*).

In summary, the knockout of CAST in a knock-in mouse model of HD resulted in a worsening of the molecular HD-related hallmarks including elevated formation of huntingtin fragments and increased amount of respective aggregates. These observations emphasize the important role of calpains in the pathogenesis of HD and suggest targeting this pathway as a therapeutic approach for this devastating disorder.

Author contribution statements

Experimental design: JJW, HPN

Conduction of experiments: JJW, MN, JH, HPN

Data analysis: JJW, MN

D. Calpain-1 ablation in the YAC84 mouse model of SCA3

Jonasz J. Weber[1,2], Olaf Riess[1,2], Jeannette Hübener-Schmid[1,2*]

[1] Institute of Medical Genetics and Applied Genomics, University of Tuebingen, Tuebingen, Germany

[2] Centre for Rare Diseases, University of Tuebingen, Tuebingen, Germany

Introduction

In our previous study, we reported on the exacerbation of the neurological phenotype in a SCA3 mouse model, which was caused by a genetic ablation of the endogenous calpain inhibitor calpastatin (CAST) (*Accepted paper a*). We showed that both calpain-1 and calpain-2 cleave wild type and mutant ataxin-3, and that the lack of CAST led to an elevated fragmentation and aggregation of ataxin-3 *in vivo*. This was accompanied by an accelerated neurodegeneration in the cerebellum. These observations emphasize the important role of the calpain system in the molecular pathogenesis of SCA3. In addition, our investigations highlighted two distinct genetic strategies to ameliorate the disease phenotype: First, the overexpression of CAST to suppress calpain activity and second, the knockout of calpain-1 or calpain-2 to lower ataxin-3 cleavage. The first approach has already been reported in a recent study, where adeno-associated viral vector-based overexpression of CAST in mouse models of SCA3 improved both the molecular and histological phenotype (Simões *et al.*, 2012). Thus, we aimed at investigating the effect of a calpain-1 knockout (*Capn1*$^{-/-}$) in a SCA3 animal model. For this, we crossbred the YAC transgenic mouse model for SCA3 (YAC84) with mice featuring a genetically inactivated *Capn1* gene (Azam *et al.*, 2001; Cemal *et al.*, 2002).

To investigate the molecular effects of calpain-1 ablation in mouse brain, we analysed the activation state of the calpain system, including levels of CAST and fragmentation of the calpain substrates α-spectrin and p35. The impact on endogenous and transgenic, polyQ-expanded ataxin-3 was surveyed by measuring full-length levels, cleavage and aggregation of ataxin-3.

Materials and Methods

Animals

All mouse experiments were conducted after approval by the local ethics committee at the Regierungspraesidium Tuebingen in accordance with the German Animal Welfare Act and the guidelines of the Federation of European Laboratory Animal Science Associations, based on European Union legislation (Directive 2010/63/EU). Homozygous calpain-1 knockout (*Capn1*$^{-/-}$) and hemizygous YAC84 mice bred on a C57BL/6 background were maintained and genotyped as previously described (Azam *et al.*, 2001; Cemal *et al.*, 2002). Both models were crossbred to obtain for groups of mice with 3 animals per group: wild type (WT), *Capn1*$^{-/-}$, hemizygous YAC84, and YAC84/*Capn1*$^{-/-}$. Animals were sacrificed at 3 months of age by CO_2 inhalation. Whole brains were immediately dissected on ice, snap-frozen in liquid nitrogen and stored at –80°C for further analysis.

Further materials and methods

Information on tissue preparation and lysis, western blot analysis, and antibodies can be found under *Accepted papers e* and *g.* Details on TR-FRET based measurements of ataxin-3 are described in *Accepted paper a*.

Results

Activation of the calpain system is reduced in Capn1$^{-/-}$ mice

To confirm the knockout of calpain-1 in single (*Capn1*$^{-/-}$) and double mutant animals (YAC84/*Capn1*$^{-/-}$), we performed western blotting of whole brain samples at 3 months of age. Detection of calpain-1 showed the complete absence of the specific band below 80 kDa when compared to wild type and single mutant (YAC84) animals (Fig. 1a). As a response to the genetic calpain-1 depletion, levels of CAST increased and calpain-specific cleavage of α-spectrin and p35 were reduced (Fig. 1a and b). This observation points to a substantial contribution of the calpain-1 enzyme to the baseline fragmentation of the analysed substrates, which was apparently not compensated by another member of the calpain family.

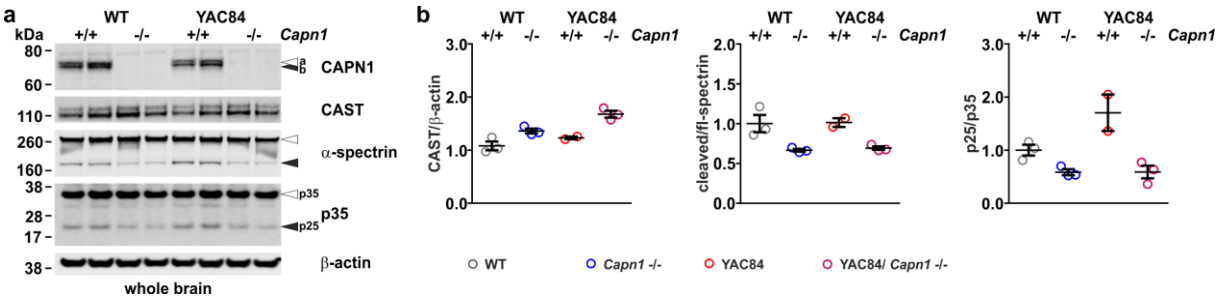

Figure 1. Calpain-1 knockout leads to a downregulation of the calpain system. (**a**) To confirm the calpain-1 knockout (*Capn1*$^{-/-}$) on protein level, whole brain lysates of 3-month-old mice were analysed using western blotting. Activation of the calpain system was assessed by detecting CAST levels and fragmentation state of calpain substrates α-spectrin and p35. Actin served as a loading control. White arrowheads = full-length proteins, black arrowheads = processed/fragmented proteins. (**b**) Quantification of protein levels and fragment ratio shows reduced overall calpain activation in *Capn1*$^{-/-}$ animals. Horizontal lines represent the means ± s.e.m. of two to three animals per group.

Ataxin-3 levels are elevated and cleavage is lowered in calpain-1 knockout animals

As calpain-1 was shown to cleave ataxin-3 *in vitro* and its knockout might therefore reduce ataxin-3 fragmentation, we analysed whole brain samples of 3-month-old mice by western blotting to survey full-length levels and fragments of ataxin-3. Detection with the ataxin-3-specific antibody 1H9 revealed a different fragmentation patter of ataxin-3 in YAC84 mice, when compared wild type animals, featuring additional cleavage bands (Fig. 2a, red arrowheads a_2 and b_2). These marginally bigger fragments appeared to be specific N-terminal breakdown products of the transgenic human ataxin-3, which cannot be explained by an expectedly much stronger polyQ-dependent size shift. Furthermore, immunostaining with 1H9 showed a slight increase in full-length ataxin-3 (Fig. 2a and b). This was accompanied by a reduction of fragment b_1 in *Capn1*$^{-/-}$ animals and b_1 and b_2 in double mutant YAC84/*Capn1*$^{-/-}$ mice (Fig. 2a and 2b). However, fragments a_1 and a_2 showed increased levels when knocking out calpain-1. This observation suggests that these larger fragments are further processed by calpain-1 and are themselves formed in calpain- or at least calpain-1-independent manner.

To confirm the increase of full-length transgenic ataxin-3, we performed TR-FRET analysis to detect only the overexpressed, polyQ-expanded protein in whole brain homogenates. As seen in western blotting, TR-FRET measurements showed an increase of full-length ataxin-3 in YAC84/*Capn1*$^{-/-}$ mice when compared to YAC84 animals (Fig. 3a), which seems to be a direct effect of the lowered calpain-dependent fragmentation.

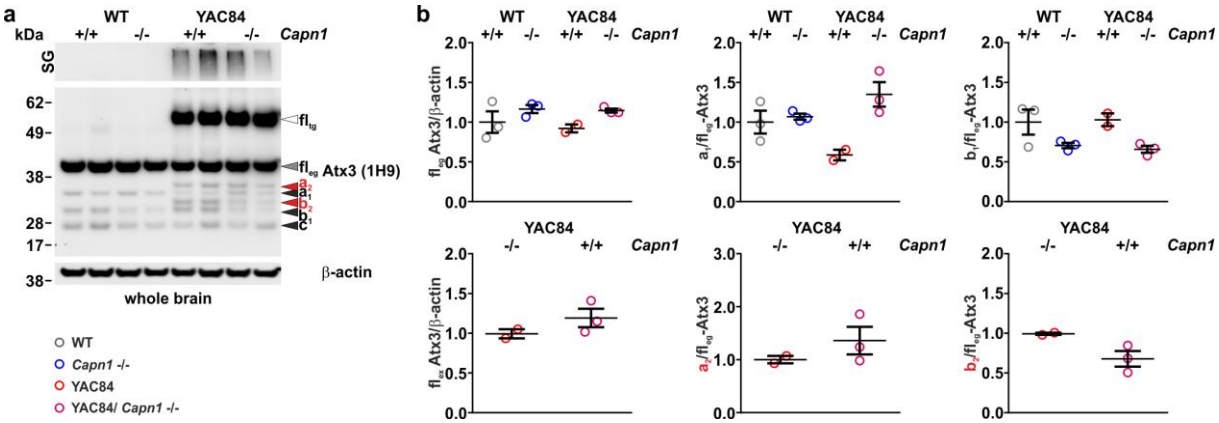

Figure 2. Calpain-1 knockout reduces cleavage of ataxin-3. (**a**) The effect of calpain-1 knockout (*Capn1*$^{-/-}$) on ataxin-3 cleavage was analysed in whole brain lysates of mice at 3 months of age using the ataxin-3 antibody 1H9. Ataxin-3 fragments are indicated with black and red arrowheads (labelled with a_1, a_2, b_1, b_2, and c). Red arrowheads indicate ataxin-3 fragments specifically formed in YAC84 animals. Detection of the blotted stacking gel (SG) shows ataxin-3 aggregates in YAC84 animals. Actin served as a loading control. WT = wild type; fl = full-length; tg = transgenic ataxin-3; eg = endogenous ataxin-3. (**b**) Quantification of ataxin-3 full-length levels and fragment ratios. Full-length transgenic and endogenous ataxin-3 shows a slight increase in *Capn1*$^{-/-}$ animals. Fragment a_1 and a_2 levels exhibit an increase, whereas levels of fragment b_1 and b_2 are reduced. Horizontal lines represent the means ± s.e.m. of two to three animals per group.

Ataxin-3 aggregation levels are not altered in mice with a calpain-1 *knockout*

Proteolytic fragmentation of polyQ proteins has been suggested as the source of toxic and aggregation-prone breakdown products and thus as a contributing factor to the formation of protein aggregates. To investigate effects of the calpain-1 knockout on ataxin-3 aggregation *in vivo*, we performed filter retardation assays to measure the aggregate load in whole brain homogenates of YAC84 animals with and without the genetic depletion of calpain-1. However, detection with the ataxin-3-specific antibody 1H9 showed no major changes in the aggregate levels in YAC84/*Capn1*$^{-/-}$ animals of 3 months of age (Fig. 3b) when compared to YAC84 mice.

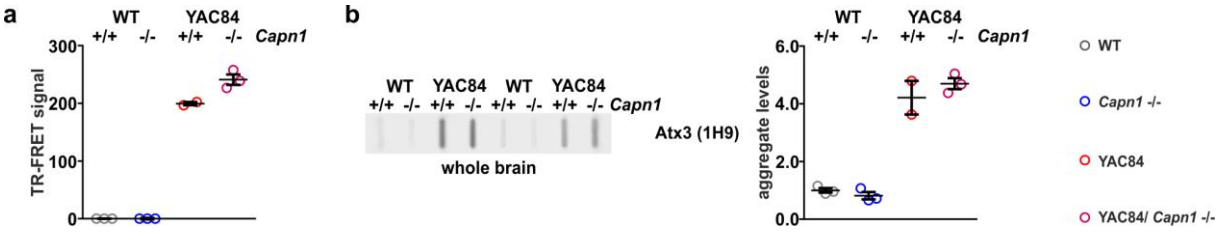

Figure 3. Transgenic ataxin-3 levels increase upon calpain-1 knockout. (**a**) TR-FRET analysis of whole brain homogenates of 3-month-old mice was performed to further validate effects of the calpain-1 knockout (*Capn1*$^{-/-}$) on ataxin-3 levels. Knockout of calpain-1 leads to an increase of the transgenic ataxin-3 signal in YAC84 animals, indicative of elevated levels as seen before by western blotting. (**b**) Ataxin-3 aggregation levels in whole brain homogenates were investigated using filter retardation assays. Signal quantification did not show any clear changes in the aggregate load of YAC84/*Capn1*$^{-/-}$ mice at 3 months of age, when compared to YAC84 animals. Horizontal lines represent the means ± s.e.m. of two to three animals per group.

Calpain-1 knockout leads to increased CAST levels in muscle tissue

The knockout animals used in this study exhibit a global inactivation of calpain-1 in all tissues. To investigate the impact of the calpain-1 knockout in peripheral tissue, we analysed the calpain system and ataxin-3 cleavage in lysates of femoral muscle tissue. Western blot analysis confirmed the knockout of calpain-1 on protein level (Fig. 4a). The lack of calpain-1 expression led to a distinct elevation of CAST levels, whereas alterations of α-spectrin cleavage were not clearly detectable (Fig. 4b). As ataxin-3 is also expressed in muscle tissue, we investigated full-length levels and ataxin-3 fragmentation in our samples. Compared to brain tissue, ataxin-3 showed a slightly different fragmentation pattern in muscle tissue with strongly elevated levels of fragment c (Fig. 4b). As seen for fragmentation of the calpain substrate α-spectrin, cleavage of ataxin-3 was not obviously changed and the samples showed certain variability. However, qualitatively, fragment b_1 showed a trend towards reduced and fragment a_1 toward increased levels (Fig. 4b).

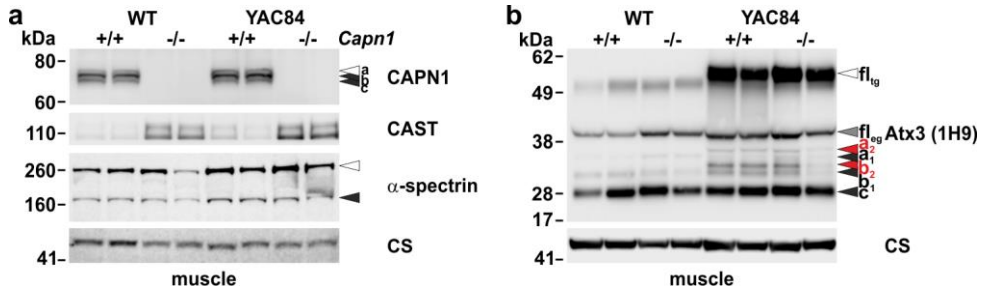

Figure 4. Calpain-1 knockout affects the calpain system in muscle tissue. (**a**) To analyse the calpain-1 knockout in non-neuronal tissue, lysates of femoral muscle tissue of 3-month-old mice were investigated by western blotting. Activation of the calpain system was assessed by detecting CAST levels and fragmentation state of calpain substrate α-spectrin. Citrate synthase (CS) served as a loading control. White arrowheads = full-length proteins, black arrowheads = processed/fragmented proteins. As in neuronal tissue *Capn1*$^{-/-}$ leads to a decrease of calpain system activation in muscle tissue. (**b**) Ataxin-3 fragmentation in femoral muscle tissue lysates was assessed by western blotting with the ataxin-3 antibody 1H9. Ataxin-3 fragments are indicated with black and red arrowheads (labelled with a_1, a_2, b_1, b_2, and c). Citrate synthase (CS) served as a loading control. fl = full-length, tg = transgenic ataxin-3, eg = endogenous ataxin-3.

Discussion

We investigated the genetic inactivation of calpain-1 in the YAC84 mouse model of SCA3 as a possible strategy for lowering calpain-mediated cleavage of polyQ-expanded ataxin-3. The fragmentation of the disease protein is discussed as an important source for toxic fragments and seeds for formation of aggregates, and its reduction might alleviate the disease progression.

Our previous study has shown that calpain-1 and calpain-2 cleave wild type and polyQ-expanded ataxin-3 and overactivation of the calpain system by knocking out the endogenous inhibitor CAST led to a worsening of the SCA3 phenotype *in vivo* (*Accepted paper a*). Investigations performed by other researches demonstrated, that a reduction of calpain activity by overexpressing CAST or by pharmacological inhibition reduced ataxin-3 cleavage and fragmentation, and prevented cerebellar degeneration and motor behavioural deficits (Simões *et al.*, 2012, 2014). Thus, genetic ablation of one of the calpain isoforms, which was associated with polyQ-expanded ataxin-3 cleavage, might represent a further option to ameliorate disease-related molecular and phenotypic abnormalities in a mouse model of SCA3.

For this, we crossbred *Capn1*$^{-/-}$ animals with YAC84 SCA3 mice and investigated the effect of the knockout on ataxin-3 levels, fragmentation and aggregation at 3 months of age (Azam *et al.*, 2001; Cemal *et al.*, 2002). Using western blot analysis, we confirmed the knockout of calpain-1 not only in whole brain but also in muscle tissue, and observed a downregulation of the calpain system activity. Furthermore, we observed a reduction of specific calpain-dependent breakdown products of ataxin-3 in *Capn1*$^{-/-}$ and YAC84/*Capn1*$^{-/-}$ mice and, as a consequence of it, an increase of ataxin-3 full-length levels. However, we did not observe the anticipated reduction of ataxin-3 aggregation in YAC84/*Capn1*$^{-/-}$ mice.

The lack of a clear effect of the calpain-1 knockout on aggregation can be due to different factors. One limitation might be the comparatively early time point of investigations at three months of age, despite both hemizygous and homozygous YACQ84 mice were shown to have robust intranuclear accumulation of mutant ataxin-3 at as early as six to eight weeks of age (do Carmo Costa *et al.*, 2013). However, there might be differences between cleavage of ataxin-3 by calpain-1 or by other calpains, producing fragments with different toxicities and aggregation propensities. For example, in Huntington disease (HD), a strong association of the disease phenotype especially with caspase-6-mediated cleavage of huntingtin was discovered, which was circumvented in a mouse model expressing caspase-6 cleavage-resistant, polyQ-expanded huntingtin (Graham *et al.*, 2006). In this regard, crossbreeding

YAC84 mice with a calpain-2 knockout model and a comparison with our YAC84/*Capn1*$^{-/-}$ might throw light on this matter. Of particular note in this regard is that a homozygous knockout of calpain-2 is lethal and obtaining adult mice is only possible under a conditional knockout in which calpain-2 is still expressed in the placenta (Takano *et al.*, 2011). Furthermore, very recent publications are indicating that targeting calpain-1 as a therapeutic strategy should be approached with caution, as *Capn1* null-mutations in patients resulted in cerebellar ataxia and limb spasticity and a calpain-1 knockout in mice led to an abnormal cerebellar development (Liu *et al.*, 2016; Y. Wang *et al.*, 2016). With reference to this, our rotarod assessments of YAC84/*Capn1*$^{-/-}$ but also *Capn1*$^{-/-}$ mice showed certain deficits in motor behaviour when compared to YAC84 or wild type animals (data not shown).

Taken together, knockout of calpain-1 seems to reduce cleavage of endogenous and transgenic, polyQ-expanded ataxin-3 in animals, but without leading to a reduced aggregation in mice at 3 months of age. Our behavioural data and recent publications are pointing to rather diametrically opposite effects of the knockout as the genetic inactivation of calpain-1 might exacerbate the observed ataxic phenotype in SCA3 mice. Thus, genetically targeting calpain-1 as a treatment for SCA3 might represent a therapeutic impasse.

Author contribution statements

Experimental design: JHS, OR

Conduction of experiments: JJW, JHS

Data analysis: JJW, JHS

E. Calpain-dependent cleavage of huntingtin

Jonasz J. Weber[1,2], Midea M. Ortiz-Rios[1,2], Huu P. Nguyen[1,2]

[1] Institute of Medical Genetics and Applied Genomics, University of Tuebingen, Tuebingen, Germany
[2] Centre for Rare Diseases, University of Tuebingen, Tuebingen, Germany

Introduction

Following the *toxic fragment hypothesis*, proteolytic fragments of mutant huntingtin are suggested as mediators of neurotoxic effects, which ultimately cause neuronal death (Wellington and Hayden, 1997). Underpinning this conjecture, the accumulation and aggregation of N-terminal polyglutamine (polyQ)-containing fragments of the HD protein huntingtin has been observed in animal models as well as in HD patient brain tissue (DiFiglia *et al.*, 1997; Mende-Mueller *et al.*, 2001; Toneff *et al.*, 2002; Wang *et al.*, 2008). In consequence, a row of cell and animal models of HD overexpressing N-terminal huntingtin fragments has been generated, which display increased cell death, aggravated phenotypes or an earlier disease onset (Mangiarini *et al.*, 1996; Cooper *et al.*, 1998; Hackam *et al.*, 1999; Schilling, Becher, *et al.*, 1999; Igarashi *et al.*, 2003).

On these grounds, many researchers have focussed on the identification of enzymes responsible for proteolysis of huntingtin or on the localization of cleavage sites within the disease protein. Since then, various groups of proteases have been associated with the cleavage of huntingtin. Amongst them, caspases and calpains appeared to be the most important contributors and a long list of their cleavage sites has been identified, mainly localized between amino acids 400 and 600 of the huntingtin protein (Goldberg *et al.*, 1996; Gafni and Ellerby, 2002; Ehrnhoefer *et al.*, 2011). Further investigations demonstrated that preventing cleavage by inhibiting specific proteases or by mutating their recognition sites, ameliorated the disease phenotype both in cell and animals models of HD and might therefore represent an promising therapeutic approach to treat this fatal disorder (Wellington *et al.*, 2000; Gafni *et al.*, 2004; Graham *et al.*, 2010).

Several studies described calpain-dependent cleavage of huntingtin in cell models, neuronal tissue of animal models and *post mortem* patient brain (Kim *et al.*, 2001; Gafni and Ellerby, 2002). Calpains, a group of Ca^{2+}-activated cysteine proteases, were reported to cleave huntingtin at residues 469 and 536 and mutating these sites for rendering huntingtin calpain-

resistant reduced the formation of toxic and aggregation-prone fragments (Gafni *et al.*, 2004). However, as huntingtin constitutes a large protein of more than three thousand amino acids and previously analysed calpain-dependent fragmentation patterns appeared to be more complex, the number of calpain cleavage sites within huntingtin is probably much higher.

In our experiments, we focussed on analysing the proteolytic fragmentation of huntingtin by calpains. Our aims were to test whether huntingtin is cleaved by both calpain-1 and calpain-2 *in vitro* and to model calpain-dependent cleavage in HD cell lines. Furthermore, using a mass spectrometry-based approach, we sought to identify further calpain cleavage sites in the huntingtin protein, which might contribute to the formation of toxic huntingtin fragments.

Materials and Methods

Cell culture

For overexpression of HA-tagged huntingtin 15Q and 128Q, HEK 293T (ATCC: CRL-11268) cells were transfected 24 h post-seeding with pCI-neo vectors containing the respective cDNA and harvested 48 h after transfection. Attractene (QIAGEN) was used as a transfection reagent according to manufacturer's instructions. Immortalized murine striatal precursor cell lines of HD (ST*Hdh)* were purchased from Coriell Cell Repositories (Coriell Institute for Medical Research) and utilized in an undifferentiated state. All cell lines were maintained in Dulbecco's Modified Eagle Medium (DMEM) supplemented with 10% fetal calf serum, 1% penicillin/streptomycin (all Thermo Fisher Scientific) at 37°C and 5% CO_2. Media for ST*Hdh* cells was additionally supplemented with 1% geneticin (Biochrome).

Calpain activation assays in vitro

Calpain activation assays *in vitro* were described elsewhere (see *Accepted paper g*). A modification of the protocol comprises the application of the calpain inhibitor ALLN (N-Acetyl-L-leucyl-L-leucyl-L-norleucinal) at a concentration of 100 µM as a negative control.

Gel staining for mass-spectrometry sampling

To obtain material for mass spectrometry analysis of cleavage sites in huntingtin, RIPA-lysates of HEK 293T transfected with HA-huntingtin 15Q and HA-huntingtin 128Q, untreated or incubated with $CaCl_2$ for calpain activation, were separated on NuPAGE Novex 7% Tris-Acetate gels (Thermo Fisher Scientific). After electrophoresis, gels were stained using the Coomassie G-250-based protein gel stain SimplyBlue™ SafeStain (Thermo Fisher Scientific), following the manufacturer's protocol. Gel areas were excised with a scalpel, samples transferred to 1.5 ml reaction tubes and stored at 4°C.

In silico cleavage site prediction using the GPS-CCD tool

Cleavage likelihood score was computed using the using the GPS-CCD (group-based prediction system-calpain cleavage detector) software (Z. Liu *et al.*, 2011). Predictions were based on a wild type huntingtin reference sequence (UniProt identifier: P42858-1 with 15 glutamines). Scores for amino acid positions 1150-1200 were graphically visualized using GraphPad Prism 6.00 for Windows (GraphPad Software Inc.).

Further materials and methods

Information on cell lysis, western blot analysis, and antibodies can be found under *Accepted papers e* and *g.*

Mass spectrometry analyses and data interpretation was conducted as a service by the Proteome Center Tuebingen, Interfaculty Institute for Cell Biology, University of Tuebingen, Tuebingen, in collaboration with the Quantitative Biology Center (QBiC), University of Tuebingen, Tuebingen, Germany.

Results

Calpain cleavage of huntingtin can be induced in immortalized striatal precursor cells of HD

To reconfirm previous findings on calpain-dependent cleavage of huntingtin and to get a closer look at calpain-derived fragmentation patterns, we performed *in vitro* calpain cleavage assays using lysates of undifferentiated ST*Hdh*^{Q7} and ST*Hdh*^{Q111} cells. These cell lines were derived from wild type and homozygous *Hdh*^{Q111} mice, and represent immortalized striatal precursor cells with a potential of differentiation into neuron-like cells (Wheeler *et al.*, 1999; Trettel *et al.*, 2000).

We incubated respective cell lysates with recombinant calpain-1 and calpain-2 upon addition of calcium chloride ($CaCl_2$) to activate the applied enzymes. The induced fragmentation was analysed by western blotting using the huntingtin-specific antibody (D7F7, epitope around amino acid position 1220). We observed a time-dependent increase in huntingtin fragments with a wide range of molecular weights and a correlating reduction of the full-length protein (Fig. 1a and b). Cleavage of huntingtin was abolished by the addition of the calpain-specific inhibitor ALLN. The fragmentation patterns did not show clear differences, when comparing huntingtin cleavage by calpain-1 with calpain-2. However, the over-all fragmentation appeared to be weaker in lysates of ST*Hdh*^{Q111}, which can be explained by a decreased expression level of polyQ-expanded huntingtin in this cell line. Interestingly, detection of endogenous calpain-1 in samples incubated with recombinant calpain-2, showed a parallel activation of the endogenous enzyme due to addition of $CaCl_2$ (Fig. 1b).

To evaluate the effects of endogenous calpain activation, we incubated lysates of ST*Hdh*^{Q7} and ST*Hdh*^{Q111} cells only with $CaCl_2$ and performed western blotting of thereby generated samples. Successful induction of the calpain activity was validated by detecting the activation state of calpain-1 and the fragment formation of the known calpain substrate α-spectrin (Fig. 1c). The calpain-dependent cleavage of huntingtin was reproduced, but occurred expectedly to a weaker extent then in set-ups with recombinant calpains (Fig. 1c). Interestingly, in all experimental set-ups, we observed a time-dependent generation of a calpain-independent cleavage product of huntingtin in lysates of ST*Hdh*^{Q111} but not of ST*Hdh*^{Q7} cells (Fig. 1a, b, c; black arrows), which was not prevented when incubating with calpain inhibitors ALLN or CI III. The origin of this fragment remains unclarified, but preliminary results from additional experiments, which included a pan-caspase inhibitor, ruled out a caspase-dependent origin of this breakdown product (data not shown).

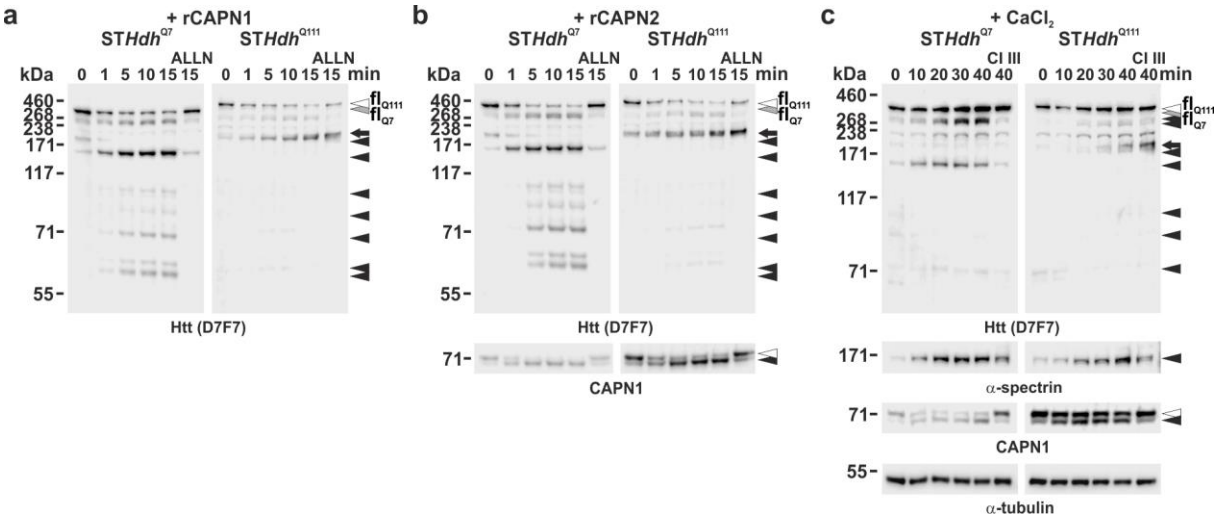

Figure 1. Calpain activation assays *in vitro* with or without recombinant calpains confirm the calpain-dependent cleavage of huntingtin in ST*Hdh* cell extracts. ST*Hdh* cell lysates were diluted in calpain reaction buffer. After addition of recombinant calpain-1 (rCAPN1, **a**) or calpain-2 (rCAPN2, **b**), samples were incubated at room temperature for the indicated times. To inhibit calpain activity, 100 µM of calpain inhibitor ALLN were added to the respective control reaction. Samples were analysed using western blotting and immunostaining with huntingtin (D7F7) and calpain-1 antibodies. (**c**) To activate endogenous calpains, ST*Hdh* cell lysates were diluted in calpain reaction buffer and incubated with 2 mM calcium chloride ($CaCl_2$) for the indicated times at room temperature. To inhibit calpain activity, 100 µM calpain inhibitor III (CI III) were added. Samples were analysed using western blotting and immunostaining with huntingtin (D7F7), α-spectrin and calpain-1 antibodies. Tubulin served as a loading control. White arrowheads indicate full-length proteins; black arrowheads highlight proteolytically processed proteins. Black arrows indicate a calpain cleavage-independent fragment. fl_{Q7} and fl_{Q111} = full-length huntingtin 7Q and 111Q.

Overexpressed human huntingtin is cleaved by calpains in vitro

As ST*Hdh* cells express only wild type and polyglutamine-expanded huntingtin of murine origin, we sought to repeat our experiments with human huntingtin constructs. For this purpose, we transfected HEK 293T cells with HA-tagged huntingtin containing 15 or 128 glutamines and subjected lysates to *in vitro* calpain activation assay with recombinant calpain-1 and calpain-2. Western blotting showed the formation of N-terminal and polyQ-independent C-terminal fragments of huntingtin as detected with the antibodies 2166 (epitope at amino acid 445-459) and D7F7 (epitope around amino acid position 1220) (Fig. 2a-d). As known for calpain cleavage of huntingtin in ST*Hdh* cells, fragmentation patterns induced by calpain-1 and calpain-2 did not differ. This observation points to equivalent recognition of the same cleavage sites by both proteases. Likewise, the C-terminal cleavage pattern of HA-huntingtin 15Q and 128Q was comparable. However, N-terminal breakdown products induced by calpain activation could be hardly detected, pointing to a stronger further processing or aggregation of generated polyQ-containing fragments.

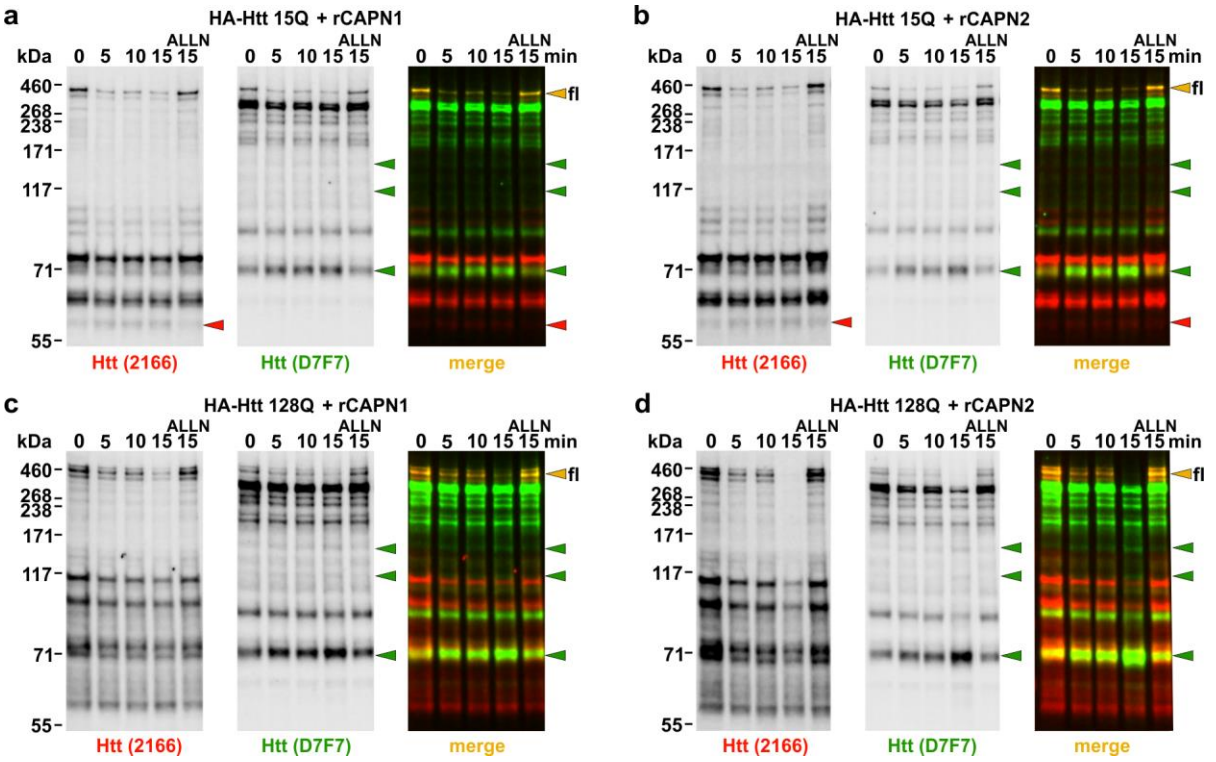

Figure 2. Overexpressed wild type and mutant huntingtin are cleaved by calpain-1 and calpain-2 *in vitro.* HEK 293T cells expressing human HA-tagged huntingtin with 15Q (**a** and **b**) or 128Q (**c** and **d**) were lysed in calpain reaction buffer and incubated with recombinant calpain-1 (rCAPN1, **a** and **c**) or calpain-2 (rCAPN2, **b** and **d**) for up to 15 min. To inhibit calpain activity, 100 µM ALLN were added to the respective control reaction. Subsequent western blot analysis using the huntingtin-specific antibodies 2166 (epitope at amino acids 445-459) and D7F7 (epitope around amino acid 1220) revealed several, mainly polyQ-independent huntingtin-fragments accumulating upon calpain activation (red and green arrowheads). fl = full length huntingtin.

Calpain activation leads to proteolysis of overexpressed human huntingtin in living cells

To repeat our experiments under more physiological conditions, we treated HEK 293T cells transfected with HA-huntingtin 15Q and 128Q with the Ca^{2+} ionophore ionomycin to activate endogenous calpains. Western blotting of calpain-1 and a-spectrin cleavage confirmed the activation of the calpain system (Fig. 3b). When detecting huntingtin with the antibodies 2166 and D7F7, differences in N-terminal fragmentation pattern could be observed, showing a set of fragments shifting upwards in a polyQ-dependent manner (Fig. 3a, red arrowheads). However, both huntingtin variants were proteolytically processed with a comparable efficiency, resulting in the formation of fragments of similar intensities. Interestingly, huntingtin fragmentation appeared to give rise to two large polyQ-independent fragments, which can be observed just below the full-length protein (Fig 3a, uppermost green arrowheads, bdp_{LCter}). These fragments point to the existence to a yet unidentified, rather C-terminal calpain cleavage sites.

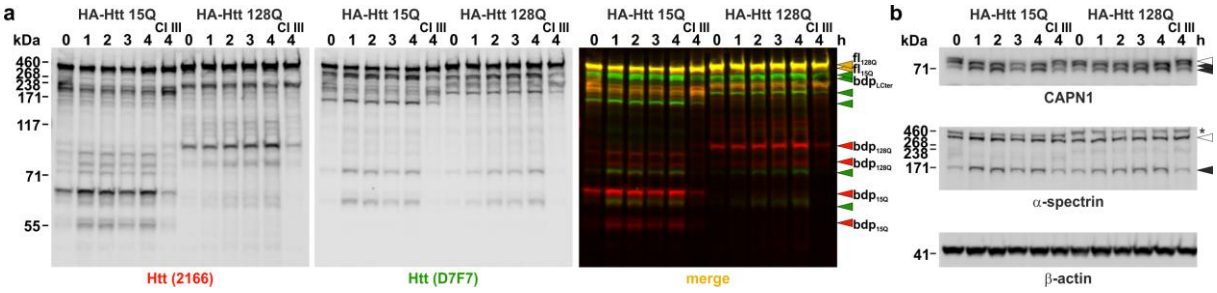

Figure 3. Cell-based activation of calpains leads to fragmentation of wild type and mutant huntingtin. HEK 293T cells expressing human HA-tagged huntingtin with 15Q or 128Q were treated with ionomycin to activate endogenous calpains for up to 4 h. To inhibit calpain activity, cells were pre-incubated with 25 µM calpain inhibitor III (CI III) for 1 h before ionomycin treatment. (**a**) Western blot analysis using huntingtin-specific antibodies 2166 (epitope at amino acids 445-459) and D7F7 (epitope around amino acid 1220) detected a time-dependent formation of several polyQ-containing and -non-containing fragments upon calpain activation (red and green arrowheads). fl_{15Q} and fl_{128Q} = full-length huntingtin 15Q and 128Q; bdp = breakdown product, LCter = large C-terminal fragments. (**b**) Activation of the calpain system was validated by detecting calpain-1 activation and α-spectrin cleavage. Actin served as loading control. Asterisk indicates redetection of huntingtin in the α-spectrin blot.

Identification of a calpain cleavage site between amino acids 1167 and 1168

Calpain activation in cells expressing HA-tagged huntingtin, revealed the existence of two large calpain cleavage-dependent C-terminal huntingtin breakdown products. To localize the cleavage sites within huntingtin, which are responsible for the generation of these fragments, we performed mass spectrometric analysis of huntingtin and huntingtin fragments without or after calpain activation. For this, we incubated lysates of wild type and polyQ-expanded HA-huntingtin transfected HEK 293T cells with $CaCl_2$ to activate calpains and loaded the samples on Tris-Acetate gels. A control set of samples was transferred on nitrocellulose membrane and immunodetected with the D7F7 antibody to confirm a successful cleavage induction of huntingtin (Fig. 4a). After total protein staining of the gel, areas were excised which contain the full-length protein or the high-molecular huntingtin fragments of interest (Fig. 4b). Thereby isolated fractions were analysed using mass spectrometry to identify non-tryptic peptides, when comparing samples with and without calpain activation. Despite limitations in coverage of the total huntingtin sequence, a peptide corresponding to cleavage between amino acid positions T1167 and N1168 in HA-huntingtin 15Q could be identified (Fig. 4c). In addition, computation of the likelihood for calpain cleavage within the region of interest of huntingtin further endorsed the identification of a cleavage site after amino acid T1167 (Fig. 4d). A potential cleavage at this site could explain the formation of one of the observed large C-terminal fragments, which can be detected by the D7F7 but not by the 2166 antibody.

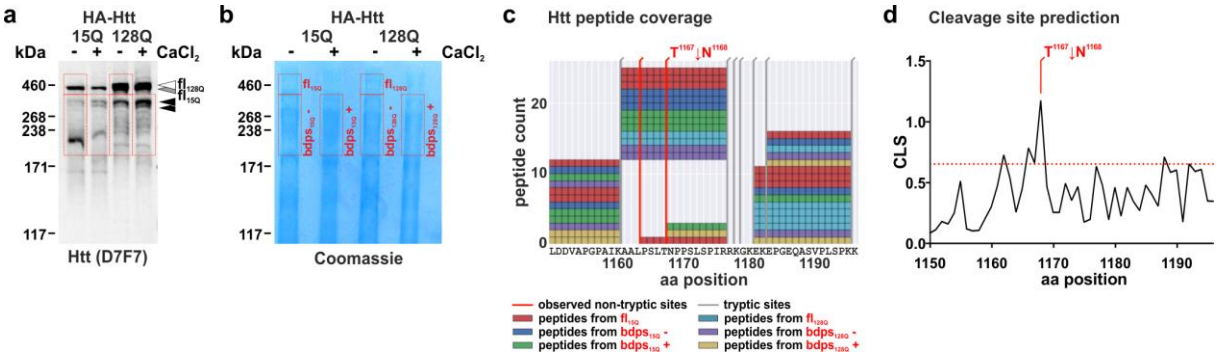

Figure 4. Identification of calpain cleavage sites within huntingtin by mass spectrometry. Lysates of HEK 293T cells transfected with HA-huntingtin 15Q and 128Q were incubated for 2 h with 2 mM $CaCl_2$ (+) to induce calpain-dependent cleavage of huntingtin and analysed via western blotting and mass spectrometry. (**a**) Western blot analysis using the huntingtin-specific antibody D7F7 shows decrease of full-length huntingtin (fl_{15Q} or fl_{128Q}) and an accumulation of polyQ-independent, high-molecular huntingtin fragments (black arrowheads). (**b**) To prepare material for mass spectrometry analysis, samples were run on a Tris-Acetate gel and visualized using Coomassie. Respective areas in the gel (red boxes) were excised containing only full-length huntingtin (fl_{15Q} or fl_{128Q}) or sections enriched for high-molecular huntingtin fragments ($bdps_{15Q}$ or $bdps_{128Q}$) with (+) or without (-) cleavage-induction by addition of $CaCl_2$. (**c**) Mass spectrometry analysis identified a specific non-tryptic and presumably calpain-dependent cleavage event located between amino acid (aa) positions T1167 and N1168 in the human huntingtin 15Q reference sequence. Representative peptide coverage blot of the huntingtin 15Q sequence between amino acids 1150 and 1995 shows tryptic and non-tryptic peptides as detected in the excised gel sections. (**d**) Calpain cleavage site prediction within in the region of interest using the GPS-CCD tool shows a high cleavage likelihood after amino acid T1167 of human huntingtin (UniProt identifier: P42858-1 with 15 glutamines). The red dotted line indicates maximum default cut-off value of 0.654. CLS = cleavage likelihood score.

Discussion

Proteolysis of polyQ-expanded huntingtin was shown to be an important key event in the molecular pathogenesis of HD and calpains were identified as one of the major groups of enzymes executing cleavage of the disease protein (Gafni and Ellerby, 2002; Gafni *et al.*, 2004; Ehrnhoefer *et al.*, 2011). Although previous studies have analysed calpain-dependent fragmentation of huntingtin and identified several cleavage sites within the protein, the impact of certain cleavage fragments remains nebulous. Therefore, we focused on reproducing calpain cleavage of huntingtin in different cell models of HD and to identify new calpain cleavage sites.

In our experiments, we showed that wild type and polyQ-expanded huntingtin are cleaved both by calpain-1 and calpain-2 *in vitro*, producing comparable fragmentation patterns. Cell-based assays did not show differences in fragmentation efficiency between wild type and polyQ-expanded huntingtin. However, N-terminal fragments of huntingtin with 128 glutamines showed an expected, polyQ-dependent size shift. Our observations accentuate that calpain cleavage of huntingtin is a physiological process, though toxicity and aggregation propensity of formed fragments reportedly depend on the length of the embedded polyQ stretch (Cooper *et al.*, 1998). Interestingly, a recent publication demonstrated that polyQ-independent breakdown products of huntingtin can evoke additional negative effects by compromising the endoplasmic reticulum (El-Daher *et al.*, 2015). Moreover, different N-terminal and C-terminal portions of the huntingtin protein seem to share similarities with *Saccharomyces cerevisiae* autophagic proteins and overexpression of C-terminal Atg11-like huntingtin fragments in rat primary cortical neurons induced cell death (Ochaba *et al.*, 2014). These findings demand further investigations on C-terminal cleavage events and the identification of proteases responsible for it.

In a further, preliminary approach, we sought to localize a calpain cleavage site, which might explain the origin of a large C-terminal fragment of huntingtin. Using mass spectrometry analysis, we identified a probable cleavage site between amino acids T1167 and N1168 within the huntingtin 15Q reference sequence. However, the identified cleavage site requires a further validation, which could be achieved by site directed mutagenesis.

Taken together, our investigations confirm the occurrence of huntingtin fragmentation by calpains and contribute to the search for calpain cleavage sites in the disease protein, which can help to clarify the role of polyQ-dependent and -independent huntingtin fragments in the pathogenesis of HD.

Author contribution statements

Experimental design: JJW, HPN

Conduction of experiments: JJW, MMOR

Data analysis: JJW

Acknowledgements

We are grateful to Prof. Dr. Michael R. Hayden, Department of Medical Genetics, University of British Columbia, Vancouver, Canada, for providing us with the huntingtin expression constructs.

Appendix II: Accepted papers

The accepted papers comprise:

a. Hübener *et al.*, 2013, *Human Molecular Genetics*.

b. Nguyen *et al.*, 2013, *PLoS One*.

c. Weber *et al.*, 2014, *BioMed Research International*.

d. Clemens *et al.*, 2015, *Brain*.

e. Weber *et al.*, 2016, *Rare Diseases*.

f. Schmidt *et al.*, 2016, *Journal of Neurochemistry*.

g. Weber *et al.*, 2017, *Brain*.

a. Hübener *et al.*, 2013, *Human Molecular Genetics*.

This is a pre-copyedited, author-produced version of an article accepted for publication in *Brain* following peer review. The version of record “Jeannette Hübener, Jonasz Jeremiasz Weber, Claudia Richter, Lisa Honold, Andreas Weiss, Fabronia Murad, Peter Breuer, Ullrich Wüllner, Peter Bellstedt, Francois Paquet-Durand, Jiro Takano, Takaomi C. Saido, Olaf Riess, Huu Phuc Nguyen; Calpain-mediated ataxin-3 cleavage in the molecular pathogenesis of spinocerebellar ataxia type 3 (SCA3), Human Molecular Genetics, Volume 22, Issue 3, 1 February 2013, Pages 508–518” is available online at: https://doi.org/10.1093/hmg/dds449.

Calpain mediated ataxin-3 cleavage in the molecular pathogenesis of spinocerebellar ataxia type 3 (SCA3)

Jeannette Hübener[1,#,*], Jonasz Jeremiasz Weber[1,#], Claudia Richter[1], Lisa Honold[1], Andreas Weiss[2], Fabronia Murad[1], Peter Breuer[3], Ullrich Wüllner[3], Peter Bellstedt[1], Francois Paquet-Durand[4], Jiro Takano[5], Takaomi C. Saido[5], Olaf Riess[1], Huu Phuc Nguyen[1]

[1] Department of Medical Genetics, University of Tuebingen, 72076 Tuebingen, Germany

[2] Neuroscience Discovery, Novartis Institutes for BioMedical Research, Novartis Pharma AG, CH-4002 Basel, Switzerland

[3] Department of Neurology, University of Bonn, 53127 Bonn, Germany

[4] Centre for Ophthalmology, Institute for Ophthalmic Research, University of Tuebingen, 72076 Tuebingen, Germany

[5] RIKEN Brain Science Institute, Laboratory for Proteolytic Neuroscience, 351-0198 Saitama, Japan

* Address for correspondence: Jeannette Hübener, PhD, Institute of Medical Genetics and Applied Genomics, University of Tuebingen, Calwerstrasse 7, 72076 Tuebingen, Germany, Phone: +49-7071-2972276, Fax: +49-7071-295171, Email: jeannette.huebener@med.uni tuebingen.de

# These authors contributed equally to this work.

a. Hübener et al., 2013, Human Molecular Genetics.

Abstract

Spinocerebellar Ataxia Type 3 (SCA3) is pathologically characterized by the formation of intranuclear aggregates which contain ataxin-3, the mutated protein in SCA3, in a specific subtype of neurons. It has been proposed that ataxin-3 is cleaved by proteolytic enzymes, in particular by calpains and caspases, eventually leading to the formation of aggregates. In our study, we examined the ability of calpains to cleave ataxin-3 *in vitro* and *in vivo*. We demonstrated in cell culture and mouse brain homogenates that cleavage of overexpressed ataxin-3 by calpains and in particular by calpain-2 occur and that polyglutamine expanded ataxin-3 is more sensitive to calpain degradation. Based on these results, we investigated the influence of calpains on the pathogenesis of SCA3 *in vivo*. For this purpose, we enhanced calpain activity in a SCA3 transgenic mouse model by knocking out the endogenous calpain inhibitor calpastatin. Double-mutant mice demonstrated an aggravated neurological phenotype with an increased number of nuclear aggregates and accelerated neurodegeneration in the cerebellum. This study confirms the critical importance of calcium-dependent calpain-type proteases in the pathogenesis of SCA3 and suggests that manipulating the ataxin-3 cleavage pathway and the regulation of intracellular calcium homeostasis may represent novel targets for therapeutic intervention in SCA3.

Introduction

Neurodegenerative diseases such as Parkinson disease (PD), Huntington disease (HD) or the Spinocerebellar Ataxia group (SCA) are proposed to share common pathogenic mechanisms, including generation of toxic fragments by cytoplasmic cleavage, aggregate formation and neurodegeneration in disease specific neurons (1, 2). For polyglutamine diseases such as HD and SCA pathogenesis models suggest cytoplasmic cleavage of the mutant protein leading to nuclear translocation of fragments containing the polyQ tract (3, 4). Further studies revealed a much higher toxicity of fragments or truncated polyQ proteins with a shifted propensity to aggregate compared to expanded full-length polyglutamine proteins (reviewed in 5, 6). Therefore, cleavage of disease proteins by proteases (e.g. caspases or calpains) is proposed to represent an important step in the pathogenesis of neurodegenerative diseases. For Spinocerebellar Ataxia Type 3 (SCA3), caused by an expanded polyglutamine tract in the encoded ataxin-3 protein, cleavage by caspases (7-11) or calpains (12-14) is controversially discussed. The latter studies did, however, show that the calpain-dependent formation of polyglutamine containing fragments is triggered by calcium in neuroblastoma cells (12) and in patient-specific induced pluripotent stem cell (iPSC)-derived neurons (13). In iPS cells, generation of fragments and aggregate formation were not suppressed after treatment with caspase-1, caspase-3, or pan-caspase inhibitors. In contrast, treatment with ALLN or calpeptin (both calpain inhibitors) resulted in complete disappearance of aggregates (13). Additionally, overexpression of calpastatin, the only known endogenous calpain inhibitor, inhibited cleavage and prevented aggregation of ataxin-3 in neuroblastoma cells (12) and mouse brain (14). Both studies indicated that the occurrence of specific cleavage products was closely correlated with the aggregation process and demonstrated that calpain proteolysis may initiate a harmful aggregation cascade.

The calpain system originally comprised three different important proteins in neurons: the two best characterized members of the calpain family, calpain-1 and calpain-2 and calpastatin, whose only known function is to inhibit these calpains (15). Calpain-1 is activated by calcium concentrations in the µM range, whereas calpain-2 is activated by mM levels of calcium *in vitro*. As the activation of calpains is an irreversible process, calpain activation must be strictly controlled. Calpastatin binds to the inhibitory domain on both sides of the active site cleft in a reversible manner to inhibit calpains *in vivo* (16). The calpain system is also critical for development, as mice lacking the common regulatory 30 kDa calpain subunit (17) or calpain-2 (18) die prenatally, whereas mice lacking calpain-1 (19) or calpastatin (20) are phenotypically normal.

a. Hübener et al., 2013, Human Molecular Genetics.

To gain more insight into the impact of proteolytic cleavage of ataxin-3 *in vivo*, we investigated whether enhancing calpain cleavage modifies polyQ-expanded ataxin-3 in terms of cellular toxicity and formation of aggregates. Therefore, SCA3 transgenic mice overexpressing human ataxin-3 with 140Q (21) were crossbred with mice lacking the intracellular calpain inhibitor calpastatin (Cast KO; 20). We focused on the question whether ataxin-3 is cleaved by calpain-1 or calpain-2 in mouse brain *in vivo* and how this process would influence aggregate formation and neuropathology. In summary, we demonstrate for the first time that ataxin-3 is a substrate of calpain-1 and calpain-2 *in vitro* and *in vivo* and that these proteases present promising targets for therapeutic intervention.

Results

Ataxin-3 is a sensitive calpain substrate in vitro

To determine whether ataxin-3 is a calpain sensitive substrate *in vitro*, we investigated cleavage of overexpressed ataxin-3 with different polyglutamine lengths (15Q, 77Q, 148Q) in HEK293T cells. After incubation with 2 mM $CaCl_2$ and either recombinant calpain-1 or calpain-2 for up to 45 min ataxin-3 was cleaved more efficiently with recombinant calpain-2. Whereas most of full-length ataxin-3 was still detectable after 45 min of calpain-1 incubation (Fig. 1A-C), the length of the polyglutamine tract modulates calpain-2 cleavage of ataxin-3 (Fig. 1D-F). Full-length ataxin-3 with 15Q is nearly fully cleaved by calpain-2 after 45 min of incubation (Fig. 1D). On the other hand, cell lysates with an expanded polyglutamine tract revealed a complete cleavage of full-length ataxin-3 after 30 min (77Q) or 15 min (148Q) of incubation, respectively (Fig. 1E, F). Clearly, an N-terminal derived cleavage fragment of around 30 kDa was detected after calpain-1 and -2 cleavage independently of the polyQ lengths (Fig. 1A-F). Inhibition of calpain cleavage by incubation with ALLN resulted in no fragmentation of full-length ataxin-3 regardless of the polyglutamine length indicating that the observed cleaved ataxin-3 fragments were generated by calpain cleavage.

Generation of double-mutant Cast KO (-/-)/SCA3 mice

To further investigate the role of calpain cleavage in the pathogenesis of SCA3 *in vivo*, we crossbred calpastatin knock-out mice (20) with our SCA3 disease model (21). This SCA3 mouse model exhibits striking intergenerational instability of the expanded CAG stretch which modifies age at onset of symptoms and progression of the disease as it has been described for other polyQ models as well (22-26). SCA3 mice with 140Q demonstrated an ataxic and neurological phenotype as well as premature death, starting at the age of 6 to 9 months. In subsequent experiments, we therefore only used mice with 140Q, which are referred to as SCA3 in the following data. We confirmed that mutant ataxin-3 was expressed and calpastatin was knocked out in brains of double-mutant mice (dm-mice) by Western blot and immunohistochemical analyses whereas both mutant ataxin-3 and endogenous calpastatin were expressed in single-transgenic SCA 3 mice (st-mice) (data not shown). We also confirmed for each mouse the polyQ size of 140.

Calpastatin activity determines calpain cleavage rate of ataxin-3 ex vivo

To determine cleavage rates of endogenous and overexpressed ataxin-3 *ex vivo* when calpastatin is normally expressed or fully abolished, we used brain homogenates from 3

independent animals of wildtype mice, homozygous calpastatin knock-out mice [Cast KO (-/-)] as well as SCA3 st- and dm-mice [Cast KO (-/-)/SCA3] in a cleavage assay. Here we found that endogenous ataxin-3 in brain homogenates from wildtype mice was sensitively cleaved by calpain-1 and calpain-2 in the presence of 2 mM calcium, respectively. However, cleavage by calpain-2 occurs more rapidly and more efficiently. For both enzymes, calpain-1 and calpain-2, the same N-terminal derived ataxin-3 specific cleavage fragments at around 30 kDa (Fig. 2A, E) were detected as seen before in the cell culture analyses (Fig. 1). Specificity of calpain cleavage was confirmed by incubation with the calpain inhibitor ALLN. Knocking out calpastatin completely, we observed a faster degradation of endogenous mouse ataxin-3 after incubation with calpain-1 (Fig. 2B) as well as an increased amount of the 30 kDa cleavage fragment (Fig. 2I). However, cleavage by calpain-2 occurred immediately and more efficiently and revealed a very strong 30 kDa cleavage fragment after 5 min of incubation (Fig. 2F, J). Analyzing mice with overexpressed human ataxin-3 demonstrated that after 5 min of incubation with calpain-1 and calpain-2 almost no overexpressed protein is detectable (Fig. 2C, G). Similar results were found after knocking out calpastatin (Fig. 2D, H). The 30 kDa N-terminal derived cleavage fragment occurred independently from overexpressed human ataxin-3 as it is also seen in wildtype and Cast KO (-/-) mice (Fig. 2C, D, G, H). Quantification of the 30 kDa cleavage fragment demonstrated a more rapidly produced fragment if calpastatin is knocked out completely independently of the expression of a polyglutamine expanded human ataxin-3. The results were similar using either calpain-1 or calpain-2 (Fig. 2I, J).

Calpastatin knock-out increases mutant ataxin-3 fragmentation upon calcium stimulation

To quantify soluble mutant ataxin-3, we applied a highly sensitive time-resolved Förster resonance energy transfer (TR-FRET) assay, using the ataxin-3 antibody 1H9 (terbium cryptate-labeled) and the expanded polyQ specific MW1 (D2-labeled; Fig. 3A). Both antibodies are flanking a previously described potential cleavage site of ataxin-3 at amino acid position 260 (12) and exhibit fluorescence energy transfer in close proximity. Using the TR-FRET assay, we assessed the amount of soluble mutant ataxin-3 in the various genotypes in native cerebellar brain lysates, and additionally upon increased calpain-1 or calpain-2 activation via calcium stimulation over time (TR-FRET). As expected, since the MW1 antibody is specific against an expanded polyQ stretch (≥6CAGs), almost no ataxin-3 signal was observed in Cast KO (-/-) and wildtype mice. In contrast, in st-line SCA3 and in dm-mice a TR-FRET signal was detected. Notably, the signal intensity in the dm-mice was only half of that of the st-line SCA3. After calcium stimulation, the FRET signal decreases in

cerebellar brain lysates of st-line and dm-mice to half of the normal level (Fig. 3B). This indicates that decreased detection of soluble mutant ataxin-3 after calcium induction was due to increased calpain cleavage at amino acid position 260 (Fig. 3A).

Knock-out of calpastatin leads to an increased number of aggregates and neurodegeneration in SCA3 mice

Aggregate formation was analyzed in brain regions with high expression of calpain-1 and calpain-2 (confirmed by the ALLEN brain atlas; www.brain-map.org) as well as SCA3 transgene expression, including cerebellum and pons. Using ataxin-3 immunostaining of brain slices, we found the highest number of ataxin-3 positive nuclear inclusions (NII) in dm-mice at the age of 12 months. Significantly fewer aggregates were detected in mice of the st-line SCA3 confirmed by quantitative analysis of aggregates per cell in the cerebellum and pons (Fig. 4A, B). Furthermore, even in SCA3 mice, in which calpastatin is knocked out heterozygously [Cast KO (+/-)/SCA3], the number of neurons with NII is dramatically increased compared to st-line SCA3 (Fig. 4) suggesting that loss of one calpastatin allele was sufficient to enhance the formation of aggregates. Immunofluorescence staining with calpain-1 or calpain-2 antibodies revealed no co-localization of calpains with aggregates (data not shown). To investigate whether the aggravated phenotype in dm-mice was due to alterations in neuronal pathology and neurodegeneration, we performed toluidine blue staining and immunostaining with an antibody against neurofilament in the cerebellum of all genotypes at the age of 12 months. Immunostaining with a neurofilament antibody and toluidine blue revealed a strong atrophy of Purkinje cells in the st-line SCA3 and the dm-mice, but nearly no aberrant cells in Cast KO (-/-) mice and wildtype controls, respectively (Fig. 5A). Quantitative analysis of the percentage of degenerated, atrophic cells of toluidine blue staining revealed significantly more neurodegeneration in dm-mice compared to st-line SCA3 ($p \leq 0.001$), Cast KO (-/-), or wildtype mice ($p \leq 0.001$). However, the neurofilament staining revealed only significant differences of both disease lines compared to the controls but not between st-line SCA3 and dm-mice (Fig. 5B).

Depletion of calpastatin induces an advanced and more severe behavior phenotype in SCA3 Mice

To assess the ataxic and neurological phenotype of the mouse models, we performed rotarod tests and monitored survival rate as well as body weight. Measuring the body weight every second week, a significant decrease in body weight in the st-line SCA3 and both dm-lines [Cast KO (+/-)/SCA3 and Cast KO (-/-)/SCA3] compared to controls was found starting

at the age of 24 weeks. Whereas wildtype mice and mice of Cast KO (-/-) line continuously gained weight up to the age of 60 weeks, the st-line SCA3 and both dm-lines progressively lost weight, in the end more than 1/3 of the body weight of control mice. On the other hand, we did not find any significant differences between both control groups [wildtype and Cast KO (-/-)] and between the disease lines (SCA3, and both dm-lines, Fig. 6A), respectively. The progressive loss of body weight resulted in a premature death of all disease lines, shown in the Kaplan-Meier curve (Fig. 6B). Although, there was a clear tendency that heterozygous or homozygous knock-out of calpastatin in SCA3 mice lead to a decreased life span compared to st-line SCA3, this difference did not reach significance. In confirmation to the published data of Takano et al. (20), the Cast KO (-/-) showed no premature death (Fig. 6B). Furthermore, the disease lines (SCA3, both dm-lines) showed neurological symptoms with tremor, clasping and gait abnormalities from the age of 40 weeks onwards. To detect motor coordination abnormalities in the different lines, we performed rotarod tests. Dm-mice showed impaired motor capabilities on the rotarod with a significant difference starting at the age of 32 weeks for Cast KO (+/-)/SCA3 mice and at the age of 44 weeks for Cast KO (-/-)/SCA3 mice, whereas no significant coordination deficits were detectable in the st-line SCA3 or Cast KO (-/-) mice at this age (Fig. 6C). While it is surprising that Cast KO (+/-)/SCA3 mice seemingly show an earlier onset of motor deficit in the rotarod test at the age of 32 weeks, it should be noted that there was no significant difference between Cast KO (+/-)/SCA3 and Cast KO (-/-)/SCA3 mice. Also, it has to be kept in mind that Cast KO (-/-)/SCA3 mice started to die earlier (Fig. 6B). This has reduced the number of available mice for the rotarod test in the Cast KO (-/-)/SCA3 mice group to a larger extent and therefore has reduced the statistical power in this group. Moreover, the surviving mice in the Cast KO (-/-)/SCA3 group might have a milder phenotype leading to this slightly better performance on the rotarod.

Discussion

Caspases (7-11) and calpains (12-14) have been demonstrated to be involved in the proteolysis of ataxin-3. To gain more insight into the role of proteolytic cleavage in the pathogenesis of SCA3, we focused on calpain cleavage, specifically if ataxin-3 is a calpain-1 or calpain-2 sensitive substrate, as it was previously shown for huntingtin (27). Identifying the key protease that cleaves ataxin-3 is of particular importance as this will path the way for developing a targeted therapy. We demonstrated that overexpressed ataxin-3 is cleaved more efficiently by calpain-2 than by calpain-1 and that expanded ataxin-3 seems to be more sensitive to calpain degradation. That calpain-2 can cleave ataxin-3 more efficiently can be further supported by the expression pattern of calpain-1 and calpain-2 in wildtype C57Bl/6 mice as shown in the database of the ALLEN brains atlas (www.brain-map.org). Calpain-2 is highly expressed in the most affected brain areas by SCA3 including cerebellum, pons and medulla oblongata (expression value ≥ 2.5). In contrast, calpain-1 shows only a very low expression in the cerebellum (expression value ≤ 0.5) but normal expression values in the pons and medulla (≤ 2.0), respectively.

Our *in vitro* results were confirmed *in vivo* as we showed that endogenous wildtype murine and overexpressed human expanded ataxin-3 are calpain-2 sensitive substrates independently of the polyQ length. Furthermore, by knocking out calpastatin, endogenous and polyQ-expanded ataxin-3 is further destabilized. These results suggest that modifying the level of calpains (in particular of calpain-2) or of calpastatin will influence the rate of proteolysis of ataxin-3 and subsequently the generation of potentially toxic fragments ultimately leading to neurodegeneration. Indeed, knocking out calpastatin in our SCA3 transgenic mouse model (21) lead to a worsening of behavioral and neuropathological abnormalities. This is in agreement with reports that in the brain of patients, transgenic mice and cell models of Alzheimer Disease, as well as in animal models for retinal neurodegeneration, calpastatin depletion can act upstream of calpains to activate a calcium-dependent cascade of protein kinase activation, hyperphosphorylation, and proteolysis resulting in neurodegeneration (28, 29). Therefore, it has been proposed that calpastatin acts as a positive regulator against unwanted protein cleavage during calpain activation (15) and under pathological conditions as a negative regulator of calpains (20, 30). Calpastatin therefore is an attractive target for developing therapeutic approaches in SCA3, in particular as neither overexpression (28) nor ablation of calpastatin (20) has an effect on normal nervous system function in mice under physiological conditions.

Based on our findings we propose a role of ataxin-3 cleavage by calpains in the pathogenesis of SCA3. By applying a new assay (TR-FRET) to detect the level of soluble

mutant ataxin-3, we found less soluble mutant ataxin-3 in dm-mice compared to st-line SCA3 suggesting cleavage of ataxin-3 within the 63 amino acids separating the binding sites of the antibodies 1H9 and MW1. Interestingly, Haacke et al. (12) proposed a cleavage site for calpain-2 in ataxin-3 at amino acid position 260, which is positioned between the two antibodies we used. The fragments derived from cleaving ataxin-3 around this position have been shown to be highly susceptible to aggregation (12) and are associated with toxicity (31). Interestingly, we have previously described a genetrap mouse model, which expresses 259 amino acids N-terminal of ataxin-3 and which partially mimics a possible cleavage at position 260. In these mice we observed SCA3-like symptoms and a strong cytoplasmic accumulation of the N-terminal part of the protein in the brain (32). Additionally, a calculation of the molecular weight of the first 259 amino acids of the mouse and human ataxin-3 protein using a Protein Molecular Weight Calculator (Science gateway) revealed a fragment size of 29.7 kDa for mouse and 29.93 kDa for human N-terminal ataxin-3 (first 259 aa). The calculated size is consistent with the detected 30 kDa N-terminal fragment in the presented cleavage assays of overexpressed ataxin-3 in cell culture and mouse brain homogenates. In addition, C-terminal fragments including the polyQ stretch have a much higher toxicity and propensity to aggregate than expanded full-length polyglutamine proteins (31). In support of this hypothesis we found a significantly increased number of aggregates in the granular layer of the cerebellum in dm-mice.

In summary, our results indicate that endogenous murine ataxin-3 and human expanded ataxin-3 are cleaved by calpains, especially by calpain-2, and that increased proteolytic cleavage of ataxin-3 results in a more severe and faster progressing neurological phenotype. Therefore, aberrant activation of calpains and consequently enhanced proteolytic cleavage of ataxin-3 may play a pivotal role in SCA3 pathogenesis. Thus, the ataxin-3 cleavage pathway and the molecules involved in it, in particular calpastatin, may represent potential targets for therapeutic intervention in SCA3. This perspective is particularly exciting since calpain inhibitors entering the brain are already in clinical trials (33).

Materials and methods

Expression constructs

In order to generate ataxin-3 constructs with C-terminal V5 tag, the stop codon of ataxin-3 (ataxin-3c isoform containing a third UIM, NM_004993.5) was replaced by an XbaI restriction site via PCR using the reverse primer MJDnoStopXbaRev (TAAAGtctagaTTTTTTTCCTTCTGTTTT). Full-length ataxin-3 was then cloned into the vector pcDNA 3.1/V5-His (Life Technologies) using BamHI and XbaI. Expanded CAG repeats (77 and 148 CAG, respectively) were inserted into the constructs by employing Esp3I and PpuMI.

Cell culture

HEK293T cells were maintained in Dulbecco´s modified eagle medium supplemented with 10% fetal calf serum, 1% non-essential amino acids and 1% penicillin/ streptomycin at 37°C in 5% CO2. Transient transfections with V5-tagged ataxin-3 constructs with different polyglutamine length (15Q, 77Q, 148Q) were performed using Attractene transfection reagent (QIAGEN) following the manufacturer's instructions followed by 72 h incubation. To obtain protein lysates HEK293T cells were mechanically homogenized in calpain reaction buffer (2 mM HEPES/KOH pH 7.6, 10 mM KCl, 1.5 mM $MgCl_2$, 1 mM DTT) using a QIAshredder homogenizer (QIAGEN) according to manufacturer's instructions.

Preparation of brain homogenates

Dissected mouse brains were homogenized in 1x PBS buffer with 1% Triton-X 100 and Complete Protease Inhibitor without EDTA (Roche Applied Science) using a Dounce homogenizer (Fisher Scientific).

Calpain activation assay

For *in vitro* calpain activation assays of cell culture lysates or brain homogenates, 200 ng of total protein were incubated with calpain-1 or calpain-2 in calpain reaction buffer containing 2 mM $CaCl_2$ at room temperature for indicated time points. To inhibit calpain activity, 100 µM N-acetylleucylleucylnorleucinal (ALLN; Sigma Aldrich, Inc.) were added to the respective reactions. All reactions were quenched by adding 5 x Laemmli buffer and denatured for 5 min at 95°C prior to Western blot analysis. For quantification of the 30 kDa fragment 3 brain samples of each indicated genotype were used. A ratio with loading control GAPDH and time point zero was calculated following quantification with ImageJ.

Generation and genotyping of the double-mutant mouse model

Hemizygous SCA3 mice overexpressing human ataxin-3 containing 140 CAGs under the control of the Prp promoter (21) were crossbred with homozygous calpastatin knock-out mice [Cast KO (-/-), (20)] to generate double-mutant mice (dm-) that were hemizygous for the calpastatin knock-out and heterozygote for mutant ataxin-3 (Cast KO (+/-)/SCA3). In a second breeding step, Cast KO (+/-)/SCA3 mice were mated with hemizygous Cast KO (+/-) or homozygous Cast KO (-/-) mice to obtain Cast KO (-/-), st-SCA3, double-mutant Cast KO (+/-)/SCA3 and double-mutant Cast KO (-/-)/SCA3 mice. Offspring with the expected Mendelian distribution of genotypes for both breeding steps were achieved (data not shown). For genotyping, we used the primers and conditions described in the respective publications. The number of CAG-repeats for all animals was analyzed using the primers pre-CAG-for (5´-GCTAAGTATGCAAGGTAGTTCC-3´) and post-CAG-rev (5´-CAAGTGCTCTGAACTGGTG-3´). The forward primer is labeled at the 5´end with the fluorescent dye Cy5. The PCR amplicon length was then analyzed on the Beckman coulter sequencer (CEQ 8000 Cycle Sequencer, Krefeld, Germany).

Western blot analysis

Western blot analyses were performed as previously described (21). Antibodies were used at the following dilutions: mouse anti-ATXN3 (1:4000; MAB 5360; clone 1H9; Millipore), rabbit anti-calpain-1 (1:2500 in 3% BSA; ab39170), rabbit anti-calpain-2 (1:2500; ab39168) (both from Abcam), rabbit anti-murine calpastatin (1:2000; Ref. 20), mouse anti-GAPDH (1:5000; sc-47724; Santa Cruz Biotechnology, Inc.), as well as peroxidase-conjugated secondary antibodies goat anti-mouse (1:2000; 115-035-003; Jackson Immuno-Research) and donkey anti-rabbit (1:3333; NA934; GE Healthcare Biosciences).

Immunohistochemistry

Immunohistochemistry was performed as previously described (21). The following antibodies were used: rabbit anti-ATXN3 (1:1000; Ref. 34), rabbit anti-calpain-1 (1:100; ab39170), rabbit anti-calpain-2 (1:100; ab39168) (both from Abcam), rabbit anti-murine calpastatin (1:2000; Ref. 19) and mouse anti-neurofilament (1:500; M0762; DakoCytomation), as well as fluorescence-coupled antibodies rabbit anti-Cy2 (1:50) and mouse anti-Cy3 (1:100) (both from Dianova). Staining with toluidine blue (Sigma Aldrich, Inc.) was done for 10 min in 0.2% toluidine blue in sodium acetate buffer. Dehydration steps with 70, 96 and 100% ethanol were then performed for 5 min each. Aggregates and neurodegenerative cells were manually

counted from three independent individuals in the cerebellum and pons from three animals of each indicated genotype at the age of 12 months. For quantifying aggregates or neurodegenerative cells four fields per brain region were counted on three different sections of each mouse.

a. Hübener et al., 2013, Human Molecular Genetics.

Time-resolved FRET assay

Cerebellar samples from indicated genotypes were homogenized in homogenization buffer (10% PBS, 1% Triton X, Complete without EDTA). After diluting lysates 1:1 in homogenization buffer, reactions were carried out by adding 3 µM or 2 mM $CaCl_2$, to activate calpain-1 or calpain-2 respectively, and incubation for 5 min at 30°C. Reactions were terminated by adding 100 pmol ALLN and 2.5 µmol EDTA. As control, samples were incubated under the same conditions with 3 µm or 2 mM $CaCl_2$ and 100 µM ALLN. Reactions were stopped by addition of pure 2.5 µmol EDTA. Polyglutamine specific antibody MW1 was developed by Paul Patterson (35) and obtained from the Developmental Studies Hybridoma Bank developed under the auspices of the NICHD and maintained by The University of Iowa (Department of Biological Sciences, Iowa City, IA 52242). Ataxin-3 antibody was obtained from Millipore (1H9; Mab5360). MW1 antibody was labeled with acceptor fluorophore D2. Ataxin-3 antibody was labeled with terbium-cryptate (Tb) as donor fluorophore. TR-FRET detection protocol was performed as previously described (36). In short, 5 µl sample and 1 µl detection buffer (50 mM NaH_2PO_4, 400 mM NaF, 0.1% BSA and 0.05% Tween + antibodies) was pipette into low-volume wells of an opaque 384-microtiter plate and incubated for 20 h at 4°C. Final detection antibody amounts per well were 0.3 ng Ataxin-3-Tb and 10 ng MW1-D2. TR-FRET quantification was performed with an Envision reader (PerkinElmer). The terbium donor fluorophore was excited at 320 nm. After a time-delay of 100 µs, emission signal of D2 was detected at 665 nm. All signals are reported as the percentage signal intensity over the lysis buffer background signal.

Phenotype analysis

Body weight was determined every second week for 8 to 10 animals per group starting at the age of 4 weeks. Behavioral experiments were performed in the dark cycle when mice were more active. Behavioral testing began at the age of 8 weeks and was repeated every 8 weeks until the age of 44 weeks. For rotarod tests, mice were placed on an accelerating rotating rod (TSE) at the same time of the day for five consecutive days. Three training sessions (each with acceleration from 4 to 16 rpm in 2 min) were followed by two test sessions. Each test trial started with rotation at 4 rpm and accelerated to a maximum of 40 rpm within 5 min. The amount of time that elapsed before the mouse fell off the rod was recorded. The trials within the same day were performed approximately 1 h apart. Eight to 10 age- and sex-matched animals were analyzed per group. All experiments were conducted in a blind-coded manner with respect to genotype until an overt phenotype was visible. The survival rate was measured by recording the life span of mice that died naturally. As the

license to carry out experiments on mice requires that mice are euthanized when disease exceeds defined, moderately severe, humane end points, only a relatively small number of animals were used to determine survival rate: wildtype: n=28; Cast KO (-/-): n=8; SCA3: n=5; Cast KO (+/-)/SCA3: n=16; Cast KO (-/-)/SCA3: n=7.

Statistical analysis

All data were analyzed by using JMP® version 8.0 (SAS Institute, Inc., Cory, NC, USA). Rotarod tests, survival rate, measurement of body weight, TR-FRET assay and immunohistochemistry were investigated by an unpaired Student´s t-test with a significance threshold of $p<0.05$. All results are presented as means ± standard error mean.

a. Hübener et al., 2013, Human Molecular Genetics.

Acknowledgements

We thank Dr. Thorsten Schmidt for providing us the V5-tagged ataxin-3 constructs and Anna Sowa for critical reading of the manuscript. Part of this work was supported by the fortune program (1987-1-0) to Jeannette Hübener and by the Charlotte and Tistou Kerstan foundation to Francois Paquet-Durand.

Conflict of Interest Statement: None declared.

References

1. Gusella, J.F. and MacDonald, M.E. (2000) Molecular genetics: unmasking polyglutamine triggers in neurodegenerative disease. *Nat. Rev. Neurosci.*, **1**, 109-115. [Review]

2. Zoghbi, H.Y. and Orr, H.T. (2000) Glutamine repeats and neurodegeneration. *Annu. Rev. Neurosci*., **23**, 217-247. [Review]

3. Schöls, L., Bauer, P., Schmidt, T., Schulte, T. and Riess, O. (2004) Autosomal dominant cerebellar ataxias: clinical features, genetics, and pathogenesis. *Lancet Neurol*., **3**, 291-304. [Review]

4. Antony, P.M., Mäntele, S., Mollenkopf, P., Boy, J., Kehlenbach, R.H., Riess, O. and Schmidt, T. (2009) Identification and functional dissection of localization signals within ataxin-3. *Neurobiol. Dis*., **36**, 280-292.

5. Ross, C.A., Wood, J.D., Schilling, G., Peters, M.F., Nucifora, F.C. Jr, Cooper, J.K., Sharp, A.H., Margolis, R.L. and Borchelt, D.R. (1999) Polyglutamine pathogenesis. *Philos. Trans. R. Soc. Lond. B. Biol. Sci*., **354**, 1005-1011. [Review]

6. Ross, C.A. and Poirier, M.A. (2004) Protein aggregation and neurodegenerative disease. *Nat. Med*., **10**, Suppl, 10-17. [Review]

7. Wellington, C.L., Ellerby, L.M., Hackam, A.S., Margolis, R.L., Trifiro, M.A., Singaraja, R., McCutcheon, K., Salvesen, G.S., Propp, S.S., Bromm, M. *et al.* (1998) Caspase cleavage of gene products associated with triplet expansion disorders generates truncated fragments containing the polyglutamine tract. *J. Biol. Chem*., **273**, 9158-9167.

8. Berke, S., Schmied, F.A., Brunt, E.R., Ellerby, L.M. and Paulson, H.L. (2004) Caspasemediated proteolysis of the polyglutamine disease protein ataxin-3. *J. Neurochem*., **89**, 908-918.

9. Goti, D., Katzen, S.M., Mez, J., Kurtis, N., Kiluk, J., Ben-Haiem, L., Jenkins, N.A., Copelang, N.G., Kakizuka, A., Sharp, A.H. *et al.* (2004) A mutant ataxin-3 putative-cleavage fragment in brains of Machado-Joseph disease patients and transgenic mice is cytotoxic above a critical concentration. *J. Neurosci*., **24**, 10266-10279.

10. Pozzi, C., Valtorta, M., Tedeschi, G., Galbusera, E., Pastori, V., Bigi, A., Nonnis, S., Grassi, E. and Fusi, P. (2008) Study of subcellular localization and proteolysis of ataxin-3. *Neurobiol. Dis*., **30**, 190-200.

11. Jung, J., Xu, K., Lessing, D. and Bonini, N.M. (2009) Preventing ataxin-3 protein cleavage mitigates degeneration in a Drosophila model of SCA3. *Hum. Mol. Genet*., **18**, 4843-4852.

12. Haacke, A., Hartl, F.U. and Breuer, P. (2007) Calpain inhibition is sufficient to suppress aggregation of polyglutamine-expanded ataxin-3. *J. Biol. Chem*., **26**, 18851-18856.

13. Koch, P., Breuer, P., Peitz, M., Jungverdorben, J., Kesavan, J., Poppe, D., Doerr, J., Ladewig, J., Mertens, J., Tüting, T. *et al*. (2011) Excitation-induced ataxin-3 aggregation in neurons from patients with Machado-Joseph disease. *Nature*, **480**, 543-546.

14. Simoes, A.T., Goncalves, N., Koeppen, A., Deglon, N., Kügler, S., Duarte, C.B. and Pereira de Almeida, L. (2012) Calpastatin-mediated inhibition of calpains in the mouse brain prevents mutant ataxin-3 proteolysis, nuclear localization and aggregation, relieving Machado-Joseph disease. *Brain*, **135**, 2428-2439.

15. Goll, D.E., Thompson, V.F., Li, H., Wei, W. and Cong, J. (2003) The calpain system. *Physiol. Rev.*, **83**, 731-801. [Review]

16. Hanna, R.A., Campbell, R.L. and Davies, P.L. (2008) Calcium-bound structure of calpain and its mechanism of inhibition by calpastatin. *Nature*, **456**, 409-412.

17. Zimmerman, U.J., Boring, L., Pak, J.H., Mukerjee, N. and Wang, K.K. (2000) The calpain small subunit gene is essential: its inactivation results in embryonic lethality. *IUBMB Life*, **50**, 63-68.

18. Dutt, P., Croall, D.E., Arthur, J.S.C., De Veyra, T., Williams, K., Elce, J.S. and Greer, P.A. (2006) M-Calpain is required for preimplantation embryonic development in mice. *BMC Dev. Biol.*, **24**, 6:3.

19. Azam, M., Andrabi, S.S., Sahr, K.E., Kamath, L., Kuliopulos, A. and Chishti, A.H. (2001) Disruption of the mouse μ-calpain gene reveals an essential role in platelet function. *Mol. Cell Biol.*, **21**, 2213-2220.

20. Takano, J., Tomioka, M., Tsubuki, S., Higuchi, M., Iwara, N., Itohara, S., Maki, M. And Saido, T.C. (2005) Calpain mediates excitotoxic DNA fragmentation via mitochondrial pathways in adult brains: evidence from calpastatin mutant mice. *J. Biol. Chem*., **280**, 16175-16184.

21. Bichelmeier, U., Schmidt, T., Hübener, J., Boy, J., Rüttiger, L., Häbig, K., Poths, S., Bonin, M., Knipper, M., Schmidt, W.J. *et al*. (2007) Nuclear localization of ataxin-3 is required for the manifestation of symptoms in SCA3: *in vivo* evidence. *J. Neurosci*., **27**, 7418-7428.

22. Shelbourne, P.F., Killeen, N., Hevner, R.F., Johnston, H.M., Tecott, L., Lewandoski, M., Ennis, M., Ramirez, L., Li, Z., Iannicola, C. *et al.* (1999) A Huntington´s disease CAG expansion at the murine Hdh locus is unstable and associated with behavioural abnormalities in mice. *Hum. Mol. Genet*., **8**, 763-774.

23. Lorenzetti, D., Watase, K., Xu, B., Matzuk, M.M., Orr, H.T. and Zoghbi, H.Y. (2000) Repeat instability and motor incoordination in mice with a targeted expanded CAG repeat in the Sca1 locus. *Hum. Mol. Genet.,* **9**, 779-785.

24. Dragileva, E., Hendricks, A., Teed, A., Gillis, T., Lopez, E.T., Friedberg, E.C., Kucherlapati, R., Edelmann, W., Lunetta, K.L., MacDonald, M.E. *et al.* (2009) Intergenerational and striatal CAG repeat instability in Huntington´s disease knock-in mice involve different DNA repair genes. *Neurobiol. Dis*., **33**, 37-47.

25. Morton, A.J., Glynn, D., Leavens, W., Zheng, Z., Faull, R.L., Skepper, J.N. and Wight, J.M. (2009) Paradoxical delay in the onset of disease caused by super-long CAG repeat expansions in R6/2 mice. *Neurobiol. Dis*., **33**, 331-334.

26. Boy, J., Schmidt, T., Schumann, U., Grasshoff, U., Unser, S., Holzmann, C., Schmitt, I., Karl, T., Laccone, F., Wolburg, H. *et al.* (2010) A transgenic mouse model of spinocerebellar ataxia type 3 resembling late disease onset and gender-specific instability of CAG repeats. *Neurobiol. Dis*., **37**, 284-293.

27. Gafni, J. and Ellerby, L.M. (2002) Calpain activation in Huntington's disease. *J. Neurosci*., **22**, 4842-4849. [Review]

28. Rao, M.V., Mohan, P.S., Peterhoff, C.M., Yang, D.S., Schmidt, S.D., Stavrides, P.D., Campbell, J., Chen, Y., Jiang, Y., Paskevich, P.A. *et al.* (2008) Marked calpastatin (Cast) depletion in Alzheimer's disease accelerates cytoskeleton disruption and neurodegeneration: neuroprotection by CAST overexpression. *Neurobiol. Dis*., **28**, 12241-12254.

29. Paquet-Durand, F., Johnson, L. and Ekstrom, P. (2007) Calpain activity in retinal degeneration. *J. Neurosci. Res.*, **85**, 693-702.

30. Paquet-Durand, F., Sanges, D., McCall, J., Silvia, J., van Veen, T., Marigo, V. and Ekström, P. (2010) Photoreceptor rescue and toxicity induced by different calpain inhibitors. *J. Neurochem.*, **115**, 930-940.

31. Ikeda, H., Yamagucki, M., Sugai, S., Aze, Y., Narumiya, S. and Kakizuka, A. (1996) Expanded polyglutamine in the Machado-Joseph disease protein induces cell death *in vitro* and *in vivo*. *Nat. Genet.*, **13**, 196-202.

a. Hübener et al., 2013, Human Molecular Genetics.

32. Hübener, J., Vauti, F., Funke, C., Wolburg, H., Ye, Y., Schmidt, T., Wolburg-Buchholz, K., Schmitt, I., Gardyan, A., Driessen, S. *et al.* (2011) N-terminal ataxin-3 causes neurological symptoms with inclusions, endoplasmic reticulum stress and ribosomal dislocation. *Brain*, **134**, 1925-1942.

33. Donkor, I.O. (2011) Calpain inhibitors: a survey of compounds reported in the patent and scientific literature. *Expert. Opin. Ther. Pat*., **21**, 601-636.

34. Haacke, A., Broadley, S.A., Boteva, R., Tzvetkov, N., Hartl, F.U. and Breuer, P. (2006) Proteolytic cleavage of polyglutamine-expanded ataxin-3 is critical for aggregation and sequestration of non-expanded ataxin-3. *Hum. Mol. Genet*., **15**, 555-568.

35. Ko, J., Ou, S. and Patterson, P.H. (2001) New anti-huntingtin monoclonal antibodies: implications for huntingtin conformation and its binding proteins. *Brain Res. Bull*., **56**, 319-329.

36. Weiss, A., Abramowski, D., Bibel, M., Bodner, R., Chopra, V., DiFiglia, M., Fox, J., Kegel, K., Klein, C., Grueninger, S. *et al.* (2009) Single-step detection of mutant huntingtin in animal and human tissues: A bioassay for Huntington's disease. *Anal. Biochem*., **39**, 8-15.

Abbreviations

Cast – calpastatin, dm – double-mutant, SCA3 – Spinocerebellar Ataxia Type 3, st – single transgenic

Figures and Legends to Figures

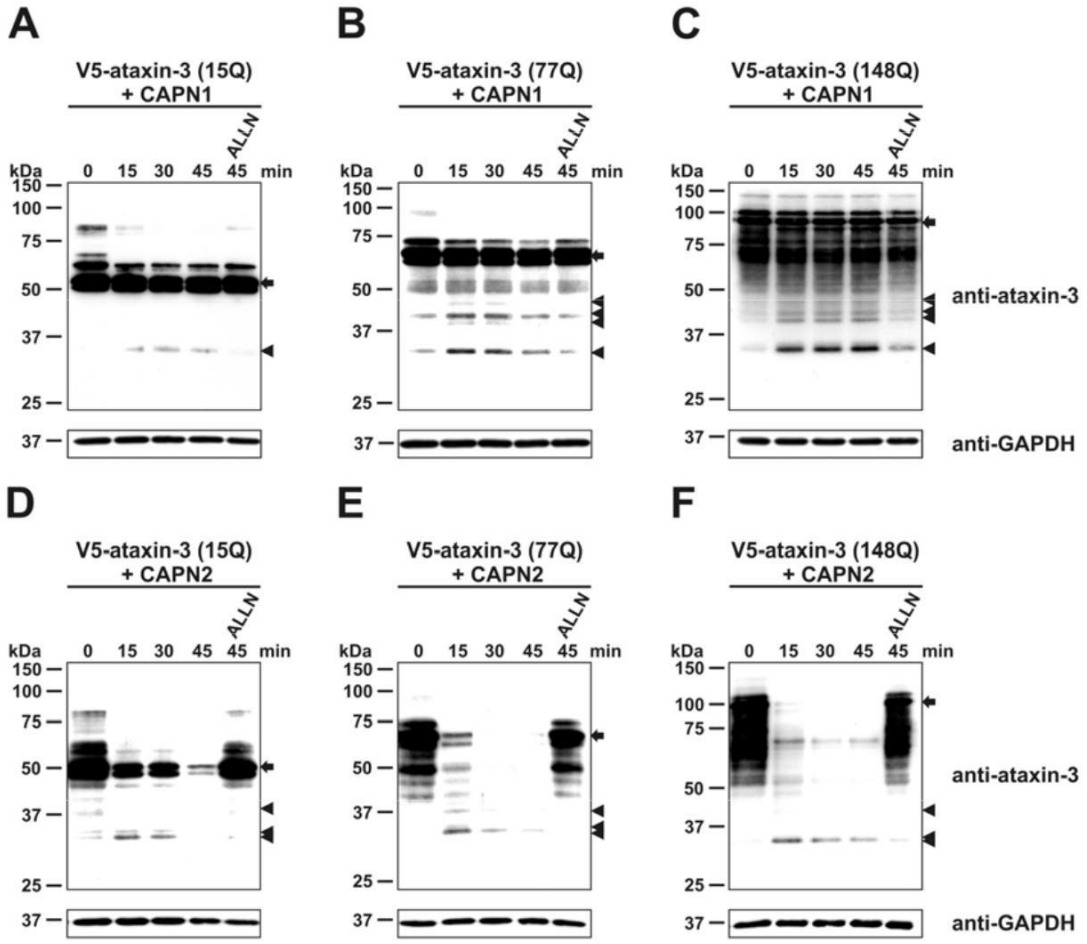

Figure 1. Overexpressed ataxin-3 can be cleaved more efficiently by calpain-2. Protein lysates from HEK293T cells transfected with V5-tagged ataxin-3 with different polyQ lengths (15Q, 77Q, 148Q) were incubated with recombinant calpain-1 (A-C) or calpain-2 (D-F) and 2 mM calcium for up to 45 min. Full-length ataxin-3 is indicated by an arrow, arrowheads show cleavage derived fragments. Where indicated, calpain inhibitor ALLN was added. Whereas incubation with recombinant calpain-1 revealed a weak cleavage of full-length ataxin-3 independently from the polyglutamine length (A-C), cleavage by calpain-2 lead to a more efficient fragmentation of full-length ataxin-3, which is dependent on the polyglutamine length (D-F). Calpain-1 and -2 cleavage results in an identical N-terminal cleavage fragment (around 30 kDa). As loading control GAPDH is shown.

a. Hübener et al., 2013, Human Molecular Genetics.

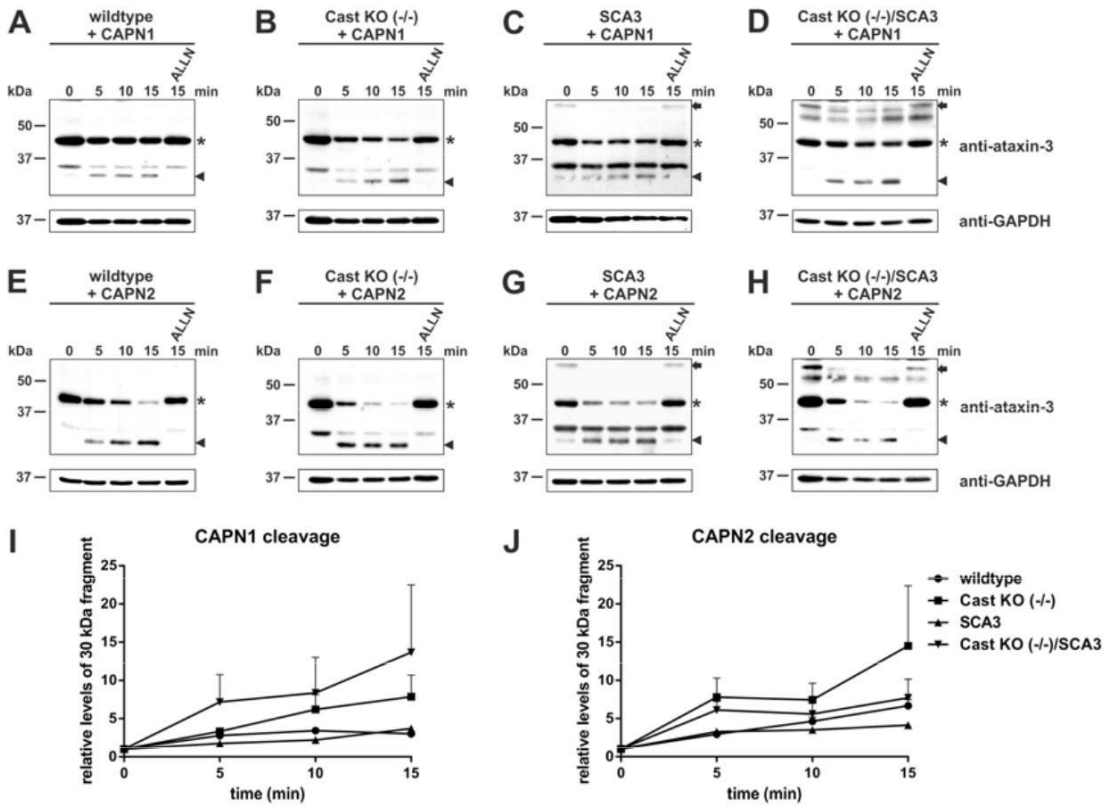

Figure 2. Calpastatin deficiency increases endogenous ataxin-3 cleavage. Whole brain homogenates of the indicated animals were incubated up to 15 min with 2 mM calcium and recombinant calpain-1 (A-D) or -2 (E-H), respectively. Stars highlight endogenous mouse ataxin-3, arrows indicate human overexpressed full-length ataxin-3 with expanded polyQ and arrowheads point to an N-terminal derived cleavage fragment. A-D) Cleavage of ataxin-3 by recombinant calpain-1 occurs slowly; after 15 min of incubation only little endogenous or overexpressed ataxin-3 is cleaved. E-H) Ataxin-3 cleavage by recombinant calpain-2 revealed an increased cleavage rate, which is enhanced when calpastatin (Cast) is knocked out. Both calpain-1 and calpain-2 cleavage results in a 30 kDa N-terminal derived fragment, respectively. Densitometric quantification of the 30 kDa fragment relative to time point zero and loading control GAPDH revealed more accumulation of the cleavage fragment if calpastatin is knocked out completely over time (I, J). SEM = standard error of mean.

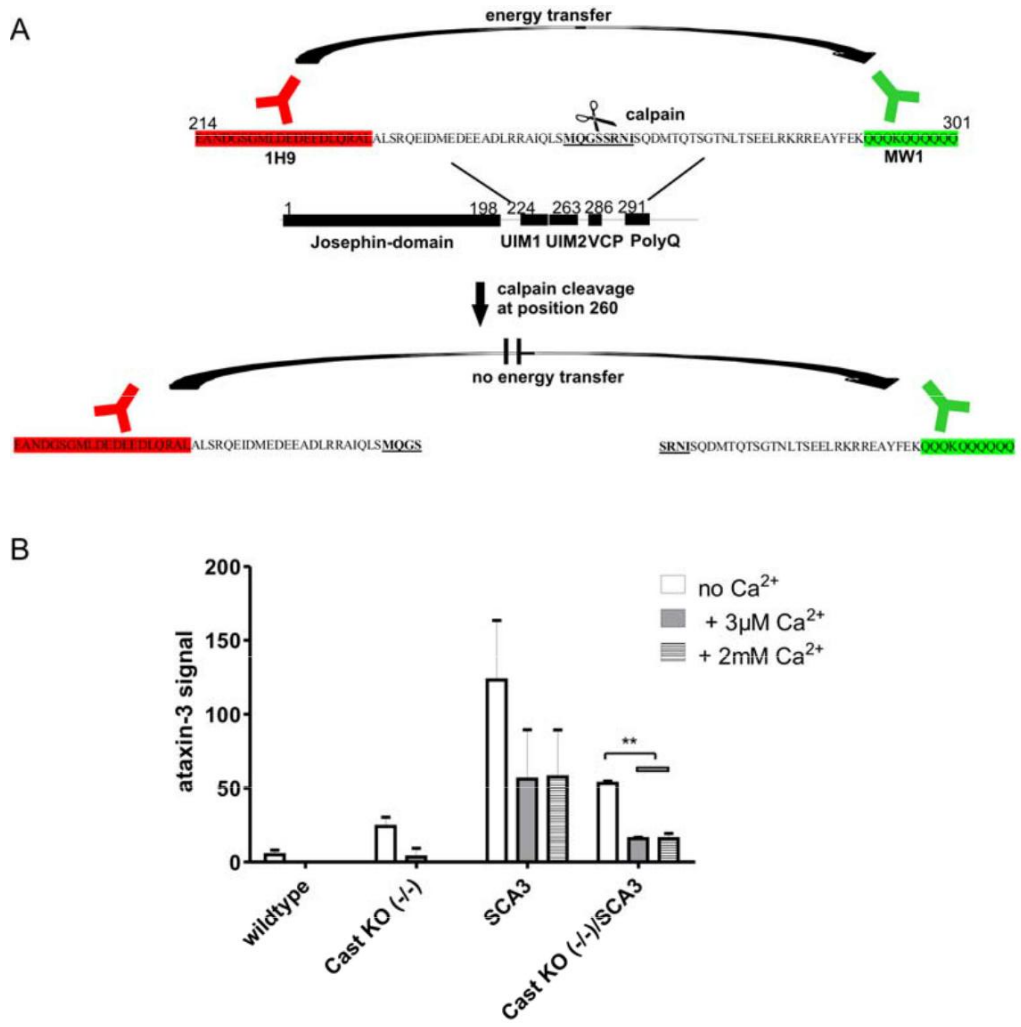

Figure 3. Calpastatin knock-out increases mutant ataxin-3 fragmentation upon calcium stimulation. A) Schematic representations of antibody binding sites in context of the ataxin-3 protein and the principal of the TR-FRET assay. B) TR-FRET analysis of cerebellar protein lysates of mice with indicated genotypes at the age of 12 months, without calcium stimulation or with appropriate calcium levels for calpain-1 or calpain-2 activation. In wildtype and Cast KO (-/-) mice only a background signal is detectable. Specific signals were found in st-line SCA3 and dm-mice. Importantly, the signal intensity in the dm-mice was only half of that of SCA3 single transgenic mice. Upon calcium stimulation the ataxin-3 specific signal decreases significantly in dm-mice. Bars represent means of three different mice per genotype. ** $p \leq 0.01$.

a. Hübener et al., 2013, Human Molecular Genetics.

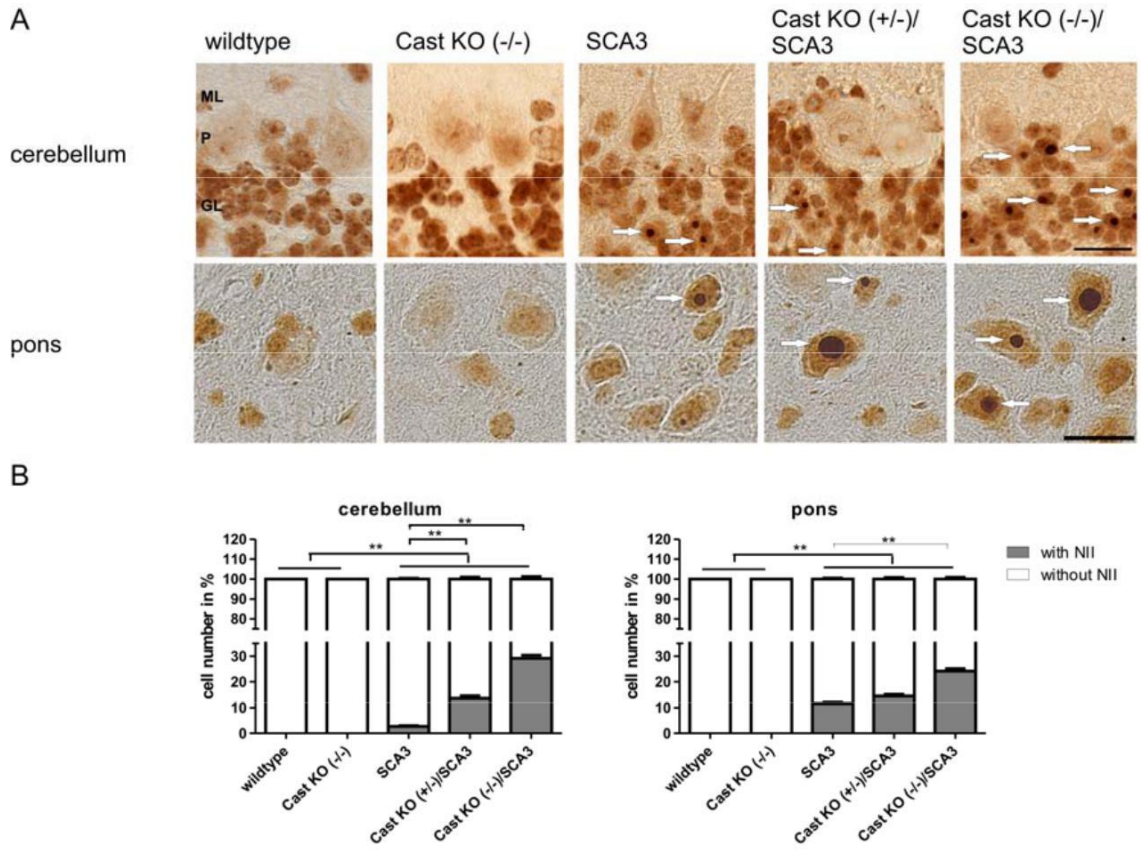

Figure 4. Increased number of nuclear inclusions in the dt-mutant lines. A) Sections stained with an ataxin-3 specific antibody (1H9) revealed ataxin-3 positive nuclear inclusions in the cerebellum and pons (indicated by an arrow). Notably, in the dm-lines with heterozygous or homozygous loss of calpastatin function, an increased number of aggregates were detected. No nuclear inclusions were found in wildtype and Cast KO (-/-) mice. Scale bar = 20 µm. B) Quantitative analysis of aggregates per cells in the cerebellum and pons revealed significant less aggregates in the st-line SCA3 compared to both dm-lines (** p≤0.001). Results are means ± SEM.

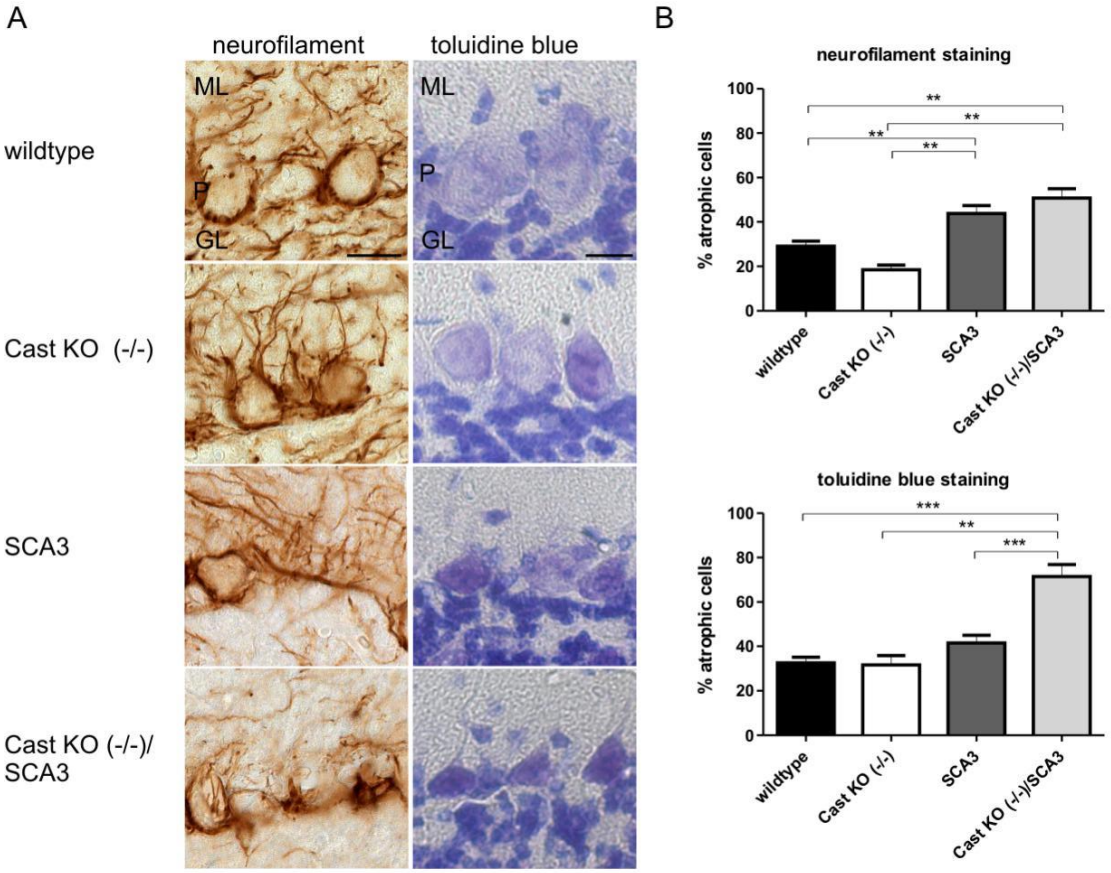

Figure 5. Calpastatin knock-out leads to enhanced neurodegeneration in the cerebellum of SCA3 mice. A) In 12 months old mice striking atrophy of Purkinje cells was detected in the st-line SCA3 and the dm-line indicated by empty baskets in the neurofilament staining and by dark blue staining of Purkinje cells by toluidine blue. Scale bar = 20µm. B) Quantitative analysis revealed more severe neurodegeneration in the dm-mice and st-line SCA3 compared to controls. Furthermore, toluidine blue staining demonstrated significant more neurodegeneration of Purkinje cells in dm-mice compared to the st-line SCA3 (** $p \leq 0.01$; *** $p \leq 0.001$). Results are means ± SEM.

a. Hübener et al., 2013, Human Molecular Genetics.

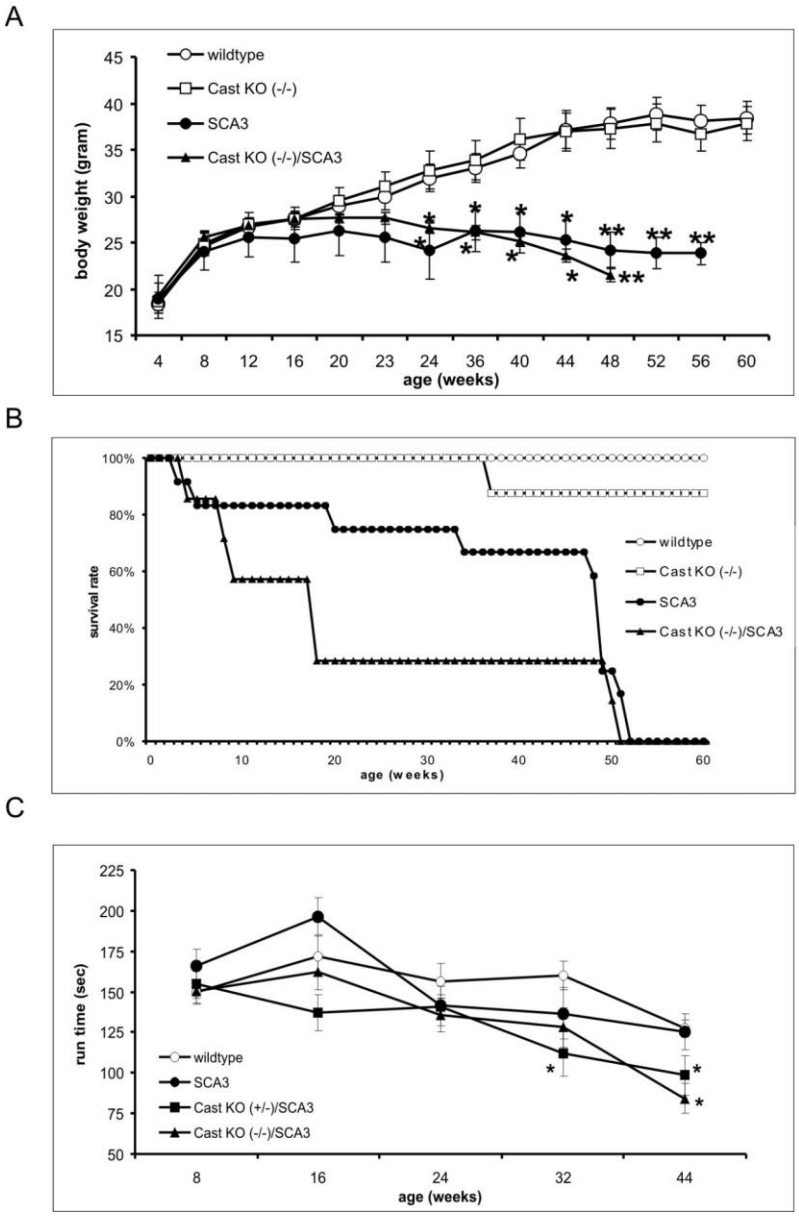

Figure 6. Calpastatin knock-out aggravates behavioral deficits in SCA3 mice. A) Body weight measurements revealed a significant reduction of body weight starting from the age of 24 weeks in the st-line SCA3 and dm-lines compared to controls. No significant differences were found between the disease lines. B) Cumulative survival using Kaplan-Meier estimator revealed premature death in the disease lines (st-line SCA3 and the dm-lines) compared to controls. Between the disease lines no significant differences in the survival rate were detected (p=0.226). C) Rotarod analysis demonstrated abnormalities in balance and motor coordination in animals of dm-lines. No differences were found between wildtype and the st-line for SCA3 (p=0.899. Results are means ± SEM. (*p≤0.05; **p≤0.01)

b. Nguyen *et al.*, 2013, *PLoS One*.

b. Nguyen et al., 2013, PLoS One.

OPEN ACCESS Freely available online

Cerebellar Soluble Mutant Ataxin-3 Level Decreases during Disease Progression in Spinocerebellar Ataxia Type 3 Mice

Huu Phuc Nguyen[1☯], Jeannette Hübener[1*☯], Jonasz Jeremiasz Weber[1], Stephan Grueninger[2], Olaf Riess[1], Andreas Weiss[2,3]

1 Institute of Medical Genetics and Applied Genomics, University of Tuebingen, Tuebingen, Germany, **2** Neuroscience Discovery, Novartis Institute for BioMedical Research, Basel, Switzerland, **3** IRBM Promidis, Pomezia, Italy

Abstract

Spinocerebellar Ataxia Type 3 (SCA3), also known as Machado-Joseph disease, is an autosomal dominantly inherited neurodegenerative disease caused by an expanded polyglutamine stretch in the ataxin-3 protein. A pathological hallmark of the disease is cerebellar and brainstem atrophy, which correlates with the formation of intranuclear aggregates in a specific subset of neurons. Several studies have demonstrated that the formation of aggregates depends on the generation of aggregation-prone and toxic intracellular ataxin-3 fragments after proteolytic cleavage of the full-length protein. Despite this observed increase in aggregated mutant ataxin-3, information on soluble mutant ataxin-3 levels in brain tissue is lacking. A quantitative method to analyze soluble levels will be a useful tool to characterize disease progression or to screen and identify therapeutic compounds modulating the level of toxic soluble ataxin-3. In the present study we describe the development and application of a quantitative and easily applicable immunoassay for quantification of soluble mutant ataxin-3 in human cell lines and brain samples of transgenic SCA3 mice. Consistent with observations in Huntington disease, transgenic SCA3 mice reveal a tendency for decrease of soluble mutant ataxin-3 during disease progression in fractions of the cerebellum, which is inversely correlated with aggregate formation and phenotypic aggravation. Our analyses demonstrate that the time-resolved Förster resonance energy transfer immunoassay is a highly sensitive and easy method to measure the level of soluble mutant ataxin-3 in biological samples. Of interest, we observed a tendency for decrease of soluble mutant ataxin-3 only in the cerebellum of transgenic SCA3 mice, one of the most affected brain regions in Spinocerebellar Ataxia Type 3 but not in whole brain tissue, indicative of a brain region selective change in mutant ataxin-3 protein homeostasis.

Citation: Nguyen HP, Hübener J, Weber JJ, Grueninger S, Riess O, et al. (2013) Cerebellar Soluble Mutant Ataxin-3 Level Decreases during Disease Progression in Spinocerebellar Ataxia Type 3 Mice. PLoS ONE 8(4): e62043. doi:10.1371/journal.pone.0062043

Editor: Harm H. Kampinga, UMCG, The Netherlands

Received November 28, 2012; **Accepted** March 17, 2013; **Published** April 23, 2013

Funding: The study was supported by the fortüne program of the University of Tuebingen (No. 1987-10 to Jeannette Hübener). The funders had no role in study design, data collection and analysis, decision to publish, or preparation of the manuscript.

Competing Interests: The authors have the following interests: Dr. Andreas Weiss and Stephan Grueninger were both employees of Novartis Institute for biomedical Research, Switzerland. Currently, Dr. Andreas Weiss is working at IRBM Promidis. There are no patents, products in development or marketed products to declare. This does not alter the authors' adherence to all the PLOS ONE policies on sharing data and materials.

* E-mail: Jeannette.huebener@med.uni-tuebingen.de

☯ These authors contributed equally to this work.

Introduction

A common feature of polyglutamine diseases such as Huntington disease (HD) or the group of Spinocerebellar Ataxias (SCA), including Spinocerebellar Ataxia Type 3 (SCA3), is the formation of intranuclear aggregates in specific subtypes of neurons containing the misfolded disease protein [1]. The question if these aggregates have a toxic role in neurons is controversially discussed and so far unresolved [2,3]. For SCA3 a relationship between processing of the disease protein ataxin-3 and disease progression was shown in tissue of transgenic mice and SCA3 patients where an increasing amount of ataxin-3 fragmentation was linked to disease severity [4]. Very recently, different studies revealed a proteolytic cleavage of mutant ataxin-3 by calpains [5–7] which results in the formation of highly aggregation-prone polyQ-containing fragments [5]. Therefore, analysis of soluble mutant ataxin-3 thus offers potential for evaluating the efficacy of possible therapeutic agents or as a biomarker for SCA3 disease progression.

Biomarker research in the field of neurodegenerative diseases gained increased interest in the last years due to the difficult monitoring and heterogeneous clinical nature of these disorders in which disease progression likely occurs over decades prior to appearance of first clinical symptoms. Blood- or cerebrospinal fluid-based biomarkers in neurodegenerative diseases are thus of major importance in context of disease risk prediction, improvement of diagnosis and prognosis, and optimization of therapeutic studies. In part, application of biomarker diagnostic in the clinical routine depends on the establishment of novel technologies in this field [8].

As aggregation of disease causing proteins is a hallmark in post mortem brains of patients with neurodegenerative diseases, quantification of their soluble and aggregated conformations are

potential useful readouts for biomarker development [9]. Time-resolved Förster resonance energy transfer (TR-FRET) immunoassays have been shown to be a robust and reliable method for detection of soluble and aggregated mutant huntingtin, the disease protein in HD, in a high spectrum of biological material including cellular, animal and human samples [10]. In addition, the quantification of the soluble and aggregated disease protein species using similar TR-FRET immunoassay based analyses is currently being investigated as potential biomarkers in Alzheimer disease (AD) [11] and Parkinson disease (PD) [12,13]. In the last months different groups implemented and modified this technique to also analyze the ratio between soluble and aggregated disease protein [9] or the ratio of oligomerization of proteins [13,14].

We thus chose to investigate levels of soluble mutant ataxin-3 during disease progression in brain tissue of SCA3 transgenic mice. In summary, we were able to develop a new robust, reproducible and sensitive TR-FRET immunoassay to analyze the level of soluble polyglutamine-expanded ataxin-3 in cellular and animal tissue and found that soluble mutant ataxin-3 levels show a tendency for decrease specifically in the cerebellum, one of the most affected brain regions in SCA3.

Materials and Methods

Ethics Statement

This study was carried out in strict accordance with the recommendations in the Guide for the Care and Use of Laboratory Animals of the University of Tuebingen, Germany. The protocols were approved by Institutional Animal Care and Use Committee (IACUC) of the University of Tuebingen.

Antibodies

In this study two different antibodies (1H9 and MW1) were used, both bind to the ataxin-3 protein. 1H9 antibody (MAB5360, Millipore) recognizes a 20 amino acid polypeptide 63 amino acids upstream of the disease causing polyglutamine tract (epitope E214 to L233) and the MW1 antibody, which binds specifically elongated and mutated polyQ-stretches. The MW1 antibody was developed by Paul Patterson [15] and obtained from the Developmental Studies Hybridoma Bank developed under the auspices of the NICHD and maintained by The University of Iowa, Department of Biological Sciences, Iowa City, IA 52242.

Cellular Model

HEK293T cells were grown in Dulbeccos modified eagle medium supplemented with 10% fetal calf serum, 1% non-essential amino acids and 1% penicillin/streptomycin at 37°C in 5% CO_2. Cells were plated in 96-well tissue culture plates, immediately transfected with V5-tagged ataxin-3 constructs (containing 15, 77 and 148 CAG repeats) using Attractene transfection reagent according to the manufacturer's instructions (Qiagen) and subsequently incubated for 24 h.

Animal Model

The generation and first characterization of the SCA3 transgenic mouse model used here has been described previously [16]. Briefly, a full-length ataxin-3 construct (isoform c) containing 70 CAG repeats under the control of a 3.4 kb fragment of the murine prion protein (Prp) promoter was used to generated SCA3 transgenic mice. The mice developed a severe neurological phenotype with gait ataxia and tremor beginning at the age of 10 months [16].

Sample Preparation

Brain samples were generated by sonication of adult mouse brains (whole brains or cerebellum) in 10x v/w of ice-cold lysis buffer (PBS +1% TritonX100+1X protease inhibitor cocktail (Roche)). HEK293T cell lysates were prepared by removal of cell culture medium and addition of lysis buffer to the adherent cells. Cells were lysed for 30 min under 300 rpm at 4°C. Total protein concentration was quantified by BCA assay (Pierce).

Time-resolved FRET Immunoassay

1H9 was labeled with donor Lumi4-Tb-fluorophore (Cisbio). MW1 was labeled with D2 acceptor fluorophore (Cisbio). After optimization of antibody titers and incubation conditions, quantification of mutant ataxin-3 levels was performed in low volume polystyrene 384 microtiter plates (Greiner Bio-One) with 5 µl sample volume and addition of 1 µl antibody solution (50 mM $NaHPO_4$+400 mM NaF +0.1% BSA +0.05% Tween-20+0.3 ng/µl 1H9-Tb +10 ng/µl MW1-D2). Plates were then incubated at 4°C for 20 h and analyzed by time-resolved fluorescence at 620 nm and 665 nm on an Envision Multilabel reader (Perkin Elmer).

Immunohistochemistry

For aggregate analysis, brains of 12 and 22 months old mice (3 of each genotype) were fixed by perfusion with 4% paraformaldehyde. Afterwards, 7 µm sections of paraffin-embedded brain tissue were processed and stained as previously described [16]. Primary antibody (ataxin-3, clone 1H9, Millipore) binding was performed in a 1:4000 dilution overnight at 4°C. Antibody binding was visualized by peroxidase labeling using vectastain elite avidin and biotinylated enzyme complex kit with 3,3′-diaminobenzidine substrate following the manufacturers instructions. Quantification of number and size of ataxin-3 positive inclusions was performed by analyzing ten visual fields (spread from lobule 6 to 10) on three different sections per analyzed mouse using an x63 objective on a Zeiss Axiovert image microscope. Image acquisition and quantification of number and size of aggregates in the granular layer of the cerebellum was done blinded using ImageJ analysis software (National Institutes of Health, NIH). The average number and size of inclusions was calculated for each animal and data are presented as the mean ± standard deviation.

Immunofluorescence Double Staining

Calbindin immunostaining of 3 mice per genotype and age was used to analyze the progression of neuronal dysfunction in the cerebellum of SCA3 transgenic mice compared to wildtype littermates. For double-fluorescence staining, 7 µm sections of paraffin-embedded brain tissue were incubated with the polyclonal anti-calbindin D-28K antibody (1:1000 Swant Swiss antibodies) and monoclonal anti-ataxin-3 antibody (clone 1H9; 1:500; Millipore) overnight at 4°C, followed by incubation with the corresponding fluorescence-coupled secondary antibodies (rabbit anti-Cy2 (1:50) and mouse anti-Cy3 (1:100); both from Dianova). Cell nuclei were stained with the fluorescent chromatin dye 4',6-diamidino-2-phenylindole (DAPI).

Quantification of calbindin immunoreactivity was performed by screening 10 fields in the cerebellum (lobule 6 to 10) on three different sections per analyzed mouse using an x40 objective on a Zeiss Axiovert image microscope. Optical densitometry analysis was done using ImageJ analysis software. Values are presented as the mean value of calbindin optical density per analyzed field ± standard deviation (u.a. = arbitrary unit).

b. Nguyen et al., 2013, PLoS One.

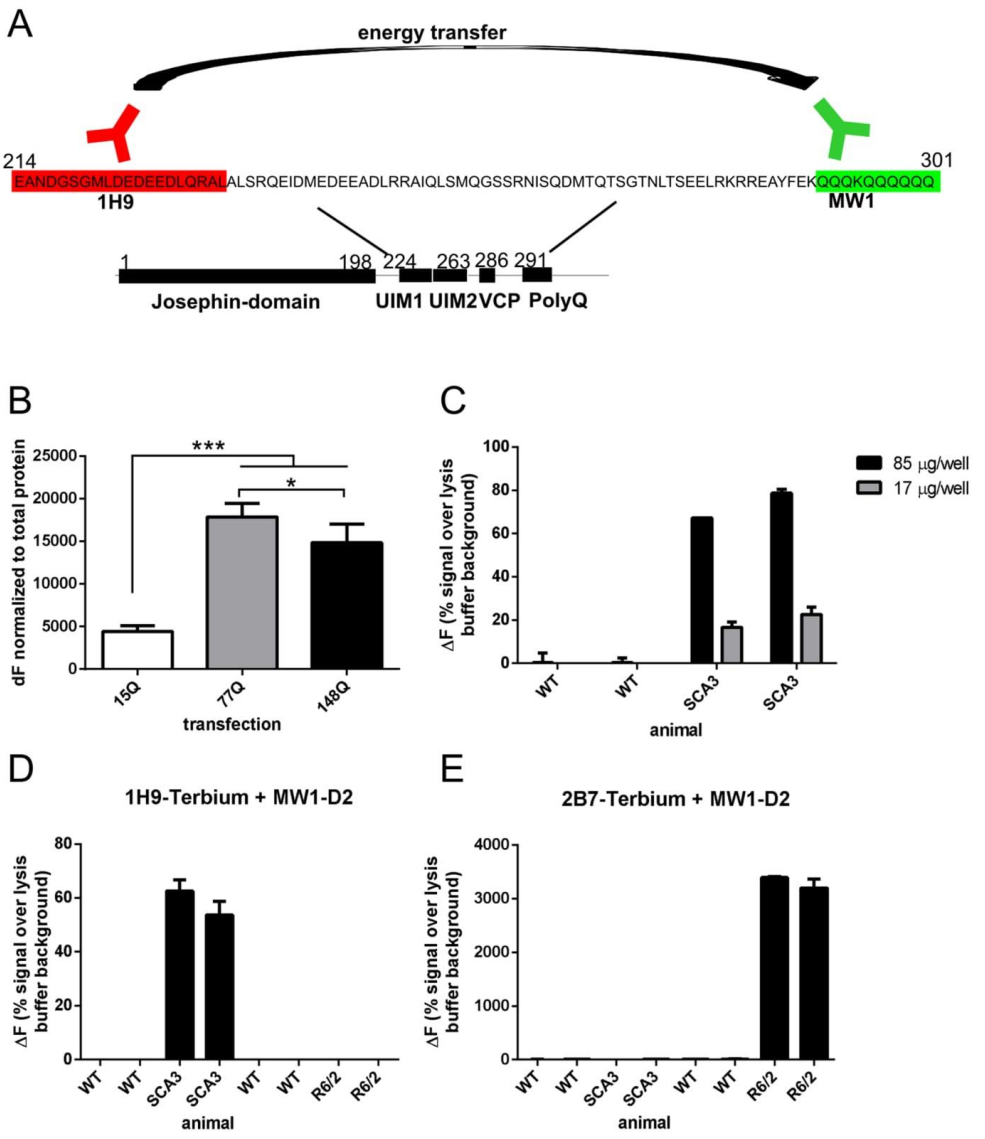

Figure 1. Establishing a TR-FRET based immunoassay to detect soluble ataxin-3 levels. A) Schematic illustration of antibody binding sites in context of the ataxin-3 protein and the principal of the TR-FRET immunoassay. By using this antibody combination (1H9 and MW1) only ataxin-3 with more than 6 CAG repeats can be detected (no detection of wildtype mouse ataxin-3) since the MW1 antibody is specific against an expanded polyQ-stretch. B) Measuring mutant ataxin-3 levels in HEK293T cells transiently transfected with ataxin-3 with different polyQ-lengths (15Q, 77Q, 148Q) revealed a detection of mutant ataxin-3 with 15, 77 and 148 polyglutamine repeats. Furthermore, ataxin-3 with a highly elongated polyQ-repeat (77 or 148Q) can be detected more efficiently than ataxin-3 with a normal, non-expanded repeat (15Q, ***$p<0.001$). Formation of aggregates was only found in cells transfected with ataxin-3-148Q but not with ataxin-3-77Q, which is associated with a significant reduction of soluble ataxin-3-148Q compared to ataxin-3-77Q (*$p<0.05$). C) To validate detectable protein amounts in mouse brain homogenates different concentrations of protein levels were tested. Whereas in wildtype lysates only a background noise signal was measured, in SCA3 transgenic whole brain lysates a protein concentration dependent TR-FRET signal was detected. D, E) To validate the specificity of the used antibody combinations for the disease

protein ataxin-3 (1H9– MW1) or huntingtin (2B7– MW1) a detection of protein in ataxin-3 transgenic mice (SCA3), huntingtin transgenic mice (R6/2) and wildtype mice was carried out. The antibody combination for ataxin-3 (1H9– MW1) showed only a specific signal in SCA3 transgenic mice, whereas the antibodies tailored for huntingtin (2B7– MW1) only detect in R6/2 huntingtin transgenic mice. Bars represent averages and standard error of the mean n = 6.
doi:10.1371/journal.pone.0062043.g001

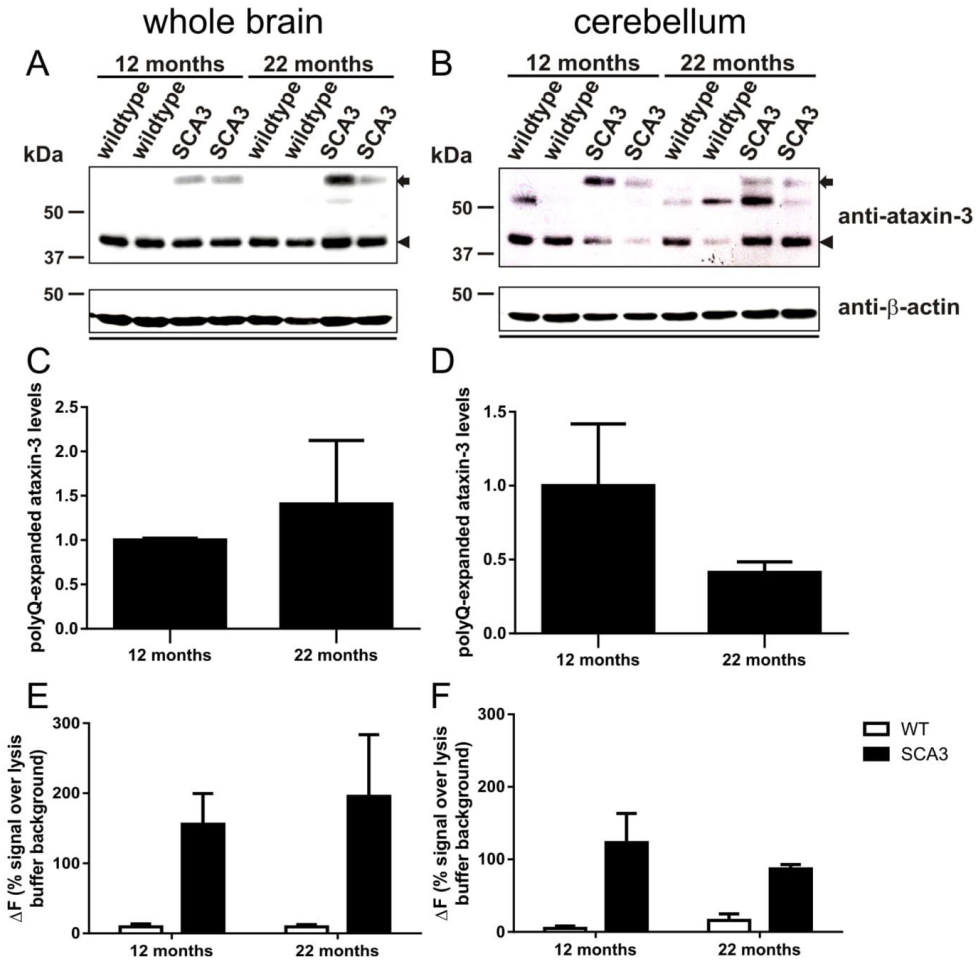

Figure 2. Western blot and TR-FRET analyses revealed an age dependent decrease of soluble mutant ataxin-3 levels in cerebellum. A–D) Two animals of the indicated genotypes per age were immunoblotted and detected with an ataxin-3 (clone 1H9) antibody. In all samples the endogenous ataxin-3 at 42 kDa was detected (indicated by an arrow head). In transgenic SCA3 mice a protein band at 60 kDa revealed the human ataxin-3 protein with 70Qs (arrow). Whole brain lysates showed similar expression levels of overexpressed human ataxin-3 in SCA3 transgenic mice at the age of 12 and 22 months (A and densitometric analysis in C; p = 0.6). In the cerebellum, one of the mainly affected brain areas in SCA3, less overexpressed ataxin-3 is detectable at the age of 22 months compared to 12 months of age (B). Densitometric analysis confirmed this observation (D, p = 0.3). As loading control actin is shown. E, F) Analysis of these samples by TR-FRET detection revealed similar levels of ataxin-3 in SCA3 transgenic mice in whole brain lysates at the age of 12 and 22 months (p = 0.52; E). In comparison in homogenates of the cerebellum the level of overexpressed ataxin-3 in SCA3 transgenic mice decreases in an age dependent manner, although this did not reach statistical significance (p = 0.19, F). Bars represent averages and standard deviation of biological triplicates.
doi:10.1371/journal.pone.0062043.g002

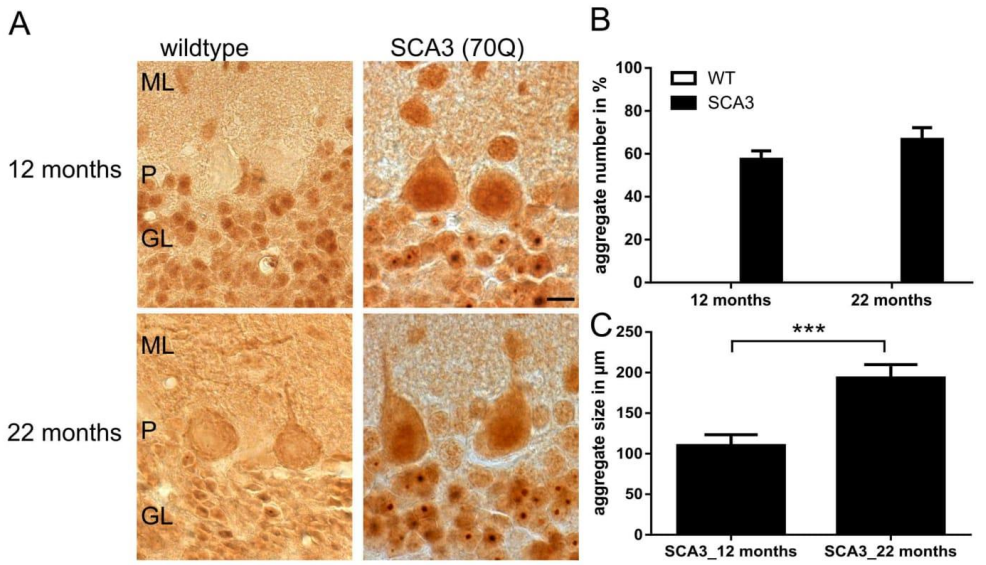

Figure 3. The number of ataxin-3 positive aggregates is inversely correlated with the level of soluble ataxin-3 in Western blot and TR-FRET analyses. A) shows representative immunohistochemical staining with an antibody against ataxin-3 (clone 1H9) in SCA3 transgenic mice compared to sex- and age-matched wildtype controls at the age of 12 and 22 months. No aggregates are detectable in wildtype animals. However, in SCA3 transgenic mice increasing numbers of aggregates are found at the age of 22 months compared to 12 months (A), but this did not reach significance ($p = 0.076$) after counting three independent animals per genotype (B). C) Measuring the size of aggregates in the granular layer of the cerebellum on the other hand revealed significant larger aggregates with disease progression in SCA3 transgenic mice (***$p<0.001$). Scale bar = 20 µm, ML = molecular layer, P = Purkinje cells and GL = granular layer.
doi:10.1371/journal.pone.0062043.g003

Western Blot

Western Blot analyses were carried out as previously described [16]. Immunodetection was performed using following antibodies: monoclonal mouse anti-ataxin-3 antibody (1:2500, clone 1H9, Millipore), monoclonal mouse anti-β-actin antibody (1:10,000, clone AC-15, Sigma), HRP-conjugated goat anti-mouse antibody (1:2500, GE Healthcare).

AGERA

AGERA (agarose gel electrophoresis for resolving aggregates) method and isolation of cytoplasmic and nuclear fractions were performed as previously described [17]. Cytoplasmic and nuclear fractions of brain samples from 6 months old mice (wildtype, SCA3 transgenic, R6/2) were run on a long 1% agarose gel and immunoblotted with specific antibodies for both ataxin-3 (clone 1H9, MAB5360, Millipore) and huntingtin (MW8).

Data Analysis

Unless otherwise indicated, TR-FRET signals are presented as ΔF values, which normalize the emission of the TR-FRET-dependent signal of the D2 acceptor fluorophore (665 nm) to that of the FRET-independent Terbum-cryptate donor fluorophore (620 nm) after subtracting the assay buffer background fluorescence. This method takes advantage of the internal reference fluorescence intensity of the donor fluorophore, thereby providing a HTT protein signal corrected for potential assay-interfering artifacts such as turbidity, light scattering or quenching capability of the sample, differences in sample volume due to slight pipetting variability, and day-to-day assay fluctuation caused by differences in excitation lamp energy. As a final step, the percentage TR-FRET signal increase over background is then normalized to total protein content of the sample as determined by BCA assay.

Statistical Analysis

All data were analyzed using Prism 6.0 software, GraphPad. Standard two-way ANOVA (data not matched) to assess the effects of genotype and age and Bonferroni *post hoc* tests were conducted to compare individual genotype effects at individual ages. Data are presented as mean ± SEM. Differences were considered significant if $p<0.05$.

Results and Discussion

Establishing a TR-FRET based Immunoassay to Detect Soluble Ataxin-3 Levels

To investigate the levels of soluble mutant ataxin-3 during disease progression, we aimed to develop a robust and easy-to-use TR-FRET immunoassay suitable for analysis of cellular and animal samples. To achieve this aim, we focused on the immunoassay antibody pair 1H9 and MW1, which should specifically bind to mutant but not wildtype ataxin-3. Higher specificity for the mutant form is a direct result of both antibodies binding in proximity to each other with the MW1 antibody recognizing the elongated and mutated polyglutamine region [15],

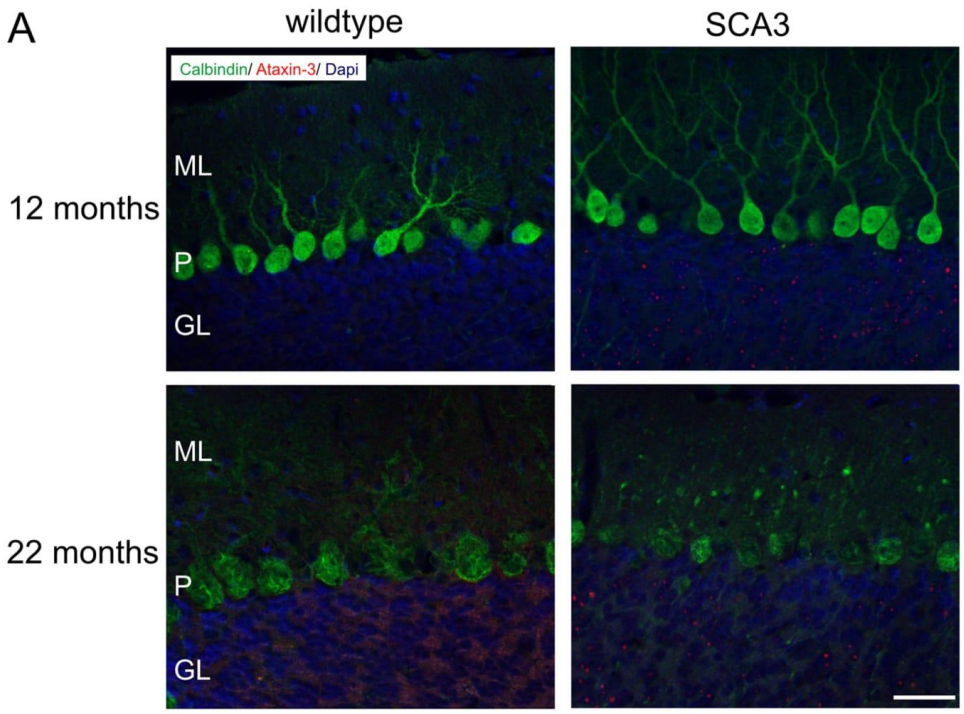
A
wildtype
SCA3
Calbindin/ Ataxin-3/ Dapi
12 months
22 months
ML
P
GL
ML
P
GL

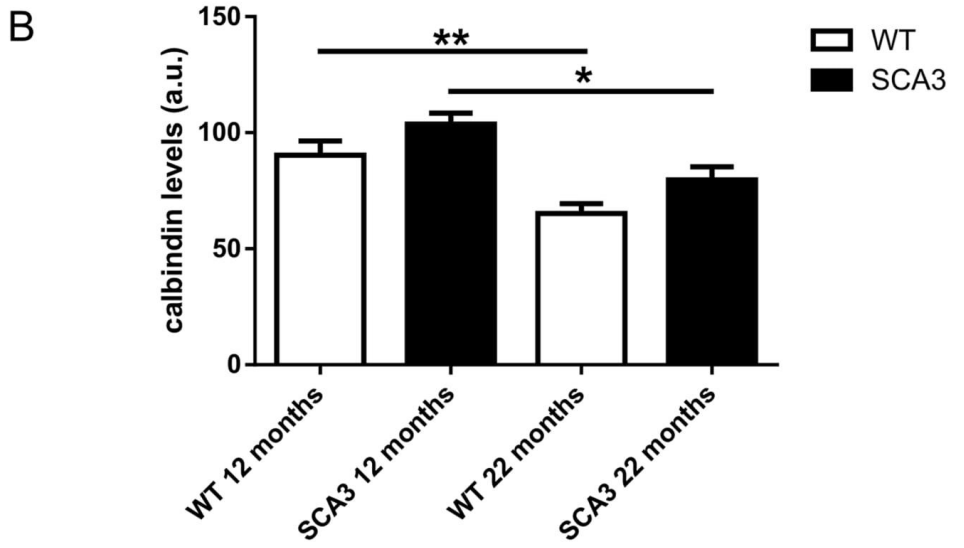
B
150
100
50
0
calbindin levels (a.u.)
**
*
WT
SCA3
WT 12 months
SCA3 12 months
WT 22 months
SCA3 22 months

Figure 4. Calbindin immunoreactivity showed reduced arborization of Purkinje cells with age independently from transgene expression. A) Double-immunofluorescence staining with calbindin (green) and ataxin-3 (clone 1H9, red) revealed aggregates in the granular layer of the cerebellum but not in the Purkinje cell layer of SCA3 transgenic mice. Calbindin staining of the Purkinje cells demonstrated shrinkage and loss of cells as well as a reduction of arborization of Purkinje cells with age in both, wildtype and SCA3 transgenic mice. B) Quantification of optical densitometry of calbindin showed a loss of immunoreactivity with age in both genotypes, respectively (*$p<0.05$; **$p<0.01$; a.u. = arbitrary units). Scale bar = 20 μm, ML = molecular layer, P = Purkinje cells and GL = granular layer.
doi:10.1371/journal.pone.0062043.g004

whereas the 1H9 antibody recognizes a sequence 58 amino acids N-terminal to the MW1 (schematic illustration in Fig. 1A). Prior to in-depth analysis of biological material we optimized the assay protocol for lysis buffer conditions (Sup. Fig. S1), the donor:-acceptor antibody titers and incubation conditions (Sup. Fig. S2). Following optimization, all analyzed samples were subsequently lysed in PBS buffer supplemented with 1% TritonX100 and incubated with 0.3 ng/μl 1H9-Tb and 10 ng/μl MW1-D2 at 4°C for 20 h.

Next, we transfected HEK293T cells with ataxin-3 constructs with different polyglutamine length (15Q, 77Q and 148Q) and monitored the expression level of the respective ataxin-3 using the TR-FRET immunoassay. As expected, ataxin-3 with a highly elongated polyglutamine repeats (77 or 148Q) can be detected more efficiently than ataxin-3 with a normal non-expanded repeat (15Q; $p<0.001$, Fig. 1B). The most frequent non-expanded allele found in normal individuals is 14 glutamines [18]. While our analysis revealed that the wildtype length can also be detected by the assay, the sensitivity for mutant over wildtype proved to be highly increased. Additionally, overexpressing human ataxin-3 with 148 or 77 glutamines in HEK293T cells results in aggregate formation only in cells transfected with ataxin-3-148Q but not in cells transfected with ataxin-3-77Q (data not shown). Notably, this is associated with a significant reduction of soluble ataxin-3-148Q compared to levels of ataxin-3-77Q as detected by TR-FRET analyses (Fig. 1B, $p<0.05$).

We then proceeded to assess mutant ataxin-3 detection in crude brain homogenates of 6 months old wildtype and SCA3 transgenic mice overexpressing human mutant ataxin-3. Mutant ataxin-3 could be readily quantified with high specificity over endogenous wildtype ataxin-3 in these samples (Fig. 1C). Further, to validate the specificity of the used antibody combinations for mutant ataxin-3 over other mutant polyglutamine containing proteins such as mutant huntingtin we tested the specificity in brain lysates of SCA3 and R6/2 mice, the most commonly used HD mouse model [19]. As expected, the antibody combination 1H9 and MW1 shows a mutant ataxin-3 specific signal in SCA3 transgenic mice, whereas the antibodies 2B7 and MW1 specifically bind to mutant huntingtin in transgenic Huntington mice (Fig. 1D, E).

Ataxin-3 Detection in Cerebellar Samples Reveals a Tendency for Decrease in Soluble polyQ-expanded Ataxin-3 during Disease Progression

After establishing the assay for ataxin-3 we analyzed if the assay is suitable to measure disease progression in tissue samples from transgenic SCA3 mice. Therefore, we monitored the level of soluble mutant ataxin-3 with 70 glutamines in whole brain homogenates or cerebellar lysates from transgenic SCA3 mice [16] at the age of 12 and 22 months compared to age- and sex-matched wildtype controls.

As represented by Menzies et al., (2010) the transgenic SCA3 mice with 70 glutamines (line 70.61, Ref. 16) did not longer demonstrate as severe a phenotype as previously reported [20]. Now, SCA3 transgenic mice developed first neurological symptoms including gait ataxia and tremor at the age of ten months, which progressively worsen with weight loss and result in a premature death at the age of 22 to 23 months. Using rotarod performance to measure motor coordination in these mice demonstrated a decreased ability to walk starting at the age of 10 weeks [20]. Immunohistochemical staining demonstrated first aggregates at the age of 3 months. In a first step, to measure a possible reduction of soluble mutant ataxin-3 with disease progression we analyzed whole brain lysates on Western blot (Fig. 2A, C) and by TR-FRET (Fig. 2E) and found similar levels of soluble ataxin-3 at the age of 12 and 22 months ($p = 0.62$ for Western blot analyses and $p = 0.52$ for TR-FRET). In contrast, in one of the main pathogenesis areas of SCA3, the cerebellum [21], both techniques revealed less soluble ataxin-3 at the age of 22 months compared to 12 months of age (Fig. 2B, D, F), although this decrease did not reach statistical significance (Western blot: $p = 0.3$; TR-FRET: $p = 0.19$). In both TR-FRET analyses, whole brain and cerebellum, the specific signal of polyQ-expanded ataxin-3 was up to 200% higher than in wildtype mice, which demonstrated that the endogenous mouse ataxin-3 with around 6 glutamines is nearly undetected with this method (Fig. 2E, F). A reduction of soluble levels of mutant ataxin-3 in the cerebellum could possibly be an effect of increased aggregate formation with disease progression in these transgenic mice. Therefore, we analyzed the aggregate load in cerebellar slices of transgenic SCA3 mice at the age of 12 and 22 months by immunohistochemical staining using 1H9 antibody. As described earlier, in wildtype controls no aggregates were detectable [16]. However, in SCA3 transgenic mice up to 70% of granular cells in the cerebellum showed aggregates in the nucleus, whereas at the age of 12 months less aggregates (up to 55%) were found (Fig. 3A). A quantification of the aggregate load demonstrated a tendency of an increased number of aggregates in cerebellar neurons at the age of 22 months, but this did not reach significance after counting three independent transgenic animals per genotype (Fig. 3B, $p = 0.07$). Additionally, the quantification of the aggregate size revealed significant larger aggregates at the age of 22 months compared to 12 months of age (Figure 3C, $p<0.001$). Presence of nuclear, but also cytoplasmic aggregates in SCA3 transgenic mouse brains was further validated with AGERA (Sup. Fig. S3). To investigate the association of aggregate formation and neuronal degeneration in the cerebellum of SCA3 transgenic mice we performed double immunofluorescence staining with calbindin (green signal) and ataxin-3 antibodies (clone 1H9, red signal). Similar to the immunohistochemistry data (Figure 3) staining with ataxin-3 revealed a higher aggregate load in 22 months old SCA3 transgenic mice compared to 12 months old SCA3 mice. Furthermore, staining with calbindin demonstrated shrinkage and loss of Purkinje cells as well as a reduced arborization of these cells with age in both wildtype and SCA3 transgenic mice (Figure 4A, B).

In summary, with the combination of the techniques applied (Western blot, immunohistochemistry and TR-FRET) we confirmed the hypothesis that the level of soluble polyQ-expanded ataxin-3 in the cerebellum of transgenic mice decreases with disease progression, whereas the aggregate load in the same brain region inversely correlates with this observation. Similar results were found in Huntington disease mice (R6/2) where also an

inverse correlation between the level of soluble mutant huntingtin and aggregate formation was observed [9,22]. These findings demonstrate that in these two distinct polyglutamine diseases, Huntington disease and SCA3, the soluble level of the disease protein correlates with disease progression and, therefore, possibly representing a biomarker for these disorders. In both, HD and SCA3, it is known that the disease protein has to be proteolytically cleaved by caspases and/or calpains before the formation of nuclear aggregates occurs. The cleavage separates the expanded polyglutamine tract from the rest of the protein, subsequently allowing the polyQ-tract to translocate to the nucleus and form intranuclear aggregates. For huntingtin, the cleavage sites of caspases [23–26] and calpains [27,28] are well known. However for ataxin-3, there is an ongoing discussion whether caspases [4,23,29–31] or calpains [5–7] can cleave ataxin-3. Very recently, it was convincingly shown that calpains can proteolyze ataxin-3 [5–7] and different cleavage sites have been proposed [32]. Therefore, in another study we utilized our novel TR-FRET immunoassay to investigate whether a hypothetical cleavage site around amino acid position 260 [32] in the ataxin-3 protein, which is located between the both antibodies used for TR-FRET, is indeed a cleavage site for calpains. To this end, we treated cerebellar lysates of SCA3 transgenic mice with appropriate calcium levels to activate calpain-1 or calpain-2. Under these conditions we found that the TR-FRET signal is decreased by half compared to the native, untreated ataxin-3 signal [6] indicating that decreased detection of soluble mutant ataxin-3 after calcium induction was due to increased calpain cleavage at amino acid position 260. This demonstrates that our TR-FRET immunoassay cannot only be applied to measure the level of soluble mutant ataxin-3 but by use of specific antibody combinations it can be of great value to investigate specific pathomechanisms such as identifying cleavage sites of ataxin-3.

Conclusions

In summary, we described the adaptation of a new robust, specific, reproducible and sensitive time-resolved Förster resonance energy transfer (TR-FRET) immunoassay to analyze the level of soluble polyglutamine-expanded ataxin-3 in cellular and animal tissue. Using this assay we were able to detect a tendency for a decrease of soluble polyQ-expanded ataxin-3 in mouse brain lysates, particularly in the cerebellum, with disease progression. In line with this observation, we found more nuclear aggregates in the respective brain region and therefore described an inverse correlation between level of soluble ataxin-3 and aggregate formation.

To identify biomarkers of neurodegenerative diseases a simple and sensitive assay is needed. As shown for AD, HD, and PD, the TR-FRET immunoassay is a technique, which can be very useful for this implement. Therefore, the adaptation of the assay to SCA3 will help to understand pathomechanisms, monitor disease progression in different patient material (e.g. blood, cerebrospinal fluid) and help to evaluate the efficiency of therapeutic strategies.

Supporting Information

Figure S1 Determination of optimal lysis buffer composition for mutant ataxin-3 extraction and subsequent TR-FRET detection. Wildtype and SCA3 transgenic mouse brain were homogenized with the indicated lysis buffers. Homogenates were adjusted to identical total protein concentrations and subjected to TR-FRET detection.
(TIF)

Figure S2 Optimization of donor:acceptor antibody ratios and kinetics for TR-FRET detection of mutant ataxin-3. SCA3 transgenic mouse brain homogenate was analyzed with different antibody titers and assay incubation conditions. Samples were incubated at either room temperature or at 4°C for the indicated duration. Incubation for 22 h at 4°C with 0.3 ng/well 1H9-Terbium and 3 ng/well MW1-D2 antibody yielded the maximum signal over background window. These conditions were subsequently used for further analysis of biological samples in this report. Bars represent averages and standard deviation of n = 3.
(TIF)

Figure S3 Analysis of ataxin-3 aggregates in mouse brain by AGERA. Representative example of an AGERA blot of mouse brain samples from ataxin-3 mice with 70 glutamines compared to wildtype controls and Huntington transgenic R6/2 mice. Both ataxin-3 transgenic as well as R6/2 transgenic mice showed aggregates in the cytoplasmic (C) and nuclear (N) fraction using specific antibodies for both ataxin-3 (1H9) and huntingtin (MW8). In the R6/2 mice aggregates are significantly larger than in SCA3 transgenic mice. No aggregates were found in wildtype mice.
(TIF)

Acknowledgments

The authors thank Nicolas Casadai for technical help with the ImageJ software for quantifying size and number of aggregate.

Author Contributions

Conceived and designed the experiments: HPN JH OR. Performed the experiments: JH JJW SG AW. Analyzed the data: JH JJW AW. Contributed reagents/materials/analysis tools: SG AW. Wrote the paper: HPN JH AW.

References

1. Riess O, Rüb U, Pastore A, Bauer P, Schöls L (2008) SCA3: neurological features, pathogenesis and animal models. Cerebellum 7: 125–137.
2. Michalik A, Van Broeckhoven C (2003) Pathogenesis of polyglutamine disorders: aggregation revisited. Hum Mol Genet 12 Spec No 2: R173–86.
3. Williams AJ, Paulson HL (2008) Polyglutamine neurodegeneration: protein misfolding revisited. Trends Neurosci 31: 521–528.
4. Goti D, Katzen SM, Mez J, Kurtis N, Kiluk J, et al. (2004) A mutant ataxin-3 putative-cleavage fragment in brains of Machado-Joseph disease patients and transgenic mice is cytotoxic above a critical concentration. J Neurosci 24: 10266–10279.
5. Koch P, Breuer P, Peitz M, Jungverdorben J, Kesavan J, et al. (2011) Excitation-induced ataxin-3 aggregation in neurons from patients with Machado-Joseph disease. Nature 480: 543–546.
6. Hübener J, Weber JJ, Richter C, Honold L, Weiss A, et al. (2013) Calpain mediated ataxin-3 cleavage in the molecular pathogenesis of Spinocerebellar Ataxia Type 3 (SCA3). Hum Mol Genet 22: 508–518.
7. Simoes AT, Goncalves N, Koeppen A, Deglon N, Kügler S, et al. (2012) Calpastatin-mediated inhibition of calpains in the mouse brain prevents mutant ataxin-3 proteolysis, nuclear localization and aggregation, relieving Machado-Joseph disease. Brain 135: 2428–2439.
8. Bertram L, Hampel H (2011) The role of genetics for biomarker development in neurodegeneration. Prog Neurobiol 95: 501–504.
9. Baldo B, Paganetti P, Grueninger S, Marcellin D, Kaltenbach LS, et al. (2012) TR-FRET-based duplex immunoassay reveals an inverse correlation of soluble and aggregated mutant huntingtin in Huntingtons disease. Chem Biol 19: 264–275.
10. Weiss A, Abramowski D, Bibel M, Bodner R, Chopra V, et al. (2009) Single-step detection of mutant huntingtin in animal and human tissues: A bioassay for Huntingtons disease. Anal Biochem 395: 8–15.
11. Ran C, Zhao W, Moir RD, Moore A (2011) Non-conjugated small molecule FRET for differentiating monomers from high molecular weight amyloid beta species. PLoS One 6: e19362.

12. Kaminski Schierle GS, Bertoncini CW, Chan FTS, van der Goot AT, Schwendler S, et al. (2011) A FRET Sensor for non-invasive imaging of amyloid formation in vivo. Chem Phys Chem 12: 673–680.
13. Bidinosti M, Shimshek DR, Mollenbauer B, Marcellin D, Schweizer T, et al. (2012) Novel one-step immunoassays to quantify α-synuclein: applications for biomarker development and high-throughput screening. J Biol Chem 287: 33691–33705.
14. Cottet M, Faklaris O, Maurel D, Scholler P, Doumazane E, et al. (2012) BRET and time-resolved FRET strategy to study GPCR oligomerization: from cell lines toward native tissues. Front Endocrinol (Lausanne) 3: 92.
15. Ko J, Ou S, Patterson PH (2001) New anti-huntingtin monoclonal antibodies: implications for huntingtin conformation and its binding proteins. Brain Res Bull 56: 319–329.
16. Bichelmeier U, Schmidt T, Hübener J, Boy J, Rüttiger L, et al. (2007) Nuclear localization of ataxin-3 is required for the manifestation of symptoms in SCA3: in vivo evidence. J Neurosci 27: 7418–7428.
17. Weiss A, Klein C, Woodman B, Sathasivam K, Bibel M, et al. (2008) Sensitive biochemical aggregate detection reveals aggregation onset before symptom development in cellular and murine models of Huntingtons disease. J Neurochem 104: 846–858.
18. Maruyama H, Nakamura S, Matsuyama Z, Sakai T, Doyu M, et al. (1995) Molecular features of the CAG repeats and clinical manifestation of Machado-Joseph disease. Hum Mol Genet 4: 807–812.
19. Mangiarini L, Sathasivam K, Seller M, Cozens B, Harper A, et al. (1996) Exon 1 of the HD gene with an expanded CAG repeat is sufficient to cause a progressive neurological phenotype in transgenic mice. Cell 87: 493–506.
20. Menzies FM, Huebener J, Renna M, Bonin M, Riess O, et al. (2010) Autophagy induction reduces mutant ataxin-3 levels and toxicity in a mouse model of Spinocerebellar ataxia type 3. Brain 133: 93–104.
21. Seidel K, Siswanto S, Brunt ERP, den Dunnen W, Korf HW, et al. (2012) Brain pathology of spinocerebellar ataxias. Acta Neuropathol 124: 1–21. 22.
22. Cowin RM, Roscic A, Bui N, Graham D, Paganetti P, et al. (2012) Neuronal aggregates are associated with phenotypic onset in the R6/2 Huntington's disease transgenic mouse. Behav Brain Res 229: 308–319.
23. Wellington CL, Ellerby LM, Hackam AS, Margolis RL, Trifiro MA, et al. (1998) Caspase cleavage of gene products associated with triplet expansion disorders generates truncated fragments containing the polyglutamine tract. J Biol Chem 273: 9158–9167.
24. Kim J, Yi Y, Sapp E, Wang Y, Cuiffo B, et al. (2001) Caspase 3-cleaved N-terminal fragments of wildtype and mutant huntingtin are present in normal and Huntington's disease brains, associated with membranes, and undergo calpain-dependent proteolysis. Proc Natl Acad Sci U S A 98: 12784–12789.
25. Hermel E, Gafni J, Propp SS, Leavitt BR, Wellington CL, et al. (2004) Specific caspase interactions and amplification are involved in selective neuronal vulnerability in Huntington's disease. Cell Death Differ 11: 424–438.
26. Graham RK, Deng Y, Slow EJ, Haigh B, Bissada N, et al. (2006) Cleavage at the caspase-6 site is required for neuronal dysfunction and degeneration due to mutant huntingtin. Cell 125: 1179–1191.
27. Gafni J, Ellerby LM (2002) Calpain activation in Huntington's disease. J Neurosci 22: 4842–4849.
28. Gafni J, Hermel E, Young JE, Wellington CL, Hayden MR, et al. (2004) Inhibition of calpain cleavage of huntingtin reduces toxicity: accumulation of calpain/caspase fragments in the nucleus. J Biol Chem 279: 20211–20220.
29. Berke S, Schmied FA, Brunt ER, Ellerby LM, Paulson HL (2004) Caspase-mediated proteolysis of the polyglutamine disease protein ataxin-3. J Neurochem 89: 908–918.
30. Pozzi C, Valtorta M, Tedeschi G, Galbusera E, Pastori V, et al. (2008) Study of subcellular localization and proteolysis of ataxin-3. Neurobiol Dis 30: 190–200.
31. Jung J, Xu K, Lessing D, Bonini NM (2009) Preventing ataxin-3 protein cleavage mitigates degeneration in a Drosophila model of SCA3. Hum Mol Genet 18: 4843–4852.
32. Haacke A, Hartl FU, Breuer P (2007) Calpain inhibition is sufficient to suppress aggregation of polyglutamine-expanded ataxin-3. J Biol Chem 26: 18851–18856.

c. Weber *et al.*, 2014, *BioMed Research International*.

“Jonasz Jeremiasz Weber, Anna Sergeevna Sowa, Tina Binder, Jeannette Hübener (2014) From Pathways to Targets: Understanding the Mechanisms behind Polyglutamine Disease. BioMed Research International, Volume 2014, Article ID 701758.” Available online at: http://dx.doi.org/10.1155/2014/701758.

Hindawi Publishing Corporation
BioMed Research International
Volume 2014, Article ID 701758, 22 pages
http://dx.doi.org/10.1155/2014/701758

Review Article

From Pathways to Targets: Understanding the Mechanisms behind Polyglutamine Disease

Jonasz Jeremiasz Weber,[1,2] Anna Sergeevna Sowa,[1,2] Tina Binder,[1,2] and Jeannette Hübener[1,2]

[1] *Institute of Medical Genetics and Applied Genomics, University of Tübingen, Calwerstraße 7, 72076 Tübingen, Germany*
[2] *Rare Disease Center, Calwerstraße 7, 72076 Tübingen, Germany*

Correspondence should be addressed to Jeannette Hübener; jeannette.huebener@med.uni-tuebingen.de

Received 9 May 2014; Accepted 3 September 2014; Published 21 September 2014

Academic Editor: Yiying Zhang

The history of polyglutamine diseases dates back approximately 20 years to the discovery of a polyglutamine repeat in the androgen receptor of SBMA followed by the identification of similar expansion mutations in Huntington's disease, SCA1, DRPLA, and the other spinocerebellar ataxias. This common molecular feature of polyglutamine diseases suggests shared mechanisms in disease pathology and neurodegeneration of disease specific brain regions. In this review, we discuss the main pathogenic pathways including proteolytic processing, nuclear shuttling and aggregation, mitochondrial dysfunction, and clearance of misfolded polyglutamine proteins and point out possible targets for treatment.

1. Introduction

Polyglutamine (polyQ) diseases are inherited, fatal neurodegenerative disorders caused by an expansion of a coding trinucleotide (CAG) repeat, which is translated to an abnormally elongated glutamine (Q) tract in the respective mutant proteins. There are nine known polyQ diseases: dentatorubral-pallidoluysian atrophy (DRPLA), Huntington's disease (HD), spinal-bulbar muscular atrophy (SBMA), and six spinocerebellar ataxias (SCA 1, 2, 3, 6, 7, and 17). Except for SBMA, which is X-linked, members of this disease group are inherited in an autosomal dominant manner [1]. It also appears that the shared expansion of polyQ tract confers some shared neurodegenerative pathways on the diseases. Although the region of the brain that is affected differs according to each disease, the observed cell death is aggravated by the trafficking of the protein to specific cellular compartments where it can increase the rate of aggregation. Both nuclear and cytoplasmic aggregates are present in polyQ diseases and contain parts of the respective disease proteins, ubiquitin, and several important homeostatic proteins [2]. The recruitment of ubiquitin, heat shock proteins, and proteasomal subunits into these aggregates implies that protein quality control mechanisms such as the ubiquitin-proteasome system (UPS) are involved in polyQ pathogenesis [3]. It has also been discussed that the cleaved protein is more toxic than the full-length variant. An initial proteolytic cleavage of the respective disease proteins may generate a fragment containing the elongated polyQ stretch which is more aggregate prone and hence more toxic for the cell [4, 5]. What is also interesting about this group of proteins is that although they are all ubiquitously expressed in embryonic stages and adulthood, the pathology of the disease only occurs in neuronal cells [6]. One possible explanation for this phenomenon is the high energy demand of neurons and hence their dependency on oxidative energy metabolism. This points dysfunctional mitochondria as a shared mechanism of neurodegeneration [7]. In this review we focus on what we consider to be the most important pathways in pathology of Huntington's disease and spinocerebellar ataxias: proteolytic processing, nuclear

shuttling and aggregation, mitochondrial dysfunction, and intracellular protein degradation systems (Figure 1).

2. Proteolytic Processing

Early studies of the common characteristics of polyQ diseases revealed that small fragments of mutant proteins containing the expanded polyQ stretch harbored cytotoxic characteristics [8, 9]. Proteolytic cleavage, the proposed source of these breakdown products, was suggested as an early or initial step in the molecular disease development. This mechanistic concept is commonly known as the *toxic fragment hypothesis* [10]. The presence of proteolytically derived fragments of mutant proteins was reported for all polyQ diseases introduced in this review, namely, SCA 1 [11], SCA 2 [12], SCA 3 [13, 14], SCA 6 [15], SCA 7 [16, 17] SCA 17 [18], and HD [19, 20]. Currently, several classes of endogenous proteases have been linked to the proteolysis of polyQ proteins including the groups of caspases [21–24] and calpains [20, 25–29].

For SCA 1 and 2, neither an inherent cytotoxicity and aggregation propensity nor a clear impact on pathology is evident for mutant protein fragments, demanding further characterization [11, 12]. For ataxin-2, the disease protein in SCA 2, mutant fragment constructs were shown to exhibit an aggregate formation potential *in vitro* [30], but further studies revealed a decreased cytotoxicity of N-terminally truncated mutant ataxin-2 compared to the full-length protein [31]. Even so, for the majority of polyQ diseases a correlation between proteolytic processing of mutant proteins and disease progression is generally accepted.

In a SCA 3 cell model, the expression of a fragment of ataxin-3 containing an elongated polyQ stretch induced apoptosis and cell death as well as a severe ataxia in a mouse model, showing a more rapid manifestation of a SCA 3-reminiscent phenotype when compared to mice expressing full-length mutant ataxin-3 [8]. In addition, polyQ-containing ataxin-3 fragments were shown to form aggregates on their own and were also able to recruit full-length protein into the insoluble inclusions [32, 33]. In HD, *in vitro* data showed that the progressive truncation of mutant huntingtin (mHtt) protein and the length of the polyQ expansion correlate with the aggregation propensity and an increase in apoptotic stress [34, 35]. Mouse studies revealed a similar result when animals expressing the polyQ expanded exon 1 of huntingtin (Htt) showed a progressive neurological phenotype recapitulating characteristics of HD. This suggests that the N-terminal polyQ-containing portion of Htt was sufficient to induce neurodegeneration *in vivo* [9]. An important observation is that these disease fragments were detectable in human HD and SCA 3 brain and lymphoblasts [13, 20, 36] and were found to be an important component of neuronal intranuclear inclusions [37–39]. Similar results were retrieved from two mouse models of SCA 7 expressing polyQ expanded ataxin-7. In brain tissue of these animals N-terminal ataxin-7 fragments were observed which appeared in nuclear aggregates in correlation with onset of the disease phenotype [16, 17]. As with much of the current research on polyQ diseases, not all observations are in agreement. An HD mouse model expressing a polyQ expanded fragment of Htt encompassing exons 1 and 2 exhibited neither neurotoxic effects nor an HD phenotype, despite the presence of nuclear inclusions [40]. This illustrates that not all fragment species feature neuropathological characteristics. Another noteworthy investigation made on a SCA 3 gene trap mouse model showed that expression of a fusion protein comprising β-galactosidase and the N-terminal portion of ataxin-3 without the polyglutamine tract led to the formation of cytoplasmic inclusion bodies and to a phenotype reminiscent of the neurological symptoms observed in SCA 3 mice and patients [41]. Furthermore, C-terminal polyQ fragments of the α1A calcium channel, disease protein in SCA 6, showed a polyQ independent cytotoxic nature. However, the expansion of the polyQ stretch within the fragment resulted in its increased resistance to proteolysis entailing an accumulation of this toxic species [15].

The first proteases which were shown to cleave polyQ expanded proteins were caspases. This family of cysteine proteases is associated with apoptotic pathways and inflammation but is also known to be involved in a variety of other cellular functions like cell proliferation, differentiation, and migration [42, 43].

Caspases are involved in cell death mechanisms and an increase in activation of caspases has been detected in the course of polyQ diseases. Presence of apoptotic cell death and caspase activation was shown in human HD brains as well as in mouse and cell models of HD [44–51], although this goes against previous studies that did not find apoptotic nuclei in the R6/2 mouse model of HD [52]. Cell death pathways and caspases were also reported to be switched on in other polyQ diseases like SCA 3 [8, 53] and SCA 7 [54, 55]. In the case of SCA 7, activated caspase-3 was recruited into inclusions in cell culture and human SCA 7 brain, and its expression was upregulated in cortical neurons [54]. In general, inhibition of caspases has been shown to ameliorate disease progression and phenotype in HD mice [44, 49].

Within the polyQ diseases reviewed, the first discovery of caspase-mediated cleavage of a disease-causing protein was made for HD [21]. This *in vitro* study indicated a specificity of caspase-3 for huntingtin and a polyQ expansion dependent cleavage. Further studies identified caspase-1 dependent cleavage of huntingtin and confirmed caspase-3-mediated fragmentation, whereas caspases-7 and -8 appeared not to cleave full-length huntingtin [22]. Moreover, caspase-3 selectively processed expanded huntingtin and resulting N-terminal fragments formed cytoplasmic and nuclear inclusions [48]. Direct evidence for caspase-mediated huntingtin cleavage was gained from early stage HD postmortem human tissue and transgenic mice. In these brain tissues, not only mutant but also wild type huntingtin are substrates for caspase cleavage. The early disease stage of these samples suggests that caspase-mediated proteolysis of mHtt may precede neurodegeneration [23].

Multiple studies have begun to elucidate the specific caspases responsible for cleavage of huntingtin. A broad inhibition of caspases with Z-VAD-FMK in clonal striatal cells led to a reduction of specific huntingtin fragments and an increased viability without changing levels of inclusions,

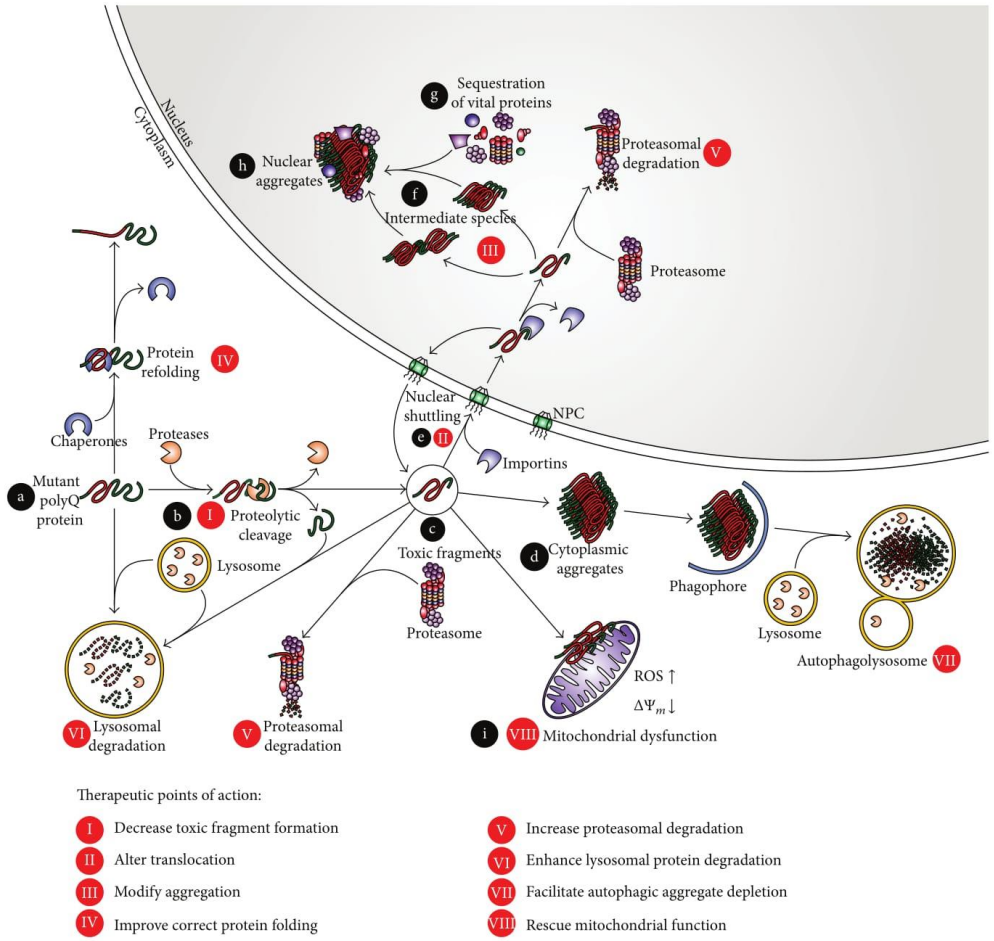

FIGURE 1: A model of the common molecular mechanisms behind polyglutamine pathology. Schematic illustration of the intracellular fate of the polyglutamine (polyQ) expanded protein, from the unprocessed mutant protein to a protein aggregate. The mutant protein (a) is proteolytically processed by endogenous enzymes (b) forming toxic fragments (c). These fragments form aggregates in the cytoplasm (d). Alternatively, toxic breakdown products can translocate into the nucleus (e) and generate nuclear aggregates (h) by forming intermediate species (f) and sequestering further vital proteins (g). Accumulation of polyQ species can damage important cellular components and lead, for example, to mitochondrial dysfunction (i). The visualized pathways point possible sites for therapeutic engagement: prevention of proteolytic events (I) can decrease levels of toxic fragments. Alteration of nuclear shuttling (II) and modulation of aggregation (III) can ameliorate the detrimental effects of toxic species. As polyQ expansions lead to misfolded proteins, structural refolding assisted by enhanced chaperone activity (IV) might be beneficial. An increased degradation of polyQ proteins and aggregates via proteasomal (V), lysosomal (VI), and autophagosomal (VII) pathways can reduce the amounts of toxic species inside the cell. Finally, attenuating the consequences of polyQ toxicity (VIII), like impaired mitochondrial function, can improve the cellular viability.

whereas treatment with the caspase-3 specific inhibitor Z-DEVD-FMK reduced aggregates without changing cleavage or increasing cell viability [46]. The generation of mouse lines expressing caspase-3 and caspase-6 resistant polyQ expanded huntingtin by eliminating specific cleavage sites unveiled a strong relevance of cleavage at the 586 amino acid caspase-6 site of huntingtin. Removing the caspase-6, but not caspase-3, recognition sites in mHtt appeared to be sufficient to protect from neuronal dysfunction and neurodegeneration *in vivo* [56]. A further study showed that caspase-6, but not

caspase-3, is activated before the onset of motor abnormalities in murine and human HD brain. Caspase-6 activation correlated directly with the size of the polyQ expansion and inversely with the age at onset [56]. Moreover, medium spiny neurons (MSNs) expressing caspase-6 resistant mHtt showed a decreased susceptibility for NMDAR-induced excitotoxicity and no caspase-6 activation compared to MSNs expressing unmodified mHtt [56–58]. By contrast, two caspase-6 knockout HD mouse models showed that production of a 586 amino acid derived proteolytic fragment was not prevented in the brain, disagreeing with a direct involvement of caspase-6 in mHtt cleavage [59, 60].

Correlating with the results for huntingtin, caspases-1 and -3, but not caspases-7 and -8, were reported to cleave ataxin-3 *in vitro* producing specific fragments [22]. The impact of caspase cleavage was confirmed in a cell based model, showing that predominantly caspase-1-mediated fragmentation of expanded ataxin-3 resulted in increased aggregation and treatment with caspase inhibitors prevented inclusion formation *in vitro* [61]. Interestingly, a different *in vitro* study showed that mutant ataxin-3 was cleaved to a lesser extent than wild-type ataxin-3 after a common initial proteolytic step, suggesting that generated mutant fragments cannot be further degraded. This may result in an accumulation of aggregation-prone expanded ataxin-3 fragment species [62]. In a *Drosophila* model cleavage of ataxin-3 appeared to be conserved and also caspase-mediated, featuring neuronal loss which was mitigated by a sextuplet caspase site mutation in ataxin-3 [63]. A recent publication reported involvement of CDK5 in caspase-mediated ataxin-3 cleavage, showing that RNAi of CDK5 in a *Drosophila* model for SCA 3 resulted in an enhanced SCA 3 toxicity [64]. Contrary to results pointing to an involvement of caspases in the molecular pathology of SCA 3, an *in vitro* study based on patient-derived iPSCs demonstrated that upon excitotoxic stress ataxin-3 cleavage and aggregation were prevented neither by pharmacological inhibition of caspases-1 and -3 nor by treatment with a pan-caspase inhibitor but was abolished by inhibiting calpain activity [65].

In the case of SCA 7, *in vitro* assays identified caspase-7 as the responsible proteolytic enzyme for ataxin-7 fragmentation. The mutation of two specific caspase-cleavage sites in ataxin-7 not only resulted in a resistance of polyQ expanded ataxin-7 to caspase cleavage but also attenuated cell death, aggregate formation, and transcriptional interference in cells. Fragments of ataxin-7 corresponding to products of caspase-7 cleavage were also found in SCA 7 mice, which furthermore exhibited an increased caspase-7 activation and recruitment into the nucleus by expanded ataxin-7 [24]. Nonetheless, full-length expanded ataxin-7 can form inclusions without evidence for cleavage [54].

TBP (TATA-binding protein), the disease protein in SCA 17, was reported to show fragmentation and fragment-dependent formation of aggregates in SCA 17 mice [18], but *in vitro* assays did not show a TBP substrate-specificity for caspases [22], suggesting different proteolytic enzymes to be involved in truncation of TBP.

A second group of proteolytic enzymes that were associated with cleavage of polyQ expanded proteins are calpains, a class of calcium-dependent cysteine proteases. These ubiquitously expressed enzymes exhibit a multitude of regulatory cellular functions and are specialized in modulating structure, localization, and activity of their substrates [66, 67].

In human HD tissue and in brains of HD mouse models an increased expression level of calpains, namely, of calpains-1, -5, -7, and -10, and elevated enzyme activity have been reported [25, 26, 68, 69]. Interestingly, an age-dependent attenuation of calpain activity was observed in an HD mouse model, suggesting alterations in calcium signaling mechanism with disease progression [70]. Furthermore, wild-type and mutant huntingtin were identified as calpain substrates and calpain-dependent proteolytic cleavage products of huntingtin were detected in murine and human HD tissue [25, 27, 46, 71]. Caspase-3 cleavage derived huntingtin fragments undergo further proteolysis by calpains, generating smaller products and suggesting a proteolytic pathway of serial processing events [20]. Additionally, calpain-derived mHtt fragments were shown to accumulate in the nucleus [26], which correlates with cytotoxicity and aggregation in HD [34, 35]. In cell models, the inhibition of calpain cleavage of mutant huntingtin by mutating putative cleavage sites within the huntingtin protein resulted in a decreased proteolysis, aggregation, and toxicity [26]. The mutation of Ser-536 to aspartic acid in order to mimic phosphorylation abolished huntingtin proteolysis at this cleavage site and reduced mutant huntingtin toxicity, pointing to an involvement of phosphorylation events as modulators of calpain cleavage [72]. Concurrent with their activation after ischemic injury, calpains were also shown to cleave full-length huntingtin in infarcted rat cortex and striatum producing N-terminal fragments [73].

Although initial studies stating that an involvement of calpains in SCA 3 was not detectable [61, 63], calpain-dependent proteolysis of ataxin-3 has been reported corresponding to observations in HD [28, 29, 65]. Several putative calpain cleavage sites within the ataxin-3 protein were identified [28, 29, 65, 74], accounting for the generation of a C-terminal polyQ-containing and aggregation-prone fragment [33]. After activation of calpains *in vitro,* fragments of respective sizes were generated. This effect was suppressed when the endogenous calpain inhibitor calpastatin (CAST) was coexpressed in treated cells and aggregation of mutant ataxin-3 was induced or decreased [28]. In a double mutant CAST KO/SCA 3 mouse model, the knockout of the endogenous calpain inhibitor led to higher ataxin-3 fragmentation, amplified aggregate load, increased neurodegeneration, and, in conclusion, to a more severe behavioral phenotype [29]. Reciprocally, overexpression of CAST using adenoassociated viral vectors in a lentiviral mouse model of SCA 3 resulted in reduced ataxin-3 proteolysis and in decreased size and number of intranuclear inclusions of ataxin-3 and neuroprotection via calpain inhibition [74]. In line with these observations, CAST was shown to be depleted in murine and human SCA 3 brain tissue [74]. The neuronal specificity of the molecular mechanisms underlying SCA 3 pathology has been demonstrated by an approach using SCA 3 patient-derived IPSCs. After neuronal differentiation and glutamate-induced calcium influx, excitation-induced ataxin-3 cleavage

and aggregation were triggered. This was observed only in neurons, not in glial cells or fibroblasts, and was abolished by calpain inhibition [65].

Although caspases and calpains are reported to account for the majority of cleavage effects on polyQ expanded disease proteins, several fragmentation events could not be explained by their proteolytic activity. An important group of enzymes to consider is the lysosomal cathepsins, which has been shown to process mutant huntingtin. An involvement of cathepsins-D, -B, -L, and -Z [75–77] has been indicated to produce fragments termed cp-A and cp-B [78]. For the cp-A fragment it was illustrated that the protease responsible for its formation has cathepsin-D-like properties in immortalized neurons and gamma-secretase-like properties in primary neurons, pointing to a cell type specific involvement of different proteolytic enzymes [79]. A further screen for identification of novel proteases using 514 protease-specific siRNAs detected 11 enzymes including three members of the matrix metalloproteinase (MMP) family cleaving huntingtin. When knocking down the most promising candidate MMP-10 in a striatal cell line cleavage of mutant huntingtin was prevented. In line with this work, MMPs were shown to be upregulated in HD mouse models and loss of function of *Drosophila* MMP homologs also ameliorated mutant huntingtin-induced neuronal dysfunction [80]. A very interesting novel explanation for the appearance of toxic fragments of huntingtin is that observed missplicing of huntingtin transcripts accounts for shortened N-terminal huntingtin variants [81]. A likewise fascinating attempt to explain ataxin-3 cleavage was done by showing that the intrinsic proteolytic property of ataxin-3's Josephin domain may lead to an autolytic processing of the disease protein [82]. However, C14A ataxin-3 mutants lacking proteolytic activity exhibited no differences neither in subcellular localization nor in proteolysis [62].

As a multitude of publications show that proteolytic processing of polyQ expanded proteins by a variety of enzymes represents a pivotal step in the molecular pathomechanism of polyQ diseases, modulating the activity of cleavage-responsible proteases or decreasing the levels of toxic fragments could be reasonable approaches for therapeutic treatment.

There are various ways to approach treatment. One method is to inhibit the proteolytic activity of caspases, calpains, cathepsins, or MMPs directly. Using such methods beneficial effects were achieved for HD [26, 46, 80, 83, 84] and SCA 3 [28, 61, 63, 65]. But attention should be paid to potential adverse effects as well [84]. A similar approach is to target the expression of endogenous inhibitors, such as calpastatin, as was done in SCA 3 [28, 29, 74].

A second approach is to modulate alternate pathways and achieve off-target benefits. Treating R6/2 mice with a tetracycline derivative delayed disease progression and death by reducing the levels of caspases-1 and -3 [42] through upstream regulation of Apaf-1 [85]. Reducing elevated calpain activity in HD mice also had beneficial off-target benefits [68, 69]. In addition, CDK5 was reported to act against caspase cleavage of huntingtin by phosphorylation at S434 [86]. In SCA 3, decreasing CDK5 levels via RNAi in *Drosophila* enhanced mutant ataxin-3 toxicity [64]. Another option is to use a genetic approach to modulate cleavage such as induction of exon 12 skipping in huntingtin pre-mRNA using oligonucleotides. This modification prevented the translation of the caspase-targeted region around amino acid 586 and thereby inhibited the formation of an N-terminal fragment implicated in HD toxicity [87].

3. Aggregation

As the pathological hallmark of polyQ diseases [1], aggregation has been widely discussed as therapeutic target. Although it serves as an easy readout for screens, cell models, and neuropathology, the exact role of aggregates in the neurodegeneration observed in polyQ diseases is still under debate. In the field of polyQ diseases, aggregates were identified as intranuclear inclusions in mouse models of Huntington's disease [52] and subsequently confirmed in HD patients [37, 88]. This was quickly followed by an identification of aggregates containing the disease protein in SCA 3 [32, 38] and SCA 1 [89] and cytoplasmic aggregates in SCA 6 [90], SCA 7 [54, 91], and SCA 17 [92]. In SCA 2, the initial reports of the absence of aggregation [93, 94] have since been challenged [95, 96].

What was initially observed as large fibrillar inclusions is most likely the end stage of protein aggregation and nucleation. The beginning steps feature monomeric species which transform into oligomeric structures and protofibrils/fibrils, although the correlation between these intermediates may not be linear. Some of these species may be direct pathway intermediates while others may not be directly relevant to the inclusion formation seen in patients [97]. Recent advances are being made and assays developed which will help in studying this pathway of aggregation, monomer addition, and isolating specific aggregate species [98]. Work in the field of HD on oligomer formation is bringing the field closer to understanding the mechanisms behind nucleation. The conversion of monomers to oligomers in HD is described as a packing of the N-terminal Htt segment into the oligomer core [98], elongation of fibrils follows, and a third step involves the ability of oligomers to seed monomer elongation. The work suggests that oligomer dissociation rates are similar to association rates and that oligomers serve as both on-pathway and off-pathway intermediates in fibril formation. It seems important to thus consider the aggregation pathway as an ebb and flow of intermediates which feed into multiple pathways. Ataxin-3 was also shown to have a multistep aggregation process where the first step involves the aggregation of the protein independent of the polyQ domain and a second step which is unique to the polyQ expansion and produces highly stable amyloid-like aggregates [99]. In a discussion about aggregation pathways, it is also important to note that kinetic differences between nucleation and protein folding in the nucleus and in the cytoplasm probably play a large role in the observed differences we see in inclusions between nuclear protein aggregates such as in SCA 1 and SCA 3 and cytoplasmic proteins such as SCA 2 and SCA 6 [100]. For HD, the study of the aggregation pathway pointed to

"at least three" aggregation pathways which can be influenced by various inhibitors, molecules, and interactions [101]. Inhibiting each pathway has different effects on neurotoxicity. The same was shown for ataxin-3 where different amyloid aggregates affect Ca^{2+} regulation by different mechanisms [102]. Altering the specific pathways of aggregation is a potential therapeutic strategy which may not decrease the total amount of aggregation but could decrease neurotoxicity.

A widely discussed topic is the exact cytotoxic nature of aggregates. By looking at the specific location of inclusions in patient brains, a discrepancy arose between the neurons which have the inclusions and the neurons which are known to degenerate [103]. In HD, the medium spiny neurons which are selectively lost present with much less aggregation than the large interneurons [103]. This and similar findings suggest that the large aggregates are protective. But the other work, such as in SCA 1, reiterates the relationship between aggregates and cytotoxicity. Patients who have a specific histidine interruption in the expanded polyQ tract of ataxin-1 have a decreased amount of aggregation and absence of disease [104]. The issue with such findings is that it does not provide insight into what is happening with intermediate oligomeric species which are more correlated to the onset of symptoms than to the formation of large protein aggregates [105, 106].

Just to highlight how complex it is to tease out the exact role of aggregates, in SCA 7 and SCA 6, different types of nuclear inclusions were identified. In SCA 7, they differ in their size, composition, and distribution of key proteins [54, 91] and detection with a p62 antibody found different subsets of cytoplasmic aggregates in SCA 6 [107]. Furthering our understanding of the interplay between neuronal types can tell us more about the effect of aggregation in specific populations and how that affects the health of surrounding cells. It is difficult to come to a conclusive decision on aggregation and to pull apart the protective properties from the cytotoxic ones without further information.

The discussion on toxicity of aggregates is also relevant for the screening of large libraries of therapeutic compounds or genetic modifiers. Using aggregation as readout is intuitive since if any part of the pathways of aggregation is toxic, then reducing the eventual product of large readout aggregates could also be considered reducing the intermediate toxic species. However, the field should be cautious about blocking the conversion of toxic oligomeric species to possible beneficial aggregates or shifting the balance of different conformation in an unfavorable direction [108]. It is also possible to look at increasing the overall rate of aggregation which could decrease the amount of time in which toxic intermediates can do damage but would cause an overall increase in total large aggregates. Targeting the depletion of specific species with antibodies or upregulated clearance is also a therapeutic possibility. Also, although extracellular aggregate transmission has not been proven for polyglutamine diseases, it could be possible to target the prion-like spread of smaller fibrils and oligomers [109, 110].

In general, a focus on aggregation has allowed the field to gain knowledge about various biological pathways involved in polyQ induced neurodegeneration. As previously described, cleavage plays a large role in the kinetics of aggregation and the mechanisms of toxicity. In the search for intermediate steps between proteolysis and aggregation, it was demonstrated in various cell models that polyQ-containing fragments or polyQ stretches themselves are generally able to form soluble oligomeric structures, mediating cytotoxicity and representing a starting point for subsequent aggregation [111–113]. These oligomeric species could also be identified in brain tissue of HD mouse models and patients [113, 114].

Looking at aggregates has also allowed us to see the recruitment of proteasomal subunits and look into the dysregulation of the ubiquitin system in neurodegeneration. But aggregation is slowly becoming an avoided topic in polyQ research. Hopefully recent advances in understanding aggregate intermediates will open a door to a better analysis of aggregation in neurodegeneration. This can lead to a renewed interest in understanding the complexity behind protein folding and nucleation in polyQ diseases.

4. Nuclear Transport

One aspect relevant to both of the aggregation of these proteins and to their general function is their ability to shuttle between the nucleus and cytoplasm. This transport modulates how they both perform their regular function and cause neurodegeneration. Nuclear transport encompasses many features of protein function such as transcription, avoidance of protein clearance machinery, import of a toxic fragment, and many other cellular processes. The current evidence suggests that the nucleus is a large site of toxicity in cells and blocking nuclear transport in animal models has shown that this pathway is a possible therapeutic target [109, 115, 116]. In general, nuclear entry is a highly controlled process and at the heart of that regulation is the nuclear pore complex which serves as a selective gatekeeper of entry [117]. The nuclear pore complex recognizes a group of proteins known as karyopherins which are carrying protein cargo for entry and exit out of the nucleus. Karyopherins recognize their cargo by the presence of specific nuclear localization signal (NLS) and nuclear export signal (NES) on proteins (reviewed by [118]). The most direct way for a protein to be transported by a karyopherin is to have an identifiable NLS or NES (or combination), but secondary features such as the visibility of this signal and posttranslational modifications such as phosphorylation and cleavage which alter the signal also play a large role.

Within the polyQ diseases discussed here, NES and/or NLS have been found for the disease proteins of SCA 1, SCA 3, SCA 7, and HD [11, 119–123].

In SCA 1, specifically, it has been shown that regulation of nuclear localization is relevant to disease progression and ataxin-1 stability. It was shown early on that blocking the NLS on ataxin-1 prevents the protein from causing neurodegeneration *in vivo* [11]. It was later explained that phosphorylation at S776 and the subsequent binding and release from 14-3-3 can mask the NLS, stabilize ataxin-1, and

modulate its localization [124] which is important for the nuclear interaction of ataxin-1 with splicing factors RBM17 and U2AF65 [125]. 14-3-3 is a protein that is involved in regulating many cellular processes by binding phosphorylation sites and the example of ataxin-1 demonstrates how factors outside of direct nuclear shuttling influence localization and affect the direct pathomechanisms of disease.

SCA 3 and HD have been the two most widely studied in the possible therapeutic regulation of transport to modify disease. The focus on nuclear transport has been a consequence of studies where fusing mutant fragments of Htt to exogenous NES prevented nuclear transport and inhibited the toxicity of the fragment [126, 127] and the reverse happened when it was fused to an NLS [126]. This work was reproduced in a mouse model which had a shorter lifespan correlated to an added NLS [128]. It has been difficult to tie together the cellular events that cause transport with the known pathways of nuclear entry. It is known, for example, that ataxin-3 and huntingtin enter the nucleus in response to cellular stress and heat shock, but the exact mechanism of transport is not elucidated [129–131]. Also, phosphorylation of both proteins has been linked to nuclear transport. Phosphorylation of huntingtin on N17 releases it from the endoplasmic reticulum to allow nuclear entry but also prevents export from the nucleus during stress response [132] and modulates its neurotoxicity [133]. In the case of ataxin-3, CK-2 dependent phosphorylation of S340 and S352 within the third UIM (ubiquitin interacting motif) has been suggested to control nuclear entry [134]. The current research is also focused on understanding the karyopherins involved in the recognition of the NLS and NES sites of these proteins with the aim of modulating disease. CRM1, or exportin-1, has been shown to interact with both ataxin-3 and huntingtin NES sites [132, 135] and suggested to be an exporter of ataxin-7 [122]. Karyopherins B1 and B2 have also been published as possible mediators of huntingtin localization which act on a putative huntingtin NLS [136]. Cellular and oxidative stress were shown to alter the activity of CRM1 and to affect the localization of polyQ proteins by posttranslational modifications of karyopherins or subsets of the nuclear pore complex [137].

Also of note is the importance of the NLS site in SBMA. The androgen receptor (AR) is kept in the cytoplasm by heat shock proteins which mask this nuclear localization site but, upon binding to the androgen ligand, the NLS is exposed and the androgen receptor translocates to the nucleus where it activates androgen-responsive genes (reviewed in [138]). The presence of the androgen receptor in the nucleus in the presence of the ligand is considered necessary for disease development as mice with an NLS deletion showed delayed onset of phenotype and reduced motor deficit [139]. It is important to note this nuclear function of the AR as the proteins in SCA 1, SCA 3, and HD may also have similar important roles in the nucleus, although aggravating their nuclear presence may overwhelm those beneficial roles and cause neurotoxicity.

In those polyQ diseases where an NLS or NES has not been identified, localization of the protein has still proved to be important to pathogenesis. Recent work using a polyQ antibody has demonstrated that the localization of ataxin-2 within the cell corresponds to disease stages of SCA 2. Cytoplasmic presence corresponded to early stage and nuclear presence and aggregation to final stages of the disease [140]. The mislocalization of ataxin-2 has also been shown to be a potent modifier of ALS/TDP43 toxicity [141] and it has also been suggested that ataxin-2 is important for SCA 3 neurodegeneration. This points to the possibility that the localization of ataxin-2 is important in modulating other neurodegenerative diseases [142]. In SCA 6, the C-terminal peptide of the alpha 1A subunit of the P/Q-type voltage-gated calcium channel with the expanded polyQ tract is also toxic to cells depending on its nuclear localization [143]. Although the exact mechanism behind this translocation is not known, the current hypothesis is that it is important for disease progression.

One way to affect localization is to target the polyQ expansion of the protein. It was shown that the expansion of the CAG repeat in Htt reduces its interaction with Tpr, a nuclear pore protein, which is involved in nuclear export [144] and the expansion of ataxins-3 and -7 has also been linked to nuclear retention [122, 145].

Overall, nuclear trafficking and localization are a summation of many processes that happen within the cell starting from cleavage of the protein, aggregation, modulation of mitochondrial response, and involving all functions of the protein such as transcriptional regulation. The list of proteins with altered subcellular localization in neurodegeneration includes NFkB, ERK1/2, TDP43, Smad, E2F1, CREB, and many others [146]. Because of this wide breadth of cellular mechanisms involved in nuclear localization, it should always be considered an aspect of therapeutic intervention.

5. Clearance Mechanisms

It is known that polyQ proteins are associated with the formation of intracellular aggregates, possibly through the formation of toxic fragments, but the important question of what clearance mechanisms are involved remains. The two main clearance routes of organelles and proteins in eukaryotic cells are the ubiquitin-proteasome system (UPS) together with heat shock response and the autophagy-lysosomal pathway. While proteasomes predominantly degrade short-lived nuclear and cytoplasmic proteins as well as misfolded and unfolded proteins from the endoplasmic reticulum, the autophagic system can degrade organelles and cytoplasmic protein complexes [147, 148].

The interplay of heat shock proteins, chaperones, and the UPS is important for protein clearance [149]. During oxidative or cellular stress heat shock proteins are dramatically upregulated. They bind to misfolded proteins and remodel them back to their native formation. If refolding is not possible, degradation by the proteasome is initiated. Failure in one of the systems can be compensated partially by the upregulation of the other, but prolonged failure results in protein aggregation and dysfunctional homeostasis of cells [150]. Many wild-type ataxins as well as huntingtin have been shown to interact with components of the UPS under

normal conditions. Yeast two hybrid assays demonstrated an interaction of ataxin-3 and the ubiquitin and proteasome binding factors HHR23A and HHR23B [151, 152]. Ataxin-1 was shown to interact with the ubiquitin-like protein A1Up [153], the ubiquitin-specific protease USP7 [154], and the E2 ubiquitin-conjugation enzyme UbcH6 [155, 156]. Moreover, ataxin-7 was indicated to interact with the S4 subunit of the 19S proteasome [157].

In line with the fact that normal function of polyQ proteins involves interaction with the quality control system is the knowledge that molecular heat shock proteins, ubiquitin, and proteasomal subunits are found in neuronal aggregates in postmortem brains of patients. In HD patients and animal models, aside from the N-terminal part of mHtt, ubiquitin, molecular chaperones including GRP78/BiP, HSP70, and HSP40, and the 20S, 19S, and 11S subunits of the 26S proteasome were also found ([37, 158], reviewed in [159]). Similar results were described for SCA 1 [160], for SCA 3 [161], and for SCA 7 [54, 157]. Together, these findings indicate that ubiquitin, heat shock proteins, and subcomplexes of the 26S proteasome are redistributed to the site of polyQ protein degradation.

The carboxyl terminus of the HSC70-interacting protein (CHIP) is a HSP70 cochaperone as well as an E3 ubiquitin ligase that protects cells from proteotoxic stress. The ability of CHIP to interact with HSP70 and function as a ubiquitin ligase places CHIP in a pivotal position in protein quality control [162] and makes CHIP a frequently analyzed protein in polyQ refolding and degradation. It was shown that CHIP directly interacts and colocalizes to ataxin-1, ataxin-3, and huntingtin aggregates [163, 164]. Additionally, CHIP promotes ubiquitination of wild-type and mutant ataxins-1 and -3 and huntingtin as well as decreasing steady state levels of mutant ataxins-1 and -3 and huntingtin by inducing degradation. Therefore, CHIP suppresses aggregation and toxicity in cell culture and *Drosophila* [163, 164]. Suppression of CHIP resulted in an increased formation of microaggregates and toxicity in a SCA 3 transgenic mouse model [165]. Moreover, overexpression of CHIP together with ataxin-1 led to reduction of ataxin-1 solubility and thus increased formation of aggregates [166]. Another HSP70-dependent E3 ligase that is shown to act redundantly to CHIP on some substrates is parkin [167]. Parkin (*PARK2*, mutated in an autosomal recessive form of PD), which mediates the targeting of proteins for proteasomal degradation, is known to interact and modulate ataxin-2 and ataxin-3 but not ataxin-1 [166, 168–171]. Wild-type and polyQ expanded ataxin-3 deubiquitinate parkin directly and parkin ubiquitinates and facilitates the clearance of wild-type and mutant ataxin-2 and ataxin-3 by proteasomal degradation [168–170]. Additionally, it was demonstrated that parkin forms a complex with the expanded polyQ protein, HSP70, and the proteasome. This decreases cytotoxicity in SCA 2 and SCA 3 by reducing proteasomal impairment. No direct interaction of huntingtin and parkin has been described to date although studies confirmed the colocalization of parkin and huntingtin in mouse brain as well as in patient samples [168]. Additionally, a partial suppression of parkin in an HD mouse model slightly aggravates the neurological phenotype [172]. The interaction or modulation of polyQ disease proteins by parkin can offer an explanation of the parkinsonian phenotype in SCA 2 and SCA 3. Also it is noteworthy that ataxin-1 interacts and is modulated by an E2 ubiquitin-conjugation enzyme, called UbcH6, which regulates the transcriptional repression of expanded ataxin-1 and the rate of ataxin-1 degradation [155, 156]. The binding and ubiquitination of huntingtin by the E2 ubiquitin-conjugation enzyme E2-25K is not influenced by the length of the polyQ stretch [173]. But it is shown that the expression of E2-25K modulates the aggregation and toxicity of mutant huntingtin and that E2-25k is recruited to aggregates in HD and SCA 3 patients [174]. Together these findings indicate a clear influence and impairment of the UPS in all polyQ diseases discussed with the exception of SCA 6. Here, the proteasome has not been implicated in disease progression and there is no evidence for the ubiquitination of aggregates.

Unfolding and remodeling of proteins is necessary for them to pass through the narrow pore of the proteasome barrel, which thus precludes clearance of oligomers and aggregated proteins [175]. A number of polyQ diseases have been associated with decreased chaperone and proteasome activity in patients, cell, and animal models of SCA 1, SCA 3, SCA 7, SCA 17, and HD [176–182]. Nonetheless, there was work demonstrating that, in a SCA 7 knock-in mouse model, no significant impairment of the UPS was found [183]. Also, in recent studies on HD degradation, rapid and complete clearance of polyQ expanded huntingtin in neuronal cells and *in vitro* was shown [184] and dynamic and reversible recruitment of proteasomal subunits into inclusion bodies was observed in living cells [185]. In addition, several groups demonstrated that inhibition of the proteasome in cell culture and mammalian cells results in increased aggregation and cytotoxicity in SCA 3 and HD [181, 186], whereas an overexpression of p45 (ATPase of 19S subunit of proteasome) stimulates degradation of ataxin-3 [187]. Whether the proteasomal enzymatic machinery is able to cleave between successive glutamine residues remains unclear [184, 185, 188–190].

One widely accepted theory is that degradation of misfolded polyQ proteins is a team effort between autophagy and the UPS. Besides the above mentioned involvement of the UPS it is known that the aggregation-prone polyQ proteins and fragments strongly depend on autophagy for their clearance [191]. In SCA 7, the unmodified truncated protein was shown to be degraded via macroautophagy *in vitro* [192] and it was shown that macroautophagy and proteasomal degradation play a role in degrading mHtt [76, 184]. In these studies they demonstrated that blocking autophagy resulted in reduced cell viability and increased number of aggregates and stimulating autophagy promoted clearance of wild-type and mutant huntingtin as well as its caspase derived N-terminal fragment of huntingtin [76]. Specifically targeting the N-terminal huntingtin for the UPS decreased its levels and thus decreased aggregation [184]. Furthermore, it was shown that a polymorphism in an autophagy related gene (ATG7) modulates the age at onset of HD patients [193, 194].

For SCA 1, SCA 3, SCA 6, and SCA 7 an increased susceptibility of cytoplasmic aggregates to autophagic degradation

was shown compared to nuclear polyQ inclusions [195–200]. Impairment of the autophagic system is demonstrated by an increased number of autophagosomes, endosomal-lysosomal-like organelles, and multiple vesicular bodies. This was shown in brain and lymphoblasts of HD patients and in primary neurons and brain of HD transgenic mice [52, 201–203]. Characterization of a SCA 1 transgenic mouse model also indicated changes in the autophagic flux by vacuolar formation with autophagic origin and significant altered LC3-II/-I ratio [204]. Similar results were found in ataxin-7 transgenic mice where LC3 levels were significantly altered and wild-type ataxin-7 levels were stabilized by autophagy whereas no stabilizing effects were described for mutant ataxin-7 [196]. Additionally, it was shown that full-length and cleaved fragments of ataxin-7 are differentially degraded. While full-length wild-type and mutant ataxin-7 was primarily found in the nucleus and therefore degraded by the UPS, fragments of ataxin-7 which were located in both the cytoplasm and nucleus were found to be degraded similarly by autophagy and the UPS [197]. Pharmacological activation of autophagy by treatment with a p53 inhibitor led to increased autophagic activity together with reduced ataxin-7 toxicity and therefore represents a possible therapeutic approach in the treatment of SCA 7 [205].

p62 acts as a cargo receptor for degradation of ubiquitinated targets by autophagy [206]. Studies in human post-mortem brain samples from SCA 3, SCA 6, and HD patients revealed p62 positive cytoplasmic, axonal, and nuclear aggregates. This again indicates an involvement of the autophagic system in the clearance of aggregated polyQ proteins [107, 207, 208]. p62 also contributes to recruitment of proteasomes to nuclear aggregates of ataxin-1 and to the degradation of ataxin-1 [209]. As discussed earlier, mammalian proteasomes may not be able to cleave (polyQ) sequences and seem to release polyQ-rich peptides. An initial study about a cytosolic enzyme called puromycin-sensitive aminopeptidase (PSA) showed that it is able to digest polyQ sequences [210]. However, in cultured cells, *Drosophila*, and mouse muscles, PSA overexpression decreased aggregate content and toxicity of mutant huntingtin and mutant ataxin-3 by enhancing autophagy [211].

As discussed earlier in this review, aggregates including polyQ protein fragments are believed to cause neuronal death. Therefore, reducing the amount of aggregates is an important therapeutic strategy. This reduction can be achieved by enhancing the above described mechanisms: chaperone mediated refolding of polyQ proteins or degradation of misfolded proteins by autophagy or the UPS. Heat shock proteins were shown to accumulate in aggregates of HD, SCA 1, SCA 3, and SCA 7 and this led to an interest in modulating the molecular chaperone machinery as a possible therapeutic strategy for polyQ diseases. An overexpression of HSP40/HDJ-2 suppressed ataxin-3 and ataxin-1 aggregation *in vitro* [3, 160], but not in huntingtin exon 1 overexpressing cell lines [185]. Moreover, modulation of the chaperone system in HD, SCA 1, SCA 3, and SCA 17 studied *in vitro* [212, 213], yeast [214], *C. elegans* [215], *Drosophila* [216], mammalian cells [186, 217–219], and animal models [220–226] demonstrated controversial results. As the overexpression of single members or the combination of different members of the molecular chaperone system gave controversial and transient effects, the development of combinatorial therapies was proposed. Combining treatment with histone deacetylase (HDAC) inhibitors was promoted in recent years. It was shown that the oral administration of 17-(allylamino)-17-demethoxygeldanamycin (17-AAG) markedly suppressed eye degeneration, inclusion formation, and lethality in a SCA 3 *Drosophila* model and also neurodegeneration in an HD *Drosophila* model by induction of HSP70, HSP40, and HSP90 expression [227]. Valproic acid (VPA) an antiepileptic drug which also acts as an HDAC inhibitor and promotes expression of small molecules including HSP70 was shown to alleviate the phenotype of SCA 3 in *Drosophila* [228] and in HD transgenic mice [229]. Furthermore, a combined treatment of lithium (induces autophagy and downregulates HDAC1) and VPA produced several beneficial effects and prolonged median survival in HD transgenic mice [230]. In HD patients, valproic acid is discussed to have beneficial effects on psychiatric symptoms [231] but was also shown to have side effects like developing Parkinson's syndrome with an axial dystonia [232]. The HDAC inhibitor sodium butyrate was shown to delay the onset, ameliorate the neurological phenotype, improve the survival in SCA 3 transgenic mice, and improve the survival of neurons in an ataxin-7 cell model [55, 233]. An analog of this compound, sodium phenylbutyrate, was successfully tested in HD mice [234] and was shown to be safe and well tolerated by HD patients [235], but a phase II clinical trial (started 2006) was abandoned with no cited results.

Although attempts at modulating the proteasome system have been made, upregulation of this pathway is challenging and thus attention has shifted to enhancing autophagy [236]. In polyQ diseases, it has been demonstrated that modulation of one system has direct effects on the other. An HSP90 inhibitor (17-DMAG) resulted in a reduction of neuropathology in a SCA 3 transgenic mouse model although the biggest induction was of LC3-II and beclin and not in heat shock proteins as expected [237]. Beclin modulation has been previously shown to rescue motor symptoms and ataxin-3 clearance in a lentiviral-based rat model [199, 200] and in HD cell culture and primary neurons [237, 238].

Autophagy can also be upregulated by mTOR-(mammalian target of rapamycin-) dependent and mTOR-independent pathways. Autophagy can be induced in all mammalian cell types by rapamycin, an inhibitor of mTOR. Rapamycin treatment of cells expressing aggregation-prone polyQ disease proteins enhanced the degradation of polyQ proteins, reduced the number of aggregates, and protected cells, flies, and mice from mutant protein-associated degradation in SCA 3 and HD [239–241]. Lithium, which is normally used to treat bipolar disorders, was shown to have beneficial effects in polyQ diseases by an mTOR-independent pathway. It targets various intracellular enzymes, including glycogen synthase kinase 3β and inositol monophosphatase by lowering inositol and IP3 levels [242]. Induction of autophagy by lithium led to enhanced clearance of autophagy substrates, like mutant huntingtin fragments as well as mutant ataxin-1 and ataxin-3 *in vitro*, in

Drosophila and mouse models [240, 243–246]. Additionally, a combinatory treatment of lithium and rapamycin protected an HD *Drosophila* model against neurodegeneration by enhancing macroautophagy [247]. Other substances having a beneficial effect on mutant huntingtin toxicity and clearance by activating an mTOR-independent pathway are rilmenidine and trehalose [248]. Trehalose together with rapamycin again showed an additive effect on the clearance of mutant huntingtin [249]. Very recently, the first nanomedical approach in treating HD was presented. It was demonstrated that europium hydroxide nanorods reduced huntingtin aggregation by inducing autophagic flux [250].

6. Mitochondrial Dysfunction

As the field of research in polyQ diseases is progressing, more is understood about the common mechanisms behind neurodegeneration. Over the last decade an emerging role in the pathogenesis of several neurodegenerative disorders such as Alzheimer's disease (AD), Parkinson's disease (PD), and amyotrophic lateral sclerosis (ALS) [251, 252] has been assigned to mitochondrial dysfunction and impaired energy metabolism. This can be explained by the high energy demands of neuronal cells and their inability to produce ATP by glycolysis and hence dependence on functional mitochondria for oxidative phosphorylation. Recent findings also support the involvement of dysfunctional mitochondria in polyglutamine diseases. Most insights were gained in the field of Huntington's disease but several studies also highlight the role of mitochondria in the pathology of spinocerebellar ataxias.

Metabolic defects and loss of body weight at early stages of the disease are well described symptoms of polyQ disease patients in HD [253, 254], SCA 1 [255], and SCA 3 [256] as well as in the respective disease mouse models [9, 41, 257]. For HD and SCA 3 patients, an inverse correlation between body mass index and CAG repeat number was reported [256, 258]. In SCA 1 patients this weight loss appears despite a balance between energy intake and expenditure and patients show an increase of energy expenditure and fat oxidation at a resting state which might be a cause of altered autonomic nervous system activity and gait ataxia [255].

Another common feature of polyQ diseases is metabolic alterations. Advanced magnetic resonance imaging techniques are used to study alterations in metabolite concentrations in distinct brain regions of patients and mouse models. Increased lactate production was found in cortex and basal ganglia of HD patients [259] while cerebellum and brain stem of SCA 1 patients showed decreased total NAA (N-acetylaspartate + N-acetylglutamate, tNAA) concentrations and elevated glutamine, total creatine, and myoinositol concentrations compared to controls [260, 261]. The levels of tNAA and myoinositol correlated with patients' ataxia scores. Similar changes in metabolite concentrations were seen in conditional SCA 1 and a SCA 1 knock-in mouse models. Interestingly, the metabolite levels almost went back to baseline when expression of the transgene was suppressed at early stages of the disease in the conditional mouse model and alterations in metabolite levels were observed in knock-in mice months before any pathology was detected [261, 262].

Apart from alterations in metabolite concentrations, oxidative stress and changes in ATP production caused by deranged respiratory chain complex activities indicate mitochondrial dysfunction in polyQ disease. As previously reviewed, HD patients show reduced complexes II, III, and IV activities in putamen and caudate, while alterations in complex I activity were found in muscles only [263]. Several studies also point to dysfunctional respiratory chain complex and increased oxidative stress in SCA 2, 3, and 12 [264–270]. Decreased complex II activity was found in lymphoblasts from SCA 3 patients, in cells from transgenic mice and in SCA 3 cell models [269]. In cells expressing human, polyQ expanded ataxin-3, decreased activities of the antioxidant enzymes catalase, glutathione reductase and superoxide dismutase, and consequently mitochondrial DNA damage were detected [266]. Similar findings of increased catalase levels and DNA damage were gained from SCA 3 patient samples compared to healthy controls [270]. A recent study also suggests that the disease characteristic aggregates can be reduced in a neuronal SCA 3 cell model by treatment with an extract of *Gardenia jasminoides* which was shown to reduce the production of reactive oxygen species [271].

While the precise pathways which lead to the observed problems in mitochondrial bioenergetics remain elusive, localization of polyQ disease causing proteins to the mitochondria and their actions at the mitochondria have been subjects of intensive research. For SCA 3, it is known that both normal and polyQ expanded ataxin-3 localize to mitochondria [62] and that degradation of polyQ expanded ataxin-3 via the UPS is promoted by an ubiquitin ligase in the outer mitochondrial membrane called MITOL [272]. Localization to the mitochondria was also shown for mutant huntingtin. Also, mitochondria from HD patient lymphoblasts and from brain of transgenic mice expressing full-length mHtt had decreased membrane potential and defects in mitochondrial calcium handling [273].

An important role in regulating mitochondria mediated cell death in polyQ disease has been ascribed to the B-cell lymphoma 2 (Bcl-2) family of proteins. These proteins regulate the permeability of the outer mitochondrial membrane and thereby control cell survival, morphology, dynamics, and membrane potential of mitochondria. Bcl-2 family members can be both prosurvival and proapoptotic. The main family members inhibiting cell death are Bcl-2 and B-cell lymphoma-extra large (Bcl-xL) while the BH3-only proteins Bax and Bcl-2 antagonist (Bak) form pores in the mitochondrial membrane and thus initiate apoptosis. For SCA 3 and SCA 7 it was shown that the mRNA and protein levels of Bcl-xL were downregulated in cerebellar neurons when polyQ expanded ataxin-3 and ataxin-7, respectively, were overexpressed leading to activation of caspase-3 and caspase-9, two main caspases involved in mitochondrial induced apoptosis [53, 274]. Recently, it was shown that a direct interaction between ataxin-3 and Bcl-xL exists and suggested that ataxin-3 promotes the interaction between Bcl-xL and Bax [274]. SCA 3 and SCA 7 *in vivo* models also showed increased levels of Bax mRNA and protein which

can be explained by increased levels of active phospho-p53, a transcription factor known to enhance the transcription of Bax [53, 274–276]. Similarly, Bax levels were found to be increased in HD cell and mouse models [51, 268, 277] as well as in the caudate nucleus of HD patients compared to healthy individuals [278]. Moreover, polyQ expanded ataxin-3 was found to decrease mRNA and protein levels of the prosurvival Bcl-2 by affecting Bcl-2 mRNA stability [279, 280]. For HD, the alterations of Bcl-2 levels remain controversial. While expression of mHtt decreased Bcl-2 protein levels in different cell lines and in brain of HD mouse models [281–283], other studies did not find alterations in well studied models like R6/1 [284].

PolyQ proteins are also known to influence the transcription of multiple genes coding for important mitochondrial proteins. One example is the impairment of peroxisome proliferator-activated receptor-γ (PPAR-γ) coactivator-1α (PGC-1α) expression and function. PGC-1α is a transcriptional master coactivator controlling mitochondrial biogenesis, metabolism, and antioxidant defense [285–287]. Alterations in levels and activity of PGC-1α have been found in HD patients and mouse models [288, 289] and polymorphisms of PGC-1α have been described to modify the age at onset in HD patients [290]. PGC-1α has also been considered a potential therapeutic target by showing that PGC-1α levels were restored and phenotype and survival of HD mice were improved by treatment with bezafibrate, a pan-PPAR agonist [291]. While PGC-1α emerges as an important player in HD pathogenesis, little is known about the involvement of this master coactivator in other polyQ disorders. The question also remains: whether this mechanism is exclusive to HD or is a common feature of many polyQ diseases.

Apart from changes in mitochondrial bioenergetics and transcription of important proteins associated with mitochondrial function and cell death, alterations in shape and motility of mitochondria have been observed in HD. Both retrograde and anterograde mitochondrial transport along axons were shown to be impaired by mHtt in cultured neurons of mouse and rat models [292, 293]. While fragmented mitochondria have been reported for many HD cell models and patients over the last decades, recent studies link this observation to GTPase dynamin related protein-1 (DRP-1). DRP-1 is one of the shaping proteins which regulate mitochondrial fission and fusion. Costa et al. [294] described a higher basal activity of calcineurin which phosphorylates DRP-1 and thereby increases its activity and translocation to mitochondria thus leading to mitochondrial fragmentation in HD models. A direct interaction between mHtt and Drp-1 and an increased enzymatic activity were also shown in brain tissue of HD patients and an HD mouse model [295]. Since the balance between fission and fusion is known to be crucial for mitochondrial function and since neuronal death caused by increased mitochondrial fragmentation has been reported for other neurodegenerative disorders like AD and PD [251], it seems that a better understanding of this pathway would be insightful into understanding the mechanisms and possible therapeutic opportunities in polyglutamine diseases.

7. Concluding Remarks

The neurodegenerative disorders belonging to the group of polyglutamine diseases reviewed here share features such as an inverse correlation of the CAG length with age at onset, neurological features as main presentations of the disease, and an autosomal dominant mode of inheritance. The polyglutamine expansion in these unrelated proteins converges them into common pathogenic mechanisms which can result in corresponding therapeutic interventions. In this review we describe these pathways and possible points of therapeutic entry. First, it is possible to target the stability and conversion of the expanded protein by enhancing protein refolding and degradation or preventing proteolytic cleavage and creation of the toxic fragment. Another option is to decrease the ability of the protein to reach the site of toxicity by altering its ability to translocate between the nucleus and cytoplasm. Enhancing the lysosomal and proteasomal degradation and facilitating autophagic aggregate clearance are exciting current prospects for therapy. Also, modifying the pathways of aggregation remains a viable therapeutic approach as does facilitating mitochondrial health and function. Overall, the field of polyglutamine disease offers many possibilities for disease intervention (Figure 1), although no current therapy is available.

Abbreviations

AD: Alzheimer's disease
ALS: Amyotrophic lateral sclerosis
AR: Androgen receptor
ATP: Adenosine triphosphate
Bak: Bcl-2 homologous antagonist/killer
Bax: Bcl-2-associated X protein
Bcl-2: B-cell lymphoma 2
Bcl-xL: B-cell lymphoma-extra large
CAST: Calpastatin
CDK: Cyclin-dependent kinase
CHIP: C-terminus of the HSC70-interacting protein
DRP-1: GTPase dynamin related protein-1
DRPLA: Dentatorubral-pallidoluysian atrophy
HD: Huntington's disease
HDAC: Histone deacetylase
HSP: Heat shock protein
Htt: Huntingtin
iPSC: Induced pluripotent stem cell
mHtt: Mutant huntingtin
MITOL: Mitochondrial ubiquitin ligase
MMP: Matrix metalloproteinase
MSNs: Medium spiny neurons
mTOR: Mammalian target of rapamycin
NES: Nuclear export signal
NLS: Nuclear localization signal
NMDAR: N-Methyl-D-aspartate (NDMA) receptor
PSA: Puromycin-sensitive aminopeptidase
PD: Parkinson's disease

polyQ: Polyglutamine
PGC-1α: Peroxisome proliferator-activated receptor-γ (PPAR-γ) coactivator-1α
SBMA: Spinal-bulbar muscular atrophy
SCA: Spinocerebellar ataxia
TBP: TATA-binding protein
tNAA: N-Acetylaspartate + N-acetylglutamate
UIM: Ubiquitin interacting motif
UPS: Ubiquitin-proteasome system
VPA: Valproic acid.

Conflict of Interests

Any financial conflict of interests is disclosed by all sides.

Authors' Contribution

All authors contributed equally to this study.

Acknowledgments

Jonasz Jeremiasz Weber receives funding from the Baden-Württemberg Stiftung (International Frontier Research, Project "Inhibition of Proteolytic Digestion of Disease Proteins as Therapeutic Target in Neurodegenerative Diseases," P-BWS-SPII/3-08). The German Center for Neurodegenerative Diseases (DZNE) supported this work by funding Tina Binder. The work leading to this invention has received funding from the European Community's Seventh Framework Programme FP7/2010 under Grant Agreement no. 264508 to Anna Sergeevna Sowa. Jeannette Hübener receives funding from the German Research Foundation (DFG, HU 1770/3-1) and Treuhandstiftung der Caritas Stiftung Deutschland "Stiftung Hoffnung." The research leading to these results has received funding from the European Community's Seventh Framework Programme (FP7/2007–2013) under Grant Agreement no. 2012-305121 "Integrated European—Omics Research Project for Diagnosis and Therapy in Rare Neuromuscular and Neurodegenerative Diseases (NEUROMICS)."

References

[1] H. T. Orr and H. Y. Zoghbi, "Trinucleotide repeat disorders," *Annual Review of Neuroscience*, vol. 30, pp. 575–621, 2007.

[2] L. S. Havel, S. Li, and X.-J. Li, "Nuclear accumulation of polyglutamine disease proteins and neuropathology," *Molecular Brain*, vol. 2, no. 1, article 21, 2009.

[3] Y. Chai, S. L. Koppenhafer, N. M. Bonini, and H. L. Paulson, "Analysis of the role of heat shock protein (Hsp) molecular chaperones in polyglutamine disease," *Journal of Neuroscience*, vol. 19, no. 23, pp. 10338–10347, 1999.

[4] J. L. Marsh, H. Walker, H. Theisen et al., "Expanded polyglutamine peptides alone are intrinsically cytotoxic and cause neurodegeneration in Drosophila," *Human Molecular Genetics*, vol. 9, no. 1, pp. 13–25, 2000.

[5] M. L. Duennwald, S. Jagadish, P. J. Muchowski, and S. Lindquist, "Flanking sequences profoundly alter polyglutamine toxicity in yeast," *Proceedings of the National Academy of Sciences of the United States of America*, vol. 103, no. 29, pp. 11045–11050, 2006.

[6] D. Cohen-Carmon and E. Meshorer, "Polyglutamine (polyQ) disorders: the chromatin connection," *Nucleus*, vol. 3, no. 5, pp. 433–441, 2012.

[7] E. A. Schon and G. Manfredi, "Neuronal degeneration and mitochondrial dysfunction," *Journal of Clinical Investigation*, vol. 111, no. 3, pp. 303–312, 2003.

[8] H. Ikeda, M. Yamaguchi, S. Sugai, Y. Aze, S. Narumiya, and A. Kakizuka, "Expanded polyglutamine in the Machado-Joseph disease protein induces cell death in vitro and in vivo," *Nature Genetics*, vol. 13, no. 2, pp. 198–202, 1996.

[9] L. Mangiarini, K. Sathasivam, M. Seller et al., "Exon I of the HD gene with an expanded CAG repeat is sufficient to cause a progressive neurological phenotype in transgenic mice," *Cell*, vol. 87, no. 3, pp. 493–506, 1996.

[10] C. L. Wellington and M. R. Hayden, "Of molecular interactions, mice and mechanisms: new insights into Huntington's disease," *Current Opinion in Neurology*, vol. 10, no. 4, pp. 291–298, 1997.

[11] I. A. Klement, P. J. Skinner, M. D. Kaytor et al., "Ataxin-1 nuclear localization and aggregation: role in polyglutarnine- induced disease in SCA1 transgenic mice," *Cell*, vol. 95, no. 1, pp. 41–53, 1998.

[12] D. P. Huynh, K. Figueroa, N. Hoang, and S.-M. Pulst, "Nuclear localization or inclusion body formation of ataxin-2 are not necessary for SCA2 pathogenesis in mouse or human," *Nature Genetics*, vol. 26, no. 1, pp. 44–50, 2000.

[13] D. Goti, S. M. Katzen, J. Mez et al., "A mutant ataxin-3 putative-cleavage fragment in brains of Machado-Joseph disease patients and transgenic mice is cytotoxic above a critical concentration," *Journal of Neuroscience*, vol. 24, no. 45, pp. 10266–10279, 2004.

[14] V. F. Colomer Gould, D. Goti, D. Pearce et al., "A Mutant ataxin-3 fragment results from processing at a site N-terminal to amino acid 190 in brain of Machado-Joseph disease-like transgenic mice," *Neurobiology of Disease*, vol. 27, no. 3, pp. 362–369, 2007.

[15] T. Kubodera, T. Yokota, K. Ohwada et al., "Proteolytic cleavage and cellular toxicity of the human α1A calcium channel in spinocerebellar ataxia type 6," *Neuroscience Letters*, vol. 341, no. 1, pp. 74–78, 2003.

[16] G. Yvert, K. S. Lindenberg, S. Picaud, G. B. Landwehrmeyer, J.-A. Sahel, and J.-L. Mandel, "Expanded polyglutamines induce neurodegeneration and trans-neuronal alterations in cerebellum and retina of SCA7 transgenic mice," *Human Molecular Genetics*, vol. 9, no. 17, pp. 2491–2506, 2000.

[17] G. A. Garden, R. T. Libby, Y.-H. Fu et al., "Polyglutamine-expanded ataxin-7 promotes non-cell-autonomous purkinje cell degeneration and displays proteolytic cleavage in ataxic transgenic mice," *Journal of Neuroscience*, vol. 22, no. 12, pp. 4897–4905, 2002.

[18] M. J. Friedman, C.-E. Wang, X.-J. Li, and S. Li, "Polyglutamine expansion reduces the association of TATA-binding protein with DNA and induces DNA binding-independent neurotoxicity," *Journal of Biological Chemistry*, vol. 283, no. 13, pp. 8283–8290, 2008.

[19] C.-A. Gutekunst, S.-H. Li, H. Yi et al., "Nuclear and neuropil aggregates in Huntington's disease: relationship to neuropathology," *Journal of Neuroscience*, vol. 19, no. 7, pp. 2522–2534, 1999.

[20] Y. J. Kim, Y. Yi, E. Sapp et al., "Caspase 3-cleaved N-terminal fragments of wild-type and mutant huntingtin are present in normal and Huntington's disease brains, associate with membranes, and undergo calpaindependent proteolysis," *Proceedings of the National Academy of Sciences of the United States of America*, vol. 98, no. 22, pp. 12784–12789, 2001.

[21] Y. P. Goldberg, D. W. Nicholson, D. M. Rasper et al., "Cleavage of huntingtin by apopain, a proapoptotic cysteine protease, is modulated by the polyglutamine tract," *Nature Genetics*, vol. 13, no. 4, pp. 442–449, 1996.

[22] C. L. Wellington, L. M. Ellerby, A. S. Hackam et al., "Caspase cleavage of gene products associated with triplet expansion disorders generates truncated fragments containing the polyglutamine tract," *Journal of Biological Chemistry*, vol. 273, no. 15, pp. 9158–9167, 1998.

[23] C. L. Wellington, L. M. Ellerby, C.-A. Gutekunst et al., "Caspase cleavage of mutant huntingtin precedes neurodegeneration in Huntington's disease," *Journal of Neuroscience*, vol. 22, no. 18, pp. 7862–7872, 2002.

[24] J. E. Young, L. Gouw, S. Propp et al., "Proteolytic cleavage of ataxin-7 by caspase-7 modulates cellular toxicity and transcriptional dysregulation," *Journal of Biological Chemistry*, vol. 282, no. 41, pp. 30150–30160, 2007.

[25] J. Gafni and L. M. Ellerby, "Calpain Activation in Huntington's Disease," *Journal of Neuroscience*, vol. 22, no. 12, pp. 4842–4849, 2002.

[26] J. Gafni, E. Hermel, J. E. Young, C. L. Wellington, M. R. Hayden, and L. M. Ellerby, "Inhibition of calpain cleavage of Huntingtin reduces toxicity: accumulation of calpain/caspase fragments in the nucleus," *Journal of Biological Chemistry*, vol. 279, no. 19, pp. 20211–20220, 2004.

[27] D. Goffredo, D. Rigamonti, M. Tartari et al., "Calcium-dependent cleavage of endogenous wild-type huntingtin in primary cortical neurons," *Journal of Biological Chemistry*, vol. 277, no. 42, pp. 39594–39598, 2002.

[28] A. Haacke, F. U. Hartl, and P. Breuer, "Calpain inhibition is sufficient to suppress aggregation of polyglutamine-expanded ataxin-3," *Journal of Biological Chemistry*, vol. 282, no. 26, pp. 18851–18856, 2007.

[29] J. Hübener, J. J. Weber, C. Richter et al., "Calpain-mediated ataxin-3 cleavage in the molecular pathogenesis of spinocerebellar ataxia type 3 (SCA3)," *Human Molecular Genetics*, vol. 22, no. 3, pp. 508–518, 2013.

[30] K. Nozaki, O. Onodera, H. Takano, and S. Tsuji, "Amino acid sequences flanking polyglutamine stretches influence their potential for aggregate formation," *NeuroReport*, vol. 12, no. 15, pp. 3357–3364, 2001.

[31] H. Ng, S.-M. Pulst, and D. P. Huynh, "Ataxin-2 mediated cell death is dependent on domains downstream of the polyQ repeat," *Experimental Neurology*, vol. 208, no. 2, pp. 207–215, 2007.

[32] H. L. Paulson, M. K. Perez, Y. Trottier et al., "Intranuclear inclusions of expanded polyglutamine protein in spinocerebellar ataxia type 3," *Neuron*, vol. 19, no. 2, pp. 333–344, 1997.

[33] A. Haacke, S. A. Broadley, R. Boteva, N. Tzvetkov, F. U. Hartl, and P. Breuer, "Proteolytic cleavage of polyglutamine-expanded ataxin-3 is critical for aggregation and sequestration of non-expanded ataxin-3," *Human Molecular Genetics*, vol. 15, no. 4, pp. 555–568, 2006.

[34] A. S. Hackam, R. Singaraja, C. L. Wellington et al., "The influence of huntingtin protein size on nuclear localization and cellular toxicity," *Journal of Cell Biology*, vol. 141, no. 5, pp. 1097–1105, 1998.

[35] D. Martindale, A. Hackam, A. Wieczorek et al., "Length of huntingtin and its polyglutamine tract influences localization and frequency of intracellular aggregates," *Nature Genetics*, vol. 18, no. 2, pp. 150–154, 1998.

[36] T. Toneff, L. Mende-Mueller, Y. Wu et al., "Comparison of huntingtin proteolytic fragments in human lymphoblast cell lines and human brain," *Journal of Neurochemistry*, vol. 82, no. 1, pp. 84–92, 2002.

[37] M. DiFiglia, E. Sapp, K. O. Chase et al., "Aggregation of huntingtin in neuronal intranuclear inclusions and dystrophic neurites in brain," *Science*, vol. 277, no. 5334, pp. 1990–1993, 1997.

[38] T. Schmidt, G. Bernhard Landwehrmeyer, I. Schmitt et al., "An isoform of ataxin-3 accumulates in the nucleus of neuronal cells in affected brain regions of SCA3 patients," *Brain Pathology*, vol. 8, no. 4, pp. 669–679, 1998.

[39] K. A. Sieradzan, A. O. Mechan, L. Jones, E. E. Wanker, N. Nukina, and D. M. A. Mann, "Huntington's disease intranuclear inclusions contain truncated, ubiquitinated huntingtin protein," *Experimental Neurology*, vol. 156, no. 1, pp. 92–99, 1999.

[40] E. J. Slow, R. K. Graham, A. P. Osmand et al., "Absence of behavioral abnormalities and neurodegeneration in vivo despite widespread neuronal huntingtin inclusions," *Proceedings of the National Academy of Sciences of the United States of America*, vol. 102, no. 32, pp. 11402–11407, 2005.

[41] J. Hübener, F. Vauti, C. Funke et al., "N-terminal ataxin-3 causes neurological symptoms with inclusions, endoplasmic reticulum stress and ribosomal dislocation," *Brain*, vol. 134, no. 7, pp. 1925–1942, 2011.

[42] J. Li and J. Yuan, "Caspases in apoptosis and beyond," *Oncogene*, vol. 27, no. 48, pp. 6194–6206, 2008.

[43] D. R. McIlwain, T. Berger, and T. W. Mak, "Caspase functions in cell death and disease," *Cold Spring Harbor Perspectives in Biology*, vol. 5, no. 4, p. a008656, 2013.

[44] M. Chen, V. O. Ona, M. Li et al., "Minocycline inhibits caspase-1 and caspase-3 expression and delays mortality in a transgenic mouse model of Huntington disease," *Nature Medicine*, vol. 6, no. 7, pp. 797–801, 2000.

[45] E. Hermel, J. Gafni, S. S. Propp et al., "Specific caspase interactions and amplification are involved in selective neuronal vulnerability in Huntington's disease," *Cell Death and Differentiation*, vol. 11, no. 4, pp. 424–438, 2004.

[46] M. Kim, H.-S. Lee, G. LaForet et al., "Mutant Huntingtin expression in clonal striatal cells: dissociation of inclusion formation and neuronal survival by caspase inhibition," *Journal of Neuroscience*, vol. 19, no. 3, pp. 964–973, 1999.

[47] C. Portera-Cailliau, J. C. Hedreen, D. L. Price, and V. E. Koliatsos, "Evidence for apoptotic cell death in Huntington disease and excitotoxic animal models," *Journal of Neuroscience*, vol. 15, no. 5, pp. 3775–3787, 1995.

[48] A. Lunkes and J.-L. Mandel, "A cellular model that recapitulates major pathogenic steps of Huntington's disease," *Human Molecular Genetics*, vol. 7, no. 9, pp. 1355–1361, 1998.

[49] V. O. Ona, M. Li, J. P. G. Vonsattel et al., "Inhibition of caspase-1 slows disease progression in a mouse model of Huntington's disease," *Nature*, vol. 399, no. 6733, pp. 263–267, 1999.

[50] S.-H. Li, S. Lam, A. L. Cheng, and X.-J. Li, "Intranuclear huntingtin increases the expression of caspase-1 and induces apoptosis," *Human Molecular Genetics*, vol. 9, no. 19, pp. 2859–2867, 2000.

[51] Y. Zhang, V. O. Ona, M. Li et al., "Sequential activation of individual caspases, and of alterations in Bcl-2 proapoptotic signals in a mouse model of Huntington's disease," *Journal of Neurochemistry*, vol. 87, no. 5, pp. 1184–1192, 2003.

[52] S. W. Davies, M. Turmaine, B. A. Cozens et al., "Formation of neuronal intranuclear inclusions underlies the neurological

dysfunction in mice transgenic for the HD mutation," *Cell*, vol. 90, no. 3, pp. 537–548, 1997.

[53] A.-H. Chou, T.-H. Yeh, Y.-L. Kuo et al., "Polyglutamine-expanded ataxin-3 activates mitochondrial apoptotic pathway by upregulating Bax and downregulating Bcl-xL," *Neurobiology of Disease*, vol. 21, no. 2, pp. 333–345, 2006.

[54] C. Zander, J. Takahashi, K. H. El Hachimi et al., "Similarities between spinocerebellar ataxia type 7 (SCA7) cell models and human brain: Proteins recruited in inclusions and activation of caspase-3," *Human Molecular Genetics*, vol. 10, no. 22, pp. 2569–2579, 2001.

[55] M. Latouche, C. Lasbleiz, E. Martin et al., "A conditional pan-neuronal Drosophila model of spinocerebellar ataxia 7 with a reversible adult phenotype suitable for identifying modifier genes," *Journal of Neuroscience*, vol. 27, no. 10, pp. 2483–2492, 2007.

[56] R. K. Graham, Y. Deng, J. Carroll et al., "Cleavage at the 586 amino acid caspase-6 site in mutant huntingtin influences caspase-6 activation in vivo," *Journal of Neuroscience*, vol. 30, no. 45, pp. 15019–15029, 2010.

[57] R. K. Graham, Y. Deng, E. J. Slow et al., "Cleavage at the caspase-6 site is required for neuronal dysfunction and degeneration due to mutant huntingtin," *Cell*, vol. 125, no. 6, pp. 1179–1191, 2006.

[58] A. J. Milnerwood, C. M. Gladding, M. A. Pouladi et al., "Early increase in extrasynaptic NMDA receptor signaling and expression contributes to phenotype onset in Huntington's disease mice," *Neuron*, vol. 65, no. 2, pp. 178–190, 2010.

[59] J. Gafni, T. Papanikolaou, F. Degiacomo et al., "Caspase-6 activity in a BACHD mouse modulates steady-state levels of mutant huntingtin protein but is not necessary for production of a 586 amino acid proteolytic fragment," *Journal of Neuroscience*, vol. 32, no. 22, pp. 7454–7465, 2012.

[60] C. Landles, A. Weiss, S. Franklin, D. Howland, and G. P. Bates, "Caspase-6 does not contribute to the proteolysis of mutant huntingtin in the HdhQ150 Knock-in mouse model of Huntington's disease," *PLoS Currents*, Article ID e4fd085bfc9973, 2012.

[61] S. J. Berke, F. A. Schmied, E. R. Brunt, L. M. Ellerby, and H. L. Paulson, "Caspase-mediated proteolysis of the polyglutamine disease protein ataxin-3," *Journal of Neurochemistry*, vol. 89, no. 4, pp. 908–918, 2004.

[62] C. Pozzi, M. Valtorta, G. Tedeschi et al., "Study of subcellular localization and proteolysis of ataxin-3," *Neurobiology of Disease*, vol. 30, no. 2, pp. 190–200, 2008.

[63] J. Jung, K. Xu, D. Lessing, and N. M. Bonini, "Preventing Ataxin-3 protein cleavage mitigates degeneration in a Drosophila model of SCA3," *Human Molecular Genetics*, vol. 18, no. 24, pp. 4843–4852, 2009.

[64] J. Liman, S. Deeg, A. Voigt et al., "CDK5 protects from caspase-induced ataxin-3 cleavage and neurodegeneration," *Journal of Neurochemistry*, vol. 129, no. 6, pp. 1013–1023, 2014.

[65] P. Koch, P. Breuer, M. Peitz et al., "Excitation-induced ataxin-3 aggregation in neurons from patients with Machado-Joseph disease," *Nature*, vol. 480, no. 7378, pp. 543–546, 2011.

[66] H. Sorimachi, S. Hata, and Y. Ono, "Calpain chronicle-an enzyme family under multidisciplinary characterization," *Proceedings of the Japan Academy Series B: Physical and Biological Sciences*, vol. 87, no. 6, pp. 287–327, 2011.

[67] M. A. Smith and R. G. Schnellmann, "Calpains, mitochondria, and apoptosis," *Cardiovascular Research*, vol. 96, no. 1, pp. 32–37, 2012.

[68] C. M. Cowan, M. M. Y. Fan, J. Fan et al., "Polyglutamine-modulated striatal calpain activity in YAC transgenic huntington disease mouse model: impact on NMDA receptor function and toxicity," *Journal of Neuroscience*, vol. 28, no. 48, pp. 12725–12735, 2008.

[69] C. M. Gladding, M. D. Sepers, J. Xu et al., "Calpain and STriatal-Enriched protein tyrosine Phosphatase (STEP) activation contribute to extrasynaptic NMDA receptor localization in a huntington's disease mouse model," *Human Molecular Genetics*, vol. 21, no. 17, pp. 3739–3752, 2012.

[70] A. Dau, C. M. Gladding, M. D. Sepers, and L. A. Raymond, "Chronic blockade of extrasynaptic NMDA receptors ameliorates synaptic dysfunction and pro-death signaling in Huntington disease transgenic mice," *Neurobiology of Disease*, vol. 62, pp. 533–542, 2014.

[71] C. Landles, K. Sathasivam, A. Weiss et al., "Proteolysis of mutant huntingtin produces an exon 1 fragment that accumulates as an aggregated protein in neuronal nuclei in huntington disease," *Journal of Biological Chemistry*, vol. 285, no. 12, pp. 8808–8823, 2010.

[72] B. Schilling, J. Gafni, C. Torcassi et al., "Huntingtin phosphorylation sites mapped by mass spectrometry: modulation of cleavage and toxicity," *Journal of Biological Chemistry*, vol. 281, no. 33, pp. 23686–23697, 2006.

[73] M. Kim, J.-K. Roh, B. W. Yoon et al., "Huntingtin is degraded to small fragments by calpain after ischemic injury," *Experimental Neurology*, vol. 183, no. 1, pp. 109–115, 2003.

[74] A. T. Simões, N. Gonçalves, A. Koeppen et al., "Calpastatin-mediated inhibition of calpains in the mouse brain prevents mutant ataxin 3 proteolysis, nuclear localization and aggregation, relieving Machado-Joseph disease," *Brain*, vol. 135, no. 8, pp. 2428–2439, 2012.

[75] Y. J. Kim, E. Sapp, B. G. Cuiffo et al., "Lysosomal proteases are involved in generation of N-terminal huntingtin fragments," *Neurobiology of Disease*, vol. 22, no. 2, pp. 346–356, 2006.

[76] Z.-H. Qin, Y. Wang, K. B. Kegel et al., "Autophagy regulates the processing of amino terminal huntingtin fragments," *Human Molecular Genetics*, vol. 12, no. 24, pp. 3231–3244, 2003.

[77] T. Ratovitski, E. Chighladze, E. Waldron, R. R. Hirschhorn, and C. A. Ross, "Cysteine proteases bleomycin hydrolase and cathepsin Z mediate N-terminal proteolysis and toxicity of mutant huntingtin," *Journal of Biological Chemistry*, vol. 286, no. 14, pp. 12578–12589, 2011.

[78] A. Lunkes, K. S. Lindenberg, L. Ben-Haem et al., "Proteases acting on mutant huntingtin generate cleaved products that differentially build up cytoplasmic and nuclear inclusions," *Molecular Cell*, vol. 10, no. 2, pp. 259–269, 2002.

[79] K. B. Kegel, E. Sapp, J. Alexander et al., "Huntingtin cleavage product A forms in neurons and is reduced by gamma-secretase inhibitors," *Molecular Neurodegeneration*, vol. 5, no. 1, article 58, 2010.

[80] J. P. Miller, J. Holcomb, I. Al-Ramahi et al., "Matrix metalloproteinases are modifiers of huntingtin proteolysis and toxicity in Huntington's disease," *Neuron*, vol. 67, no. 2, pp. 199–212, 2010.

[81] K. Sathasivam, A. Neueder, T. A. Gipson et al., "Aberrant splicing of HTT generates the pathogenic exon 1 protein in Huntington disease," *Proceedings of the National Academy of Sciences of the United States of America*, vol. 110, no. 6, pp. 2366–2370, 2013.

[82] P. L. Mauri, M. Riva, D. Ambu et al., "Ataxin-3 is subject to autolytic cleavage," *The FEBS Journal*, vol. 273, no. 18, pp. 4277–4286, 2006.

[83] C. L. Wellington, R. Singaraja, L. Ellerby et al., "Inhibiting caspase cleavage of huntingtin reduces toxicity and aggregate formation in neuronal and nonneuronal cells," *Journal of Biological Chemistry*, vol. 275, no. 26, pp. 19831–19838, 2000.

[84] T. Ratovitski, M. Nakamura, J. D'Ambola et al., "N-terminal proteolysis of full-length mutant huntingtin in an inducible PC12 cell model of Huntington's disease," *Cell Cycle*, vol. 6, no. 23, pp. 2970–2981, 2007.

[85] M. Sancho, A. E. Herrera, A. Gortat et al., "Minocycline inhibits cell death and decreases mutant Huntingtin aggregation by targeting Apaf-1," *Human Molecular Genetics*, vol. 20, no. 18, pp. 3545–3553, 2011.

[86] S. Luo, C. Vacher, J. E. Davies, and D. C. Rubinsztein, "Cdk5 phosphorylation of huntingtin reduces its cleavage by caspases: implications for mutant huntingtin toxicity," *Journal of Cell Biology*, vol. 169, no. 4, pp. 647–656, 2005.

[87] M. M. Evers, H.-D. Tran, I. Zalachoras et al., "Preventing formation of toxic N-terminal huntingtin fragments through antisense oligonucleotide-mediated protein modification," *Nucleic Acid Therapeutics*, vol. 24, no. 1, pp. 4–12, 2014.

[88] M. W. Becher, J. A. Kotzuk, A. H. Sharp et al., "Intranuclear neuronal inclusions in Huntington's disease and dentatorubral and pallidoluysian atrophy: correlation between the density of inclusions and IT15 CAG triplet repeat length," *Neurobiology of Disease*, vol. 4, no. 6, pp. 387–397, 1998.

[89] P. J. Skinner, B. T. Koshy, C. J. Cummings et al., "Ataxin-1 with an expanded glutamine tract alters nuclear matrix- associated structures," *Nature*, vol. 389, no. 6654, pp. 971–974, 1997.

[90] K. Ishikawa, H. Fujigasaki, H. Saegusa et al., "Abundant expression and cytoplasmic aggregations of α1A voltage-dependent calcium channel protein associated with neurodegeneration in spinocerebellar ataxia type 6," *Human Molecular Genetics*, vol. 8, no. 7, pp. 1185–1193, 1999.

[91] J. Takahashi, H. Fujigasaki, C. Zander et al., "Two populations of neuronal intranuclear inclusions in SCA7 differ in size and promyelocytic leukaemia protein content," *Brain*, vol. 125, no. 7, pp. 1534–1543, 2002.

[92] K. Nakamura, S.-Y. Jeong, T. Uchihara et al., "SCA17, a novel autosomal dominant cerebellar ataxia caused by an expanded polyglutamine in TATA-binding protein," *Human Molecular Genetics*, vol. 10, no. 14, pp. 1441–1448, 2001.

[93] A. Durr, D. Smadja, G. Cancel et al., "Autosomal dominant cerebellar ataxia type I in Martinique (French West Indies). Clinical and neuropathological analysis of 53 patients from three unrelated SCA2 families," *Brain*, vol. 118, no. 6, pp. 1573–1581, 1995.

[94] D. P. Huynh, M. R. Del Bigio, D. H. Ho, and S. M. Pulst, "Expression of ataxin-2 in brains from normal individuals and patients with Alzheimer's disease and spinocerebellar ataxia 2," *Annals of Neurology*, vol. 45, no. 2, pp. 232–241, 1999.

[95] S. Koyano, T. Uchihara, H. Fujigasaki, A. Nakamura, S. Yagishita, and K. Iwabuchi, "Neuronal intranuclear inclusions in spinocerebellar ataxia type 2: triple-labeling immunofluorescent study," *Neuroscience Letters*, vol. 273, no. 2, pp. 117–120, 1999.

[96] J. T. Pang, P. Giunti, S. Chamberlain et al., "Neuronal intranuclear inclusions in SCA2: a genetic, morphological and immunohistochemical study of two cases," *Brain*, vol. 125, no. 3, pp. 656–663, 2002.

[97] R. Kodali and R. Wetzel, "Polymorphism in the intermediates and products of amyloid assembly," *Current Opinion in Structural Biology*, vol. 17, no. 1, pp. 48–57, 2007.

[98] M. Jayaraman, A. K. Thakur, K. Kar, R. Kodali, and R. Wetzel, "Assays for studying nucleated aggregation of polyglutamine proteins," *Methods*, vol. 53, no. 3, pp. 246–254, 2011.

[99] A. M. Ellisdon, B. Thomas, and S. P. Bottomley, "The two-stage pathway of ataxin-3 fibrillogenesis involves a polyglutamine-independent step," *Journal of Biological Chemistry*, vol. 281, no. 25, pp. 16888–16896, 2006.

[100] J. Stöhr, "Prion protein aggregation and fibrillogenesis in vitro," *Sub-cellular biochemistry*, vol. 65, pp. 91–108, 2012.

[101] M. Jayaraman, R. Mishra, R. Kodali et al., "Kinetically competing huntingtin aggregation pathways control amyloid polymorphism and properties," *Biochemistry*, vol. 51, no. 13, pp. 2706–2716, 2012.

[102] F. Pellistri, M. Bucciantini, G. Invernizzi et al., "Different ataxin-3 amyloid aggregates induce intracellular Ca2+ deregulation by different mechanisms in cerebellar granule cells," *Biochimica et Biophysica Acta—Molecular Cell Research*, vol. 1833, no. 12, pp. 3155–3165, 2013.

[103] S. Kuemmerle, C. A. Gutekunst, A. M. Klein et al., "Huntington aggregates may not predict neuronal death in Huntingtons disease," *Annals of Neurology*, vol. 46, no. 6, pp. 842–849, 1999.

[104] S. Sen, D. Dash, S. Pasha, and S. K. Brahmachari, "Role of histidine interruption in mitigating the pathological effects of long polyglutamine stretches in SCA1: a molecular approach," *Protein Science*, vol. 12, no. 5, pp. 953–962, 2003.

[105] M. Bucciantini, E. Giannoni, F. Chiti et al., "Inherent toxicity of aggregates implies a common mechanism for protein misfolding diseases," *Nature*, vol. 416, no. 6880, pp. 507–511, 2002.

[106] A. Weiss, C. Klein, B. Woodman et al., "Sensitive biochemical aggregate detection reveals aggregation onset before symptom development in cellular and murine models of Huntington's disease," *Journal of Neurochemistry*, vol. 104, no. 3, pp. 846–858, 2008.

[107] K. Seidel, E. R. P. Brunt, R. A. I. de Vos et al., "The p62 antibody reveals various cytoplasmic protein aggregates in spinocerebellar ataxia Type 6," *Clinical Neuropathology*, vol. 28, no. 5, pp. 344–349, 2009.

[108] Y. Nekooki-Machida, M. Kurosawa, N. Nukina, K. Ito, T. Oda, and M. Tanaka, "Distinct conformations of in vitro and in vivo amyloids of huntingtin-exon1 show different cytotoxicity," *Proceedings of the National Academy of Sciences of the United States of America*, vol. 106, no. 24, pp. 9679–9684, 2009.

[109] W. Yang, J. R. Dunlap, R. B. Andrews, and R. Wetzel, "Aggregated polyglutamine peptides delivered to nuclei are toxic to mammalian cells," *Human Molecular Genetics*, vol. 11, no. 23, pp. 2905–2917, 2002.

[110] P.-H. Ren, J. E. Lauckner, I. Kachirskaia, J. E. Heuser, R. Melki, and R. R. Kopito, "Cytoplasmic penetration and persistent infection of mammalian cells by polyglutamine aggregates," *Nature Cell Biology*, vol. 11, no. 2, pp. 219–225, 2009.

[111] S. Iuchi, G. Hoffner, P. Verbeke, P. Djian, and H. Green, "Oligomeric and polymeric aggregates formed by proteins containing expanded polyglutamine," *Proceedings of the National Academy of Sciences of the United States of America*, vol. 100, no. 5, pp. 2409–2414, 2003.

[112] T. Takahashi, S. Kikuchi, S. Katada, Y. Nagai, M. Nishizawa, and O. Onodera, "Soluble polyglutamine oligomers formed prior to inclusion body formation are cytotoxic," *Human Molecular Genetics*, vol. 17, no. 3, pp. 345–356, 2008.

[113] J. Legleiter, E. Mitchell, G. P. Lotz et al., "Mutant huntingtin fragments form oligomers in a polyglutamine length-dependent

manner in vitro and in vivo," *Journal of Biological Chemistry*, vol. 285, no. 19, pp. 14777–14790, 2010.

[114] K. Sathasivam, A. Lane, J. Legleiter et al., "Identical oligomeric and fibrillar structures captured from the brains of R6/2 and knock-in mouse models of Huntington's disease," *Human Molecular Genetics*, vol. 19, no. 1, pp. 65–78, 2009.

[115] W. S. Jackson, S. J. Tallaksen-Greene, R. L. Albin, and P. J. Detloff, "Nucleocytoplasmic transport signals affect the age at onset of abnormalities in knock-in mice expressing polyglutamine within an ectopic protein context," *Human Molecular Genetics*, vol. 12, no. 13, pp. 1621–1629, 2003.

[116] U. Bichelmeier, T. Schmidt, J. Hübener et al., "Nuclear localization of ataxin-3 is required for the manifestation of symptoms in SCA3:in vivo evidence," *Journal of Neuroscience*, vol. 27, no. 28, pp. 7418–7428, 2007.

[117] K. Ribbeck and D. Görlich, "The permeability barrier of nuclear pore complexes appears to operate via hydrophobic exclusion," *The EMBO Journal*, vol. 21, no. 11, pp. 2664–2671, 2002.

[118] L. F. Pemberton and B. M. Paschal, "Mechanisms of receptor-mediated nuclear import and nuclear export," *Traffic*, vol. 6, no. 3, pp. 187–198, 2005.

[119] M. D. Kaytor, L. A. Duvick, P. J. Skinner, M. D. Koob, L. P. W. Ranum, and H. T. Orr, "Nuclear localization of the spinocerebellar ataxia type 7 protein, ataxin-7," *Human Molecular Genetics*, vol. 8, no. 9, pp. 1657–1664, 1999.

[120] J. Xia, D. H. Lee, J. Taylor, M. Vandelft, and R. Truant, "Huntingtin contains a highly conserved nuclear export signal," *Human Molecular Genetics*, vol. 12, no. 12, pp. 1393–1403, 2003.

[121] S. Irwin, M. Vandelft, D. Pinchev et al., "RNA association and nucleocytoplasmic shuttling by ataxin-1," *Journal of Cell Science*, vol. 118, no. 1, pp. 233–242, 2005.

[122] J. Taylor, S. K. Grote, J. Xia et al., "Ataxin-7 can export from the nucleus via a conserved exportin-dependent signal," *Journal of Biological Chemistry*, vol. 281, no. 5, pp. 2730–2739, 2006.

[123] P. M. A. Antony, S. Mäntele, P. Mollenkopf et al., "Identification and functional dissection of localization signals within ataxin-3," *Neurobiology of Disease*, vol. 36, no. 2, pp. 280–292, 2009.

[124] S. Lai, B. O'Callaghan, H. Y. Zoghbi, and H. T. Orr, "14-3-3 Binding to ataxin-1(ATXN1) regulates its dephosphorylation at Ser-776 and transport to the nucleus," *Journal of Biological Chemistry*, vol. 286, no. 40, pp. 34606–34616, 2011.

[125] J. Lim, J. Crespo-Barreto, P. Jafar-Nejad et al., "Opposing effects of polyglutamine expansion on native protein complexes contribute to SCA1," *Nature*, vol. 452, no. 7188, pp. 713–718, 2008.

[126] M. F. Peters, F. C. Nucifora Jr., J. Kushi et al., "Nuclear targeting of mutant huntingtin increases toxicity," *Molecular and Cellular Neurosciences*, vol. 14, no. 2, pp. 121–128, 1999.

[127] F. Saudou, S. Finkbeiner, D. Devys, and M. E. Greenberg, "Huntingtin acts in the nucleus to induce apoptosis but death does not correlate with the formation of intranuclear inclusions," *Cell*, vol. 95, no. 1, pp. 55–56, 1998.

[128] G. Schilling, A. V. Savonenko, A. Klevytska et al., "Nuclear-targeting of mutant huntingtin fragments produces Huntington's disease-like phenotypes in transgenic mice," *Human Molecular Genetics*, vol. 13, no. 15, pp. 1599–1610, 2004.

[129] R. S. Atwal, J. Xia, D. Pinchev, J. Taylor, R. M. Epand, and R. Truant, "Huntingtin has a membrane association signal that can modulate huntingtin aggregation, nuclear entry and toxicity," *Human Molecular Genetics*, vol. 16, no. 21, pp. 2600–2615, 2007.

[130] C. P. Reina, X. Zhong, and R. N. Pittman, "Proteotoxic stress increases nuclear localization of ataxin-3," *Human Molecular Genetics*, vol. 19, no. 2, pp. 235–249, 2009.

[131] L. Munsie, N. Caron, R. S. Atwal et al., "Mutant huntingtin causes defective actin remodeling during stress: defining a new role for transglutaminase 2 in neurodegenerative disease," *Human Molecular Genetics*, vol. 20, no. 10, pp. 1937–1951, 2011.

[132] T. Maiuri, T. Woloshansky, J. Xia, and R. Truant, "The huntingtin N17 domain is a multifunctional CRM1 and ran-dependent nuclear and cilial export signal," *Human Molecular Genetics*, vol. 22, no. 7, pp. 1383–1394, 2013.

[133] E. E. Watkin, N. Arbez, E. Waldron-Roby et al., "Phosphorylation of mutant huntingtin at serine 116 modulates neuronal toxicity," *PLoS ONE*, vol. 9, no. 2, Article ID e88284, 2014.

[134] T. Mueller, P. Breuer, I. Schmitt, J. Walter, B. O. Evert, and U. Wüllner, "CK2-dependent phosphorylation determines cellular localization and stability of ataxin-3," *Human Molecular Genetics*, vol. 18, no. 17, pp. 3334–3343, 2009.

[135] W. M. Chan, H. Tsoi, C. C. Wu et al., "Expanded polyglutamine domain possesses nuclear export activity which modulates subcellular localization and toxicity of polyQ disease protein via exportin-1," *Human Molecular Genetics*, vol. 20, no. 9, pp. 1738–1750, 2011.

[136] C. R. Desmond, R. S. Atwal, J. Xia, and R. Truant, "Identification of a karyopherin $\beta1/\beta2$ proline-tyrosine nuclear localization signal in huntingtin protein," *The Journal of Biological Chemistry*, vol. 287, no. 47, pp. 39626–39633, 2012.

[137] V. P. Patel and C. T. Chu, "Nuclear transport, oxidative stress, and neurodegeneration," *International Journal of Clinical and Experimental Pathology*, vol. 4, no. 3, pp. 215–229, 2011.

[138] M. Katsuno, F. Tanaka, H. Adachi et al., "Pathogenesis and therapy of spinal and bulbar muscular atrophy (SBMA)," *Progress in Neurobiology*, vol. 99, no. 3, pp. 246–256, 2012.

[139] H. I. Montie, M. S. Cho, L. Holder et al., "Cytoplasmic retention of polyglutamine-expanded androgen receptor ameliorates disease via autophagy in a mouse model of spinal and bulbar muscular atrophy," *Human Molecular Genetics*, vol. 18, no. 11, pp. 1937–1950, 2009.

[140] S. Koyano, S. Yagishita, Y. Kuroiwa, F. Tanaka, and T. Uchihara, "Neuropathological staging of spinocerebellar ataxia type 2 by semiquantitative 1C2-positive neuron typing. Nuclear translocation of cytoplasmic 1C2 underlies disease progression of spinocerebellar ataxia type 2," *Brain Pathology*, 2014.

[141] A. C. Elden, H.-J. Kim, M. P. Hart et al., "Ataxin-2 intermediate-length polyglutamine expansions are associated with increased risk for ALS," *Nature*, vol. 466, no. 7310, pp. 1069–1075, 2010.

[142] D. Lessing and N. M. Bonini, "Polyglutamine genes interact to modulate the severity and progression of neurodegeneration in Drosophila," *PLoS Biology*, vol. 6, no. 2, article e29, pp. 0266–0274, 2008.

[143] H. B. Kordasiewicz, R. M. Thompson, H. B. Clark, and C. M. Gomez, "C-termini of P/Q-type Ca^{2+} channel $\alpha1A$ subunits translocate to nuclei and promote polyglutamine-mediated toxicity," *Human Molecular Genetics*, vol. 15, no. 10, pp. 1587–1599, 2006.

[144] J. Cornett, F. Cao, C.-E. Wang et al., "Polyglutamine expansion of huntingtin impairs its nuclear export," *Nature Genetics*, vol. 37, no. 2, pp. 198–204, 2005.

[145] Y. Chai, J. Shao, V. M. Miller, A. Williams, and H. L. Paulson, "Live-cell imaging reveals divergent intracellular dynamics of polyglutamine disease proteins and supports a sequestration

model of pathogenesis," *Proceedings of the National Academy of Sciences of the United States of America*, vol. 99, no. 14, pp. 9310–9315, 2002.

[146] C. T. Chu, E. D. Plowey, Y. Wang, V. Patel, and K. L. Jordan-Sciutto, "Location, location, location: altered transcription factor trafficking in neurodegeneration," *Journal of Neuropathology and Experimental Neurology*, vol. 66, no. 10, pp. 873–883, 2007.

[147] T. Yorimitsu and D. J. Klionsky, "Autophagy: molecular machinery for self-eating," *Cell Death and Differentiation*, vol. 12, supplement 2, pp. 1542–1552, 2005.

[148] A. Ciechanover, "The ubiquitin proteolytic system: From a vague idea, through basic mechanisms, and onto human diseases and drug targeting," *Neurology*, vol. 66, no. 2, pp. S7–S19, 2006.

[149] S. Wickner, M. R. Maurizi, and S. Gottesman, "Posttranslational quality control: folding, refolding, and degrading proteins," *Science*, vol. 286, no. 5446, pp. 1888–1893, 1999.

[150] M. Kästle and T. Grune, "Interactions of the proteasomal system with chaperones: protein triage and protein quality control," *Progress in Molecular Biology and Translational Science*, vol. 109, pp. 113–160, 2012.

[151] G.-H. Wang, N. Sawai, S. Kotliarova, I. Kanazawa, and N. Nukina, "Ataxin-3, the MJD1 gene product, interacts with the two human homologs of yeast DNA repair protein RAD23, HHR23A and HHR23B," *Human Molecular Genetics*, vol. 9, no. 12, pp. 1795–1803, 2000.

[152] E. W. Doss-Pepe, E. S. Stenroos, W. G. Johnson, and K. Madura, "Ataxin-3 interactions with Rad23 and valosin-containing protein and its associations with ubiquitin chains and the proteasome are consistent with a role in ubiquitin-mediated proteolysis," *Molecular and Cellular Biology*, vol. 23, no. 18, pp. 6469–6483, 2003.

[153] J. D. Davidson, B. Riley, E. N. Burright, L. A. Duvick, H. Y. Zoghbi, and H. T. Orr, "Identification and characterization of an ataxin-1-interacting protein: A1Up, a ubiquitin-like nuclear protein," *Human Molecular Genetics*, vol. 9, no. 15, pp. 2305–2312, 2000.

[154] S. Hong, S.-J. Kim, S. Ka, I. Choi, and S. Kang, "USP7, a ubiquitin-specific protease, interacts with ataxin-1, the SCA1 gene product," *Molecular and Cellular Neuroscience*, vol. 20, no. 2, pp. 298–306, 2002.

[155] S. Hong, S. Lee, S.-G. Cho, and S. Kang, "UbcH6 interacts with and ubiquitinates the SCA1 gene product ataxin-1," *Biochemical and Biophysical Research Communications*, vol. 371, no. 2, pp. 256–260, 2008.

[156] S. Lee, S. Hong, and S. Kang, "The ubiquitin-conjugating enzyme UbcH6 regulates the transcriptional repression activity of the SCA1 gene product ataxin-1," *Biochemical and Biophysical Research Communications*, vol. 372, no. 4, pp. 735–740, 2008.

[157] A. Matilla, C. Gorbea, D. D. Einum et al., "Association of ataxin-7 with the proteasome subunit S4 of the 19S regulatory complex," *Human Molecular Genetics*, vol. 10, no. 24, pp. 2821–2831, 2001.

[158] S. Waelter, A. Boeddrich, R. Lurz et al., "Accumulation of mutant huntingtin fragments in aggresome-like inclusion bodies as a result of insufficient protein degradation," *Molecular Biology of the Cell*, vol. 12, no. 5, pp. 1393–1407, 2001.

[159] M. Arrasate and S. Finkbeiner, "Protein aggregates in Huntington's disease," *Experimental Neurology*, vol. 238, no. 1, pp. 1–11, 2012.

[160] C. J. Cummings, M. A. Mancini, B. Antalffy, D. B. DeFranco, H. T. Orr, and H. Y. Zoghbi, "Chaperone suppression of aggregation and altered subcellular proteasome localization imply protein misfolding in SCA1," *Nature Genetics*, vol. 19, no. 2, pp. 148–154, 1998.

[161] T. Schmidt, K. S. Lindenberg, A. Krebs et al., "Protein surveillance machinery in brains with spinocerebellar ataxia type 3: redistribution and differential recruitment of 26S proteasome subunits and chaperones to neuronal intranuclear inclusions," *Annals of Neurology*, vol. 51, no. 3, pp. 302–310, 2002.

[162] M. F. N. Rosser, E. Washburn, P. J. Muchowski, C. Patterson, and D. M. Cyr, "Chaperone functions of the E3 ubiquitin ligase CHIP," *Journal of Biological Chemistry*, vol. 282, no. 31, pp. 22267–22277, 2007.

[163] N. R. Jana, P. Dikshit, A. Goswami et al., "Co-chaperone CHIP associates with expanded polyglutamine protein and promotes their degradation by proteasomes," *Journal of Biological Chemistry*, vol. 280, no. 12, pp. 11635–11640, 2005.

[164] I. Al-Ramahi, Y. C. Lam, H.-K. Chen et al., "CHIP protects from the neurotoxicity of expanded and wild-type ataxin-1 and promotes their ubiquitination and degradation," *Journal of Biological Chemistry*, vol. 281, no. 36, pp. 26714–26724, 2006.

[165] A. J. Williams, T. M. Knutson, V. F. Colomer Gould, and H. L. Paulson, "In vivo suppression of polyglutamine neurotoxicity by C-terminus of Hsp70-interacting protein (CHIP) supports an aggregation model of pathogenesis," *Neurobiology of Disease*, vol. 33, no. 3, pp. 342–353, 2009.

[166] J. Y. Choi, J. H. Ryu, H.-S. Kim et al., "Co-chaperone CHIP promotes aggregation of ataxin-1," *Molecular and Cellular Neuroscience*, vol. 34, no. 1, pp. 69–79, 2007.

[167] Y. Morishima, A. M. Wang, Z. Yu, W. B. Pratt, Y. Osawa, and A. P. Lieberman, "CHIP deletion reveals functional redundancy of E3 ligases in promoting degradation of both signaling proteins and expanded glutamine proteins," *Human Molecular Genetics*, vol. 17, no. 24, pp. 3942–3952, 2008.

[168] Y. C. Tsai, P. S. Fishman, N. V. Thakor, and G. A. Oyler, "Parkin facilitates the elimination of expanded polyglutamine proteins and leads to preservation of proteasome function," *Journal of Biological Chemistry*, vol. 278, no. 24, pp. 22044–22055, 2003.

[169] D. P. Huynh, D. T. Nguyen, J. B. Pulst-Korenberg, A. Brice, and S.-M. Pulst, "Parkin is an E3 ubiquitin-ligase for normal and mutant ataxin-2 and prevents ataxin-2-induced cell death," *Experimental Neurology*, vol. 203, no. 2, pp. 531–541, 2007.

[170] T. M. Durcan, M. Kontogiannea, T. Thorarinsdottir et al., "The machado-joseph disease-associated mutant form of ataxin-3 regulates parkin ubiquitination and stability," *Human Molecular Genetics*, vol. 20, no. 1, pp. 141–154, 2011.

[171] T. M. Durcan, M. Kontogiannea, N. Bedard, S. S. Wing, and E. A. Fon, "Ataxin-3 deubiquitination is coupled to parkin ubiquitination via E2 ubiquitin-conjugating enzyme," *Journal of Biological Chemistry*, vol. 287, no. 1, pp. 531–541, 2012.

[172] I. Rubio, J. A. Rodríguez-Navarro, C. Tomás-Zapico et al., "Effects of partial suppression of parkin on huntingtin mutant R6/1 mice," *Brain Research*, vol. 1281, pp. 91–100, 2009.

[173] M. A. Kalchman, R. K. Graham, G. Xia et al., "Huntingtin is ubiquitinated and interacts with a specific ubiquitin-conjugating enzyme," *Journal of Biological Chemistry*, vol. 271, no. 32, pp. 19385–19394, 1996.

[174] R. de Pril, D. F. Fischer, R. A. C. Roos, and F. W. van Leeuwen, "Ubiquitin-conjugating enzyme E2-25K increases aggregate formation and cell death in polyglutamine diseases," *Molecular and Cellular Neuroscience*, vol. 34, no. 1, pp. 10–19, 2007.

[175] I. Weinhofer, S. Forss-Petter, M. Žigman, and J. Berger, "Aggregate formation inhibits proteasomal degradation of polyglutamine proteins," *Human Molecular Genetics*, vol. 11, no. 22, pp. 2689–2700, 2002.

[176] N. R. Jana, E. A. Zemskov, G.-H. Wang, and N. Nukina, "Altered proteasomal function due to the expression of polyglutamine-expanded truncated N-terminal huntingtin induces apoptosis by caspase activation through mitochondrial cytochrome c release," *Human Molecular Genetics*, vol. 10, no. 10, pp. 1049–1059, 2001.

[177] H. Seo, K.-C. Sonntag, and O. Isacson, "Generalized brain and skin proteasome inhibition in Huntington's disease," *Annals of Neurology*, vol. 56, no. 3, pp. 319–328, 2004.

[178] Y. Park, S. Hong, S.-J. Kim, and S. Kang, "Proteasome function is inhibited by polyglutamine-expanded ataxin-1, the SCA1 gene product," *Molecules and Cells*, vol. 19, no. 1, pp. 23–30, 2005.

[179] M. Díaz-Hernández, A. G. Valera, M. A. Morán et al., "Inhibition of 26S proteasome activity by huntingtin filaments but not inclusion bodies isolated from mouse and human brain," *Journal of Neurochemistry*, vol. 98, no. 5, pp. 1585–1596, 2006.

[180] L. A. Khan, P. O. Bauer, H. Miyazaki, K. S. Lindenberg, B. G. Landwehrmeyer, and N. Nukina, "Expanded polyglutamines impair synaptic transmission and ubiquitin-proteasome system in Caenorhabditis elegans," *Journal of Neurochemistry*, vol. 98, no. 2, pp. 576–587, 2006.

[181] H.-L. Wang, C.-Y. He, A.-H. Chou, T.-H. Yeh, Y.-L. Chen, and A. H. Li, "Polyglutamine-expanded ataxin-7 decreases nuclear translocation of NF-κB p65 and impairs NF-κB activity by inhibiting proteasome activity of cerebellar neurons," *Cellular Signalling*, vol. 19, no. 3, pp. 573–581, 2007.

[182] S. Yang, S. Huang, M. A. Gaertig, X.-J. Li, and S. Li, "Age-dependent decrease in chaperone activity impairs MANF expression, leading to Purkinje cell degeneration in inducible SCA17 mice," *Neuron*, vol. 81, no. 2, pp. 349–365, 2014.

[183] A. B. Bowman, S.-Y. Yoo, N. P. Dantuma, and H. Y. Zoghbi, "Neuronal dysfunction in a polyglutamine disease model occurs in the absence of ubiquitin-proteasome system impairment and inversely correlates with the degree of nuclear inclusion formation," *Human Molecular Genetics*, vol. 14, no. 5, pp. 679–691, 2005.

[184] K. Juenemann, S. Schipper-Krom, A. Wiemhoefer, A. Kloss, A. S. Sanz, and E. A. J. Reits, "Expanded polyglutamine-containing N-terminal huntingtin fragments are entirely degraded by mammalian proteasomes," *Journal of Biological Chemistry*, vol. 288, no. 38, pp. 27068–27084, 2013.

[185] S. Schipper-Krom, K. Juenemann, A. H. Jansen et al., "Dynamic recruitment of active proteasomes into polyglutamine initiated inclusion bodies," *The FEBS Letters*, vol. 588, no. 1, pp. 151–159, 2014.

[186] A. Wyttenbach, J. Carmichael, J. Swartz et al., "Effects of heat shock, heat shock protein 40 (HDJ-2), and proteasome inhibition on protein aggregation in cellular models of Huntington's disease," *Proceedings of the National Academy of Sciences of the United States of America*, vol. 97, no. 6, pp. 2898–2903, 2000.

[187] H. Wang, N. Jia, E. Fei et al., "p45, an ATPase subunit of the 19S proteasome, targets the polyglutamine disease protein ataxin-3 to the proteasome," *Journal of Neurochemistry*, vol. 101, no. 6, pp. 1651–1661, 2007.

[188] P. Venkatraman, R. Wetzel, M. Tanaka, N. Nukina, and A. L. Goldberg, "Eukaryotic proteasomes cannot digest polyglutamine sequences and release them during degradation of polyglutamine-containing proteins," *Molecular Cell*, vol. 14, no. 1, pp. 95–104, 2004.

[189] C. I. Holmberg, K. E. Staniszewski, K. N. Mensah, A. Matouschek, and R. I. Morimoto, "Inefficient degradation of truncated polyglutamine proteins by the proteasome," *The EMBO Journal*, vol. 23, no. 21, pp. 4307–4318, 2004.

[190] G. Pratt and M. Rechsteiner, "Proteasomes cleave at multiple sites within polyglutamine tracts: activation by PA28γ(K188E)," *Journal of Biological Chemistry*, vol. 283, no. 19, pp. 12919–12925, 2008.

[191] B. Ravikumar, R. Duden, and D. C. Rubinsztein, "Aggregate-prone proteins with polyglutamine and polyalanine expansions are degraded by autophagy," *Human Molecular Genetics*, vol. 11, no. 9, pp. 1107–1117, 2002.

[192] S. Mookerjee, T. Papanikolaou, S. J. Guyenet et al., "Post-translational modification of ataxin-7 at lysine 257 prevents autophagy-mediated turnover of an N-terminal caspase-7 cleavage fragment," *Journal of Neuroscience*, vol. 29, no. 48, pp. 15134–15144, 2009.

[193] S. Metzger, M. Saukko, H. Van Che et al., "Age at onset in Huntington's disease is modified by the autophagy pathway: implication of the V471A polymorphism in Atg7," *Human Genetics*, vol. 128, no. 4, pp. 453–459, 2010.

[194] S. Metzger, C. Walter, REGISTRY Investigators of the European Huntington's Disease Network et al., "The V471A polymorphism in autophagy-related gene ATG7 modifies age at onset specifically in Italian Huntington disease patients," *PLoS ONE*, vol. 8, no. 7, Article ID e68951, 2013.

[195] A. Iwata, J. C. Christianson, M. Bucci et al., "Increased susceptibility of cytoplasmic over nuclear polyglutamine aggregates to autophagic degradation," *Proceedings of the National Academy of Sciences of the United States of America*, vol. 102, no. 37, pp. 13135–13140, 2005.

[196] C. Duncan, T. Papanikolaou, and L. M. Ellerby, "Autophagy: polyQ toxic fragment turnover," *Autophagy*, vol. 6, no. 2, pp. 312–314, 2010.

[197] X. Yu, A. Ajayi, N. R. Boga, and A.-L. Ström, "Differential degradation of full-length and cleaved ataxin-7 fragments in a novel stable inducible SCA7 model," *Journal of Molecular Neuroscience*, vol. 47, no. 2, pp. 219–233, 2012.

[198] T. Unno, M. Wakamori, M. Koike et al., "Development of Purkinje cell degeneration in a knockin mouse model reveals lysosomal involvement in the pathogenesis of SCA6," *Proceedings of the National Academy of Sciences of the United States of America*, vol. 109, no. 43, pp. 17693–17698, 2012.

[199] I. Nascimento-Ferreira, T. Santos-Ferreira, L. Sousa-Ferreira et al., "Overexpression of the autophagic beclin-1 protein clears mutant ataxin-3 and alleviates Machado-Joseph disease," *Brain*, vol. 134, no. 5, pp. 1400–1415, 2011.

[200] I. Nascimento-Ferreira, C. Nóbrega, A. Vasconcelos-Ferreira et al., "Beclin 1 mitigates motor and neuropathological deficits in genetic mouse models of Machado-Joseph disease," *Brain*, vol. 136, no. 7, pp. 2173–2188, 2013.

[201] E. Sapp, C. Schwarz, K. Chase et al., "Huntingtin localization in brains of normal and Huntington's disease patients," *Annals of Neurology*, vol. 42, no. 4, pp. 604–612, 1997.

[202] Å. Petersén, K. E. Larsen, G. G. Behr et al., "Expanded CAG repeats in exon 1 of the Huntington's disease gene stimulate dopamine-mediated striatal neuron autophagy and degeneration," *Human Molecular Genetics*, vol. 10, no. 12, pp. 1243–1254, 2001.

[203] E. Nagata, A. Sawa, C. A. Ross, and S. H. Snyder, "Autophagosome-like vacuole formation in Huntington's disease lymphoblasts," *NeuroReport*, vol. 15, no. 8, pp. 1325–1328, 2004.

[204] P. J. S. Vig, Q. Shao, S. H. Subramony, M. E. Lopez, and E. Safaya, "Bergmann glial S100B activates myo-inositol monophosphatase 1 and Co-localizes to Purkinje cell vacuoles in SCA1 transgenic mice," *Cerebellum*, vol. 8, no. 3, pp. 231–244, 2009.

[205] X. Yu, A. Muñoz-Alarcón, A. Ajayi et al., "Inhibition of autophagy via p53-mediated disruption of ULK1 in a SCA7 polyglutamine disease model," *Journal of Molecular Neuroscience*, vol. 50, no. 3, pp. 586–599, 2013.

[206] S. Pankiv, T. H. Clausen, T. Lamark et al., "p62/SQSTM1 binds directly to Atg8/LC3 to facilitate degradation of ubiquitinated protein aggregates by autophagy," *Journal of Biological Chemistry*, vol. 282, no. 33, pp. 24131–24145, 2007.

[207] U. Nagaoka, K. Kim, R. J. Nihar et al., "Increased expression of p62 in expanded polyglutamine-expressing cells and its association with polyglutamine inclusions," *Journal of Neurochemistry*, vol. 91, no. 1, pp. 57–68, 2004.

[208] K. Seidel, W. F. A. Den Dunnen, C. Schultz et al., "Axonal inclusions in spinocerebellar ataxia type 3," *Acta Neuropathologica*, vol. 120, no. 4, pp. 449–460, 2010.

[209] S. Pankiv, T. Lamark, J.-A. Bruun, A. Øvervatn, G. Bjørkøy, and T. Johansen, "Nucleocytoplasmic shuttling of p62/SQSTM1 and its role in recruitment of nuclear polyubiquitinated proteins to promyelocytic leukemia bodies," *Journal of Biological Chemistry*, vol. 285, no. 8, pp. 5941–5953, 2010.

[210] N. Bhutani, P. Venkatraman, and A. L. Goldberg, "Puromycin-sensitive aminopeptidase is the major peptidase responsible for digesting polyglutamine sequences released by proteasomes during protein degradation," *The EMBO Journal*, vol. 26, no. 5, pp. 1385–1396, 2007.

[211] F. M. Menzies, R. Hourez, S. Imarisio et al., "Puromycin-sensitive aminopeptidase protects against aggregation-prone proteins via autophagy," *Human Molecular Genetics*, vol. 19, no. 23, pp. 4573–4586, 2010.

[212] P. J. Muchowski, G. Schaffar, A. Sittler, E. E. Wanker, M. K. Hayer-Hartl, and F. U. Hartl, "Hsp70 and Hsp40 chaperones can inhibit self-assembly of polyglutamine proteins into amyloid-like fibrils," *Proceedings of the National Academy of Sciences of the United States of America*, vol. 97, no. 14, pp. 7841–7846, 2000.

[213] M. J. Friedman, S. Li, and X.-J. Li, "Activation of gene transcription by heat shock protein 27 may contribute to its neuronal protection," *Journal of Biological Chemistry*, vol. 284, no. 41, pp. 27944–27951, 2009.

[214] S. Krobitsch and S. Lindquist, "Aggregation of huntingtin in yeast varies with the length of the polyglutamine expansion and the expression of chaperone proteins," *Proceedings of the National Academy of Sciences of the United States of America*, vol. 97, no. 4, pp. 1589–1594, 2000.

[215] S. H. Satyal, E. Schmidt, K. Kitagawa et al., "Polyglutamine aggregates alter protein folding homeostasis in Caenorhabditis elegans," *Proceedings of the National Academy of Sciences of the United States of America*, vol. 97, no. 11, pp. 5750–5755, 2000.

[216] J. M. Warrick, H. Y. E. Chan, G. L. Gray-Board, Y. Chai, H. L. Paulson, and N. M. Bonini, "Suppression of polyglutamine-mediated neurodegeneration in Drosophila by the molecular chaperone HSP70," *Nature Genetics*, vol. 23, no. 4, pp. 425–428, 1999.

[217] N. R. Jana, M. Tanaka, G.-H. Wang, and N. Nukina, "Polyglutamine length-dependent interaction of Hsp40 and Hsp70 family chaperones with truncated N-terminal huntingtin: their role in suppression of aggregation and cellular toxicity," *Human Molecular Genetics*, vol. 9, no. 13, pp. 2009–2018, 2000.

[218] H. Zhou, S.-H. Li, and X.-J. Li, "Chaperone suppression of cellular toxicity of huntingtin is independent of polyglutamine aggregation," *Journal of Biological Chemistry*, vol. 276, no. 51, pp. 48417–48424, 2001.

[219] A. Wyttenbach, O. Sauvageot, J. Carmichael, C. Diaz-Latoud, A.-P. Arrigo, and D. C. Rubinsztein, "Heat shock protein 27 prevents cellular polyglutamine toxicity and suppresses the increase of reactive oxygen species caused by huntingtin," *Human Molecular Genetics*, vol. 11, no. 9, pp. 1137–1151, 2002.

[220] C. J. Cummings, Y. Sun, P. Opal et al., "Over-expression of inducible HSP70 chaperone suppresses neuropathology and improves motor function in SCA1 mice," *Human Molecular Genetics*, vol. 10, no. 14, pp. 1511–1518, 2001.

[221] O. Hansson, J. Nylandsted, R. F. Castilho, M. Leist, M. Jäättelä, and P. Brundin, "Overexpression of heat shock protein 70 in R6/2 Huntington's disease mice has only modest effects on disease progression," *Brain Research*, vol. 970, no. 1-2, pp. 47–57, 2003.

[222] D. G. Hay, K. Sathasivam, S. Tobaben et al., "Progressive decrease in chaperone protein levels in a mouse model of Huntington's disease and induction of stress proteins as a therapeutic approach," *Human Molecular Genetics*, vol. 13, no. 13, pp. 1389–1405, 2004.

[223] M. Fujimoto, E. Takaki, T. Hayashi et al., "Active HSF1 significantly suppresses polyglutamine aggregate formation in cellular and mouse models," *Journal of Biological Chemistry*, vol. 280, no. 41, pp. 34908–34916, 2005.

[224] C. Vacher, L. Garcia-Oroz, and D. C. Rubinsztein, "Overexpression of yeast hsp104 reduces polyglutamine aggregation and prolongs survival of a transgenic mouse model of Huntington's disease," *Human Molecular Genetics*, vol. 14, no. 22, pp. 3425–3433, 2005.

[225] V. Perrin, E. Régulier, T. Abbas-Terki et al., "Neuroprotection by Hsp104 and Hsp27 in lentiviral-based rat models of Huntington's disease," *Molecular Therapy*, vol. 15, no. 5, pp. 903–911, 2007.

[226] A. Zourlidou, T. Gidalevitz, M. Kristiansen et al., "Hsp27 overexpression in the R6/2 mouse model of Huntington's disease: Chronic neurodegeneration does not induce Hsp27 activation," *Human Molecular Genetics*, vol. 16, no. 9, pp. 1078–1090, 2007.

[227] N. Fujikake, Y. Nagai, H. A. Popiel, Y. Okamoto, M. Yamaguchi, and T. Toda, "Heat shock transcription factor 1-activating compounds suppress polyglutamine-induced neurodegeneration through induction of multiple molecular chaperones," *Journal of Biological Chemistry*, vol. 283, no. 38, pp. 26188–26197, 2008.

[228] J. Yi, L. Zhang, B. Tang et al., "Sodium valproate alleviates neurodegeneration in SCA3/MJD via suppressing apoptosis and rescuing the hypoacetylation levels of histone H3 and H4," *PLoS ONE*, vol. 8, no. 1, Article ID e54792, 2013.

[229] D. Zádori, A. Geisz, E. Vámos, L. Vécsei, and P. Klivényi, "Valproate ameliorates the survival and the motor performance in a transgenic mouse model of Huntington's disease," *Pharmacology Biochemistry and Behavior*, vol. 94, no. 1, pp. 148–153, 2009.

[230] C.-T. Chiu, G. Liu, P. Leeds, and D.-M. Chuang, "Combined treatment with the mood stabilizers lithium and valproate produces multiple beneficial effects in transgenic mouse models of huntington's disease," *Neuropsychopharmacology*, vol. 36, no. 12, pp. 2406–2421, 2011.

[231] E. Unti, S. Mazzucchi, L. Kiferle, U. Bonuccelli, and R. Ceravolo, "Q09 Valproic Acid for the treatment of aggressiveness in Huntington's disease: 1-year follow-up," *Journal of Neurology, Neurosurgery & Psychiatry*, vol. 83, p. A57, 2012.

[232] Z. Salazar, L. Tschopp, C. Calandra, and F. Micheli, "Pisa syndrome and Parkinson secondary to valproic acid in Huntington's disease," *Movement Disorders*, vol. 23, no. 16, pp. 2430–2431, 2008.

[233] A.-H. Chou, S.-Y. Chen, T.-H. Yeh, Y.-H. Weng, and H.-L. Wang, "HDAC inhibitor sodium butyrate reverses transcriptional downregulation and ameliorates ataxic symptoms in a transgenic mouse model of SCA3," *Neurobiology of Disease*, vol. 41, no. 2, pp. 481–488, 2011.

[234] G. Gardian, S. E. Browne, D.-K. Choi et al., "Neuroprotective effects of phenylbutyrate in the N171-82Q transgenic mouse model of Huntington's disease," *Journal of Biological Chemistry*, vol. 280, no. 1, pp. 556–563, 2005.

[235] P. Hogarth, L. Lovrecic, and D. Krainc, "Sodium phenylbutyrate in Huntington's disease: a dose-finding study," *Movement Disorders*, vol. 22, no. 13, pp. 1962–1964, 2007.

[236] L. M. Watson, J. Scholefield, L. Jacquie Greenberg, and M. J. A. Wood, "Polyglutamine disease: from pathogenesis to therapy," *South African Medical Journal*, vol. 102, no. 6, pp. 481–484, 2012.

[237] A. Silva-Fernandes, S. Duarte-Silva, A. Neves-Carvalho et al., "Chronic Treatment with 17-DMAG Improves Balance and Coordination in A New Mouse Model of Machado-Joseph Disease," *Neurotherapeutics*, vol. 11, no. 2, pp. 433–449, 2014.

[238] J.-C. Wu, L. Qi, Y. Wang et al., "The regulation of N-terminal Huntingtin (Htt552) accumulation by Beclin1," *Acta Pharmacologica Sinica*, vol. 33, no. 6, pp. 743–751, 2012.

[239] B. Ravikumar, C. Vacher, Z. Berger et al., "Inhibition of mTOR induces autophagy and reduces toxicity of polyglutamine expansions in fly and mouse models of Huntington disease," *Nature Genetics*, vol. 36, no. 6, pp. 585–595, 2004.

[240] Z. Berger, E. K. Ttofi, C. H. Michel et al., "Lithium rescues toxicity of aggregate-prone proteins in Drosophila by perturbing Wnt pathway," *Human Molecular Genetics*, vol. 14, no. 20, pp. 3003–3011, 2005.

[241] F. M. Menzies, J. Huebener, M. Renna, M. Bonin, O. Riess, and D. C. Rubinsztein, "Autophagy induction reduces mutant ataxin-3 levels and toxicity in a mouse model of spinocerebellar ataxia type 3," *Brain*, vol. 133, no. 1, pp. 93–104, 2010.

[242] S. Sarkar and D. C. Rubinsztein, "Inositol and IP3 levels regulate autophagy: biology and therapeutic speculations," *Autophagy*, vol. 2, no. 2, pp. 132–134, 2006.

[243] J. Carmichael, K. L. Sugars, Y. P. Bao, and D. C. Rubinsztein, "Glycogen synthase kinase-3β inhibitors prevent cellular polyglutamine toxicity caused by the Huntington's disease mutation," *Journal of Biological Chemistry*, vol. 277, no. 37, pp. 33791–33798, 2002.

[244] K. Watase, J. R. Gatchel, Y. Sun et al., "Lithium therapy improves neurological function and hippocampal dendritic arborization in a spinocerebellar ataxia type 1 mouse model," *PLoS Medicine*, vol. 4, no. 5, article e182, pp. 0836–0847, 2007.

[245] D.-D. Jia, L. Zhang, Z. Chen et al., "Lithium chloride alleviates neurodegeneration partly by inhibiting activity of GSK3β in a SCA3 drosophila model," *Cerebellum*, vol. 12, no. 6, pp. 892–901, 2013.

[246] S. Wu, S.-D. Zheng, H.-L. Huang et al., "Lithium down-regulates histone deacetylase 1 (HDAC1) and induces degradation of mutant huntingtin," *Journal of Biological Chemistry*, vol. 288, no. 49, pp. 35500–35510, 2013.

[247] S. Sarkar, G. Krishna, S. Imarisio, S. Saiki, C. J. O'Kane, and D. C. Rubinsztein, "A rational mechanism for combination treatment of Huntington's disease using lithium and rapamycin," *Human Molecular Genetics*, vol. 17, no. 2, pp. 170–178, 2008.

[248] C. Rose, F. M. Menzies, M. Renna et al., "Rilmenidine attenuates toxicity of polyglutamine expansions in a mouse model of Huntington's disease," *Human Molecular Genetics*, vol. 19, no. 11, pp. 2144–2153, 2010.

[249] S. Sarkar, J. E. Davies, Z. Huang, A. Tunnacliffe, and D. C. Rubinsztein, "Trehalose, a novel mTOR-independent autophagy enhancer, accelerates the clearance of mutant huntingtin and α-synuclein," *Journal of Biological Chemistry*, vol. 282, no. 8, pp. 5641–5652, 2007.

[250] P.-F. Wei, L. Zhang, S. K. Nethi et al., "Accelerating the clearance of mutant huntingtin protein aggregates through autophagy induction by europium hydroxide nanorods," *Biomaterials*, vol. 35, no. 3, pp. 899–907, 2014.

[251] M. B. Moura, L. S. dos Santos, and B. van Houten, "Mitochondrial dysfunction in neurodegenerative diseases and cancer," *Environmental and Molecular Mutagenesis*, vol. 51, no. 5, pp. 391–405, 2010.

[252] W. Tan, P. Pasinelli, and D. Trotti, "Role of mitochondria in mutant SOD1 linked amyotrophic lateral sclerosis," *Biochimica et Biophysica Acta—Molecular Basis of Disease*, vol. 1842, no. 8, pp. 1295–1301, 2014.

[253] K. L. Leenders, R. S. Frackowiak, N. Quinn, and C. D. Marsden, "Brain energy metabolism and dopaminergic function in Huntington's disease measured in vivo using positron emission tomography," *Movement Disorders*, vol. 1, no. 1, pp. 69–77, 1986.

[254] L. Djoussé, B. Knowlton, L. A. Cupples, K. Marder, I. Shoulson, and R. H. Myers, "Weight loss in early stage of Huntington's disease," *Neurology*, vol. 59, no. 9, pp. 1325–1330, 2002.

[255] A. Mähler, J. Steiniger, M. Endres, F. Paul, M. Boschmann, and S. Doss, "Increased catabolic state in spinocerebellar ataxia type 1 patients," *Cerebellum*, pp. 1–7, 2014.

[256] J. A. M. Saute, A. C. F. da Silva, G. N. Souza et al., "Body mass index is inversely correlated with the expanded CAG repeat length in SCA3/MJD patients," *Cerebellum*, vol. 11, no. 3, pp. 771–774, 2012.

[257] P. Jafar-Nejad, C. S. Ward, R. Richman, H. T. Orr, and H. Y. Zoghbi, "Regional rescue of spinocerebellar ataxia type 1 phenotypes by 14-3-3ε haploinsufficiency in mice underscores complex pathogenicity in neurodegeneration," *Proceedings of the National Academy of Sciences of the United States of America*, vol. 108, no. 5, pp. 2142–2147, 2011.

[258] N. A. Aziz, J. M. M. Van Der Burg, G. B. Landwehrmeyer, P. Brundin, T. Stijnen, and R. A. C. Roos, "Weight loss in Huntington disease increases with higher CAG repeat number," *Neurology*, vol. 71, no. 19, pp. 1505–1513, 2008.

[259] B. G. Jenkins, W. J. Koroshetz, M. F. Beal, and B. R. Rosen, "Evidence for impairment of energy metabolism in vivo in Huntington's disease using localized 1H NMR spectroscopy," *Neurology*, vol. 43, no. 12, pp. 2689–2695, 1993.

[260] L. Guerrini, F. Lolli, A. Ginestroni et al., "Brainstem neurodegeneration correlates with clinical dysfunction in SCA1 but not in SCA2. A quantitative volumetric, diffusion and proton spectroscopy MR study," *Brain*, vol. 127, no. 8, pp. 1785–1795, 2004.

[261] G. Öz, C. D. Nelson, D. M. Koski et al., "Noninvasive detection of presymptomatic and progressive neurodegeneration in a mouse model of spinocerebellar ataxia type 1," *Journal of Neuroscience*, vol. 30, no. 10, pp. 3831–3838, 2010.

[262] U. E. Emir, H. Brent Clark, M. L. Vollmers, L. E. Eberly, and G. Öz, "Non-invasive detection of neurochemical changes prior to overt pathology in a mouse model of spinocerebellar ataxia type 1," *Journal of Neurochemistry*, vol. 127, no. 5, pp. 660–668, 2013.

[263] V. Costa and L. Scorrano, "Shaping the role of mitochondria in the pathogenesis of Huntington's disease," *The EMBO Journal*, vol. 31, no. 8, pp. 1853–1864, 2012.

[264] D. K. Simon, K. Zheng, L. Velázquez et al., "Mitochondrial complex I gene variant associated with early age at onset in spinocerebellar ataxia type 2," *Archives of Neurology*, vol. 64, no. 7, pp. 1042–1044, 2007.

[265] R. K. Dagda, R. A. Merrill, J. T. Cribbs et al., "The spinocerebellar ataxia 12 gene product and protein phosphatase 2A regulatory subunit Bβ2 antagonizes neuronal survival by promoting mitochondrial fission," *Journal of Biological Chemistry*, vol. 283, no. 52, pp. 36241–36248, 2008.

[266] Y.-C. Yu, C.-L. Kuo, W.-L. Cheng, C.-S. Liu, and M. Hsieh, "Decreased antioxidant enzyme activity and increased mitochondrial DNA damage in cellular models of Machado-Joseph disease," *Journal of Neuroscience Research*, vol. 87, no. 8, pp. 1884–1891, 2009.

[267] Y.-C. Wang, C.-M. Lee, L.-C. Lee et al., "Mitochondrial dysfunction and oxidative stress contribute to the pathogenesis of spinocerebellar ataxia type 12 (SCA12)," *Journal of Biological Chemistry*, vol. 286, no. 24, pp. 21742–21754, 2011.

[268] J. M. García-Martínez, E. Pérez-Navarro, X. Xifró et al., "BH3-only proteins Bid and BimEL are differentially involved in neuronal dysfunction in mouse models of Huntington's disease," *Journal of Neuroscience Research*, vol. 85, no. 12, pp. 2756–2769, 2007.

[269] M. N. Laço, C. R. Oliveira, H. L. Paulson, and A. C. Rego, "Compromised mitochondrial complex II in models of Machado-Joseph disease," *Acta Biochimica et Biophysica Sinica*, vol. 1822, no. 2, pp. 139–149, 2012.

[270] L. S. Pacheco, A. F. da Silveira, A. Trott et al., "Association between Machado-Joseph disease and oxidative stress biomarkers," *Mutation Research—Genetic Toxicology and Environmental Mutagenesis*, vol. 757, no. 2, pp. 99–103, 2013.

[271] K.-H. Chang, W.-L. Chen, Y.-R. Wu et al., "Aqueous extract of Gardenia jasminoides targeting oxidative stress to reduce polyQ aggregation in cell models of spinocerebellar ataxia 3," *Neuropharmacology*, vol. 81, pp. 166–175, 2014.

[272] A. Sugiura, R. Yonashiro, T. Fukuda et al., "A mitochondrial ubiquitin ligase MITOL controls cell toxicity of polyglutamine-expanded protein," *Mitochondrion*, vol. 11, no. 1, pp. 139–146, 2011.

[273] A. V. Panov, C.-A. Gutekunst, B. R. Leavitt et al., "Early mitochondrial calcium defects in Huntington's disease are a direct effect of polyglutamines," *Nature Neuroscience*, vol. 5, no. 8, pp. 731–736, 2002.

[274] H.-L. Wang, T.-H. Yeh, A.-H. Chou et al., "Polyglutamine-expanded ataxin-7 activates mitochondrial apoptotic pathway of cerebellar neurons by upregulating Bax and downregulating Bcl-xL," *Cellular Signalling*, vol. 18, no. 4, pp. 541–552, 2006.

[275] H.-L. Wang, A.-H. Chou, A.-C. Lin, S.-Y. Chen, Y.-H. Weng, and T.-H. Yeh, "Polyglutamine-expanded ataxin-7 upregulates Bax expression by activating p53 in cerebellar and inferior olivary neurons," *Experimental Neurology*, vol. 224, no. 2, pp. 486–494, 2010.

[276] A.-H. Chou, A.-C. Lin, K.-Y. Hong et al., "P53 activation mediates polyglutamine-expanded ataxin-3 upregulation of Bax expression in cerebellar and pontine nuclei neurons," *Neurochemistry International*, vol. 58, no. 2, pp. 145–152, 2011.

[277] B.-I. Bae, H. Xu, S. Igarashi et al., "p53 mediates cellular dysfunction and behavioral abnormalities in Huntington's disease," *Neuron*, vol. 47, no. 1, pp. 29–41, 2005.

[278] J. C. Vis, E. Schipper, H. de Boer-van et al., "Expression pattern of apoptosis-related markers in Huntington's disease," *Acta Neuropathologica*, vol. 109, no. 3, pp. 321–328, 2005.

[279] H.-F. Tsai, H.-J. Tsai, and M. Hsieh, "Full-length expanded ataxin-3 enhances mitochondrial-mediated cell death and decreases Bcl-2 expression in human neuroblastoma cells," *Biochemical and Biophysical Research Communications*, vol. 324, no. 4, pp. 1274–1282, 2004.

[280] C.-L. Tien, F.-C. Wen, and M. Hsieh, "The polyglutamine-expanded protein ataxin-3 decreases bcl-2 mRNA stability," *Biochemical and Biophysical Research Communications*, vol. 365, no. 2, pp. 232–238, 2008.

[281] W. Duan, Q. Peng, N. Masuda et al., "Sertraline slows disease progression and increases neurogenesis in N171-82Q mouse model of Huntington's disease," *Neurobiology of Disease*, vol. 30, no. 3, pp. 312–322, 2008.

[282] T.-C. Ju, H.-M. Chen, J.-T. Lin et al., "Nuclear translocation of AMPK-α1 potentiates striatal neurodegeneration in Huntington's disease," *The Journal of Cell Biology*, vol. 194, no. 2, pp. 209–227, 2011.

[283] C. Ruiz, M. J. Casarejos, I. Rubio et al., "The dopaminergic stabilizer, (-)-OSU6162, rescues striatal neurons with normal and expanded polyglutamine chains in huntingtin protein from exposure to free radicals and mitochondrial toxins," *Brain Research*, vol. 1459, pp. 100–112, 2012.

[284] A. V. F. Teles, T. R. Rosenstock, C. S. Okuno, G. S. Lopes, C. R. Bertoncini, and S. S. Smaili, "Increase in bax expression and apoptosis are associated in Huntington's disease progression," *Neuroscience Letters*, vol. 438, no. 1, pp. 59–63, 2008.

[285] P. Puigserver, Z. Wu, C. W. Park, R. Graves, M. Wright, and B. M. Spiegelman, "A cold-inducible coactivator of nuclear receptors linked to adaptive thermogenesis," *Cell*, vol. 92, no. 6, pp. 829–839, 1998.

[286] D. P. Kelly and R. C. Scarpulla, "Transcriptional regulatory circuits controlling mitochondrial biogenesis and function," *Genes & Development*, vol. 18, no. 4, pp. 357–368, 2004.

[287] C. Handschin and B. M. Spiegelman, "Peroxisome proliferator-activated receptor γ coactivator 1 coactivators, energy homeostasis, and metabolism," *Endocrine Reviews*, vol. 27, no. 7, pp. 728–735, 2006.

[288] L. Cui, H. Jeong, F. Borovecki, C. N. Parkhurst, N. Tanese, and D. Krainc, "Transcriptional repression of PGC-1α by mutant huntingtin leads to mitochondrial dysfunction and neurodegeneration," *Cell*, vol. 127, no. 1, pp. 59–69, 2006.

[289] P. Weydt, V. V. Pineda, A. E. Torrence et al., "Thermoregulatory and metabolic defects in Huntington's disease transgenic mice implicate PGC-1α in Huntington's disease neurodegeneration," *Cell Metabolism*, vol. 4, no. 5, pp. 349–362, 2006.

[290] P. Weydt, S. M. Soyal, C. Gellera et al., "The gene coding for PGC-1α modifies age at onset in Huntington's disease," *Molecular Neurodegeneration*, vol. 4, article 3, 2009.

[291] A. Johri, N. Y. Calingasan, T. M. Hennessey et al., "Pharmacologic activation of mitochondrial biogenesis exerts widespread beneficial effects in a transgenic mouse model of Huntington's disease," *Human Molecular Genetics*, vol. 21, no. 5, pp. 1124–1137, 2012.

[292] D. T. Chang, G. L. Rintoul, S. Pandipati, and I. J. Reynolds, "Mutant huntingtin aggregates impair mitochondrial movement and trafficking in cortical neurons," *Neurobiology of Disease*, vol. 22, no. 2, pp. 388–400, 2006.

[293] A. L. Orr, S. Li, C.-E. Wang et al., "N-terminal mutant huntingtin associates with mitochondria and impairs mitochondrial trafficking," *The Journal of Neuroscience*, vol. 28, no. 11, pp. 2783–2792, 2008.

[294] V. Costa, M. Giacomello, R. Hudec et al., "Mitochondrial fission and cristae disruption increase the response of cell models of Huntington's disease to apoptotic stimuli," *EMBO Molecular Medicine*, vol. 2, no. 12, pp. 490–503, 2010.

[295] U. Shirendeb, A. P. Reddy, M. Manczak et al., "Abnormal mitochondrial dynamics, mitochondrial loss and mutant huntingtin oligomers in Huntington's disease: implications for selective neuronal damage," *Human Molecular Genetics*, vol. 20, no. 7, pp. 1438–1455, 2011.

d. Clemens *et al.*, 2015, *Brain*.

Olesoxime suppresses calpain activation and mutant huntingtin fragmentation in the BACHD rat

Laura E. Clemens[#,1,2,3], Jonasz J. Weber[#,1,2], Tanja T. Wlodkowski[1,2,4], Libo Yu-Taeger[1,2], Magali Michaud[5], Carsten Calaminus[6], Schamim H. Eckert[7] , Janett Gaca[7,8], Andreas Weiss[9,10], Janine C. D. Magg[1,2], Erik K. H. Jansson[1,2], Gunter P. Eckert[7], Bernd J. Pichler[6], Thierry Bordet[5,11], Rebecca M. Pruss[5], Olaf Riess[1,2] and Huu P. Nguyen*[,1,2]

[1] Institute of Medical Genetics and Applied Genomics, University of Tuebingen, Calwerstrasse 7, 72076 Tuebingen, Germany

[2] Centre for Rare Diseases, University of Tuebingen, Calwerstrasse 7, 72076 Tuebingen, Germany

[3] Current institution: QPS Austria, Research and Development, Parkring 12, 8074 Grambach, Austria

[4] Current institution: Pediatric Nephrology Division, Heidelberg University Hospital, Im Neuenheimer Feld 430, 69120 Heidelberg, Germany

[5] Trophos SA., Parc Scientifique de Luminy Case 931, 13288 Marseille Cedex 9, France

[6] Werner Siemens Imaging Center, Department of Preclinical Imaging and Radiopharmacy, University of Tuebingen, Roentgenweg 13, 72076 Tuebingen, Germany

[7] Department of Pharmacology, Goethe University Frankfurt am Main, Max-von-Laue Str. 9, 60438 Frankfurt, Germany

[8] Current institution: Merz Pharmaceuticals, Eckenheimer Landstraße 100, 60318 Frankfurt am Main, Germany

[9] Novartis Institutes for BioMedical Research, Klybeckstrasse 141, 4057 Basel, Switzerland.

[10] Current institution: Evotec AG, Manfred Eigen Campus, Essener Bogen 7, 22419 Hamburg, Germany

[11] Current institution: AFM Téléthon, Biotherapies Institute for Rare Diseases, 1 Rue de l'Internationale, Evry 91002, France

[#] These authors contributed equally

* Corresponding author: Dr. Huu Phuc Nguyen, Institute of Medical Genetics and Applied Genomics, Centre for Rare Diseases, University of Tuebingen, Calwerstrasse 7, Tuebingen, Germany, Phone: +49 7071 29 72283, Fax: +49 7071 29 5228, Email: hoa.nguyen@med.uni-tuebingen.de

d. Clemens et al., 2015, Brain.

Abstract

Huntington disease is a fatal human neurodegenerative disorder caused by a CAG repeat expansion in the HTT gene, which translates into a mutant huntingtin protein. A key event in the molecular pathogenesis of Huntington disease is the proteolytic cleavage of mutant huntingtin, leading to the accumulation of toxic protein fragments. Mutant huntingtin cleavage has been linked to the overactivation of proteases due to mitochondrial dysfunction and calcium derangements. Here, we investigated the therapeutic potential of olesoxime, a mitochondria-targeting, neuroprotective compound, in the BACHD rat model of Huntington disease. BACHD rats were treated with olesoxime via the food for 12 months. *In vivo* analysis covered motor impairments, cognitive deficits, mood disturbances and brain atrophy. *Ex vivo* analyses addressed olesoxime's effect on mutant huntingtin aggregation and cleavage, as well as brain mitochondria function. Olesoxime improved cognitive and psychiatric phenotypes, and ameliorated cortical thinning in the BACHD rat. The treatment reduced cerebral mutant huntingtin aggregates and nuclear accumulation. Further analysis revealed a cortex-specific overactivation of calpain in untreated BACHD rats. Treated BACHD rats instead showed significantly reduced levels of mutant huntingtin fragments due to the suppression of calpain-mediated cleavage. In addition, olesoxime reduced the amount of mutant huntingtin fragments associated with mitochondria, restored a respiration deficit, and enhanced the expression of fusion and outer-membrane transport proteins. In conclusion, we discovered the calpain proteolytic system, a key player in Huntington disease and other neurodegenerative disorders, as a target of olesoxime. Our findings suggest that olesoxime exerts its beneficial effects by improving mitochondrial function, which results in reduced calpain activation. The observed alleviation of behavioral and neuropathological phenotypes encourages further investigations on the use of olesoxime as a therapeutic for Huntington disease.

Keywords: Huntington disease, olesoxime, calpain, mitochondrial dysfunction, mutant huntingtin aggregates

Abbreviations: BACHD rat = Huntington disease rat model expressing full-length mutant huntingtin from a bacterial artificial chromosome, Htt = endogenous rat huntingtin protein, Htt = total huntingtin protein, mHTT = mutant human huntingtin protein, polyQ = poly-glutamine, WT = wild type.

Introduction

Huntington disease, a fatal human neurodegenerative disorder, results from a CAG repeat expansion in exon 1 of HTT (The Huntington's Disease Collaborative Research Group, 1993). The mutation translates into an elongated polyQ tract close to the N-terminus of the mutant huntingtin protein, mHTT (Persichetti et al., 1995). Huntington disease patients suffer from a broad range of symptoms including motor, psychiatric, cognitive and metabolic disturbances (Vonsattel and DiFiglia, 1998), which are associated with neuronal dysfunction, and the selective degeneration of cortical and striatal projection neurons (Poudel et al., 2014; Tabrizi et al., 2011).

The intrinsic toxicity of mHTT has been linked to the formation of N-terminal protein fragments (Nagai et al., 2007; Rigamonti et al., 2000; Wang et al., 2008). These fragments interfere with important intracellular pathways (Zuccato et al., 2010), accumulate in the nucleus (Landles et al., 2010), and form protein aggregates in nucleus and cytoplasm (Cooper et al., 1998; Li and Li, 1998), which is a hallmark of Huntington disease (Gutekunst et al., 1999). Mutant HTT fragments derive from proteolytic cleavage of the full-length protein. Several classes of proteolytic enzymes have been identified to mediate this process, including calpains (Gafni and Ellerby, 2002), caspases (Goldberg et al., 1996), cathepsins (Kim et al., 2006) and matrix-metalloproteinases (Miller et al., 2010). Calpains, which play a general role in neurodegenerative processes (Yang et al., 2013), are overactivated in Huntington disease (Gafni and Ellerby, 2002), and inhibition of the calpain-mediated cleavage of mHTT has been found to ameliorate Huntington disease-related pathologies (Gafni et al., 2004).

Calpains are activated in response to cytosolic Ca^{2+} currents (Goll et al., 2003), and Ca^{2+} homeostasis is disrupted at several levels in Huntington disease (Miller and Bezprozvanny, 2010). Moreover, Ca^{2+} derangements have been considered to be causal for the neuronal damage in Huntington disease, as the selective demise of vulnerable neurons is thought to result from their particular sensitivity to excitotoxicity, which is characterized by intracellular Ca^{2+} overload and subsequent cell death (Fan and Raymond, 2007). Mitochondria are particularly involved in this process, as they are crucial for maintaining low intracellular Ca^{2+} levels, and pivotal for triggering cell death programs, when their buffering capacity is exhausted (Calì et al., 2012). Mutant HTT affects mitochondrial function by directly binding to the outer mitochondrial membrane (Choo et al., 2004; Gellerich et al., 2008; Panov et al., 2002; Rockabrand et al., 2007; Wang et al., 2009), and by disturbing the transcription of nuclear-encoded mitochondrial effector genes (Bae et al., 2005; Cui et al., 2006). As a

consequence, mitochondrial Ca^{2+} handling ability is impaired, making cells more susceptible to excitotoxic insults (Panov et al., 2003; Tang et al., 2005).

The current study was designed to evaluate the therapeutic potential of the orphan drug candidate, olesoxime (Bordet et al., 2007), on disease-related phenotypes of the BACHD rat model of Huntington disease (Yu-Taeger et al., 2012). Olesoxime is a small cholesterol-like molecule, which accumulates at the site of mitochondria (Bordet et al., 2010). Olesoxime's mechanism of action is not fully understood, although it has been shown to inhibit mitochondrial permeability transition (Bordet et al., 2010; Gouarné et al., 2013, 2015), which is a Ca^{2+}-sensitive process that can trigger cell death (Lemasters et al., 2009). Olesoxime has demonstrated therapeutic efficacy in several neurodegenerative diseases (Bordet et al., 2007; Eckmann et al., 2013; Richter et al., 2014; Sunyach et al., 2012) and peripheral neuropathies (Bordet et al., 2008; Rovini et al., 2010; Xiao et al., 2009, 2012), and just recently yielded impressive beneficial effects on motor function in a phase II clinical trial in spinal muscular atrophy patients (Dessaud et al., 2014).

Here, we found that olesoxime treatment ameliorated psychiatric and cognitive abnormalities in the BACHD rat. The treatment, further, increased their frontal cortex thickness, and improved mitochondrial function. Prominently, it appeared that the main effect of olesoxime was to reduce Huntington disease-related calpain overactivation. Thereby, the formation of mHTT fragments was drastically decreased. This yet undiscovered function opens a new view on olesoxime's mechanism of action, and highlights it as a novel tool for reducing calpain activation and the accumulation of toxic mHTT fragments.

Materials and Methods

Ethical statement

Behavioral experiments were performed at the University of Tuebingen, by individuals with appropriate training and experience. Experiments were approved by the local ethics committee at Regierungspraesidium Tuebingen, and carried out in accordance with the German Animal Welfare Act and the guidelines of the Federation of European Laboratory Animal Science Associations, based on European Union legislation (Directive 2010/63/EU).

The BACHD rat

The BACHD rat of line TG5 (Crl:CD(SD)-Tg(HTT*97Q)21.2Hpn/Hpn), in the following referred to as BACHD rat, overexpresses full-length *HTT* with 97 CAA/CAG repeats on a BAC (bacterial artificial chromosome) (Yu-Taeger et al., 2012). The construct has previously been used to generate the BACHD mouse (Gray et al., 2008).

General husbandry and genotyping

All rats were bred at the University of Tuebingen and study groups derived from a total of 24 different breedings in order to reduce possible litter bias. Male BACHD rats, hemizygous for mHTT, and male WT littermates from respective breedings were spread across study groups. The rats were weaned and genotyped at 21 days of age. Genotyping was confirmed at the end of the study when the animals were sacrificed, and followed established protocols (Yu-Taeger et al., 2012). From weaning on, the animals were kept in autoclavable plastic cages with high lids (38 cm x 55 cm wide, 24.5 cm high). Cages contained 3 l of autoclaved wooden bedding and were cleaned twice a week. Food (initially standard rat chow: Ssniff V1534-000, SSNIFF Germany, later changed to: Altromin C1000, Altromin, Lage, Germany, details under *Olesoxime treatment and experimental groups*) and tap water were delivered *ad libitum*. Housing conditions followed the European Convention for the Protection of Vertebrate Animals used for Experimental and other Scientific Purposes (ETS 123, appendix A: Guidelines for accommodation and care of animals). The environmental conditions in the housing room were kept at 21–23 °C ambient temperature, 55 +/- 10 % humidity and a 12/12 h light/dark cycle with lights off at 1:00 p.m. and lights on at 1:00 a.m. during winter, or with lights off at 2:00 p.m. and lights on at 2:00 a.m. during summer.

Olesoxime treatment and experimental groups

The study included two cohorts of rats. Cohort I served a longitudinal study to assess the treatment effect on relevant behavioral, neuropathological and molecular phenotypes (Suppl. Fig. 1). This cohort was composed of 30 WT (15 treated, 15 non-treated) and 30 BACHD rats (15 treated, 15 non-treated), kept in groups of four of mixed genotype (two WT rats and two BACHD rats per cage). Two weeks after weaning (5 weeks of age), food was changed from regular rodent chow (as stated above) to either control diet or the same diet loaded with 0.6 mg/g olesoxime (provided by Trophos SA, Marseille, France). Behavioral characterization was carried out until the age of 13 months and was followed by MRI and *post mortem* analyses.

Cohort II was used for the measurement of olesoxime concentration in plasma and brain as well as its distribution in different brain areas (nine olesoxime-treated and three non-treated control animals per genotype). These rats were kept in groups of three of the same genotype. Olesoxime-containing or control diet was administered for 2 weeks starting at the age of 4 months.

Body weight and food intake were measured as safety parameters for the olesoxime treatment. Body weight was measured weekly. For food intake measurements, the rats were housed individually for 70 hours in an automated behavioral test system (PhenoMaster, TSE Systems, Germany) at 2, 4, 6, 8 and 12 months of age. Test protocol, system specifications and data analysis were the same as described in detail in (Clemens et al., 2014).

Clasping behavior

Clasping behavior was investigated as a measure of a striatum-based motor dysfunction (Soll et al., 2013). In order to detect hind limb clasping, each animal was lifted on its tail for approximately 2 s. The test was performed weekly from 5 weeks until the age of 10 months (total of 33 observations). The clasping frequency in % of all observations was analyzed.

Rotarod test

The animals were trained to walk on an accelerating rod (Rat Rotarod 7750, Ugo Basile, Italy) in order to assess fore limb/hind limb coordination at 2, 4 and 8 months of age as a measure of striatum-based motor dysfunction (Bergeron et al., 2014). Rats were given four daily trials at 2 months of age, or three daily trials at older ages, during a total of 5 consecutive days. Trials were separated by one-hour intervals. The experiments were run during the dark phase. During the first 3 days, the rats were trained to a stable performance.

At this stage, the maximum rotation speed of the rod was set to 12 rpm (increasing from 2 to 12 rpm over 30 s), and trials lasted either 120 s, or until the rat had been falling off the rod for a total of five times. The *number of falls* served as the performance readout. On the last 2 days, the rats' maximum motor capacity was tested. For this, the rotation speed of the rod increased from 4 to 40 rpm over 240 s and the trials lasted either 300 s or until the rat had been falling off the rod for a total of five times. The total amount of time the animals spent on the rod (excluding the time spent not running during falls) was measured and analyzed as the animals' running capacity. The number of rats included in the analysis decreased, as an increasing number of particularly BACHD rats refused to stay on the rod at older ages (as discussed previously in (Abada, Nguyen, Schreiber, et al., 2013; Yu-Taeger et al., 2012)).

Simple Swim test

At the age of 7 months, cognitive abilities were investigated using a simple swim test. The animals were trained to swim to a hidden platform placed at one end of a rectangular water tank of 150 x 25 x 40 cm (adapted from (Van Raamsdonk et al., 2005)). Training was carried out in dimmed red light during the dark phase, alternating between cages with placebo- and olesoxime-treated rats. During an initial training phase, the animals were placed into the middle of the tank facing away from the platform, forcing them to turn around to reach it. The training was carried out on 2 consecutive days in 3 x 3 trials on the first and 3 trials on the following day. On the third day, the platform was repositioned to the opposite side (*reversal*) and the rats' performance was measured again on 2 consecutive days. In this reversal training, the rats needed to swim straight ahead in order to reach the platform. The rats were trained in 3 x 3 trials on the first day and 3 trials on the second day. Individual blocks of trials were separated by one hour. The water kept room temperature, and was colored with non-toxic black paint (Marabu Fingerfarbe, Marabu GmbH & Co. KG). The water tank was virtually divided into four areas: the starting area, the area opposite to the platform, the area towards the platform and the platform. The trials were videotaped and tracked using TSE VideoMot 2 equipment (TSE Systems, Germany). Raw data on time and distance covered before reaching the platform as well as swim speed were exported from the software, sorted according to genotype and treatment, and analyzed as average values for each block of three trials, using a script for R statistics developed at the University of Tuebingen.

d. Clemens et al., 2015, Brain.

Elevated plus maze

The rats' preference for exploring the closed rather than the open arms of an EPM was assessed as a measurement of anxiety-like behavior at 13 months of age. The setup comprised four arms (12 cm wide and 42 cm long), connected by a 12 x 12 cm central area. Two of the arms were enclosed by 42 cm high walls (closed arms), while the other two arms had no walls (open arms). The arena was positioned 52 cm above ground. The experimental room was lit with white light, leaving the open arms exposed to light, while the closed arms remained substantially darker. The test was carried out for all rats on one day during the early dark phase, and cages with placebo- and olesoxime-treated rats were tested in an alternating order. At the start of each trial, a rat was placed inside the central area of the maze, facing one of the open arms, and allowed to freely explore the maze for a total of 5 min. The time spent in the open arms of the EPM was measured and subsequently analyzed as % of the total trial duration.

Magnetic resonance imaging

MRI was performed at the Werner Siemens Imaging Center (Tuebingen, Germany). For this purpose, the rats were anaesthetized with 2 % isoflurane and maintained at 1.2 % vaporized in 100 % O_2 at a flow rate of 1.5 l/min. Body temperature and ventilation rate were monitored throughout the MRI acquisition, with body temperature kept in the stable range of 37 ± 0.5 °C. Anatomical T2WIs were acquired with a rat brain surface coil using a 3D-spoiled turbo spin echo sequence (256 x 160 matrix, 25 x 25 mm^2 FOV, repetition time (TR) = 3000 ms, echo time (TE) = 205 ms, slice thickness = 0.22 mm). For MRI data evaluation, image analysis was performed using Inveon Research Workplace software (Siemens Healthcare, Erlangen, Germany) and referring to the rat brain atlas (*The Rat Brain in Stereotaxic coordinates*, 6^{th} edition, 2006). Size differences in whole brain, cerebellum and striatum were determined with high accuracy by measuring the respective volume, as these brain regions have a clear delimitation in MRI. By contrast, differences in the size of the cerebral cortex were evaluated more accurately by measuring the thickness of the frontal part at -1.56 mm relative to bregma at the most dorsal point of the corpus callosum.

Measurement of olesoxime concentration

The concentration of olesoxime in plasma and brain samples was measured via HPLC-MS at Trophos SA. (Marseille, France) using the Alliance® HPLC System (Waters S.A.S.). Samples were collected as explained below and thawed at room temperature. Plasma was mixed with

150 µl of acetonitrile, vortexed for 10 s and centrifuged for 10 min at 16,100 rpm. Brain tissue was first homogenized at a concentration of 1 g/ml in HBSS (10 mM HEPES, 141 mM NaCl, 4 mM KCl, 28 mM $CaCl_2$, 1 mM $MgSO_4$, 1 mM NaH_2PO_4). Homogenates were then mixed with 300 µl dichloromethane, vortexed for 10 s and centrifuged for 10 min at 16,100 rpm. The organic phase was collected, evaporated at low pressure and 40 °C and resolubilized in 110 µl acetonitrile. Assays were run once. Calculations were performed against a calibration curve prepared from olesoxime-spiked, normal rat plasma or brain homogenate, respectively.

Blood sampling

Blood was collected from rats of cohort I during the longitudinal study at 3, 6, 9 and 13 months of age, and from rats of cohort II after two weeks of olesoxime treatment at 4 months of age. For cohort I, blood was collected by puncturing the animals' tail veins (the procedure did not require anesthesia), while for cohort II, blood was sampled retro-orbitally *post mortem*. In either case, sampling was carried out within two hours during the late light phase to minimize variation based on circadian rhythms. Blood was collected into EDTA-coated tubes on ice. Samples were centrifuged at 1,500 x g for 10 min, plasma was removed, transferred into cryotubes and stored at -80 °C.

Brain tissue sampling

For immunohistochemical techniques, the rats were deeply anesthetized with an intraperitoneal injection of ketamin/xylazin (100 mg/kg or 5–8 mg/kg respectively) and perfused transcardially with 4 % PFA in PBS (pH 7.4). Brains were removed and stored at 4 °C in 0.5 % PFA in PBS (pH 7.4).

For all other analyses, the animals were sacrificed by CO_2 inhalation. Brains were immediately dissected on ice and whole brain, or brain regions, were sampled. Tissue was shock-frozen in liquid nitrogen and either stored at -80 °C or immediately processed in order to obtain live mitochondria for high-resolution respirometry. Tissue sampling was performed within 2 hours during the late light phase to minimize variation based on any circadian phase-related changes.

Isolation of mitochondria and high resolution respirometry

Mitochondria were isolated from the frontal brain and respiration was measured at the Department of Pharmacology, Goethe University Frankfurt, Germany. For this purpose,

tissue samples were homogenized in respiration media (20 mM HEPES, 110 mM sucrose, 0.5 mM EGTA, 3 mM magnesium dichloride, 60 mM lactobionic acid, 20 mM taurine, 10 mM potassium dihydrogenphosphate and 1 g/l essentially fatty acid-free BSA, pH 7.4) containing 4 % protease inhibitors (Complete® Protease Inhibitor, Roche). Homogenates were centrifuged at 1,400 x g for 7 min, supernatant was collected and centrifuged at 1,400 x g for 3 min and finally recollected and centrifuged at 10,000 x g for 5 min in order to pellet the mitochondria-containing fraction. Pellets were gently resuspended in respiration media, aliquots for the determination of protein concentration and citrate synthase activity (procedure described below) were collected, frozen in liquid nitrogen and stored at -80 °C, while respiration was recorded immediately.

Respiration was measured with the Oxygraph (Oroboros, Austria), which allows the measurement of mitochondrial respiration in two samples simultaneously. Analysis was made using sample pairs of different genotypes (WT and BACHD) but identical treatment (placebo or olesoxime). Data was acquired with DatLab software, version 4.3.2.7. The rate of mitochondrial respiration was monitored at 37 °C according to a protocol by Prof. Dr. Erich Gnaiger (University of Innsbruck, Austria) (Kuznetsov et al., 2002). A series of substrates and inhibitors were added to the samples in sequence to assess the function of different components of the mitochondrial respiratory chain. The capacity for oxidative phosphorylation was measured after addition of the complex I substrates (CI_{OXPHOS}) glutamate (G; 5 mM), malate (M; 2 mM) and ADP (D; 2 mM), followed by the addition of succinate, the substrate for complex II ($CI+II_{OXPHOS}$, state P). Blocking the ATP synthase via addition of oligomycin, further allowed for the measurement of respiration driven by the mitochondrial proton leak only. Subsequent titration of the artificial uncoupler FCCP (trifluorocarbonylcyanide phenylhydrazone), injected in steps of 1 µM up to 4 µM until saturation occurred) revealed the maximum capacity of the ETC. Afterwards, addition of the complex I inhibitor rotenone revealed uncoupled CII activity (CII_{ETS}). Residual oxygen consumption (oxygen consumption caused by enzymes not belonging to the ETC) was measured after inhibition of complex III with 2.5 µM antimycin A, and subtracted from all measurements. Cytochrome C oxidase (complex IV) activity was determined after addition of 0.5 mM TMPD (tetramethylphenylenediamine), an artificial substrate and 2 mM ascorbate, which keeps TMPD in the reduced state. Complex IV respiration was corrected for the auto-oxidation rate of TMPD, determined by addition of azide (≥100 mM).

Respiration data were normalized to citrate synthase activity, a marker for mitochondrial mass (Kuznetsov et al., 2002). Citrate synthase activity was assessed spectrophotometrically. For this purpose, samples were thawed and diluted 1:2 in deionized

water. Reaction media (0.1 M Tris-HCl, 0.1 mM DTNB (5,5-dithiobis-2-nitrobenzoic acid), 0.5 mM oxaloacetate, 50 µM EDTA, 0.31 mM acetyl coenzyme A, 5 mM triethanolamine hydrochloride) were warmed for 5 min at 30 °C, samples were added, and the formation of TNB (5-thio-2-nitrobenzoic acid) was measured immediately via absorbance at 412 nm.

Immunohistochemistry

PFA-fixed brains were embedded in gelatin blocks (16 brains per block) and cut serially into 40 µm thick coronal sections (performed by NeuroScience Associates, Knoxville, USA). Sections were stored in antigen-preserve solution (Fisher Scientific, USA) at -20 °C. Free-floating staining was performed at room temperature, as described previously (Osmand et al., 2006). Briefly, a series of 24 sections were warmed up at room temperature for 2 h and incubated for 30 min in 0.5 % $NaBH_4$ for blocking purpose. After washing, the sections were probed overnight with sheep polyclonal S830 antibody (1:20,000, kindly provided by Prof. Dr. Gillian Bates, King's College London, UK) for the detection of N-terminal mHTT. On the next day, the sections were incubated with biotinylated rabbit anti-sheep IgG secondary antibody (1:1000, BA-6000, Vector Laboratories) for 2 h and subsequently with avidin-enzyme complex (Vectastain® Elite ABC Kit Rabbit IgG, Linaris) for 1 h. In order to further enhance the signal, biotinylated thyramine plus 0.001 % H_2O_2 was added for 10 min and the sections were once more incubated with avidin-biotin complex. Color development was achieved with nickel-DAB-H_2O_2 (0.6 % nickel, 0.01 % DAB and 0.001 % H_2O_2) dissolved in TI buffer (0.05 M Tris, 0.05 M imidazole). Nissl staining was performed using 1 % thionine acetate to visualize nuclei. Sections were mounted and stored at room temperature.

Images were acquired using a Zeiss Axioplan microscope (Pl 10x ocular, Plan-NEOFLUAR 40x/0.75 objective, AxioCam MRc) and Axiovision 4.8 software (Zeiss, Germany). Images were exported from Axiovision in tiff format, and imported into Corel Draw X5, where they were cropped to display the region of interest, and moderately adjusted in brightness, contrast and saturation to better visualize the structures of interest. The aforementioned adjustments did in no way change the information that was subject to analysis, namely the total number of S830-positive nuclei and cytoplasmic aggregates. The quantification, i.e. counting the number of cytoplasmic aggregates and the number of nuclei positive for mHTT staining, was performed manually.

d. Clemens et al., 2015, Brain.

Immunoblotting

Immunoblotting was performed with striatal and cortical tissue as well as mitochondrial membranes isolated from cerebral hemispheres.

Striata and cortices were thawed and homogenized on ice in TES buffer (50 mM Tris, 2 mM EDTA, 100 mM NaCl, pH 7.5) containing protease inhibitors (4 % Complete® Protease Inhibitor, Roche). Homogenates were diluted 1:10 in TNES buffer (90 % TES buffer, 10 % Igepal CA630), incubated for 1 h at 4 °C and centrifuged 2 x 30 min at 16,100 x g. Supernatant (cell lysates) were collected and stored at -80 °C in 10 % glycerin.

Mitochondria-enriched heavy membrane fractions were isolated from cerebral hemispheres (brain stem, cerebellum and olfactory bulbs had been removed). Tissue was homogenized on ice in HEPES buffer (10 mM HEPES, 0.32 M sucrose, 1 mM EDTA, pH 7.4) and centrifuged at 585 x g for 10 min. Supernatant was collected and further centrifuged twice at 17.400 x g for 20 min. Pellets were resuspended and layered over a Ficoll density gradient (7.5 % and 13 %, w/v). After 60 min of ultracentrifugation at 87,300 x g, the pellet, which at this point contained the mitochondrial fraction, was sampled, resuspended in 5 mM Tris-HCl and stored at -20 °C.

At the time of immunoblotting, all samples were thawed on ice, and the protein concentration was measured spectrophotometrically using Bradford reagent. Western blot analysis was performed according to standard procedures. Briefly, 15 µg of mitochondrial protein or 30 µg of protein from tissue lysates were assayed using SDS-PAGE on Tris-glycine or purchased Tris-acetate gels (Life Technologies). Proteins were transferred on nitrocellulose or PVDF membranes, and probed overnight at 4 °C with the primary antibody (Supplementary Table 1). One hour of incubation with a respective HRP-conjugated secondary or IRDye antibody (Supplementary Table 1) at room temperature followed. Chemiluminescence and fluorescence signals were detected with the LI-COR ODYSSEY FC Imaging system (LI-COR Biosciences). Protein levels were quantified by densitometry using ImageJ (Abràmoff et al., 2004).

Filter retardation assay

For the detection of SDS-insoluble HTT species, 30 µg of cortical or striatal proteins were diluted in 100 µl DPBS (Life Technologies) with 2 % SDS and incubated for 5 min at room temperature. A nitrocellulose membrane (0.45 µm; Bio-Rad) was equilibrated in 0.1 % SDS in DPBS and samples were filtered through this membrane using a Minifold II Slot Blot System (Schleicher & Schuell). The membrane was then washed twice with DPBS and

blocked with 5 % SlimFast (Unilever) in TBS for 1 h at room temperature. Retained SDS-insoluble HTT was detected using anti-HTT primary antibody (1:1000; clone 1HU-4C8, MAB2166, EMD Millipore) and the respective anti-mouse HRP-conjugated secondary antibody. Chemiluminescence signals were detected with the LI-COR ODYSSEY FC Imaging system and quantified using the ODYSSEY® Server software version 4.1 (both LI-COR Biosciences).

Calpain activation assays

In vitro calpain activation assays of brain lysates were performed as previously described (Hübener et al., 2013). Briefly, 30 µg of protein from TNES lysates were diluted in 40 µl calpain reaction buffer (20 mM HEPES/KOH pH 7.6, 10 mM KCl, 1.5 mM $MgCl_2$, 1 mM dithiothreitol). The positive control was incubated with 20 ng of recombinant calpain-1 (EMD Millipore), and 2 mM $CaCl_2$ for indicated times at room temperature, while the negative control was pretreated with 100 µM of the calpain inhibitor CI-III (carbobenzoxy-valinyl-phenylalaninal) (EMD Millipore) prior to calpain-1 addition. Calpain activity of all samples was quenched by addition of 4 x NuPAGE LDS sample buffer (Life technologies) and heat denaturation for 10 min at 70 °C. Samples were subsequently assayed by immunoblotting, as described above.

TR-FRET for soluble mHTT detection

TR-FRET was performed with cortical and striatal lysates (sampled as described under *Immunoblotting*), and conducted according to Baldo *et al*. at Novartis (Basel, Switzerland) (Baldo et al., 2012). Briefly, samples were ultra-centrifuged at 80,000 x g for 90 min. Supernatant was transferred to 384-microtiter plates, diluted 1:5 in detection buffer (50 mM NaH_2PO_4, 400 mM NaF, 0.1 % BSA, and 0.05 % Tween) and probed with fluorophore-labeled antibodies 2B7-Tb and MW1-d2 in a ratio of 1:10. TR-FRET was read with an EnVision Reader (PerkinElmer, Waltham). After the excitation of the donor fluorophore Tb at 320 nm and a time delay of 100 ms, the resulting Tb and d2 emission signals were read at 620 nm and 665 nm, respectively.

Experimental design

Sample size estimation was based on behavioral data previously obtained for the BACHD rat. Fifteen animals per genotype and treatment group were assigned to the Rotarod test, 12

to the simple swim test, five to the elevated plus maze and 10 to MRI analysis. *Ex vivo* analyses were planned with five rats per group. The final assignment differed slightly from this, as one cage of placebo-treated rats originally intended for the elevated plus maze and mitochondrial respiration analysis was used in addition for MRI measurements. Furthermore, three animals died during the study (without any bias regarding genotype or treatment groups). For *ex vivo* analyses, a final number of three to five rats per group were used, as sample material was limited.

During behavioral studies, the experimenter was blind to the animals' genotype, but not treatment, as the cages had to be labeled to ensure that the right kind of food, either placebo or olesoxime-loaded pellets, was provided at all times. Aggregate count was performed by one observer, who was blind to genotype and treatment group.

The *n* analyzed, refers to the biological replicate of individual animals of a given genotype and treatment group, except for drug concentration analysis in brain regions, where samples from two to three individuals were pooled in order to reach a proper amount of sample material.

Statistical analysis

Data were analyzed and graphed using GraphPad Prism 6.00 for Windows (GraphPad Software, San Diego California USA, http://www.graphpad.com). Values refer to group mean and standard error of the mean (s.e.m.) for all figures, and group mean and standard deviation (SD) for Table 1. The α-level was set to 0.05. Complete data sets proved to be normally distributed. Longitudinal data were analyzed using repeated measurements two-way ANOVA (2way rmANOVA) with time (e.g. age or trial) as a within-group factor and group (e.g. genotype and treatment) as between-group factor. Single data sets were analyzed using regular two-way ANOVAs (2way ANOVA) to identify genotype and treatment effects. For both, 2way rmANOVA and 2way ANOVA, the results are implemented in each graph and specify the respective between-group factors. Fisher's LSD was performed as ANOVA posttest, and did not account for multiple comparisons, favoring false positive over false negative results in this first evaluation of olesoxime effects on HD-related phenotypes. There was one two-group comparison (treatment effects specific to BACHD rats), which was analyzed using a Student's *t*-test. Results from two-way ANOVAs and Fisher's LSD posttest, and posttest as well as *t*-test results for the comparisons * WT versus BACHD rats, $^{\#}$ untreated versus treated WT and $^{+}$ untreated versus treated BACHD rats are indicated in respective figures, with ns: not significant, $*/^{\#}/^{+}$: $P < 0.05$; $**/^{\#\#}/^{++}$: $P \leq 0.01$ and $***/^{\#\#\#}/^{+++}$: $P \leq 0.001$.

Some behavioral data were excluded from the analysis based on predefined criteria or technical problems. Concerning technical problems, the data could either not be properly acquired or the acquired data were inconclusive (as explained in detail below). We did not predefine exclusion criteria for outliers, or exclude data in order to reach a normal distribution. Moreover, the values we excluded were spread equally among groups, suggesting that it did not have a biological meaning or exclusion was skewing the results. Food intake measurements: Nine of the 60 animals were excluded from the analysis, because in at least one of the five measurements (at 2, 4, 6, 8 or 12 months of age), the food got stuck in the food basket leaving the animal unable to reach it and resulting in unreasonably low values for food intake during the respective night. Rotarod test: no data were excluded, but the number of rats available for analysis decreased with age, as an increasing number of mainly BACHD rats refused to stay on the rod at older ages (as discussed previously in (Abada, Nguyen, Schreiber, et al., 2013; Yu-Taeger et al., 2012)); Simple swim test: the tracking software produced a variety of errors, which made it necessary to exclude animals with individual erroneous runs.; EPM: one of the 20 animals was excluded from the analysis, as it did not move at all during the test; MRI: two of the 40 animals were excluded from the analysis, as they moved their heads during measurements and no sharp images could be acquired; Drug concentration analysis: two of the 16 samples were excluded as they had far higher drug concentrations than the rest of the rats. The high drug load in the two animals is considered to be due to food intake just prior to blood sampling, as we did not food deprive the animals; *Ex vivo* analyses: no data were excluded. Numbers of animals analyzed in each experiment are listed in Supplementary Table 2.

d. Clemens et al., 2015, Brain.

Results

A time line and overview over the parameters assessed in this study is given in Supplementary Figure 1.

Olesoxime ameliorates cognitive and psychiatric phenotypes of BACHD rats

We previously reported that BACHD rats show a broad range of behavioral abnormalities reminiscent of the symptoms found in Huntington disease patients (Abada, Nguyen, Ellenbroek, et al., 2013; Abada, Nguyen, Schreiber, et al., 2013; Yu-Taeger et al., 2012). The cognitive phenotype of the BACHD rat is characterized by difficulties in strategy shifting (Abada, Nguyen, Ellenbroek, et al., 2013). Accordingly, we found 7 months old BACHD rats to display reversal learning deficits in a simple swim test. Untreated, but not olesoxime-treated BACHD rats, needed longer to find a hidden platform after the platform had been relocated (Fig. 1A). Swim speed did not differ between groups (data not shown), suggesting that BACHD rats' general ability to swim was not impaired.

Anxiety-related changes were assessed by measuring the time spent on the open arms of an elevated plus maze at 13 months of age. In line with our previous findings (Yu-Taeger et al., 2012), BACHD rats spent a significantly higher amount of time on the open arms than WT rats. Olesoxime treatment clearly ameliorated this phenotype (Fig. 1B).

Longitudinal assessment of clasping behavior and Rotarod performance were carried out as common tests of striatum-based motor dysfunction (Bergeron et al., 2014; Soll et al., 2013). BACHD rats showed hind limb clasping, similar to previous cohorts (Yu-Taeger et al., 2012) (Fig. 1C). Furthermore, Rotarod performance, which is among the earliest pathological phenotypes detected in the BACHD rat (Yu-Taeger et al., 2012), was found to be impaired at 2, 4 and 8 months of age (Fig. 1D). Olesoxime treatment, which started when the motor abnormalities were already manifested, did not reverse the pathology (Fig. 1C and D).

Olesoxime increases frontal cortex thickness

Olesoxime has been ascribed with neuroprotective properties, as it was found to increase the survival of neurons expressing disease proteins (Bordet et al., 2010; Gouarné et al., 2013, 2015). We performed MRI scans in 13 months old rats in order to evaluate, if olesoxime was able to ameliorate brain atrophy observed in BACHD rats (Yu-Taeger et al., 2012). BACHD rats had significantly smaller cerebra (Fig. 1E), striata (Fig. 1F) and prefrontal cortices (Fig. 1G) compared to their WT littermates. While olesoxime treatment did not significantly

affect cerebral or striatal volume (Fig. 1E, F), frontal cortex thickness was significantly increased, pointing to a region-specific neuroprotective effect of olesoxime (Fig. 1G).

Olesoxime is enriched in prefrontal and frontal cortex

After finding significant beneficial but apparently region-specific effects of olesoxime, we analyzed the drug concentration in plasma and brain regions in a separate cohort of rats after 2 weeks of olesoxime treatment at 4 months of age (cohort II). Analysis revealed similar plasma levels as found for the main cohort at 3 months of age (cohort I) (Fig. 1H), which were presumed to lie in the pharmacologically active range of olesoxime based on the results of previous studies (Bordet et al., 2007, 2010; Richter et al., 2014). Furthermore, BACHD rats tended to have higher plasma (Fig. 1H) and brain (Fig. 1I) olesoxime levels than WT rats. In addition, we detected significant differences in the olesoxime concentration among brain regions, with highest concentrations measured in prefrontal and frontal cortex (Fig. 1I). The general trend to higher olesoxime concentrations in BACHD rats was not the result of increased food intake (data not shown) and there was no difference in body weight between genotype or treatment groups, thus the results might point to altered pharmacokinetics of olesoxime in the BACHD rat.

Olesoxime reduces mHTT aggregates and nuclear accumulation

Aggregation and nuclear accumulation of mHTT are prominent neuropathological features of Huntington disease (Gutekunst et al., 1999). Consistent with our previous results (Yu-Taeger et al., 2012), 13 months old BACHD rats show mHTT aggregates (reflected by distinct S830-positive punctae) and nuclear accumulation (reflected by S830-positive nuclei) in variable magnitude throughout the brain (Fig. 2, Fig. 3A and B). Aggregates were found predominantly in cortex, hypothalamus and amygdala. Mutant HTT nuclear accumulation prevailed in cortex, lateral striatum and hippocampus. Similar to Huntington disease patients (Gutekunst et al., 1999), cerebral cortex hosted a high amount of mHTT aggregates and nuclear accumulation of mHTT, while neither form was abundant in the central caudate putamen, the major part of striatum. Olesoxime-treated BACHD rats showed a significant reduction in both aggregate load and nuclear mHTT accumulation (Fig. 2, Fig. 3A and B). Moreover, not only the number of aggregates and mHTT-positive nuclei was reduced due to olesoxime treatment, but also aggregate size and the density of mHTT in the nuclei of olesoxime-treated BACHD rats seemed to be lowered.

The results from immunohistochemical staining were validated using a filter retardation assay to detect the amount of non-soluble, and thus aggregated, mHTT in cortical and striatal lysates from untreated and olesoxime-treated BACHD rats. In both, cortical and striatal samples, aggregated mHTT was significantly reduced due to olesoxime treatment (Fig. 3C).

Olesoxime decreases mHTT fragments and increases full-length mHTT by reducing calpain-mediated cleavage

To further investigate the cause and consequences of reduced mHTT aggregate formation and nuclear accumulation, we analyzed the levels of soluble full-length and truncated forms of mHTT in cortical and striatal lysates from 13 months old rats BACHD and WT rats.

Total levels of soluble mHTT were measured by TR-FRET analysis as described previously (Baldo et al., 2012). Consistent with the reduction of aggregated mHTT throughout the cortex, soluble mHTT levels were highly increased in the cortices but not striata from olesoxime-treated BACHD rats (Fig. 3D).

As mHTT fragments are particularly prone to aggregate formation (Cooper et al., 1998; Li and Li, 1998; Martindale et al., 1998) and nuclear accumulation (Davies et al., 1997; DiFiglia et al., 1997; Zhou et al., 2003), we further quantified the levels of truncated mHTT by western blot analysis (Fig. 3E–G). By using the HTT-specific D7F7 antibody (epitope around proline 1220 of human HTT) to detect mHTT as well as endogenous rat huntingtin (Htt), and the polyQ-specific 1C2 antibody to detect mHTT only, we obtained a variety of protein fragments in cortex and striatum of both WT and BACHD rats (Fig. 3E). Untreated BACHD rats showed clearly enhanced fragmentation of mHTT in cortex (Fig. 3E and F) but not striatum (Fig. 3E and G). In addition, the cortex samples from untreated BACHD rats contained a variety of shorter HTT fragments that were not detectable in cortical samples from WT rats, or striatal samples of either genotype (Fig. 3E). Olesoxime treatment reduced HTT fragmentation in BACHD rats below WT level in both cortex and striatum (Fig. 3E–G). Similar to the TR-FRET analysis, olesoxime-treated BACHD rats showed a significant increase in full-length mHTT, specifically in cortex (Fig. 3E and F).

Based on the apparent influence of olesoxime on mHTT proteolysis, we then investigated the origin of mHTT fragments by analyzing the activity of calpains and caspases, the main contributors to proteolytic cleavage of mHTT (Gafni and Ellerby, 2002; Goldberg et al., 1996). We did not find marked differences between genotype or treatment groups in the expression levels of caspase-3, or the activation status of caspase-6 in either cortex or striatum (data not shown). On the other hand, strong activation of the calpain system was detected specifically in cortex (Fig. 4A) but not striatum (Fig. 4B) of untreated BACHD rats. While the expression

levels of full-length calpain-1, calpain-2 and calpain-10 were unchanged (data not shown), overactivation of the calpain system was evidenced by a distinct increase in processed calpain-1, elevated levels of the cleaved form of the calpain substrate α-spectrin, and decreased levels of the endogenous calpain inhibitor calpastatin (Fig. 4A). Olesoxime treatment reversed the dysregulation by decreasing active calpain-1, increasing calpastatin levels, and reducing α-spectrin cleavage (Fig. 4A). Even though calpain activity was not increased in the striata of untreated BACHD compared to WT rats, olesoxime reduced calpain-1 activation and spectrin cleavage also in this brain region, while no significant effects on calpastatin levels were detected (Fig. 4B).

In order to validate that the cortical mHTT fragments reduced by olesoxime treatment were calpain-derived, we performed *in vitro* calpain cleavage assays on cortical lysates (Fig. 4C and D). Incubation with recombinant calpain-1 resulted in increased fragmentation accompanied by a decrease in the levels of both full-length HTT and mHTT (Fig. 4C). The accumulation of HTT and mHTT fragments was calpain-1 concentration dependent, and concerned a variety of rather N-terminal and rather C-terminal fragments as detected by double-immunostaining with D7F7 and the N-terminal 4C8 antibody (epitope between amino acids 181 and 810) (Fig. 4D). Calpain dependency was further confirmed by addition of the specific calpain inhibitor CI-III, which abolished the fragmentation. *In vitro* calpain activation resulted in a clear fragmentation of HTT in WT rats, resembling the fragmentation pattern found in BACHD rats. Fragmentation was also enhanced in BACHD rats, although the effect was less strong due to high basal fragmentation of mHTT. These results suggest that calpain cleavage constituted the major contributor to proteolytic cleavage in the BACHD rat and that the additional small fragments found in BACHD rat cortex, which were cleared by olesoxime treatment, derived from enhanced calpain-mediated cleavage.

Olesoxime reduces mitochondria-associated HTT fragments and improves mitochondrial function

Given that olesoxime accumulates at the site of mitochondria (Bordet et al., 2010), we investigated the impact of olesoxime on mitochondrial properties.

First, we analyzed the activation status of the calpain system in mitochondria-enriched heavy membrane fractions isolated from the cerebra of 13 months old, placebo- and olesoxime-treated, WT and BACHD rats (Fig. 5A), as calpains are also located in mitochondria (Arrington et al., 2006; Badugu et al., 2008; Smith and Schnellmann, 2012). Enrichment in mitochondrial protein in the mitochondrial fractions is demonstrated by higher citrate synthase levels compared to whole cell lysate (Fig. 5A and B). Calpain activation was not

increased in the mitochondrial fractions of untreated BACHD rats (Fig. 5A). However, olesoxime treatment repressed mitochondrial calpain activity in both BACHD and WT rat samples, as indicated by a reduced amount of active calpain-1 and cleaved α-spectrin, as well as increased amounts of calpastatin (Fig. 5A).

As HTT and mHTT are known to associate with mitochondria (Choo et al., 2004; Gellerich et al., 2008; Orr et al., 2008), we further investigated their presence and cleavage in the mitochondrial fractions from WT and BACHD rats (Fig. 5B). Full-length protein as well as truncated forms of Htt and mHTT were detected. More mitochondria-associated fragments of HTT were found in untreated BACHD compared to WT rats. Olesoxime treatment reduced the amount of HTT fragments associated with mitochondria, in both WT and BACHD rats. In the BACHD rat, olesoxime additionally increased mitochondria-associated full-length Htt and mHTT. Together with the results on whole cell lysate, these findings indicate that olesoxime mediates a genotype-independent reduction in mitochondrial calpain activation, and reduces tissue-specific, whole cell calpain overactivation in the Huntington disease context of the BACHD rat.

To test if olesoxime affected mitochondrial function, we further investigated mitochondrial respiratory chain activity (Fig. 5C) and the expression of mitochondrial proteins (Table 1). Mitochondrial function has not been assessed in the BACHD rat previously. Mitochondria isolated from 13 months old untreated BACHD rat cerebra showed an overall lower oxygen consumption rate compared to WT rats, and olesoxime treatment reduced this respiration deficit (Fig. 5C). Expression levels of mitochondrial proteins were not strikingly altered in 13 months old untreated BACHD compared to WT rats, but olesoxime strongly affected the protein expression in BACHD and WT rats in a differential manner (Table 1). While we observed a general increase in the expression of many mitochondrial proteins in cortex and striatum of olesoxime-treated WT rats, indicative of an overall increase in mitochondrial mass, we detected more specific effects in BACHD rats with olesoxime treatment. In cortex, olesoxime increased the expression of ATP synthase and the fusion-promoting proteins Mfn 1, Mfn 2 and Opa 1, while the expression of fission-promoting proteins was either unaffected (Fis 1) or decreased (Drp 1), suggesting a higher capacity for respiration and fusion processes in this tissue due to olesoxime treatment. Olesoxime further dramatically increased the expression of the outer mitochondrial membrane transporter TOM 20, in both cortex and striatum of the BACHD rat. This finding led us to consider a general effect of olesoxime on transport across the mitochondrial membrane, and particularly the exchange of Ca^{2+}, as the overactivation of calpain found in BACHD rat cortex might be due to a mitochondrial Ca^{2+} buffering deficit.

Olesoxime affects the expression of proteins involved in Ca^{2+} homeostasis

It had been demonstrated that calpain-derived fragments of mHTT are formed in response to Ca^{2+} stress (Gafni et al., 2004). Olesoxime might influence Ca^{2+} homeostasis, as it interacts with VDAC (Bordet et al., 2007), which is involved in intracellular Ca^{2+} translocation (Gincel et al., 2001; Min et al., 2012; Szabadkai et al., 2006). Western blot analysis revealed no alteration in VDAC 1/2 expression in 13 months old untreated BACHD compared to WT rats, but a dramatic increase in the expression of both isoforms in cortex (Fig. 6A) and striatum (Fig. 6B) from olesoxime-treated BACHD rats. The strong effect on VDAC expression was also seen in cortex of WT rats (Fig. 6A).

We further analyzed the levels of the endoplasmic reticulum-associated Ca^{2+}-transporter IP3R 1, as it is implicated in neurodegenerative diseases (Stutzmann and Mattson, 2011). Specifically, IP3R 1 protein expression is upregulated in response to elevated Ca^{2+} levels (Genazzani et al., 1999), and excessive IP3R 1-mediated Ca^{2+}-release into the cytosol primes apoptosis (Stutzmann and Mattson, 2011). Furthermore, both interaction with mHTT and calpain cleavage, have been shown to facilitate IP3R 1 activity upon stimulation, and render neurons more vulnerable to excitotoxic stimuli (Kopil et al., 2012; Tang et al., 2003). We found the levels of IP3R 1 to be increased in cortex (Fig. 6A) of untreated BACHD compared to WT rats. While no significant effect of olesoxime treatment on IP3R 1 was found in WT rats, olesoxime normalized IP3R 1 expression in the cortex from BACHD rats (Fig. 6A and B).

d. Clemens et al., 2015, Brain.

Discussion

Olesoxime is a mitochondria-targeting neuroprotective compound (Bordet et al., 2007, 2010) that has shown potential as a treatment for several neurodegenerative diseases (Bordet et al., 2008; Eckmann et al., 2013; Richter et al., 2014; Rovini et al., 2010; Sunyach et al., 2012; Xiao et al., 2009, 2012). We show here that olesoxime exhibited highly beneficial effects on disease-related phenotypes in a Huntington disease animal model. Importantly, the treatment effects appeared to be conveyed through a previously unknown function of olesoxime, to reduce proteolysis. In Huntington disease, proteolytic cleavage of mHTT results in the generation and accumulation of toxic mHTT fragments (Gafni and Ellerby, 2002; Goldberg et al., 1996; Kim et al., 2006; Miller et al., 2010), which are thought to be crucial for disease pathogenesis (Nagai et al., 2007; Rigamonti et al., 2000; Wang et al., 2008). Consistent with this, olesoxime-treated BACHD rats showed reduced activation of the calpain system, reduced amounts of mHTT fragments, aggregates and nuclear mHTT accumulation, as well as behavioral and neuropathological improvements. Inhibition of mHTT cleavage has previously been targeted in Huntington disease models by genetic manipulations (Gafni et al., 2004; Graham et al., 2006; Miller et al., 2010), or the use of protease inhibitor (Bizat et al., 2003), revealing beneficial effects (Bizat et al., 2003; Gafni et al., 2004; Graham et al., 2006; Miller et al., 2010). However, olesoxime is the first small molecule identified to reduce the level of mHTT fragments in a safe and simple approach: the compound can be administered orally, has been shown to be safe and well-tolerated clinically (Lenglet et al., 2014), and its neuroprotective activity has recently been demonstrated in a pivotal clinical trial in spinal muscular atrophy patients (Dessaud et al., 2014). Thus, our findings highly encourage further investigations of olesoxime for use as a therapeutic for Huntington disease. Still, some questions arose from the present study, which need to be addressed further.

Are the beneficial effects of olesoxime restricted to specific brain regions?

The current results indicate that olesoxime reaches higher concentrations in the frontal and prefrontal cortex compared to other brain regions, when given orally. In line with this, both *in vivo* and *ex vivo* analyses indicated a predominant cortical effect of olesoxime treatment. MRI results revealed increased frontal cortex thickness, while atrophy of other brain areas such as the striatum was not alleviated. Further, olesoxime-treated BACHD rats showed a selective improvement of reversal learning and anxiety deficits, while motor phenotypes remained. Important in this regard is that lesion studies have tied attentional set shifting difficulties and reduced anxiety in the elevated plus maze to the prefrontal and frontal cortex

(Birrell and Brown, 2000; Shah and Treit, 2003), while motor performance crucially involves the striatum (Bergeron et al., 2014; Soll et al., 2013). Thus, it is possible that the apparent selective effect on behavior was a result of the uneven distribution of olesoxime. However, it is important to note that olesoxime still exerted strong effects on mHTT fragmentation and nuclear accumulation in striatum, despite its lower concentration. The reason for olesoxime not mitigating more striatum-based phenotypes could thus be that neuronal pathologies differ among brain regions. Most notably, the overactivation of the calpain system seemed to be a cortex-specific phenotype in the BACHD rat, and appeared to play a major role in olesoxime's beneficial effects. It is possible that striatal neurons suffer more from other mHTT-mediated deficits, and that neuronal dysfunction thus persisted, despite sufficient olesoxime concentrations.

An alternative hypothesis on the selective effects of olesoxime might be that some deficits, such as the Rotarod phenotype, were already manifest prior to the start of olesoxime treatment in the current study. Similar results have been obtained in a recent study on the effect of cholesterol oximes on the pathological phenotypes of Parkinson disease mice. The compounds ameliorated non-motor phenotypes and gene expression changes in mitochondrial genes, but were not able to reverse motor dysfunction with onset prior to the start of treatment (Richter et al., 2014). The fact that olesoxime treatment did not generally ameliorate brain atrophy in BACHD rats could have the same cause, as we recently reported that smaller body and brain sizes among BACHD rats derive from growth impairment rather than progressive degeneration (Jansson et al., 2014).

What is the primary target of olesoxime?

It has previously been proposed that the presence of mHTT might initiate a vicious cycle, in which mitochondrial dysfunction leads to reduced Ca^{2+} buffering, subsequent protease activation and generation of mHTT fragments that further enhance the cytotoxic events (Bizat et al., 2003; Petersén et al., 1999). Accordingly, we observed a respiratory chain deficit, along with increased calpain activation and mHTT fragmentation in BACHD rats, pathologies which were all alleviated by olesoxime (Fig. 7). Thus, we suggest that olesoxime interfered with the vicious cycle by stabilizing mitochondria.

It is conceivable that mitochondria were the primary effectors of olesoxime treatment, since olesoxime concentrates at this site (Bordet et al., 2010), and cholesterol-oximes have been shown to affect the expression of genes important for mitochondrial function (Richter et al., 2014). Such gene expression changes include the up-regulation of Mfn 1 and down-regulation of Drp 1, consistent with our findings on protein level. Importantly, abnormally

increased fission activity has recently been shown to contribute to the cellular pathology in Huntington disease (Costa and Scorrano, 2012). Counteracting this by inhibiting fission or enhancing fusion, further, has been found to ameliorate Huntington disease-related phenotypes (Costa et al., 2010; Song et al., 2011; Wang et al., 2009). This is possibly due to improved mitochondrial Ca^{2+} handling, as suppressing fission or enhancing fusion generally renders neurons less susceptible to excitotoxic stress (Grohm et al., 2012; Jahani-Asl et al., 2011; Kushnareva et al., 2013; Nguyen et al., 2011).

Another interesting effect of olesoxime is a modulation of mitochondrial membrane fluidity. We reported earlier that olesoxime was able to reverse an increase in mitochondrial membrane fluidity observed in the BACHD rat and two other Huntington disease models (Eckmann et al., 2014). We further showed that olesoxime-treated BACHD rats had significantly higher mitochondrial membrane cholesterol levels than untreated BACHD rats, which might be causal for the reduction in membrane fluidity (Eckmann et al., 2014). Here, we demonstrate that olesoxime dramatically increased the levels of the outer mitochondrial membrane transporter VDAC, which is involved in mitochondrial cholesterol import (Rone et al., 2009). The additional increase in the levels of the outer mitochondrial membrane import component TOM 20 suggests that olesoxime exerted a general beneficial effect on transport processes across the mitochondrial membrane. It had been argued before that energetic deficits and impaired Ca^{2+} homeostasis might be the result of impaired communication between mitochondria and cytoplasm due to the accumulation of mHTT on the outer mitochondrial membrane (Gellerich et al., 2008, 2010). A recent study further specifically demonstrated that mHTT impairs mitochondrial protein import by interaction with the inner membrane transport complex TIM 23, and that overexpression of TIM23 leads to restoration of protein import and prevention of cell death (Yano et al., 2014). Thus, there are several indications that the mitochondrial membrane environment is modulated by olesoxime, which might connect to its beneficial effects.

We hypothesized that the compound had exerted its beneficial effects by improving mitochondrial function, thereby stabilizing Ca^{2+} homeostasis, decreasing Ca^{2+}-related calpain-1 activation and aborting the generation of toxic mHtt fragments as well as their exaggerated negative influence on mitochondria (Fig. 87). Since Ca^{2+} levels, Ca^{2+} handling or the effects of olesoxime on Ca^{2+} balance could not be directly evaluated in this study, the proposed mechanism remains hypothetical. However, the finding of overactive calpain-1 itself and the increased protein levels of IP3R 1 in untreated BACHD rats, as well as the restorative effects of olesoxime on these parameters, strongly support the idea of improved

Ca^{2+} homeostasis, if not as primary effect then at least as part of olesoxime's mechanism of action.

Nonetheless, lacking a clear mechanism of action, it will be difficult to develop pharmacodynamic biomarkers, which will be crucial for conducting successful clinical efficacy trials. This has for instance been proven true for well-tolerated antioxidant molecules such as cysteamine (CYTE-I-HD study), creatine (CREST-E study), ethyl-EPA (TREND-HD study), and coenzyme Q10 (2CARE study). While these small molecules targeting mitochondrial function showed efficacy in some rodent models (Ferrante et al., 2000; Hickey et al., 2012; Yang et al., 2009) (although there is also conflicting data (Menalled et al., 2010)), they mainly yielded negative findings in the clinics, emphasizing the urgent need for pharmacodynamics biomarkers. However, olesoxime is the first small molecule to modulate soluble levels of mHTT, which can be quantified in CSF, plasma and other tissues from animal models and HD patients using a TR-FRET (Baldo et al., 2012; Weiss et al., 2012) or mHTT immunoassay (Wild et al., 2015), and could therefore potentially serve as a biomarker.

Can it be beneficial to reduce mHTT aggregation?

We observed a reduction in mHTT aggregation in olesoxime-treated BACHD rats. It is widely accepted that aggregates are not the most toxic species of mHTT, and reducing aggregation has even been found to enhance Huntington disease-related pathologies (Arrasate and Finkbeiner, 2012). However, it is likely that in these cases, reduced aggregation was accompanied by an increase in mHTT fragments, as truncated mHTT, not its full-length form, is thought to mediate mHTT toxicity (Arrasate et al., 2004). This is different from our study, as olesoxime specifically reduced mHTT fragments, but led to an increase in soluble full-length mHTT and Htt. There is evidence that not only mHTT but also Htt fragments have cytotoxic properties (Hackam et al., 1998; Kim et al., 1999; Nasir et al., 1995), while the full-length form of Htt exerts protective effects (Leavitt et al., 2001; Tanaka et al., 2006). Our results further support the idea that soluble full-length mHTT is non-toxic, as we did not detect any adverse effects of olesoxime treatment *in vivo*. Suppression of mHTT cleavage and aggregation might also exert secondary beneficial effects by increasing endogenous Htt levels.

It should be noted that the reduction of mHTT aggregates in olesoxime-treated BACHD rats might not only derive from reduced cleavage, but could be an effect of increased protein degradation. Calpain activation has been shown to interfere with autophagic degradation processes (Xia et al., 2010; Yousefi et al., 2006), and inhibiting calpain activity enhances autophagy (Kim et al., 2013; Kuro et al., 2011; Menzies et al., 2014). The increase in soluble

mHTT that paralleled the decline in aggregation in the BACHD rat might, however, argue against a strong increase in mHTT degradation.

Is it relevant and safe to suppress calpain activity in neurodegenerative diseases?

The calpain proteolytic system has been recognized as an important player in neurodegenerative diseases (Getz, 2012; Haacke et al., 2007; Samantaray et al., 2008; Stifanese et al., 2014), including Huntington disease (Gafni and Ellerby, 2002). The pivotal role is underpinned by current studies addressing the mechanistic link between calpains and Ca^{2+} dysbalance (Gladding et al., 2012), mitochondrial dysfunction (Wang et al., 2014), axonal degeneration (Yang et al., 2013), inflammation (Zhang et al., 2014), and apoptosis (Sobhan et al., 2013). A variety of calpain inhibitors have been developed to counteract the detrimental effects of calpain activation, but unspecific inhibitors and strong inhibition might exert off-target and side effects (Donkor, 2014). Such effects are less likely to arise from olesoxime treatment, as this probably affects calpains indirectly, and only lowers their activation. In this regard, we recently demonstrated that decreasing calpain activity in a mouse model of Parkinson disease by cross-breeding with calpastatin-overexpressing mice, ameliorates Parkinson disease-related pathologies (Diepenbroek et al., 2014). These, as well as other data (Menzies et al., 2014), suggest that long-term reduction of calpain activity does not have deleterious effects in mice *in vivo*.

Conclusion

Our study reveals behavioral and neuropathological improvements in olesoxime-treated BACHD rats due to improved mitochondrial function, which halts a vicious cycle of mitochondrial defects and calpain-mediated cleavage of mHTT. The current findings once more emphasize the connection between mitochondrial dysfunction and the generation of calpain-derived mHTT fragments, which underlies the molecular pathogenesis of Huntington disease, and constitutes a pivotal therapeutic target. As safety, tolerance and neuroprotective properties of olesoxime have been demonstrated, both clinically and in several neurodegenerative disease models, the compound represents a promising candidate for the treatment of Huntington disease.

Acknowledgements

LEC, MM, SHE, JG, GPE, TB, RMP, OR and HPN received grants by the European Union 7th Framework Program for RTD, Project MitoTarget, Grant Agreement HEALTH-F2-2008-223388, and JJW was funded by the Baden-Wuerttemberg Foundation, Research Grant Number P-BWS-SPII/3-08.

We are grateful to all MitoTarget members for helpful discussions and further want to thank Therese Stanek and Celina Tomczak for support in animal caretaking, Jean Axfanatidis for analytical chemistry, Adriana Rathore for assisting immunohistochemical staining and microscopy, Dr. Nicolas Casadei for advice on aggregate quantification, and Julian Clemens for illustration support.

Author contributions statements

Conceptual framework for the study: HPN
Behavioral experiments and data analysis: LEC, TTW, JCDM
Blood and tissue sampling: LEC, TTW
Olesoxime blood analysis: MM, TB, RMP
MRI measurements and data analysis: CC, BJP
Immunohistochemistry, microscopy and data analysis: LEC, TTW, LY
Western blotting and data analysis: JJW, TTW, LEC
Isolation of mitochondria and high resolution respirometry: JE, SHE, GPE
Data interpretation: LEC, JJW, HPN, OR, RMP, EKHJ
Writing of the manuscript: LEC, HPN, EKHJ, JJW, OR, RMP
Illustrations: LEC, JJW

Potential Conflicts Of Interest

RMP is employed by, and holds stock and stock options on Trophos; RMP and TB are named as an inventor on patents covering the use of olesoxime assigned to Trophos; MM is currently employed by Trophos; TB has been, at the time the study was conducted, employed by Trophos, and is currently employed by AFM Téléthon; LEC is currently employed by QPS Austria, JG is currently employed by Merz Pharmaceuticals; AW has been, at the time the study was conducted, employed by Novartis, and is currently employed by Evotec.

d. Clemens et al., 2015, Brain.

References

Abada Y-SK, Nguyen HP, Ellenbroek B, Schreiber R. Reversal learning and associative memory impairments in a BACHD rat model for Huntington disease. PLoS One 2013; 8: e71633.

Abada Y-SK, Nguyen HP, Schreiber R, Ellenbroek B. Assessment of motor function, sensory motor gating and recognition memory in a novel BACHD transgenic rat model for huntington disease. PLoS One 2013; 8: e68584.

Abràmoff MD, Magalhães PJ, Sunanda J. Image Processing with ImageJ. Biophotonics Int. 2004; 11: 36–42.

Arrasate M, Finkbeiner S. Protein aggregates in Huntington's disease. Exp. Neurol. 2012; 238: 1–11.

Arrasate M, Mitra S, Schweitzer ES, Segal MR, Finkbeiner S. Inclusion body formation reduces levels of mutant huntingtin and the risk of neuronal death. Nature 2004; 431: 805–10.

Arrington DD, Van Vleet TR, Schnellmann RG. Calpain 10: a mitochondrial calpain and its role in calcium-induced mitochondrial dysfunction. Am. J. Physiol. Cell Physiol. 2006; 291: C1159–71.

Badugu R, Garcia M, Bondada V, Joshi A, Geddes JW. N terminus of calpain 1 is a mitochondrial targeting sequence. J. Biol. Chem. 2008; 283: 3409–17.

Bae B-I, Xu H, Igarashi S, Fujimuro M, Agrawal N, Taya Y, et al. p53 mediates cellular dysfunction and behavioral abnormalities in Huntington's disease. Neuron 2005; 47: 29–41.

Baldo B, Paganetti P, Grueninger S, Marcellin D, Kaltenbach LS, Lo DC, et al. TR-FRET-based duplex immunoassay reveals an inverse correlation of soluble and aggregated mutant huntingtin in huntington's disease. Chem. Biol. 2012; 19: 264–75.

Bergeron Y, Chagniel L, Bureau G, Massicotte G, Cyr M. mTOR signaling contributes to motor skill learning in mice. Front. Mol. Neurosci. 2014; 7: 26.

Birrell JM, Brown VJ. Medial frontal cortex mediates perceptual attentional set shifting in the rat. J. Neurosci. 2000; 20: 4320–4.

Bizat N, Hermel J-M, Boyer F, Jacquard C, Créminon C, Ouary S, et al. Calpain is a major cell death effector in selective striatal degeneration induced in vivo by 3-nitropropionate: implications for Huntington's disease. J. Neurosci. 2003; 23: 5020–30.

Bordet T, Berna P, Abitbol J-L, Pruss RM. Olesoxime (TRO19622): A Novel Mitochondrial-Targeted Neuroprotective Compound. Pharmaceuticals 2010; 3: 345–368.

Bordet T, Buisson B, Michaud M, Abitbol J-L, Marchand F, Grist J, et al. Specific antinociceptive activity of cholest-4-en-3-one, oxime (TRO19622) in experimental models of painful diabetic and chemotherapy-induced neuropathy. J. Pharmacol. Exp. Ther. 2008; 326: 623–32.

Bordet T, Buisson B, Michaud M, Drouot C, Galéa P, Delaage P, et al. Identification and characterization of cholest-4-en-3-one, oxime (TRO19622), a novel drug candidate for amyotrophic lateral sclerosis. J. Pharmacol. Exp. Ther. 2007; 322: 709–20.

Calì T, Ottolini D, Brini M. Mitochondrial Ca(2+) and neurodegeneration. Cell Calcium 2012; 52: 73–85.

Choo YS, Johnson GVW, MacDonald M, Detloff PJ, Lesort M. Mutant huntingtin directly increases susceptibility of mitochondria to the calcium-induced permeability transition and cytochrome c release. Hum. Mol. Genet. 2004; 13: 1407–20.

Clemens LE, Jansson EKH, Portal E, Riess O, Nguyen HP. A behavioral comparison of the common laboratory rat strains Lister Hooded, Lewis, Fischer 344 and Wistar in an automated homecage system. Genes, Brain Behav. 2014; 13: 305–321.

Cooper JK, Schilling G, Peters MF, Herring WJ, Sharp AH, Kaminsky Z, et al. Truncated N-terminal fragments of huntingtin with expanded glutamine repeats form nuclear and cytoplasmic aggregates in cell culture. Hum. Mol. Genet. 1998; 7: 783–90.

Costa V, Giacomello M, Hudec R, Lopreiato R, Ermak G, Lim D, et al. Mitochondrial fission and cristae disruption increase the response of cell models of Huntington's disease to apoptotic stimuli. EMBO Mol. Med. 2010; 2: 490–503.

Costa V, Scorrano L. Shaping the role of mitochondria in the pathogenesis of Huntington's disease. EMBO J. 2012; 31: 1853–64.

Cui L, Jeong H, Borovecki F, Parkhurst CN, Tanese N, Krainc D. Transcriptional repression of PGC-1alpha by mutant huntingtin leads to mitochondrial dysfunction and neurodegeneration. Cell 2006; 127: 59–69.

Davies SW, Turmaine M, Cozens BA, DiFiglia M, Sharp AH, Ross CA, et al. Formation of neuronal intranuclear inclusions underlies the neurological dysfunction in mice transgenic for the HD mutation. Cell 1997; 90: 537–48.

Dessaud E, Carole A, Bruno S, Patrick B, Rebecca P, Cuvier V, et al. 2014 Emerging Science Abstracts. Neurology 2014; 83: e34–e40.

Diepenbroek M, Casadei N, Esmer H, Saido TC, Takano J, Kahle PJ, et al. Overexpression of the calpain-specific inhibitor calpastatin reduces human alpha-Synuclein processing, aggregation and synaptic impairment in [A30P]αSyn transgenic mice. Hum. Mol. Genet. 2014; 23: 3975–89.

DiFiglia M, Sapp E, Chase KO, Davies SW, Bates GP, Vonsattel JP, et al. Aggregation of huntingtin in neuronal intranuclear inclusions and dystrophic neurites in brain. Science 1997; 277: 1990–3.

Donkor IO. An updated patent review of calpain inhibitors (2012 - 2014). Expert Opin. Ther. Pat. 2014: 1–15.

Eckmann J, Clemens LE, Eckert SH, Hagl S, Yu-Taeger L, Bordet T, et al. Mitochondrial Membrane Fluidity is Consistently Increased in Different Models of Huntington Disease: Restorative Effects of Olesoxime. Mol. Neurobiol. 2014

Eckmann J, Eckert SH, Leuner K, Muller WE, Eckert GP. Mitochondria: mitochondrial membranes in brain ageing and neurodegeneration. Int. J. Biochem. Cell Biol. 2013; 45: 76–80.

Fan MMY, Raymond LA. N-methyl-D-aspartate (NMDA) receptor function and excitotoxicity in Huntington's disease. Prog. Neurobiol. 2007; 81: 272–93.

Ferrante RJ, Andreassen OA, Jenkins BG, Dedeoglu A, Kuemmerle S, Kubilus JK, et al. Neuroprotective effects of creatine in a transgenic mouse model of Huntington's disease. J. Neurosci. 2000; 20: 4389–97.

Gafni J, Ellerby LM. Calpain activation in Huntington's disease. J. Neurosci. 2002; 22: 4842–9.

Gafni J, Hermel E, Young JE, Wellington CL, Hayden MR, Ellerby LM. Inhibition of calpain cleavage of huntingtin reduces toxicity: accumulation of calpain/caspase fragments in the nucleus. J. Biol. Chem. 2004; 279: 20211–20.

Gellerich FN, Gizatullina Z, Nguyen HP, Trumbeckaite S, Vielhaber S, Seppet E, et al. Impaired regulation of brain mitochondria by extramitochondrial Ca2+ in transgenic Huntington disease rats. J. Biol. Chem. 2008; 283: 30715–24.

Gellerich FN, Gizatullina Z, Trumbeckaite S, Nguyen HP, Pallas T, Arandarcikaite O, et al. The regulation of OXPHOS by extramitochondrial calcium. Biochim. Biophys. Acta 2010; 1797: 1018–27.

Genazzani AA, Carafoli E, Guerini D. Calcineurin controls inositol 1,4,5-trisphosphate type 1 receptor expression in neurons. Proc. Natl. Acad. Sci. U. S. A. 1999; 96: 5797–801.

Getz GS. Calpain inhibition as a potential treatment of Alzheimer's disease. Am. J. Pathol. 2012; 181: 388–91.

Gincel D, Zaid H, Shoshan-Barmatz V. Calcium binding and translocation by the voltage-dependent anion channel: a possible regulatory mechanism in mitochondrial function. Biochem. J. 2001; 358: 147–55.

Gladding CM, Sepers MD, Xu J, Zhang LYJ, Milnerwood AJ, Lombroso PJ, et al. Calpain and STriatal-Enriched protein tyrosine phosphatase (STEP) activation contribute to extrasynaptic NMDA receptor localization in a Huntington's disease mouse model. Hum. Mol. Genet. 2012; 21: 3739–52.

Goldberg YP, Nicholson DW, Rasper DM, Kalchman MA, Koide HB, Graham RK, et al. Cleavage of huntingtin by apopain, a proapoptotic cysteine protease, is modulated by the polyglutamine tract. Nat. Genet. 1996; 13: 442–9.

Goll DE, Thompson VF, Li H, Wei W, Cong J. The calpain system. Physiol. Rev. 2003; 83: 731–801.

Gouarné C, Giraudon-Paoli M, Seimandi M, Biscarrat C, Tardif G, Pruss RM, et al. Olesoxime protects embryonic cortical neurons from camptothecin intoxication by a mechanism distinct from BDNF. Br. J. Pharmacol. 2013; 168: 1975–88.

Gouarné C, Tracz J, Paoli MG, Deluca V, Seimandi M, Tardif G, et al. Protective role of olesoxime against wild-type α-synuclein-induced toxicity in human neuronally differentiated SHSY-5Y cells. Br. J. Pharmacol. 2015; 172: 235–45.

Graham RK, Deng Y, Slow EJ, Haigh B, Bissada N, Lu G, et al. Cleavage at the caspase-6 site is required for neuronal dysfunction and degeneration due to mutant huntingtin. Cell 2006; 125: 1179–91.

Gray M, Shirasaki DI, Cepeda C, André VM, Wilburn B, Lu X-H, et al. Full-length human mutant huntingtin with a stable polyglutamine repeat can elicit progressive and selective neuropathogenesis in BACHD mice. J. Neurosci. 2008; 28: 6182–95.

Grohm J, Kim S-W, Mamrak U, Tobaben S, Cassidy-Stone A, Nunnari J, et al. Inhibition of Drp1 provides neuroprotection in vitro and in vivo. Cell Death Differ. 2012; 19: 1446–58.

Gutekunst CA, Li SH, Yi H, Mulroy JS, Kuemmerle S, Jones R, et al. Nuclear and neuropil aggregates in Huntington's disease: relationship to neuropathology. J. Neurosci. 1999; 19: 2522–34.

Haacke A, Hartl FU, Breuer P. Calpain inhibition is sufficient to suppress aggregation of polyglutamine-expanded ataxin-3. J. Biol. Chem. 2007; 282: 18851–6.

Hackam AS, Singaraja R, Wellington CL, Metzler M, McCutcheon K, Zhang T, et al. The influence of huntingtin protein size on nuclear localization and cellular toxicity. J. Cell Biol. 1998; 141: 1097–105.

Hickey MA, Zhu C, Medvedeva V, Franich NR, Levine MS, Chesselet M-F. Evidence for behavioral benefits of early dietary supplementation with CoEnzymeQ10 in a slowly progressing mouse model of Huntington's disease. Mol. Cell. Neurosci. 2012; 49: 149–57.

Hübener J, Weber JJ, Richter C, Honold L, Weiss A, Murad F, et al. Calpain-mediated ataxin-3 cleavage in the molecular pathogenesis of spinocerebellar ataxia type 3 (SCA3). Hum. Mol. Genet. 2013; 22: 508–18.

Jahani-Asl A, Pilon-Larose K, Xu W, MacLaurin JG, Park DS, McBride HM, et al. The mitochondrial inner membrane GTPase, optic atrophy 1 (Opa1), restores mitochondrial morphology and promotes neuronal survival following excitotoxicity. J. Biol. Chem. 2011; 286: 4772–82.

Jansson EKH, Clemens LE, Riess O, Nguyen HP. Reduced Motivation in the BACHD Rat Model of Huntington Disease Is Dependent on the Choice of Food Deprivation Strategy. PLoS One 2014; 9: e105662.

Kim J-S, Wang J-H, Biel TG, Kim D-S, Flores-Toro JA, Vijayvargiya R, et al. Carbamazepine suppresses calpain-mediated autophagy impairment after ischemia/reperfusion in mouse livers. Toxicol. Appl. Pharmacol. 2013

Kim M, Lee HS, LaForet G, McIntyre C, Martin EJ, Chang P, et al. Mutant huntingtin expression in clonal striatal cells: dissociation of inclusion formation and neuronal survival by caspase inhibition. J. Neurosci. 1999; 19: 964–73.

Kim YJ, Sapp E, Cuiffo BG, Sobin L, Yoder J, Kegel KB, et al. Lysosomal proteases are involved in generation of N-terminal huntingtin fragments. Neurobiol. Dis. 2006; 22: 346–56.

Kopil CM, Siebert AP, Foskett JK, Neumar RW. Calpain-cleaved type 1 inositol 1,4,5-trisphosphate receptor impairs ER Ca(2+) buffering and causes neurodegeneration in primary cortical neurons. J. Neurochem. 2012; 123: 147–58.

Kuro M, Yoshizawa K, Uehara N, Miki H, Takahashi K, Tsubura A. Calpain inhibition restores basal autophagy and suppresses MNU-induced photoreceptor cell death in mice. In Vivo (Brooklyn). 2011; 25: 617–623.

Kushnareva YE, Gerencser AA, Bossy B, Ju W-K, White AD, Waggoner J, et al. Loss of OPA1 disturbs cellular calcium homeostasis and sensitizes for excitotoxicity. Cell Death Differ. 2013; 20: 353–65.

Kuznetsov A V, Strobl D, Ruttmann E, Königsrainer A, Margreiter R, Gnaiger E. Evaluation of mitochondrial respiratory function in small biopsies of liver. Anal. Biochem. 2002; 305: 186–94.

Landles C, Sathasivam K, Weiss A, Woodman B, Moffitt H, Finkbeiner S, et al. Proteolysis of mutant huntingtin produces an exon 1 fragment that accumulates as an aggregated protein in neuronal nuclei in Huntington disease. J. Biol. Chem. 2010; 285: 8808–23.

Leavitt BR, Guttman JA, Hodgson JG, Kimel GH, Singaraja R, Vogl AW, et al. Wild-type huntingtin reduces the cellular toxicity of mutant huntingtin in vivo. Am. J. Hum. Genet. 2001; 68: 313–24.

Lemasters JJ, Theruvath TP, Zhong Z, Nieminen A-L. Mitochondrial calcium and the permeability transition in cell death. Biochim. Biophys. Acta 2009; 1787: 1395–401.

Lenglet T, Lacomblez L, Abitbol JL, Ludolph A, Mora JS, Robberecht W, et al. A phase II-III trial of olesoxime in subjects with amyotrophic lateral sclerosis. Eur. J. Neurol. 2014; 21: 529–36.

Li SH, Li XJ. Aggregation of N-terminal huntingtin is dependent on the length of its glutamine repeats. Hum. Mol. Genet. 1998; 7: 777–82.

Martindale D, Hackam A, Wieczorek A, Ellerby L, Wellington C, McCutcheon K, et al. Length of huntingtin and its polyglutamine tract influences localization and frequency of intracellular aggregates. Nat. Genet. 1998; 18: 150–4.

Menalled LB, Patry M, Ragland N, Lowden PAS, Goodman J, Minnich J, et al. Comprehensive behavioral testing in the R6/2 mouse model of Huntington's disease shows no benefit from CoQ10 or minocycline. PLoS One 2010; 5: e9793.

Menzies FM, Garcia-Arencibia M, Imarisio S, O'Sullivan NC, Ricketts T, Kent BA, et al. Calpain inhibition mediates autophagy-dependent protection against polyglutamine toxicity. Cell Death Differ. 2014; 22: 433–44.

Miller BR, Bezprozvanny I. Corticostriatal circuit dysfunction in Huntington's disease: intersection of glutamate, dopamine and calcium. Future Neurol. 2010; 5: 735–756.

Miller JP, Holcomb J, Al-Ramahi I, de Haro M, Gafni J, Zhang N, et al. Matrix metalloproteinases are modifiers of huntingtin proteolysis and toxicity in Huntington's disease. Neuron 2010; 67: 199–212.

Min CK, Yeom DR, Lee K-E, Kwon H-K, Kang M, Kim Y-S, et al. Coupling of ryanodine receptor 2 and voltage-dependent anion channel 2 is essential for Ca2+ transfer from the sarcoplasmic reticulum to the mitochondria in the heart. Biochem. J. 2012; 447: 371–9.

Nagai Y, Inui T, Popiel HA, Fujikake N, Hasegawa K, Urade Y, et al. A toxic monomeric conformer of the polyglutamine protein. Nat. Struct. Mol. Biol. 2007; 14: 332–40.

Nasir J, Floresco SB, O'Kusky JR, Diewert VM, Richman JM, Zeisler J, et al. Targeted disruption of the Huntington's disease gene results in embryonic lethality and behavioral and morphological changes in heterozygotes. Cell 1995; 81: 811–23.

Nguyen D, Alavi M V, Kim K-Y, Kang T, Scott RT, Noh YH, et al. A new vicious cycle involving glutamate excitotoxicity, oxidative stress and mitochondrial dynamics. Cell Death Dis. 2011; 2: e240.

Orr AL, Li S, Wang C-E, Li H, Wang J, Rong J, et al. N-terminal mutant huntingtin associates with mitochondria and impairs mitochondrial trafficking. J. Neurosci. 2008; 28: 2783–92.

Osmand AP, Berthelier V, Wetzel R. Imaging polyglutamine deposits in brain tissue. Methods Enzymol. 2006; 412: 106–22.

Panov A V, Burke JR, Strittmatter WJ, Greenamyre JT. In vitro effects of polyglutamine tracts on Ca2+-dependent depolarization of rat and human mitochondria: relevance to Huntington's disease. Arch. Biochem. Biophys. 2003; 410: 1–6.

Panov A V, Gutekunst C-A, Leavitt BR, Hayden MR, Burke JR, Strittmatter WJ, et al. Early mitochondrial calcium defects in Huntington's disease are a direct effect of polyglutamines. Nat. Neurosci. 2002; 5: 731–6.

Persichetti F, Ambrose CM, Ge P, McNeil SM, Srinidhi J, Anderson MA, et al. Normal and expanded Huntington's disease gene alleles produce distinguishable proteins due to translation across the CAG repeat. Mol. Med. 1995; 1: 374–83.

Petersén A, Mani K, Brundin P. Recent advances on the pathogenesis of Huntington's disease. Exp. Neurol. 1999; 157: 1–18.

Poudel GR, Egan GF, Churchyard A, Chua P, Stout JC, Georgiou-Karistianis N. Abnormal synchrony of resting state networks in premanifest and symptomatic Huntington disease: the IMAGE-HD study. J. Psychiatry Neurosci. 2014; 39: 87–96.

Van Raamsdonk JM, Pearson J, Slow EJ, Hossain SM, Leavitt BR, Hayden MR. Cognitive dysfunction precedes neuropathology and motor abnormalities in the YAC128 mouse model of Huntington's disease. J. Neurosci. 2005; 25: 4169–80.

Richter F, Gao F, Medvedeva V, Lee P, Bove N, Fleming SM, et al. Chronic administration of cholesterol oximes in mice increases transcription of cytoprotective genes and improves transcriptome alterations induced by alpha-synuclein overexpression in nigrostriatal dopaminergic neurons. Neurobiol. Dis. 2014; 69: 263–75.

Rigamonti D, Bauer JH, De-Fraja C, Conti L, Sipione S, Sciorati C, et al. Wild-type huntingtin protects from apoptosis upstream of caspase-3. J. Neurosci. 2000; 20: 3705–13.

Rockabrand E, Slepko N, Pantalone A, Nukala VN, Kazantsev A, Marsh JL, et al. The first 17 amino acids of Huntingtin modulate its sub-cellular localization, aggregation and effects on calcium homeostasis. Hum. Mol. Genet. 2007; 16: 61–77.

Rone MB, Fan J, Papadopoulos V. Cholesterol transport in steroid biosynthesis: role of protein-protein interactions and implications in disease states. Biochim. Biophys. Acta 2009; 1791: 646–58.

Rovini A, Carré M, Bordet T, Pruss RM, Braguer D. Olesoxime prevents microtubule-targeting drug neurotoxicity: selective preservation of EB comets in differentiated neuronal cells. Biochem. Pharmacol. 2010; 80: 884–94.

Samantaray S, Ray SK, Banik NL. Calpain as a potential therapeutic target in Parkinson's disease. CNS Neurol. Disord. Drug Targets 2008; 7: 305–12.

Shah AA, Treit D. Excitotoxic lesions of the medial prefrontal cortex attenuate fear responses in the elevated-plus maze, social interaction and shock probe burying tests. Brain Res. 2003; 969: 183–94.

Smith M a, Schnellmann RG. Calpains, mitochondria, and apoptosis. Cardiovasc. Res. 2012; 96: 32–7.

Sobhan PK, Seervi M, Deb L, Varghese S, Soman A, Joseph J, et al. Calpain and reactive oxygen species targets Bax for mitochondrial permeabilisation and caspase activation in zerumbone induced apoptosis. PLoS One 2013; 8: e59350.

Soll LG, Grady SR, Salminen O, Marks MJ, Tapper AR. A role for α4(non-α6)* nicotinic acetylcholine receptors in motor behavior. Neuropharmacology 2013; 73: 19–30.

Song W, Chen J, Petrilli A, Liot G, Klinglmayr E, Zhou Y, et al. Mutant huntingtin binds the mitochondrial fission GTPase dynamin-related protein-1 and increases its enzymatic activity. Nat. Med. 2011; 17: 377–82.

Stifanese R, Averna M, De Tullio R, Pedrazzi M, Milanese M, Bonifacino T, et al. Role of calpain-1 in the early phase of experimental ALS. Arch. Biochem. Biophys. 2014; 562: 1–8.

Stutzmann GE, Mattson MP. Endoplasmic reticulum Ca(2+) handling in excitable cells in health and disease. Pharmacol. Rev. 2011; 63: 700–27.

Sunyach C, Michaud M, Arnoux T, Bernard-Marissal N, Aebischer J, Latyszenok V, et al. Olesoxime delays muscle denervation, astrogliosis, microglial activation and motoneuron death in an ALS mouse model. Neuropharmacology 2012; 62: 2346–52.

Szabadkai G, Bianchi K, Várnai P, De Stefani D, Wieckowski MR, Cavagna D, et al. Chaperone-mediated coupling of endoplasmic reticulum and mitochondrial Ca2+ channels. J. Cell Biol. 2006; 175: 901–11.

Tabrizi SJ, Scahill RI, Durr A, Roos RA, Leavitt BR, Jones R, et al. Biological and clinical changes in premanifest and early stage Huntington's disease in the TRACK-HD study: the 12-month longitudinal analysis. Lancet. Neurol. 2011; 10: 31–42.

Tanaka Y, Igarashi S, Nakamura M, Gafni J, Torcassi C, Schilling G, et al. Progressive phenotype and nuclear accumulation of an amino-terminal cleavage fragment in a transgenic mouse model with inducible expression of full-length mutant huntingtin. Neurobiol. Dis. 2006; 21: 381–91.

Tang T-S, Slow E, Lupu V, Stavrovskaya IG, Sugimori M, Llinás R, et al. Disturbed Ca2+ signaling and apoptosis of medium spiny neurons in Huntington's disease. Proc. Natl. Acad. Sci. U. S. A. 2005; 102: 2602–7.

Tang T-S, Tu H, Chan EYW, Maximov A, Wang Z, Wellington CL, et al. Huntingtin and huntingtin-associated protein 1 influence neuronal calcium signaling mediated by inositol-(1,4,5) triphosphate receptor type 1. Neuron 2003; 39: 227–39.

The Huntington’s Disease Collaborative Research Group. A novel gene containing a trinucleotide repeat that is expanded and unstable on Huntington’s disease chromosomes. The Huntington's Disease Collaborative Research Group. Cell 1993; 72: 971–83.

Vonsattel JP, DiFiglia M. Huntington disease. J. Neuropathol. Exp. Neurol. 1998; 57: 369–84.

Wang C-E, Tydlacka S, Orr AL, Yang S-H, Graham RK, Hayden MR, et al. Accumulation of N-terminal mutant huntingtin in mouse and monkey models implicated as a pathogenic mechanism in Huntington’s disease. Hum. Mol. Genet. 2008; 17: 2738–51.

Wang H, Lim PJ, Karbowski M, Monteiro MJ. Effects of overexpression of huntingtin proteins on mitochondrial integrity. Hum. Mol. Genet. 2009; 18: 737–52.

Wang W, Zhang F, Li L, Tang F, Siedlak SL, Fujioka H, et al. Mfn2 Couples Glutamate Excitotoxicity and Mitochondrial Dysfunction in Motor Neurons. J. Biol. Chem. 2014

Weiss A, Träger U, Wild EJ, Grueninger S, Farmer R, Landles C, et al. Mutant huntingtin fragmentation in immune cells tracks Huntington’s disease progression. J. Clin. Invest. 2012; 122: 3731–6.

Wild EJ, Boggio R, Langbehn D, Robertson N, Haider S, Miller JRC, et al. Quantification of mutant huntingtin protein in cerebrospinal fluid from Huntington’s disease patients. J. Clin. Invest. 2015

Xia H-G, Zhang L, Chen G, Zhang T, Liu J, Jin M, et al. Control of basal autophagy by calpain1 mediated cleavage of ATG5. Autophagy 2010; 6: 61–6.

Xiao WH, Zheng FY, Bennett GJ, Bordet T, Pruss RM. Olesoxime (cholest-4-en-3-one, oxime): analgesic and neuroprotective effects in a rat model of painful peripheral neuropathy produced by the chemotherapeutic agent, paclitaxel. Pain 2009; 147: 202–9.

Xiao WH, Zheng H, Bennett GJ. Characterization of oxaliplatin-induced chronic painful peripheral neuropathy in the rat and comparison with the neuropathy induced by paclitaxel. Neuroscience 2012; 203: 194–206.

Yang J, Weimer RM, Kallop D, Olsen O, Wu Z, Renier N, et al. Regulation of axon degeneration after injury and in development by the endogenous calpain inhibitor calpastatin. Neuron 2013; 80: 1175–89.

Yang L, Calingasan NY, Wille EJ, Cormier K, Smith K, Ferrante RJ, et al. Combination therapy with coenzyme Q10 and creatine produces additive neuroprotective effects in models of Parkinson’s and Huntington's diseases. J. Neurochem. 2009; 109: 1427–39.

Yano H, Baranov S V, Baranova O V, Kim J, Pan Y, Yablonska S, et al. Inhibition of mitochondrial protein import by mutant huntingtin. Nat. Neurosci. 2014

Yousefi S, Perozzo R, Schmid I, Ziemiecki A, Schaffner T, Scapozza L, et al. Calpain-mediated cleavage of Atg5 switches autophagy to apoptosis. Nat. Cell Biol. 2006; 8: 1124–32.

Yu-Taeger L, Petrasch-Parwez E, Osmand AP, Redensek A, Metzger S, Clemens LE, et al. A Novel BACHD Transgenic Rat Exhibits Characteristic Neuropathological Features of Huntington Disease. J. Neurosci. 2012; 32: 15426–15438.

Zhang J, Mao X, Zhou T, Cheng X, Lin Y. IL-17A contributes to brain ischemia reperfusion injury through calpain-TRPC6 pathway in mice. Neuroscience 2014; 274: 419–28.

Zhou H, Cao F, Wang Z, Yu Z-X, Nguyen H-P, Evans J, et al. Huntingtin forms toxic NH2-terminal fragment complexes that are promoted by the age-dependent decrease in proteasome activity. J. Cell Biol. 2003; 163: 109–18.

Zuccato C, Valenza M, Cattaneo E. Molecular mechanisms and potential therapeutical targets in Huntington’s disease. Physiol. Rev. 2010; 90: 905–81.

Figures and Figure Legends

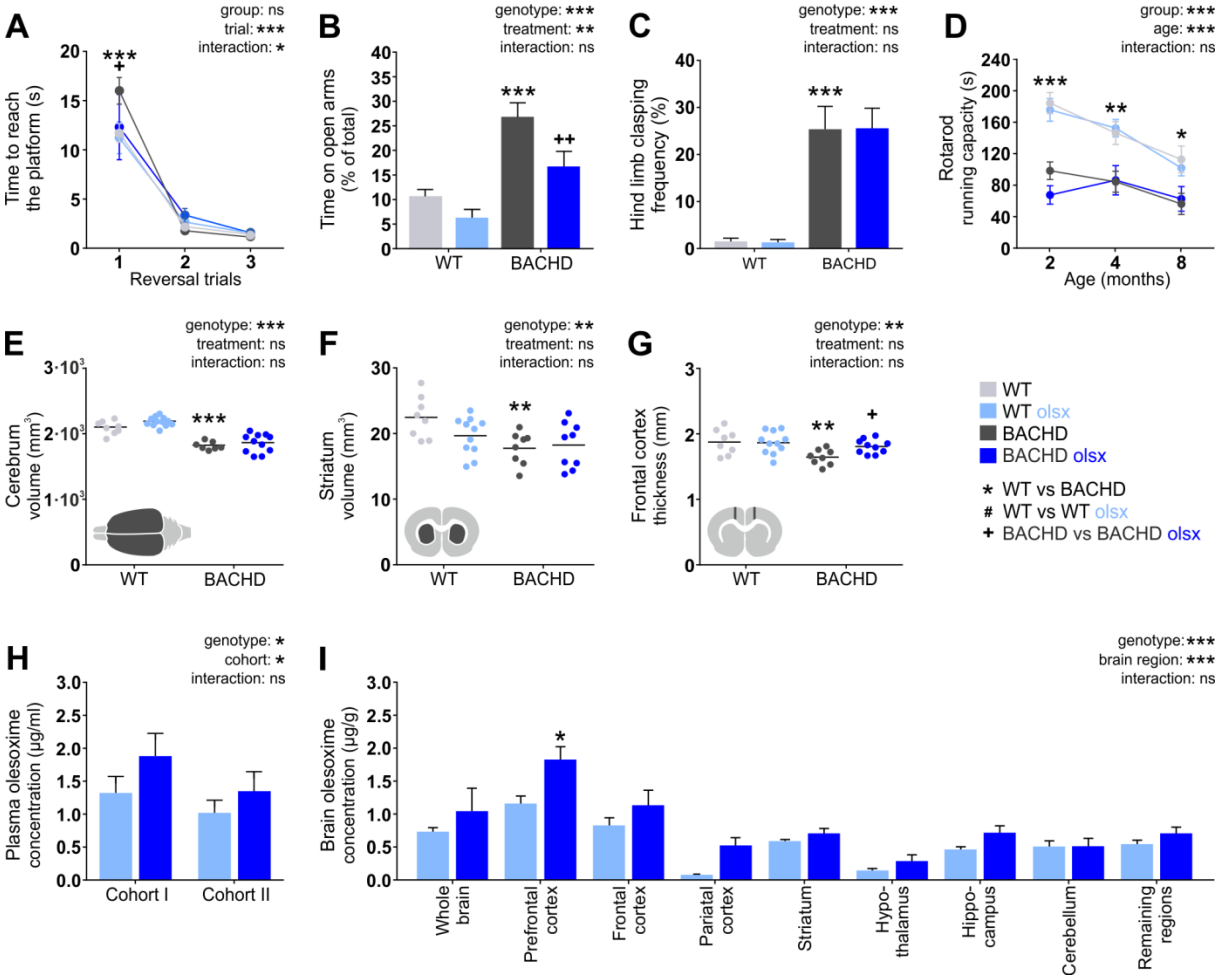

Figure 1: Olesoxime accumulates in the frontal cortex and exerts specific beneficial effects on behavioral and neuropathological phenotypes of the BACHD rat. (**A**) A simple swim test (SST) was used to assess cognitive flexibility at 7 months of age. The graph shows the time the animals needed to find a hidden platform after the position of the platform had been changed (reversal training). (**B**) Anxiety-related behavior was assessed in an elevated plus maze at 13 months of age. The graph shows the time the animals spent on the open arms of the maze relative to trial duration. (**C**) Clasping behavior was assessed weekly as an indicator for motor dysfunction. The graph displays the clasping frequency between the age of 1 and 10 months. (**D**) Motor abnormalities were further investigated longitudinally using a Rotarod test. The graph displays the mean running capacity during tests. (**E–G**) MRI was performed at 13 months of age. Images in the lower left corner illustrate the site of measurement. (**H and I**) Plasma olesoxime levels were measured in the main cohort of rats used for all *in vivo* and *ex vivo* analyses (cohort I) at 3 months of age after 7 weeks of treatment. In addition, plasma and brain olesoxime levels were determined in a second

d. Clemens et al., 2015, Brain.

cohort of rats (cohort II) at 4 months of age after 2 weeks of treatment. Olsx: olesoxime, EPM: elevated plus maze, */$^{\#}$/$^{+}$: $P < 0.05$; **/$^{\#\#}$/$^{++}$: $P \leq 0.01$ and ***/$^{\#\#\#}$/$^{+++}$: $P \leq 0.001$.

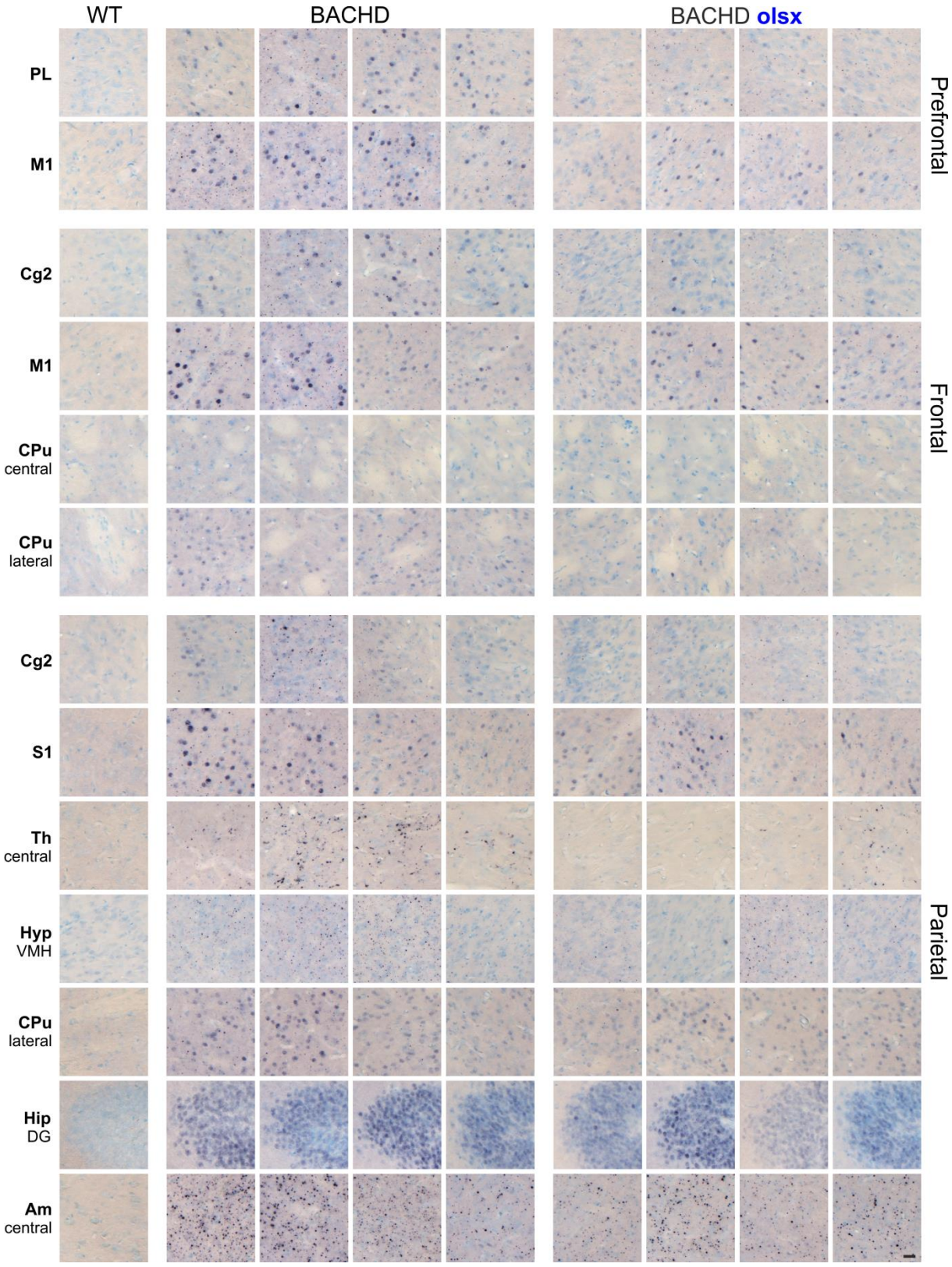

Figure 2: Effects of olesoxime on mutant huntingtin aggregates and nuclear accumulation in different brain regions. Aggregation and nuclear accumulation of mHTT were investigated in coronal brain sections from 13 months old rats, stained with S830 N-

terminal mHTT antibody. Images were taken from prefrontal, frontal and parietal brain areas. Columns display series of images from individual rats ($n_{(WT)}$ = 1, $n_{(BACHD)}$ = 4. Distinct punctae represent mHTT cytoplasmic aggregates and large circular staining represents mHTT nuclear accumulation. Black – purple staining: S830 huntingtin signal; blue staining: thionine nuclear signal. Magnification: 400 x, scale bar: 10 µM. Olsx: olesoxime, PL: prelimbic cortex, M1: motor cortex 1, Cg: cingulate cortex, CPu: caudate putamen, S: somatosensory cortex, Th: thalamus, Hyp: hypothalamus (VMH = ventro-medial hypothalamus), Hip: hippocampus, Am: amygdala.

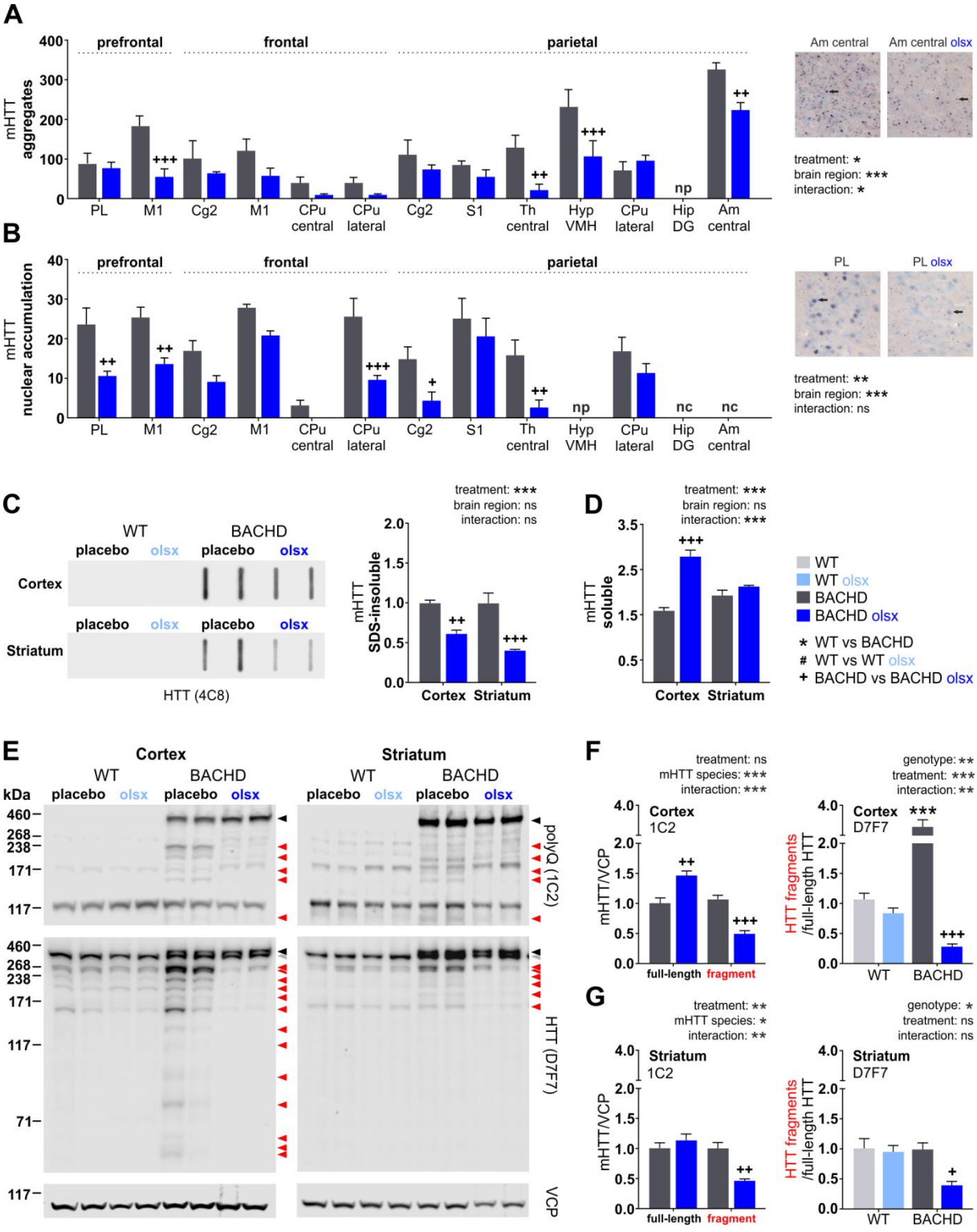

Figure 3: Olesoxime reduces mHTT aggregation, nuclear accumulation and fragmentation, and increases soluble full-length forms of mHTT. (**A and B**) Total numbers of S830-positive punctae (mHTT aggregates) and nuclei (nuclear accumulation of mHTT) were counted manually from the brain regions displayed in Figure 3. Images on the left illustrate the structures counted, with arrows pointing to mHTT aggregates or mHTT-

positive nuclei, respectively. Nc: not counted, np: not present, PL: prelimbic cortex, M1: motor cortex 1, Cg: cingulate cortex, CPu: caudate putamen, S: somatosensory cortex, Th: thalamus, Hyp: hypothalamus (VMH = ventro-medial hypothalamus), Hip: hippocampus, Am: amygdala. (**C**) SDS-insoluble proteins from cortical and striatal lysates were trapped on a nitrocellulose membrane and probed with the HTT-specific 4C8 antibody to quantify the amount of aggregated mHTT. (**D**) Levels of soluble mHTT were measured in cortical and striatal lysates from untreated and olesoxime-treated BACHD rats via TR-FRET analysis. (**E–G**) Full-length and fragment forms of mHTT were assessed in cortical and striatal lysates using the HTT-specific D7F7 and the polyQ-specific 1C2 antibodies. Black arrowheads: full-length mHTT, gray arrowhead: full-length Htt, red arrowheads: HTT fragments (1C2-positive bands in WT rats label polyQ-containing proteins other than mHTT), VCP/p97: loading control. Olsx: olesoxime, */$^{\#}$/$^{+}$: $P < 0.05$; **/$^{\#\#}$/$^{++}$: $P \leq 0.01$ and ***/$^{\#\#\#}$/$^{+++}$: $P \leq 0.001$.

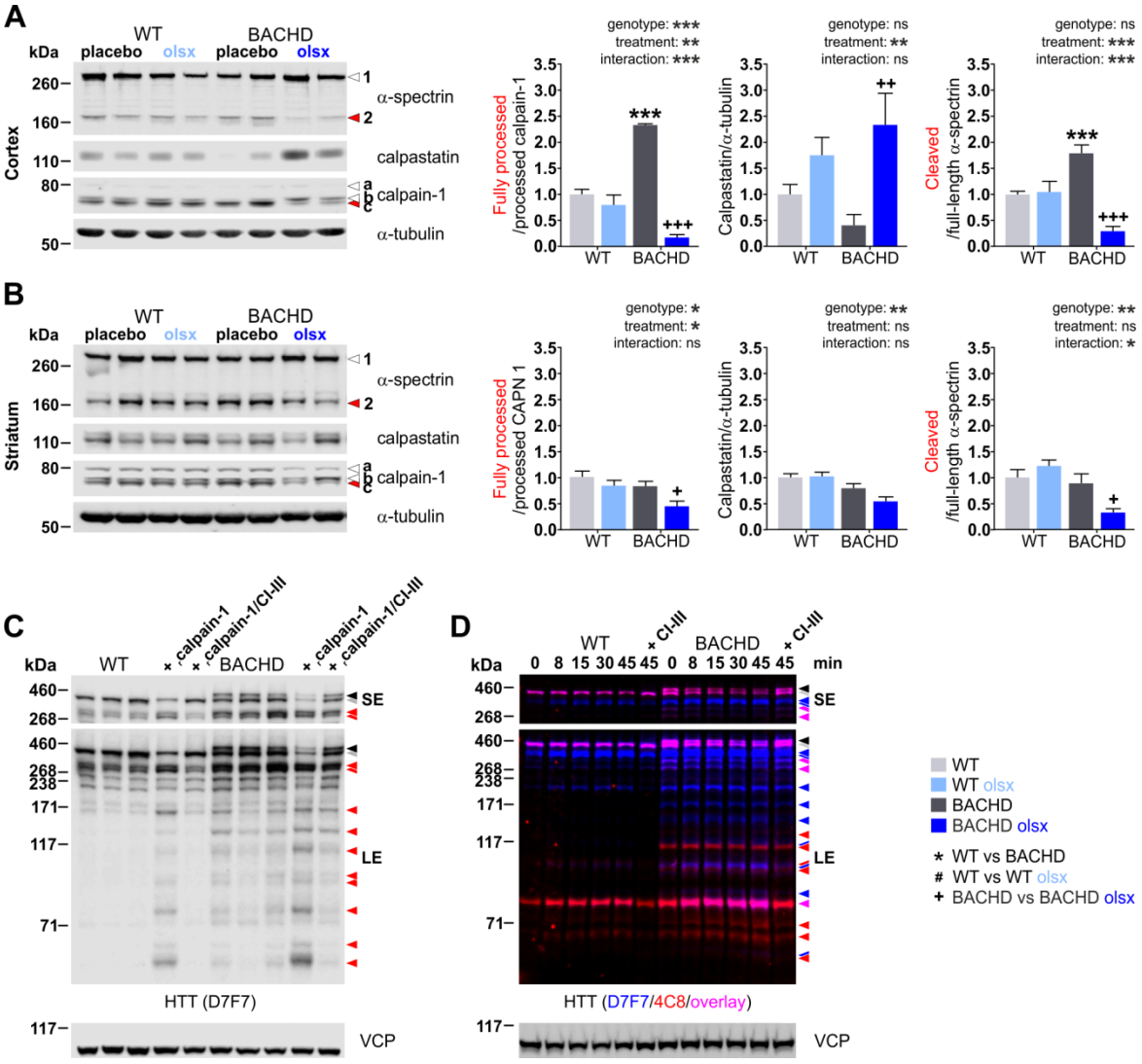

Figure 4: Olesoxime reduces the calpain-mediated cleavage of HTT, the major source of HTT fragments in the BACHD rat. (**A and B**) Calpain activation was investigated by Western blot analysis of the protease calpain-1, its endogenous inhibitor calpastatin and cleavage substrate α-spectrin, in cortical and striatal lysates from 13 months old rats. Arrowhead 1: full-length α-spectrin, arrowhead 2: α-spectrin fragment, arrowhead a: full-length calpain-1, arrowhead b: processed calpain-1, arrowhead c: further processed calpain-1 (active calpain1 refers to the ratio c/b), α-tubulin: loading control. (**C**) The dependency of HTT cleavage on calpain activity was assessed qualitatively in a calpain activation assay performed with cortical lysates from untreated, 13 months old WT and BACHD rats. Samples were treated with recombinant calpain-1 and $CaCl_2$ ($_r$calpain-1) for 15 min, or additionally pretreated with calpain inhibitor III (CI-III) to demonstrate calpain-1 specificity. HTT fragments were detected with the HTT-specific D7F7 antibody. Black arrowhead: full-length mHTT, gray arrowhead: full-length Htt, red arrowheads: HTT fragments. Shorter exposure of the

membrane was used to distinguish high molecular weight bands, while longer exposure revealed low molecular weight HTT fragments. (**D**) Another calpain activation assay was performed with cortical lysates from one untreated, 13 months old WT and BACHD rat, respectively, to illustrate the variety of N-terminal and more C-terminal HTT fragments. For this, the samples were first treated with recombinant calpain-1 and $CaCl_2$ ($_r$calpain-1) for an increasing amount of time or pretreated with calpain inhibitor III (CI-III) to demonstrate calpain-1 specificity. Samples were then probed with the HTT-specific D7F7 antibody as well as the HTT-specific 4C8 antibody, labelling central and N-terminal mHTT, respectively. The figure shows the overlay of the two detections with exclusive staining of HTT with D7F7 in blue, exclusive staining of HTT with 4C8 in red and double-staining of HTT with both antibodies in pink.. Black arrowhead: full-length mHTT, gray arrowhead: full-length Htt, blue, red and pink arrowheads: HTT fragments. Shorter exposure of the membrane was used to distinguish high molecular weight bands, while longer exposure revealed low molecular weight HTT fragments. $*/^{\#}/^{+}$: $P < 0.05$; $**/^{\#\#}/^{++}$: $P \leq 0.01$ and $***/^{\#\#\#}/^{+++}$: $P \leq 0.001$.

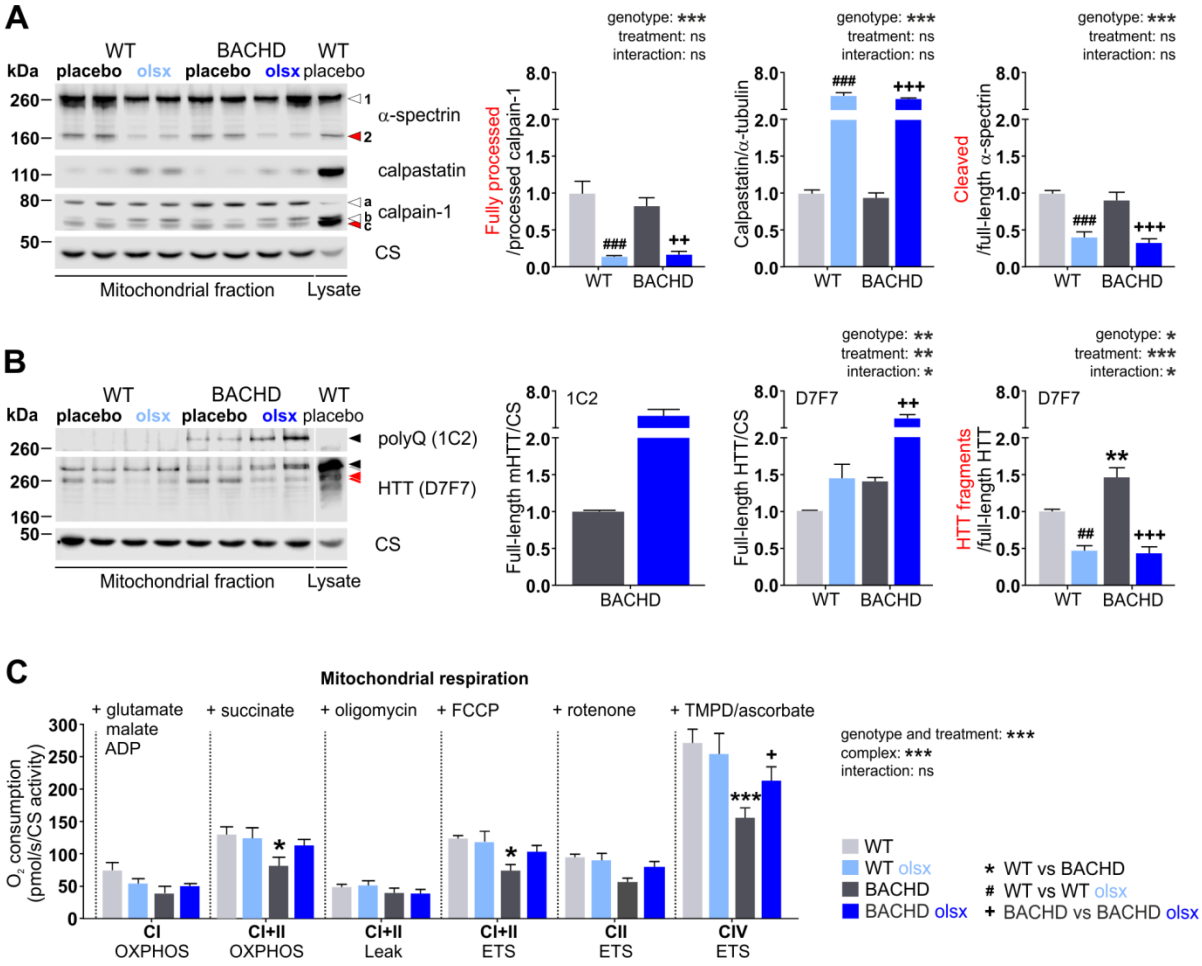

Figure 5: Olesoxime reduces the activation of mitochondrial calpains and mitochondria-associated HTT fragments and restores mild respiratory deficits in BACHD rats. (**A**) Calpain activation was investigated in cerebral mitochondria-enriched heavy membranes (mitochondrial fraction) from 13 months old rats by Western blot analysis of the protease calpain-1, its endogenous inhibitor calpastatin and cleavage substrate α-spectrin, in cortical and striatal lysates. Arrowhead 1: full-length α-spectrin, arrowhead 2: α-spectrin fragment, arrowhead a: full-length calpain-1, arrowhead b: processed calpain-1, arrowhead c: further processed calpain-1 (active calpain-1 refers to the ratio c/b), Citrate synthase (CS): loading control. (**B**) Full-length and fragment forms of mHTT were assessed in cortical and striatal lysates from 13 months old rats using the HTT-specific D7F7 and the polyQ-specific 1C2 antibodies. Black arrowheads: full-length mHTT, gray arrowhead: full-length Htt, red arrowheads: HTT fragments. One sample of WT cortex lysate was loaded to demonstrate the enrichment of the mitochondrial marker CS in the mitochondrial fraction. (**C**) Mitochondrial respiratory chain activity was assessed by measuring oxygen consumption of isolated cerebral mitochondria from 13 months old rats. Addition of substrates and inhibitors was performed as indicated in the figure and described in detail in the methods section.

d. Clemens et al., 2015, Brain.

CI_{OXPHOS} = complex I-fueled respiration; $CI+II_{OXPHOS}$ = complex I- and II-fueled respiration; $CI+II_{LEAK}$ = membrane leakage; $CI+II_{ETC}$ = maximum respiratory capacity; CII_{ETC} = maximum capacity dependent on complex II; CIV_{ETC} = maximum capacity dependent on complex IV. Oxygen consumption rates were normalized to CS activity. */$^{\#}$/$^{+}$: $P < 0.05$; **/$^{\#\#}$/$^{++}$: $P \leq 0.01$ and ***/$^{\#\#\#}$/$^{+++}$: $P \leq 0.001$.

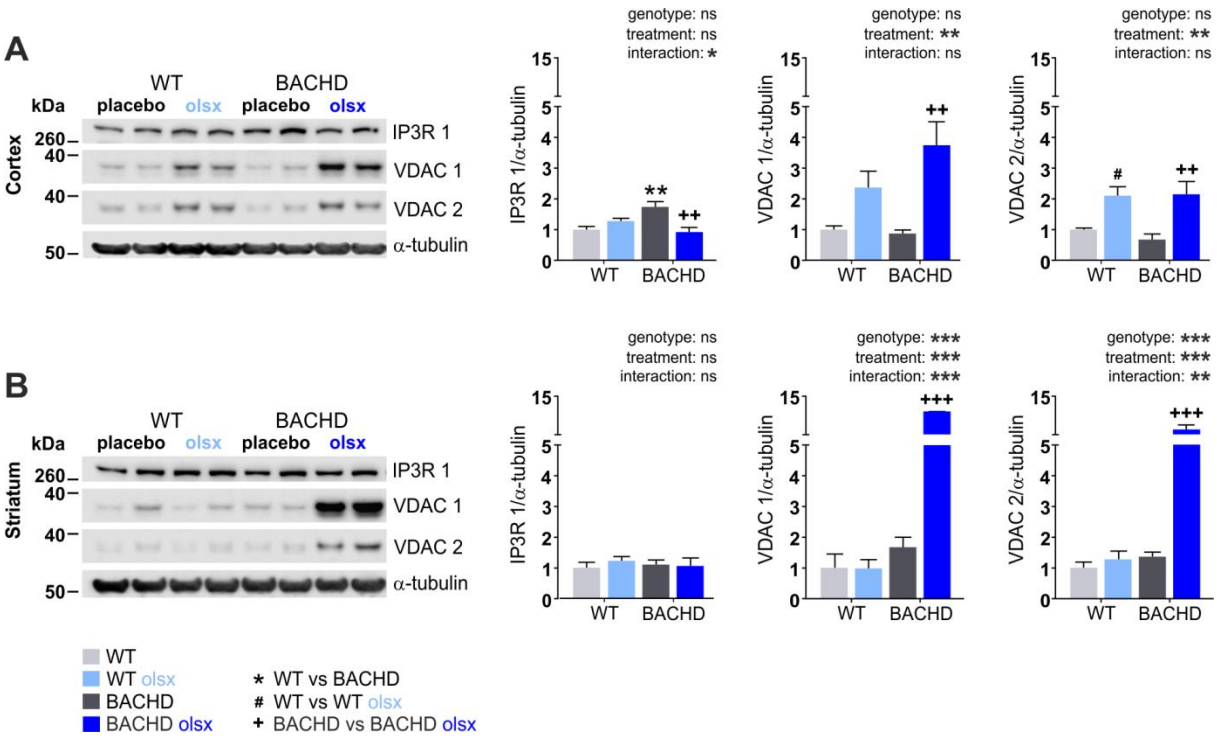

Figure 6: Olesoxime affects the expression of proteins involved in Ca^{2+} homeostasis. (**A and B**) Expression levels of the endoplasmic reticulum Ca^{2+} transporter IP3R 1, and the outer mitochondrial membrane channels VDAC 1 and VDAC 2, which are also involved in Ca^{2+} transport, were assayed in cortical and striatal lysates from 13 months old rats. α-tubulin: loading control. */#/+: $P < 0.05$; **/##/++: $P \leq 0.01$ and ***/###/+++: $P \leq 0.001$.

d. Clemens et al., 2015, Brain.

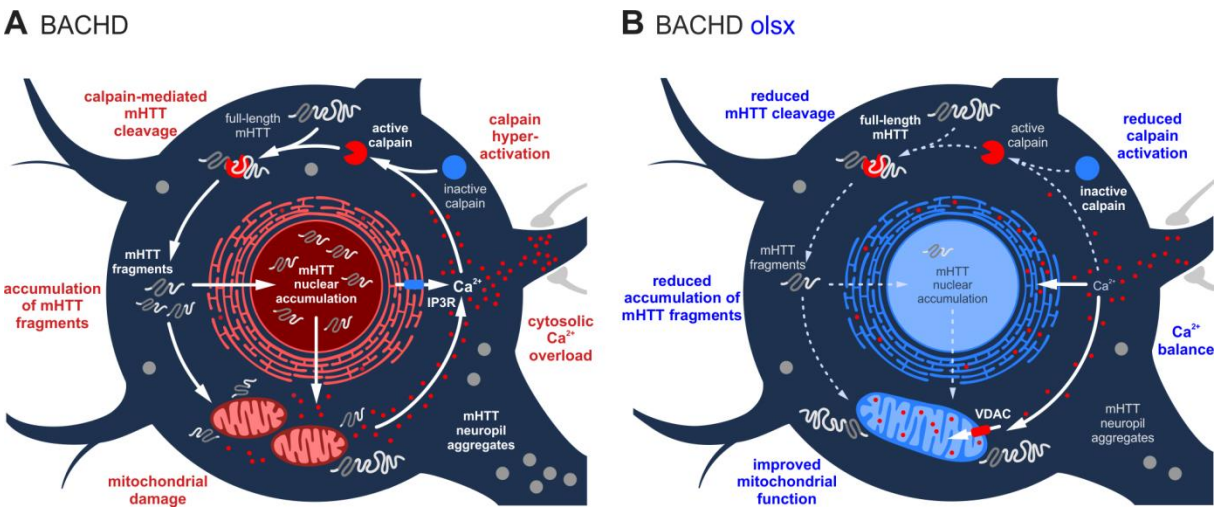

Figure 7: Schematic of the hypothetical Huntington disease-related pathology and beneficial effects of olesoxime, in a BACHD rat cortical neuron. (**A**) The presence of mHTT provokes an increase in cytosolic Ca^{2+}, leading to the overactivation of calpain, a major executer of mHTT cleavage in the BACHD rat. Enhanced calpain-mediated cleavage generates large amounts of mHTT fragments, which accumulate in cytosol and nucleus, and are recruited to form cytosolic and neuropil aggregates. Mutant HTT fragments impair mitochondrial function by transcriptional dysregulation and direct interaction, thereby reducing mitochondrial Ca^{2+}-buffering capacity, further elevating cytosolic Ca^{2+}-levels and fueling the vicious cycle. (**B**) Olesoxime interrupts this by improving mitochondrial function, reflected in increased respiratory activity, fusion protein and outer membrane transporter expression. This can in turn improve Ca^{2+} buffering, explaining the reduced calpain activation, mHTT cleavage and accumulation of mHTT fragments, as well as the decrease in cytosolic and neuropil aggregates seen in the current study.

Tables

Table 1: Expression levels of mitochondrial proteins. The table contains group means (mean), standard deviation (SD) and the number of animals analyzed (n). Individual values were related to β-actin levels and normalized to the mean expression of placebo-treated WT rats. Significant differences from 2way ANOVA and Fisher LSD posttest are indicated in bold for the comparisons * WT versus BACHD rats, # untreated versus treated WT and + untreated versus treated BACHD rats (in blue), with */#/+: $P < 0.05$; **/##/++: $P \leq 0.01$ and ***/###/+++: $P \leq 0.001$. Fusion: Mfn 1, Mfn 2, Opa 1. Fission: Drp 1, Fis 1, Matrix: citrate synthase (CS). Inner membrane: ATP synthase (ATP 5A). Outer membrane: translocase of the outer mitochondrial membrane (TOM 20).

		Cortex				**Striatum**			
		WT **placebo**	WT **olsx**	BACHD **placebo**	BACHD **olsx**	WT **placebo**	WT **olsx**	BACHD **placebo**	BACHD **olsx**
Mfn 1	*mean*	1,00	**1,33$^{\#\#}$**	**0,77***	**1,18^{++}**	1,00	1,66	1,10	0,96
	SD	0,18	0,11	0,16	0,14	0,32	0,36	0,57	0,71
	n	4	4	4	4	3	4	4	3
Mfn 2	*mean*	1,00	1,17	0,93	**1,87^{++}**	1,00	2,41	1,63	1,63
	SD	0,16	0,29	0,38	0,39	0,11	0,37	0,90	1,63
	n	4	4	4	4	3	4	4	3
Opa 1	*mean*	1,00	**1,84$^{\#\#}$**	0,96	**2,33^{+++}**	1,00	1,90	1,39	1,37
	SD	0,40	0,30	0,29	0,52	0,49	0,55	0,60	0,88
	n	4	4	4	4	3	4	4	3
Drp 1	*mean*	1,00	0,92	0,84	**0,52^{++}**	1,00	1,36	0,98	1,04
	SD	0,06	0,14	0,14	0,05	0,04	0,52	0,15	0,27
	n	4	4	4	4	3	4	4	4
Fis 1	*mean*	1,00	**1,40$^{\#}$**	1,23	1,17	1,00	**2,16$^{\#}$**	2,08	1,31
	SD	0,13	0,33	0,15	0,31	0,29	0,70	0,93	0,34
	n	4	4	4	4	3	4	4	3
CS	*mean*	1,00	**1,95$^{\#}$**	1,23	1,86	1,00	**1,64$^{\#}$**	1,11	0,94
	SD	0,56	0,94	0,33	0,22	0,11	0,36	0,33	0,22
	n	4	4	4	4	3	4	4	3
ATP 5A	*mean*	1,00	1,85	0,78	**3,20^{++}**	1,00	1,51	1,68	1,68
	SD	0,10	0,66	0,09	1,53	0,19	0,47	1,01	0,39
	n	4	4	4	4	3	4	4	3
TOM 20	*mean*	1,00	2,05	1,36	**3,19^{+}**	1,00	1,36	1,34	**8,24^{++}**
	SD	0,30	0,99	0,51	1,42	0,78	1,26	0,88	4,68
	n	4	4	4	4	4	4	4	4

e. Weber *et al.*, 2016, *Rare Diseases*.

“Jonasz J. Weber, Midea M. Ortiz Rios, Olaf Riess, Laura E. Clemens, Huu P. Nguyen (2016) The calpain-suppressing effects of olesoxime in Huntington’s disease. Rare Dis. 4(1): e1153778.” Available online at: http://dx.doi.org/10.1080/21675511.2016.1153778.

RARE DISEASES
2016, VOL. 4, NO. 1, e1153778 (9 pages)
http://dx.doi.org/10.1080/21675511.2016.1153778

Taylor & Francis
Taylor & Francis Group

ADDENDUM

OPEN ACCESS

The calpain-suppressing effects of olesoxime in Huntington's disease

Jonasz J. Weber[a,b], Midea M. Ortiz Rios[a,b], Olaf Riess[a,b], Laura E. Clemens[a,b,c,†], and Huu P. Nguyen[a,b,†]

[a]Institute of Medical Genetics and Applied Genomics, University of Tuebingen, Tuebingen, Germany; [b]Centre for Rare Diseases, University of Tuebingen, Tuebingen, Germany; [c]Current institution: QPS Austria, Grambach, Austria

ABSTRACT

Olesoxime, a small molecule drug candidate, has recently attracted attention due to its significant beneficial effects in models of several neurodegenerative disorders including Huntington's disease. Olesoxime's neuroprotective effects have been assumed to be conveyed through a direct, positive influence on mitochondrial function. In a long-term treatment study in BACHD rats, the latest rat model of Huntington's disease, olesoxime revealed a positive influence on mitochondrial function and improved specific behavioral and neuropathological phenotypes. Moreover, a novel target of the compound was discovered, as olesoxime was found to suppress the activation of the calpain proteolytic system, a major contributor to the cleavage of the disease-causing mutant huntingtin protein into toxic fragments, and key player in degenerative processes in general. Results from a second model of Huntington's disease, the *Hdh*^{Q111} knock-in mouse, confirm olesoxime's calpain-suppressing effects and support the therapeutic value of olesoxime for Huntington's disease and other disorders involving calpain overactivation.

ARTICLE HISTORY
Received 2 December 2015
Revised 25 January 2016
Accepted 4 February 2016

KEYWORDS
BACHD rat; calpain; *Hdh*^{Q111} knock-in mouse; huntingtin fragments; Huntington's disease; mutant huntingtin aggregates; neurodegeneration; olesoxime; polyglutamine diseases; proteolysis

The therapeutic compound olesoxime

Olesoxime is a cholesterol derivative, which was discovered in a small-molecule screen for neuroprotective compounds at Trophos SA, Marseille.[1] In the initial screening, primary motor neurons were deprived of serum, incubated in the presence or absence of olesoxime, and survival was monitored.[1] The screen revealed highly beneficial effects of the compound. Further assays on neurons subjected to other pathological stimuli all showed increased survival.[2]

Binding and localization analysis revealed that the compound concentrates at the site of mitochondria[2] and interacts with the voltage-dependent anion channel (VDAC)[3] as well as the translocator protein (TSPO)[4] on the outer mitochondrial membrane.[1] As these proteins are considered to play a role in mitochondrial permeability transition (mPT),[5] it was proposed that olesoxime's mechanism of neuroprotection was the inhibition of mPT and subsequent cell death.[1] In accordance with this idea, olesoxime was found to prevent cell death induced by various toxins[1,2,6] to a similar magnitude as cyclosporine A, a potent mPT inhibitor. Further studies discovered a variety of interesting aspects around olesoxime's molecular effects, but the exact mechanism of cytoprotection remained elusive. Olesoxime was reported to prevent cytochrome *c* release from mitochondria and the subsequent activation of caspases in the cytosol.[7] These effects did not seem to derive from improved mitochondrial Ca^{2+} handling or inhibition of Ca^{2+} release.[2] Olesoxime further did not directly inhibit caspases, activate prosurvival kinases or modulate the transcription of proapoptotic genes via the transcriptional regulator p53.[7] Besides the direct effect on the initiation of mitochondria-mediated apoptosis, olesoxime was found to promote microtubule-based neurite outgrowth and microtubule-dependent mitochondrial transport, specifically in differentiated neuronal cells,[8] and to improve oligodendrocyte-mediated remyelination.[9]

In vivo studies demonstrated consistently beneficial outcomes regarding neuroprotection and regeneration in animal models of motor neuron diseases[1,2,10] as well as neurodegenerative disorders,[2,9,11] and neuroprotective

CONTACT Huu P. Nguyen hoa.nguyen@med.uni-tuebingen.de University of Tuebingen, Institute of Medical Genetics and Applied Genomics, Calwerstrasse 7, 72076 Tuebingen, Germany.

Color versions of one or more of the figures in the article can be found online at www.tandfonline.com/krad.

Addendum to: Clemens LE, et al. Olesoxime suppresses calpain activation and mutant huntingtin fragmentation in the BACHD rat. Brain 2015; 138:3632-53; http://dx.doi.org/10.1093/brain/awv290

[†]These authors equally contributed to this work.

and antinociceptive effects in models of peripheral neuropathies.[8,12-14]

The therapeutic potential of olesoxime was further investigated in clinical trials on motor neuron diseases. Olesoxime showed excellent safety and tolerability in the patients.[2] Moreover, the treatment was easy to apply, as olesoxime reaches the brain in sufficient amount upon oral administration of one daily dose,[15] and therefore medication does not involve invasive or time-consuming procedures. Two trials, one on survival in end-stage amyotrophic lateral sclerosis (ALS) patients[15] and one on motor symptom onset in early stage spinal muscular atrophy (SMA) patients[16] were conducted. The ALS trial revealed a negative outcome, while the trial on SMA patients showed striking beneficial effects on the clinical end point, suggesting better efficacy of olesoxime in early phases of disease.

As *in vitro* data pointed to positive effects of cholesterol-oximes in Huntington's disease (HD),[17] and as mitochondrial dysfunction is considered to contribute substantially to the HD pathology,[18] it was considered to be of significant interest to investigate the potential therapeutic effects of olesoxime in an *in vivo* model of this disorder.

Main effects of olesoxime in the BACHD rat model of HD

BACHD rats were treated with olesoxime, supplied via the food, from the age of 5 weeks until the age of 13 months. The rats' behavior as well as their neuropathological phenotypes were investigated.[19]

Olesoxime-treated BACHD rats showed specific improvements in behavior and neuropathology compared to placebo-treated BACHD rats. These concerned the selective amelioration of cognitive and psychiatric abnormalities, increased cortical thickness and a significant reduction in the aggregation and nuclear accumulation of the disease-causing mutant huntingtin (HTT) protein throughout the brain. The drug effect appeared to be the result of reduced calpain-mediated proteolysis, which was found to be the main source of mutant and wild type HTT fragments in the BACHD rat. Furthermore, olesoxime seemed to have influenced mitochondria in several ways: Olesoxime treatment led to a restoration of respiratory function, reduced the association of HTT fragments with mitochondria and modulated the levels of several mitochondrial proteins involved in mitochondrial cholesterol import, metabolite exchange, respiratory chain function, Ca^{2+} homeostasis, calpain activation and mitochondrial dynamics. Thus, it was hypothesized that the compound had exerted its beneficial effects by improving mitochondrial function, thereby stabilizing Ca^{2+} homeostasis, decreasing Ca^{2+}-related calpain activation and aborting the generation of toxic HTT fragments, as well as their exaggerated negative influence on mitochondria.

Validation of olesoxime's effects in other models of HD

The beneficial effects of olesoxime in HD are not restricted to the BACHD rat model. Several analyses have been performed, or are ongoing, in the *Hdh*^{Q111} knock-in mouse[20] as well as in ST*Hdh*^{Q111} cells, a stable cell line derived from striatal progenitor cells of this mouse model[21] (Fig. 1). Evaluating olesoxime's effects in these models represents a relevant extension of the BACHD rat study in terms of validating the initial results and determining their general importance for HD. *Hdh*^{Q111} knock-in mice represent a particularly valuable model, as they provide a more precise reproduction of the human genetic conditions due to the polyQ mutation being inserted into the mouse huntingtin gene (*Hdh*). The intact genetic context as well expression of the mHTT protein on an endogenous level, result in a slow progressing phenotype, which might better resemble the symptoms observed in HD patients.[23]

Olesoxime has been found to restore abnormally high mitochondrial membrane fluidity not only in the BACHD rat, but also in *Hdh*^{Q111} knock-in mice and ST*Hdh*^{Q111} cells.[22] Moreover, olesoxime's prominent effects on calpain activation and HTT fragmentation reported for the BACHD rat could be reproduced in the *Hdh*$^{Q111/Q111}$ knock-in mouse (Fig. 2 and 3). Compared to wild type mice, 3 months old knock-in mice showed significantly increased levels of large and small fragments containing the N-terminal (Fig. 2A, *4C8 detection*) and/or middle (Fig. 2B, *D7F7 detection*) part of HTT. In addition, HTT aggregation was already moderately increased at this young age (Fig. 2C, *4C8 and 1C2 detections*), all of which is indicative of enhanced HTT cleavage. In accordance with this, as well as in line with the results obtained from BACHD rats,[19] calpain-1 was found to be

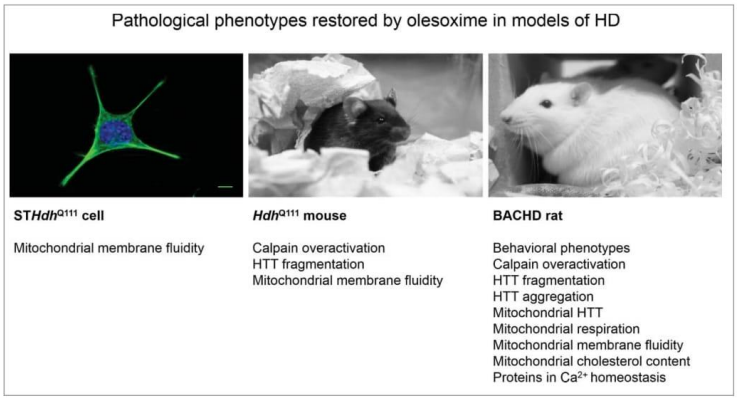

Figure 1. Overview of pathological phenotypes restored by olesoxime in models of HD. The effect of olesoxime on pathological phenotypes has been studied in 3 models of HD: the ST*Hdh*^{Q111} cell line, the *Hdh*^{Q111} knock-in mouse and the BACHD rat.

overactivated in the knock-in mice, as demonstrated by an increased ratio of fully processed to processed calpain-1, increased levels of the cleaved form of the calpain substrate α (alpha)-spectrin, see labeling in Fig. 3A as well as reduced levels of its endogenous inhibitor calpastatin (Fig. 3A). A possible reason for this overactivation could be intracellular Ca^{2+} derangements, as elevated protein levels of IP3R 1 were detected as well (Fig. 3B).

Olesoxime treatment, which had been started prenatally, via feeding the dams with olesoxime-loaded diet, significantly reduced both HTT fragmentation (Fig. 2A and B) and calpain overactivation (Fig. 3A), similar as in the BACHD rat.[19] Other effects found in the rats, such as reduced HTT aggregation, as well as reduced IP3R 1 and increased VDAC 1 and TOM20 levels,[19] did not reach statistical significance in the knock-in mice, although trends were apparent (Fig. 3B). This might be ascribed to the fact that these phenotypes were mostly not very strong from the start.

Additional insight into the causal relationship between olesoxime's effects on mitochondrial function, Ca^{2+} homeostasis, calpain activation, HTT fragmentation and HTT aggregation might be gained by studying the compound's therapeutic effects in a fragment model of HD. Due to the constitutive expression of mHTT fragments through the transgene in such a model, the effects on HTT fragment generation can be assumed to be marginal, potentially enabling the dissection of direct effects of olesoxime on mitochondrial function from indirect treatment effects via reduced fragment generation.

Olesoxime's mechanism of action

Although Ca^{2+} levels or Ca^{2+} handling were not directly measured in our studies, the overactivation of the Ca^{2+}-dependent protease calpain-1 (Fig. 2) as well as the increased protein levels of the endoplasmic reticulum Ca^{2+} exporter IP3R 1 in BACHD rats[19] and *Hdh*^{Q111} knock-in mice (Fig. 3) suggest a baseline disturbance of Ca^{2+} homeostasis in these models. The ameliorating effects of olesoxime on these parameters (although only in trend for IP3R 1 levels in *Hdh*^{Q111} knock-in mice) further support the idea that Ca^{2+} homeostasis is somehow involved in olesoxime's mechanism of action. The direct effects of olesoxime on Ca^{2+} balance are currently under investigation in several HD cell models including the ST*Hdh*$^{Q111/Q111}$ cell line.

Brain region-selective effects of olesoxime

Olesoxime was found to ameliorate deficits, which were restricted to the cortex and not present in the striatum of the BACHD rat.[19] The absence of increased IP3R 1 levels, calpain-1 overactivation and extensive HTT fragmentation in the striatum were interpreted as an indicator of a compensatory reduction in Ca^{2+} sensitivity in this brain region, since this had been reported earlier for HD mouse models including the *Hdh*^{Q111} knock-in mouse. [24]

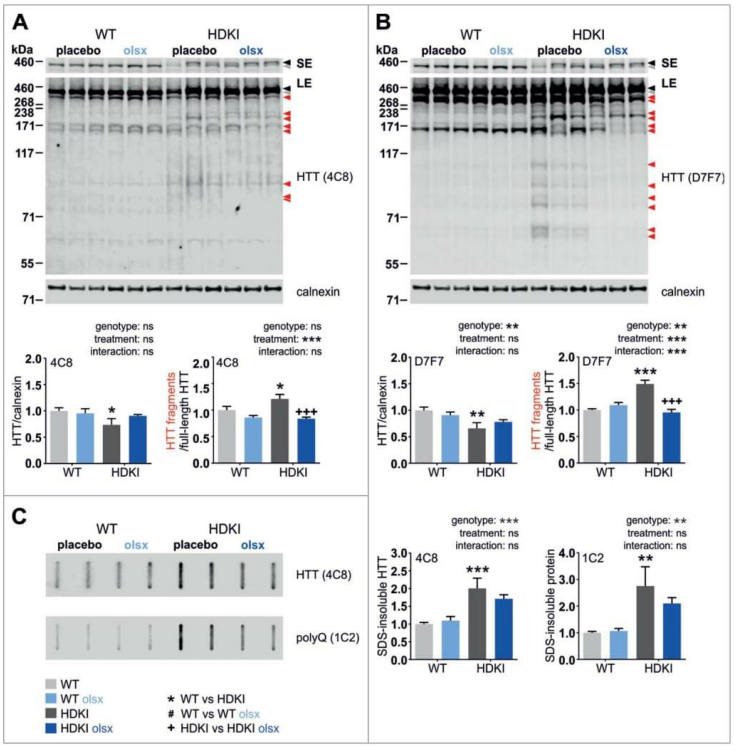

Figure 2. Olesoxime treatment reduces mHTT fragmentation in *Hdh*^{Q111} knock-in mice. Effects of olesoxime on HTT fragmentation were analyzed by western blotting of half brain lysates from 3 months old wild type (WT) and heterozygous *Hdh*^{Q111} knock-in mice (HDKI) receiving placebo or olesoxime-loaded diet (olsx). Full-length and fragment forms of HTT were assessed using the HTT-specific antibodies 4C8 (A) and D7F7 (B). Black arrowheads: full-length mHTT, gray arrowhead: full-length HTT, red arrowheads: HTT fragments, calnexin: loading control. SE: short exposure; LE: long exposure. (**C**) SDS-insoluble proteins were trapped on a nitrocellulose membrane and probed with the HTT-specific antibody 4C8 or the polyQ-specific antibody 1C2 to quantify the amount of aggregated HTT. Data were analyzed using 2-way ANOVA and Fisher LSD posttest; $^{*}/^{\#}/^{+}$: $P < 0.05$; $^{**}/^{\#\#}/^{++}$: $P \leq 0.01$ and $^{***}/^{\#\#\#}/^{+++}$: $P \leq 0.001$.

Data from 6 months old knock-in mice show that calpain overactivation is specifically found in the striatum and not in the cortex of these animals, as an increased ratio of fully processed to processed calpain-1 as well as increased levels of the cleaved form of alpha-spectrin (see comment above or Fig. 3A) were found to be restricted to the striatum (Fig. 4). Further analysis of samples from 12 months old mice is still outstanding and will reveal, if the phenotype is reversed to cortical instead of striatal calpain overactivation at this older age, and then resembles the results obtained from BACHD rats. In line with the increased striatal calpain activation, mutant HTT aggregates are also predominantly detected in the striatum and not in the cortex at earlier ages in the *Hdh*^{Q111} knock-in mice (unpublished data).

Importantly, the fact that olesoxime treatment was effective in restoring calpain overactivation in the striatum of *Hdh*^{Q111} knock-in mice, suggests that the compound is capable of affecting this pathology independent of the brain region it is found in at a given time or in a given animal model.

Phenotype-Specific effects of olesoxime

Olesoxime had failed to ameliorate some pathological phenotypes in the BACHD rat. Pathologies with particularly early onset, such as Rotarod performance[25]

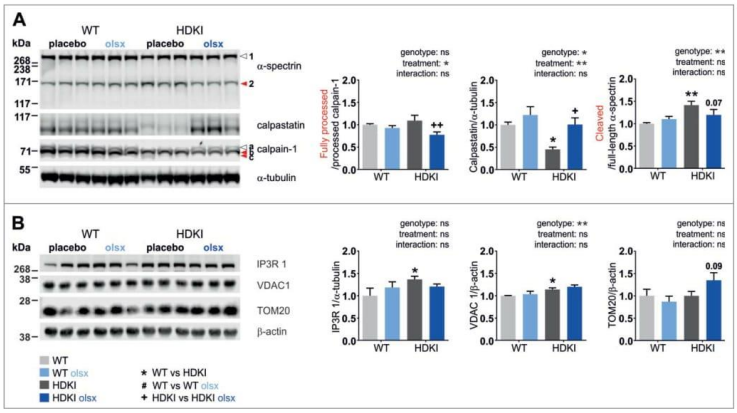

Figure 3. The calpain-suppressing effects of olesoxime are replicated in *Hdh*^{Q111} knock-in mice. The calpain-suppressing effects of olesoxime were investigated by protein gel blot analysis of half brain lysate from 3 months old wild type (WT) and heterozygous *Hdh*^{Q111} knock-in mice (HDKI) receiving placebo or olesoxime-loaded diet (olsx). (A) Calpain activation was assessed based on the processing of calpain-1, protein levels of the endogenous calpain inhibitor calpastatin and the cleavage of the calpain substrate α-spectrin. Arrowhead 1: full-length α-spectrin, arrowhead 2: α-spectrin fragment, arrowhead a: full-length calpain-1, arrowhead b: processed calpain-1, arrowhead c: fully processed calpain-1 (active calpain-1 refers to the ratio c/b), α-tubulin: loading control. (B) Expression levels of the endoplasmic reticulum Ca^{2+} transporter IP3R 1, outer mitochondrial membrane channel VDAC 1 and mitochondrial import receptor subunit TOM20 were assayed. β-actin: loading control. Data were analyzed using 2-way ANOVA and Fisher LSD posttest; $^{*}/^{\#}/^{+}$: $P < 0.05$; $^{**}/^{\#\#}/^{++}$: $P \leq 0.01$ and $^{***}/^{\#\#\#}/^{+++}$: $P \leq 0.001$.

or whole brain size (which correlates with reduced body length due to a developmental deficit[26]), did not show improvement upon olesoxime treatment. However, it is possible that the compound is not *per se* incapable of restoring such phenotypes, but that the treatment might have simply started too late to reverse

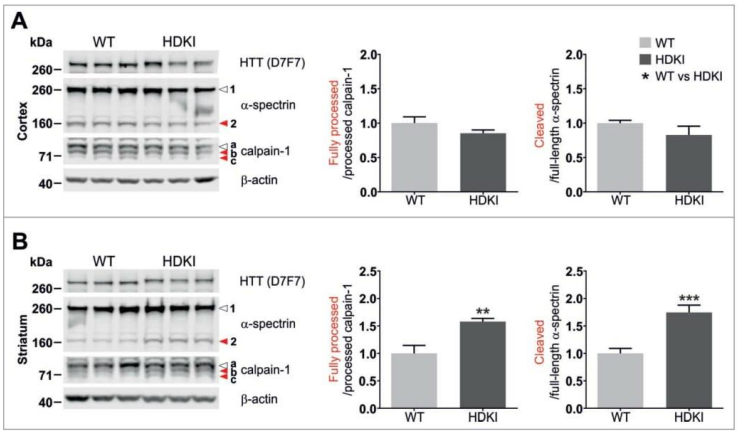

Figure 4. Calpain overactivation is restricted to the striatum in 6 months old *Hdh*^{Q111} knock-in mice. Calpain activation was assessed by western blot analysis of cortical (A) and striatal (B) lysates from 6 months old wild type (WT) and homozygous *Hdh*^{Q111} knock-in mice (HDKI), based on the processing of calpain-1 and the cleavage of its substrate α-spectrin. Arrowhead 1: full-length α-spectrin, arrowhead 2: α-spectrin fragment, arrowhead a: full-length calpain-1, arrowhead b: processed calpain-1, arrowhead c: fully processed calpain-1 (active calpain-1 refers to the ratio c/b), β-actin: loading control. Data were analyzed using unpaired Student's *t*-test; $^{*}/^{\#}/^{+}$: $P < 0.05$; **: $P \leq 0.01$ and ***: $P \leq 0.001$.

pathologies that were already manifest. In this regard, olesoxime treatment of late stage ALS patients did not yield significant improvements,[15] while treatment of children and young patients with SMA had significant, beneficial effects.[16] Also, the compound was highly effective in preclinical studies on ALS models, in which treatment had started early.[10] These findings might indicate that olesoxime is most effective when applied at earliest stages of disease, although it is clear that the direct comparison of preclinical and clinical outcomes from two different diseases is difficult. Therefore, it would be of particular interest to investigate the specific effects of an earlier start of olesoxime treatment on phenotypes that were not ameliorated by the later onset of treatment in the BACHD rat.

Earliest start of treatment was achieved in the Hdh^{Q111} knock-in mouse by feeding olesoxime already to the parental animals during breeding, as the drug crosses the placental barrier and is secreted into the dam's milk (Rebecca Pruss, personal communication). The data further demonstrate that calpain overactivation is an early phenotype, and that olesoxime effectively suppresses this pathology also after shorter treatment duration.

Summary and conclusion

The new data confirm that olesoxime suppresses calpain activation and HTT fragmentation *in vivo*, and strengthen its potential as a treatment for HD. Olesoxime had been presumed to improve mitochondrial function and, through this, restore Ca^{2+} balance as well as downstream pathological events. Deciphering olesoxime's exact mechanism of action might be of great value for the understanding of neurodegenerative processes and the development of effective treatments, also, but not only, for HD.

Methods

Ethical statement

All experiments described herein involving animals were carried out by persons with appropriate training and expertise. Operating procedures were approved by the local ethics committees and carried out in accordance with the guidelines of the Federation of European Laboratory Animal Science Associations and the German Animal Welfare Act, based on European Union legislation (Directive 2010/63/EU).

Animals

Hdh^{Q111} knock-in mice were kindly provided by Dr. Marcy MacDonald (Harvard Medical School, Boston, USA) and bred on C57BL/6 background for more than 10 generations in our laboratory.

The mice were kept under controlled environmental conditions of 21–23°C ambient temperature, 55 +/− 10 % humidity and a 12/12 h light/dark cycle, in groups of same sex in standard type III autoclavable plastic cages with wooden bedding and nesting material. Food and tap water were delivered *ad libitum*.

In order to investigate the effect of olesoxime on calpain activation in Hdh^{Q111} knock-in mice, breeding pairs of wild type and heterozygous Hdh^{Q111} knock-in mice received either placebo or olesoxime-loaded food pellets (Altromin C1000, 0.6 g/kg olesoxime). Offspring from these breeding pairs was weaned and genotyped at 21 days of age, and maintained on the respective diet. Five mice per genotype and treatment, of mixed sex, were sacrificed at 3 months of age for *ex vivo* analyses.

To study brain region-specific calpain activation in Hdh^{Q111} knock-in mice, 6 homozygous mice were sacrificed at the age of 6 months.

Brain tissue sampling

The animals were sacrificed by CO_2 inhalation. Brains were immediately dissected on ice and whole brain, or brain regions, were sampled. Tissue was shock-frozen in liquid nitrogen and stored at −80°C. Tissue sampling was performed within 2 hours during the late light phase to minimize variation based on any circadian phase-related changes.

Immunoblotting

Immunoblotting was performed with half brain lysates from 3 months old mice (olesoxime effect on calpain activation) or striatal and cortical lysates from 6 months old mice (region-specific calpain activation). For the former, mouse brains previously stored at −80°C were first placed on dry ice and cut in half along the medial longitudinal fissure. Half brains were then thawed and homogenized on ice in RIPA buffer (50 mM Tris, 150 mM NaCl, 1% Triton X-100, pH 7.5) containing protease inhibitors (cOmplete® Protease Inhibitor

Cocktail, Roche). Homogenates were diluted 1:10 in RIPA detergent (5% sodium deoxycholate and 1% sodium dodecyl sulfate in RIPA buffer, pH 7.5) and incubated for 25 min at 4°C. For preparation of the half brain lysates, homogenates were centrifuged for 15 min at 16,100 *g*. The supernatant was collected and stored at −80°C containing 10% glycerol. Striatal and cortical lysates were generated by homogenizing the respective tissue on ice in TES buffer (50 mM Tris, 2 mM EDTA, 100 mM NaCl, pH 7.5) containing protease inhibitors (cOmplete® Protease Inhibitor Cocktail, Roche). Homogenates were diluted 1:10 in TNES buffer (90% TES buffer, 10% Igepal CA630), incubated for 1 h at 4°C and centrifuged twice for 30 min at 16,100 *g*. The supernatant was collected and stored at −80°C containing 10% glycerol.

At the time of immunoblotting, all samples were thawed on ice and the protein concentration was measured spectrophotometrically using Bradford reagent. Western blot analysis was performed according to standard procedures. Briefly, 30 μg of lysate protein were assayed by SDS-PAGE using homemade Bis-Tris polyacrylamide gels or purchased Bolt® Bis-Tris or NuPAGE® Tris-Acetate gels (Life Technologies). Proteins were transferred on nitrocellulose membranes and probed overnight at 4°C with the respective primary antibody: mouse anti-β-actin (1:10,000; clone AC-15, A5441, Sigma Aldrich), rabbit anti-calnexin (1:1000; C4731, Sigma Aldrich) rabbit anti-calpain-1 (1:1000; ab39170, Abcam), rabbit anti-calpastatin (1:1000; 4146, Cell Signaling), rabbit anti-huntingtin (1:1000; clone D7F7, #5656, Cell Signaling), mouse anti-huntingtin (1:500; clone 4C8, MAB2166, EMD Millipore), rabbit anti-IP3R 1 (1:1000; ab5804; Abcam), mouse anti-polyglutamine-expansion diseases marker (1:1000; clone 5TF1-1C, MAB1574, EMD Millipore), mouse anti-α-spectrin (1:1000; clone AA6, EMD Millipore), rabbit anti-TOM20 (1:500; sc-11415, Santa Cruz), mouse anti-α-tubulin (1:5000; clone DM1A, CP06, EMD Millipore), and rabbit anti-VDAC1 (1:10,000; AB10527, EMD Millipore). One hour of incubation with a respective HRP-conjugated secondary (sheep anti-mouse or donkey anti-rabbit 1:2500, GE Healthcare) or IRDye® antibody (goat anti-mouse, donkey anti-mouse or goat anti-rabbit, 1:10,000; LI-COR Biosciences) at room temperature followed. Chemiluminescence and fluorescence signals were detected with the LI-COR ODYSSEY FC Imaging system (LI-COR Biosciences). Protein levels were quantified by densitometry using Image Studio™ Lite software version. 4.0 (LI-COR Biosciences) or ImageJ[27].

Filter retardation assay

For the detection of SDS-insoluble HTT species, 25 μg homogenate protein were diluted in 100 μl DPBS (Life Technologies) with 2% SDS and 50 mM DTT, and incubated for 5 min at 95°C. A nitrocellulose membrane (0.45 μm; Bio-Rad) was equilibrated in 0.1% SDS in DPBS and samples were filtered through this membrane using a Minifold II Slot Blot System (Schleicher & Schuell). The membrane was then washed twice with TBS and blocked with 5% SlimFast (Unilever) in TBS for 1 h at room temperature. Retained SDS-insoluble HTT was detected using the primary antibodies mouse anti-HTT (1:1000; clone 1HU-4C8, MAB2166, EMD Millipore) and mouse anti-polyglutamine-expansion diseases marker (1:1000; clone 5TF1-1C, MAB1574, EMD Millipore) as well as respective anti-mouse IRDye® 800CW secondary antibodies (1:10,000; LI-COR Biosciences). Fluorescence signals were detected with the LI-COR ODYSSEY FC Imaging system and quantified using the ODYSSEY® Server software version 4.1 (both LI-COR Biosciences).

Abbreviations

BACHD rat — Huntington's disease rat model expressing full-length mutant huntingtin from a bacterial artificial chromosome

Disclosure of potential conflicts of interest

No potential conflicts of interest were disclosed.

Acknowledgments

We are grateful to all collaborators from past and present studies on the potential benefits of olesoxime as a treatment for HD.

Funding

LEC, OR and HPN received grants by the European Union 7th Framework Program for RTD, Project MitoTarget, Grant Agreement HEALTH-F2-2008-223388, and JJW was funded by the Baden-Wuerttemberg Foundation, Research Grant Number P-BWS-SPII/3-08.

References

[1] Bordet T, Buisson B, Michaud M, Drouot C, Galéa P, Delaage P, Akentieva NP, Evers AS, Covey DF, Ostuni M A, et al. Identification and characterization of cholest-4-en-3-one, oxime (TRO19622), a novel drug candidate for amyotrophic lateral sclerosis. J Pharmacol Exp Ther [Internet] 2007; 322:709-20. Available from: http://www.ncbi.nlm.nih.gov/pubmed/17496168; PMID:17496168; http://dx.doi.org/10.1124/jpet.107.123000

[2] Bordet T, Berna P, Abitbol JL, Pruss RM. Olesoxime (TRO19622): A novel mitochondrial-targeted neuroprotective compound. Pharmaceuticals 2010; 3:345-68; http://dx.doi.org/10.3390/ph3020345

[3] Colombini M. VDAC: the channel at the interface between mitochondria and the cytosol. Mol Cell Biochem 256-257:107-15; PMID:14977174

[4] Gatliff J, Campanella M. The 18 kDa translocator protein (TSPO): a new perspective in mitochondrial biology. Curr Mol Med 2012; 12:356-68; PMID:22364127

[5] Veenman L, Shandalov Y, Gavish M. VDAC activation by the 18 kDa translocator protein (TSPO), implications for apoptosis. J Bioenerg Biomembr 2008; 40:199-205; PMID:18670869; http://dx.doi.org/10.1007/s10863-008-9142-1

[6] Gouarné C, Tracz J, Paoli MG, Deluca V, Seimandi M, Tardif G, Xilouri M, Stefanis L, Bordet T, Pruss RM. Protective role of olesoxime against wild-type α-synuclein-induced toxicity in human neuronally differentiated SHSY-5Y cells. Br J Pharmacol [Internet] 2015; 172:235-45. Available from: http://doi.wiley.com/10.1111/bph.12939; PMID: 25220617; http://dx.doi.org/10.1111/bph.12939

[7] Gouarné C, Giraudon-Paoli M, Seimandi M, Biscarrat C, Tardif G, Pruss RM, Bordet T. Olesoxime protects embryonic cortical neurons from camptothecin intoxication by a mechanism distinct from BDNF. Br J Pharmacol 2013; 168:1975-88; PMID:23278424; http://dx.doi.org/10.1111/bph.12094

[8] Rovini A, Carré M, Bordet T, Pruss RM, Braguer D. Olesoxime prevents microtubule-targeting drug neurotoxicity: selective preservation of EB comets in differentiated neuronal cells. Biochem Pharmacol 2010; 80:884-94; PMID:20417191; http://dx.doi.org/10.1016/j.bcp.2010.04.018

[9] Magalon K, Zimmer C, Cayre M, Khaldi J, Bourbon C, Robles I, Tardif G, Viola A, Pruss RM, Bordet T, et al. Olesoxime accelerates myelination and promotes repair in models of demyelination. Ann Neurol 2012; 71:213-26; PMID:22367994; http://dx.doi.org/10.1002/ana.22593

[10] Sunyach C, Michaud M, Arnoux T, Bernard-Marissal N, Aebischer J, Latyszenok V, Gouarné C, Raoul C, Pruss RM, Bordet T, et al. Olesoxime delays muscle denervation, astrogliosis, microglial activation and motoneuron death in an ALS mouse model. Neuropharmacology 2012; 62:2346-52; PMID:22369784; http://dx.doi.org/10.1016/j.neuropharm.2012.02.013

[11] Richter F, Gao F, Medvedeva V, Lee P, Bove N, Fleming SM, Michaud M, Lemesre V, Patassini S, De La Rosa K, et al. Chronic administration of cholesterol oximes in mice increases transcription of cytoprotective genes and improves transcriptome alterations induced by alpha-synuclein overexpression in nigrostriatal dopaminergic neurons. Neurobiol Dis 2014; 69:263-75; PMID:24844147; http://dx.doi.org/10.1016/j.nbd.2014.05.012

[12] Bordet T, Buisson B, Michaud M, Abitbol J-L, Marchand F, Grist J, Andriambeloson E, Malcangio M, Pruss RM. Specific antinociceptive activity of cholest-4-en-3-one, oxime (TRO19622) in experimental models of painful diabetic and chemotherapy-induced neuropathy. J Pharmacol Exp Ther 2008; 326:623-32; PMID:18492948; http://dx.doi.org/10.1124/jpet.108.139410

[13] Xiao WH, Zheng FY, Bennett GJ, Bordet T, Pruss RM. Olesoxime (cholest-4-en-3-one, oxime): analgesic and neuroprotective effects in a rat model of painful peripheral neuropathy produced by the chemotherapeutic agent, paclitaxel. Pain 2009; 147:202-9; PMID:19833436; http://dx.doi.org/10.1016/j.pain.2009.09.006

[14] Xiao WH, Zheng H, Bennett GJ. Characterization of oxaliplatin-induced chronic painful peripheral neuropathy in the rat and comparison with the neuropathy induced by paclitaxel. Neuroscience 2012; 203:194-206; PMID:22200546; http://dx.doi.org/10.1016/j.neuroscience.2011.12.023

[15] Lenglet T, Lacomblez L, Abitbol JL, Ludolph a., Mora JS, Robberecht W, Shaw PJ, Pruss RM, Cuvier V, Meininger V. A phase II-III trial of olesoxime in subjects with amyotrophic lateral sclerosis. Eur J Neurol 2014; 21:529-36; PMID:24447620; http://dx.doi.org/10.1111/ene.12344

[16] Dessaud E, Carole A, Bruno S, Patrick B, Rebecca P, Cuvier V, Hauke W, Enrico B, Mcdonald C, Watson C, et al. A Phase II study to assess safety and efficacy of olesoxime (TRO19622) in 3-25 year-old Spinal Muscular Atrophy (SMA) patients. Neurol Emerg Abstr 2014; 83:e34-40

[17] Valenza M, Rigamonti D, Goffredo D, Zuccato C, Fenu S, Jamot L, Strand A, Tarditi A, Woodman B, Racchi M, et al. Dysfunction of the cholesterol biosynthetic pathway in Huntington's disease. J Neurosci 2005; 25:9932-9; PMID:16251441; http://dx.doi.org/10.1523/JNEUROSCI.3355-05.2005

[18] Browne SE. Mitochondria and Huntington's disease pathogenesis: insight from genetic and chemical models. Ann N Y Acad Sci 2008; 1147:358-82; PMID:19076457; http://dx.doi.org/10.1196/annals.1427.018

[19] Clemens LE, Weber JJ, Wlodkowski TT, Yu-Taeger L, Michaud M, Calaminus C, Eckert SH, Gaca J, Weiss A, Magg JCD, et al. Olesoxime suppresses calpain activation and mutant huntingtin fragmentation in the BACHD rat. Brain 2015; 138:3632-53; http://dx.doi.org/10.1093/brain/awv290

[20] Wheeler VC, White JK, Gutekunst CA, Vrbanac V, Weaver M, Li XJ, Li SH, Yi H, Vonsattel JP, Gusella JF, et al. Long glutamine tracts cause nuclear localization of

a novel form of huntingtin in medium spiny striatal neurons in HdhQ92 and HdhQ111 knock-in mice. Hum Mol Genet 2000; 9:503-13; PMID:10699173; http://dx.doi.org/10.1093/hmg/9.4.503

[21] Trettel F, Rigamonti D, Hilditch-Maguire P, Wheeler VC, Sharp a H, Persichetti F, Cattaneo E, MacDonald ME. Dominant phenotypes produced by the HD mutation in STHdh(Q111) striatal cells. Hum Mol Genet 2000; 9:2799-809; PMID:11092756; http://dx.doi.org/10.1093/hmg/9.19.2799

[22] Eckmann J, Clemens LE, Eckert SH, Hagl S, Yu-Taeger L, Bordet T, Pruss RM, Muller WE, Leuner K, Nguyen HP, et al. Mitochondrial membrane fluidity is consistently increased in different models of huntington disease: restorative effects of olesoxime. Mol Neurobiol 2014; 50:107-18; PMID:24633813

[23] Menalled LB. Knock-in mouse models of Huntington's disease. NeuroRx 2005; 2:465-70; PMID:16389309; http://dx.doi.org/10.1602/neurorx.2.3.465

[24] Brustovetsky N, LaFrance R, Purl KJ, Brustovetsky T, Keene CD, Low WC, Dubinsky JM. Age-dependent changes in the calcium sensitivity of striatal mitochondria in mouse models of Huntington's Disease. J Neurochem 2005; 93:1361-70; PMID:15935052; http://dx.doi.org/10.1111/j.1471-4159.2005.03036.x

[25] Yu-Taeger L, Petrasch-Parwez E, Osmand AP, Redensek A, Metzger S, Clemens LE, Park L, Howland D, Calaminus C, Gu X, et al. A novel BACHD transgenic rat exhibits characteristic neuropathological features of huntington disease. J Neurosci 2012; 32:15426-38; PMID:23115180; http://dx.doi.org/10.1523/JNEUROSCI.1148-12.2012

[26] Jansson EKH, Clemens LE, Riess O, Nguyen HP. Reduced motivation in the BACHD rat model of huntington disease is dependent on the choice of food deprivation strategy. PLoS One 2014; 9:e105662; PMID:25144554; http://dx.doi.org/10.1371/journal.pone.0105662

[27] Abràmoff MD, Magalhães PJ, Sunanda J. Image processing with ImageJ. Biophotonics Int 2004; 11:36-42.

f. Schmidt *et al.*, 2016, *Journal of Neurochemistry*.

Journal of Neurochemistry JNC

JOURNAL OF NEUROCHEMISTRY | 2016 | 138 | 150–162 doi: 10.1111/jnc.13606

ORIGINAL ARTICLE

In vivo assessment of riluzole as a potential therapeutic drug for spinocerebellar ataxia type 3

Jana Schmidt,[1] Thorsten Schmidt,[1] Matthias Golla, Lisa Lehmann, Jonasz Jeremiasz Weber, Jeannette Hübener-Schmid and Olaf Riess

Institute of Medical Genetics and Applied Genomics and Center for Rare Diseases, University of Tuebingen, Tuebingen, Germany

Abstract

Spinocerebellar ataxia type 3 (SCA3) is an autosomal dominantly inherited neurodegenerative disorder for which no curative therapy is available. The cause of this disease is the expansion of a CAG repeat in the so-called *ATXN3* gene leading to an expanded polyglutamine stretch in the ataxin-3 protein. Although the function of ataxin-3 has been defined as a deubiquitinating enzyme, the pathogenic pathway underlying SCA3 remains to be deciphered. Besides others, also the glutamatergic system seems to be altered in SCA3. The antiglutamatergic substance riluzole has thus been suggested as a potential therapeutic agent for SCA3. To assess whether riluzole is effective in the treatment of SCA3 *in vivo*, we used a phenotypically well-characterized conditional mouse model previously generated by us. Treatment with 10 mg/kg riluzole in the drinking water was started when mice showed impairment in rotarod performance. Post-symptomatic treatment with riluzole carried out for a period of 10 months led to reduction of the soluble ataxin-3 level and an increase in ataxin-3 positive accumulations, but did not improve motor deficits measured by rotarod. There was also no positive effect on home cage behavior or body weight. We even observed a pronounced reduction of calbindin expression in Purkinje cells in riluzole-treated mice. Thus, long-term treatment with riluzole was not able to alleviate disease symptoms observed in transgenic SCA3 mice and should be considered with caution in the treatment of human patients.

Keywords: mouse model, polyglutamine disease, riluzole, spinocerebellar ataxia type 3.

J. Neurochem. (2016) **138**, 150–162.

Spinocerebellar ataxia type 3, also known as Machado–Joseph disease (MJD), is the most common autosomal dominantly inherited ataxia worldwide (Riess *et al.* 2008). The cause of this neurodegenerative disease is the expansion of a CAG repeat in the *ATXN3* gene, leading to an expanded polyglutamine tract in the ataxin-3 protein. Hence, spinocerebellar ataxia type 3 (SCA3) belongs to the group of so-called polyglutamine diseases comprising nine disorders [spinocerebellar ataxia type 1, 2, 3, 6, 7 and 17, Huntington's disease (HD), dentatorubralpallidoluysian atrophy and spinal and bulbar muscular atrophy] (Gatchel and Zoghbi 2005).

Brain regions affected by neuronal loss include mainly the cerebellum, pontine nuclei, substantia nigra, striatum, thalamus, and spinal cord. Dysfunction and degeneration in these regions lead to a wide range of symptoms including progressive ataxia, spasticity, dystonia, dysarthria, ophthalmoplegia, and neuropathy (reviewed in Matos *et al.* 2011). As of yet, no curative therapy for this devastating disease exists.

Received August 13, 2015; revised manuscript received February 25, 2016; accepted February 26, 2016.

Address correspondence and reprint requests to Thorsten Schmidt, PhD, Institute of Medical Genetics and Applied Genomics, University of Tuebingen, Calwerstrasse 7, 72076 Tuebingen, Germany. E-mail: thorsten.schmidt@med.uni-tuebingen.de

[1]These authors contributed equally to this work.

Abbreviations used: ALS, amyotrophic lateral sclerosis; ATXN3, ataxin-3; con, control; con-rilu, control with riluzole; DRPLA, dentatorubralpallidoluysian atrophy; dtg, double transgenic; dtg-rilu, double transgenic with riluzole; eg, endogenous; FALS, familial amyotrophic lateral sclerosis; HD, Huntington's disease; ICARS, International Cooperative Ataxia Rating Scale; MJD, Machado-Joseph disease; NMDA, *N*-methyl-D-aspartate; pmn, progressive motor neuropathy; PrP, prion protein promoter; SBMA, spinal and bulbar muscular atrophy; SCA1, 3, 7, spinocerebellar ataxia type 1, 3, 7; SDHA, succinate dehydrogenase complex; SPF, specific pathogen free; TBP, TATA-binding protein; tg, transgenic; TRE, tetracycline responsive element; TR-FRET, time-resolved Förster resonance energy transfer; tTA, tetracycline transactivator; YWHAZ, tyrosine 3-monooxygenase/tryptophan 5-monooxygenase activation protein zeta.

The pathogenesis of SCA3 is widely unknown. In particular, processes that lead to neurodegeneration still need to be defined. Several hypotheses have been published, mostly based on cell cultures. Besides altered protein degradation (Chai *et al.* 1999; Schmidt *et al.* 2002), transcriptional dysregulation (Chai *et al.* 2001, 2002; Chou *et al.* 2008), and mitochondrial dysfunction (Tsai *et al.* 2004; Yu *et al.* 2009) also an impaired glutamate transmission has been identified in SCA3 (Chou *et al.* 2008; Koch *et al.* 2011; Konno *et al.* 2014). This has led researchers to investigate whether targeting the glutamatergic pathway could be an option to treat SCA3. In a randomized, double-blind, placebo-controlled pilot study, it has been demonstrated that the antiglutamatergic drug riluzole has a beneficial impact on patients with cerebellar ataxia of different etiologies (Ristori *et al.* 2010). After a period of only 8 weeks of riluzole treatment, a reduction of ICARS scores (International Cooperative Ataxia Rating Scale, Trouillas *et al.* 1997) by at least five points was observed. Thus, the authors suggest riluzole as a potential symptomatic therapy for cerebellar ataxias (Ristori *et al.* 2010). However, none of the patients in this trial suffered from SCA3. A recently published study by the same group, conducted over a longer period (12 months), achieved comparable results (Romano *et al.* 2015), but it is not clear whether SCA3 patients were included.

Riluzole has a broad variety of actions, including the inhibition of glutamate release from nerve terminals by inactivation of voltage-gated sodium channels and blockade of NMDA receptors, a subtype of glutamate receptors (Doble 1996; Danbolt 2001). Riluzole was also proven to open small conductance Ca^{2+}-activated potassium channels (Cao *et al.* 2002). In several studies, neuroprotective actions of riluzole have been investigated (Martin *et al.* 1993; Hubert *et al.* 1994; Albo *et al.* 2004; Wang *et al.* 2004).

In HD, as SCA3 also caused by polyglutamine expansion, riluzole inhibits huntingtin aggregate formation in cell-free systems, cell culture, as well as in primary neuronal cultures (Heiser *et al.* 2002; Hockly *et al.* 2006; Ortega *et al.* 2010). However, in a mouse model of spinocerebellar ataxia type 1 (SCA1) ($SCA1^{154Q}$), no attenuation of motor deficits measured by rotarod was observed (Nag *et al.* 2013).

For preclinical testing of potential beneficial effects of riluzole in SCA3, we used an inducible mouse model for SCA3 previously generated and characterized by us (Boy *et al.* 2009). Applying the Tet-Off system (Gossen and Bujard 1992) under the control of a prion protein promoter (Prp, Tremblay *et al.* 1998), leading to strong expression of the transgene in the cerebellum (Boy *et al.* 2006, 2009; Nuber *et al.* 2008), double transgenic mice of this model develop a phenotype resembling that of human patients of SCA3. Mice show a progressive neurological phenotype characterized by hyperactivity, reduced anxiety, impaired motor learning, weak rotarod performance, reduced weight, and intranuclear inclusion bodies (Boy *et al.* 2009).

In this study, treatment with 10 mg/kg riluzole in the drinking water over a period of 10 months was unable to alter the motor phenotype of double transgenic PrP/SCA3 mice, but did reduce the amount of soluble ataxin-3 protein and unexpectedly led to increased Purkinje cell damage.

Materials and methods

Animals

All experiments were conducted in our previously generated inducible mouse model of SCA3 (Boy *et al.* 2009). To generate Tet-Off double transgenic mice, the hamster prion protein promoter mouse line for the expression of tetracycline transactivator (tTA) ($Tg(Prnp\text{-}tTA)FVByPrnp^{0/0}$), referred to as PrP, was crossbred to the SCA3 responder line 2904. This responder line contains three ataxin-3 transgene copies with ~ 80, ~ 65, and ~ 60 CAG repeats (Boy *et al.* 2009).

In order to exclude influences by hormones, only male mice being either single transgenic for the SCA3 responder (serving as controls) or double transgenic for both the promoter and the responder transgene (serving as disease mice) were used. Both groups were homozygous for the SCA3 responder transgene and double transgenic mice in addition were heterozygous for the PrP promoter transgene. In the following, double transgenic PrP/SCA3 mice will be designated dtg and single transgenic controls con.

Mice were kept on a 12 h light/dark cycle and had *ad libitum* access to food and water. All research and animal care procedures were approved by the district government (HG3/11; Tuebingen, Germany) and performed according to international guidelines for the use of laboratory animals in the FORS animal facility in Tuebingen, Germany.

In total, 81 mice were included in this study and were randomly assigned to the following groups: con, $n = 19$; con-rilu, $n = 19$; dtg, $n = 21$; dtg-rilu, $n = 22$. According to power analysis using the PASS Modul of the NCSS2000 statistic program (NCSS 2000; Kaysville, UT, USA), a group size for rotarod tests of 20 animals would have been sufficient to reveal a 30% difference, with a power of 80% and $p < 0.05$.

Mice were housed specific pathogen free in Type II long cages on lignocel aspen bedding in groups up to five mice per cage. Animal welfare was routinely monitored by the caretakers of the animal facility and the veterinary service of the University of Tuebingen. The experimenter was blinded for the genetic status of the mice during both treatment and behavioral tests, but was aware of the treatment status (receiving riluzole or not). The order of mice for behavioral tests was independent of their genetic status or the treatment group.

Genotyping

Transgenic animals were identified using DNA extracted from ear biopsy tissue (Roche High Pure PCR Template Preparation Kit; Roche Applied Science, Mannheim, Germany). PCR analyses were carried out for promoter mice using primers specific for the tTA sequence: tTA-F, 5′-GACGAGCTCCACTTAGACGG-3′; tTA-R, 5′-TACTCGTCAATTCCAAGGGC-3′. PCR analyses of responder mice were carried out with primers specific for the tetracycline-responsive element (TRE) vector: TRE-Seq/PCR-F, 5′-CGCCT

GGAGACGCCATCC-3′; TRE-Seq/PCR-R, 5′-CCACACCTCCCC CTGAAC-3′.

To distinguish between mice that are hetero- or homozygous for either or both of the transgene constructs (PrP promoter or SCA3 responder), real-time PCR analysis was performed using hybridization probes. Duplex PCR reactions were carried out on a LightCycler 480 Real-Time PCR System (Roche Applied Science). Sample mixtures (10 µl) contained 1 µl of genomic mouse DNA, 5 pmol of each transgene primer, 10 pmol of β-2-microglobulin as the reference gene, 1.5 pmol of each hybridization probe, and 1× LightCycler 480 Probes Master Reaction-Mix (Roche Applied Science). The primer sequences to recognize the promoter region were: tTA-LC-F, 5′-GTAATAACGCTAAAAGTTTTAGATG-3′; tTA-LC-R, 5′-CGGCATACTATCAGTAGTAGG T-3′. The primer sequences to recognize the responder region were: TRE-LC-F, 5′-GGTGGGAGGCCTATATAAG-3′; TRE-LC-R, 5′-TACCGAGC TCGAATTCG-3′). Primer sequences to recognize the reference gene β-2-microglobulin were: β-2-micro-LC-F, 5′-TAGATAGCT-GAGCAATAAATCTTCA-3′; β-2-micro-LC-R, 5′-AATTAGGCC TCTTTGCTTTAC-3′. Probe sequences to hybridize with the promoter region were: tTA-LC-FL, 5′-GGCATTTTACTTTAGGT TGCGTATTGGA-FL-3′; tTA-LC-610, 5′-Red 610-GATCAA-GAGCATCAAGTCGCTAAAGAAGAA-PH-3′. Probe sequences to hybridize with the responder region were: TRE-LC-FL, 5′-GGAG ACGCCATCCACGCTGT-FL-3′; TRE-LC-640, 5′-Red 640-TTGACCTCCATAGAAGACACCGGG-PH-3′. Probe sequences to hybridize with the reference gene region were: β-2-micro-LC-FL, 5′-GTTGATCATATGCCAAACCCTCTGTACTTC-FL-3′; β-2-micro-LC-670, 5′-Red 670-CATTACTTGGATGCAGTTACT-CATCTTTGG-PH-3′. To calculate the zygosity of the transgenes, the $2^{-\Delta\Delta Ct}$ method (Livak and Schmittgen 2001) was used.

Riluzole treatment

Riluzole (Rilutek®; Sanofi-Aventis Deutschland GmbH, Frankfurt, Germany) was applied in a concentration of 10 mg/kg body weight in the drinking water. To prepare the riluzole drinking solution, Rilutek® tablets were dissolved in tap water and exposed to ultrasound for 1 h. Following that, the solution was cleared by filtering it through a paper filter. Drinking volume of mice was determined using the LabMaster system (TSE Systems GmbH, Bad Homburg, Germany).

Rotarod

To measure the motor coordination abilities and balance of the transgenic mice, Rotarod analyses were performed. At a maximum illumination of 100 lux, mice were tested on an accelerating Rotarod (TSE Systems GmbH), which began at 4 rpm and accelerated to 40 rpm over 300 s (5 min). Three trials per test day were carried out, with a 15 min rest between trials. In each trial, the latency to fall off the rotating rod was recorded (Brown *et al.* 2005; Green *et al.* 2005). The tests were repeated approximately every 6 weeks. In order to increase the challenge, at 40 weeks of age, an initial speed of 10 rpm was used.

Home cage activity

To analyze the spontaneous home cage activity of the mice, the LabMaster system (TSE Systems GmbH) was used. The mouse cages were placed into sensor frames, the number of beam brakes was counted and the total activity, ambulatory and fine movements, as well as rearings, were quantified. In addition, drinking and feeding behavior was analyzed. The analysis was performed for 23 h, starting with 3–4.5 h of light phase, continuing with 12 h of darkness and concluding with an additional 8–6.5 h of light. For analysis, beam breaks were counted in 15 min intervals. In each run, 12 mice were analyzed in parallel using 12 separate test systems. In order to exclude any bias, to serve as internal control, and for reproduction, both transgenic and control as well as untreated and treated mice were routinely analyzed in parallel and were randomly distributed between the test systems.

RNA expression analysis

RNA isolation from frozen cerebellar tissue was performed using QIAzol and RNeasy Midi Kit (Qiagen, Hilden, Germany) according to manufacturer's instructions. For reverse transcription, QuantiTect Reverse Transcription Kit (Qiagen) was used. Relative expression was analyzed in triplicates using a Lightcycler 480 system (Roche Applied Science) and primers specific for transgenic *ATXN3* (MJD-LC-F1: 5′-AATGGATGGCTCAGGAAT GT-3′ and MJD-LC-R2: 5′-TGATGTCTGTGTCATATCTTGAGATA-3′) and primers for TBP (*TATA-binding protein*: TBP-m-F: 5′-TCTATTTTGGAAG AGCAACAAAGAC-3′ and TBP-m-R: 5′-GAGGCTGCTGCAG TTGCTA-3′); SDHA (*Succinate dehydrogenase complex*: SDHA-m-F: 5′-GCAGCACAGGGAGGTATCA-3′ and SDHA-m-R: 5′-CTCAACCACAGAGGCAGGA-3′); and YWHAZ (tyrosine 3-monooxygenase/tryptophan 5-monooxygenase activation protein zeta: YWHAZ-m-F: 5′-AGACGGAAGGTGCTGAGAAA-3′ and YWHAZ-m-R: 5′-TCAAGAACTTTTCCAAAAGAGACA-3′) as reference genes. Relative transgenic *ATXN3* expression was determined using the Lightcycler 480 system software.

Western blot

For protein isolation, brain homogenates (see time-resolved Förster resonance energy transfer, TR-FRET) without Triton-X-100 were taken and cleared of debris by centrifugation [15 min each, 20 000 relative centrifugal force (rcf), 4°C]. The clarified protein extract was supplemented with glycerol (VWR International, Darmstadt, Germany) to a final concentration of 10% and stored at −80°C. For the determination of the protein concentration, a protein assay (Protein Assay Dye Reagent Concentrate; Bio-Rad, Munich, Germany) based on the method described by Bradford (1976) was used according to the manufacturer's instructions. Protein lysates (30 µg of each) were mixed with loading buffer (80 mM Tris, pH 6.8, 0.1 M dithiothreitol, 2% sodium dodecyl sulfate (SDS), 10% glycerol, bromophenol blue), denatured, and analyzed in polyacrylamide gel electrophoresis buffer (192 mM glycine, 25 mM Tris, 1% SDS) by SDS–polyacrylamide gel electrophoresis (Blue Vertical 100/C; Serva, Heidelberg, Germany) according to the method described by Laemmli (1970). Separated proteins were transferred to polyvinylidene difluoride membranes (Immobilon-P Transfer membrane; Millipore, Schwalbach, Germany) in transfer buffer (0.2 M glycine, 25 mM Tris, 10% methanol).

Analysis of ataxin-3 cleavage fragments was performed using 4-12% Bolt Bis-Tris Plus gradient gels (Thermo Fisher Scientific, Schwerte, Germany) and SeeBlue Plus2 Pre-Stained Standard (Thermo Fisher Scientific) was used for molecular weight estimation. Proteins were transferred on Amersham Protran Premium 0.2 µm

nitrocellulose membranes (GE Healthcare, Freiburg, Germany) using Bicine/Bis-Tris transfer buffer (25 mM bicine, 25 mM Bis-Tris pH 7.2, 1 mM EDTA, 15% methanol) and a TE22 Transfer Tank (Hoefer, Holliston, MA, USA) at 80 V for 2 h.

The detection of proteins was performed essentially as described previously (Schmidt *et al.* 1998). Briefly, the membrane was blocked for 2 h at 20–25°C in 5% dry milk in Tris-buffered saline TWEEN 20 (TBST) buffer (10 mM Tris, pH 7.5, 0.15 M NaCl, 0.1% TWEEN 20). The primary antibody was diluted in TBST. The 1H9 antibody against ataxin-3 (MAB5360; Merck Millipore, Darmstadt, Germany) and the β-actin antibody were purchased from Millipore and Sigma-Aldrich (St Louis, Mo, USA), respectively. After incubation for 2 h, the membrane was washed four times (15 min each) with TBST. The membrane was incubated for 75 min with secondary antibody that was coupled to horseradish peroxidase (GE Healthcare Life Sciences, Freiburg, Germany). After four washing steps with TBST (15 min each), bands were visualized using the enhanced chemiluminescence method (GE Healthcare Life Sciences) and Odyssey LC imaging system (LI-COR Biosciences, Lincoln, NB, USA).

Time-resolved Förster resonance energy transfer

Mice were killed by CO_2 inhalation, and the tissue was freshly prepared, immediately snap frozen, and stored at −80°C. For TR-FRET sample preparation, tissue was homogenized with a Dounce tissue grinder in Dulbecco's Phosphate-Buffered Saline (DPBS) buffer (GIBCO Life Technologies, Darmstadt, Germany) supplemented with a protease inhibitor cocktail (Complete, Roche Molecular Biochemicals). For TR-FRET measurement, TritonX-100 to a final concentration of 1% was added. The 1H9 antibody against ataxin-3 (MAB5360; Merck Millipore) was labelled with donor Lumi4-Tb-fluorophore (Cisbio, Codolet, France) and the MW1 antibody against polyglutamine stretches (Developmental Studies Hybridoma Bank, Iowa City, IA, USA) was labeled with D2 acceptor fluorophore (Cisbio). Quantification of soluble transgenic ataxin-3 levels was performed in 384 microtiter plates with 5 µl sample volume and addition of 1 µl antibody solution (50 mM NaHPO4 + 400 mM NaF + 0.1% bovine serum albumin + 0.05% Tween-20 + 0.3 ng/ml 1H9-Tb + 10 ng/ml MW1-D2). Time-resolved fluorescence was measured at 620 nm and 665 nm on an EnVision Multilabel reader with a TRF laser to lower background noise (Perkin Elmer, Waltham, MA, USA).

Immunohistochemistry and immunofluorescence

Mice were deeply anaesthetized by CO_2 inhalation and transcardially perfused using 4% paraformaldehyde in 0.1 M PBS. Brains were removed from the skull and postfixed overnight in fixative, embedded in paraffin and cut into 7 µm sagittal sections. After rehydrating, the sections in xylene and a graded alcohol series, slides were microwaved for 15 min in 10 mM sodium citrate, pH 6.0. Slides were washed with PBS, followed by 5% normal goat serum in PBS supplemented with 0.3% Triton X-100. After washing with PBS three times for 10 min each, the primary antibody (diluted in PBS containing 3% goat serum) was added and incubated at 4°C overnight in a humid chamber. The polyclonal ataxin-3 antibody (1 : 1000) was generated by us (Schmidt *et al.* 1998) and the mouse monoclonal 1H9 antibody against ataxin-3 (MAB5360; 1 : 500) was purchased from Merck Millipore. After washing the slides with PBS, the secondary antibody coupled with biotin (Vector Laboratories, Burlingame, CA, USA) and diluted in PBS containing 1.5% goat serum was added and incubated for 30 min at 20–25°C. After a brief wash with PBS, sections were incubated in an ABC enhancer complex coupled with peroxidase (Vector Laboratories) for 30 min at 20–25°C. After washing with PBS, the substrate (DAB; Sigma-Aldrich) was added, and the reaction was stopped in distilled water once the desired degree of staining was reached. Finally, slides were dehydrated again and mounted using CV Mount (Leica, Bensheim, Germany).

The immunofluorescence staining of paraffin-embedded sections was performed essentially as described above, but with normal donkey serum used for blocking. The polyclonal calbindin antibody (1 : 500) was purchased from Swant Swiss Antibodies (Marly, Switzerland). The secondary antibody was Cy2-coupled anti-rabbit (Dianova, Hamburg, Germany). 4',6-diamidino-2-phenylindole (DAPI) was added in the following washing steps and sections were coverslipped with Mowiol (Merck, Darmstadt, Germany) supplemented with 2.5% 1,4-diazabicyclo[2.2.2]octane (DABCO; Sigma-Aldrich) and stored at 4°C.

To visualize staining, an Axioplan 2 imaging microscope (Carl Zeiss Microimaging, Oberkochen, Germany) was used with suitable filter sets. The microscope was equipped with an Axio-Cam MR color digital camera and an Axio-Cam MRm black and white digital camera for fluorescence analyses (Carl Zeiss Microimaging) and the AxioVision 4.8 software package (Carl Zeiss). For investigation of ataxin-3 stained cells in the cerebellum, 17–20 randomly chosen areas were analyzed. Intensity of ataxin-3 positive cells (30 cells per group) in cortical tissue was measured using *ImageJ* analysis software (U. S. National Institutes of Health, Bethesda, MD, USA, http://imagej.nih.gov/ij/). Optical densitometry of calbindin-stained Purkinje cells was performed on 35 cells per animal, which corresponds to 105 cells per group, using *ImageJ* analysis software.

Statistical analysis

Data are presented as mean ± SEM. Results are reported significant if $p < 0.05$. Two-way ANOVA with Bonferroni post-tests was used to analyze rotarod performance and body weight. In order to compensate for weight differences influencing rotarod results, ANCOVA using JMP in addition was performed. In general, home cage activity, immunohistochemistry and expression analyses were analyzed using unpaired Student's *t*-test.

Results

In this study, we assessed whether the antiglutamatergic drug riluzole has therapeutic potential in the treatment of spinocerebellar ataxia type 3. To do so, we used our previously generated inducible mouse model for SCA3 (Boy *et al.* 2009) and treated already phenotypic mice of this model with riluzole. We chose a daily riluzole dose of 10 mg/kg body weight, equaling 62 µg/ml, in the drinking water. This concentration has been successfully used before in mouse studies for familial amyotrophic lateral sclerosis, HD, and depression (Gurney *et al.* 1996; Schiefer *et al.* 2002; Gourley

et al. 2012). A dose of 10 mg/kg in mice corresponds to a human equivalent dose based on the body surface area (Reagan-Shaw *et al.* 2008) of approx. 50 mg/day.

Effect of riluzole treatment on the motor phenotype of SCA3 mice

To measure the effect of riluzole treatment on motor coordination, rotarod tests were performed. At eleven weeks of age, double transgenic mice (dtg) over-expressing ataxin-3 performed significantly worse compared to single transgenic controls (Fig. 1a). Riluzole treatment in a concentration of 10 mg/kg started at the age of 13 weeks. Treatment lasted for 10 months until mice were 13 months old and had no impact on the survival of treated mice compared with untreated mice until this age. In rotarod tests in the following 6 months, double transgenic mice with and without riluzole treatment (dtg, dtg-rilu) always showed significantly poorer performances compared to treated single transgenic controls (con-rilu). To increase the challenge, an initial starting rotation of 10 rpm instead of 4 rpm was used at 40 weeks of age (Fig. 1b). As observed before (Boy *et al.* 2009), double transgenic SCA3 mice (either with or without riluzole treatment) always had a significantly lower body weight compared with single transgenic controls (Fig. 1c). To compensate for these differences in body weight, rotarod results in Fig. 1(b) are corrected by performing ANCOVA using JMP. Taken together, there was no difference in rotarod performance between double transgenic untreated mice and double transgenic mice which were treated with riluzole. Both double transgenic groups performed worse compared to controls. Untreated double transgenic mice even showed a slightly (though not significant) better rotarod performance than riluzole-treated double transgenic mice. Thus, riluzole treatment had no beneficial effect on the rotarod phenotype measured in this mouse model.

Effect of riluzole treatment on the overall activity of SCA3 mice

To measure the home cage behavior, we used the PhenoMaster/LabMaster – Modular Animal Monitoring System (TSE Systems GmbH). This measurement was performed to analyze whether riluzole treatment has an influence on the overall activity and especially on the hyperactivity phenotype observed in the PrP/SCA3 (dtg) model (Boy *et al.* 2009). Each measurement was conducted for 23 h. Results are depicted in beam breaks throughout the whole cage (Fig. 2). The first test was conducted before riluzole treatment was started, when mice were 3 months (12 weeks) old. In this test, double transgenic mice showed a higher overall activity compared to single transgenic controls, especially pronounced toward the end of the dark phase (Fig. 2a, a3), reflecting the hyperactivity phenotype observed before in this SCA3 mouse model (Boy *et al.* 2009).

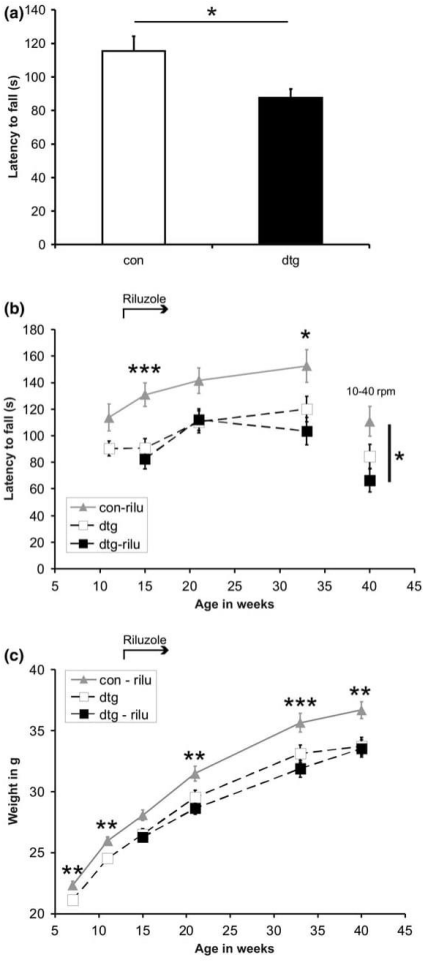

Fig. 1 Rotarod results and body weight of riluzole-treated mice. (a) At the age of 11 weeks, double transgenic mice (dtg, $n = 39$) performed significantly worse in the rotarod test compared to single transgenic controls (con, $n = 19$). (b) From the age of 13 weeks, dtg and control mice were treated with 10 mg/kg riluzole in the drinking water. Rotarod data were analyzed using Two-way ANOVA after correction for body weight by performing ANCOVA analyses using JMP. Over a period of approx. 6 months, controls treated with riluzole (con-rilu) always performed significantly better than treated dtg mice (dtg-rilu, $n = 19$). At 40 weeks of age, the protocol was changed to a higher initial rotation speed (10 rpm instead of 4 rpm) in order to increase the challenge. (c) Both dtg ($n = 16$) and treated dtg mice (dtg-rilu, $n = 19$) always had lower body weights compared to same aged control littermates which were treated with riluzole (con-rilu, $n = 19$). $^*p < 0.05$, $^{**}p < 0.005$, $^{***}p < 0.0005$.

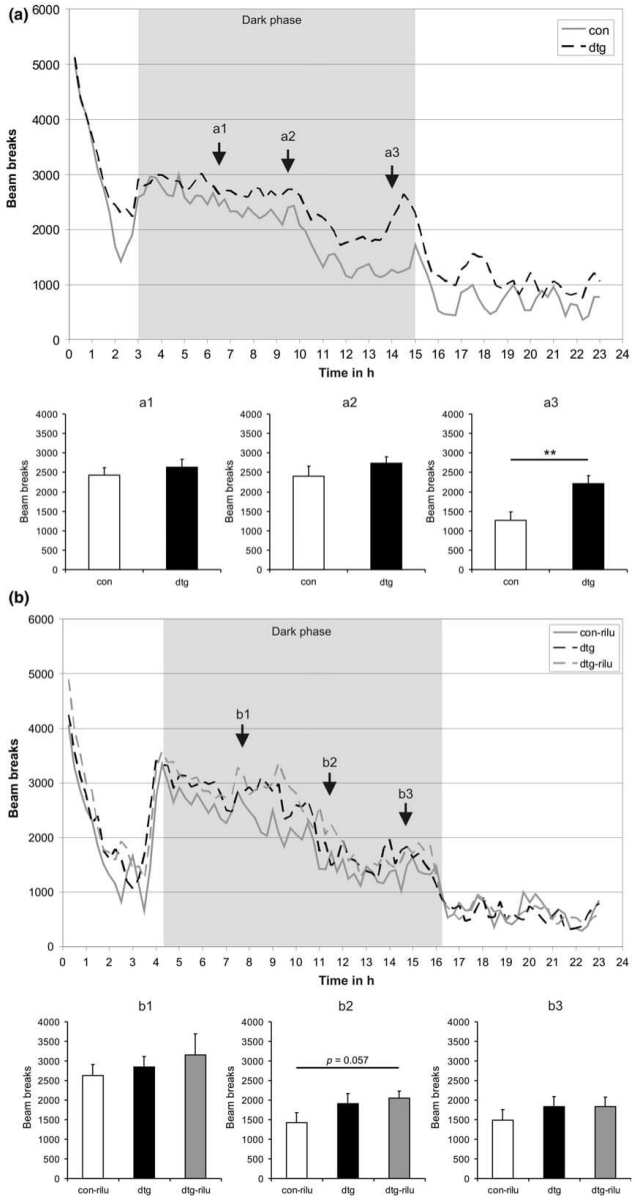

Fig. 2 Home cage activity of riluzole-treated mice. Each measurement was conducted for 23 h. Depicted are the counted beam breaks throughout the whole cage. (a) In the first test at the age of 3 months (12 weeks), before riluzole treatment was started, double transgenic mice (dtg, $n = 39$) showed a higher overall activity compared to single transgenic controls (con, $n = 19$), especially pronounced toward the end of the dark phase (a3). (b) The second test was performed at the age of 13 months, when mice had been treated with 10 mg/kg of riluzole for 10 months. Double transgenic mice (dtg, $n = 16$) were again more active compared to controls (con-rilu, $n = 16$). Double transgenic mice treated with riluzole (dtg-rilu, $n = 19$) showed an overall activity comparable to untreated mice, thus riluzole treatment showed no effect on the hyperactivity phenotype in these spinocerebellar ataxia type 3 mice. a1, a2, a3 and b1, b2, b3 depict three time points in each run for a more detailed analysis. $*p < 0.05$, $**p < 0.005$.

The second test was performed at the age of 13 months, when mice had been treated with 10 mg/kg of riluzole for 10 months. Double transgenic mice were again more active compared with controls. Treated mice showed an overall activity comparable to those that were untreated, demonstrating that riluzole treatment has no

effect on the hyperactivity phenotype in this model (Fig. 2b).

Using the LabMaster system, we also measured the drink and food intake of the mice. Measuring the intake of drinking water was important for the calculation of the riluzole concentration in the drinking water to ensure continuous daily intake of 10 mg/kg. The conducted tests revealed no significant differences in the intake of food or water between the analyzed mouse groups (data not shown).

Effects of riluzole on soluble transgenic ataxin-3 protein

Soluble ataxin-3 protein was first analyzed by western blot. In the cerebellar tissue of 5-month-old mice, a slight reduction in transgenic ataxin-3 protein in riluzole-treated double transgenic mice (dtg-rilu) compared to untreated mice (dtg) was seen (Fig. 3a). Performing TR-FRET analyses of the same cerebellar samples, this reduction of transgenic ataxin-3 in riluzole-treated double transgenic mice (dtg-rilu) could be confirmed (Fig. 3b), although it did not reach significance. However, in the cortical tissue of the same mice, lower levels of transgenic ataxin-3 protein in dtg-rilu mice was measured using TR-FRET (**$p = 0.0026$, Fig. 3c). Following up on the level of soluble transgenic ataxin-3 protein in older mice (13 months of age) which were treated with riluzole for a long period (10 months), a marked reduction of ataxin-3 signal in dtg-rilu mice was

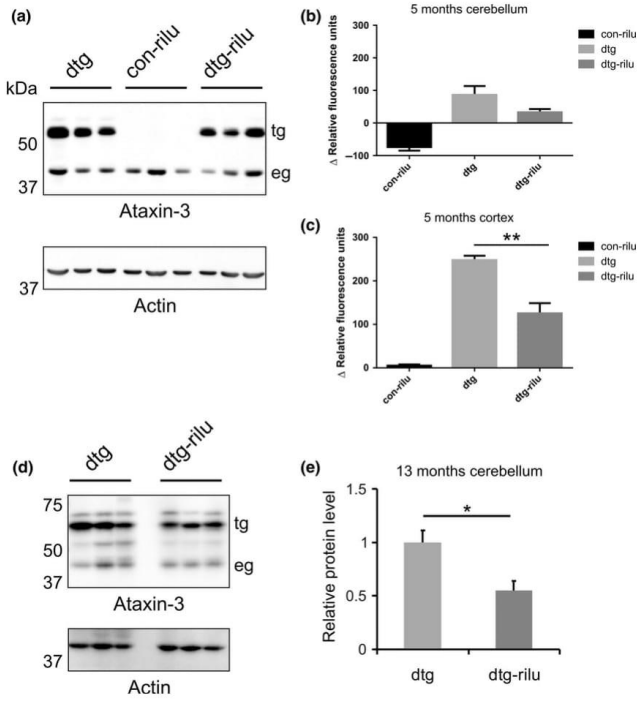

Fig. 3 The effects of riluzole treatment on soluble ataxin-3 levels. (a) Western blot analysis of cerebellar tissue of 5 month old mice, which were untreated or treated with riluzole for 10 weeks. (b) TR-FRET measurements of the same cerebellar samples, although not significant, revealed lower values for double transgenic mice which were treated with riluzole (dtg-rilu) compared to untreated double transgenics (dtg). (c) Also, using TR-FRET in cortical tissue of the same mice, a highly significant reduction of transgenic ataxin-3 became evident (**$p = 0.0026$). (d) Western blot analysis of cerebellar tissue of 13 month old mice, which were untreated or treated for 10 months. Quantification of this blot (e) showed significantly lower levels of soluble transgenic ataxin-3 protein (tg) in riluzole-treated double transgenic mice (dtg-rilu) compared to untreated mice (dtg) (*$p = 0.037$). Three mice per group were analyzed. Groups are: dtg – untreated double transgenic mice; con-rilu – riluzole-treated control mice; dtg-rilu – riluzole-treated double transgenic mice. To analyze transgenic (tg) and endogenous ataxin-3 protein (eg) by western blot an anti-ataxin-3 antibody (1H9) was used and the detection with a beta-actin antibody served as loading control. *$p < 0.05$, **$p < 0.005$.

already detected by western blot analysis of cerebellar tissue (Fig. 3d). Quantification of western blot signals revealed an approximate 50% lower level of transgenic ataxin-3 protein in riluzole-treated double transgenic mice (dtg-rilu) compared to untreated mice (dtg) (Fig. 3e).

Relative *ATXN3* expression and the ataxin-3 fragments, number and intensity of ataxin-3 positive cells

As we observed a significant reduction of soluble ataxin-3 in riluzole-treated double transgenic mice, we wanted to investigate the reason behind this reduction. To do so, we first performed mRNA analyses to determine the relative expression of transgenic *ATXN3* in untreated and riluzole-treated double transgenic mice. This analysis revealed an up-regulation of transgenic *ATXN3* expression in riluzole-treated double transgenic mice compared with untreated double transgenic mice, which was not significant (Fig. 4a).

In a next step, we analyzed whether the amount of ataxin-3 cleavage fragments is altered in riluzole-treated double transgenic mice. Western blot analyses of cerebellar samples of 13-month-old double transgenic mice with and without riluzole treatment for 10 months were performed. These analyses revealed no higher abundance of ataxin-3 cleavage fragments in treated mice. Furthermore, not only was the signal for transgenic ataxin-3 protein weaker in riluzole-treated mice but also were signals for a ~ 34 kDa cleavage fragment (Fig. 4b). After ruling out the possibility that reduced soluble ataxin-3 protein levels in riluzole-treated mice are based on changes in mRNA expression or alterations in ataxin-3 cleavage, we performed immunohistochemical analysis on brain sections. Sections of double transgenic mice and double transgenic mice treated with riluzole were stained with an anti-ataxin-3 antibody. In the cerebella of riluzole-treated double transgenic mice (dtg-rilu), more ataxin-3 positive cells per mm^2 were detected (Fig. 4c).

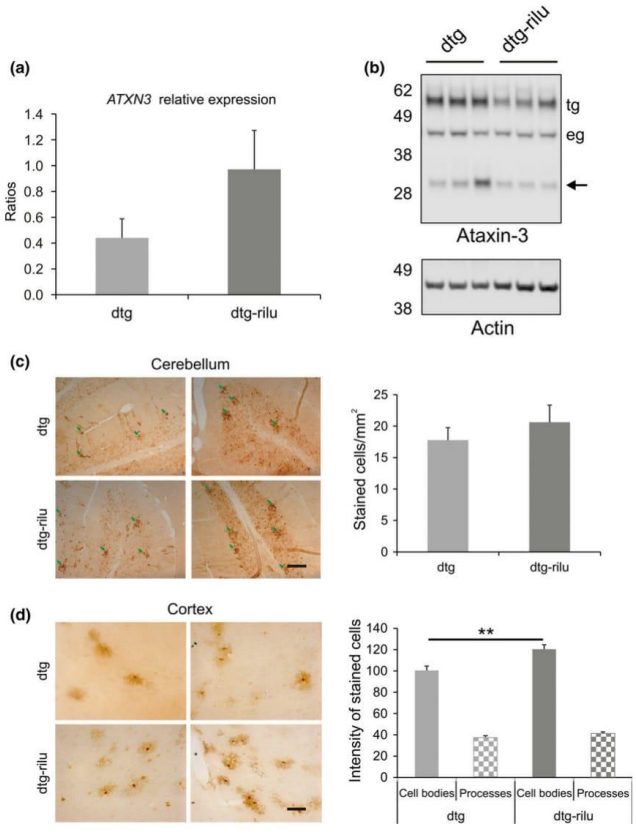

Fig. 4 ATXN3 mRNA analysis, fragments and number and intensity of ataxin-3 positive cells. (a) Messenger RNA expression level of transgenic ATXN3 is not significantly up-regulated in riluzole-treated double transgenic mice (dtg-rilu, $n = 4$) compared to untreated mice (dtg, $n = 4$). (b) Western blot analysis to investigate ataxin-3 cleavage upon riluzole treatment. Analyzed mice were 13 months old and either double transgenic (dtg, $n = 3$), or double transgenic and treated with riluzole for 10 months (dtg-rilu, $n = 3$). Upon detection with an anti-ataxin-3 antibody (1H9), signals for transgenic ataxin-3 protein (tg) and a ~ 34 kDa cleavage fragment (arrow) were weaker in riluzole-treated mice (dtg-rilu) compared to untreated mice (dtg). A beta-actin antibody served as loading control. eg, endogenous ataxin-3 protein (c) Brain sections were stained using an anti-ataxin-3 antibody and positive cells (green arrows) in the cerebellum were counted. The number of stained cells/mm^2 was slightly higher in cerebellar of riluzole-treated double transgenic mice (dtg-rilu). (d) Brain sections were stained with an anti-ataxin-3 antibody (1H9). Measurement of the intensities of cell bodies and processes of stained cortical cells revealed significantly higher values for cell bodies of riluzole-treated double transgenic mice (dtg-rilu). Scale bars: (c) 100 μm; (d) 50 μm; $^{**}p < 0.05$.

The analysis of the intensity of ataxin-3 positive cells in cortical brain regions revealed significantly higher values for cell bodies of riluzole-treated double transgenic mice (Fig. 4d), suggesting that more transgenic ataxin-3 protein accumulated in cell bodies in these mice.

Taken together, these results indicate that the measured decrease of soluble ataxin-3 protein in dtg-rilu mice is not based on a lower expression level or increased cleavage, but is rather caused by an increased accumulation of transgenic ataxin-3 protein.

Damaged Purkinje cells in double transgenic mice treated with riluzole

In the initial analysis of PrP/SCA3 mice (dtg), dysfunctional Purkinje cells were observed (Boy *et al.* 2009). To evaluate the impact of riluzole treatment on Purkinje cells in this study, the total number of Purkinje cells was determined. Brain sections of double transgenic mice and double transgenic mice treated with riluzole were stained with calbindin to visualize Purkinje cells (Fig. 5a). Analyzed mice were 13 months old and riluzole treatment was carried out for 10 months. Purkinje cells of all cerebellar lobules (Cb2-10) were counted and Purkinje cells/mm were quantified. Most lobules showed lower Purkinje cell numbers in treated double transgenic mice (dtg-rilu) compared to untreated mice (dtg) (Fig. 5b). The number of calbindin positive Purkinje cells over all lobules was reduced in riluzole-treated mice (dtg-rilu), although not reaching statistical significance ($p = 0.066$) (Fig. 5c).

Calbindin is also a marker for Purkinje cell quality. It was shown that loss of calbindin expression leads to deficits in motor coordination (Barski *et al.* 2003). To functionally evaluate Purkinje cells, we performed optical densitometry on paraffin sections after fluorescence staining with a calbindin antibody (Fig. 5d). Quantification revealed that riluzole-treated double transgenic mice (dtg-rilu) showed significantly lower fluorescence intensities ($*p = 0.037$) compared to untreated double transgenic mice, suggesting that more Purkinje cells in these mice are functionally disturbed (Fig. 5e).

In further analyses, counting Purkinje cells of brain sections revealed a reduction of calbindin positive cells in dtg-rilu mice, but no change in the number of neurofilament-stained cells (data not shown) indicating that the observed reduction in calbindin signaling in dtg-rilu mice is based on a loss of calbindin expression and not on an actual loss of Purkinje cells. Also, these analyses revealed no effect on the number of calbindin or neurofilament positive cells in the brains of riluzole-treated controls compared to untreated controls (data not shown).

Discussion

In a pilot study on ataxia patients of different etiologies, treatment with riluzole showed beneficial effects after only 8 weeks. However, no SCA3 patient was included in this study (Ristori *et al.* 2010). Also, a second very recent study carried out by the same group reported positive results from riluzole treatment over a period of 12 months (Romano *et al.* 2015). But again, it is not clear whether SCA3 patients were included in this trial.

Riluzole (benzothiazole; Rilutek®) is licensed to be applied in the treatment of amyotrophic lateral sclerosis where it prolongs survival of patients by 2–3 months (Miller *et al.* 2003; Orrell 2010). Riluzole has also been tested as a therapeutic agent in models of several neurological diseases other than ALS. Mice suffering from progressive motor neuropathy (*pmn*) showed delayed onset of paralysis and increased lifespan after riluzole treatment (Kennel *et al.* 2000). Riluzole delays neuromuscular dysfunction in a mouse model of motor neuron disease (Ishiyama *et al.* 2004) and slows down the progression of multiple sclerosis in humans (Killestein *et al.* 2005).

One function of riluzole is to inhibit the release of glutamate from nerve terminals, thereby acting against toxic actions of excessive glutamate. Glutamate excitotoxicity is suggested to also contribute to pathogenic processes seen in polyglutamine diseases (Ross and Cleveland 2006) and in particular, in SCA3 (Koch *et al.* 2011). Results of the analyses of a YAC mouse model strengthened the evidence that excitotoxicity also plays a role in the pathogenesis of Huntington's disease (Hodgson *et al.* 1999). Furthermore, in a microarray study of mice transgenic for SCA1, five of nine genes specifically altered in SCA1 were associated with the glutamate signaling pathway in Purkinje cells (Serra *et al.* 2004) and modulating glutamate receptors positively impacted the phenotype in SCA1 mice (Notartomaso *et al.* 2013). For SCA7, directing the expression of a pathogenically expanded ataxin-7 to Bergmann glial cells, astrocytic cells responsible for the removal of glutamate from synapses of Purkinje cells, led to a strong ataxia phenotype in mice (Custer *et al.* 2006). This suggests that glutamate excitotoxicity may also play a crucial role in the pathogenesis of SCA7. Subsequently, it has been demonstrated that the expression of proteins involved in the glutamatergic transmission is significantly down-regulated in a mouse model of SCA3 (Chou *et al.* 2008). This down-regulation could lead to disturbances in the glutamate signaling that could be corrected by riluzole. Riluzole is also known to open small conductance calcium-activated potassium channels (Cao *et al.* 2002), which have been shown to play a critical regulatory role in the firing rate of neurons in deep cerebellar nuclei. Openers of these channels may reduce neuronal hyperexcitability and thus therapeutically benefit cerebellar ataxia (Shakkottai *et al.* 2004).

Based on the above listed patients, mouse and cellular studies, we evaluated the effect of riluzole as a potential long term treatment strategy for SCA3 in our transgenic PrP/SCA3 mouse model. However, long term treatment with

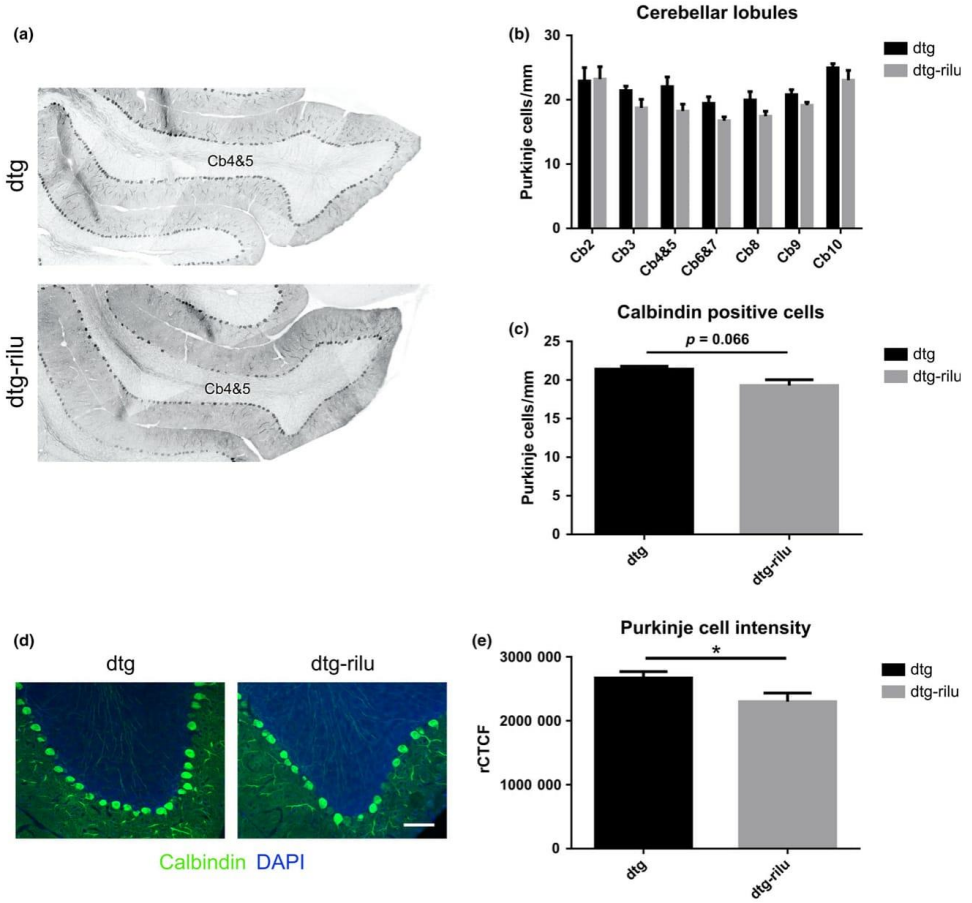

Fig. 5 Purkinje cell density and intensity in riluzole-treated mice. (a) Overview representation of mouse cerebellar lobules 4 and 5 (Cb4&5) of a double transgenic (dtg) and a double transgenic mouse treated with riluzole (dtg-rilu) after calbindin fluorescence staining. (b) Quantification of calbindin stained Purkinje cells of cerebellar lobules 2–10. Analyzed mice were 13 months old and either double transgenic (dtg, $n = 3$) or double transgenic and treated with riluzole for 10 months (dtg-rilu, $n = 3$). For most lobules calbindin positive Purkinje cells/mm were less in dtg-rilu mice compared to untreated dtg mice. Two-way ANOVA analysis over all lobules revealed significant differences between double transgenic und riluzole-treated double transgenic mice ($F_{(1,28)} = 10.70$, $p = 0.0028$). (c) In total, the number of calbindin positive Purkinje cells per mm (cells/mm) were less in riluzole-treated mice (dtg-rilu), although not reaching statistical significance ($p = 0.066$). (d) Fluorescence staining of Purkinje cells using a calbindin antibody (green) and DAPI (blue) to visualize nuclei. (e) Quantification of optical densitometry of calbindin stained Purkinje cells. Analyzed mice were 13 months old and either double transgenic (dtg, $n = 3$) or double transgenic and treated with riluzole for 10 months (dtg-rilu, $n = 3$). The intensity of Purkinje cells of double transgenic mice which were treated with riluzole is significantly lower than the intensity of double transgenics without treatment ($*p = 0.037$). Abbreviations: rCTCF, relative corrected total cell fluorescence. Scale bar: D, 100 μm; $*p < 0.05$.

10 mg/kg riluzole in the drinking water over a period of 10 months led to no improvement of the rotarod performance. Riluzole-treated double transgenic mice even showed a worsening of the performance in the rotarod task. Moreover, no positive effect on body weight or home cage activity was measurable.

Other mouse models of polyglutamine diseases also failed to show improvement of the motor phenotype after riluzole

treatment. Treatment with riluzole of a Huntington's disease model (R6/2 mice) had no beneficial effect on motor coordination or locomotor activity, but led to prolonged survival and improved body weight (Schiefer *et al.* 2002). In a following study on R6/2 mice, no improvement in the disease phenotype at all was measured (Hockly *et al.* 2006). Furthermore, no attenuation of motor deficits measured by rotarod was achieved by treating $SCA1^{154Q}$ mice with riluzole (Nag *et al.* 2013).

However, in this study, we could show that treating double transgenic SCA3 mice with riluzole leads to decreased levels of soluble transgenic ataxin-3 protein accompanied by an increase in ataxin-3 positive accumulates in transgene expressing cells in cerebellum and cortex.

The PrP/SCA3 mouse model used here, shows strong expression of expanded ataxin-3 in astrocytes of the cerebellum, namely in Bergmann glial cells. As we proved in the initial analysis of this model, this leads to Purkinje cell dysfunction, thus causing the measured motor phenotype (Boy *et al.* 2009).

Astrocytes influence the duration and strength of synaptic signals by clearing glutamate from the synaptic cleft; failure to clear glutamate from the synapse leads to excitotoxic neurodegeneration (Rothstein *et al.* 1996). In the cerebellum, Bergmann glial cells are responsible for most of the glutamate clearance from the synaptic clefts of climbing and parallel fibers (Mohebiany and Schneider 2013).

Riluzole-treated PrP/SCA3 mice showed a higher number of damaged Purkinje cells. The number as well as the intensity of calbindin positive Purkinje cells was reduced. Calbindin is an endogenous calcium-buffering protein and loss of calbindin expression leads to disturbances in Ca^{2+} signaling, causing deficits in motor coordination (Barski *et al.* 2003).

Recently, it was found that riluzole paradoxically enhanced glutamate-induced glutamate release from cultured astrocytes (Hayashida *et al.* 2010; Yoshizumi *et al.* 2012). Also recently, Koch *et al.* (2011) proposed a model in which Ca^{2+} influx induced by neurotransmitter like glutamate leads to calpain-mediated ataxin-3 cleavage and aggregate formation. These findings could offer an explanation for the results presented here: Riluzole treatment of PrP/SCA3 mice led to a stronger glutamate release in mutant ataxin-3 expressing cells resulting in an excessive influx of Ca^{2+}. This caused the observed increase in mutant ataxin-3 positive protein accumulates in Bergmann glial cells and ultimately damaged Purkinje cells.

The study conducted here might serve as the first *in vivo* evidence for riluzole acting as a glutamate release enhancer in astrocytes instead of having protective effects. According to our data, one should be cautious about using riluzole in the treatment of SCA3 patients.

Acknowledgements and conflict of interest disclosure

This study was supported by the National Ataxia Foundation to J.S. The authors declare no conflict of interest.

All experiments were conducted in compliance with the ARRIVE guidelines.

References

Albo F., Pieri M. and Zona C. (2004) Modulation of AMPA receptors in spinal motor neurons by the neuroprotective agent riluzole. *J. Neurosci. Res.* **78**, 200–207.

Barski J. J., Hartmann J., Rose C. R., Hoebeek F., Morl K., Noll-Hussong M., De Zeeuw C. I., Konnerth A. and Meyer M. (2003) Calbindin in cerebellar Purkinje cells is a critical determinant of the precision of motor coordination. *J. Neurosci.* **23**, 3469–3477.

Boy J., Leergaard T. B., Schmidt T. *et al.* (2006) Expression mapping of tetracycline-responsive prion protein promoter: digital atlasing for generating cell-specific disease models. *NeuroImage* **33**, 449–462.

Boy J., Schmidt T., Wolburg H. *et al.* (2009) Reversibility of symptoms in a conditional mouse model of spinocerebellar ataxia type 3. *Hum. Mol. Genet.* **18**, 4282–4295.

Bradford M. M. (1976) A rapid and sensitive method for the quantitation of microgram quantities of protein utilizing the principle of protein-dye binding. *Anal. Biochem.* **72**, 248–254.

Brown S. D., Chambon P. and de Angelis M. H. (2005) EMPReSS: standardized phenotype screens for functional annotation of the mouse genome. *Nat. Genet.* **37**, 1155.

Cao Y. J., Dreixler J. C., Couey J. J. and Houamed K. M. (2002) Modulation of recombinant and native neuronal SK channels by the neuroprotective drug riluzole. *Eur. J. Pharmacol.* **449**, 47–54.

Chai Y., Koppenhafer S. L., Shoesmith S. J., Perez M. K. and Paulson H. L. (1999) Evidence for proteasome involvement in polyglutamine disease: localization to nuclear inclusions in SCA3/MJD and suppression of polyglutamine aggregation in vitro. *Hum. Mol. Genet.* **8**, 673–682.

Chai Y., Wu L., Griffin J. D. and Paulson H. L. (2001) The role of protein composition in specifying nuclear inclusion formation in polyglutamine disease. *J. Biol. Chem.* **276**, 44889–44897.

Chai Y., Shao J., Miller V. M., Williams A. and Paulson H. L. (2002) Live-cell imaging reveals divergent intracellular dynamics of polyglutamine disease proteins and supports a sequestration model of pathogenesis. *Proc. Natl Acad. Sci. USA* **99**, 9310–9315.

Chou A. H., Yeh T. H., Ouyang P., Chen Y. L., Chen S. Y. and Wang H. L. (2008) Polyglutamine-expanded ataxin-3 causes cerebellar dysfunction of SCA3 transgenic mice by inducing transcriptional dysregulation. *Neurobiol. Dis.* **31**, 89–101.

Custer S. K., Garden G. A., Gill N. *et al.* (2006) Bergmann glia expression of polyglutamine-expanded ataxin-7 produces neurodegeneration by impairing glutamate transport. *Nat. Neurosci.* **9**, 1302–1311.

Danbolt N. C. (2001) Glutamate uptake. *Prog. Neurobiol.* **65**, 1–105.

Doble A. (1996) The pharmacology and mechanism of action of riluzole. *Neurology* **47**, S233–S241.

Gatchel J. R. and Zoghbi H. Y. (2005) Diseases of unstable repeat expansion: mechanisms and common principles. *Nat. Rev.* **6**, 743–755.

Gossen M. and Bujard H. (1992) Tight control of gene expression in mammalian cells by tetracycline-responsive promoters. *Proc. Natl Acad. Sci. USA* **89**, 5547–5551.

Gourley S. L., Espitia J. W., Sanacora G. and Taylor J. R. (2012) Antidepressant-like properties of oral riluzole and utility of incentive disengagement models of depression in mice. *Psychopharmacology* **219**, 805–814.

Green E. C., Gkoutos G. V., Lad H. V., Blake A., Weekes J. and Hancock J. M. (2005) EMPReSS: European mouse phenotyping resource for standardized screens. *Bioinformatics (Oxford, England)* **21**, 2930–2931.

Gurney M. E., Cutting F. B., Zhai P., Doble A., Taylor C. P., Andrus P. K. and Hall E. D. (1996) Benefit of vitamin E, riluzole, and gabapentin in a transgenic model of familial amyotrophic lateral sclerosis. *Ann. Neurol.* **39**, 147–157.

Hayashida K., Parker R. A. and Eisenach J. C. (2010) Activation of glutamate transporters in the locus coeruleus paradoxically activates descending inhibition in rats. *Brain Res.* **1317**, 80–86.

Heiser V., Engemann S., Brocker W. *et al.* (2002) Identification of benzothiazoles as potential polyglutamine aggregation inhibitors of Huntington's disease by using an automated filter retardation assay. *Proc. Natl Acad. Sci. USA* **99**(Suppl 4), 16400–16406.

Hockly E., Tse J., Barker A. L. *et al.* (2006) Evaluation of the benzothiazole aggregation inhibitors riluzole and PGL-135 as therapeutics for Huntington's disease. *Neurobiol. Dis.* **21**, 228–236.

Hodgson J. G., Agopyan N., Gutekunst C. A. *et al.* (1999) A YAC mouse model for Huntington's disease with full-length mutant huntingtin, cytoplasmic toxicity, and selective striatal neurodegeneration. *Neuron* **23**, 181–192.

Hubert J. P., Delumeau J. C., Glowinski J., Premont J. and Doble A. (1994) Antagonism by riluzole of entry of calcium evoked by NMDA and veratridine in rat cultured granule cells: evidence for a dual mechanism of action. *Br. J. Pharmacol.* **113**, 261–267.

Ishiyama T., Okada R., Nishibe H., Mitsumoto H. and Nakayama C. (2004) Riluzole slows the progression of neuromuscular dysfunction in the wobbler mouse motor neuron disease. *Brain Res.* **1019**, 226–236.

Kennel P., Revah F., Bohme G. A., Bejuit R., Gallix P., Stutzmann J. M., Imperato A. and Pratt J. (2000) Riluzole prolongs survival and delays muscle strength deterioration in mice with progressive motor neuronopathy (pmn). *J. Neurol. Sci.* **180**, 55–61.

Killestein J., Kalkers N. F. and Polman C. H. (2005) Glutamate inhibition in MS: the neuroprotective properties of riluzole. *J. Neurol. Sci.* **233**, 113–115.

Koch P., Breuer P., Peitz M. *et al.* (2011) Excitation-induced ataxin-3 aggregation in neurons from patients with Machado-Joseph disease. *Nature* **480**, 543–546.

Konno A., Shuvaev A. N., Miyake N. *et al.* (2014) Mutant ataxin-3 with an abnormally expanded polyglutamine chain disrupts dendritic development and metabotropic glutamate receptor signaling in mouse cerebellar Purkinje cells. *Cerebellum* **13**, 29–41.

Laemmli U. K. (1970) Cleavage of structural proteins during the assembly of the head of bacteriophage T4. *Nature* **227**, 680–685.

Livak K. J. and Schmittgen T. D. (2001) Analysis of relative gene expression data using real-time quantitative PCR and the 2(-Delta Delta C(T)) method. *Methods (San Diego Calif* **25**, 402–408.

Martin D., Thompson M. A. and Nadler J. V. (1993) The neuroprotective agent riluzole inhibits release of glutamate and aspartate from slices of hippocampal area CA1. *Eur. J. Pharmacol.* **250**, 473–476.

Matos C. A., de Macedo-Ribeiro S. and Carvalho A. L. (2011) Polyglutamine diseases: the special case of ataxin-3 and Machado-Joseph disease. *Prog. Neurobiol.* **95**, 26–48.

Miller R. G., Mitchell J. D., Lyon M. and Moore D. H. (2003) Riluzole for amyotrophic lateral sclerosis (ALS)/motor neuron disease (MND). *Amyotroph. Lateral Scler. Other Motor Neuron Disord.* **4**, 191–206.

Mohebiany A. N. and Schneider R. (2013) Glutamate excitotoxicity in the cerebellum mediated by IL-1beta. *J. Neurosci.* **33**, 18353–18355.

Nag N., Tarlac V. and Storey E. (2013) Assessing the efficacy of specific cerebellomodulatory drugs for use as therapy for spinocerebellar ataxia type 1. *Cerebellum* **12**, 74–82.

Notartomaso S., Zappulla C., Biagioni F. *et al.* (2013) Pharmacological enhancement of mGlu1 metabotropic glutamate receptors causes a prolonged symptomatic benefit in a mouse model of spinocerebellar ataxia type 1. *Mol. Brain* **6**, 48.

Nuber S., Petrasch-Parwez E., Winner B. *et al.* (2008) Neurodegeneration and motor dysfunction in a conditional model of Parkinson's disease. *J. Neurosci.* **28**, 2471–2484.

Orrell R. W. (2010) Motor neuron disease: systematic reviews of treatment for ALS and SMA. *Br. Med. Bull.* **93**, 145–159.

Ortega Z., Diaz-Hernandez M., Maynard C. J., Hernandez F., Dantuma N. P. and Lucas J. J. (2010) Acute polyglutamine expression in inducible mouse model unravels ubiquitin/proteasome system impairment and permanent recovery attributable to aggregate formation. *J. Neurosci.* **30**, 3675–3688.

Reagan-Shaw S., Nihal M. and Ahmad N. (2008) Dose translation from animal to human studies revisited. *FASEB J.* **22**, 659–661.

Riess O., Rub U., Pastore A., Bauer P. and Schols L. (2008) SCA3: neurological features, pathogenesis and animal models. *Cerebellum* **7**, 125–137.

Ristori G., Romano S., Visconti A., Cannoni S., Spadaro M., Frontali M., Pontieri F. E., Vanacore N. and Salvetti M. (2010) Riluzole in cerebellar ataxia: a randomized, double-blind, placebo-controlled pilot trial. *Neurology* **74**, 839–845.

Romano S., Coarelli G., Marcotulli C. *et al.* (2015) Riluzole in patients with hereditary cerebellar ataxia: a randomised, double-blind, placebo-controlled trial. *Lancet Neurol.* **14**, 985–991.

Ross C. A. and Cleveland D. W. (2006) Intercellular miscommunication in polyglutamine pathogenesis. *Nat. Neurosci.* **9**, 1205–1206.

Rothstein J. D., Dykes-Hoberg M., Pardo C. A. *et al.* (1996) Knockout of glutamate transporters reveals a major role for astroglial transport in excitotoxicity and clearance of glutamate. *Neuron* **16**, 675–686.

Schiefer J., Landwehrmeyer G. B., Luesse H. G., Sprunken A., Puls C., Milkereit A., Milkereit E. and Kosinski C. M. (2002) Riluzole prolongs survival time and alters nuclear inclusion formation in a transgenic mouse model of Huntington's disease. *Mov. Disord.* **17**, 748–757.

Schmidt T., Landwehrmeyer G. B., Schmitt I. *et al.* (1998) An isoform of ataxin-3 accumulates in the nucleus of neuronal cells in affected brain regions of SCA3 patients. *Brain Pathol.* **8**, 669–679.

Schmidt T., Lindenberg K. S., Krebs A., Schols L., Laccone F., Herms J., Rechsteiner M., Riess O. and Landwehrmeyer G. B. (2002) Protein surveillance machinery in brains with spinocerebellar ataxia type 3: redistribution and differential recruitment of 26S proteasome subunits and chaperones to neuronal intranuclear inclusions. *Ann. Neurol.* **51**, 302–310.

Serra H. G., Byam C. E., Lande J. D., Tousey S. K., Zoghbi H. Y. and Orr H. T. (2004) Gene profiling links SCA1 pathophysiology to glutamate signaling in Purkinje cells of transgenic mice. *Hum. Mol. Genet.* **13**, 2535–2543.

Shakkottai V. G., Chou C. H., Oddo S., Sailer C. A., Knaus H. G., Gutman G. A., Barish M. E., LaFerla F. M. and Chandy K. G. (2004) Enhanced neuronal excitability in the absence of neurodegeneration induces cerebellar ataxia. *J. Clin. Investig.* **113**, 582–590.

Tremblay P., Meiner Z., Galou M. *et al.* (1998) Doxycycline control of prion protein transgene expression modulates prion disease in mice. *Proc. Natl Acad. Sci. USA* **95**, 12580–12585.

Trouillas P., Takayanagi T., Hallett M. *et al.* (1997) International Cooperative Ataxia Rating Scale for pharmacological assessment of the cerebellar syndrome. The Ataxia Neuropharmacology Committee of the World Federation of Neurology. *J. Neurol. Sci.* **145**, 205–211.

Tsai H. F., Tsai H. J. and Hsieh M. (2004) Full-length expanded ataxin-3 enhances mitochondrial-mediated cell death and decreases Bcl-2 expression in human neuroblastoma cells. *Biochem. Biophys. Res. Commun.* **324**, 1274–1282.

Wang S. J., Wang K. Y. and Wang W. C. (2004) Mechanisms underlying the riluzole inhibition of glutamate release from rat cerebral cortex nerve terminals (synaptosomes). *Neuroscience* **125**, 191–201.

Yoshizumi M., Eisenach J. C. and Hayashida K. (2012) Riluzole and gabapentinoids activate glutamate transporters to facilitate glutamate-induced glutamate release from cultured astrocytes. *Eur. J. Pharmacol.* **677**, 87–92.

Yu Y. C., Kuo C. L., Cheng W. L., Liu C. S. and Hsieh M. (2009) Decreased antioxidant enzyme activity and increased mitochondrial DNA damage in cellular models of Machado-Joseph disease. *J. Neurosci. Res.* **87**, 1884–1891.

g. Weber *et al.*, 2017, *Brain*.

This is a pre-copyedited, author-produced version of an article accepted for publication in *Brain* following peer review. The version of record “Jonasz J. Weber, Matthias Golla, Giambattista Guaitoli, Pimthanya Wanichawan, Stefanie N. Hayer, Stefan Hauser, Ann-Christin Krahl, Maike Nagel, Sebastian Samer, Eleonora Aronica, Cathrine R. Carlson, Ludger Schöls, Olaf Riess, Christian J. Gloeckner, Huu P. Nguyen, Jeannette Hübener-Schmid; A combinatorial approach to identify calpain cleavage sites in the Machado-Joseph disease protein ataxin-3, Brain, Volume 140, Issue 5, 1 May 2017, Pages 1280–1299” is available online at: https://doi.org/10.1093/brain/awx039.

A combinatorial approach to identify calpain cleavage sites in the Machado-Joseph disease protein ataxin-3

Jonasz Jeremiasz Weber[1,2], Matthias Golla[1,2], Giambattista Guaitoli[3,4], Pimthanya Wanichawan[5], Stefanie Nicole Hayer[4,6], Stefan Hauser[4], Ann-Christin Krahl[7], Maike Nagel[1,2], Sebastian Samer[1,2,8], Eleonora Aronica[9,10], Cathrine Rein Carlson[5], Ludger Schöls[4,6], Olaf Riess[1,2], Christian Johannes Gloeckner[3,4], Huu Phuc Nguyen[1,2], Jeannette Hübener-Schmid[1,2,*]

[1] Institute of Medical Genetics and Applied Genomics, University of Tübingen, Tübingen, Germany

[2] Centre for Rare Diseases, University of Tübingen, Tübingen, Germany

[3] Center for Ophthalmology, Institute for Ophthalmic Research, University of Tübingen, Tübingen, Germany

[4] German Center for Neurodegenerative Diseases (DZNE), Tübingen, Germany

[5] Institute for Experimental Medical Research, Oslo University Hospital and University of Oslo, Oslo, Norway

[6] Department of Neurodegenerative Diseases, Hertie-Institute for Clinical Brain Research & Center of Neurology, University of Tübingen, Tübingen, Germany

[7] Paediatric Hematology and Oncology, University Children's Hospital Tübingen, Tübingen, Germany

[8] Werner Reichardt Centre for Integrative Neuroscience, University of Tuebingen, Tübingen, Germany

[9] Department of (Neuro)Pathology, Academic Medical Center, University of Amsterdam, Amsterdam, The Netherlands

[10] Swammerdam Institute for Life Sciences, Center for Neuroscience, University of Amsterdam, Amsterdam, The Netherlands

* Corresponding author: Dr. Jeannette Hübener-Schmid, Institute of Medical Genetics and Applied Genomics, University of Tübingen, Calwerstraße 7, 72076 Tübingen, Germany, Phone: +49 7071 29 72276, E-mail: jeannette.huebener@med.uni-tuebingen.de

g. Weber et al., 2017, Brain.

Abstract

Ataxin-3, the disease protein in Machado-Joseph disease, is known to be proteolytically modified by various enzymes including two major families of proteases, caspases and calpains. This processing results in the generation of toxic fragments of the polyglutamine-expanded protein. Although various approaches were undertaken to identify cleavage sites within ataxin-3 and to evaluate the impact of fragments on the molecular pathogenesis of Machado-Joseph disease, calpain-mediated cleavage of the disease protein and the localization of cleavage sites remained unclear. Here, we report on the first precise localization of calpain cleavage sites in ataxin-3 and on the characterization of the thereof resulting breakdown products. After confirming the occurrence of calpain-derived fragmentation of ataxin-3 in patient-derived cell lines and post mortem brain tissue, we combined in silico prediction tools, western blot analysis, mass spectrometry, and peptide overlay assays to identify calpain cleavage sites. We found that ataxin-3 is primarily cleaved at two sites, namely at amino acid positions D208 and S256 and mutating amino acids at both cleavage sites to tryptophan nearly abolished ataxin-3 fragmentation. Furthermore, analysis of calpain cleavage-derived fragments showed distinct aggregation propensities and toxicities of C-terminal polyglutamine-containing breakdown products. Our data elucidate the important role of ataxin-3 proteolysis in the pathogenesis of Machado-Joseph disease and further emphasize the relevance of targeting this disease pathway as a treatment strategy in neurodegenerative disorders.

Keywords: ataxin-3/ calpains/ cleavage sites/ Machado Joseph disease/ Spinocerebellar ataxia type 3

Abbreviations: ataxin-3 = Atx3, calpastatin = CAST, Machado-Joseph disease = MJD, polyglutamine = polyQ

Introduction

Proteolytic cleavage of disease proteins has been proposed as a key event in the molecular pathogenesis of various neurodegenerative diseases like Alzheimer's (De Strooper, 2010) and Parkinson's disease (Xilouri et al., 2013), or the group of polyglutamine (polyQ) disorders (Weber et al., 2014). This posttranslational processing constitutes the source for fragments of mutant proteins, which exhibit elevated cytotoxic characteristics and aggregation propensities, ultimately leading to cell death and neurodegeneration. The discovery of this mechanism led to the formulation of the so called toxic fragment hypothesis (Wellington and Hayden, 1997).

The presence of proteolytically derived breakdown products has been reported for all polyQ diseases, and was intensively investigated in Machado-Joseph disease (MJD; also known as Spinocerebellar ataxia type 3, SCA3), Spinocerebellar ataxia type 7, and Huntington's disease (DiFiglia et al., 1997; Goti et al., 2004; Wellington et al., 1998; Yvert et al., 2000). Since then, research has focused on the identification of enzymes responsible for the fragmentation of the involved proteins, as they represent an auspicious target for pharmacological treatments of these incurable diseases (Tarlac and Storey, 2003).

Ataxin-3, the disease protein in MJD, was shown to be a substrate for mainly two families of proteases: caspases and calpains (Berke et al., 2004; Haacke et al., 2007; Hübener et al., 2013; Jung et al., 2009; Koch et al., 2011; Wellington et al., 1998). Caspases are cysteine proteases which usually cleave after a C-terminal aspartate residue and are known to be involved in apoptotic and inflammatory pathways, but also to play a crucial role in cell proliferation, differentiation, and migration (Li and Yuan, 2008; McIlwain et al., 2013). Calpains, a class of Ca^{2+}-dependent regulatory cysteine proteases, show a more complex selection for the cleavage site recognition motif and are specialized in modulating structure, localization, and activity of their substrates (Smith and Schnellmann, 2012; Sorimachi et al., 2011).

Although both groups of enzymes are reportedly active in processing ataxin-3, most recent research has zeroed in on calpains, as their intrinsic Ca^{2+}-sensitivity directly links these proteases with the disrupted Ca^{2+} homoeostasis observed in MJD and other neurodegenerative diseases (Bezprozvanny, 2009; Chen et al., 2008; Koch et al., 2011). First *in vivo* studies demonstrated beneficial effects on neuropathology and behavioural phenotype of MJD animals, when inhibiting calpain activity pharmacologically or overexpressing the endogenous calpain inhibitor calpastatin (CAST) (Simoes et al., 2012; Simões et al., 2014).

g. Weber et al., 2017, Brain.

Several putative calpain cleavage sites within ataxin-3 were described and their localization narrowed down to positions around amino acids 60, 200, 260 (Haacke et al., 2007), 190 (Colomer Gould et al., 2007), or 154 and 220, respectively (Simoes et al., 2012). Concordantly, C-terminal fragment constructs comprising amino acids which encompass the polyQ tract, showed a notably enhanced cytotoxicity and aggregation propensity compared to full-length mutant ataxin-3 (Haacke et al., 2006; Ikeda et al., 1996; Invernizzi et al., 2012; Paulson et al., 1997). However, the exact sites and the impact of the consequent fragments remain elusive.

Here, we report on the successful precise identification and characterization of calpain cleavage sites within the ataxin-3 protein. After confirming our previous results that ataxin-3 is cleaved both by calpain-1 and calpain-2 *in vitro*, and that calpain-derived cleavage fragments can be observed in animal models of MJD (Hübener et al., 2013), we now verified the existence of these specific breakdown products in patient-derived cell lines and MJD post mortem brain tissue. In addition, we engaged in the determination of cleavage sites using an elaborated combination of in silico prediction tools, western blot analysis, mass spectrometry, and peptide overlay assays. By this means, we detected four prominent calpain cleavage sites in the ataxin-3 protein, with two major sites at amino acids D208 and S256. Furthermore, we effectively abolished calpain cleavage of ataxin-3 by exchanging amino acids at identified sites by triple-tryptophan motifs and analysed the impact of ataxin-3 proteolysis by overexpressing cleavage site-corresponding fragment constructs. Our data pave the way for subsequent *in vivo* studies and help to better understand calpain-dependent proteolytic events in MJD as a target for pharmacological treatments.

Materials and methods

Ethical statement on human research

Informed consent was acquired for all patients from whom skin biopsies were obtained. Skin biopsies and experiments on human material were approved by the ethics committee of the University of Tübingen (NEUROMICS No. 598/2011BO1). Tissue was obtained and used in accordance with the Declaration of Helsinki.

Prediction of calpain cleavage sites in silico

In silico prediction of the calpain cleavage sites in the ataxin-3 protein (isoform 2; UniProt identifier: P54252-2) was performed using the GPS-CCD (group-based prediction system-calpain cleavage detector) software (Liu et al., 2011). Scores for every amino acid position were graphically visualized using GraphPad Prism 6.00 for Windows (GraphPad Software Inc.).

Expression constructs

The pDsRed2-ER vector was obtained from Clontech (Takara Bio). For generation of Strep/FLAG-tagged ataxin-3 constructs, ataxin-3 (cDNA for isoform 2; UniProt identifier: P54252-2) 15Q and 62Q was cloned into the pDEST-(N)SF TAP by Gateway cloning as described previously (Gloeckner et al., 2007). Calpain cleavage site mutated ataxin-3 constructs were cloned by inserting gBlocks® Gene Fragments (Integrated DNA Technologies), comprising the altered cleavage site sequence, into pEGFP-N1 ataxin-3 vectors (thankfully provided by Thorsten Schmidt). For penta-alanine (5A) mutations at amino acid sites H187, D208 and S256 restriction enzymes SpeI and XmnI were used. For triple-tryptophan (3W) mutations at sites H187, D208 and S256, SpeI was replaced by SacII. Gene fragments featuring 5A and 3W mutations at amino acid site T277 were inserted using SacII and BbsI. For calpain cleavage-corresponding fragment constructs, DNA fragments were generated by amplifying respective sequences of the ataxin-3 isoform 2 cDNA by PCR. Primer pairs used for amplification added HindIII (5') and KpnI (3') restriction sites flanking the PCR products. Sequences were cloned into a pEGFP-N1 vector via aforementioned restrictions sites. Expanded CAG repeats (148 CAG) were integrated into the constructs employing enzymes XmnI and PpuMI. All restriction enzymes used for cloning were obtained from NEB. Correct cloning of the constructs was confirmed by Sanger sequencing and functional overexpression tested by transient transfection in HEK 293T cells.

g. Weber et al., 2017, Brain.

Cell culture and transfection

Cell culture experiments were performed with HEK 293T cells (ATCC: CRL-11268), SV40-immortalized human fibroblasts, generated from skin biopsies of an MJD patient (23 and 67 CAG repeats) and an age- and gender-matched control (14 and 21 CAG repeats) (Supplementary Table 1), human primary fibroblasts and human fibroblast-derived iPS cells.
HEK 293T cells and SV-40-immortalized human fibroblasts were cultured in Dulbecco's modified eagle's medium (DMEM) GlutaMAX™ supplemented with 10% fetal calf serum (FCS), 1% non-essential amino acids (MEM NEAA) and 1% Antibiotic-Antimycotic (all Gibco®, Thermo Fisher Scientific) at 37°C in 5% CO_2. Transfection of HEK 293T cells was done using Attractene reagent (Qiagen) according to the manufacturer's protocol.
For overexpression of SF-tagged ataxin-3 and subsequent protein purification, HEK 293T cells were cultured in 14 cm dishes in DMEM medium (PAA) supplemented with 10% FCS (PAA) and appropriate antibiotics. Cells were transfected at a confluence between 50 - 70% with 8 µg plasmid DNA/dish using polyethyleneimine PEI (Polysciences) solution as described previously (Ben-Zimra et al., 2002). After transfection, cells were cultured for 48 h.

Reprogramming of fibroblasts to iPSCs

Skin biopsies were obtained from 3 MJD patients and 4 healthy controls (Supplementary Table 1). Each biopsy was dissected and left undistributed in fibroblast medium consisting of DMEM high glucose with 10% FCS for 10 days at 37 °C and 5% CO_2 to allow fibroblasts to grow out from the biopsy. Expansion of skin fibroblast was achieved by medium change every 2-3 days. For reprogramming $1x10^5$ fibroblasts were electroporated (Nucleofector 2D, Lonza) with a total of 1 µg per plasmid carrying the sequences for hOCT4, hSOX2, hKLF4, hL-MYC and hLIN28 and cultured in fibroblast medium for 1 day (Okita et al., 2011). After 2 days of cultivation in fibroblast medium containing 2 µg/L FGF-2 (Peprotech), cells were transferred to Essential 8 (E8) medium containing 100 µM NaB (Sigma-Aldrich). After approx. 21 - 28 days, iPSC colonies were picked manually and further expanded on Matrigel-coated 6-well dishes cultivated with E8 medium. After reaching confluency cells were split in a ratio of 1:6 – 1:12 with PBS/EDTA (0.02% EDTA in DPBS) and further expanded. At passage 7 - 10, iPSCs were harvested for analysis or frozen in E8 medium with 40% KOSR (Gibco®, Thermo Fisher Scientific), 10% DMSO (Sigma-Aldrich), and 1 µM Y-27632 (Abcam Biochemicals). Generated iPSCs were carefully characterized including exclusion of plasmid-integration, screening for genomic aberrations, resequencing of mutation site, confirmation of expression of pluripotency markers, and verifying the *in vitro* differentiation potential (as example see Hauser *et al*., 2016) (data not shown).

Neuronal differentiation of iPSCs

For differentiation of iPSCs to cortical neurons (iCNs) a protocol published from Shi and colleagues was applied (Shi *et al.*, 2012). Briefly, neural induction was achieved by dual SMAD inhibition (10 µM SB431542 and 500 nM LDN-193189 (both Sigma-Aldrich)) and cultivation in 3N medium. Medium was changed every day and cells collected at day 10 by dissociation with Accutase (Thermo Fisher Scientific) followed by replating in 3N medium supplemented with 20 ng/ml FGF2. At day 12, FGF2 was withdrawn and cells were further cultivated in 3N medium with medium change every other day. Cell cultures were passage once more by dissociation with Accutase and replated at a density of 400,000 cells per cm^2 on poly-ornithine and Matrigel-coated 6-well plates. Medium was changed every other day and cell-based calpain activation assay was performed at day 36.

Fluorescence microscopy of differentiated neurons

Differentiated cortical neurons were fixed at day 36 in 4% paraformaldehyde in DPBS for 15 min and washed 3 times with DPBS. Blocking solution (DPBS supplemented with 1% FBS and 0.1% Triton X-100) was added for 45 min and cells were incubated with first primary antibody mouse anti-β-III-tubulin (TUJ1)(1:1000; clone SDL.3D10, T8660, Sigma Aldrich) for 1 h at room temperature. After 3 times washing in DPBS, secondary antibody anti-mouse Alexa Fluor® 488 (1:500; Thermo Fisher Scientific)) was applied and incubated for 1 h at room temperature in the dark. Afterwards, cells were incubated with second primary antibody rat anti-CTIP2 (1:500; clone 25B6, ab18465, Abcam). Subsequently, coverslides were incubated with secondary antibody anti-rat Alexa Fluor® 568 (1:500; Thermo Fisher Scientific). After 3 washing steps in DPBS, nuclear counterstaining was achieved by adding DAPI (1:10,000) for 15 min at room temperature. Cells were embedded in ProLong® Diamond Antifade Mountant (Thermo Fisher Scientific) and images were taken with Axio Imager Z1 with ApoTome (Zeiss).

Confocal microscopy

For confocal microscopy of HEK 293T cells, cells were seeded on 8-well Millicell® EZ slides (Merck Millipore), transfected with respective constructs and cultured for 48 h. Subsequently, cells were pre-fixed with 0.4% paraformaldehyde in DPBS for 15 min at 37°C and fixed with 4% paraformaldehyde in DPBS for another 15 min at room temperature. After washing twice with DPBS for 5 min, the media chamber was removed and cells mounted with VECTASHIELD® Antifade Mounting Medium with DAPI (Vector Laboratories). Fluorescent

images were taken on a confocal laser-scanning microscope (Zeiss, LSM 710), using a 40× 1.3 NA oil objective and the pinhole set to one airy unit. Zeiss ZEN 2011 was used as imaging software.

FACS analysis

For measuring viability of cells transfected with EGFP-tagged ataxin-3 constructs, cells were cultured for 72 h post transfection and subsequently stained with Zombie NIR™ Fixable Viability Kit (BioLegend) according to the manufacturer's standard cell staining protocol. Afterwards, cells were fixed with 1% paraformaldehyde in DPBS for 30 min at 4°C and analysed using a FACS LSR II cytofluorometer with FACS-DIVA software version 6.1.3 (BD Bioscience). To exclude untransfected cells, only GFP-positive cells were analysed for Zombie NIR staining. As a positive control for cell death and for defining the gating strategy, cells were treated with 5 mM H_2O_2 overnight prior to the staining (Supplementary Fig. 1).

Cell-based calpain inhibition and activation assay

For activation of endogenous calpains, cell medium was aspirated and replaced by Opti-MEM® I Reduced Serum Media (Gibco®, Thermo Fisher Scientific). For negative control, cells were pre-treated with 10 µM of the calpain inhibitor CI III (carbobenzoxy-valinyl-phenylalaninal) (Merck Millipore) for 1 h. Calpain activation was triggered by incubating cells with 1 µM of the Ca^{2+} ionophore ionomycin (Sigma-Aldrich) and 5 mM $CaCl_2$ for 1 h at 37°C in 5% CO_2. To decrease baseline activity of calpains, cells were solely treated with 10 µM of the calpain inhibitor CI III or with DMSO as vehicle control for 2 h.

Lysate preparation and western blotting

Cell lysates were prepared as follows: Transfected and treated HEK 293T cells were detached by rinsing with cold DPBS (Gibco®, Thermo Fisher Scientific). Treated MJD patient- and control-derived SV40-immortalized fibroblasts were collected by trypsinization followed by pelleting at 300 × g for 5 min and washing with cold DPBS. All cells were again pelleted at 300 × g for 5 min and lysed in RIPA buffer (50 mM Tris pH 7.5, 150 mM NaCl, 0.1% SDS, 0.5% sodium deoxycholate and 1% Triton X-100), containing cOmplete® protease inhibitor cocktail (Roche) for 25 min on ice, while vortexing every 5 min. Samples were centrifuged at 13,200 × g for 15 min at 4°C. Afterwards, the supernatant was transferred into a pre-cooled reaction tube, adding glycerol to final concentration of 10%. Lysates of human cerebellar tissue were obtained by homogenizing the sample in RIPA buffer containing cOmplete® protease inhibitor cocktail using a ULTRA-TURRAX® disperser

(VWR). Homogenates were incubated for 25 min on ice and centrifuged at 13,200 × g for 30 min at 4°C. The supernatant was transferred into a pre-cooled reaction tube and mixed with glycerol to a final concentration of 10%. Protein concentrations of RIPA lysates were measured spectrophotometrically using Bradford reagent (Bio-Rad Laboratories).

Western blotting was performed according to standard procedures. Briefly, 30 µg of protein were mixed with 4 × LDS sample buffer (1 M Tris Base pH 8.5, 2 mM EDTA, 8% LDS, 40% glycerol, 0.075% CBB G, 0.025% phenol red) and 100 mM DTT, and heat denatured for 10 min at 70°C. Subsequently, protein samples were separated electrophoretically using home-made 10% Bis-Tris gels, 4-12% Bolt® Bis-Tris gradient gels or 7% NuPAGE® Tris-Acetate gels (both Thermo Fisher Scientific) with respective electrophoresis buffers, MES buffer (50 mM MES, 50 mM Tris Base pH 7.3, 0.1% SDS, 1 mM EDTA) or Tris-Acetate running buffer (50 mM Tricine, 50 mM Tris Base pH 8.25, 0.1% SDS). Proteins were transferred on Amersham™ Protran™ Premium 0.2 µm nitrocellulose membranes (GE Healthcare) using Bicine/Bis-Tris transfer buffer (25 mM Bicine, 25 mM Bis-Tris pH 7.2, 1 mM EDTA, 15% methanol) and a TE22 Transfer Tank (Hoefer) at 80 V for 2 h.

For detecting total protein on the blot after transfer, membranes were stained using SYPRO® Ruby Protein Blot Stain (Thermo Fisher Scientific) according to manufacturer's protocol. Afterwards, membranes were blocked for 1 h with 5% SlimFast (Unilever) in TBS (Tris-buffered saline) at room temperature, and probed overnight at 4°C with primary antibodies diluted in TBS-T (TBS with 0.1% Tween 20). Afterwards, western blots were incubated at room temperature for 1 h with the respective HRP-conjugated secondary antibodies. For a detailed list of primary and secondary antibodies, see Supplementary Materials and Methods. Chemiluminescence and fluorescence signals were detected using the LI-COR ODYSSEY® FC and quantified with ODYSSEY® Server software version 4.1 (LI-COR Biosciences).

Cytoplasmic/nuclear fractionation

For separation of cytoplasmic and nuclear proteins, the REAP (Rapid, Efficient And Practical) fractionation method was utilized with minor modifications (Suzuki et al., 2010). Briefly, transfected HEK 293T cells were detached by rinsing with cold DPBS and pelleted at 300 × g. Pellets were resuspended in DPBS-N (DPBS, 0.1% NP-40, and cOmplete® protease inhibitor). An aliquot was taken as total cell sample. The remainder was centrifuged for 10 s at 10,000 × g. The supernatant was transferred into a fresh tube and declared as the cytoplasmic fraction. The pellet was washed once with DPBS-N and centrifuged again for 10 s at 10,000 × g. The supernatant was discarded and the pellet, containing the nuclear

fraction, was resuspended in 1 × LDS buffer with 100 mM DTT. Total cell sample and cytoplasmic fraction were mixed with 1 × LDS buffer with 100 mM DTT, ultrasonicated for 10 s and analysed by western blotting. Purity of obtained fractions was confirmed by western blotting using α-tubulin as a cytoplasmic marker and histone H3 as a nuclear marker (antibody mouse anti-histone H3; 1:2000; clone mAbcam 10799, Abcam).

Protein purification

Purification of Strep/FLAG (SF)-tagged ataxin-3 from HEK 293T cells was performed as described previously (Gloeckner et al., 2009, 2010). Briefly, after removal of the medium cells were lysed in 1 ml lysis/washing buffer (50 mM TRIS pH 7.4, 100 mM NaCl) supplemented with 0.55% NP-40 and cOmplete® protease inhibitor cocktail, per 14 cm dish. Incubation with lysis buffer was then performed for 40 min at 4 °C on a shaker. Cell debris and nuclei were removed by centrifugation of the lysates at 10,000 × g for 10 min. Cleared lysates were incubated with Strep-Tactin® Superflow® resin (IBA) for 1 h at 4 °C. Beads were transferred to micro-spin columns (GE Healthcare) and washed 5 × with 500 µl washing buffer prior final elution using 400 µl elution buffer (washing buffer supplemented with 200 mM D-desthiobiotin [IBA]).

Calpain activation assay in vitro

In vitro calpain activation assays using purified recombinant proteins or cell extracts were per formed as previously described (Hübener et al., 2013). Briefly, for calpain cleavage of recombinant ataxin-3, 5 µg of His_6-ataxin-3 (R&D Systems) or purified SF-tagged ataxin-3 were diluted in 400 µl calpain reaction buffer (20 mM HEPES/KOH pH 7.6, 10 mM KCl, 1.5 mM $MgCl_2$, 1 mM DTT). The positive control was incubated with recombinant calpain-1 or calpain-2 (Merck Millipore), and 2 mM $CaCl_2$ for indicated molar ratios and times at room temperature. Calpain activity of all samples was quenched by adding 100 µM ALLN (N-Acetyl-L-leucyl-L-leucyl-L-norleucinal) (Merck Millipore) and 20 mM EDTA. When needed, 100 µM of the pan-caspase inhibitor Q-VD-OPh (Merck Millipore) were added to block caspase activation.

For *in vitro* calpain activation using cell culture lysates, cell pellets were incubated in calpain lysis/reaction buffer (20 mM HEPES/KOH pH 7.6, 10 mM KCl, 1.5 mM $MgCl_2$, 1 mM DTT, 0.1% Triton X-100) for 25 min on ice, while vortexing every 5 min. Samples were centrifuged at 13,200 × g for 15 min at 4°C. Afterwards, the supernatant was transferred into a pre-cooled reaction tube and protein concentrations were measured spectrophotometrically using Bradford reagent. Lysates were diluted in calpain reaction buffer to obtain a final protein

concentration of 1.5 µg/ µl. For negative control, lysates were pre-incubated with 100 µM of the calpain inhibitor CI III for 10 min on ice. To activate endogenous calpains, 2 mM $CaCl_2$ were added and incubated at 37°C under constant agitation for indicated times. For quenching the reaction and further western blot analysis, as described above, samples were mixed with 4 × LDS sample buffer and 100 mM DTT, and heat denatured for 10 min at 70°C.

Quantitative mass spectrometric analysis

Strep/FLAG (SF)-tagged ataxin-3 with 15Q or 62Q repeats was either expressed in HEK 293T cells cultured in heavy (lysine-8; aginine-10) or light (lysine-0, arginine-0) SILAC medium and purified via the Strep-tag II as described previously (Gloeckner et al., 2009). For calpain cleavage induction, 5 µg of purified heavy-labelled ataxin-3 was incubated with recombinant calpain-1 or calpain-2 as described above. Calpain-treated and control samples were mixed in a 1:1 ratio and samples were precipitated by chloroform/methanol and re-dissolved in 50 mM ammonium bicarbonate, containing 0.2% RapiGest (Waters), reduced with DTT and alkylated with iodoacetamide. In addition, a reverse experiment was performed by switching the labels between the conditions. Proteolysis was carried out by adding GluC or AspN (both NEB) at 37°C o/n. The RapiGest surfactant was hydrolysed and removed and samples were further purified via C18-StageTips (Thermo Fisher Scientific) following standard protocols. Samples were subsequently analysed by LC-MSMS using a nano-flow HPLC system (Dionex Ultimate 3000 RSLC, Thermo Fisher Scientific) coupled to a Q-Exactive Plus tandem mass spectrometer (Thermo Fisher Scientific). In order to identify peptides specific to the calpain cleavage, quantification of the resulting MS-data was performed. The raw data were directly analysed by the MaxQuant software ver. 1.5.2.8 (Cox et al., 2009) allowing protein identification and quantification with the following Andromeda search-engine parameters: database: custom ataxin-3 database (66 entries), containing typical protein IDs previously identified in ataxin-3 affinity purifications, carbamidomethyl as fixed modification as well as N-terminal protein acetylation as variable modification with the heavy/light (H/L) isotope pairs lysine-0/arinine-0 and lysine-8/arginine-10 for quantification. As enzyme either GluC or AspN and semi-specific cleavage mode were chosen. The initial mass accuracy (MS) for mass recalibration was set to 20 ppm. For MSMS spectra, the mass accuracy was set to 0.1 Da. The FDR (false discovery rate) threshold was set to 0.01. Razor-peptides and peptides with N-terminal acetylation or methionine oxidation were included into protein quantification. Downstream analysis and graphical representation was carried out using Perseus ver. 1.5.2.6. Peptides corresponding to ataxin-3 appearing at least in one forward (H: calpain treatment; L: control condition) and one reverse experiment (label switch)

were filtered out. Each condition (“Ratio H/L normalized” values of MaxQuant output) was then re-normalized by division by their medians. A combined analysis was performed for the calpain-1/2 isoforms and the different ataxin-3 polyQ repeats, 15Q and 62Q. Peptides with a normalized H/L ratio greater than 2 in the forward experiment and a normalized H/L ratio below 0.5 in the reverse condition were considered as robust hits.

Peptide array synthesis, calpain overlay and immunodetection

Putative calpain cleavage sites in ataxin-3 and alanine or tryptophan mutations thereof were synthesized as 20-mer peptides on cellulose membranes using a Multipep automated peptide synthesizer (INTAVIS Bioanalytical Instruments AG) (Frank and Overwin, 1996).
Calpain overlay experiments were performed as previously described (Wanichawan et al., 2014). Shortly, the peptide array membranes were first activated in methanol for 10 seconds followed by three washes of 10 min in TBS-T. Thereafter, the membranes were blocked in 1% casein overnight at 4°C before overlaying with 1 µg/ml of calpain-1 (human erythrocytes, 208713, Calbiochem) or calpain-2 (porcine kidney, 208715, Calbiochem) in calpain buffer (20 mM HEPES pH 7.5, 10 mM EGTA, 0.1% Triton X-100, 20 mM $CaCl_2$) overnight at 4°C with gentle agitation. Membranes incubated without any calpain protein were used as negative control. The membranes were then washed five times for 5 min in TBS-T and incubated with primary antibody rabbit anti-calpain (1:1000; sc-30064, Santa Cruz) for 1 h at room temperature, washed five times for 5 min in TBS-T, and incubated with the HRP-conjugated secondary antibody donkey anti-rabbit IgG (NA934V, GE Healthcare). Chemiluminescence signals were developed by ECL Prime western blotting detection reagent (RPN 2232, GE Healthcare) and detected using ImageQuant™ LAS-4000 imager (Fujifilm). Densitometric analysis of detected signals was performed using the ImageJ software (Schneider et al., 2012).

Filter retardation assay

For the detection of SDS-insoluble ataxin-3 species, transfected HEK 293T cells were homogenized in DPBS-T (DPBS with 1% Triton X-100 and cOmplete® protease inhibitor cocktail) by ultrasonication for 10 s. Protein concentrations of the homogenates were determined spectrophotometrically using Bradford reagent and 12.5 µg of total protein were diluted in DPBS containing 2% SDS and 50 mM DTT. Samples were heat denatured for 5 min at 95°C and cooled down to room temperature to prevent precipitation of SDS. A nitrocellulose membrane (Amersham™ Protran™ 0.45 µm, GE Healthcare) was equilibrated in 0.1% SDS in DPBS and samples were filtered through this membrane using a Minifold® II

Slot Blot System (Schleicher & Schuell). The membrane was rinsed once with TBS and blocked with 5% SlimFast in TBS for 1h at room temperature. Membranes were detected using the standard immunodetection protocol, see section *western blotting*. Retained SDS-insoluble ataxin-3 was detected using the antibodies mouse rabbit anti-ataxin-3 (1:500; SA3637, Schmidt et al. 1998) or rabbit anti-ubiquitin (1:500; Z 0458, Dako, Agilent Technologies).

Denaturing detergent agarose gel electrophoresis (DDAGE)

Electrophoretical separation and analysis of high molecular species of ataxin-3 was performed according to the protocol for semi-denaturing detergent agarose gel electrophoresis (SDD-AGE) (Halfmann and Lindquist, 2008), with the modifications stated below. For sample preparation, 25 µg of cell homogenate were mixed with 4 × loading buffer (2 × TAE buffer, 40% glycerol, 8% SDS, 0.05% bromophenol blue) with 50 mM DTT, and heat denatured for 5 min at 95°C. Samples were electrophoretically separated on a 0.75% TAE agarose Gel with 0.1% SDS using a PerfectBlue Gelsystem Mini S (Peqlab) at 3 V per cm gel length. Afterwards, proteins were transferred on Amersham™ Protran™ Premium 0.2 µm nitrocellulose membranes (GE Healthcare) using Bicine/Bis-Tris transfer buffer with 10% methanol, and a TE22 Transfer Tank (Hoefer) at 80 V for 2 h. Membranes were detected using the standard immunodetection protocol, see section *western blotting*. For detecting high molecular species of ataxin-3, antibodies rabbit anti-ataxin-3 (1:500; SA3637, Schmidt et al. 1998) or rabbit anti-ubiquitin (1:500; Z 0458, Dako, Agilent Technologies) were applied. Huntingtin was detected as a loading control using a rabbit anti-huntingtin antibody (1:1000; clone D7F7, #5656, Cell Signaling).

Statistical analysis

Statistical analysis was performed with GraphPad Prism 6.00 for Windows (GraphPad Software Inc.). Statistical significance of data sets obtained by western blot, DDAGE and FACS was determined using One-way-ANOVA and Tukey post-test. For calpain overlay experiments, statistical differences were tested using One-way ANOVA with Bonferroni post-test. *P*-values <0.05 were considered as statistically significant, with $*P < 0.05$, $**P < 0.01$ and $***P < 0.001$.

g. Weber et al., 2017, Brain.

Results

In silico prediction of calpain cleavage sites in the ataxin-3 protein

The precise mechanism of cleavage site-recognition by calpains remains elusive, making predictions of putative cleavage sites a challenging task. Many structural features of the substrate protein seem to contribute to its specificity including determinants like primary/secondary protein structures or PEST regions (sequences rich in proline, glutamic acid, serine, and threonine) (duVerle et al., 2011; Liu et al., 2011; Tompa et al., 2004).
In order to perform an *in silico* prediction approach for calpain cleavage sites within the ataxin-3 protein, we utilized the GPS-CCD tool (Group-based Prediction System - Calpain Cleavage Detector; freely available at http://ccd.biocuckoo.org/), which is based on a data set of 368 experimentally verified sites in 130 substrate proteins (Liu et al., 2011). Using the canonical protein sequence of the ataxin-3 isoform 2 (UniProt identifier: P54252-2), we could identify 24 major sites with a cleavage likelihood score above the maximum default cut-off value of 0.654. High scores for the polyQ repeat were considered as an artefact of the prediction. To narrow down the choice of promising sites, we selected those with protruding cleavage likelihood scores in comparison to the surrounding region (Fig. 1A). A detailed list with the main sites is given in Supplementary Table 2.

Calpain-1 and calpain-2 cleave wild-type and mutant ataxin-3 at similar sites in vitro

To reconfirm ataxin-3 as a substrate for calpains *in vitro*, we performed calpain activation assays by incubating recombinant His_6-ataxin-3 22Q with increasing amounts of recombinant calpain-1 and calpain-2. Using a set of antibodies with epitopes along the ataxin-3 sequence (Fig. 1B), we investigated resulting fragments via western blotting and observed comparable cleavage patterns for both calpains with corresponding N-terminal and C-terminal ataxin-3 fragments (Fig. 1C and D). Furthermore, when repeating the experiment with Strep/FLAG (SF)-tagged ataxin-3 15Q and 62Q in a time-dependent manner, no major differences between wild-type and polyQ-expanded ataxin-3 fragments became apparent (Supplementary Fig. 2). However, on closer examination of resulting cleavage patterns, we identified a consistent group of presumably N-terminal ataxin-3 breakdown products and labelled them with letters ‘a’ to ‘e’ according to their expected cleavage site position from the N- to the C-terminus (Fig. 1C and D, Supplementary Fig. 2). Overall, these data suggest that wild-type and polyQ-expanded ataxin-3 are cleaved mainly at similar cleavage sites by both calpain-1 and calpain-2.

Calpain-dependent ataxin-3 cleavage is present in patient-derived cells and post mortem brain tissue

After modelling calpain-cleavage *in vitro*, we sought to investigate the presence of calpain-dependent ataxin-3 cleavage in patient-derived cell lines and *post mortem* brain tissues. For this purpose, we treated SV40-immortalized fibroblasts, which were derived from a MJD patient and age- and gender-matched control, with the calpain inhibitor CI III for 2 h. Western blotting revealed that pharmacologic suppression of calpain activity, as verified by decreased levels of calpain-cleaved α-spectrin (black arrowhead; Fig. 2A), a lower ratio of active to inactive calpain-1 and elevated levels of CAST (Fig. 2A), led to the reduction of a predominant ataxin-3 fragment in both cell lines (‘c’; Fig. 2A), pointing to its calpain cleavage-dependent origin. When triggering calpain activity in lysates of immortalized fibroblasts by adding $CaCl_2$ (Fig. 2B) or treating the cells with the ionophore ionomycin (Fig. 2C), we could concordantly increase the levels of fragment ‘c’. Furthermore, we detected two further calpain-derived fragments (‘b’ and ‘d’; Fig. 2C) of minor intensity using an antibody guided against the N-terminus of ataxin-3.

In addition to the investigations on immortalized fibroblasts, we analysed ataxin-3 cleavage in primary fibroblasts, induced pluripotent stem (iPS) cells and iPS-derived differentiated cortical neurons (iCNs) of further MJD patients and healthy controls. By this, we reconfirmed the appearance of the predominant, presumably calpain-derived fragment ‘c’ (Fig. 3A). According to expectations, treating iPS cells but also iCNs with ionomycin led to further fragmentation of ataxin-3 and elevated levels of fragment ‘c’ (Fig. 3B-D) and to a weaker extent fragment ‘d’ (Fig. 3D), which was prevented by pre-incubation with CI III. Ultimately, western blotting of *post mortem* cerebellar tissue of a MJD patient and a respective control unveiled the appearance of calpain-dependent ataxin-3 cleavage *in vivo* (Fig. 3E, Supplementary Fig. 3).

In summary, calpains cleave ataxin-3 in both, patient and control-derived cell lines, and in *post mortem* brain tissue, emphasizing the physiological relevance of calpain-mediated proteolysis of ataxin-3.

Deletion constructs help to unveil calpain cleavage sites in ataxin-3

As we reconfirmed calpain-dependent ataxin-3 cleavage *in vitro* and additionally observed fragmentation of the disease protein in patient-derived cell lines and *post mortem* tissue, we raised the question at which particular sites ataxin-3 is proteolytically processed by calpains.

To exclude that the observed ataxin-3 fragments are resulting from caspase-dependent cleavage as an indirect effect of calpain activation, we initially performed a control

experiment with lysates of EGFP-ataxin-3 15Q and 148Q expressing HEK 293T cells. Activation of calpains by addition of $CaCl_2$ induced ataxin-3 cleavage, which could be prevented by the calpain inhibitor, ALLN. However, administration of the pan-caspase inhibitor Q-VD-OPh could not prevent cleavage of ataxin-3, which demonstrated the calpain-dependent origin of arising fragments (Supplementary Fig. 4).

In a first attempt to screen for cleavage regions, we utilized EGFP-tagged deletion constructs of ataxin-3 lacking C-terminal portions of the protein, which were overexpressed in HEK 293T cells. After activating calpains via ionomycin administration, we analysed the cleavage patterns of the deletion constructs by western blotting (Fig. 4A). By comparing fragmentation between the deletion constructs and correlating disappearance of specific fragments with lacking C-terminal portions of ataxin-3, we were able to narrow down cleavage sites to regions between amino acids 321-366 (fragment ‘a’), 244-259 (fragment ‘c’), 198-243 (fragment ‘d’), and right before position 198 (fragment ‘e’) (Fig. 4B). However, the region which comprises the fragment ‘b’ cleavage site could not be clearly defined via this approach.

Mass spectrometry reveals calpain cleavage sites within ataxin-3

After roughly estimating calpain cleavage sites using ataxin-3 deletion constructs, we performed a quantitative mass spectrometric approach to precisely map these sites in ataxin-3. Strep/FLAG (SF)-tagged ataxin-3 15Q or 62Q was expressed in HEK 293T cells grown either in heavy or light SILAC medium and purified afterwards. Heavy-labelled ataxin-3 was incubated with calpain-1 or calpain-2 and mixed with an untreated light-labelled ataxin-3 control in a 1:1 ratio. To rule-out labelling artefacts, a reverse experiment was performed by switching the labels between the conditions. A scheme of the mass spectrometric mapping approach and the representative control western blots of calpain-cleaved heavy-labelled ataxin-3 are shown in Fig. 5A, B and C. The mixture was then subsequently subjected to proteolytic cleavage with either GluC, cleaving C-terminal from glutamate, or AspN, cleaving N-terminally from aspartate. For the final analysis, only peptides were considered which were identified in a forward as well as in a reverse experiment. The method allowed the identification of calpain cleavage sites via the peptides significantly enriched in the calpain-treated condition. Peptides enriched by at least two-fold in the forward experiment and decreased by at least two-fold in the reverse experiment were considered as robust hits. In addition, an outlier analysis, the Significance A test (Cox and Mann, 2008) was performed for forward and reverse experiments separately. These peptides showed semi-canonical cleavage patterns for GluC and AspN supporting the assumption that

the observed non-canonical cleavage sites correspond to calpain cleavage sites. By this approach the sites H187 and D208 (GluC condition) as well as S256 and G259 (AspN condition) could be identified. H187 and D208 showed Significance A values of $p<0.001$ in the forward as well as reverse experiment. G259 showed a Significance A of $p<0.005$ in both experiments. For S256 the Significance A test returned values for the forward and reverse experiment of $p=0.061$ and $p=0.0001$, respectively. Scatter plots showing a combined analysis for the GluC and AspN secondary proteolytic cleavage for the different polyQ repeat lengths and calpain-1/2 isoforms are presented in Fig. 5D and E.

Triple tryptophan substitutions as a strategy to reduce cleavage likelihood

Standard approaches to prevent calpain cleavage of substrates comprise alanine substitutions of up to 10 amino acids or deletion mutagenesis of whole cleavage sites (Gafni et al., 2004; Wanichawan et al., 2014). To optimize this approach, we computed effects on the cleavage likelihood when replacing one to five amino acids of a predicted site by proteinogenic amino acids. Exchanging a single amino acid did not lead to marked alterations of the cleavage likelihood (Supplementary Fig. 5A). However, replacing three or five amino acids led to a strong reduction of the cleavage likelihood, only when introducing cysteine (triple: - 51%, quintuple: - 81%), tryptophan (triple: - 77%, quintuple: - 85%), or tyrosine residues (triple: - 58%, quintuple: - 62%), as exemplarily predicted for site D208 (Supplementary Fig. 5B and C). Interestingly, classical alanine substitutions barely reduced likelihood or rather caused an increase (triple: + 19% quintuple: - 1%). As cysteines and tyrosines are known to be eminent targets of posttranslational modifications, we selected the lesser effected tryptophan as a triplet for mutagenesis of putative cleavage sites together with quintuple alanine substitutions as a classical approach (Fig. 6A).

Calpain overlay of 20-mer ataxin-3 peptide arrays shows reduced binding after triple tryptophan substitution

In order to verify cleavage sites and to prove that a triple tryptophan substitution is indeed reducing cleavage likelihood or substrate recognition as seen *in silico*, we performed calpain overlay assays using an array of immobilized 20-mer peptides which represent sequences around predicted cleavage sites in ataxin-3. Peptides were synthesized as unchanged sequences, or featuring triple tryptophan or quintuple alanine substitutions at predicted sites. Peptides were spotted and immobilized on a membrane and overlaid by calpain-1 or calpain-2. Calpain-specific immunodetection visualized binding of calpains to the respective motifs and verified sequences around sites H187, D208 and S256 (Fig. 6B-D), which we

previously mapped by mass spectrometry, as calpain recognition motifs. Furthermore, peptides representing putative sites T277 and, to a weaker extent, E349 exhibited calpain binding, indicating further cleavage positions (Fig. 6E, Supplementary Fig. 6A). On the other hand, peptides comprising sites L62, S309, and G327, did not show any immunoreactivity for calpains (Supplementary Fig. 6B-D). When introducing a tryptophan triplet at putative cleavage sites, we observed marked reductions of the calpain immunoreactivity for all investigated peptides, except for site S256 and calpain-1 (Fig. 6D). However, quintuple alanine substitutions showed only a clear reduction for sites H187 and T277, with an even stronger decrease for the latter site when compared to a tryptophan triplet (Fig. 6B and E). Notably, introduction of five alanines increased the binding of calpain-2 at site D208 and calpain-1 at site S256 (Fig. 6C and D).

Triple tryptophan mutagenesis of putative calpain cleavage sites reduced ataxin-3 fragmentation

After observing decreased calpain binding to ataxin-3 peptides featuring tryptophan mutations at putative cleavage sites, we sought to confirm these effects on the full ataxin-3 protein. As cell-based calpain cleavage induction primarily gave rise to fragments ‘c’ and ‘d’, we focused on sites, which not only were identified by mass spectrometry and calpain overlay assays but also presumably represent the origin of the two aforementioned breakdown products. For this, we generated C-terminally EGFP-tagged ataxin-3 15Q and 148Q constructs featuring quintuple alanine or triple tryptophan substitutions on cleavage positions D208, S256 or both sites. Following overexpression of respective ataxin-3 variants in HEK 293T cells, we subjected lysates to *in vitro* calpain activation assays and analysed resulting ataxin-3 fragmentation patterns using N-terminally binding and EGFP-specific antibodies on western blots. When comparing unmodified ataxin-3 with variants carrying quintuple alanine substitutions at positions D208 or S256, only a reduction of the N-terminal fragment corresponding to cleavage at amino acid S256 was observed (Fig. 7A and B). However, mutagenesis using tryptophan triplets at positions D208 or S256 nearly abolished respective N-terminal cleavage products (Fig. 7A and B). According to expectations, triple tryptophan exchanges also led to a concurrent reduction of corresponding C-terminal ataxin-3 15Q and 148Q fragments (Fig. 7C and D). Interestingly, mutating both sites led to an enhanced formation of an additional fragment, likely to correspond to cleavage site T277 (‘b’; Fig. 7C and D). It should be mentioned that the cleavage of ataxin-3 is very weak at baseline, making it difficult to identify alterations of the fragmentation pattern in an uninduced state. Cell-based activation of calpains by administering ionomycin, however, revealed a strongly

reduced formation of fragments ‘c’ and ‘d’ in ataxin-3 carrying tryptophan triplets at positions D208 and S256, when compared to unmutated ataxin-3 using western blotting (Fig. 7E). In retrospect to our previous fragment labelling, we were able to assign the detected fragment ‘c’ to cleavage site S256 and fragment ‘d’ to cleavage site D208. An overview of all predicted and identified calpain cleavage sites in our study can be found in Fig. 8A.
In summary, cleavage site mutagenesis using tryptophan triplets turned out as an effective approach to decrease calpain cleavage of ataxin-3.

Fragment constructs as a tool for modelling aggregation and toxicity of calpain-cleaved ataxin-3

As calpain cleavage of overexpressed ataxin-3 was low at baseline, and in addition, stimuli which activate calpains are leading to detrimental side effects for treated cells, we generated EGFP-labelled ataxin-3 fragment constructs representing breakdown products at identified calpain cleavage sites D208 and S256 (Fig. 8B) and overexpressed them in HEK 293T cells (Fig. 8C and F).
Overexpression of C-terminal polyQ-expanded fragment constructs corresponding to cleavage at both sites, D208 and S256, led to a strong accumulation of high molecular and SDS-insoluble ataxin-3 species when compared to full-length ataxin-3 148Q. Furthermore, these ataxin-3 aggregates showed a marked ubiquitination (Fig. 8D). Confocal microscopy of cells expressing the C-terminal fragment constructs together with the endoplasmic reticulum (ER)-labelling protein DsRed2-ER revealed a mainly cytoplasmic to perinuclear formation of occasionally massive ataxin-3 aggregates (Fig. 8E, Supplementary Fig. 7). On the other hand, respective N-terminal ataxin-3 fragment constructs did not aggregate (Fig. 8G). To analyse the impact of C-terminal polyQ-expanded fragment constructs on viability, we performed FACS analyses of transfected (EGFP-positive) HEK 293T cells. Our investigations showed distinctly elevated cell death, when overexpressing both polyQ-expanded fragment constructs in comparison to full-length ataxin-3 148Q (Fig. 8H).
Fragmentation of ataxin-3 by calpains or caspases was hypothesized to lead to a separation of the intrinsic N-terminally located nuclear export signals and the C-terminally located nuclear localisation signals, which might cause a relocation of C-terminal polyQ fragments to the nucleus. To investigate this, we overexpressed full-length and fragment constructs of ataxin-3 in HEK 293T cells and analysed localization using cytoplasmic/nuclear fractionation and confocal imaging (Supplementary Fig. 8). Subcellular fractionation pointed to a mainly cytoplasmic localization of both full-length ataxin-3 and its fragment constructs, regardless of their N- or C-terminal origin (Supplementary Fig. 8A and B). C-terminal fragments did not

specifically demonstrate a shift toward the nucleus. Furthermore, microscopy showed a mainly diffuse distribution of all ataxin-3 variants within the cell, confirming the absence of a nuclear shift of C-terminal fragment constructs (Supplementary Fig. 8C and D).

Taken together, C-terminal polyQ-expanded fragment constructs of ataxin-3, representing calpain cleavage at positions D208 or S256, feature a higher aggregation propensity and elevated cytotoxicity when compared to the polyQ-expanded full-length protein. However, these fragments do not show alterations in the cellular localization when compared to intact ataxin-3.

Discussion

The discovery of proteolytic ataxin-3 cleavage as a relevant contributor to the molecular pathogenesis of MJD opened up further possibilities to develop more directed therapeutics against this highly disabling disorder. Till this day, mainly caspases and calpains were associated with ataxin-3 fragmentation and genetic or pharmacologic inhibition of these enzymes, or modification of recognition sites within their substrates seems to be a promising approach. In particular, inhibition of calpains *in vivo* was investigated intensively, showing that overexpression of CAST using adeno-associated viral vectors in a lentiviral mouse model of MJD did not only reduce ataxin-3 proteolysis but also decreased ataxin-3 aggregation and mediated neuroprotection (Simoes et al., 2012). In line with these observations, the oral administration of the calpain inhibitor BDA-410 exerted comparable beneficial effects on fragmentation, aggregation and neurodegeneration (Simões et al., 2014). On the other hand, non-specific or excessive inhibition of enzymes might lead to adverse effects due to disturbance of their physiological functions (Baudry and Bi, 2016; Donkor, 2011; Kudelova et al., 2015; Li and Sheng, 2012).

In our study, we focussed on the identification of calpain cleavage sites in ataxin-3 and on their genetic modification to prevent proteolytic processing at determined positions. Previous investigations on caspase-dependent fragmentation of ataxin-3 could already identify major caspase cleavage sites within this disease protein and mutagenesis of specific aspartate residues partially blocked ataxin-3 fragmentation (Berke et al., 2004). These findings were translated into a *Drosophila* model of MJD, which exhibited a slowed down progression of neurodegeneration when expressing caspase cleavage-resistant, polyQ-expanded ataxin-3 (Jung et al., 2009). Although localization of putative calpain cleavage sites has been narrowed down by western blotting or Edman N-terminal sequencing, exact sites remained unknown or lacked further confirmation by site-directed mutagenesis (Haacke et al., 2007; Simoes et al., 2012).

Here, in our combinatorial approach, we were not only able to precisely localize calpain cleavage sites within ataxin-3, but also confirmed elected sites by mutating surrounding amino acids to render them less calpain cleavage-prone. In our *in vitro* and cell-based assays, we first reconfirmed wild-type and polyQ-expanded ataxin-3 as substrates for both calpain-1 and calpain-2. We did not detect differences between specificities and cleavage patterns regardless of expected polyQ-dependent size shifts. These observations add to results from studies using only recombinant calpain-2 (Haacke et al., 2007). Furthermore, the lack of differences in cleavage efficiency between calpain-1 and calpain-2 stands in contrast with our previous study, where we detected stronger ataxin-3 cleavage by calpain-2

g. Weber et al., 2017, Brain.

(Hübener et al., 2013). Although previous attempts failed to identify proteolytic fragments in human MJD brain tissue or to associate them with specific proteases (Berke et al., 2004; Goti et al., 2004), we unequivocally observed calpain-dependent ataxin-3 fragmentation in patient- and control-derived fibroblasts, iPS cell lines and post mortem brain tissue at baseline. In this respect, a previous study reported on calpain-dependent ataxin 3 cleavage and aggregation in patient-specific iPSC-derived neurons after inducing Ca^{2+} influx via NMDA or glutamate administration (Koch et al., 2011). More recent investigations using similar approaches, however, could not reproduce the glutamate-induced ataxin-3 aggregation (Hansen et al., 2016).

To analyse observed ataxin-3 fragments and to identify calpain-cleavage sites within the protein sequence, we first predicted cleavage sites in ataxin-3 in silico using the GPS-CCD tool. After comparing predicted sites with results obtained by quantitative mass spectrometry and calpain overlay assays, we were able to identify four major cleavage sites at positions H187, D208, S256, and T277, matching with previous results obtained by Edman sequencing (Haacke et al., 2007). However, cleavage sites at amino acids Q154 or G220 as proposed in a more recent publication (Simoes et al., 2012) were neither observed in our experiments nor reached high scores in our in silico prediction. By correlating expected fragment sizes with the prior observed cleavage patterns, sites D208 and S256 emerged as primary calpain targets. Interestingly, these two cleavage sites co-localize with known phospho-sites in ataxin-3, namely sites T207 and S256. The not yet intensively investigated site T207 was predicted to be phosphorylated by CK2 (Mueller et al., 2009; Trottier et al., 1998). Site S256 was shown to be targeted by GSK 3β and the dephospho-mimetic variant S256A of polyQ-expanded ataxin-3 was shown to be highly aggregation-prone when compared to unchanged or phospho-mimetic S256D ataxin-3 (Fei et al., 2007). Together with our findings, these observations underline the huge relevance of both investigated sites for the protein homoeostasis of ataxin-3 and reveal the modulation of phosphorylation as a putative approach to manipulate ataxin-3 cleavage. In line with this, phosphorylation of huntingtin, the disease protein in Huntington's disease, was shown to reduce its cleavage by caspases (Luo et al., 2005).

In order to prevent ataxin-3 fragmentation by cleavage site-directed mutagenesis, we sought to modify common approaches based on polyalanine substitutions or cleavage site deletions (Gafni et al., 2004; Wanichawan et al., 2014). Although mutagenesis of single amino acids following the 'P2-P1 rule' of substrate recognition has been shown to be sufficient in preventing calpain cleavage (Hirao and Takahashi, 1984; Sasaki et al., 1984; Stabach et al., 1997; Kaczmarek et al., 2012), further studies could not confirm the preference of calpains

for any particular residues or demonstrated that alteration of the sequence at only one position was not sufficient to block calpain-dependent cleavage (Sakai et al., 1987; Banik et al., 1994; Garg et al., 2011). Due to these inconsistencies, we decided on using *in silico* prediction to test the effects of a single to multiple amino acid substitutions by all proteinogenic amino acids. By this approach, we identified a triple tryptophan motif as the most potent mutation to decrease cleavage likelihood. Calpain overlay assays of cleavage-site containing peptides carrying this triplet confirmed a significant reduction of calpain binding, which was more efficient than a penta-alanine substitution. Finally, this effect was corroborated by generating wild-type and polyQ-expanded ataxin-3 variants featuring penta-alanine and triple tryptophan mutations at cleavage sites D208 and S256. Thus, triple tryptophan substitutions constitute a potent way to prevent calpain cleavage at mutated recognition motifs, which can be applied to further calpain substrates.

To further characterize the impact of cleavage-site corresponding fragments, we generated respective EGFP-tagged ataxin-3 constructs comprising N- and C-terminal portions of the wild-type and polyQ-expanded protein. It should be noted that our C-terminal fragment construct 257Cter corresponds directly to a prior generated construct, whose sequence was based on results of unspecified limited proteolysis experiments with recombinant ataxin-3 (Haacke et al., 2006). Only overexpression of C-terminal polyQ-expanded ataxin-3 led to a massive accumulation of ubiquitin-positive aggregates, which markedly exceeded aggregation of full-length ataxin-3 and increased cell death. This corresponds to cell and animal models of MJD, which show strong ataxin-3 accumulations, apoptosis and a more rapid manifestation of MJD-reminiscent phenotypes when compared to the expression of full-length mutant ataxin-3 (Breuer et al., 2010; Ikeda et al., 1996; Paulson et al., 1997). The excessive ubiquitination of C-terminal fragment-derived aggregates, but not of aggregates composed of full-length polyQ-expanded ataxin-3, might be due to the elevated misfolding of truncated ataxin-3 species, which has been suggested earlier as a trigger for ubiquitination (Jana and Nukina, 2004). Confocal microscopy of aggregates formed by our C-terminal fragment constructs exhibited a mainly cytoplasmic localization. Interestingly, a recent histological study on the aggregation pathology in the brainstem of SCA2 and MJD patients revealed the severity of cytoplasmic aggregates as the best predictor of neurodegeneration in both polyQ disorders, while an inverse correlation of neurodegeneration and nuclear aggregates was seen in MJD brain tissue (Seidel et al., 2016). In addition to it, a further study, which investigated aggregate toxicity of artificial β-sheet proteins, as well as fragments of polyQ-expanded huntingtin and TAR DNA binding protein-43 (TDP-43), discovered that cytoplasmic but not nuclear aggregation interfered with nucleocytoplasmic protein and RNA

transport maybe contributing to the cellular pathology in proteinopathies (Woerner et al., 2016). These findings suggest a rather protective role of aggregates localized in the cell nucleus. On the other hand, N-terminal fragment constructs did not show any SDS-insoluble or high molecular aggregation when overexpressed in cell culture, consistent with earlier *in vitro* experiments (Perez et al., 1998), but out of line with our observations in a N-terminal fragment mouse model of MJD (Hübener et al., 2011). As fragmentation of ataxin-3 was connected to a separation of N-terminally located nuclear export signals (NES) and C-terminally located nuclear localisation signals (NLS) (Antony et al., 2009), we analysed the subcellular localization of ataxin-3. Our C-terminal fragment constructs 209Cter and 257Cter, which both contain NLS 273 and lack NES 77 and NES 141, did not exhibit a trend towards nuclear localization. These observations accord with previous investigations which showed that the endogenous NLS signal is not active and C-terminal ataxin-3 fragments without the NES might shuttle in and out of the nucleus (Breuer et al., 2010). The nuclear accumulation of mutant ataxin-3, however, might be triggered by alternative NLS-independent processes.

In summary, we report on the identification of calpain cleavage sites within the ataxin-3 protein and on the successful cleavage prevention by substituting recognition motifs by tryptophan triplets. Furthermore, we could characterize calpain cleavage-derived fragments of ataxin-3. A still pending but not less important further step in analysing ataxin-3 cleavage and arising fragments will be the characterization of our generated cleavage site-mutant constructs *in vivo*. Only a physiological expression of the modified ataxin-3 variants in the correct organic context and a time-dependent manner can give us the chance to assess the impact of proteolytic cleavage on the molecular pathogenesis MJD. This approach was exemplified by previous studies, which were investigating caspase-dependent cleavage of ataxin-3 in *Drosophila* or polyQ-expanded huntingtin in mice (Graham et al., 2006; Jung et al., 2009). In addition, further investigations of C- or even N-terminal ataxin-3 fragments should be undertaken, as, for instance, polyQ-independent fragments of huntingtin showed deleterious effects on autophagy or vesicle transport (El-Daher et al., 2015; Martin et al., 2014).

On a final note, our precise identification of calpain cleavage sites enables the development of an alternative possibility to prevent ataxin-3 fragmentation by skipping exons that contain the respective calpain recognition motif. This concept has already been tested for Huntington's disease by using antisense oligonucleotides that induce skipping of exon 12 in huntingtin pre-mRNA, and thereby abolish the formation of a toxic N-terminal huntingtin fragment (Evers et al., 2014). On the other hand, focusing on the correction or removal of the

expanded CAG repeat might still represent a more specific approach (An et al., 2012; Evers et al., 2013).

Overall, our data emphasize the biological relevance of calpain-mediated ataxin-3 cleavage and underline this proteolytic pathway as a potential therapeutic target for treating MJD.

g. Weber et al., 2017, Brain.

Acknowledgements

We want to thank Wilfred F.A. den Dunnen, Department of Pathology and Medical Biology, University Medical Center Groningen, University of Groningen, Groningen, The Netherlands, for his contribution in collecting human brain tissue samples. We are grateful to Tina Harmuth for generating SV40-immortalized fibroblasts. Furthermore, we want to thank Daniel Weishäupl and Nicolas L.P. Casadei for helpful remarks and fruitful discussions.

Funding

This study was funded by the German Research Foundation (DFG, research grant number HU1770/3-1). JJW was funded by the Baden-Wuerttemberg Foundation (research grant number P-BWS-SPII/3-08). EA is supported by EU Joint Programme–Neurodegenerative Disease Research (JPND; NEuroGeM) and The Netherlands Organization for Health Research and Development (ZonMw).

Author contributions statements

The conceptual framework for the study was developed by JHS, JJW, HPN and OR. Cloning was performed by JHS and MG. All cell culture experiments, protein expression and aggregation analyses were done by JJW and MG. SNH, SH and LS designed and conducted the iPS cell culture experiments. Subcellular fractionation was done by MN. Confocal images were acquired by SS. Calpain activation assays were performed by JJW. FACS-based viability analyses were performed by ACK. GG and CJG developed and conducted mass spectrometry analyses for identification of calpain cleavage sites. Calpain overlay assays were performed by PW and CRC. EA contributed to the selection and collection of brain tissues. All data were analysed and interpreted by JJW, JHS, CJG, and CRC. Illustrations were created by JJW. The manuscript was written by JJW, CJG, and JHS.

References

An MC, Zhang N, Scott G, Montoro D, Wittkop T, Mooney S, et al. Genetic correction of huntington's disease phenotypes in induced pluripotent stem cells. Cell Stem Cell 2012; 11: 253–263.

Antony PMA, Mäntele S, Mollenkopf P, Boy J, Kehlenbach RH, Riess O, et al. Identification and functional dissection of localization signals within ataxin-3. Neurobiol. Dis. 2009; 36: 280–292.

Banik NL, Chou CH, Deibler GE, Krutzch HC, Hogan EL. Peptide bond specificity of calpain: proteolysis of human myelin basic protein. J. Neurosci. Res. 1994; 37: 489–96.

Baudry M, Bi X. Calpain-1 and Calpain-2: The Yin and Yang of Synaptic Plasticity and Neurodegeneration. Trends Neurosci. 2016; xx: 1–11.

Ben-Zimra M, Koler M, Orly J. Transcription of cholesterol side-chain cleavage cytochrome P450 in the placenta: activating protein-2 assumes the role of steroidogenic factor-1 by binding to an overlapping promoter element. Mol. Endocrinol. 2002; 16: 1864–80.

Berke SJS, Schmied FA, Brunt ER, Ellerby LM, Paulson HL. Caspase-mediated proteolysis of the polyglutamine disease protein ataxin-3. J. Neurochem. 2004; 89: 908–18.

Bezprozvanny I. Calcium signaling and neurodegenerative diseases. Trends Mol. Med. 2009; 15: 89–100.

Breuer P, Haacke A, Evert BO, Wüllner U. Nuclear aggregation of polyglutamine-expanded ataxin-3: fragments escape the cytoplasmic quality control. J. Biol. Chem. 2010; 285: 6532–7.

Chen X, Tang TS, Tu H, Nelson O, Pook M, Hammer R, et al. Deranged calcium signaling and neurodegeneration in spinocerebellar ataxia type 3. J Neurosci 2008; 28: 12713–12724.

Colomer Gould VF, Goti D, Pearce D, Gonzalez GA, Gao H, Bermudez de Leon M, et al. A mutant ataxin-3 fragment results from processing at a site N-terminal to amino acid 190 in brain of Machado-Joseph disease-like transgenic mice. Neurobiol. Dis. 2007; 27: 362–9.

Cox J, Mann M. MaxQuant enables high peptide identification rates, individualized p.p.b.-range mass accuracies and proteome-wide protein quantification. Nat. Biotechnol. 2008; 26: 1367–72.

g. Weber et al., 2017, Brain.

Cox J, Matic I, Hilger M, Nagaraj N, Selbach M, Olsen J V, et al. A practical guide to the MaxQuant computational platform for SILAC-based quantitative proteomics. Nat. Protoc. 2009; 4: 698–705.

DiFiglia M, Sapp E, Chase KO, Davies SW, Bates GP, Vonsattel JP, et al. Aggregation of huntingtin in neuronal intranuclear inclusions and dystrophic neurites in brain. Science 1997; 277: 1990–3.

Donkor IO. Calpain inhibitors: a survey of compounds reported in the patent and scientific literature. Expert Opin. Ther. Pat. 2011; 21: 601–636.

duVerle D a., Ono Y, Sorimachi H, Mamitsuka H. Calpain cleavage prediction using multiple kernel learning. PLoS One 2011; 6(5).

El-Daher M-T, Hangen E, Bruyère J, Poizat G, Al-Ramahi I, Pardo R, et al. Huntingtin proteolysis releases non-polyQ fragments that cause toxicity through dynamin 1 dysregulation. EMBO J. 2015; 34: 2255–71.

Evers MM, Tran H-D, Zalachoras I, Meijer OC, den Dunnen JT, van Ommen G-JB, et al. Preventing formation of toxic N-terminal huntingtin fragments through antisense oligonucleotide-mediated protein modification. Nucleic Acid Ther. 2014; 24: 4–12.

Evers MM, Tran HD, Zalachoras I, Pepers B a., Meijer OC, den Dunnen JT, et al. Ataxin-3 protein modification as a treatment strategy for spinocerebellar ataxia type 3: Removal of the CAG containing exon. Neurobiol. Dis. 2013; 58: 49–56.

Fei E, Jia N, Zhang T, Ma X, Wang H, Liu C, et al. Phosphorylation of ataxin-3 by glycogen synthase kinase 3β at serine 256 regulates the aggregation of ataxin-3. Biochem. Biophys. Res. Commun. 2007; 357: 487–492.

Frank R, Overwin H. SPOT Synthesis: Epitope Analysis with Arrays of Synthetic Peptides Prepared on Cellulose Membranes. In: Epitope Mapping Protocols. 1996. p. 149–170.

Gafni J, Hermel E, Young JE, Wellington CL, Hayden MR, Ellerby LM. Inhibition of calpain cleavage of Huntingtin reduces toxicity: Accumulation of calpain/caspase fragments in the nucleus. J. Biol. Chem. 2004; 279: 20211–20220.

Garg S, Timm T, Mandelkow EM, Mandelkow E, Wang Y. Cleavage of Tau by calpain in Alzheimer's disease: The quest for the toxic 17 kD fragment. Neurobiol. Aging 2011; 32: 1–14.

Gloeckner CJ, Boldt K, Schumacher A, Roepman R, Ueffing M. A novel tandem affinity purification strategy for the efficient isolation and characterisation of native protein complexes. Proteomics 2007; 7: 4228–4234.

Gloeckner CJ, Boldt K, Ueffing M. Strep/FLAG tandem affinity purification (SF-TAP) to study protein interactions. Curr. Protoc. Protein Sci. 2009: 1–19.

Gloeckner CJ, Boldt K, Von Zweydorf F, Helm S, Wiesent L, Sarioglu H, et al. Phosphopeptide analysis reveals two discrete clusters of phosphorylation in the N-terminus and the Roc domain of the Parkinson-disease associated protein kinase LRRK2. J. Proteome Res. 2010; 9: 1738–1745.

Goti D, Katzen SM, Mez J, Kurtis N, Kiluk J, Ben-Haïem L, et al. A Mutant Ataxin-3 Putative-Cleavage Fragment in Brains of Machado-Joseph Disease Patients and Transgenic Mice Is Cytotoxic above a Critical Concentration. J. Neurosci. 2004; 24: 10266–10279.

Graham RK, Deng Y, Slow EJ, Haigh B, Bissada N, Lu G, et al. Cleavage at the Caspase-6 Site Is Required for Neuronal Dysfunction and Degeneration Due to Mutant Huntingtin. Cell 2006; 125: 1179–1191.

Haacke A, Broadley S a., Boteva R, Tzvetkov N, Hartl FU, Breuer P. Proteolytic cleavage of polyglutamine-expanded ataxin-3 is critical for aggregation and sequestration of non-expanded ataxin-3. Hum. Mol. Genet. 2006; 15: 555–68.

Haacke A, Hartl FU, Breuer P. Calpain inhibition is sufficient to suppress aggregation of polyglutamine-expanded ataxin-3. J. Biol. Chem. 2007; 282: 18851–6.

Halfmann R, Lindquist S. Screening for amyloid aggregation by Semi-Denaturing Detergent-Agarose Gel Electrophoresis. J. Vis. Exp. 2008: 20–22.

Hansen SK, Stummann TC, Borland H, Hasholt LF, Tümer Z, Nielsen JE, et al. Induced pluripotent stem cell - derived neurons for the study of spinocerebellar ataxia type 3. Stem Cell Res. 2016; 17: 306–317.

Hauser S, Höflinger P, Theurer Y, Rattay TW, Schöls L. Generation of induced pluripotent stem cells (iPSCs) from a hereditary spastic paraplegia patient carrying a homozygous Y275X mutation in CYP7B1 (SPG5). Stem Cell Res. 2016; 17: 437–440.

Hirao T, Takahashi K. Purification and characterization of a calcium-activated neutral protease from monkey brain and its action on neuropeptides. J. Biochem. 1984; 96: 775–84.

g. Weber et al., 2017, Brain.

Hübener J, Vauti F, Funke C, Wolburg H, Ye Y, Schmidt T, et al. N-terminal ataxin-3 causes neurological symptoms with inclusions, endoplasmic reticulum stress and ribosomal dislocation. Brain 2011; 134: 1925–42.

Hübener J, Weber JJ, Richter C, Honold L, Weiss A, Murad F, et al. Calpain-mediated ataxin-3 cleavage in the molecular pathogenesis of spinocerebellar ataxia type 3 (SCA3). Hum. Mol. Genet. 2013; 22: 508–18.

Ikeda H, Yamaguchi M, Sugai S, Aze Y, Narumiya S, Kakizuka A. Expanded polyglutamine in the Machado-Joseph disease protein induces cell death in vitro and in vivo. Nat. Genet. 1996; 13: 196–202.

Invernizzi G, Aprile FA, Natalello A, Ghisleni A, Penco A, Relini A, et al. The relationship between aggregation and toxicity of polyglutamine-containing ataxin-3 in the intracellular environment of Escherichia coli. PLoS One 2012; 7: e51890.

Jana NR, Nukina N. Misfolding promotes the ubiquitination of polyglutamine-expanded ataxin-3, the defective gene product in SCA3/MJD. Neurotox. Res. 2004; 6: 523–533.

Jung J, Xu K, Lessing D, Bonini NM. Preventing Ataxin-3 protein cleavage mitigates degeneration in a Drosophila model of SCA3. Hum. Mol. Genet. 2009; 18: 4843–52.

Kaczmarek JS, Riccio A, Clapham DE. Calpain cleaves and activates the TRPC5 channel to participate in semaphorin 3A-induced neuronal growth cone collapse. Proc. Natl. Acad. Sci. 2012; 109: 7888–7892.

Koch P, Breuer P, Peitz M, Jungverdorben J, Kesavan J, Poppe D, et al. Excitation-induced ataxin-3 aggregation in neurons from patients with Machado–Joseph disease. Nature 2011: 0–5.

Kudelova J, Fleischmannova J, Adamova E, Matalova E. Pharmacological caspase inhibitors: research towards therapeutic perspectives. J. Physiol. Pharmacol. 2015; 66: 473–82.

Li J, Yuan J. Caspases in apoptosis and beyond. Oncogene 2008; 27: 6194–206.

Li Z, Sheng M. Caspases in synaptic plasticity. Mol. Brain 2012; 5: 15.

Liu Z, Cao J, Gao X, Ma Q, Ren J, Xue Y. GPS-CCD: a novel computational program for the prediction of calpain cleavage sites. PLoS One 2011; 6: e19001.

Luo S, Vacher C, Davies JE, Rubinsztein DC. Cdk5 phosphorylation of huntingtin reduces its cleavage by caspases: implications for mutant huntingtin toxicity. J. Cell Biol. 2005; 169: 647–56.

Martin DDO, Heit RJ, Yap MC, Davidson MW, Hayden MR, Berthiaume LG. Identification of a post-translationally myristoylated autophagy-inducing domain released by caspase cleavage of Huntingtin. Hum. Mol. Genet. 2014; 23: 1–14.

McIlwain DR, Berger T, Mak TW. Caspase functions in cell death and disease. Cold Spring Harb. Perspect. Biol. 2013; 5: a008656.

Mueller T, Breuer P, Schmitt I, Walter J, Evert BO, Wüllner U. CK2-dependent phosphorylation determines cellular localization and stability of ataxin-3. Hum. Mol. Genet. 2009; 18: 3334–3343.

Okita K, Matsumura Y, Sato Y, Okada A, Morizane A, Okamoto S, et al. A more efficient method to generate integration-free human iPS cells. Nat. Methods 2011; 8: 409–412.

Paulson HL, Perez MK, Trottier Y, Trojanowski JQ, Subramony SH, Das SS, et al. Intranuclear inclusions of expanded polyglutamine protein in spinocerebellar ataxia type 3. Neuron 1997; 19: 333–44.

Perez MK, Paulson HL, Pendse SJ, Saionz SJ, Bonini NM, Pittman RN. Recruitment and the role of nuclear localization in polyglutamine-mediated aggregation. J. Cell Biol. 1998; 143: 1457–70.

Sakai K, Akanuma H, Imahori K, Kawashima S. A unique specificity of a calcium activated neutral protease indicated in histone hydrolysis. J. Biochem. 1987; 101: 911–8.

Sasaki T, Kikuchi T, Yumoto N, Yoshimura N, Murachi T. Comparative specificity and kinetic studies on porcine calpain I and calpain II with naturally occurring peptides and synthetic fluorogenic substrates. J. Biol. Chem. 1984; 259: 12489–94.

Schmidt T, Landwehrmeyer GB, Schmitt I, Trottier Y, Auburger G, Laccone F, et al. An isoform of ataxin-3 accumulates in the nucleus of neuronal cells in affected brain regions of SCA3 patients. Brain Pathol. 1998; 8: 669–79.

Schneider CA, Rasband WS, Eliceiri KW. NIH Image to ImageJ: 25 years of image analysis. Nat. Methods 2012; 9: 671–675.

Seidel K, Siswanto S, Fredrich M, Bouzrou M, den Dunnen WFA, Özerden I, et al. On the distribution of intranuclear and cytoplasmic aggregates in the brainstem of patients with spinocerebellar ataxia type 2 and 3. Brain Pathol. 2016.

g. Weber et al., 2017, Brain.

Shi Y, Kirwan P, Livesey FJ. Directed differentiation of human pluripotent stem cells to cerebral cortex neurons and neural networks. Nat. Protoc. 2012; 7: 1836–46.

Simoes AT, Goncalves N, Koeppen A, Deglon N, Kugler S, Duarte CB, et al. Calpastatin-mediated inhibition of calpains in the mouse brain prevents mutant ataxin 3 proteolysis, nuclear localization and aggregation, relieving Machado-Joseph disease. Brain 2012; 135: 2428–2439.

Simões AT, Gonçalves N, Nobre RJ, Duarte CB, Pereira de Almeida L. Calpain inhibition reduces ataxin-3 cleavage alleviating neuropathology and motor impairments in mouse models of Machado-Joseph disease. Hum. Mol. Genet. 2014; 23: 4932–44.

Smith M a, Schnellmann RG. Calpains, mitochondria, and apoptosis. Cardiovasc. Res. 2012; 96: 32–7.

Sorimachi H, Hata S, Ono Y. Calpain chronicle--an enzyme family under multidisciplinary characterization. Proc. Jpn. Acad. Ser. B. Phys. Biol. Sci. 2011; 87: 287–327.

Stabach PR, Cianci CD, Glantz SB, Zhang Z, Morrow JS. Site-directed mutagenesis of alpha II spectrin at codon 1175 modulates its mu-calpain susceptibility. Biochemistry 1997; 36: 57–65.

De Strooper B. Proteases and proteolysis in Alzheimer disease: a multifactorial view on the disease process. Physiol. Rev. 2010; 90: 465–494.

Suzuki K, Bose P, Leong-Quong RY, Fujita DJ, Riabowol K. REAP: A two minute cell fractionation method. BMC Res. Notes 2010; 3: 294. Tarlac V, Storey E. Role of proteolysis in polyglutamine disorders. J. Neurosci. Res. 2003; 74: 406–16.

Tompa P, Buzder-Lantos P, Tantos A, Farkas A, Szilágyi A, Bánóczi Z, et al. On the sequential determinants of calpain cleavage. J. Biol. Chem. 2004; 279: 20775–20785.

Trottier Y, Cancel G, An-Gourfinkel I, Lutz Y, Weber C, Brice a, et al. Heterogeneous intracellular localization and expression of ataxin-3. Neurobiol. Dis. 1998; 5: 335–347.

Wanichawan P, Hafver TL, Hodne K, Aronsen JM, Lunde IG, Dalhus B, et al. Molecular Basis of Calpain Cleavage and Inactivation of the Sodium-Calcium Exchanger 1 in Heart Failure. J. Biol. Chem. 2014; 289: 33984–33998.

Weber JJ, Sowa AS, Binder T, Hübener J. From pathways to targets: Understanding the mechanisms behind polyglutamine disease. Biomed Res. Int. 2014; 2014: 1–22.

Wellington CL, Ellerby LM, Hackam a S, Margolis RL, Trifiro M a, Singaraja R, et al. Caspase cleavage of gene products associated with triplet expansion disorders generates truncated fragments containing the polyglutamine tract. J. Biol. Chem. 1998; 273: 9158–67.

Wellington CL, Hayden MR. Of molecular interactions, mice and mechanisms: new insights into Huntington's disease. Curr. Opin. Neurol. 1997; 10: 291–8.

Woerner AC, Frottin F, Hornburg D, Feng LR, Meissner F, Patra M, et al. Cytoplasmic protein aggregates interfere with nucleocytoplasmic transport of protein and RNA. Science (80-.). 2016; 351: 173–176.

Xilouri M, Brekk OR, Stefanis L. Alpha-synuclein and Protein Degradation Systems: a Reciprocal Relationship. Mol. Neurobiol. 2013; 47: 537–551.

Yvert G, Lindenberg KS, Picaud S, Landwehrmeyer GB, Sahel J a, Mandel JL. Expanded polyglutamines induce neurodegeneration and trans-neuronal alterations in cerebellum and retina of SCA7 transgenic mice. Hum. Mol. Genet. 2000; 9: 2491–506.

g. Weber et al., 2017, Brain.

Figures and Figure Legends

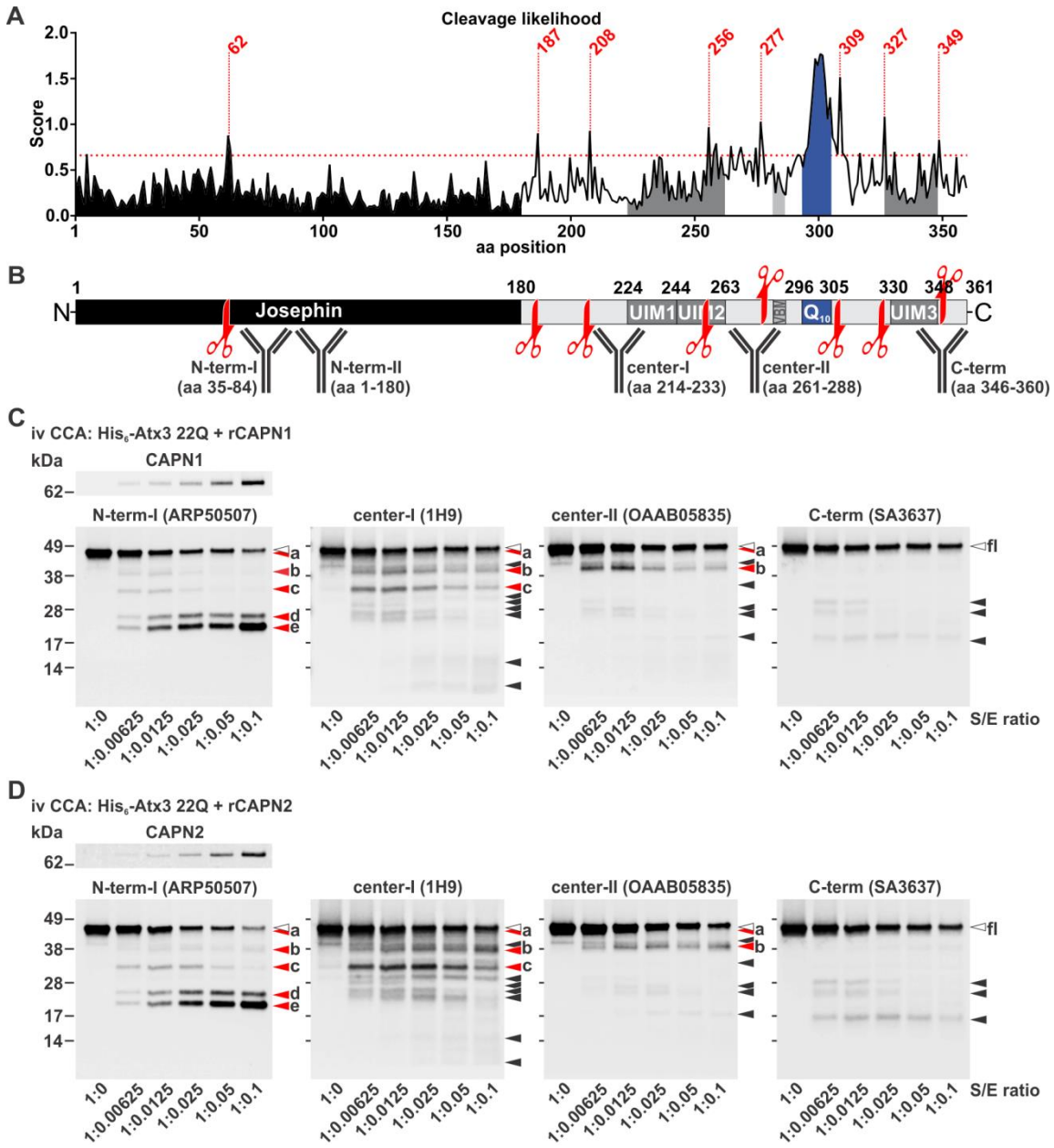

Figure 1: Calpain cleavage site prediction and calpain cleavage of ataxin-3 *in vitro*. (**A**) *In silico* prediction of calpain cleavage sites in the ataxin-3 protein (UniProt identifier: P54252-2) using the GPS-CCD tool. The red dotted line indicates maximum default cut-off value of 0.654. (**B**) Graphic representation of the ataxin-3 protein structure, highlighting domains, calpain cleavage sites (red scissors) and antibody epitopes. (**C and D**) Purified ataxin-3 (Atx3) 22Q is cleaved by recombinant calpain-1 (rCAPN1) and calpain-2 (rCAPN2) *in vitro.* Characteristic fragment patterns can be detected using four different ataxin-3-specific antibodies. iv CCA = *in vitro* calpain cleavage assay; S/E ratio = substrate/enzyme ratio; fl =

full-length. Ataxin-3 fragments are labelled with letters ‘a’ to ‘e’ according to their expected cleavage site position from the N- to the C-terminus.

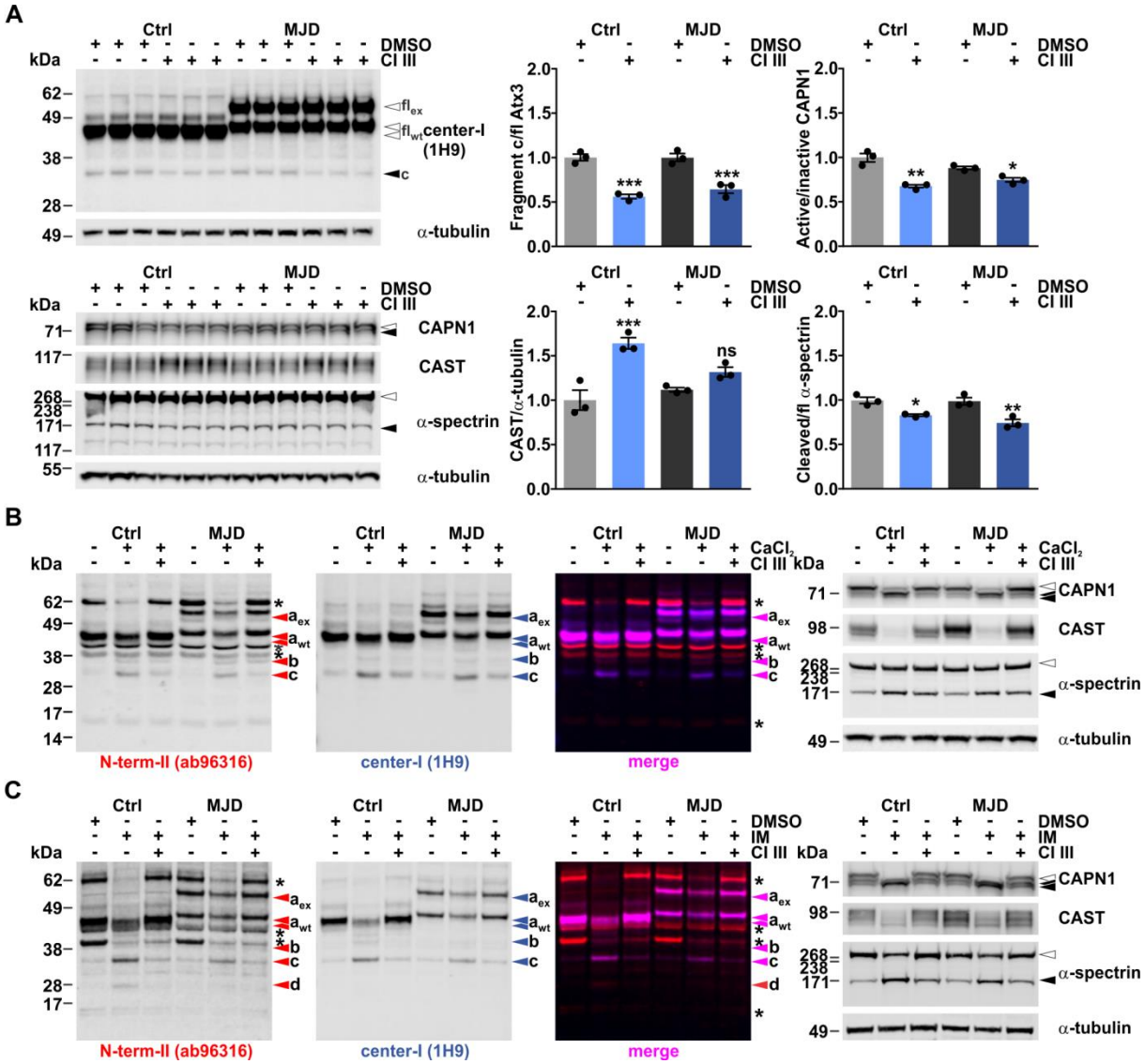

Figure 2: Ataxin-3 is cleaved by calpains in patient-derived SV40-immortalized fibroblasts. (**A**) Treating control (Ctrl) and patient-derived (MJD) SV40-immortalized fibroblasts with calpain inhibitor III (CI III) reduced levels of ataxin-3 fragment 'c' and attenuated the calpain system activation as confirmed by decreased calpain-1 activation, elevated CAST levels and decreased fragmentation of α-spectrin. Tubulin served as loading control. Densitometry analysis shows an ataxin-3 cleavage reduction by approx. 50%. Bars represent means ± SEM, relative to wild-type control and with n = 3. **P* < 0.05; ***P* < 0.01; ****P* < 0.001 (One-way ANOVA with Tukey post-test). (**B**) Calpains can be activated in cell culture lysates of control- and patient-derived SV-40-immortalized fibroblasts by addition of $CaCl_2$. Activation resulted in cleavage of wild-type and polyQ-expanded ataxin-3 featuring specific fragments ('a', 'b', and 'c'). Fragment formation was prevented by CI III treatment. Tubulin served as loading control. (**C**) Ionomycin (IM)-facilitated Ca^{2+} influx in control- and

patient-derived SV-40-immortalized fibroblasts leads to an activation of calpains and to an ataxin-3 cleavage. The fragmentation pattern is comparable to the one observed after *in vitro* calpain activation (fragment ‘a’, ‘b’, ‘c’, and, in addition, ‘d’). Pre-treatment of cell with CI III abolished ataxin-3 cleavage. Tubulin served as loading control. wt = wild-type; ex = expanded. Asterisks indicate unspecific bands.

g. Weber et al., 2017, Brain.

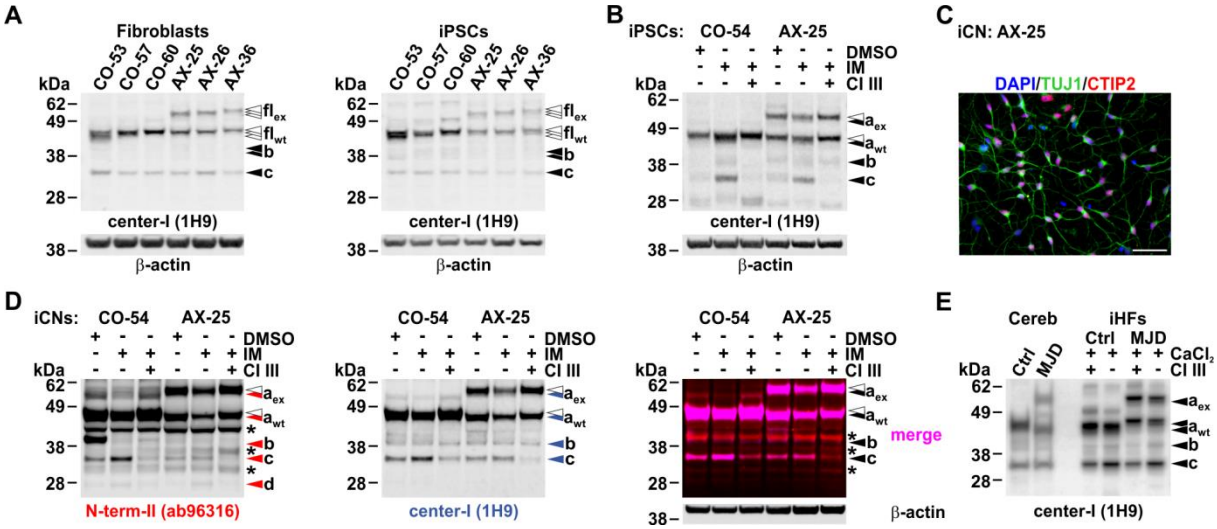

Figure 3: Calpain-dependent ataxin-3 cleavage is apparent in patient-derived fibroblasts, iPS cells and *post mortem* brain tissue. (**A**) Western blot analysis of ataxin-3 fragmentation in fibroblasts and corresponding iPS cell lines (iPSCs) derived from MJD patients and healthy controls. Detection with the ataxin-3-specific antibody 1H9 shows a predominant cleavage band between 28 and 38 kDa ('c'). Actin served as loading control. (**B**) Treatment of iPSCs from a MJD patient and a control with ionomycin (IM) leads to an increased breakdown of ataxin-3 and to elevated levels of fragments 'a', 'b' and 'c'. This effect was countered by pre-treatment with calpain inhibitor III (CI III). Actin served as loading control. (**C**) Cortical neurons differentiated (iCNs) from patient-derived iPS cells exhibit typical neuronal morphology by expressing β-III-tubulin (TUJ1, green) and the cortical layer V/VI- specific marker CTIP2 (red). Nuclei were counterstained with DAPI (blue). Scale bar = 50 µm. (**D**) iCNs from a MJD patient and a control were treated with ionomycin (IM). Treatment induced cleavage of ataxin-3 accompanied with the formation of fragments 'a', 'c' and 'd' as detected by western blot analysis. Actin served as loading control. Asterisks indicate unspecific bands. (**E**) Comparison of the fragmentation of *in vitro* cleaved ataxin-3 with ataxin-3 from human tissue. *Post mortem* cerebellar samples of a MJD patient and a control were analysed along with calpain-activated SV-40-immortalized fibroblast (iHFs) samples. Typical N-terminal ataxin-3 fragments deriving from calpain cleavage can be observed both in human brain tissue and fibroblast samples. wt = wild-type; ex = expanded.

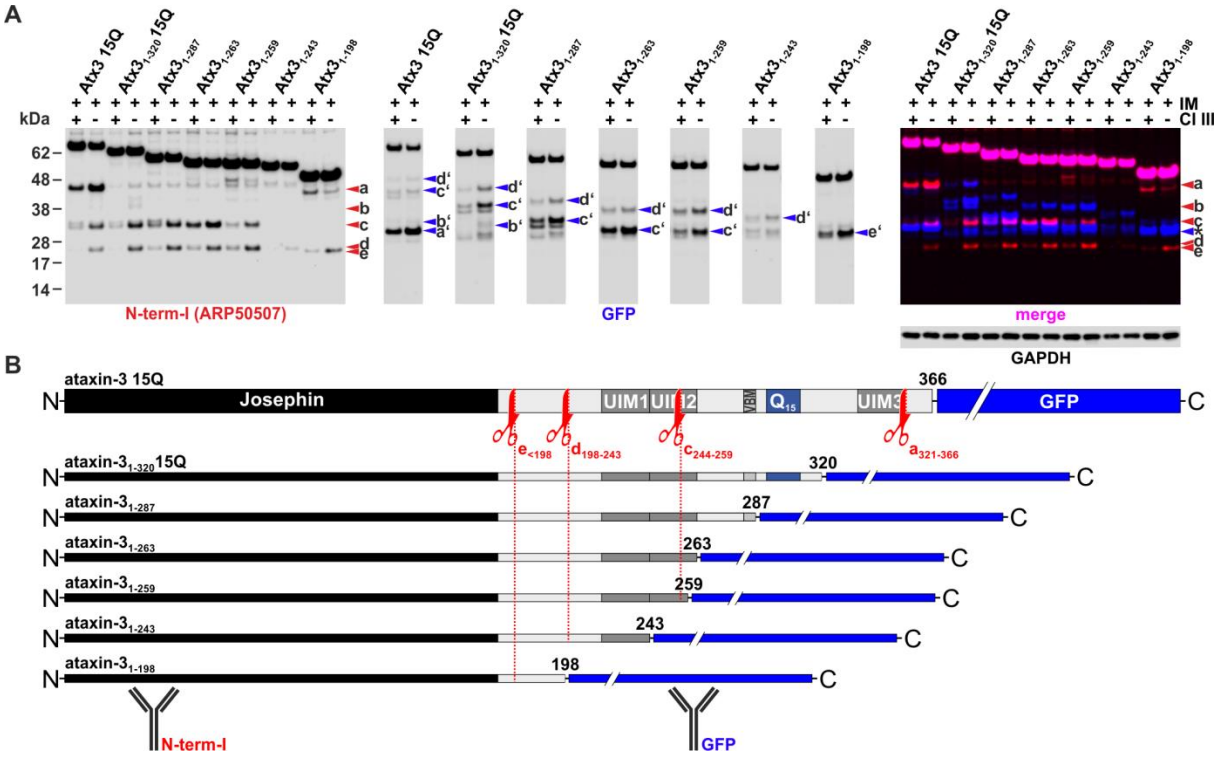

Figure 4: Deletion constructs help to unveil calpain cleavage sites in ataxin-3. (**A**) C-terminal deletion constructs of ataxin-3 display various calpain-dependent cleavage patterns attributed to the presence or absence of specific calpain cleavage sites. Constructs were overexpressed in HEK 293T cells and endogenous calpains activated by ionomycin (IM) administration. CI III treatment served as a negative control. Fragmentation patterns were analysed via western blotting. Red arrowheads labelled with ‘a’ to ‘e’ indicate N-terminal fragments of ataxin-3. C-terminal GFP-positive fragments, presumably corresponding to the N-terminal breakdown products, are marked with blue arrowheads and are respectively labelled with ‘a’’ to ‘e’’. GAPDH served as loading control. (**B**) Graphic representation of utilized ataxin-3 deletion constructs, putative cleavage regions (red scissors and dotted line) within the ataxin-3 protein and binding sites of used antibodies.

g. Weber et al., 2017, Brain.

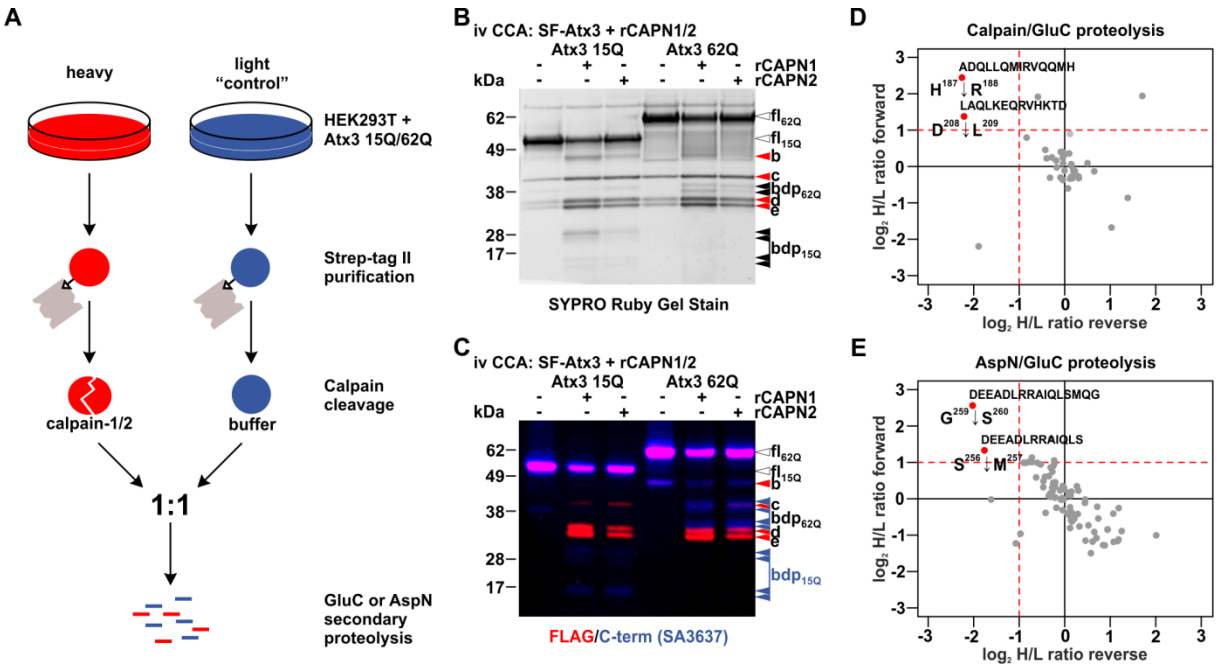

Figure 5: Cleavage sites can be identified using mass-spectrometry. (**A**) Overview of the SILAC-based quantitative mass spectrometry approach to map calpain cleavage sites. (**B and C**) For mass-spectrometry analysis, purified recombinant SF-tagged ataxin-3 15Q and 62Q were incubated with recombinant calpain-1 (rCAPN1) or calpain-2 (rCAPN2). To monitor the reaction, aliquots of the sample were analysed using SDS-PAGE. Total protein stain with SYPRO Ruby shows that ataxin-3 is cleaved by both calpains producing comparable patterns of polyQ-dependent and -independent fragments. N-terminal and C-terminal breakdown products were detected via immunodetection using antibodies against the FLAG-tag and against ataxin-3 (SA3637). iv CCA = *in vitro* calpain cleavage assay; bdp = breakdown product. (**D and E**) Scatterplots for the combined quantitative mass spectrometry approach. Log_2 median ratios of the forward experiments were plotted over the log_2 median ratios of the reverse experiments (label switch). Calpain-1/2 treatment following either a GluC or AspN secondary proteolysis allowed the identification of the calpain cleavage sites H187, D208 and S256 and G259. A minimum ratio of 2 in the forward experiments and a minimum ratio of 0.5 in the reverse experiments have been set as significance level (red line).

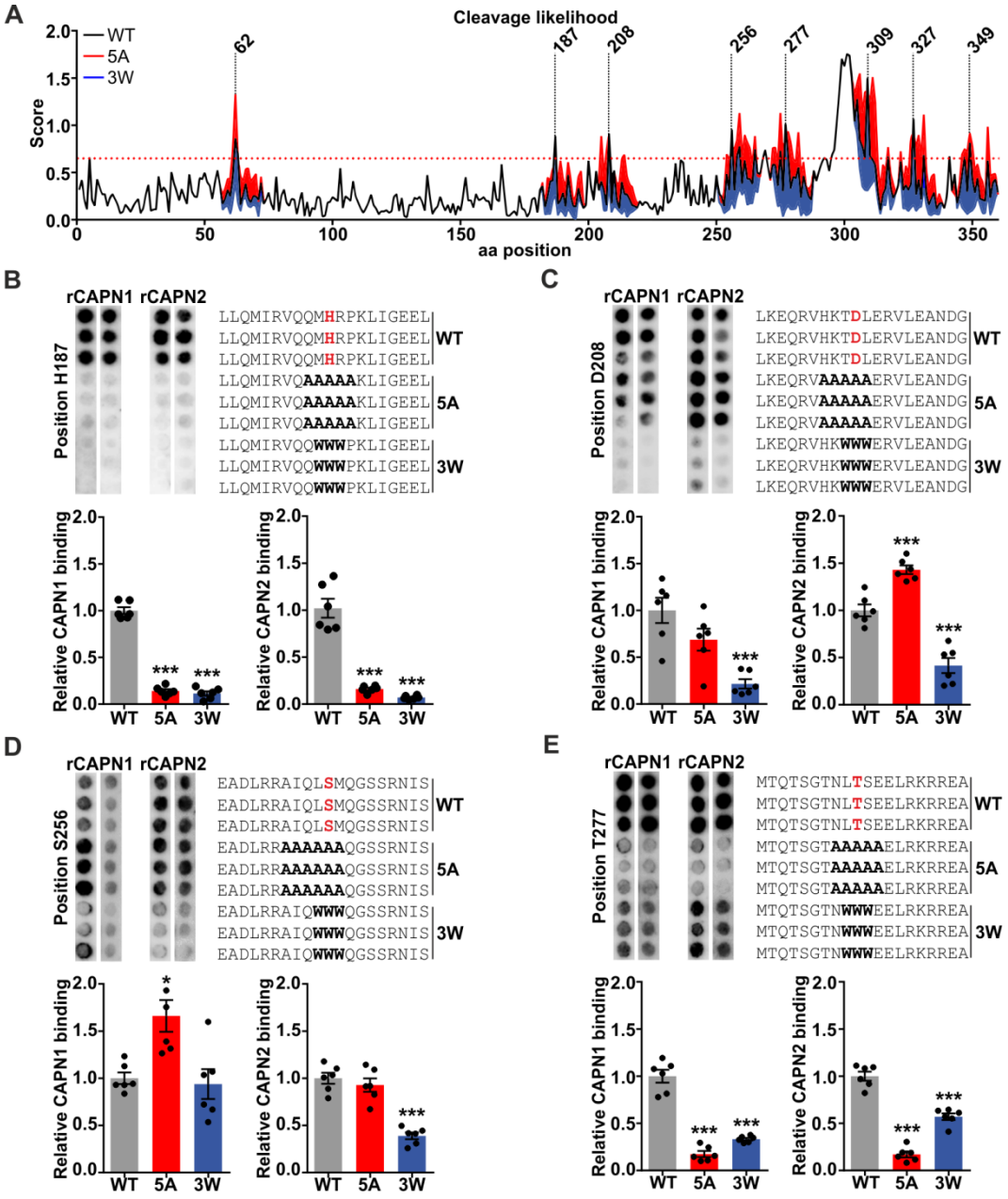

Figure 6: Overlay of 20-mer ataxin-3 peptide arrays with calpain-1 and calpain-2 shows reduced calpain binding after triple tryptophan substitution. (**A**) *In silico* prediction of calpain cleavage sites in ataxin-3 (UniProt identifier: P54252-2) using the GPS-CCD tool and effects of replacing amino acids surrounding predicted cleavage sites by five alanines or three tryptophans on calpain cleavage likelihood. The red dotted line indicates maximum default cut-off value of 0.654. (**B – F**) Calpain binding to putative cleavage sites in ataxin-3 was analysed by overlaying cleavage site-containing 20-mer ataxin-3 peptides with calpain-1 (rCAPN1) and calpain-2 (rCAPN2). Cleavage positions are located after the red-labelled amino acid. Replacement of amino acids at the putative cleavage sites H187, D208 and S256 indicates the most efficient reduction of calpain binding when introducing three

tryptophans. However, calpain binding at site T277 (**D**) is most reduced by introducing five alanines. For each site, detected peptide arrays of two representative experiments are shown. Bars represent means ± SEM, relative to wild-type sequence and n = 6. **P* < 0.05; ***P* < 0.01; ****P* < 0.001 (One-way ANOVA with Bonferroni post-test).

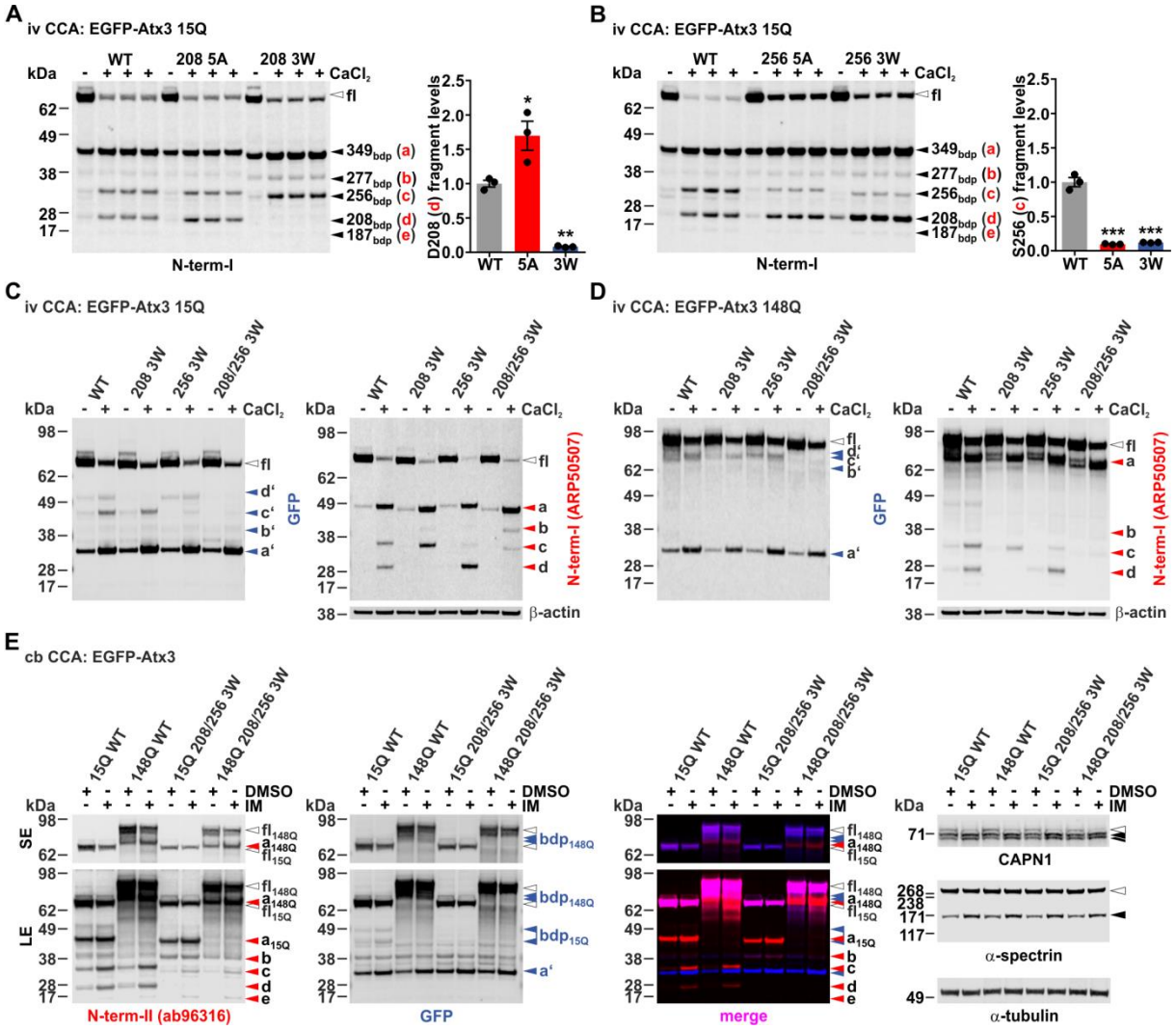

Figure 7: Mutagenesis of putative calpain cleavage sites alters fragmentation of ataxin-3. (**A and B**) Putative calpain cleavage sites within ataxin-3 15Q were mutated by a 5 alanine (5A) or a triple tryptophan (3W) exchange at positions D208 or S256. Densitometry analysis of respective fragments ('d' and 'c') induced by *in vitro* calpain cleavage assays (iv CCA) shows effects of the mutagenesis on ataxin-3 cleavage. Bars represent means ± SEM, relative to wild-type and n = 3. **P* < 0.05; ***P* < 0.01, ****P* < 0.001 (One-way ANOVA with Tukey post-test). (**C and D**) Triple tryptophan (3W) cleavage site mutations at positions D208 and S256, or at both sites in ataxin-3 15Q and 148Q show reduced levels of corresponding C-terminal (antibody: GFP) and N-terminal (antibody: N-term-I) fragments. Actin served as loading control. C-terminal ataxin-3 fragments corresponding to N-terminal fragments 'a' to 'd' are marked with an apostrophe ('a'' to 'd''). (**E**) HEK 293T cells transfected with EGFP-ataxin-3 15Q and 148Q with or without 3W mutations at positions D208 and S256 were subjected to a cell-based calpain cleavage assay (cb CCA). Detection with antibody N-term-II shows a strongly reduced occurrence of fragments 'c' and 'd' upon ionomycin (IM)-facilitated

g. Weber et al., 2017, Brain.

Ca^{2+} influx for ataxin-3 208/256 3W when compared to the unmutated variants. Activation of the calpain system was validated by detecting calpain-1 activation and α-spectrin cleavage. Tubulin served as loading control. bdp = breakdown product. SE = short exposure; LE = long exposure.

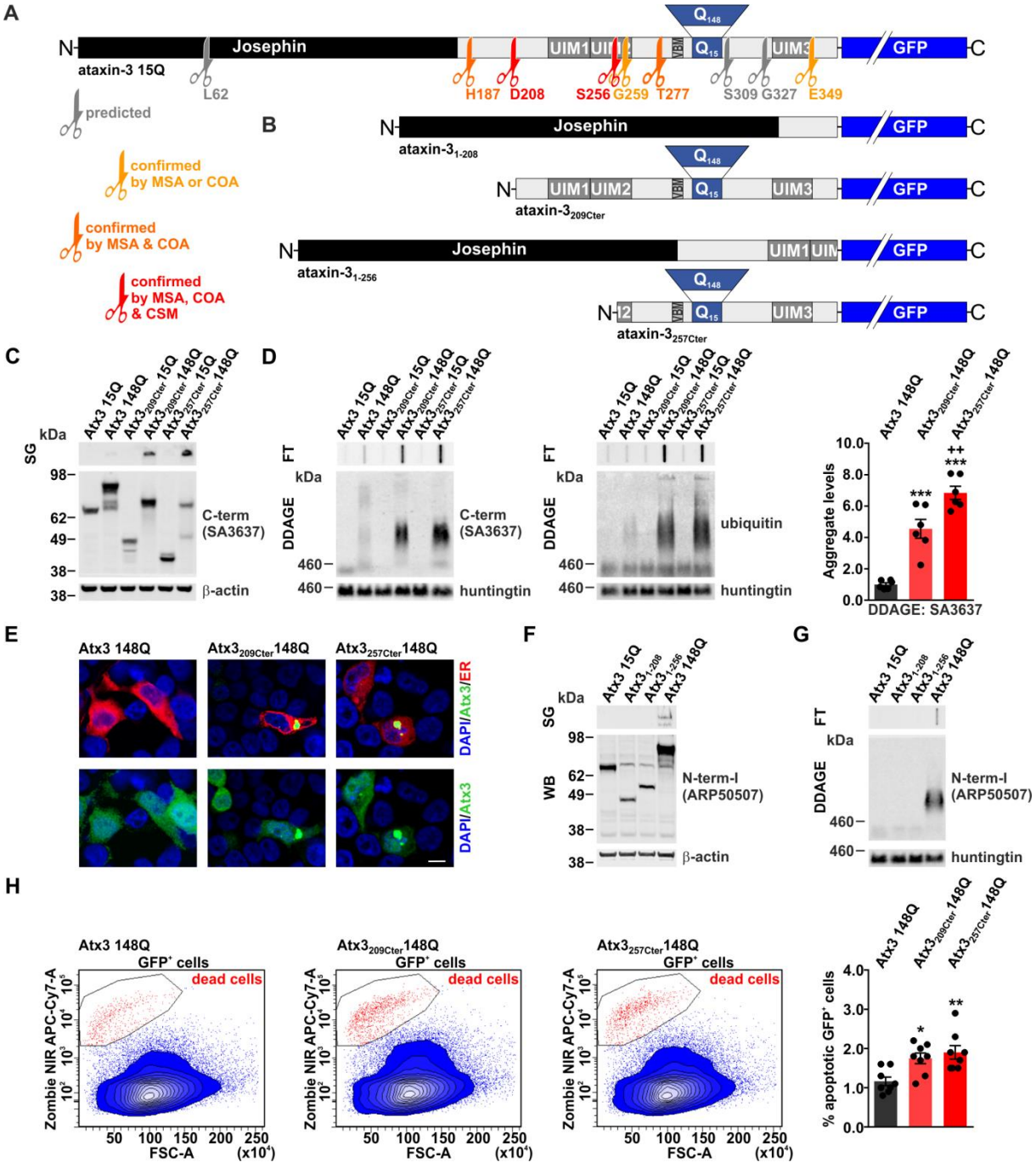

Figure 8: C-terminal calpain cleavage-corresponding fragment constructs are highly aggregation-prone and toxic. (**A**) Overview of identified calpain cleavage sites within the ataxin-3 protein. Grey scissors indicate unconfirmed but *in silico* predicted cleavage sites. Yellow scissors show cleavage sites confirmed by mass spectrometry analysis (MSA) or calpain overlay assays (COA). Orange scissors show sites confirmed by both MSA and COA. Red scissors highlight cleavage sites which were not only identified via MSA and COA but also confirmed by mutating cleavage sites (CSM). (**B**) Graphic representation of GFP-tagged N-terminal and C-terminal fragment constructs corresponding to calpain cleavage of

ataxin-3 after position D208 (1-208 and 209Cter) and S256 (1-256 and 257Cter). C-terminal fragments were generated in two different polyQ-variants (wild-type 15Q and expanded 148Q). (**C**) Overexpression of calpain cleavage-corresponding C-terminal fragment constructs in HEK 293T was analysed via western blotting (WB). Insoluble forms of ataxin-3 in the stacking gel (SG) were detected for ataxin-3 $_{209Cter}$ 148Q and ataxin-3 $_{257Cter}$ 148Q, but barely for full-length ataxin-3 148Q. Actin and huntingtin served as loading controls. (**D**) Filter retardation assays (FT) and denaturing detergent agarose gel electrophoresis (DDAGE) show elevated levels of aggregates formed by fragment constructs ataxin-3 $_{209Cter}$ 148Q and ataxin-3 $_{257Cter}$ 148Q. These aggregates show a strong ubiquitination. Densitometry of the DDAGE reveals the significant increase in aggregation by C-terminal expanded fragment constructs. Bars represent means ± SEM, relative to wild-type and n = 3. **P* < 0.05; ***P* < 0.01; ****P* < 0.001 (One-way ANOVA with Tukey post-test). (**E**) Confocal microscopy of HEK 293T cells expressing EGFP-tagged full-length ataxin-3, fragment constructs and DsRed2-ER (for highlighting the endoplasmic reticulum) shows massive and mainly cytoplasmic formation of aggregates. DAPI was used as a nuclear counter stain. Scale bar = 10 µm. (**F and G**) EGFP-tagged N-terminal ataxin-3 fragment constructs ataxin-3 $_{1-208}$ and ataxin-3 $_{1-256}$ were overexpressed in HEK 293T cells in comparison to 15Q and 148Q full-length ataxin-3 and expression analysed by WB. Overexpression of both N-terminal fragment constructs did not lead to the formation of aggregates as analysed by FT and DDAGE. Actin and huntingtin served as loading controls. (**H**) FACS based viability analysis of EGFP-positive (GFP^+) HEK 293T cells using the Zombie NIR dye reveals an increased cell death when overexpressing fragment constructs ataxin-3 $_{209Cter}$ 148Q and ataxin-3 $_{257Cter}$ 148Q in comparison to full-length ataxin-3 148Q. Bars represent means ± SEM, as percentage of GFP^+ cells, n = 8. **P* < 0.05; ***P* < 0.01 (One-way ANOVA with Tukey post-test).